DISRUPTORS ON MALE REPRODUCTION - EMERGING RISK FACTORS

EDITED BY: Qing Chen, Yankai Xia, Honggang Li, Rossella Cannarella and Panagiotis Drakopoulos

PUBLISHED IN: Frontiers in Endocrinology and Frontiers in Physiology

frontiers Research Topics

ISSN 1664-8714
ISBN 978-2-88976-407-5
DOI 10.3389/978-2-88976-407-5

About Frontiers

Frontiers is more than just an open-access publisher of scholarly articles: it is a pioneering approach to the world of academia, radically improving the way scholarly research is managed. The grand vision of Frontiers is a world where all people have an equal opportunity to seek, share and generate knowledge. Frontiers provides immediate and permanent online open access to all its publications, but this alone is not enough to realize our grand goals.

Frontiers Journal Series

The Frontiers Journal Series is a multi-tier and interdisciplinary set of open-access, online journals, promising a paradigm shift from the current review, selection and dissemination processes in academic publishing. All Frontiers journals are driven by researchers for researchers; therefore, they constitute a service to the scholarly community. At the same time, the Frontiers Journal Series operates on a revolutionary invention, the tiered publishing system, initially addressing specific communities of scholars, and gradually climbing up to broader public understanding, thus serving the interests of the lay society, too.

Dedication to Quality

Each Frontiers article is a landmark of the highest quality, thanks to genuinely collaborative interactions between authors and review editors, who include some of the world's best academicians. Research must be certified by peers before entering a stream of knowledge that may eventually reach the public - and shape society; therefore, Frontiers only applies the most rigorous and unbiased reviews.
Frontiers revolutionizes research publishing by freely delivering the most outstanding research, evaluated with no bias from both the academic and social point of view. By applying the most advanced information technologies, Frontiers is catapulting scholarly publishing into a new generation.

What are Frontiers Research Topics?

Frontiers Research Topics are very popular trademarks of the Frontiers Journals Series: they are collections of at least ten articles, all centered on a particular subject. With their unique mix of varied contributions from Original Research to Review Articles, Frontiers Research Topics unify the most influential researchers, the latest key findings and historical advances in a hot research area! Find out more on how to host your own Frontiers Research Topic or contribute to one as an author by contacting the Frontiers Editorial Office: frontiersin.org/about/contact

DISRUPTORS ON MALE REPRODUCTION - EMERGING RISK FACTORS

Topic Editors:
Qing Chen, Army Medical University, China
Yankai Xia, Nanjing Medical University, China
Honggang Li, Huazhong University of Science and Technology, China
Rossella Cannarella, University of Catania, Italy
Panagiotis Drakopoulos, University Hospital Brussels, Belgium

Citation: Chen, Q., Xia, Y., Li, H., Cannarella, R., Drakopoulos, P., eds. (2022). Disruptors on Male Reproduction - Emerging Risk Factors. Lausanne: Frontiers Media SA. doi: 10.3389/978-2-88976-407-5

Table of Contents

frontiers | Frontiers in Endocrinology

EDITORIAL
published: 31 May 2022
doi: 10.3389/fendo.2022.934098

Editorial: Disruptors on Male Reproduction - Emerging Risk Factors

Yankai Xia[1], Honggang Li[2], Rossella Cannarella[3], Panagiotis Drakopoulos[4,5,6] and Qing Chen[7]**

[1] State Key Laboratory of Reproductive Medicine, Center for Global Health, School of Public Health, Nanjing Medical University, Nanjing, China, [2] Institute of Reproductive Health, Tongji Medical College, Huazhong University of Science and Technology, Wuhan, China, [3] Department of Clinical and Experimental Medicine, University of Catania, Catania, Italy, [4] Centre for Reproductive Medicine, Universitair Ziekenhuis Brussel, Vrije Universiteit Brussel, Brussels, Belgium, [5] Department of Obstetrics and Gynaecology, University of Alexandria, Alexandria, Egypt, [6] In Vitro Fertilisation (IVF) Athens, Athens, Greece, [7] Key Lab of Medical Protection for Electromagnetic Radiation, Ministry of Education of China, Institute of Toxicology, College of Preventive Medicine, Army Medical University (Third Military Medical University), Chongqing, China

Keywords: reproduction, risk factors, lifestyle & behaviour, environmental factors, genetic susceptibility

Editorial on the Research Topic

Disruptors on Male Reproduction - Emerging Risk Factors

Over the past decades, male reproductive health has been deteriorating, partially due to the exposure to environment and lifestyle harmful factors (1, 2). With emerging and widespread harmful substances in our daily life, it becomes urgent to identify and assess their risk on male reproductive health.

Certain genetic variants could increase the susceptibility of the reproductive system to the environmental damage (3). The field of genomics has provided an extraordinary level of knowledge, aided by large-scale, unbiased genome-wide association studies (GWAS). A similar level of analysis, however, is still lacking for the influences of environmental factors on the reproductive phenotype (4, 5).

Never before, in human history, has there been such a vast multiplicity of environmental risk factors, nor has there been such expression of concern regarding their effects on health, especially on reproductive health (6). Increasing scientific evidence has shown the adverse impacts of environmental risk factors on human reproduction (7). Maternal or paternal exposure to environmental chemicals (e.g., pesticides, heavy metals, phthalates, and polycyclic aromatic hydrocarbons) can lead to a myriad of health consequences, which can manifest across individuals' lifespan and potentially be transmitted to future generations (8).

Although the risk factors of traditional environmental pollutants have been intensively investigated, their contributions could only explain a limited proportion of the reproductive damages. On the other hand, in modern society, emerging factors including novel physical factors (e.g., C-irradiation, cryopreservation, Wi-Fi), environmental chemical exposures (e.g., TiO_2 nanoparticles, $PM_{2.5}$, per-fluoroalkyl and polyfluoroalkyl substances, pesticides), biological contamination (e.g., COVID-19), behavioral and lifestyle factors (e.g., pornography use, circadian desynchrony, assisted reproductive technology) and diseases status [e.g., type 2 diabetes mellitus, obstructive sleep apnea (OSA)] have not been studied in detail. To be noted, these factors have been even less studied with regard to male reproductive damages compared to female disorders. It is urgent to understand these novel factors in terms of populational distribution/burden, impacts on male reproductive health (endocrinal disruption, sperm damage, subfecundity and infertility) as well as the underlying mechanisms.

This Research Topic aims to provide insights into the contribution of novel environmental, lifestyle and psychological factors to male reproductive damages and the mechanisms. In Volume I

OPEN ACCESS

Edited and reviewed by:
Vikas Kumar Roy,
Mizoram University, Aizawl, India

****Correspondence:***
Yankai Xia
yankaixia@njmu.edu.cn
Qing Chen
rhi@tmmu.edu.cn

Specialty section:
This article was submitted to Reproduction, a section of the journal Frontiers in Endocrinology

Received: *02 May 2022*
Accepted: *10 May 2022*
Published: *31 May 2022*

Citation:
Xia Y, Li H, Cannarella R, Drakopoulos P and Chen Q (2022) Editorial: Disruptors on Male Reproduction - Emerging Risk Factors. Front. Endocrinol. 13:934098. doi: 10.3389/fendo.2022.934098

we have accepted 18 articles and reviews, which provide interesting and exciting insights to this growing field with coverage of various potential risk factors.

Radiation is a ubiquitous environmental exposure in modern society. In the current Research Topic, Guo et al. investigated that the abscopal effects of C-irradiation on testis with regard to both structure and function and ultimately decreased sperm quality in mice. Chen et al. studied the motility, acrosomal integrity, and mitochondrial membrane potential (MMP), as well as proteomic change, of cynomolgus macaque sperm after cryopreservation. They hypothesized that AFP III may reduce the release of cytochrome C and thereby reduce sperm apoptosis by modulating the production of ROS in mitochondria. This may represent a novel molecular mechanism for cryoprotection. In addition, Jaffar et al. concluded that the long-term Wi-Fi exposure from pre-pubertal to adult age could reduce spermatogonia proliferation in the testis.

Another well celebrated example of risk factors was exposure to environmental chemicals. Although *in vitro*, Mancuso et al. highlighted the adverse effects even of subtoxic dose of TiO_2 nanoparticles on porcine prepubertal Sertoli cells (SCs) functionality and viability and, more importantly, set the basis for further *in vivo* studies, especially in chronic exposure at subtoxic dose which is closer to the human exposure to this nano agent. Calvert et al. reviewed the literature on the biological effects of perfluoroalkyl and polyfluoroalkyl substances (PFAS) exposure, with a specific focus on male reproduction, owing to its utility as a sentinel marker of general health. Shi et al. demonstrated that $PM_{2.5}$ exposure could induce spermatocyte damage and energy metabolism disorder. The activation of the aryl hydrocarbon receptor might be involved in the mechanism of male reproductive toxicity. Gao et al. suggested that a manipulation on the expression of signaling proteins regulating spermatogenesis could possibly be used to manage the toxicant-induced male reproductive dysfunction.

Environmental factors mediate changes in expression patterns can be explained by a complex network of modifications to the DNA, histone proteins and degree of DNA packaging as well as changes in DNA structure such as mitochondrial DNA copy number and chromatin integrity. Throughout our lives, epigenetic processes shape our development and enable us to adapt to a constantly changing environment. Ma et al. integrated glufosinate-ammonium (GLA) induced alterations in sperm epigenome and embryo transcriptome, and further explored their concordance, thus providing a new strategy for gamete-to-embryo toxicity assessment. Intriguingly, this study also noted that paternal GLA exposure induced aberrant transcription in both paternal and maternal alleles of preimplantation embryos, which deserves further investigation. Wang et al. concluded that bivalent chromatin structure resulted in large differences in the methylation of autism genes between manually selected spermatozoa (MSS) and Zona pellucida (ZP)-bound spermatozoa (ZPBS). Intracytoplasmic sperm injection (ICSI) using MSS, which increased the risk of methylation changes compared with ZPBS, may lead to a higher risk of autism in offspring. Liu et al. contributed to the understanding of epigenetic regulation of tet methylcytosine dioxygenase 1-Sp1 transcription factor (TET1-SP1) during spermatogonia self-renewal and proliferation. Shi et al. focused on the associations between sperm mitochondrial DNA copy number (mtDNA-CN), DNA fragmentation index (DFI), and reactive oxygen species (ROS) and embryo development as well as pregnancy outcomes in assisted reproductive technology (ART).

COVID-19 is a serious challenge to the global health systems. It has been found that the hazardous effects of COVID-19 go far beyond respiratory system, and a body of studies explored the impact of COVID-19 on male reproduction from different aspects. Guo et al. reviewed the relationship of COVID-19 and male reproduction and provided a panoramic view to understand the effect of the virus on male reproduction and a new perspective of further research for reproductive clinicians and scientists.

Behavioral and lifestyle factors may also have a substantial contribution to the damage of male reproductive health. As suggested by Cui et al., pornography use was common among male college students in China. Early contact, frequent use, and high frequency of masturbation during pornography use could lead to not only addiction trends but aberrant reproductive hormone levels and semen quality as well. Up to date, this article has received over 6,700 views and exceeded 83% of all the Frontiers articles in only 7 months. Fusco et al. aimed to provide data about pre-clinical and clinical evidence exploring the impact of circadian desynchrony on spermatogenesis. Zatecka et al. emphasized the importance of improving metabolic health not only in women of reproductive age, but also in potential fathers, in order to reduce the negative impacts of diabetes on subsequent generations. Feng et al. characterized erectile dysfunction (ED) in OSA patients.

Updated information about increasingly emerging environmental perpetrators, including physical, chemical, biological and behavioral/lifestyle risk factors can improve our understanding of male reproductive health. With the rapid evolvement of omics technologies in genomics, epigenomics, transcriptomics, proteomics and metabolomics, it is reasonable to expect that in the near future there will be plenty of studies to renew our knowledge on emerging risk factors and the attendant adverse effects on male reproductive health, as well as the underlying mechanisms. Hence, to keep the constant concern and to inspire new studies to this filed, the Volume II focusing on the same topic has started and we anticipate to receive high-quality submissions all over the world (https://www.frontiersin.org/research-topics/35111/).

AUTHOR CONTRIBUTIONS

All authors listed have made a substantial, direct and intellectual contribution to the work, and approved it for publication.

FUNDING

The work was supported by the National Key Project of Research and Development Program (Grant number: 2018YFC1004200, 2018YFC1004202) and the Ability Promotion Programme of Army Medical University (Grant number: 2021XZL01).

REFERENCES

1. Axelsson J, Bonde JP, Giwercman YL, Rylander L, Giwercman A. Gene-Environment Interaction and Male Reproductive Function. *Asian J Androl* (2010) 12(3):298–307. doi: 10.1038/aja.2010.16
2. Oliva A, Spira A, Multigner L. Contribution of Environmental Factors to the Risk of Male Infertility. *Hum Reprod* (2001) 16(8):1768–76. doi: 10.1093/humrep/16.8.1768
3. Hunter DJ. Gene-Environment Interactions in Human Diseases. *Nat Rev Genet* (2005) 6(4):287–98. doi: 10.1038/nrg1578
4. Wild CP. Complementing the Genome With an "Exposome": The Outstanding Challenge of Environmental Exposure Measurement in Molecular Epidemiology. *Cancer Epidemiol Biomarkers Prev* (2005) 14(8):1847–50. doi: 10.1158/1055-9965.Epi-05-0456
5. Vermeulen R, Schymanski EL, Barabási AL, Miller GW. The Exposome and Health: Where Chemistry Meets Biology. *Science* (2020) 367(6476):392–6. doi: 10.1126/science.aay3164
6. Bajaj JS, Misra A, Rajalakshmi M, Madan R. Environmental Release of Chemicals and Reproductive Ecology. *Environ Health Perspect* (1993) 101 (Suppl 2):125–30. doi: 10.1289/ehp.93101s2125
7. Li W, Chen B, Ding X. Environment and Reproductive Health in China: Challenges and Opportunities. *Environ Health Perspect* (2012) 120(5):A184–5. doi: 10.1289/ehp.1205117
8. Wang A, Padula A, Sirota M, Woodruff TJ. Environmental Influences on Reproductive Health: The Importance of Chemical Exposures. *Fertil Steril* (2016) 106(4):905–29. doi: 10.1016/j.fertnstert.2016.07.1076

Conflict of Interest: The authors declare that the research was conducted in the absence of any commercial or financial relationships that could be construed as a potential conflict of interest.

frontiers in Endocrinology

ORIGINAL RESEARCH
published: 10 September 2021
doi: 10.3389/fendo.2021.736384

Pornography Use Could Lead to Addiction and Was Associated With Reproductive Hormone Levels and Semen Quality: A Report From the MARHCS Study in China

Zhihong Cui[1†], Min Mo[2†], Qing Chen[2], Xiaogang Wang[2], Huan Yang[2], Niya Zhou[2], Lei Sun[2], Jinyi Liu[2], Lin Ao[2] and Jia Cao[2]*

[1] College of Pharmaceutical Sciences and Chinese Medicine, Southwest University, Chongqing, China, [2] Institute of Toxicology, College of Preventive Medicine, Army Military Medical University, Chongqing, China

OPEN ACCESS

Edited by:
Richard Ivell, University of Nottingham, United Kingdom

Reviewed by:
Zengjun Wang, Nanjing Medical University, China
Junjim Zhang, Shanghai Jiao Tong University, China

***Correspondence:**
Jia Cao
caojia1962@126.com

†These authors have contributed equally to this work and share first authorship

Specialty section:
This article was submitted to Reproduction, a section of the journal Frontiers in Endocrinology

Received: *05 July 2021*
Accepted: *17 August 2021*
Published: *10 September 2021*

Citation:
Cui Z, Mo M, Chen Q, Wang X, Yang H, Zhou N, Sun L, Liu J, Ao L and Cao J (2021) Pornography Use Could Lead to Addiction and Was Associated With Reproductive Hormone Levels and Semen Quality: A Report From the MARHCS Study in China. Front. Endocrinol. 12:736384. doi: 10.3389/fendo.2021.736384

This study aimed to investigate the situations of pornography use among male college students of China, to explore the addiction possibility for pornography use, and to study the associations between pornography use and reproductive hormone levels and semen quality. Five hundred sixty-eight participants met the inclusion criteria and finished all of the questionnaires and hormone level and semen parameter examinations. A majority of participants (except one) had pornography use experience, 94.2% participants started pornography use before college, and 95.9% participants reported they had masturbation experience when using pornography. Early contact to pornography, frequent pornography use, high amount of time spending on pornography use, and frequent masturbation during pornography use were correlated with addiction trends. Earlier pornography use was found to be associated with lower serum prolactin (PRL), follicle-stimulating hormone (FSH), and progesterone (Prog), as well as lower sperm concentration and total sperm count. Higher frequency of pornography use was associated with lower serum estrogen (E_2). In conclusion, pornography use was common among male college students in China. Early contact, high frequent use, and high frequency of masturbation during pornography use could lead to addiction trends and aberrant reproductive hormone levels and semen quality.

Keywords: pornography, addiction, reproductive hormone, semen quality, college students

INTRODUCTION

Sex demand is considered an embarrassing issue in many eastern countries, particularly in China in the past years. It is hard for adolescents to get sex information from parents or schools. At the same time, adolescents during the puberty process have high demands for sexual sensation and sex information physically and psychologically. With the quick development of the Internet, pornography has become easily accessible to all ages because of its affordability, accessibility, and anonymity (1). It was estimated that 42.7% of Internet visitors have visited pornography websites,

and 25% of Internet visitors visit pornography websites everyday (2). Adolescents are important audience for pornography works (3). An investigation among 563 US college students reported that by age 17, an overwhelming majority of boys (93%) and girls (62%) have been exposed to pornography, and boys were more likely to be exposed at an earlier age and with higher frequency (4). Similarly, situations happened in other regions (5–7). A 6-year longitudinal study showed that among middle school students of Hong Kong, from grade 7 (average age = 12.7) to grade 12, pornography consumption increased significantly, and boys were more likely to contact pornography works (8, 9). However, the pornography exposure to adolescents, especially to college students in mainland of China were not clear.

Some of the investigations showed that pornography had some positive or neutral effects on adolescents' sexual practice. For example, pornography was found to be a resource to provide information about the human body, to increase the sense of sexual competence, and to decrease the sexual shame (10). On the other hand, there are also studies suggesting its negative effects. Several publications showed that increased pornography exposure was associated with earlier and quicker onset of sexual activity (11), more permissive attitude to casual sex (12), worse mental health (5), higher likelihood to risky sexual behaviors, and more acceptance of sexual violence (13). Moreover, a recent study revealed that problematic pornography user displayed a similar neural response as the drug addicts displayed (14). A study among Canadian university students (mean age 21) showed that daily and greater pornography use was associated with a sharp rise in addictive score (15).

Pornography is a specific sexual stimulus that can cause sexually related physical and psychological reactions, including sexual imagination, sexual erection, and masturbation (16). All of these behaviors were modulated by sexual hormones and feedback to hormone secretions, which was a typical feedback loop of hypothathalamus-putuitary-gonadal axis (HPG) activity (17, 18). Adolescents, including college students, are in the late stage of puberty, which is the important process of sexual hormones and organ maturation (19). However, none of the existing studies about pornography exhibited the effects of pornography on reproductive hormones and reproductive potentials.

The purposes of this study were as follows: (1) to explicate the current situation of pornography use among Chinese college students; (2) to investigate college students' addiction trends for pornography use; and (3) to research the associations between pornography use and reproductive hormones and semen parameters.

MATERIALS AND METHODS

Participants and Procedures

All of the participants in this study originated from a cohort termed the male reproductive health in Chongqing College students (MARHCS), which began in 2013 (20). This was the second follow-up study of the cohort. Since April 2015, all volunteers who participated in the baseline survey in 2013 received our cell phone and email illustrating this study, and they scheduled an investigation time from May 23, 2015 to June 7, 2015. All volunteers were asked to complete a questionnaire and underwent a physical examination. Individuals were included if they met the following criteria: over 18 years of age; 2–7 days of abstinence; no history of inflammation of the urogenital system, epididymitis, or testicular injury; no history of incomplete orchiocatabasis; and no history of varicocele treatment. Subjects were excluded if any of the following symptoms were detected by aurologist at the physical examination stage of the investigation: an absence of prominentialaryngea, pubis, or testis; abnormal penis or breasts; varicocele; or an epididymal knob. Five hundred sixty-eight males completed the survey, and all of them had a mean coming-out age of 22.4 years (SD = 1.2). Semen samples were collected and analyzed according to WHO guideline (WHO, 2010). Abstinence duration and ejaculation time were recorded. Peripheral blood was collected under aseptic conditions. The serum was isolated by centrifugation for serum reproductive hormone measurements. The Ethics Council of the Army Medical University approved the study, and informed consent was obtained from all subjects.

Questionnaires

The questionnaires contained three parts: demographic information, lifestyle factors, and pornography use situations. The demographic information consisted of age, body mass index (BMI), and abstinence duration (days). Lifestyle factors included smoking, drinking, coffee consumption, cola consumption, and fried food consumption, which have all been reported to have an influence on semen quality (20).

The questions about pornography use situations and addictive behaviors were set according to previous studies about pornography exposure (21–25). Before the participants filled out the questionnaires, they were asked to read the definition of pornography, which included the following terms: sexually explicit material, sexually explicit media, pornography, porn, cyber-porn, Internet or online pornography, online erotica or erotica, and cyberpornography (24, 25).

Serum Collection and Reproductive Hormones Detection

All collected serum samples were taken from a low-temperature refrigerator at −80°C and then sent to the Army Medical University Affiliated Southwest Hospital Laboratory. The serum samples were then liquefied and tested of six reproductive hormone levels, including estradiol (E_2), follicle-stimulating hormone (FSH), luteinizing hormone (LH), progesterone (Prog), prolactin (PRL), and testosterone (T). The chemiluminescence method was used to determine the serum hormone levels, and the instrument was selected by Beckman's fully automated immunoassay analyzer DXI 800 (Beckman Coulter Inc., Brea, CA, USA).

Semen Collection and Analysis

Semen samples were collected by masturbation into a sterile, wide-mouth plastic container in an independent clean room. Then, the samples were incubated at 37°C for liquidation and

were analyzed within 60 min. Semen volumes were measured by weighing, assuming that 1 ml of volume equals 1 g of weight. The semen parameters (motility, progressive motility, concentration, and total sperm count) were assessed with a computer-aided sperm analysis system (SCA CASA System; Microptic S.L., Barcelona, Spain) by a well-trained laboratory technician. Sperm morphology was identified by sperm smears using a Diff-Quick staining kit (Boruide, BRED-015). All semen analyses were performed according to the WHO criteria recommendations (26).

Statistical Analysis

Semen parameters and sex hormones were presented as medians and percentiles. The Jonckheere-Terpstratest and Mann-Whitney *U* test were used to compare differences between the semen parameters of the groups. A multivariable-linear regression model was applied to exclude potential confounders (e.g., age, BMI, abstinence duration, tobacco smoking, alcohol drinking, coffee consumption, cola consumption, and fried food consumption), which have been reported to have effects on semen parameters (20). All semen parameters were log-transformed when they were nonnormally distributed. Additionally, all of the statistical data were analysis with the Statistical Package for the Social Sciences (SPSS, Chicago, IL, USA), and differences were considered statistically significant if $p < 0.05$, and all the tests were performed by two tailed.

TABLE 1 | Demographic characteristics, lifestyle factors, reproductive hormone levels, and semen parameters of the participants.

Characteristics	Values (n = 568)
Demographic characteristics	
Age (years)[a]	22.4 ± 1.2
BMI (kg/m^2)[a]	22.2 ± 2.9
Abstinence duration (days)[a]	4.1 ± 1.5
Lifestyle factors	
Tobacco smoking[b]	
Never	414 (72.9)
Quit	26 (4.6)
Current	128 (22.5)
Alcohol drinking[b]	
Never	122 (21.5)
Quit	22 (3.9)
Current	423 (74.5)
Reproductive hormones	
E_2 (pg/ml)	30.6 ± 16.7
FSH (mIU/ml)	3.5 ± 1.7
LH (mIU/ml)	4.3 ± 1.7
PRL (ng/ml)	10.4 ± 5.0
Prog (ng/ml)	0.6 ± 0.4
T (ng/ml)	3.8 ± 1.1
Semen parameters	
Volume (ml)[a]	3.8 ± 1.9
Sperm concentration (×10^6/ml)[a]	56 ± 45
Total sperm count (×10^6)[a]	203 ± 183
Total motility (%)[a]	79 ± 16
Progressive motility (%)[a]	55 ± 17
Morphological normal spermatozoa (%)[a]	11.73 ± 7.15

[a]*Values are presented as the mean ± SD.*
[b]*Value are presented no. (%).*

RESULTS

Demographic Characteristics of Participants, Lifestyles, Sex Hormones, and Semen Parameters

Descriptive results are demonstrated in **Table 1**. Five hundred sixty-eight participants met the inclusion criteria and finished the examination. The average age of the respondents was 22.4 years, and the average BMI value and abstinence duration were 22.2 (kg/m2) and 4.1 days, respectively.

The average E_2, FSH, LH, PRL, Prog, and T concentrations were 30.6 pg/ml, 3.5 mIU/ml, 4.3 mIU/ml, 10.4 ng/ml, 0.6 ng/ml, and 3.8 ng/ml respectively. The average semen volume, sperm concentration, total sperm count, total motility, progressive motility, and morphologically normal spermatozoa count were 3.8 ml, 56 million/ml, 203 million, 79%, 55%, and 11.73%, respectively.

Situations of Pornography Use

As **Table 2** shows, almost all of the male students (except one) had experienced pornography use, albeit to varying extents. A total of 84.2% of the students first searched for pornography during middle or high school, and approximately 45.3% of the students used pornography more than once per week. Additionally, approximately 51.6% of the students spent approximately 15 to 30 min using pornography at each use. Only 4.1% students reported they had never masturbated during pornography use, when asked about their masturbation frequency when using pornography. In contrast, 14.9% of the students masturbated almost every time they used pornography.

The Possibility of Addiction on Pornography Use

Approximately half of the students reported they had used less pornography in the most recent 3 months. Additionally, 6.4% of the students reported they had used pornography more than before. One hundred and eighty (31.7%) students reported that they needed more time to feel sexual excitement than ever when using pornography. Excluding students who had no sexual partners (N = 238, 42%), 6.5% (N = 37) of the students reported that it was easier for them to achieve sexual satisfaction by using pornography than with a real sexual partner. Moreover, pornography use was significantly associated with addiction possibility. Earlier contact, more frequent use, longer time, and more masturbation during pornography use were all found to be correlated with addictive possibility (**Table 3**).

Correlations Between Pornography Use and Sex Hormones

Univariate analyses were applied to estimate the associations between pornography use and sex hormones. According to the increase of ages of "first time to contact pornography" from primary school to college, the Prog, FSH, and PRL concentrations were increased from 0.4 to 0.8 ng/ml, 2.7 to 3.2 mIU/ml, and 8.5 to 10.7 ng/ml, respectively ($p < 0.05$,

TABLE 2 | The distribution of pornography use-related questions.

Characteristics	*N*	Percentage (%)
Situations for pornography use		
Q1: First time to contact with pornography information (*n* = 568)		
Primary school	57	10.0
Middle school	277	48.8
High school	201	35.4
College	32	5.8
Never	1	0.18
Q2: Pornography use frequency (*n* = 567)		
<1 time/week	310	54.6
1–2 times/week	210	37.0
>2 times/week	47	8.3
Q3: Amount of time spending on pornography use/time (*n* = 567)		
≤15 min	201	35.4
15–30 min	293	51.6
≥30 min	64	12.9
Q4: Frequency of masturbation when using pornography (*n* = 567)		
Never	23	4.1
Sometimes	295	52.0
Half of the time	129	22.8
Most of the time	92	16.2
Almost every time	28	14.9
The addiction possibility for pornography use		
Q5: Frequency of pornography use in the most recent 3 months compared with 3 months ago (*n* = 567)		
Much less than before	162	38.6
A little bit less than before	126	22.2
As much as before	243	42.9
More than before	36	6.4
Q6: Is it take more time to feel sexual excitement when using pornography compared with 3 months ago (*n* = 567)		
Yes	180	31.7
No	387	68.3
Q7: Is it easier to achieve sexual satisfaction when using pornography compared with having sex with a real partner (*n* = 567)		
Yes	37	6.5
No	292	51.5
No sex partner	238	42.0

$p < 0.05$, $p < 0.05$). The E_2 concentration decreased from 32 to 26 pg/ml according to the increase of frequency of pornography use ($p < 0.05$) (**Figure 1**).

After adjusting the potential confounders (age, BMI, abstinence duration, tobacco smoking, alcohol consumption, coffee consumption, cola consumption, and fried foods consumption), students with higher pornography use frequency had lower E_2 concentration in serum (β coefficient = −3.29; 95% confidence interval (CI), −5.14, −1.13, $p = 0.003$). Students with earlier exposure to pornography had lower PRL and Prog concentration in serum (β coefficient = 0.92; 95% CI, 0.37, 1.47, $p = 0.001$; β coefficient = 0.10; 95% CI, 0.05, 0.14, $p < 0.001$) (**Table 4**).

Correlations Between Pornography Use and Semen Parameters

Univariate analyses were applied to estimate the associations between pornography use and semen parameters. As shown in **Figure 2**, earlier pornography use, higher-frequency exposure to pornography, higher-frequency of masturbation when using pornography were associated with lower sperm concentration and total sperm count ($p < 0.05$).

Multivariable linear regression models were used to adjust the potential confounders (age, BMI, abstinence duration, tobacco smoking, alcohol consumption, coffee consumption, cola consumption, and fried foods consumption). After adjusting for potential confounders, the associations between pornography use and sperm concentration were still solid. The sperm concentration was positively associated with the ages of first time to contact with pornography (β coefficient = 11.17; 95% CI, 1.86, 21.34; $p = 0.017$) but negatively associated with masturbation frequency when using pornography (β = −7.40; 95% CI, −14.82, −0.46; $p = 0.038$). However, higher morphologically normal spermatozoa ratio (%) was found to be positively associated with masturbation frequency when using pornography (β = 7.40; 95% CI, 2.33, 12.72; $p = 0.003$) (**Table 5**).

DISCUSSION

Adolescent pornography use is a hot public health issue (27, 28). The present study is an exploratory study designed to describe pornography use among college students in China and to explore the effects of pornography use on students' reproduction health. We found that pornography use was quite common among college students in China. Pornography use was correlated with masturbation behavior and exposure to prolonged pornography may lead to addictive potential. Pornography use was also found to be significantly associated with sex hormone levels in serum and semen parameters.

TABLE 3 | Associations between pornography use and the addiction possibility for pornography use.

Addiction	First time to contact with pornography		Pornography use frequency		Amount of time spending on pornography use		Frequency of masturbation when using pornography	
	Correlation coefficient	*p*-Value	Correlation coefficient	*p*-Value	Correlation coefficient	*p*-Value	Correlation coefficient	*p*-Value
Frequency of pornography use in the most recent 3 months compared with 3 months ago	0.025	0.553	**0.260**	**<0.001**	0.035	0.405	**0.160**	**<0.001**
Is it take more time to feel sexual excitement when using pornography compared with 3 months ago	−0.007	0.866	−0.053	0.206	**−0.100**	**0.017**	0.005	0.915
Is it easier to achieve sexual satisfaction when using pornography compared with having sex with a real partner	**0.141**	**0.001**	0.075	0.076	**0.120**	**0.004**	**0.109**	**0.009**

The results in bold indicate that the variable was significantly associated with changes in semen parameters (p < 0.05).

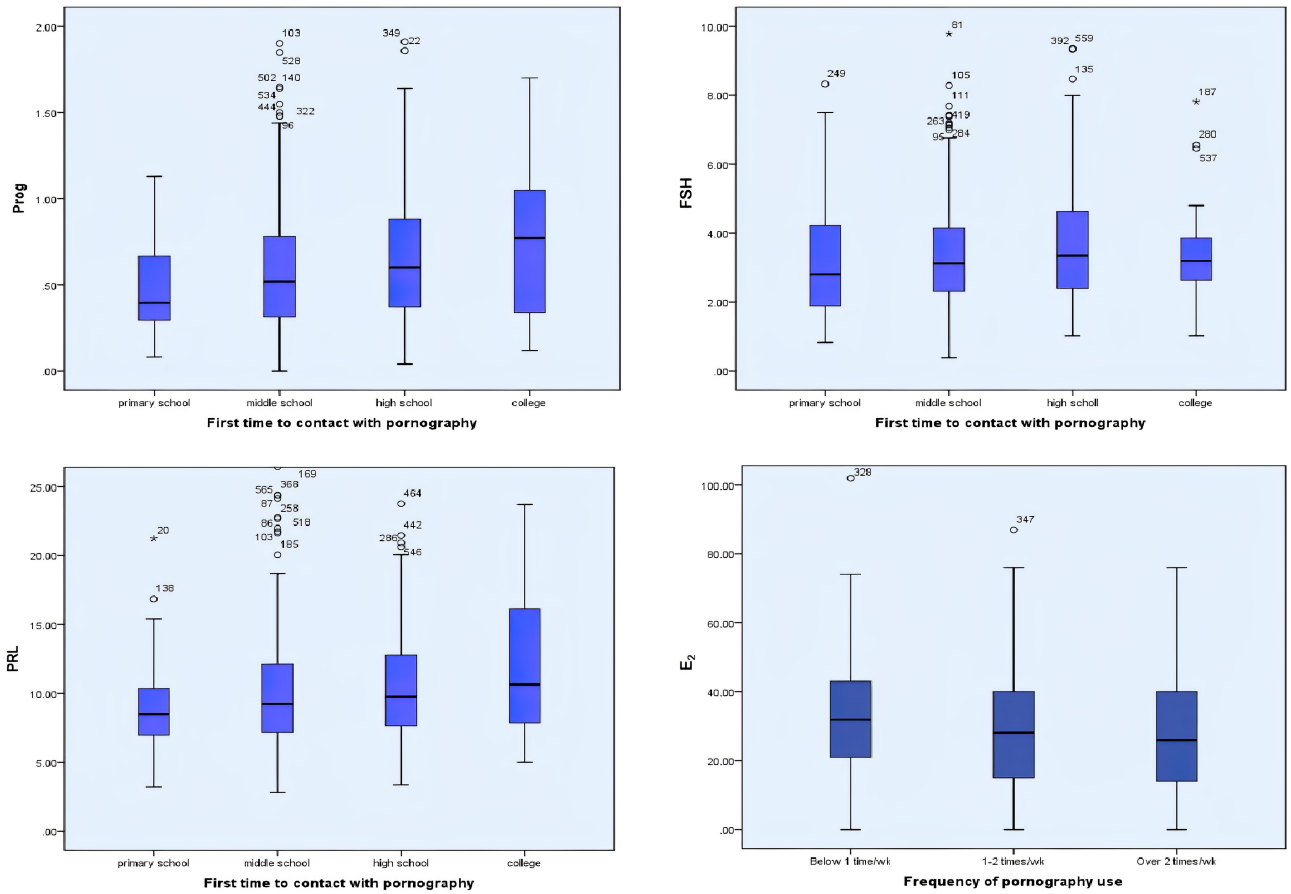

FIGURE 1 | Univariate analyses were applied to estimate the associations between pornography use and sex hormones. The ages of first-time contact pornography were positively correlated with Prog, FS, and PRL concentrations in serum ($p < 0.05$, $p < 0.05$, $p < 0.05$). The frequency of pornography use were negatively correlated with E_2 concentrations in serum ($p < 0.05$). *:extreme values.

TABLE 4 | Associations between pornography use and serum gonadal hormone levels.

Characteristics	E_2		PRL		Prog	
	β (95% CI)	*p*-Value	*β* (95% CI)	*p*-Value	*β* (95% CI)	*p*-Value
First time to contact with pornography	0.06 (–1.82, 1.94)	0.953	**0.92 (0.37, 1.47)**	**0.001**	**0.10 (0.05, 0.14)**	**0.000**
Pornography use frequency	**–3.29 (–5.14, –1.13)**	**0.003**	–0.36 (–1.01, 0.29)	0.274	–0.02 (–0.08, 0.03)	0.378
Amount of time spending on pornography use	2.12 (–0.02, 4.25)	0.052	0.33 (–0.31, 0.97)	0.318	0.02 (–0.03, 0.08)	0.399
Frequency of masturbation when using pornography	–0.99 (–2.45, 0.48)	0.185	–0.16 (–0.60, 0.27)	0.466	–0.02 (–0.05, 0.02)	0.364

The results in bold indicate that the variable was significantly associated with changes in semen parameters ($p < 0.05$). Regression coefficients were adjusted for age, abstinence duration, BMI, smoking, and alcohol drinking status. A multiple linear regression analysis was deployed. The results are presented as regression coefficients with 95% confidence intervals.

Like in other countries or areas, pornography use among college students was quite common in China. In the present study, 94.2% of college students had contacted to pornography before college, which is consistent with other recent studies in other countries (29, 30).

The American Society of Addiction Medicine (ASAM) defined "addiction" in 2011 as: Addiction is a primary, chronic disease of brain reward, motivation, memory and related circuitry. Dysfunction in these circuits leads to characteristic biological, psychological, social, and spiritual manifestation. This is reflected in an individual pathologically pursuing reward and/or relief by substance and other behavior (31). Regarding pornography addiction, the clinical diagnostic criteria is still devoid. A number of studies supported the "self-reported pornography addiction" questionnaire to access the cognitive, behavioral, and emotional aspects of problematic pornography use (21–25). The questions about pornography use situations and addictive behaviors were set according to these previous studies. Quite a

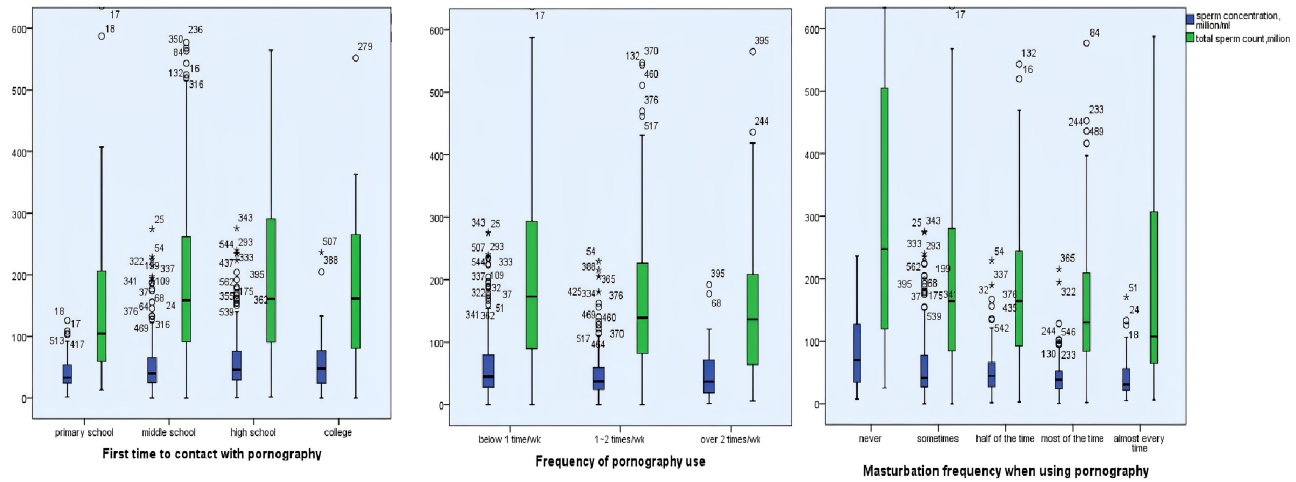

FIGURE 2 | Univariate analyses were applied to estimate the associations between pornography use and semen parameters. The ages of first-time contact pornography were positively correlated with sperm concentration and total sperm count ($p < 0.05$). The frequency of pornography use and masturbation frequency when using pornography were negatively correlated with sperm concentration and total sperm count ($p < 0.05$, $p < 0.05$). *:extreme values.

TABLE 5 | Associations between pornography use and semen parameters.

Characteristics	Sperm concentration (10^6/ml)		Total sperm count (10^6)		Morphological normal spermatozoa (%)	
	β (95% CI)	*p*-Value	*β* (95% CI)	*p*-Value	*β* (95% CI)	*p*-Value
First time to contact with pornography	**11.17 (1.86, 21.34)**	**0.017**	13.00 (–6.17, 32.17)	0.183	0.23 (–6.17, 6.91)	0.093
Pornography use frequency	–6.17 (–17.49, 3.99)	0.231	–19.09 (–42.00, 3.81)	0.102	0.00 (–7.89, 7.64)	0.992
Amount of time spending on pornography use	4.23 (–10.15, 19.40)	0.561	0.16 (–21.89, 22.20)	0.989	0.462 (7.89, 6.91)	0.883
Frequency of masturbation when using pornography	**–7.40 (–14.82, –0.46)**	**0.038**	–12.34 (–27.50, 2.82)	0.110	**7.40 (2.33, 12.72)**	**0.003**

The results in bold indicate that the variable was significantly associated with changes in semen parameters ($p < 0.05$). Regression coefficients were adjusted for age, abstinence duration, BMI, smoking, and alcohol drinking status. A multiple linear regression analysis was deployed, and all of the semen parameters were Log 10-transformed. The results are presented as back-transformed regression coefficients with 95% confidence intervals.

lot of studies led to the conclusion that frequent pornography use fitted into the addiction framework and shared a similar basic mechanism with substance addiction. The present study confirmed that pornography use might lead to addictive possibility; 31.7% of students reported they need more time to feel sexual excitement when using pornography, and nearly 6.5% of students thought it would be easier to achieve sexual satisfaction when using pornography than with a real sexual partner. Pornography has been reported to be a dopamine-producing base behavior (32). Dopamine is a neurotransmitter that is associated with activation of the brain's reward system, and its presence helps initiate feelings of enjoyment and pleasure. Moreover, a study from the Max Planck Institute for Human Development showed that frequent pornography consumption was associated with the frontostriatal network, and pornography consumption hours were negatively associated with striatum volume. Individuals with a lower striatum volume may need more external stimulation to experience pleasure and might therefore experience pornography consumption as more rewarding (33). Therefore, frequent pornography use might break the balance of the dopamine pathway. Like heroin or other drugs, frequent pornography use may cause addiction, which might be a reason for why the pornography users showed difficulty in obtaining sexual excitement.

In the present study, we found that early pornography exposure was associated with lower adult FSH, Prog, and PRL levels in serum. After adjusting with potential confounders, we still found a significant association between "the first time contact with pornography" and Prog levels in serum. During puberty, the HPG axis is initiated, and the gonadal steroid hormones are dramatically increased (18), as well as the quick development of reproductive organs. FSH is responsible for starting the process of the sperm production (spermatogenesis) by initiating spermatogenic epithelium cell division and maturation. FSH have been also reported to be related with gonadotropin levels which lead to the induction of spermatogenesis effectively (34, 35). Recent studies showed that Prog produced by cumulus cells has been associated with various physiological processes in sperm production, including stimulation of acrosome reaction. Male normal prolactin levels help maintain a high level of testosterone in the testis and affect the growth and secretion of the gonadal glands (36). Hyperprolactinemia is a high level of serum prolactin, which can interfere with the periodic release of GnRH, the elimination

of gonadotropin pulsed secretion, so that the release of LH and FSH decreased, eventually leading to hypogonadism (testosterone synthesis and secretion, spermatogenic dysfunction) (37). Thus, pornography use at an early stage may affect the function of the HPG axis and subsequently affect the secretion of steroid hormones, such as estrogen, androgen, prolactin, and progesterone, eventually affecting semen quality.

We also found that earlier pornography use was associated with lower sperm concentrations with or without adjusting to potential confounders. A majority of students are exposed to pornography before college. As we discussed in the previous section, adolescence is a key time for reproductive maturation, from sexual hormone secretion to sexual organ development. The time of puberty initiation and the time for first sexual encounter were found to be two developmental milestones associated with reproductive maturation (38). Earlier contact to pornography might lead to disturbance of sexual hormone secretion, and therefor lead to lower sperm concentration in adult semen. Besides, earlier contact to pornography might lead to higher frequency of masturbation, which is also a risk factor for lower sperm concentration. There are no other studies focused on male puberty pornography use and adult semen qualities, but some studies revealed that adolescents who were exposed to pornography were more likely to reach early sexual maturation and be higher sensation seekers (39).

The present study showed that pornography use was significantly correlated with masturbation behavior. Higher masturbation frequency during pornography use showed adverse effects on the sperm concentration and total sperm count. Masturbation was the most common behavior performed during pornography use in the present study and in other studies (40). However, a few studies have investigated the relationship between masturbation frequency during pornography use and semen parameters. A large online study on male sexual health in three European countries showed that frequent pornography use significantly increased the masturbation frequency among coupled men with decreased sexual desire (41). Additionally, higher masturbation frequency might increase the threshold of sexual arousal. Thus, we hypothesize that frequent masturbation might lead to frequent arousal and ejaculation, leading to continual hyperemia in the genitals and gonads, which could eventually affect spermatogenesis. Besides, frequent masturbation is usually accompanied with shorter abstinence time, which is also a risk factor for lower sperm concentration (20).

The present study showed that the frequency of masturbation when using pornography was negatively associated with sperm concentration while positively associated with morphological normal spermatozoa. It seems that this behavior has brought controversial effect to semen quality. Actually, it just reflects the physiology of sperm production. As the abstinence period grows, the accumulation of sperms leads to an increase in sperm concentration, while the accumulated sperms become senescent and lead to a decrease in the proportion of morphological normal spermatozoa. Vice versa, the masturbation behavior during using pornography decreased the abstinence period of the subjects, and consequently decreased the sperm concentration and increased the proportion of morphological normal spermatozoa.

The main strengths of this study were as follows. First, this was a follow-up study of MARHCS cohort. All of the participants were familiar with the study design, and they were well educated and could fully understand all of the questions, which make our results more credible. Second, our sample constituted a large healthy population with a narrow age range, and the selection of the same sampling season significantly reduced potential confounders. Third, the semen quality evaluation methods were used as per the WHO recommendations, which make our results more comparable with those of other studies.

There are some limitations to our study. First, the pornography use data were obtained *via* self-review, which raises the possibility of information bias. Secondly, the subjects of the present study were all recruited from the universities which were located in the university town of Chongqing, although the students came from different provinces all over China. The sampling season was restricted in summer and was several years ago. The population was highly homogenous, with similar ages, lifestyles, and education levels, which make it challenging to compare with other populations. Thirdly, each subject only offered one semen sample in each follow-up investigation, which might have introduced intra-individual bias to this study. Fourthly, sex is a sensitive topic for Chinese students to talk about. Thus, the pornography use data the students reported may be conservative, and the potential effects may have been underestimated. Although we adjusted for potential confounders on semen parameters and sex hormones, some other potential confounders might still exist, such as environmental exposure, psychological distress, and socioeconomic status. Whether the findings of the present study could be replicated in independent populations with different characteristics and circumstances await further studies. The results of the current study should be interpreted with caution, and further studies evaluating the relationship between pornography use and reproductive phenotypes should be conducted.

In conclusion, the present study showed that pornography use was quite common among college students in China. Our results showed pornography use was correlated with masturbation behavior and may lead to addictive behavior. This is also the first study to investigate the associations between pornography use and semen parameters. The results showed that pornography use was significantly associated with sex hormones in serum and semen parameters, which indicated that early and frequent pornography exposure may lead to adverse male reproductive outcome. Our results may have important implications for public health.

DATA AVAILABILITY STATEMENT

The raw data supporting the conclusions of this article will be made available by the authors, without undue reservation.

ETHICS STATEMENT

The studies involving human participants were reviewed and approved by The Ethics Council of the Army Medical University.

The patients/participants provided their written informed consent to participate in this study.

AUTHOR CONTRIBUTIONS

ZC and MM contributed to interpretation of the data and drafted the paper. The study was conceived and designed by ZC and JC. MM and QC contributed to statistical analyses. Data acquisition was conducted by ZC, MM, QC, XW, HY, NZ, LS, JL, and LA. All authors contributed to the article and approved the submitted version.

FUNDING

This work was supported by the Fundamental Research Funds for the Central Universities, SWU [grant number 7110100301], National Natural Science Foundation of China [grant numbers 81502788], and National Key Research and Development program of China [grant number 2017YFC1002001].

ACKNOWLEDGMENTS

We thank the participants in the study for their cooperation.

REFERENCES

1. Cooper A. Sexuality and the Internet: Surfing Into the New Millennium. *Cyber Psychol Behav* (1998) 1:187–93. doi: 10.1089/cpb.1999.2.475
2. Braithwaite SR, Coulson G, Keddington K, Fincham FD. The Influence of Pornography on Sexual Scripts and Hooking Up Among Emerging Adults in College. *Arch Sex Behav* (2015) 44:111–23. doi: 10.1007/s10508-014-0351-x
3. Peter J, Valkenburg PM. Adolescents and Pornography: A Review of 20 Years of Research. *J Sex Res* (2016) 53:509–31. doi: 10.1080/00224499.2016.1143441
4. Sabina C, Wolak J, Finkelhor D. The Nature and Dynamics of Internet Pornography Exposure for Youth. *CyberPsychol Behav* (2008) 11:691–3. doi: 10.1089/cpb.2007.0179
5. Camilleri C, Perry JT, Sammut S. Compulsive Internet Pornography Use and Mental Health: A Cross-Sectional Study in a Sample of University Students in the United States. *Front Psychol* (2021) 11:613244. doi: 10.3389/fpsyg.2020.613244
6. Madigan S, Villani V, Azzopardi C, Laut D, Smith T, Temple JR, et al. The Prevalence of Unwanted Online Sexual Exposure and Solicitation Among Youth: A Meta-Analysis. *J Adolesc Health* (2018) 63:133–41. doi: 10.1016/j.jadohealth.2018.03.012
7. Zohor Ali AA, Muhammad NA, Jamil TR, Ahmad S, Abd Aziz NA. Internet Pornography Exposures Amongst Young People in Malaysia: A Cross-Sectional Study Looking Into the Role of Gender and Perceived Realism *Versus* the Actual Sexual Activities. *Addict Behav Rep* (2021) 14:100350. doi: 10.1016/j.abrep.2021.100350
8. Shek DT, Ma CM. A Six-Year Longitudinal Study of Consumption of Pornographic Materials in Chinese Adolescents in Hong Kong. *J Pediatr Adolesc Gynecol* (2016) 29:S12–21. doi: 10.1016/j.jpag.2015.10.004
9. Ma CM, Shek DT. Consumption of Pornographic Materials in Early Adolescents in Hong Kong. *J Pediatr Adolesc Gynecol* (2013) 26:S18–25. doi: 10.1016/j.jpag.2013.03.011
10. Poulsen FO, Busby DM, Galovan AM. Pornography Use: Who Uses It and How It Is Associated With Couple Outcomes. *J Sex Res* (2013) 50:72–83. doi: 10.1080/00224499.2011.648027
11. Stulhofer A, Busko V, Landripet I. Pornography, Sexual Socialization, and Satisfaction Among Young Men. *Arch Sex Behav* (2010) 39:168–78. doi: 10.1007/s10508-008-9387-0
12. Day A. Getting the 'Blues': The Existence, Diffusion and Influence of Pornography on Young Peoples' Sexual Health in Sierra Leone. *Cult Health Sex* (2014) 16:178–89. doi: 10.1080/13691058.2013.855819.\
13. Babchishin KM, Hanson RK, VanZuylen H. Online Child Pornography Offenders are Different: A Meta-Analysis of the Characteristics of Online and Offline Sex Offenders Against Children. *Arch Sex Behav* (2015) 44:45–66. doi: 10.1007/s10508-014-0270-x
14. Voon V, Mole TB, Banca P, Porter L, Morris L, Mitchell S, et al. Neural Correlates of Sexual Cue Reactivity in Individuals With and Without Compulsive Sexual Behaviours. *PloS One* (2014) 9:e102419. doi: 10.1371/journal.pone.0102419
15. Happer C, Hodgins DC. Examining Correlates of Problematic Internet Pornography Use Among University Students. *J Behav Addict* (2016) 5:179–91. doi: 10.1556/2006.5.2016.022
16. Sun C, Bridges A, Johnson JA, Ezzell MB. Pornography and the Male Sexual Script: An Analysis of Consumption and Sexual Relations. *Arch Sex Behav* (2016) 45:983–94. doi: 10.1007/s10508-014-0391-2
17. Parhar IS, Ogawa S, Ubuka T. Reproductive Neuroendocrine Pathways of Social Behavior. *Front Endocrinol* (2016) 7:28. doi: 10.3389/fendo.2016.00028
18. Sisk CL, Zehr JL. Pubertal Hormones Organize the Adolescent Brain and Behavior. *Front Neuroendocrin* (2005) 26:163–74. doi: 10.1016/j.yfrne.2005.10.003
19. Schulz KM, Richardson HN, Zehr JL, Osetek AJ, Menard TA, Sisk CL. Gonadal Hormones Masculinize and Defeminize Reproductive Behaviors During Puberty in the Male Syrian Hamster. *Horm Behav* (2004) 45:242–9. doi: 10.1016/j.yhbeh.2003.12.007
20. Yang H, Chen Q, Zhou N, Sun L, Bao H, Tan L, et al. Lifestyles Associated With Human Semen Quality: Results From MARHCS Cohort Study in Chongqing, China. *Med (Baltimore)* (2015) 94:e1166. doi: 10.1097/MD.0000000000001166
21. Baltieri DA, Aguiar AS, de Oliveira VH, de Souza Gatti AL, de Souza Aranha ESRA. Validation of the Pornography Consumption Inventory in a Sample of Male Brazilian University Students. *J Sex Marital Ther* (2015) 41:649–60. doi: 10.1080/0092623X.2014.958793
22. Kor A, Zilcha-Mano S, Fogel YA, Mikulincer M, Reid RC, Potenza MN. Psychometric Development of the Problematic Pornography Use Scale. *Addict Behav* (2014) 39:861–8. doi: 10.1016/j.addbeh.2014.01.027
23. Grubbs JB, Exline JJ, Pargament KI, Hook JN, Carlisle RD. Transgression as Addiction: Religiosity and Moral Disapproval as Predictors of Perceived Addiction to Pornography. *Arch Sex Behav* (2015) 44:125–36. doi: 10.1007/s10508-013-0257-z
24. Harkness EL, Mullan BM, Blaszczynski A. Association Between Pornography Use and Sexual Risk Behaviors in Adult Consumers: A Systematic Review. *Cyberpsychol Behav Soc Netw* (2015) 18:59–71. doi: 10.1089/cyber.2014.0343
25. Kraus S, Rosenberg H. The Pornography Craving Questionnaire: Psychometric Properties. *Arch Sex Behav* (2014) 43:451–62. doi: 10.1007/s10508-013-0229-3
26. WHO. *WHO Laboratory Manual for the Examination and Processing of Human Semen. 5th ed*. Geneva, Switzerland: WHO Press (2010).
27. Limb M. Internet Pornography is an Urgent Public Health Issue, Conference Hears. *BMJ* (2014) 348:g4475. doi: 10.1136/bmj.g4475
28. Laws I. Better Sex Education for Children is Needed to Combat Dangers of Pornography. *BMJ* (2013) 347:f5764. doi: 10.1136/bmj.f5764
29. Mattebo M, Tyden T, Haggstrom-Nordin E, Nilsson KW, Larsson M. Pornography and Sexual Experiences Among High School Students in Sweden. *JDBP* (2014) 35:179–88. doi: 10.1097/DBP.0000000000000034
30. Mohsen J, Tai HL. The Youth Sexuality Study Task Force. Sexual Media Use by Young Adults in Hong Kong: Prevalence and Associated Factors. *Arch Sex Behav* (2003) 32:545–53. doi: 10.1023/a:1026089511526
31. American Society of Addiction Medicine (ASAM). *Public Policy Statement: Definition of Addiction*. Available at: http://www.asam.org/for-the-public/definition-of-addiction.
32. Christensen JF. Pleasure Junkies All Around! Why It Matters and Why 'The Arts' Might Be the Answer: A Biopsychological Perspective. *Proc Biol Sci* (2017) 284:20162837. doi: 10.1098/rspb.2016.2837
33. Kuhn S, Gallinat J. Brain Structure and Functional Connectivity Associated With Pornography Consumption: The Brain on Porn. *JAMA Psychiatry* (2014) 71:827–34. doi: 10.1001/jamapsychiatry.2014.93

34. Rohayem J, Hauffa BP, Zacharin M, Kliesch S, Zitzmann MGerman Adolescent Hypogonadotropic Hypogonadism Study Group. Testicular Growth and Spermatogenesis: New Goals for Pubertal Hormone Replacement in Boys With Hypogonadotropic Hypogonadism? -A Multicentre Prospective Study of hCG/rFSH Treatment Outcomes During Adolescence. *Clin Endocrinol (Oxf)* (2017) 86:75–87. doi: 10.1111/cen.13164
35. Matsumoto AM, Snyder PJ, Bhasin S, Martin K, Weber T, Winters S, et al. Stimulation of Spermatogenesis With Recombinant Human Follicle-Stimulating Hormone (Follitropin Alfa; GONAL-F): Long-Term Treatment in Azoospermic Men With Hypogonadotropic Hypogonadism. *Fertil Steril* (2009) 92:979–90. doi: 10.1016/j.fertnstert.2008.07.1742
36. Awoniyi CA, Reece MS, Hurst BS, Faber KA, Chandrashekar V, Schlaff WD. Maintenance of Sexual Function With Testosterone in the Gonadotropin-Releasing Hormone-Immunized Hypogonadotropic Infertile Male Rat. *Biol Reprod* (1993) 49:1170–6. doi: 10.1095/biolreprod49.6.1170
37. De Rosa M, Zarrilli S, Di Sarno A, Milano N, Gaccione M, Boggia B, et al. Hyperprolactinemia in Men: Clinical and Biochemical Features and Response to Treatment. *Endocrine* (2003) 20:75–82. doi: 10.1385/ENDO:20:1-2:75
38. Cornwell RE, Law Smith MJ, Boothroyd LG, Moore FR, Davis HP, Stirrat M, et al. Reproductive Strategy, Sexual Development and Attraction to Facial Characteristics. *Philos Trans R Soc Lond B Biol Sci* (2006) 361:2143–54. doi: 10.1098/rstb.2006.1936
39. Luder MT, Pittet I, Berchtold A, Akre C, Michaud PA, Suris JC. Associations Between Online Pornography and Sexual Behavior Among Adolescents: Myth or Reality? *Arch Sex Behav* (2011) 40:1027–35. doi: 10.1007/s10508-010-9714-0
40. Perry SL. Is the Link Between Pornography Use and Relational Happiness Really More About Masturbation? Results From Two National Surveys. *J Sex Res* (2020) 57:64–76. doi: 10.1080/00224499.2018.1556772
41. Carvalheira A, Traeen B, Stulhofer A. Masturbation and Pornography Use Among Coupled Heterosexual Men With Decreased Sexual Desire: How Many Roles of Masturbation? *J Sex Marital Ther* (2015) 41:626–35. doi: 10.1080/0092623X.2014.958790

Conflict of Interest: The authors declare that the research was conducted in the absence of any commercial or financial relationships that could be construed as a potential conflict of interest.

Publisher's Note: All claims expressed in this article are solely those of the authors and do not necessarily represent those of their affiliated organizations, or those of the publisher, the editors and the reviewers. Any product that may be evaluated in this article, or claim that may be made by its manufacturer, is not guaranteed or endorsed by the publisher.

frontiers in Physiology

ORIGINAL RESEARCH
published: 30 September 2021
doi: 10.3389/fphys.2021.717571

The Abscopal Effects of Cranial Irradiation Induce Testicular Damage in Mice

*Ling Guo[1,2†], Tong-Zhou Qin[1,2†], Li-Yuan Liu[1,2], Pan-Pan Lai[1,2], Yi-Zhe Xue[1,2], Yun-Tao Jing[1,2], Wei Zhang[1,2], Wei Li[3], Jing Li[1,2] and Gui-Rong Ding[1,2]**

[1] Department of Radiation Protection Medicine, School of Military Preventive Medicine, Fourth Military Medical University, Xi'an, China, [2] Ministry of Education Key Lab of Hazard Assessment and Control in Special Operational Environment, Xi'an, China, [3] Department of Histology and Embryology, School of Basic Medical Science, Fourth Military Medical University, Xi'an, China

To investigate whether the abscopal effects of cranial irradiation (C-irradiation) cause testicular damage in mice, male *C57BL/6* mice (9 weeks of age) were randomly divided into a sham irradiation group, a shielded group and a C-irradiation group and administered sham/shielded irradiation or C-irradiation at a dose rate of 2.33 Gy/min (5 Gy/d for 4 d consecutively). All mice were sacrificed at 4 weeks after C-irradiation. We calculated the testis index, observed testicular histology by haematoxylin-eosin (HE) staining and observed testicular ultrastructure by transmission electron microscopy. Western blotting was used to determine the protein levels of Bax, Bcl-2, Cleaved caspase 3, glial cell line-derived neurotrophic factor (GDNF) and stem cell factor (SCF) in the testes of mice. Immunofluorescence staining was performed to detect the expression of Cleaved caspase 3 and 3β hydroxysteroid dehydrogenase (3βHSD), and a TUNEL assay was used to confirm the location of apoptotic cells. The levels of testosterone (T), GDNF and SCF were measured by ELISA. We also evaluated the sperm quality in the cauda epididymides by measuring the sperm count, abnormality, survival rate and apoptosis rate. The results showed that there was no significant difference in testicular histology, ultrastructure or sperm quality between the shielded group and sham group. Compared with the sham/shielded group, the C-irradiation group exhibited a lower testis index and severely damaged testicular histology and ultrastructure at 4 weeks after C-irradiation. The levels of apoptosis in the testes increased markedly in the C-irradiation group, especially in spermatogonial stem cells. The levels of serum T and testicular 3βHSD did not obviously differ between the sham group and the C-irradiation group, but the levels of GDNF and SCF in the testes increased in the C-irradiation group, compared with the sham group. In addition, the sperm count and survival rate decreased in the C-irradiation group, while the abnormality and apoptosis rate increased. Under these experimental conditions, the abscopal effects of C-irradiation induced testicular damage with regard to both structure and function and ultimately decreased sperm quality in mice. These findings provide novel insights into prevention and treatment targets for male reproductive damage induced by C-irradiation.

Keywords: cranial irradiation, abscopal effect, testicular damage, apoptosis, sperm quality

OPEN ACCESS

Edited by:
Qing Chen,
Army Medical University, China

Reviewed by:
Saba Shahin,
Board of Governors Regenerative Medicine Institute, United States
Xavier D'Anglemont De Tassigny,
Universidad de Sevilla, Spain

****Correspondence:***
Gui-Rong Ding
dingzhao@fmmu.edu.cn

[†]These authors have contributed equally to this work and share first authorship

Specialty section:
This article was submitted to Reproduction, a section of the journal Frontiers in Physiology

Received: *31 May 2021*
Accepted: *07 September 2021*
Published: *30 September 2021*

Citation:
Guo L, Qin T-Z, Liu L-Y, Lai P-P, Xue Y-Z, Jing Y-T, Zhang W, Li W, Li J and Ding G-R (2021) The Abscopal Effects of Cranial Irradiation Induce Testicular Damage in Mice. Front. Physiol. 12:717571. doi: 10.3389/fphys.2021.717571

INTRODUCTION

According to recent WHO statistics, head and neck cancer is the seventh most common cancer overall (and the fifth most common cancer in men) worldwide, accounting for an estimated 888,000 new cases in 2018 (Wild et al., 2020). Notably, its incidence is increasing each year, and there is a trend towards a decreasing age at onset; thus, this disease seriously threatens human health. Cranial irradiation (C-irradiation) therapy is one of the major treatment modalities for primary and metastatic head and neck cancer (Siegel et al., 2020; Turnquist et al., 2020). Hypofractionated radiation (single dose >2.5 Gy) is a promising new strategy for radiotherapy due to its higher treatment ratio, shorter total treatment time and lower cost than conventional radiotherapy (single dose = 2.0 Gy; Azoulay et al., 2017; Isfahanian et al., 2017; Rudat et al., 2017; Vischioni et al., 2019).

Notably, cell and tissue injuries can occur in organs other than the irradiated tumour sites over the course of radiotherapy; such effects are called radiation-induced abscopal effects (RIAEs; Siva et al., 2015; Hu and Shao, 2020). Most previous literature on RIAEs has focused on the regression of nonirradiated metastatic lesions after localised tumour radiotherapy (Ishiyama et al., 2012; Siva et al., 2015; Abuodeh et al., 2016; Seggelen et al., 2020). However, RIAEs also include serious side effects in normal tissues (Aravindan et al., 2014; Tu et al., 2019). Extracranial abscopal effects of C-irradiation are particularly unusual given the brain's distinctive immune microenvironment (Lin et al., 2019). However, multiple reports have shown that C-irradiation can cause serious abscopal effects in normal peripheral tissues, such as the haemopoietic system, thymus, lungs and spleen (Koturbash et al., 2008; Lei et al., 2015; Cai et al., 2017; Mohye et al., 2017).

A recent study demonstrated that adult survivors experience a greater decline in sexual functioning after C-irradiation therapy at a dose of >22 Gy than after C-irradiation therapy at lower doses (Huang et al., 2020). To date, there have been only two reports about the abscopal effects of C-irradiation on male reproduction in animal models, which focused on DNA damage in the germline (Tamminga et al., 2008) and sperm quality impairment (Zhang et al., 2006). Overall, data on the abscopal effects of C-irradiation on distant testes are scarce, and the effects remain poorly understood. To provide a possible target for improving radiation protection and safety, we studied the abscopal effects of C-irradiation in a hypofractionated regime on the structure and function of the testes in adult mice.

MATERIALS AND METHODS

Animals

Healthy adult male C57BL/6 mice [9 weeks of age, certificate number: XK (Shaan 2014–002)] were purchased from the Laboratory Animal Center of the Fourth Military Medical University (Xi'an, China) and maintained (four mice per cage) in the animal facility (12-h light/dark cycle; temperature, 20–26°C; and humidity, 45–65%) with free access to food and water. After 1 week of adaptive feeding, the mice were randomly divided into a sham irradiation group and a C-irradiation group ($n = 16$ for each group). Notably, to ensure that no radiation leaked through the lead shield and that protection of the shielded 'bystander' tissue was complete, we added a shielded irradiation group (shielded group, eight mice). All procedures in this study were approved and conducted following the guidelines of the Animal Welfare Committee of the Fourth Military Medical University (Xi'an, China).

Procedure of C-Irradiation

For the C-irradiation group, the mice were kept in a conscious state and administered C-irradiation in four hypofractionated doses of X-rays (RAD Source RS 2000 series, Suwanee, United States; working electric current 25 mA, working voltage 160 kV) 5 Gy/d for 4 d consecutively at a dose rate of 2.33 Gy/min, which was monitored in real time by a radiation dosimeter (Radcal Accu-Dose, United States). The remainder of each mouse's body was completely protected by a 2-cm thick lead shield. The dose rate of the testes under the lead shield was 0.01 Gy/min, which was equivalent to four thousandths of the cranial dose. For the shielded group, the whole body of each mouse was placed under a 2-cm lead shield and then irradiated in the same way as the C-irradiation group. Besides, the dose rate was 0.01 Gy/min and the total does was 0.08 Gy. For the sham group, the mice were subjected to the same procedure as the mice in the C-irradiation group except for X-ray irradiation.

Sample Collection and Testis Index Calculation

The body weight of each mouse was recorded every 3 days. All mice were fed for 4 weeks after C-irradiation and then euthanized with 1% sodium pentobarbital (50 mg/kg). Immediately, the bilateral testes were quickly freed from the surrounding connective tissues and excised after transcranial perfusion with 0.9% sodium chloride. The tissues were rinsed with precooled phosphate-buffered saline (PBS), immediately weighed, snap-frozen in liquid nitrogen and stored at −80°C until analysis. The testis index was calculated using the following formula: bilateral testes weight (g)/body weight (g) × 100%.

Observation of Testicular Histology by HE Staining

After anaesthesia, mice ($n = 2$–4 for each group) were fixed *via* cardiac perfusion with 4% paraformaldehyde (PFA, pH = 7.3) after transcranial perfusion with 0.9% sodium chloride. The bilateral testes were fixed in Bouin's fixative solution (Lilai, Chengdu, China) for morphological examination. After fixation for 24 h, the fixed testes were routinely trimmed, dehydrated, embedded in paraffin and then serially sectioned on a rotary microtome (RM2135, Leica, Heidelberg, Germany) at a thickness of 4 μm. Before staining, the tissue sections were preheated at 60°C for 2 h, deparaffinised, rehydrated in graded ethanol and stained with haematoxylin-eosin (HE) according to routine protocols. Then, histological changes were observed with a light microscope (Leica).

Histological Analysis of Testis

For histological analysis of testis, the diameter of seminiferous tubules and height of seminiferous epithelium were measured using ImageJ software (NIH, MD, United States) from 50 random round or nearly round seminiferous tubules at ×100 magnification for each group, according to the methods in a previous study (Babazadeh and Najafi, 2017; Guo et al., 2019). Briefly, the diameter was calculated as the mean of the major and minor axes of the seminiferous tubules, and the height of the seminiferous epithelium was calculated as follows (average diameter – average inner diameter) of seminiferous tubule/2. In addition, according to the appearance of cells present in the seminiferous tubules, the seminiferous tubules were divided into normal or abnormal (Ibáñez et al., 2017), and the percentage of abnormal seminiferous tubules was counted from 10 random fields at ×100 magnification for each group.

Observation of Testicular Ultrastructure by Transmission Electron Microscopy

After anaesthesia, mouse testes ($n = 2$ for each group) were separated, trimmed to 1 mm × 1 mm × 1 mm samples, fixed in 3% glutaraldehyde and 1% osmic acid, dehydrated in a graded series of acetone (30, 50, 70, 80, 90, 95 and 100%) and then embedded in Araldite. Ultrathin slices (50 nm thick) were double-stained with saturated uranyl acetate and lead citrate. A transmission electron microscope (JEM-1400FLASH; JEOL Ltd., Tokyo, Japan) was used to observe the ultrastructure of seminiferous tubules. The testicular ultrastructure observed in this study included mainly Sertoli cells, Leydig cells, spermatogonia, spermatocytes and spermatids.

Western Blotting

Total testicular protein ($n = 4$ for each group) was extracted and quantified as described previously. Equal amounts of testis samples (30 μg) were subjected to 10–12% Bis-Tris gel electrophoresis and transferred to polyvinylidene fluoride immunoblot membranes (0.22 μm). The membranes were blocked with 5% non-fat milk for 2 h at room temperature and probed with primary antibodies overnight at 4°C. Primary antibodies against β-actin (20536-1-AP, 1:5000), Bcl-2 (12789-1-AP, 1:2000) and Bax (50599-2-Ig, 1:3000) were obtained from Proteintech (Wuhan, China); primary antibodies against SCF (21670–1, 1:300) were obtained from SAB (MD, United States); and primary antibodies against Cleaved caspase 3 (ab214430, 1:4000) and GDNF (ab176564, 1:2000) were obtained from Abcam (MA, United States). The following morning, the membranes were incubated with species-matched horseradish peroxidase (HRP)-conjugated secondary antibodies (1:5000, CWBIO, Beijing, China) for 2 h at room temperature and then incubated with chemiluminescent HRP substrate to visualise the bands. Quantity One 4.62 software (Bio-Rad, CA, United States) was used to analyse the optical density of each target band. To normalise the protein levels, β-actin was used as a loading control.

Immunofluorescence Staining and TUNEL Assay

After initial deparaffinization and rehydration, testis sections were processed by antigen retrieval using citrate buffer in a high-power microwave oven, treated with 3% bovine serum albumin for 30 min and incubated with a rabbit monoclonal Cleaved caspase 3 antibody (9664S, 1:200, CST, MA, United States) and a rabbit polyclonal 3β hydroxysteroid dehydrogenase (3βHSD) antibody (DF6639, 1:150, Affinity Biosciences, OH, United States) at 4°C overnight. Next day, the sections were subsequently treated with a FITC-conjugated goat anti-rabbit antibody (ab6717, 1:1000, Abcam, MA, United States). Testicular cell apoptosis was assessed by terminal deoxynucleotidyl transferase (TdT) enzymaticated dUTP nick end labelling (TUNEL) assay using an *in situ* Cell Death Detection Kit (Roche, Basel, Switzerland). Briefly, after initial deparaffinization and antigen recovery, the section was permeabilised with Triton X-100 (ST795, Beyotime, Shanghai, China), followed by 30 μl TUNEL reaction mixture for 60 min at 37°C. Negative controls were performed without the enzyme TdT. Finally, 10 random fields for each group were chosen at random for analysis using a fluorescence microscope (Leica), and the average fluorescence intensity was calculated using ImageJ software.

Detection of Testicular Secretory Function by ELISA

Blood samples were taken from the heart and centrifuged at 3000 rpm for 15 min at 4°C to obtain serum, which was stored at −80°C and used for detection of the secretory function of Leydig cells. The levels of serum testosterone (T; $n = 7$ for each group), secreted by Leydig cells, were determined with an ELISA kit (Sinoukbio, Beijing, China) according to the manufacturers' instructions. In addition, testis tissue (approximately 100 mg; $n = 5$ for each group) was lysed with PBS and homogenised to extract total proteins in a homogenisation device (Leica) under precooled conditions. After that, the levels of GDNF and SCF in the testis were measured with the ELISA kits (Elabscience, Wuhan, China) according to the manufacturers' instructions.

Detection of Sperm Quality

The cauda epididymides of each mouse were dissected out carefully, gently cut, collected in a 12-well plate containing 1 mL of sperm culture solution (Millipore, MA, United States) and then incubated at 37°C for 30 min. The sperm suspension was collected and filtered through a nylon mesh with a 38-μm pore diameter to remove tissue fragments and then used to record and calculate sperm count and abnormality according to the methods in a previous study (Guo et al., 2019). The types of abnormal sperm morphology observed in this study mainly included the folded-tail, hookless, amorphous, double-head and double-tail phenotypes according to a previous study (Chen et al., 2019). In addition, a FITC annexin V apoptosis detection kit I (BD Pharmingen, CA, United States) was applied to quantify the survival rate and apoptosis rate of sperm. Briefly, sperm samples prepared as described above

were supplemented with 1 mL of 1× annexin V binding buffer. Subsequently, the samples were washed and incubated in annexin V-FITC and propidium iodide (PI) at 37°C for 5 min in the dark and then analysed by flow cytometry (FCM; XL-MCL, Beckman Coulter, CA, United States) following the manufacturer's instructions. Four or five sperm samples were used for each group, and 15,000 sperm were analysed for each sample.

Statistical Analysis

All measurement data are expressed as the mean and standard deviation (mean ± SD) and were analysed with SPSS 20.0 statistical software (SPSS Inc., Chicago, IL, United States). For statistical analysis, two-way ANOVA with repeated measures was used to analyse the body weights of mice, one-way ANOVA followed by Tukey's multiple comparisons test was used to compare three groups and a two-tailed student's *t*-test was used to compare two groups for parametric data (data that met the normality and equal variance assumptions). All subjective analyses were performed by individuals blinded to the exposure group. All graphs were generated using GraphPad Prism 8.0 software (San Diego, CA, United States), and the results were considered statistically significant at $p < 0.05$.

RESULTS

The Abscopal Effects of C-Irradiation Damage Testicular Histology

Figure 1A shows the time schedule of C-irradiation used for the mice. Day 3 to day 0 was the irradiation time. During the whole experiment, the body weights of the mice in the shielded group decreased only on day 4 (**Figure 1B**, $p < 0.01$) and then immediately returned to the levels of the mice in the sham group, and mice in the sham and shielded groups were in good general body conditions. However, from the end of the first day of C-irradiation, mice in the C-irradiation group exhibited evident appetite loss, activity reduction and body weight loss, compared with the mice in the sham and shielded groups (**Figure 1B**, $p < 0.01$), and three mice died due to worsening health status during the first week after C-irradiation. Until 4 weeks after C-irradiation, the body weight of mice in the C-irradiation group still lagged significantly ($p < 0.01$).

In terms of the reproductive system of male mice, the testicular volume and testis index were significantly lower in the C-irradiation group than in the sham and shielded groups (**Figures 1C,D**; $p < 0.001$), but there was no significant difference between the latter two groups ($p > 0.05$). HE staining showed that the testes in the C-irradiation group had obvious pathological changes, such as vacuolation of seminiferous tubules, degeneration and necrosis of spermatogenic cells (**Figure 1E**). In addition, the diameter of the seminiferous tubules and height of the seminiferous epithelium were significantly lower, and the percentage of abnormal seminiferous tubules was higher in the C-irradiation group than in the sham and shielded groups (**Figures 1F,H**; $p < 0.001$).

Interestingly, there were no significant differences in the organ index for other peripheral organs (heart, liver, spleen, lungs, kidneys and thymus) among the three groups (**Figure S1**; $p > 0.05$). HE staining also showed that compared with the sham group, the histological structures of the other important peripheral organs had no change in the shielded group and no or only slight pathological changes in the C-irradiation group (**Figures S2–7**). All the above results indicated that the protection of the lead shield was extremely effective, and C-irradiation did not cause obvious scattering to the peripheral organs. Compared with other peripheral organs, testicular tissue was the most sensitive to the abscopal effects of C-irradiation, which could severely damage testicular histology.

The Abscopal Effects of C-Irradiation Damage the Testicular Ultrastructure

For the sham and shielded groups, the overall ultrastructure of seminiferous tubules was normal and intact (**Figure 2A**), and the spermatogenic cells in various growth cycles were closely arranged with clear cell structures, large round or oval nuclei, smooth and clear cell membranes and compact chromatin. The number of organelles in the cytoplasm was normal, and there were abundant mitochondria (**Figures 2D–F**). The intercellular bridge between the spermatogenic cells and the Sertoli cell junction complex, also called the blood-testis barrier (BTB), was complete (**Figure 2B**). For the C-irradiation group (**Figures 2A–F**), the overall ultrastructure of seminiferous tubules was severely damaged, the spermatogenic cell membrane was unclear at all levels, the perinuclear space was expanded, the nuclear membrane was dissolved, the mitochondria showed obvious swelling, cavitation was observed and the endoplasmic reticulum was dilated. Apoptosis and autophagy were suspected to be underway in testicular cells. In addition, the integrity of the BTB was disrupted. All these results suggested that the lead shield had excellent protective effects on the tissues outside the cranial region and that the abscopal effects of C-irradiation severely damaged the testicular ultrastructure.

The Abscopal Effects of C-Irradiation Increase Testicular Cell Apoptosis

Western blotting detection of apoptosis-related proteins (**Figure 3A**) showed that compared with the sham group, the C-irradiation group exhibited significantly lower relative protein level of Bcl-2 (**Figure 3B**; $p < 0.01$), significantly higher relative protein level of Bax (**Figure 3C**; $p < 0.01$), significantly lower Bcl-2/Bax ratio (**Figure 3D**; $p < 0.05$) and significantly higher relative protein level of Cleaved caspase 3 (**Figure 3E**; $p < 0.05$). Immunofluorescence staining of Cleaved caspase 3 showed that the number of Cleaved caspase 3-positive cells increased and that these cells distributed in the outermost seminiferous tubules at 4 weeks after C-irradiation (**Figures 3F–G**; $p < 0.001$). In addition,

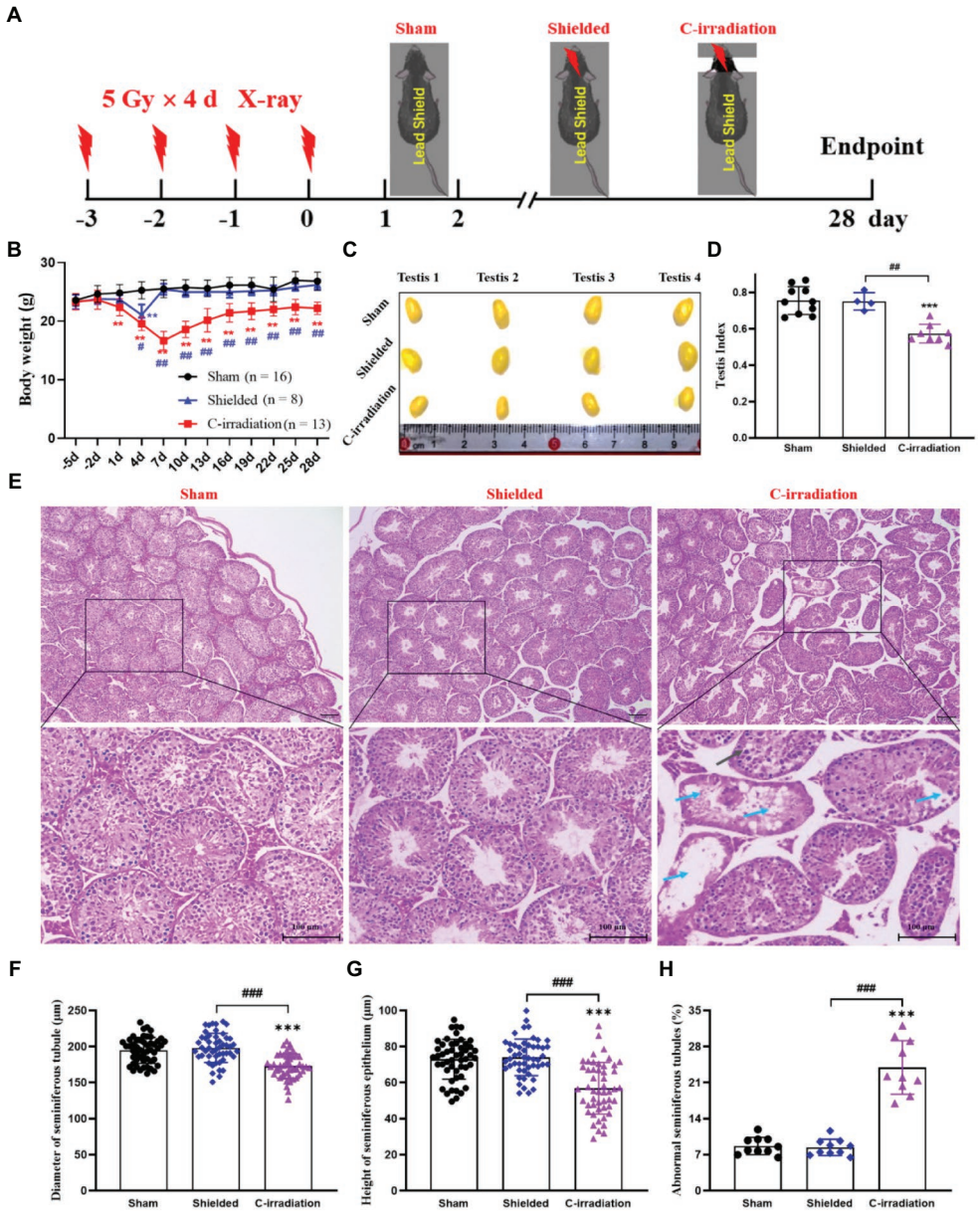

FIGURE 1 | The abscopal effects of C-irradiation damage testicular histology. **(A)** Time schedule of irradiation for mice. **(B)** Body weight of mice during experiments. **(C)** Testis volume, $n = 4$ for each group. **(D)** Testis index, $n = 10$ for the sham group. $n = 4$ for the shielded group and $n = 8$ for the C-irradiation group. **(E)** HE staining of testes, $n = 4$ for the sham and C-irradiation groups, $n = 2$ for the shielded group, bar = 100 μm. Vacuolation of seminiferous tubules (↑) and degeneration and necrosis of various spermatogenic cells (↑). **(F–G)** Diameter of seminiferous tubules and height of seminiferous epithelium calculated randomly from 50 round or nearly round cross-sections of the seminiferous tubules (long axis: short axis < 1.2:1) for each group. **(H)** Percentage of abnormal seminiferous tubules calculated from 10 random fields for each group. The values are expressed as the mean ± SD and analysed by two-way ANOVA for body weight and one-way ANOVA with Tukey's test for three-group comparisons. $^{**}p < 0.01$; $^{***}p < 0.001$ vs. sham group. $^{\#\#}p < 0.01$; $^{\#\#\#}p < 0.001$ vs. shielded group.

TUNEL staining of testis sections revealed that apoptosis of testicular cells increased obviously in the C-irradiation group compared with sham group (**Figures 3H–I**; $p < 0.001$), and the apoptotic testicular cells also located in the outermost seminiferous tubules. These results are consistent with the above results of Western blotting, suggesting that the abscopal effects of C-irradiation increase testicular cell apoptosis and more in spermatogonial stem cells (SSCs).

The Abscopal Effects of C-Irradiation Alter the Secretory Functions of the Testes

The ELISA results showed that the serum T concentration secreted by Leydig cells did not differ between the sham group and the C-irradiation group at 4 weeks after C-irradiation (**Figure 4A**; $p > 0.05$). Besides, 3βHSD, a Leydig cell specific marker, plays an important role in the synthesis of steroid hormones (Yang et al., 2017). To explore the abscopal effects

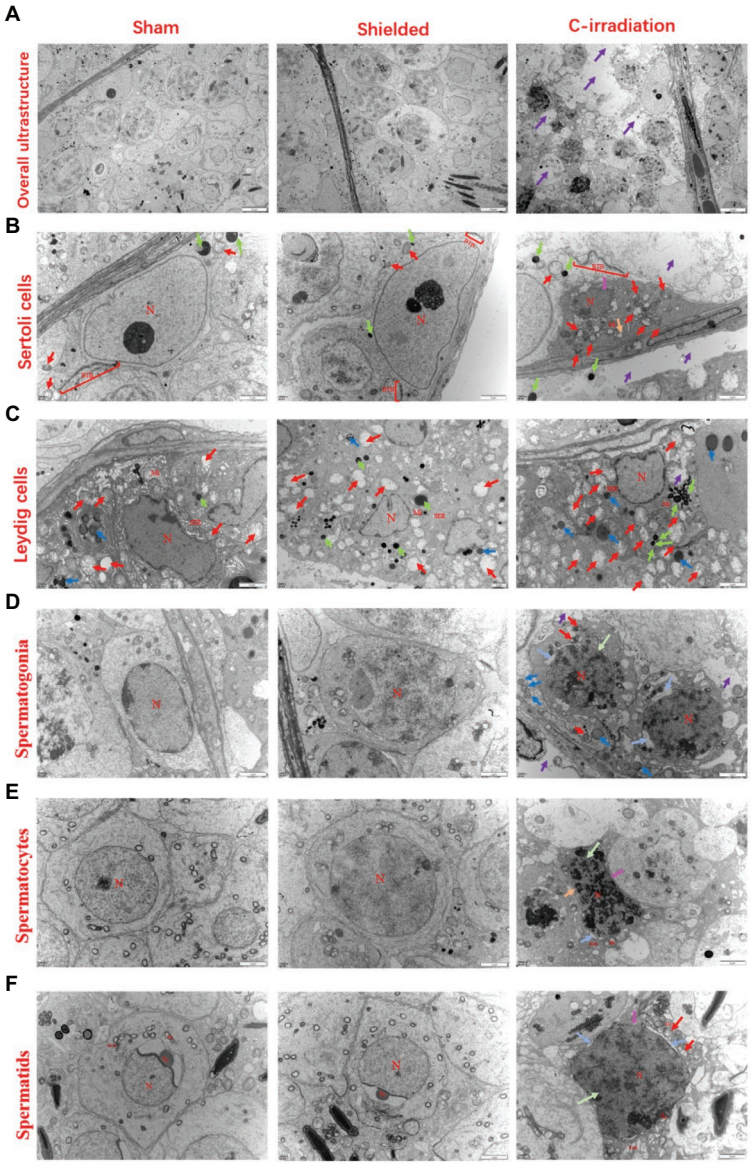

FIGURE 2 | The abscopal effects of C-irradiation damage the testicular ultrastructure. **(A)** Overall ultrastructure of seminiferous tubules. Bar = 10 μm. **(B–F)** Ultrastructure of Sertoli cells, Leydig cells, spermatogonia, spermatocytes and spermatids. Bar = 2 μm, $n = 2$ for each group. N, nucleus; Mi, mitochondrion; RER, rough endoplasmic reticulum; BTB, blood-testis barrier; and Ac, acrosome. Lipid droplets ↓, mitochondrial swelling ↓, secondary lysosomes ↓, RER dilatation ↓, loss of intracytoplasmic solutes ↓, widened perinuclear gap ↓ and suspected apoptosis ↓.

of C-irradiation on steroidogenic capacity of Leydig cells, the 3βHSD immunoreactivity in Leydig cells was detected by the immunofluorescence staining in testicular paraffin sections (**Figure 4B**). The results showed that the level of 3βHSD in testis did not differ between the sham group and the C-irradiation group at 4 weeks after C-irradiation (**Figure 4C**; $p > 0.05$), which suggested that the abscopal effects of C-irradiation do not affect the steroidogenic capacity of Leydig cells. However, the concentrations of GDNF and SCF secreted by Sertoli cells were significantly higher in the C-irradiation group at 4 weeks after C-irradiation than in the sham group (**Figures 4D,E**; $p < 0.01$). In addition, the results of Western blotting (**Figure 4F**) showed that compared with the sham group, the relative protein level of GDNF in the C-irradiation group showed an upward trend but not statistically significant (**Figure 4G**; $p > 0.05$), while the relative protein level of SCF was higher at 4 weeks after C-irradiation than of the sham group (**Figure 4H**; $p < 0.01$), which was consistent with the results of ELISA. All the results suggest that the abscopal effects of C-irradiation enhance the secretory functions of Sertoli cells at 4 weeks after C-irradiation but do not affect the secretory functions of Leydig cells, which may be related to negative feedback of damage repair during this period.

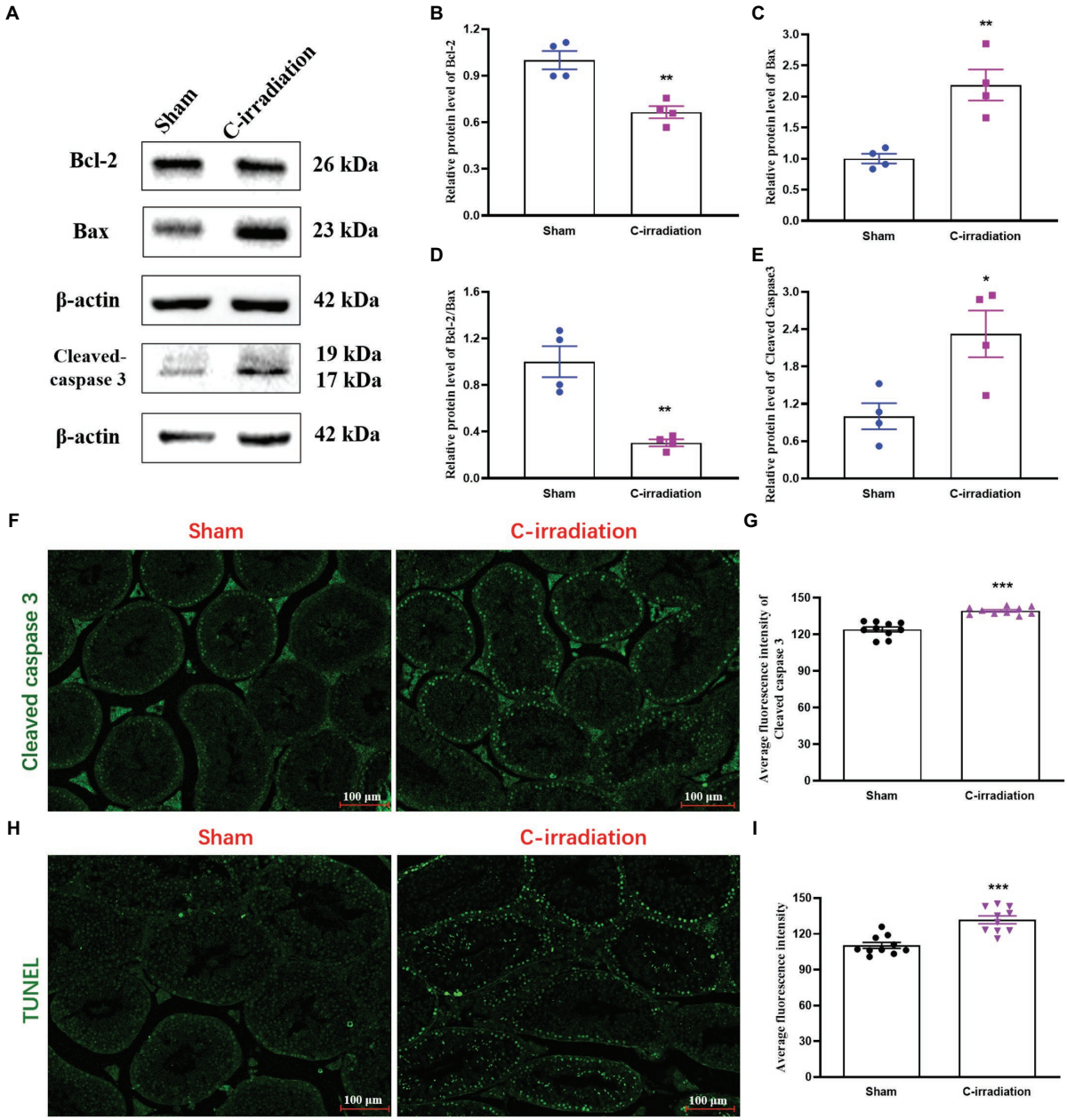

FIGURE 3 | The abscopal effects of C-irradiation increase testicular cell apoptosis. **(A)** Typical immunoblots of apoptosis-related proteins. The first three bands were from the same membrane and the last two bands were from another membrane. **(B–E)** Relative protein level of Bcl-2, Bax, Bcl-2/Bax and Cleaved caspase 3 detected by Western blotting, $n = 4$ for each group. **(F–G)** Immunofluorescence of Cleaved caspase 3 and average fluorescence intensity from 10 random fields for each group. Bar = 100 μm. **(H–I)** TUNEL staining and average fluorescence intensity from 10 random fields for each group. Bar = 100 μm. The values are expressed as the mean ± SD and analysed by two-tailed unpaired student's *t*-tests. $^{*}p < 0.05$, $^{**}p < 0.01$ and $^{***}p < 0.001$ vs. the sham group.

The Abscopal Effects of C-Irradiation Decrease Sperm Quality

The above results suggest that the testes are the most sensitive target organs to the abscopal effects of C-irradiation. To further clarify the abscopal effects of C-irradiation on testicular function in mice, we detected changes in sperm quality of the cauda epididymis at 4 weeks after C-irradiation, including sperm count, abnormality, survival rate and early and late apoptosis rate. Compared with the sham group and shielded group, the C-irradiation group exhibited marked decreases in sperm count (**Figures 5A,B**; $p < 0.01$ or 0.001). Typical types of abnormal sperm morphology observed in this study are shown in **Figure 5C**, and sperm abnormalities increased obviously in the C-irradiation group (**Figure 5D**; $p < 0.01$ or 0.001). Typical FCM pictures are shown in **Figure 5E**, where the quadrants represent dead sperm ($PI^+/FITC^-$, upper-left quadrant), late

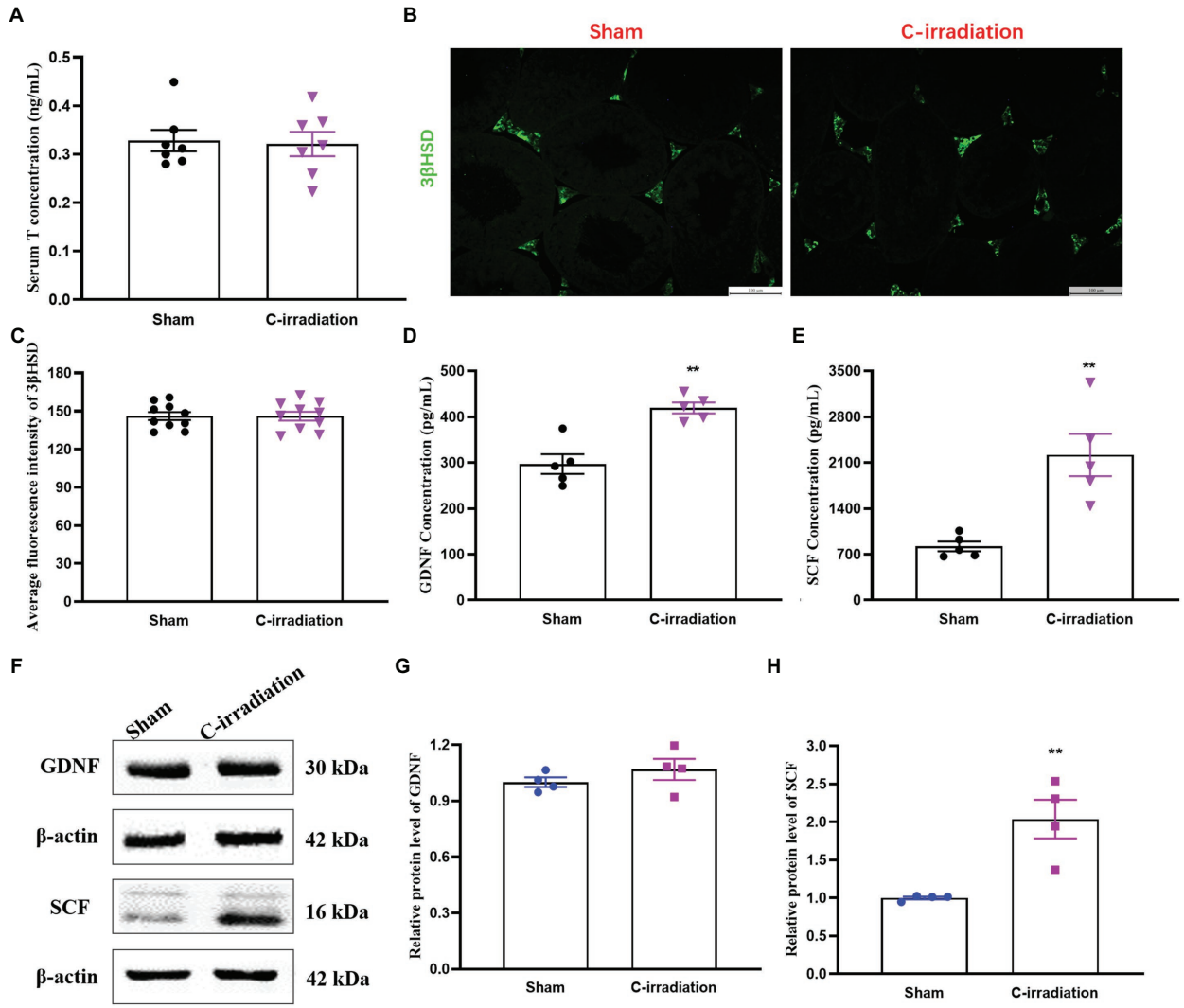

FIGURE 4 | The abscopal effects of C-irradiation affect the secretory functions of the testis. **(A)** Serum T concentrations secreted by Leydig cells, $n = 7$ for each group. **(B–C)** Immunofluorescence of 3βHSD in testis and average fluorescence intensity from 10 random fields for each group. Bar = 100 μm. **(D–E)** GDNF and SCF concentrations secreted by Sertoli cells and detected by ELISA, $n = 5$ for each group. **(F)** Typical immunoblots relating to the secretory functions of Sertoli cells. The first two bands were from the same membrane and the last two bands were from another membrane. **(G–H)** Relative protein level of GDNF and SCF detected by Western blotting, $n = 4$ for each group. The values are expressed as the mean ± SD and analysed by two-tailed unpaired student's *t*-tests. $^{**}p < 0.01$ vs. sham group.

apoptosis sperm ($PI^+/FITC^+$, upper-right quadrant), surviving sperm ($PI^-/FITC^-$, lower-left quadrant) and early apoptosis sperm ($PI^-/FITC^+$, lower-right quadrant). The survival rate of sperm decreased (**Figure 5F**; $p < 0.05$ or 0.01), and the early apoptosis rate and late apoptosis rate of sperm increased significantly at 4 weeks after C-irradiation (**Figures 5G,H**; $p < 0.05$ or 0.01 or 0.001). There were no significant changes in any of the above indexes relating to sperm quality in the shielded group, which again indicated that the lead shield had an excellent protective effect and that damage to the testes indeed arose from the abscopal effects of C-irradiation. The above results suggest that the abscopal effects of C-irradiation can damage testicular function and ultimately decrease sperm quality in mice.

DISCUSSION

With the progress of treatment technology, the survival rates of cancer patients treated with cranial irradiation significantly increased (Xu et al., 2018). Impaired fertility has been recognised as an important quality of life concern for cancer survivors of childbearing age (Muñoz et al., 2016). Thus, protection of the reproductive potential of these patients against C-irradiation damage is important. To our knowledge, this study demonstrates, for the first time, that C-irradiation induces abscopal effects to cause distal testicular damage with regard to both structure and function.

Currently, a hypofractionated dose is being carried out as a new radiotherapy strategy. Thus, 5 Gy × 4 d C-irradiation was

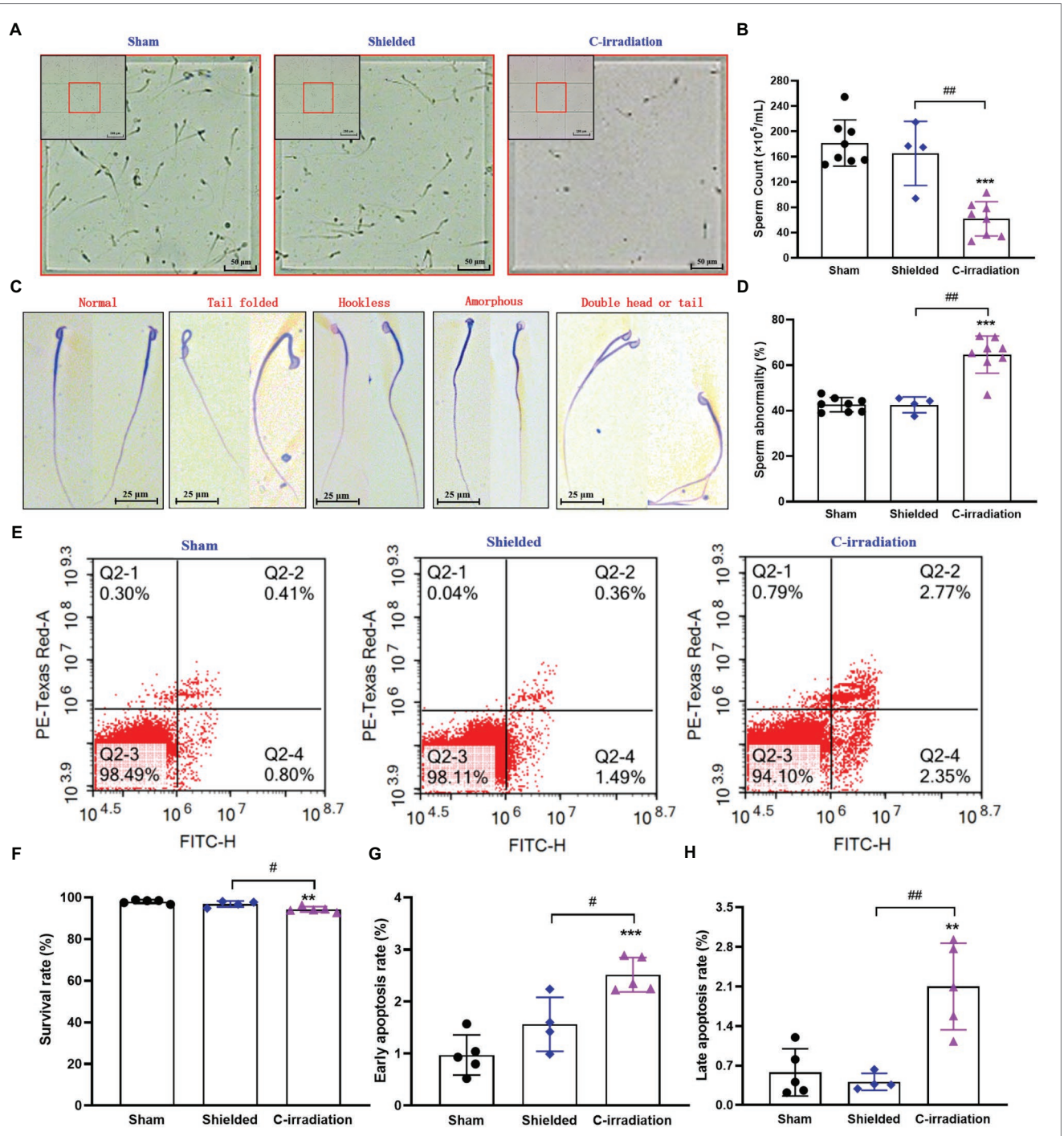

FIGURE 5 | The abscopal effects of C-irradiation decrease the sperm quality of the cauda epididymis. **(A)** Representative pictures of sperm count. Bar = 200 μm for the upper-left corner and bar = 50 μm for the magnification with red border. **(B)** Analysis of sperm count. n = 8 for the sham and C-irradiation groups and $n = 4$ for the shielded group. **(C)** Typical types of abnormal sperm morphology, including the folded-tail, hookless, amorphous, double-head and double-tail phenotypes. Bar = 25 μm. **(D)** Sperm abnormality. $n = 8$ for the sham and C-irradiation groups and $n = 4$ for the shielded group. **(E)** Representative pictures of sperm apoptosis detected by FCM. **(F–H)** Survival rate, early apoptosis rate and late apoptosis rate of sperm for analysis as noted in **(E)**. $n = 5$ for the sham and C-irradiation groups and $n = 4$ for the shielded group. The values are expressed as the mean ± SD and analysed by one-way ANOVA with Tukey's test. $^{**}p < 0.01$; $^{***}p < 0.001$ vs. sham group. $^{\#}p < 0.05$; $^{\#\#}p < 0.01$ vs. shielded group.

used to explore the damage effect of testicular tissue under shielding in the study. It is possible that X-rays are reflected while passing through tissue, resulting in a small 'scatter' dose in the protected tissue. However, a previous study demonstrated that abscopal effects are not the result of insufficient shielding or radiation scattering (Koturbash et al., 2008). Likewise,

we administered whole-body shielded irradiation to mice and found that there were no obvious changes in the histological structures of many peripheral organs (**Figure S2–7**). These results suggested that the protection of the lead shield was extremely effective and that the C-irradiation did not cause obvious scattering to the peripheral organs. We also observed the organ index values and histological structures of important peripheral organs and found that only the testis index decreased and the histological structures of the testis were significantly damaged in the C-irradiation group. All of the above results suggest that the testes are the most sensitive target organs to RIAEs and that the testicular damage in the C-irradiated mice resulted from RIAEs rather than the effects of scattered C-irradiation.

Innumerable studies have proven that the testis is highly sensitive to ionising and nonionizing radiation, which could directly induce testicular cell apoptosis in animals (Said et al., 2019; Rakici et al., 2020). Furthermore, SSCs are highly radiosensitive in spermatogenic populations (Marjault and Allemand, 2016; Qi et al., 2019). However, the sensitivity of spermatogenic populations to RIAEs is unclear. Previous studies have demonstrated that RIAEs can initiate apoptosis in distant tissues (Koturbash et al., 2008; He et al., 2020). In addition, Zhang et al. reported that fractionated irradiation (X-ray, 8 Gy × 3 d) of the right thorax damaged the ultrastructure of the BTB and increased apoptotic spermatogonia cells, which located at the outermost layer of the seminiferous epithelium of the testis (Zhang et al., 2019). The results are consistent with our findings, indicating SSCs are highly sensitive to RIAE.

The mechanism of testicular cell apoptosis directly induced by ionising radiation is mostly mediated by a p53-dependent Bax-caspase-3-mediated pathway (Shahin et al., 2018; He et al., 2020). Since the testes of mice in the C-irradiation group are not directly exposed to ionising radiation, we speculate that the mechanism of testicular cell apoptosis induced by C-irradiation is different from that induced by direct radiation. Recently, it was reported that abnormal levels of hormones secreted by the hypothalamus-pituitary gland could induce the apoptosis of testicular spermatogenic cells (Chimento et al., 2014). In our ongoing study, we found that the levels of gonadotropin-releasing hormone (GnRH) secreted by hypothalamus, luteinizing hormone (LH) and follicle stimulating hormone (FSH) secreted by pituitary increased significantly at 4 weeks after C-irradiation compared with sham group (data not shown). Probably, the testicular cell apoptosis induced by C-irradiation was caused by the abnormal secretory function of the hypothalamus and pituitary gland, and we are trying to get more evident to verify this speculation. Besides, it was reported that the PI3K/Akt pathway, a key regulator of apoptosis, played an important role in testicular damage (Huang et al., 2019; Kucukler et al., 2020; Wang et al., 2021). In addition, SCF and its receptor C-kit are upstream regulators of the PI3K/Akt pathway (Guan et al., 2020). Considering the protein level of SCF in testis increased obviously after C-irradiation compared with sham group, we speculate that another mechanism of testicular apoptosis in this study may be related to the regulation of the SCF/C-kit–PI3K/Akt pathway.

Although testicular histopathology is often considered the gold standard for the nonclinical assessment of testicular damage, male fertility also requires intact testicular function (Kenney et al., 2012; Dere et al., 2013), which depends mostly on the secretory functions of testicular somatic cells (Sertoli cells and Leydig cells; Xiong et al., 2020). T regulated by 3βHSD (Li et al., 2018), synthesised and released by Leydig cells is necessary for both spermatogenesis and the function of Sertoli cells, which secrete proteins necessary for the proliferation and self-renewal of SSCs (Zhang et al., 2006, 2015). In a previous study, 6 Gy of C-irradiation with 4 MV of nominal photon energy and a dose rate of 2.3 Gy/min induced late-onset T deficiency at 20 weeks in juvenile female rats (Xu et al., 2020). However, the levels of serum T and testicular 3βHSD were not altered at 4 weeks after 20 Gy of C-irradiation in this study. Considering the increase of upstream hormones (GnRH, FSH and LH), we speculated that it is related to negative feedback of damage repair during this period.

Spermatogenic cells are supported by surrounding Sertoli cells, which produce the factors and microenvironment required for each stage of spermatogenic cell development (Walker, 2021; You et al., 2021). The factors include GDNF, which promotes the proliferation and self-renewal of SSCs, and SCF, which encourages the differentiation of SSCs (Guo et al., 2019). The concentrations of GDNF and SCF increased at 4 weeks after 20 Gy of C-irradiation. We hypothesise that these changes are related to negative feedback regulation of testicular damage repair at 4 weeks after C-irradiation, which requires further research.

Spermatogenesis, the primary testicular function, is a complex morphological change of germ cell differentiation that involves self-renewal and differentiation of spermatogonia, meiosis of spermatocytes and spermiogenesis (Huang et al., 2021). Alteration of any stage of spermiogenesis will damage sperm quality and ultimately impact male fertility. The count, survival rate and morphology of sperm are key elements affecting fertility and function as sensitive indexes for evaluating the effects of physical and chemical factors on sperm quality. A previous study (Tamminga et al., 2008) showed that the mature sperm quality of rats decreased on day 7 after X-ray C-irradiation (10 Gy × 2 d, 3 Gy/min). Our results demonstrated that the abscopal effects of hypofractionated C-irradiation decreased the sperm quality of mice, consistent with the findings of Zhang et al.'s (2006) study. That study reported that sperm quality decreased on the 35th day after administration of 2 Gy of $^{12}C^{6+}$ ion or ^{60}Co γ-ray C-irradiation to mice. Notably, the sperm count in the C-irradiation group decreased drastically. However, in all groups, survival rates were above 93%, and total apoptosis rates were below 5%, indicating that the abscopal effects of C-irradiation mainly impaired spermatogenesis (rather than directly affecting mature sperm) and further reduced sperm quality. Such effects may explain the clinical conditions of temporary infertility and permanent sterility after C-irradiation treatment (Muñoz et al., 2016; Huang et al., 2020; Verbruggen et al., 2021).

The abscopal effects of C-irradiation are dynamic processes mediated by multiple factors, multiple pathways and multiple mechanisms, and they are not mutually exclusive. A clinical study reported that C-irradiation at doses of >22 Gy led to

gonadotropin deficiency (Haavisto et al., 2016). The hypothalamus-pituitary-gonad axis regulates spermatogenesis in mammals, and the hypothalamus and pituitary are inevitably exposed to radiation during C-irradiation therapy, which may be related to testicular damage resulting from the abscopal effects of C-irradiation. Notably, new technologies, such as gene expression profiling and proteomics, may contribute to elucidation of the mechanism and identification of the molecules involved in testicular damage induced by C-irradiation, which are the focuses of our ongoing research.

CONCLUSION

Taken together, the findings of this study indicate that the abscopal effects of C-irradiation can induce testicular damage with regard to both structure and function and ultimately decrease sperm quality in mice. These findings may have important implications for the development of strategies to improve safety and prevent radiotherapy-related reproductive damage.

DATA AVAILABILITY STATEMENT

The original contributions presented in the study are included in the article/**Supplementary Material**, and further inquiries can be directed to the corresponding author.

ETHICS STATEMENT

The animal study was reviewed and approved by the Animal Welfare Committee of Fourth Military Medical University.

AUTHOR CONTRIBUTIONS

G-RD and LG designed the research. LG, T-ZQ, L-YL, P-PL and Y-ZX performed the research. WZ and WL analysed the data. LG and T-ZQ wrote the manuscript. WL, JL and G-RD revised the manuscript. All authors approved the final manuscript for submission.

FUNDING

This work has been carried out with financial support from the Fund of National Natural Science Foundation of China (grant number: 31770905).

SUPPLEMENTARY MATERIAL

The Supplementary Material for this article can be found online at https://www.frontiersin.org/articles/10.3389/fphys.2021.717571/full#supplementary-material

REFERENCES

Abuodeh, Y., Venkat, P., and Kim, S. (2016). Systematic review of case reports on the abscopal effect. *Curr. Prob. Cancer* 40, 25–37. doi: 10.1016/j.currproblcancer.2015.10.001

Aravindan, S., Natarajan, M., Ramraj, S. K., Pandian, V., Khan, F. H., Herman, T. S., et al. (2014). Abscopal effect of low-LET gamma-radiation mediated through Rel protein signal transduction in a mouse model of nontargeted radiation response. *Cancer Gene Ther.* 21, 54–59. doi: 10.1038/cgt.2013.72

Azoulay, M., Shah, J., Pollom, E., and Soltys, S. G. (2017). New hypofractionation radiation strategies for glioblastoma. *Curr. Oncol. Rep.* 19:58. doi: 10.1007/s11912-017-0616-3

Babazadeh, M., and Najafi, G. (2017). Effect of chlorpyrifos on sperm characteristics and testicular tissue changes in adult male rats. *Vet. Res. Forum* 8, 319–326

Cai, S., Shi, G., Cheng, H., Zeng, Y., Li, G., Zhang, M., et al. (2017). Exosomal miR-7 mediates bystander autophagy in lung after focal brain irradiation in mice. *Int. J. Biol. Sci.* 13, 1287–1296. doi: 10.7150/ijbs.18890

Chen, X., Chen, T., Sun, J., Luo, J., Liu, J., Zeng, B., et al. (2019). Lower methionine/cystine ratio in low-protein diet improves animal reproductive performance by modulating methionine cycle. *Food Sci. Nutr.* 7, 2866–2874. doi: 10.1002/fsn3.1128

Chimento, A., Sirianni, R., Casaburi, I., and Pezzi, V. (2014). Role of estrogen receptors and g protein-coupled estrogen receptor in regulation of hypothalamus–pituitary–testis axis and spermatogenesis. *Front. Endocrinol.* 5, 1–8. doi: 10.3389/fendo.2014.00001

Dere, E., Anderson, L. M., Coulson, M., McIntyre, B. S., Boekelheide, K., and Chapin, R. E. (2013). SOT symposium highlight: translatable indicators of testicular toxicity: inhibin b, MicroRNAs, and sperm signatures. *Toxicol. Sci.* 136, 265–273. doi: 10.1093/toxsci/kft207

Guan, S., Zhu, Y., Wang, J., Dong, L., Zhao, Q., Wang, L., et al. (2020). A combination of semen Cuscutae and Fructus Lycii improves testicular cell proliferation and inhibits their apoptosis in rats with spermatogenic dysfunction by regulating the SCF/c-kit--PI3K--Bcl-2 pathway. *J. Ethnopharmacol.* 251, 112525–112537. doi: 10.1016/j.jep.2019.112525

Guo, L., Lin, J., Xue, Y., An, G., Zhang, J., Zhang, K., et al. (2019). Effects of 220 MHz pulsed modulated radiofrequency field on the sperm quality in rats. *Int. J. Env. Res. Pub. He.* 16, 1286–1298. doi: 10.3390/ijerph16071286

Haavisto, A., Henriksson, M., Heikkinen, R., Puukko-Viertomies, L., and Jahnukainen, K. (2016). Sexual function in male long-term survivors of childhood acute lymphoblastic leukemia. *Cancer Am. Cancer Soc.* 122, 2268–2276. doi: 10.1002/cncr.29989

He, G., Tang, A., Xie, M., Xia, W., Zhao, P., Wei, J., et al. (2020). Blood gene expression profile study revealed the activation of apoptosis and p53 signaling pathway may be the potential molecular mechanisms of ionizing radiation damage and radiation-induced bystander effects. *Dose Resp. Int. J.* 18, 1–11. doi: 10.1177/1559325820914184

Hu, S., and Shao, C. (2020). Research progress of radiation induced bystander and abscopal effects in normal tissue. *Rad. Med. Prot.* 2, 69–74. doi: 10.1016/j.radmp.2020.04.001

Huang, W., Cao, Z., Zhang, J., Ji, Q., and Li, Y. (2019). Aflatoxin B1 promotes autophagy associated with oxidative stress-related PI3K/AKT/mTOR signaling pathway in mice testis. *Environ. Pollut.* 255, 113317–113327. doi: 10.1016/j.envpol.2019.113317

Huang, S., Lu, Y., Li, S., Zhou, T., Wang, J., Xia, J., et al. (2021). Key proteins of proteome underlying sperm malformation of rats exposed to low fenvalerate doses are highly related to P53. *Environ. Toxicol.* 6, 1181–1194. doi: 10.1002/tox.23117

Huang, W., Sundquist, K., Sundquist, J., Crump, C., and Ji, J. (2020). Risk of being born preterm in offspring of survivors with childhood or adolescent central nervous system tumor in Sweden. *Int. J. Cancer* 147, 100–106. doi: 10.1002/ijc.32722

Ibáñez, C. A., Erthal, R. P., Ogo, F. M., Peres, M. N. C., Vieira, H. R., Conejo, C., et al. (2017). A high fat diet during adolescence in male rats negatively programs reproductive and metabolic function which is partially ameliorated by exercise. *Front. Physiol.* 807, 1–12. doi: 10.3389/fphys.2017.00807

Isfahanian, N., Al-Hajri, T., Marginean, H., Chang, L., and Caudrelier, J. (2017). Hypofractionation is an acceptable alternative to conventional fractionation

in the treatment of postlumpectomy ductal carcinoma in situ with radiotherapy. *Clin. Breast Cancer* 17, e77–e85. doi: 10.1016/j.clbc.2016.10.005

Ishiyama, H., Teh, B. S., Ren, H., Chiang, S., Tann, A., Blanco, A. I., et al. (2012). Spontaneous regression of thoracic metastases while progression of brain metastases after stereotactic radiosurgery and stereotactic body radiotherapy for metastatic renal cell carcinoma: Abscopal effect prevented by the blood-brain barrier? *Clin. Genitourin. Cancer* 10, 196–198. doi: 10.1016/j.clgc.2012.01.004

Kenney, L. B., Cohen, L. E., Shnorhavorian, M., Metzger, M. L., Lockart, B., Hijiya, N., et al. (2012). Male reproductive health after childhood, adolescent, and young adult cancers: A report from the Children's oncology group. *J. Clin. Oncol.* 30, 3408–3416. doi: 10.1200/JCO.2011.38.6938

Koturbash, I., Loree, J., Kutanzi, K., Koganow, C., Pogribny, I., and Kovalchuk, O. (2008). In vivo bystander effect: cranial X-irradiation leads to elevated DNA damage, altered cellular proliferation and apoptosis, and increased p53 levels in shielded spleen. *Int. J. Radiat. Oncol.* 70, 554–562. doi: 10.1016/j.ijrobp.2007.09.039

Kucukler, S., Caglayan, C., Darendelioğlu, E., and Kandemir, F. M. (2020). Morin attenuates acrylamide-induced testicular toxicity in rats by regulating the NF-κB, Bax/Bcl-2 and PI3K/Akt/mTOR signaling pathways. *Life Sci.* 261, 118301–118308. doi: 10.1016/j.lfs.2020.118301

Lei, R., Zhao, T., Li, Q., Wang, X., Ma, H., and Deng, Y. (2015). Carbon ion irradiated neural injury induced the peripheral immune effects in vitro or in vivo. *Int. J. Mol. Sci.* 16, 28334–28346. doi: 10.3390/ijms161226109

Li, L., Mu, X., Ye, L., Ze, Y., and Hong, F. (2018). Suppression of testosterone production by nanoparticulate TiO2 is associated with ERK1/2-PKA-PKC signaling pathways in rat primary cultured Leydig cells. *Int. J. Nanomed.* 13, 5909–5924. doi: 10.2147/IJN.S175608

Lin, X., Lu, T., Xie, Z., Qin, Y., Liu, M., Xie, X., et al. (2019). Extracranial abscopal effect induced by combining immunotherapy with brain radiotherapy in a patient with lung adenocarcinoma: A case report and literature review. *Thorac. Cancer* 10, 1272–1275. doi: 10.1111/1759-7714.13048

Marjault, H., and Allemand, I. (2016). Consequences of irradiation on adult spermatogenesis: Between infertility and hereditary risk. *Mutat. Res.* 770, 340–348. doi: 10.1016/j.mrrev.2016.07.004

Mohye, E. A., Abdelrazzak, A. B., Ahmed, M. T., and El-Missiry, M. A. (2017). Radiation induced bystander effects in the spleen of cranially-irradiated rats. *Br. J. Radiol.* 90, 1–11. doi: 10.1259/bjr.20170278

Muñoz, M., Santaballa, A., Seguí, M. A., Beato, C., de la Cruz, S., Espinosa, J., et al. (2016). SEOM clinical guideline of fertility preservation and reproduction in cancer patients. *Clin. Transl. Oncol.* 18, 1229–1236. doi: 10.1007/s12094-016-1587-9

Qi, L., Li, J., Le, W., and Zhang, J. (2019). Low-dose ionizing irradiation triggers apoptosis of undifferentiated spermatogonia in vivo and in vitro. *Trans. Androl. Urol.* 8, 591–600. doi: 10.21037/tau.2019.10.16

Rakici, S. Y., Guzel, A. I., Tumkaya, L., Sevim, N. H., and Mercantepe, T. (2020). Pelvic radiation-induced testicular damage: an experimental study at 1 Gray. *Syst. Biol. Reprod. Med.* 66, 89–98. doi: 10.1080/19396368.2019.1679909

Rudat, V., Nour, A., Hammoud, M., and Abou Ghaida, S. (2017). Better compliance with hypofractionation vs. conventional fractionation in adjuvant breast cancer radiotherapy. *Strahlenther. Onkol.* 193, 375–384. doi: 10.1007/s00066-017-1115-z

Said, R. S., Mohamed, H. A., and Kamal, M. M. (2019). Coenzyme Q10 mitigates ionizing radiation-induced testicular damage in rats through inhibition of oxidative stress and mitochondria-mediated apoptotic cell death. *Toxicol. Appl. Pharmacol.* 383, 1–13. doi: 10.1016/j.taap.2019.114780

Seggelen, W. O., De Vos, F. Y., Röckmann, H., van Dijk, M. R., and Verhoeff, J. J. C. (2020). Occurrence of an abscopal radiation recall phenomenon in a glioblastoma patient treated with nivolumab and re-irradiation. *Case Rep. Oncol.* 12, 896–900. doi: 10.1159/000504698

Shahin, S., Singh, S. P., and Chaturvedi, C. M. (2018). 2.45 GHz microwave radiation induced oxidative and nitrosative stress mediated testicular apoptosis: involvement of a p53 dependent bax-caspase-3 mediated pathway. *Environ. Toxicol.* 6, 1–15. doi: 10.1002/tox.22578

Siegel, R. L., Miller, K. D., and Jemal, A. (2020). Cancer statistics, 2020. *CA Cancer J. Clin.* 70, 7–30. doi: 10.3322/caac.21590

Siva, S., MacManus, M. P., Martin, R. F., and Martin, O. A. (2015). Abscopal effects of radiation therapy: A clinical review for the radiobiologist. *Cancer Lett.* 356, 82–90. doi: 10.1016/j.canlet.2013.09.018

Tamminga, J., Koturbash, I., Baker, M., Kutanzi, K., Kathiria, P., Pogribny, I. P., et al. (2008). Paternal cranial irradiation induces distant bystander DNA damage in the germline and leads to epigenetic alterations in the offspring. *Cell Cycle* 7, 1238–1245. doi: 10.4161/cc.7.9.5806

Tu, W., Dong, C., Fu, J., Pan, Y., Kobayashi, A., Furusawa, Y., et al. (2019). Both irradiated and bystander effects link with DNA repair capacity and the linear energy transfer. *Life Sci.* 222, 228–234. doi: 10.1016/j.lfs.2019.03.013

Turnquist, C., Harris, B. T., and Harris, C. C. (2020). Radiation-induced brain injury: current concepts and therapeutic strategies targeting neuroinflammation. *Neuro Oncol. Adv.* 2, 2498–2632. doi: 10.1093/noajnl/vdaa057

Verbruggen, L. C., Kok, J. L., Teepen, J. C., Janssens, G. O., de Boer, C. M., Stalpers, L. J. A., et al. (2021). Clinical characteristics of subsequent histologically confirmed meningiomas in long-term childhood cancer survivors: A Dutch LATER study. *Eur. J. Cancer* 150, 240–249. doi: 10.1016/j.ejca.2021.03.021

Vischioni, B., Petrucci, R., and Valvo, F. (2019). Hypofractionation in prostate cancer radiotherapy: A step forward towards clinical routine. *Transl. Androl. Urol.* 8, S528–S532. doi: 10.21037/tau.2019.11.06

Walker, W. H. (2021). Regulation of mammalian spermatogenesis by miRNAs. *Semin. Cell Dev. Biol.* 5, 1–8. doi: 10.1016/j.semcdb.2021.05.009

Wang, D., Zhao, W., Liu, J., Wang, Y., Yuan, C., Zhang, F., et al. (2021). Effects of HIF-1α on spermatogenesis of varicocele rats by regulating VEGF/PI3K/Akt signaling pathway. *Reprod. Sci.* 28, 1161–1174. doi: 10.1007/s43032-020-00395-0

Wild, CP, Weiderpass, E, and Stewart, BW. (2020). *World Cancer Report: Cancer Research for Cancer Prevention*. Switzerland: World Health Organization.

Xiong, L., Yang, M., Zheng, K., Wang, Z., Gu, S., Tong, J., et al. (2020). Comparison of adult testis and ovary MicroRNA expression profiles in reeves' pond turtles (Mauremys reevesii) with temperature-dependent sex determination. *Front. Genet.* 133, 1–10. doi: 10.3389/fgene.2020.00133

Xu, Y., Sun, Y., Zhou, K., Li, T., Xie, C., Zhang, Y., et al. (2018). Cranial irradiation induces hypothalamic injury and late-onset metabolic disturbances in juvenile female rats. *Dev. Neurosci.* 40, 120–133. doi: 10.1159/000487923

Xu, Y., Sun, Y., Zhou, K., Xie, C., Li, T., Wang, Y., et al. (2020). Cranial irradiation alters neuroinflammation and neural proliferation in the pituitary gland and induces late-onset hormone deficiency. *J. Cell. Mol. Med.* 24, 14571–14582. doi: 10.1111/jcmm.16086

Yang, Y., Zhang, Z., Zhang, H., Hong, K., Tang, W., Zhao, L., et al. (2017). Effects of maternal acrolein exposure during pregnancy on testicular testosterone production in fetal rats. *Mol. Med. Rep.* 16, 491–498. doi: 10.3892/mmr.2017.6624

You, X., Chen, Q., Yuan, D., Zhang, C., and Zhao, H. (2021). Common markers of testicular Sertoli cells. *Expert. Rev. Mol. Diagn.* 16, 1–14. doi: 10.1080/14737159.2021.1924060

Zhang, X. F., Choi, Y. J., Han, J. W., Kim, E., Park, J. H., Gurunathan, S., et al. (2015). Differential nanoreprotoxicity of silver nanoparticles in male somatic cells and spermatogonial stem cells. *Int. J. Nanomed.* 10, 1335–1357. doi: 10.2147/IJN.S76062

Zhang, H., Liu, B., Zhou, Q., Zhou, G., Yuan, Z., Li, W., et al. (2006). Alleviation of pre-exposure of mouse brain with low-dose $^{12}C^{6+}$ ion or ^{60}Co gamma-ray on male reproductive endocrine damages induced by subsequent high-dose irradiation. *Int. J. Androl.* 29, 592–596. doi: 10.1111/j.1365-2605.2006.00698.x

Zhang, J., Yao, D., Song, Y., Pan, Y., Zhu, L., Bai, Y., et al. (2019). Fractionated irradiation of right thorax induces abscopal damage on testes leading to decline in fertility. *Sci. Rep. U. K* 9, 1–14. doi: 10.1038/s41598-019-51772-y

Conflict of Interest: The authors declare that this research was conducted in the absence of any commercial or financial relationships that could be construed as a potential conflict of interest.

Publisher's Note: All claims expressed in this article are solely those of the authors and do not necessarily represent those of their affiliated organizations, or those of the publisher, the editors and the reviewers. Any product that may be evaluated in this article, or claim that may be made by its manufacturer, is not guaranteed or endorsed by the publisher.

frontiers in Physiology

ORIGINAL RESEARCH
published: 04 October 2021
doi: 10.3389/fphys.2021.719346

Improving Sperm Cryopreservation With Type III Antifreeze Protein: Proteomic Profiling of Cynomolgus Macaque (*Macaca fascicularis*) Sperm

Bingbing Chen[1,2†], Shengnan Wang[2†], Briauna Marie Inglis[2†], Hao Ding[2], Angbaji Suo[2], Shuai Qiu[2], Yanchao Duan[2], Xi Li[2], Shanshan Li[2], Wendell Q. Sun[1] and Wei Si[2*]*

[1] *Institute of Biothermal Science and Technology, School of Medical Instruments and Food Engineering, University of Shanghai for Science and Technology, Shanghai, China,* [2] *State Key Laboratory of Primate Biomedical Research, Institute of Primate Translational Medicine, Kunming University of Science and Technology, Kunming, China*

OPEN ACCESS

Edited by:
Qing Chen,
Army Medical University, China

Reviewed by:
Borut Kovacic,
Maribor University Medical Centre, Slovenia
Maira Bianchi Rodrigues Alves,
University of São Paulo, Brazil

***Correspondence:**
Wendell Q. Sun
wendell.q.sun@gmail.com
Wei Si
siw@lpbr.cn

† These authors have contributed equally to this work

Specialty section:
This article was submitted to Reproduction, a section of the journal Frontiers in Physiology

Received: *02 June 2021*
Accepted: *02 September 2021*
Published: *04 October 2021*

Citation:
Chen B, Wang S, Inglis BM, Ding H, Suo A, Qiu S, Duan Y, Li X, Li S, Sun WQ and Si W (2021) Improving Sperm Cryopreservation With Type III Antifreeze Protein: Proteomic Profiling of Cynomolgus Macaque (Macaca fascicularis) Sperm. Front. Physiol. 12:719346. doi: 10.3389/fphys.2021.719346

Antifreeze protein III (AFP III) is used for the cryopreservation of germ cells in various animal species. However, the exact mechanism of its cryoprotection is largely unknown at the molecular level. In this study, we investigated the motility, acrosomal integrity, and mitochondrial membrane potential (MMP), as well as proteomic change, of cynomolgus macaque sperm after cryopreservation. Sperm motility, acrosomal integrity, and MMP were lower after cryopreservation ($p < 0.001$), but significant differences in sperm motility and MMP were observed between the AFP-treated sperm sample (Cryo+AFP) and the non-treated sample (Cryo–AFP) ($p < 0.01$). A total of 141 and 32 differentially expressed proteins were, respectively, identified in cynomolgus macaque sperm cryopreserved without and with 0.1 μg/ml AFP III compared with fresh sperm. These proteins were mainly involved in the mitochondrial production of reactive oxygen species (ROS), glutathione (GSH) synthesis, and cell apoptosis. The addition of AFP III in the sperm freezing medium resulted in significant stabilization of cellular molecular functions and/or biological processes in sperm, as illustrated by the extent of proteomic changes after freezing and thawing. According to the proteomic change of differentially expressed proteins, we hypothesized a novel molecular mechanism for cryoprotection that AFP III may reduce the release of cytochrome c and thereby reduce sperm apoptosis by modulating the production of ROS in mitochondria. The molecular mechanism that AFP III acts with sperm proteins for cellular protection against cryoinjuries needs further study.

Keywords: cynomolgus macaques, sperm, cryopreservation, antifreeze protein III, proteomic profiling

INTRODUCTION

Similarities between non-human primates and humans in physiology, genetics, and behavior make primates one of the widely used animal models in biomedical research. Primate models play essential roles in human disease research, drug development, and therapeutic strategy validation. The generation of primate models has been greatly accelerated as a result of the newly developed nuclease-based genome editing tools, such as CRISPR-Cas9 technology, and improvements of

assisted reproduction technologies in primates (David, 2016). However, the cost, space, and labor required to maintain these models as living animals have created a huge burden to the biomedical community. As a result, there is an unprecedented need for optimal protocols for the maintenance of these models as cryopreserved germplasm (sperms and embryos). In combination with the established assisted reproductive technologies, such as artificial insemination, *in vitro* fertilization, and embryo transfer, in primate, cryopreservation of sperm and embryo provides efficient and cost-effective methods to safeguard primate models.

Sperm cryopreservation is an efficient method to safeguard primate models with a single mutation. However, the current protocol is not optimal. During the freezing and thawing process, sperms are exposed to several adverse events such as cold shock, intracellular ice formation, osmotic injury, pH change, oxidative stress and disruption of adenosine triphosphate (ATP) production. The stresses can inflict considerable cryo-damages on sperms (Parks and Graham, 1992; Muldrew and McGann, 1994; Gao and Critser, 2000; Johnson et al., 2000). Consequently, cryopreserved sperms show reduced motility, compromised acrosomal integrity, and low mitochondrial membrane potential (MMP), as well as impaired fertilizing capacity (Salamon and Maxwell, 1995; Gillan et al., 1997). Previously, we have successfully cryopreserved cynomolgus macaque sperm by optimizing a freezing protocol using a chemically defined medium (SpermCryo, All-round) designed for human sperm banking. However, the cryo-survival of sperm was still low after thawing compared with the traditional egg yolk-based extenders (Yan et al., 2016; Wang et al., 2019). Therefore, continued efforts are needed to optimize this freezing protocol.

Antifreeze proteins (AFPs) have thermal hysteresis ability that can inhibit ice recrystallization through binding to the surface of ice crystals to prevent the further propagation of ice crystals during freezing and thawing, especially during thawing, which can be fatal to cells (Kim et al., 2017). AFP III, the most widely used AFP, is a globular AFP with a highly stable structure formed by hydrogen bonds and hydrophobic interactions (Salvay et al., 2010). Recently, we demonstrated that supplementation of AFP III at 0.1 μg/ml to the clinical egg yolk-free medium (named "sperm freezing medium" or SFM) significantly improved the post-thaw motility and MMP (Wang et al., 2019). AFP III has also been shown to protect germ cells from a variety of animal species upon cryopreservation. However, the mechanism of its action remains largely unknown, besides the property of AFP to alter hydrogen bond dynamics in the aqueous solution (Salvay et al., 2010). Several studies have suggested that AFPs interact with membrane proteins, which can positively affect the survival of post-thaw sperms and oocytes (Lee et al., 2015; Saeed et al., 2020). The development of proteomic tools makes it possible to investigate the proteomic alteration of sperm after cryopreservation. A previous study indicated that there were 584 identified differentially expressed proteins in cryopreserved human sperm compared with the fresh sperm specimen (Li et al., 2019). A similar phenomenon about the qualitative changes of protein profiles after sperm cryopreservation has been reported in chicken, boar, ram and human sperm (Wang et al., 2013; Vilagran et al., 2014; Cheng et al., 2015; Bogle et al., 2017; Pini et al., 2018). However, there is no study about the effects of cryopreservation on non-human primate sperm proteome so far.

Therefore, the purpose of this research was to study the proteomic profiles of cynomolgus macaque sperm cryopreserved with SFM supplemented with AFP III (Wang et al., 2019) and identify the proteins affected by AFP III during the freezing and thawing process. This research has provided useful insight into the mechanism of cryoinjuries at a molecular level and illuminated the mechanisms by which antifreeze proteins may protect sperm during cryopreservation.

MATERIALS AND METHODS

Animal and Ethics

All procedures of this study were approved by the Institutional Animal Care and Use Committee, Kunming University of Science and Technology (authorization code: LPBR201701001). A total of six healthy cynomolgus macaque males (age: from 7 to 12 years old), provided by the Yunnan Key Laboratory of Primate Biomedical Research (Kunming, China), were used as semen donors. Animals were kept in an animal room with 12:12 light–dark cycle at the room temperature of 18–26°C.

Sperm Cryopreservation

Unless otherwise stated, all reagents were purchased from Millipore Sigma (St. Louis, MO, USA). The clinical egg yolk-free medium was purchased from ORIGIO (Knardrepvej, Malov, Denmark). Semen samples were collected via penile electro-ejaculation as described previously (Gould and Mann, 1988). An aliquot was taken from each semen sample which served as fresh control (referred as Fresh group). Then, each semen sample was divided into two equal parts, which were diluted by the TALP-Hepes medium containing 0.3% BSA (TH3) with 0.2 μg/ml AFP III (the Cryo+AFP group) or without AFP III (the Cryo–AFP group), respectively. Each sample was then further diluted dropwise with SFM at a ratio of 1:1 to reach a final concentration of 1×10^8 sperm/ml and allowed to sit at room temperature for 10 min. The samples were then packed into 0.5 ml cryo-straws and sealed. The cryo-straws were cooled for 30 min by holding horizontally 0.5 cm above liquid nitrogen (LN_2) and then directly plunged into LN_2 for storage. All samples were thawed by vigorously shaking for 1 min in a 37°C water bath (Wang et al., 2019).

Sperm Functional Evaluations

The motility of fresh and/or cryopreserved sperm was evaluated using a light microscope as previously described (Wang et al., 2019). Five microliters of sperm samples was placed on a pre-warmed Makler counting chamber (Sefi Medical Instruments, Haifa, Israel). At least 200 sperms per sample were counted under a light microscope under 200× magnification, and the percentage of motile sperm was determined.

The acrosomal integrity was examined by using the Alexa Flour-488-peanut agglutinin conjugate assay (Molecular Probes, Eugene, OR, USA) (Yang et al., 2011). Briefly, fresh and frozen-thawed samples were smeared on microscope slides. The slides

were air-dried and then stained with 10 μg/ml Alexa Flour-488-peanut agglutinin solution at 37°C for 30 min under dark. After staining, the slides were washed by phosphate-buffered saline (PBS) and observed under fluorescence microscope at the excitation wavelength of 488 nm and emission wavelength of 530 nm. Sperm head with an even ample green fluorescence in acrosomal region was identified as sperm with intact acrosome, while sperm head with little or no green fluorescence in acrosome region was identified as sperm with damaged acrosome. At least 200 sperms per smear were evaluated.

Mitochondrial membrane potential was evaluated by using the JC-1 (5,5′,6,6′-tetrachloro-1,1′,3,3′-tetraethyl benzimidazole carbocyanine iodide, fluorescent cationic dye) assay kit according to the instruction of the manufacturer (Smiley et al., 1991). Each sample was incubated with JC-1 at 37°C for 20 min followed by two washes. Immediately after wash, all samples were analyzed under a fluorescence microscope with the 488 nm excitation wavelength. At least 200 sperms per sample were evaluated. Sperms showing orange or yellow fluorescence due to JC-1 aggregation in mitochondria were classified as sperms with intact mitochondria. On the contrary, sperms with damaged mitochondria have a green fluorescence since the JC-1 reagent was dispersed.

Extraction of Sperm Proteins and LC-MS/MS Analysis

Sperm samples were washed with PBS twice by centrifugation at 200 g for 5 min. Proteomic analysis was performed according to the protocols provided by PTM Biolabs Inc. (Hangzhou, Zhejiang, China). In brief, samples from each of the three experimental groups in a lysis buffer were sonicated using a high-intensity ultrasonic processor three times on ice. The samples were then centrifuged at 12,000 *g* at 4°C for 10 min for supernatant collection. Protein concentration was measured with the BCA kit following the instructions of the manufacturer.

After dissolving in water containing 0.1% formic acid, the tryptic peptides were immediately loaded onto a homemade reversed-phase analytical column (25 cm length, 75 μm i.d.). At a constant flow rate of 300 nl/min on a nanoElute UHPLC system (Bruker Daltonics), peptides were separated with a gradient from 4 to 6% acetonitrile containing 0.1% formic acid in 2 min, 6–24% in 68 min, 24–32% in 14 min and climbing to 80% in 3 min, then holding at 80% for the last 3 min. The peptides were analyzed using mass spectrometry by the timsTOF Pro (Bruker Daltonics) with 1.60 kV electrospray voltage after being subjected to a Capillary source. Fragments and precursors were analyzed at an MS/MS scan range from 100 to 1,700 m/z on the TOF detector with parallel accumulation serial fragmentation (PASEF) mode of the timsTOF Pro. Precursors were selected for fragmentation with 10 PASEF-MS/MS scans and 0–5 charge states per cycle, and dynamic exclusion for 30 s.

Selection of the Differentially Expressed Proteins

Proteins were identified by using the Maxquant search engine (v.1.6.6.0) to process the MS/MS data. The proteomics data from the mass spectrometry have been uploaded to the ProteomeXchange Consortium with the dataset identifier PXD024836 via the PRIDE partner repository. The identified differentially expressed proteins were screened by DESeq with $p < 0.05$ and p-adjusted < 0.1. We obtained three sets of differentially expressed protein spectra, namely, the Cryo–AFP vs. fresh sample, the Cryo+AFP vs. fresh sample, and Cryo+AFP vs. Cryo–AFP, through the pairwise comparison among three experimental groups.

Bioinformatics Analysis and Statistical Analysis

Gene Ontology (GO) annotation was performed using the UniProt-GOA database (http://www.ebi.ac.uk/GOA/). Identified protein IDs were first converted to UniProt IDs and then mapped to GO IDs. Some identified proteins, unannotated by UniProt-GOA database, were annotated with the GO functional of the protein via the InterProScan software based on the protein sequence alignment method. The classification of differentially expressed proteins through GO was annotated on the basis of three categories: cellular component, molecular function, and biological process.

Differentially expressed proteins were annotated with the protein pathway using the Kyoto Encyclopedia of Genes and Genomes (KEGG) database. The KEGG database description of the protein was annotated by the KEGG online service tools KAAS, and the annotation result on the KEGG pathway database was mapped by using KEGG online service tools KEGG mapper.

All data were expressed as means ± SEM. The statistical analysis of sperm MMP, acrosomal integrity, and motility was performed using ANOVA and the Fisher's least-significance difference test (SPSS 16, SPSS, Chicago, IL, USA). A p-value < 0.05 is statistically significant.

RESULTS

Effect of AFP III on the Motility, Acrosomal Integrity, and Mitochondrial Membrane Potential of Cynomolgus Macaque Sperm After Cryopreservation

The motility, acrosomal integrity, and MMP of fresh sperm samples (Fresh), frozen-thawed sperm cryopreserved with AFP III (Cryo+AFP), and frozen-thawed sperm cryopreserved without AFP III (Cryo–AFP) were shown in **Table 1**. The fluorescence images of sperm acrosomal integrity and MMP were shown in **Figure 1**. Compared with fresh sperm, cryopreservation significantly decreased the motility, acrosomal integrity, and MMP of sperm ($p < 0.001$). But sperm samples that were frozen with 0.1 μg/ml AFP III (Cryo+AFP) showed significantly higher post-thaw motility and MMP than those samples frozen without AFP III (Cryo–AFP) ($p < 0.01$). No difference in acrosomal integrity was observed in two cryopreserved groups ($p > 0.05$).

TABLE 1 | The motility, acrosomal integrity, and mitochondrial membrane potential of fresh sperm and post-thaw sperm cryopreserved with or without AFP III ($n = 6$).

Group	Sperm motility (%)	Acrosomal integrity (%)	Mitochondrial membrane potential (%)
Fresh	$83.7 \pm 2.5\%^{a}$	$94.2 \pm 1.2\%^{a}$	$80.3 \pm 1.7\%^{a}$
Cryo–AFP	$31.8 \pm 2.6\%^{c}$	$81.0 \pm 2.0\%^{b}$	$51.8 \pm 2.4\%^{c}$
Cryo+AFP	$44.3 \pm 2.8\%^{b}$	$84.3 \pm 2.1\%^{b}$	$65.2 \pm 2.9\%^{b}$

Fresh, fresh sperm; Cryo–AFP, sperm cryopreserved without AFP III; Cryo+AFP, sperm cryopreserved with AFP III.
Significant difference was indicated by different superscripts in the same column ($p < 0.05$).

Identification of Cynomolgus Macaque Sperm Proteins

To determine whether there was somatic cell contamination in semen, the semen was stained with DAPI. In this study, we did not observe any somatic cell in the semen (**Supplementary Figure 1**). A total of 2,467 proteins were identified in the cynomolgus macaque sperms. Among them, 1,848 proteins were confidently quantified in six samples. Of special interest, 159 identified differential proteins were shared by sperm samples from the Fresh, Cryo–AFP, and Cryo+AFP groups (**Figure 2**; **Supplementary Table 1**). When compared with the fresh sperm sample, cryopreservation without AFP III (Cryo–AFP) resulted in the upregulation of 65 proteins and the downregulation of 76 proteins, whereas cryopreservation with AFP III (Cryo+AFP) only resulted in the upregulation of 1 protein and the downregulation of 31 proteins. This finding has clearly demonstrated that the supplementation of 0.1 μg/ml AFP III in the sperm freezing medium significantly helps the stabilization of cellular molecular functions or biological processes in sperms, as illustrated by the extent of proteomic changes after freezing and thawing. The further comparison between sperm samples cryopreserved with or without AFP III shows that the supplementation of APF III in the sperm freezing medium leads to the relative upregulation of 1 protein and the relative downregulation of 3 proteins as shown in **Figure 2A**. Based on the Venn diagram analysis of sperm differential proteins exhibited in **Figure 2B**, there were 18 differential proteins in common for both Cryo–AFP and Cryo+AFP groups when compared with the Fresh group, and 137 differential proteins different between Cryo–AFP vs. Fresh and Cryo+AFP vs. Fresh groups.

According to the UniProtKB database, 159 differential proteins with known roles in sperm function were used to further evaluate the effect of cryopreservation on cynomolgus macaque sperm function. The functions of selected sperm differential proteins including flagellated sperm motility, fertilization, mitochondrial function, heat/oxidative stress, apoptosis, metabolic process, enzymatic activity, immune response, ion binding, and others were listed in **Supplementary Table 1**.

Gene Ontology Functional Analysis

The identified differentially expressed proteins involving in biological processes, cellular components, and molecular function in GO terms between the Fresh control, Cryo–AFP and Cryo+AFP groups were shown in **Figure 3**. In **Figure 3A**, biological processes of differential proteins between Fresh and Cryo–AFP groups were primarily related to organonitrogen compound metabolic process (GO:1901564, 11 proteins), phosphorus metabolic process (GO:0006793, 8 proteins), phosphate-containing compound metabolic process (GO:0006796, 10 proteins), proteolysis (GO:0006508, 6 proteins), small molecule metabolic process (GO:0044281, 6 proteins), phosphorylation (GO:0016310, 6 proteins), regulation of protein metabolic process (GO:0051246, 6 proteins), oxidation–reduction process (GO:0055114, 5 proteins), organic acid metabolic process (GO:0006082, 5 proteins), and mitochondrion organization (GO:0007005, 4 proteins). Cellular components of differential proteins between Fresh and Cryo–AFP groups were enriched in the membrane-bound organelle (GO:0043227, 22 proteins), organelle (GO:0043226, 22 proteins), intracellular region (GO:0005622, 19 proteins), extracellular region (GO:0005576, 18 proteins), intracellular organelle (GO:0043229, 16 proteins), vesicle (GO:0031982, 12 proteins), extracellular exosome (GO:0070062, 10 proteins), extracellular vesicle (GO:1903561, 10 proteins), cytosol (GO:0005829, 9 proteins), and intracellular organelle lumen (GO:0070013, 9 proteins). The molecular function of differential proteins between Fresh and Cryo–AFP groups was enriched in catalytic activity (GO:0003824, 15 proteins), carbohydrate derivative binding (GO:0097367, 10 proteins), hydrolase activity (GO:0016787, 10 proteins), cation binding (GO:0043169, 9 proteins), adenyl ribonucleotide binding (GO:0032559, 6 proteins), nucleotide binding (GO:0000166, 6 proteins), nucleoside phosphate binding (GO:1901265, 6 proteins), ATP binding (GO:0005524, 5 proteins), cofactor binding (GO:0048037, 4 proteins), and endopeptidase activity (GO:0004175, 4 proteins).

In **Figure 3B**, biological processes of the identified differential proteins in the GO terms were basically catabolic process (GO:0009056, 5 proteins), cellular process involved in reproduction in multicellular organism (GO:0022412, 3 proteins), multi-organism reproductive process (GO:0044703, 3 proteins), and locomotion (GO:0040011, 3 proteins) between Fresh and Cryo+AFP groups. The identified differential proteins-associated cellular localizations were enriched in the extracellular region (GO:0005576, 7 proteins) and extracellular vesicle (GO:1903561, 5 proteins) between Fresh and Cryo+AFP groups.

In **Figure 3C**, biological processes of the identified differential proteins between Cryo–AFP and Cryo+AFP groups were involved in the cellular component assembly (GO:0022607, 2 proteins), microtubule cytoskeleton organization involved in mitosis (GO:1902850, 1 proteins), negative regulation of organelle assembly (GO:1902116, 1 protein), spindle localization (GO:0051653, 1 protein), positive regulation

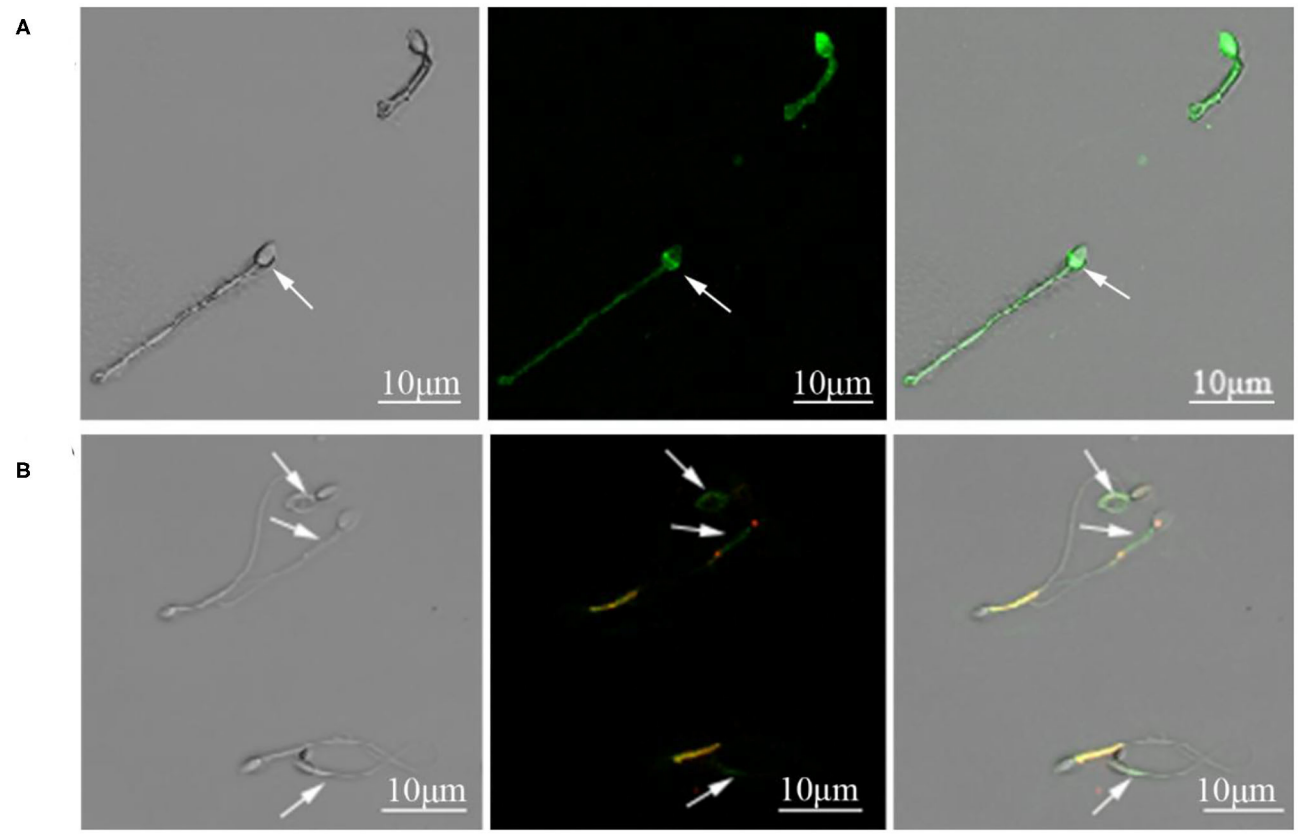

FIGURE 1 | (A) Cynomolgus macaque sperm with intact and damaged acrosomes. The arrow indicated a sperm with damaged acrosome. **(B)** Sperm with intact and damaged mitochondria function. The arrows indicated sperm with compromised mitochondrial membrane potential.

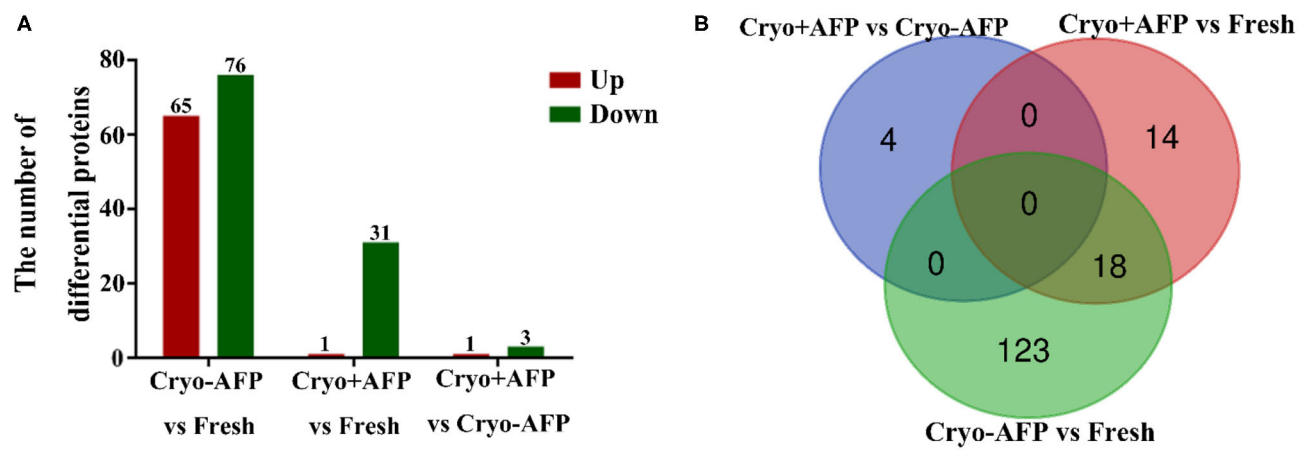

FIGURE 2 | Identification of differentially expressed proteins in cynomolgus macaque sperm. **(A)** The number of differentially identified cynomolgus macaque sperm proteins between Fresh and Cryo–AFP, between Fresh and Cryo+AFP, and between Cryo–AFP and Cryo+AFP groups. The upregulated and downregulated proteins were represented by the red and green bars, respectively. **(B)** The differences in identified differentially expressed proteins as shown by the Venn diagram between Fresh, Cryo–AFP, and Cryo+AFP groups.

of translation (GO:0045727, 1 protein), ATP synthesis-coupled electron transport (GO:0042773, 1 protein), negative regulation of cell projection organization (GO:0031345, 1 protein), positive regulation of cellular amide metabolic process (GO:0034250, 1 protein), regulation of translation (GO:0006417, 1 protein), and establishment of localization in

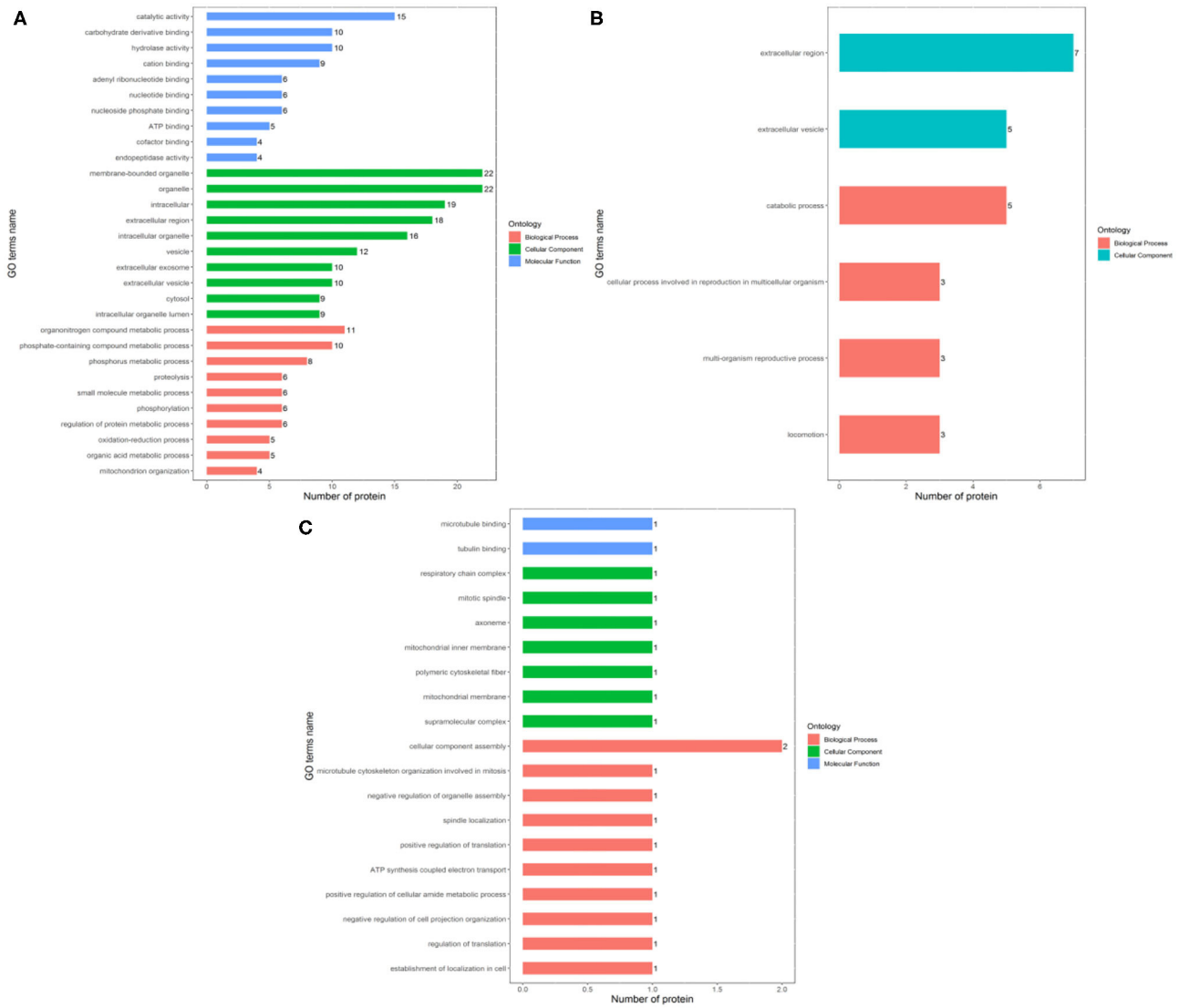

FIGURE 3 | Biological process, cellular component, and molecular function of differentially expressed proteins. **(A)** between Fresh and Cryo–AFP groups; **(B)** between Fresh and Cryo+AFP groups; **(C)** between Cryo–AFP and Cryo+AFP groups. The value represents the number of differential proteins.

the cell (GO:0051649, 1 protein). The identified differential proteins-associated cellular localizations were enriched in respiratory chain complex (GO:0098803, 1 protein), mitotic spindle (GO:0072686, 1 protein), axoneme (GO:0005930,1 protein), mitochondrial inner membrane (GO:0005743,1 proteins), polymeric cytoskeletal fiber (GO:0099513, 1 protein), mitochondrial membrane (GO:0031966, 1 protein), and supramolecular complex (GO:0099080, 1 protein). The molecular function of the identified differential proteins between Cryo–AFP and Cryo+AFP groups is enriched in microtubule binding (GO:0008017, 1 protein) and tubulin binding (GO:0015631, 1 protein).

Enrichment-Based Clustering

The enrichment analysis-based clustering of the identified differential proteins from Fresh, Cryo–AFP, and Cryo+AFP groups was exhibited in **Figure 4**. The statistical analysis of the KEGG pathway of the identified differential proteins is enriched in 2-oxocarboxylic acid metabolism, alanine, aspartate, and glutamate metabolism, citrate cycle (TCA cycle), selenocompound metabolism, thiamine metabolism, oxidative phosphorylation, Parkinson's disease, pyruvate metabolism, non-alcoholic fatty liver disease (NAFLD), cysteine and methionine metabolism, glutathione metabolism, biosynthesis of amino acids, carbon metabolism, Alzheimer disease, Huntington disease, glycolysis/gluconeogenesis, central carbon metabolism in cancer, retrograde endocannabinoid signaling, thermogenesis and metabolic pathways between the Fresh and Cryo–AFP groups; and thermogenesis, Huntington disease, Alzheimer disease, non-alcoholic fatty liver disease (NAFLD), Parkinson's disease, oxidative phosphorylation, and cardiac muscle contraction between the Cryo–AFP and Cryo+AFP

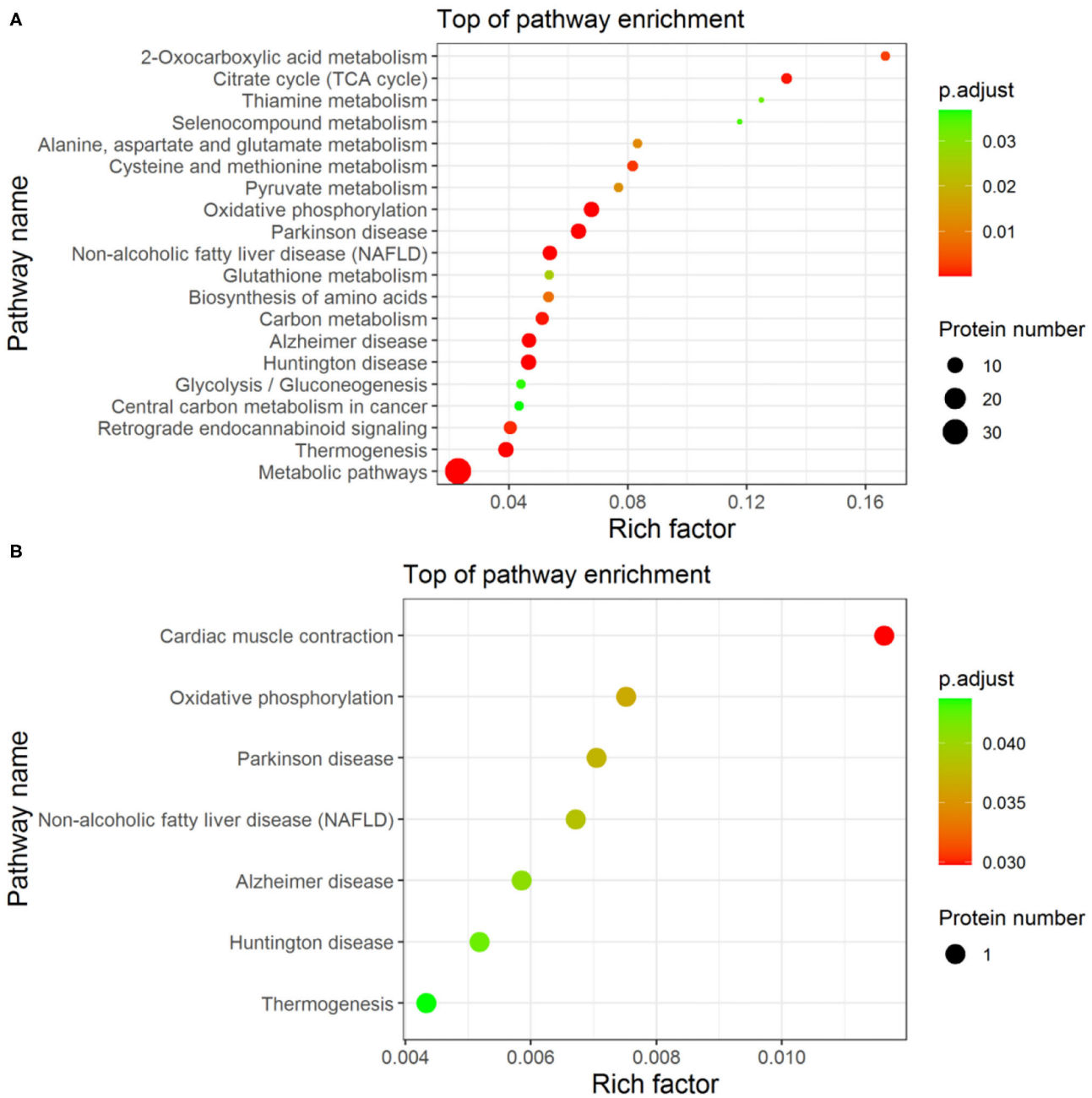

FIGURE 4 | The enrichment analysis-based clustering of the KEGG pathway. **(A)** between Fresh and Cryo–AFP groups; **(B)** between Cryo–AFP and Cryo+AFP groups.

groups. Differential proteins between the Fresh and Cryo+AFP groups were not enriched into any pathways.

DISCUSSION

In this study, we investigated the effect of AFP III on cynomolgus macaque sperm cryopreservation. The results demonstrated that sperm motility, acrosomal integrity, and MMP were decreased significantly after the freezing and thawing process. The addition of 0.1 μg/ml of AFP III into the sperm freezing medium reduced sperm damage and improved the motility and MMP of sperm after cryopreservation. Proteomic analysis showed that cryopreservation resulted in the alteration of proteomic patterns in cynomolgus macaque sperm, especially those proteins associated with flagellated sperm motility, fertilization, mitochondrial function, heat/oxidative stress, apoptosis, metabolic process, enzymatic activity, immune response, ion binding, etc. The addition of AFP III in the sperm

freezing medium protects sperm during cryopreservation by stabilizing mitochondrial function, reducing ROS production, and protecting sperm from apoptosis as evidenced by relative differential proteins by proteomic analysis.

A total of 159 differentially expressed proteins involving in sperm functions were identified after sperm cryopreservation among Fresh, Cryo–AFP, and Cryo+AFP groups. Compared with the Fresh group, 18 proteins were downregulated in both Cryo–AFP and Cryo+AFP groups. Those proteins were associated with fertilization, apoptosis, metabolic process and enzymatic activity, which likely pinpoints the main cause of the decreased sperm motility and fertility after cryopreservation (Xu et al., 2020). For example, the levels of zona pellucida binding protein (G7P1S4, ZPBP), zona pellucida binding protein 2 (A0A2K5U0C3, ZPBP2), acrosin-binding protein (A0A2K5UCT2), and phosphatidylethanolamine-binding protein 4 (A0A2K5X0P4, PEBP4) were decreased in both Cryo–AFP and Cryo+AFP groups. The loss of ZPBP, ZPBP2, and acrosin-binding protein of cryopreserved sperm could result in the deficiency to penetrate zona pellucida and initiation of acrosome reaction (Lin et al., 2007). It has been reported that the compromised acrosome reaction contributes to the subfertility of the acrosin-binding protein-deficient mice (Nagashima et al., 2019). Furthermore, the inhibition of endogenous PEBP4 expression in MCF-7 cells was found to be associated with the decreased expression of anti-apoptotic proteins such as BclXL and Bcl-2 and the increased expression of the pro-apoptotic proteins p21CIP/WAF, p53, and Bax (Wang et al., 2005). The decreased level of PEBP4 in cryopreserved sperm is likely correlated with the tendency of sperm apoptosis.

Also compared with the Fresh group, there were additional 137 differential proteins that were found either in the Cryo–AFP group (123 proteins) or in the Cryo+AFP group (14 proteins). Again, those proteins were largely associated with flagellated sperm motility, fertilization, mitochondrial function, heat/oxidative stress, apoptosis, metabolic process, enzymatic activity, immune response, and ion binding. Clearly, the changes in the proteomic patterns after freezing and thawing would have a profound negative impact on sperm motility and fertility, and the presence of AFP III in the sperm freezing medium could reduce this impact. The proteomic analysis shows that the levels of proteins related to ROS generation in mitochondrial complex, such as NDUFS8, NDUFB6, CYC1 and OCIAD1, were increased in the Cryo–AFP group when compared with Fresh group, but their levels were relatively unchanged in the Cryo+AFP group, indicating that AFP III could reduce the ROS production in mitochondrial complex I upon cryopreservation. NADH dehydrogenase (ubiquinone) iron–sulfur protein 8 (A0A2K5U649, NDUFS8) is a mitochondrial Fe–S protein in complex I (a major contributor of ROS generation) located in the inner membrane of mitochondria and participates in the electron transport chain. The upregulation of NDUFS8 increases the mitochondrial ROS production (Cheng et al., 2013). NADH dehydrogenase (ubiquinone) 1 beta subcomplex subunit 6 (A0A2K5VNL0, NDUFB6) is an accessory subunit of the multi-subunit NADH in complex I associated with ROS production, ATP generation, and cell apoptosis in the mitochondrial inner membrane. The increased expression of NDUFB6 is accompanied by the increase of ROS (Wang et al., 2020). It has been proposed that the increased ROS production during cryopreservation could lead to DNA modification, lipid peroxidation, and/or protein damages, which in turn induces cell apoptosis because of the mitochondrial cytochrome c release and the disruption of cellular homeostasis (Stokman et al., 2017). Cytochrome c 1 (A0A2K5WMQ0, CYC1), an electron carrier between complex III and complex IV in mitochondrial respiration chain located outside the mitochondrial inner membrane (Xia et al., 2002; Zhao et al., 2020), binds to APAF-1 after releasing into cytoplasm, activates pro-caspase 9, and triggers an enzymatic cascade leading to cell death (Santucci et al., 2019). Complex I activity is correlated negatively with OCIA domain-containing protein (A0A2K5VJ27, OCIAD1) expression (Shetty et al., 2018). We hypothesized that the presence of AFP III in the sperm freezing medium can reduce mitochondrial ROS production and sperm apoptosis, which may explain the higher sperm motility and MMP in the Cryo+AFP group than the Cryo–AFP group.

Another major group of differential proteins between the Fresh and Cryo–AFP and Fresh and Cryo+AFP groups is the GSH synthesis-related proteins, including gamma-ECS, lactoylglutathione lyase, and carbonyl reductase 1. GSH ensures the normal function of cell apoptosis by maintaining redox homeostasis and resisting oxidant aggression. This study detects the downregulation of gamma-ECS (A0A2K5UV75, GCLC), lactoylglutathione lyase (Q4R5F2, GLO1), and carbonyl reductase 1 (Q8MI29, CBR1) in the Cryo–AFP group when compared with the Fresh group, but not in the Cryo+AFP group. GCLC participates in the first rate-limiting reaction in GSH synthesis and feedback inhibited by GSH itself to the regulation of cellular GSH concentration (Griffith and Meister, 1979). The reduced GCLC expression increased the methylglyoxal-induced pheochromocytoma cells apoptosis (Kimura et al., 2009). By converting the spontaneously formed MGO-GSH hemithioacetal to the thioester S-D-lactoylglutathione, GLO1 acts as the rate-limiting enzyme in the primary detoxification step. GSH concentration is directly proportional to GLO1 activity. The impaired GLO1 activity is associated with the decreased GSH concentration (Sousa Silva et al., 2013; Nigro et al., 2017) and with the induced apoptosis of acute myeloid leukemia cells (Chen et al., 2015). CBR1 inactivates cellular membrane-derived lipid aldehydes to protect cells from oxidative stress and cell apoptosis. The study has found that lipid peroxidation products and oxidative stress markers were significantly lower in cells overexpressing CBR1. In contrast, the level of oxidative stress protein expressed by CBR1 knockout cells was increased (Kwon et al., 2019). Therefore, our results also suggest that AFP III could reduce ROS production by protecting the GSH synthesis-related proteins during freezing and thawing.

Furthermore, the downregulation of a non-specific serine/threonine protein kinase (A0A2K5UYV4, STK39) and a stress-induced protein (Q4R8N7, STIP1) and the upregulation of a non-specific T-complex protein 1 subunit (Q4R5J0, CCT8) were observed only in the Cryo–AFP group, but not in Cryo+AFP group after sperm cryopreservation in

this study. The suppression of STK39 significantly induces cell apoptosis in 786-0 and ACHN cells. STK39 knockdown reduces the anti-apoptosis protein Bcl-2 and increases the apoptosis-promoting protein Bax (Zhao et al., 2018). The downregulation of STIP1 increases cell apoptosis of glioma cells (Yin et al., 2019). The upregulation of CCT8 was reported to be connected to the neuronal apoptosis in adult rats with traumatic brain injury (Robles et al., 2015). Again, these findings appear to suggest a role of AFP III in preventing the apoptosis of sperm after freezing and thawing.

Of particular interest are the four differential proteins between the Cryo–AFP and Cryo+AFP groups (**Figure 2B**). The upregulated one was the ubiquinol-cytochrome-c reductase complex assembly factor 1 (A0A2K5WI39, UQCC1), whereas the downregulated ones were the cytochrome c oxidase subunit 3 (C3W4Z1, COX3), the transmembrane helical component TEX51 (A0A2K5X818), and the microtubule-associated protein (A0A2K5UU31, MAP4). Those proteins are associated with mitochondrial electron and redox function, membrane assemblies, and cytoskeleton organization. UQCC1, the complex III assembly factors, participates in the cytochrome b biogenesis (Tucker et al., 2013). COX3, the catalytic core of cytochrome c oxidase, accepts electrons from cytochrome c and subsequently transfers them to molecular oxygen to generate water (Little et al., 2018). Some previous studies have shown that cryopreservation alters the composition of sperm proteins (Wang et al., 2013; Vilagran et al., 2014; Cheng et al., 2015; Bogle et al., 2017; Pini et al., 2018; Li et al., 2019). During the freezing and thawing process, the loss of intracellular components due to damaged membranes may contribute to the considerable loss of some sperm proteins, whereas the increases of some sperm proteins can be due to secondary or tertiary structure transformations or degradation of proteins (Bogle et al., 2017). This study demonstrates that sperm cryopreservation changes the levels of some proteins in both the Cryo–AFP and Cryo+AFP groups, which results in a decrease in the number of differential proteins between the two groups. For example, the levels of 18 decreased proteins in both Cryo–AFP and Cryo+AFP groups were similar (**Supplementary Table 1**).

Previous studies demonstrate that AFP III reduces the damage of cellular structures by ice crystallization during freezing and thawing (Salvay et al., 2010; Saeed et al., 2020). AFP III can also stabilize the cell membrane, thereby reducing the sublethal damage during sperm cryopreservation (Robles et al., 2019). This study has extended our understanding of the cryoprotective role of AFP III by demonstrating that AFP III can maintain mitochondrial function and reduce ROS production and sperm apoptosis during the freezing and thawing process. The finding is consistent with the findings that the addition of AFP III successfully improved sperm motility and mitochondrial membrane potential. Sperm cryopreservation increases the production of ROS, such as superoxide and hydrogen peroxide, in many species including human and rhesus macaque (McCarthy and Meyers, 2011; Lee et al., 2015; Saeed et al., 2020). In another unpublished paper, we demonstrated that sperm cryopreservation could induce ROS production in cynomolgus monkey. AFP III has been proved to have an anti-peroxide effect in sperm cryopreservation. For example, human sperm cryopreservation with AFP III improved motility and total antioxidant capacity (TAC) levels. Meanwhile, AFP III decreased the percentage of DNA fragmentation and ROS level (Kim et al., 2017). Furthermore, ROS level was decreased in mouse oocytes vitrified with AFP III (Salvay et al., 2010). Another study also demonstrated that reduced glutathione/oxidative glutathione (GSH/GSSG) and total antioxidant capacity (TAC) were higher in bull semen cryopreservation with AFP III compared with the control group (Jang et al., 2020). In our study, the results also suggested that AFP III could protect the proteins associated with ROS production in mitochondria and GSH synthesis during sperm freezing and thawing. The proteomic evidence in this study is consistent with previous studies, suggesting the anti-peroxidative effect of AFP III. Therefore, we hypothesized that AFP III may reduce cryo-damages of sperm structures, as well as the release of cytochrome c, thereby reducing sperm apoptosis by suppressing the mitochondrial ROS production and enhancing the antioxidative function.

CONCLUSION

The addition of AFP III in the sperm freezing medium protects sperm during cryopreservation. The proteomic analysis has identified 159 proteins with known functions that are susceptible to sperm cryopreservation. The addition of 0.1 μg/ml of AFP III in the sperm freezing medium can change the outcome, significantly reducing the number of differential proteins in cryopreserved sperm. According to the biological processes and molecular functions of differentially expressed proteins, we proposed a new molecular mechanism for AFP III cryoprotection that AFP III may reduce sperm apoptosis by reducing the release of cytochrome c and the mitochondrial ROS production. The findings provide insight into the AFP III cryoprotection mechanism and a useful hint for a new strategy of developing and optimizing sperm cryopreservation. However, the mechanism of AFP III modulating the proteomic profiles upon cryopreservation needs to be studied further.

DATA AVAILABILITY STATEMENT

The datasets presented in this study can be found in online repositories. The names of the repository/repositories and accession number(s) can be found in the article/**Supplementary Material**.

ETHICS STATEMENT

The animal study was reviewed and approved by the Yunnan Key Laboratory of Primate Biomedical Research (Kunming, China) and all procedures were approved by the Institutional Animal Care and Use Committee, Kunming University of Science and Technology (authorization code: LPBR201701001), and were executed according to the Guide for Care and Use of Laboratory Animals (Commission on Life Sciences, the National Research Council, Washington, D.C.).

AUTHOR CONTRIBUTIONS

WS and BC conceptualized the study. BC, HD, and AS contributed to the formal analysis. BC, WQS, and WS contributed to the writing (review and editing). BC, SW, and BI contributed to the investigation. SQ, YD, Chen Adar, Ido Braslavsky, XL, and SL contributed to the resources. All authors have read and agreed to the published version of the manuscript.

FUNDING

This research was supported by grants from the National Key Research and Development Program of China (Grant Number: 2018YFA0801403) and Yunnan Fundamental Research Projects (Grant Number: 2018FA020).

ACKNOWLEDGMENTS

We thank Chen Adar and Ido Braslavsky for providing us with antifreeze protein III.

SUPPLEMENTARY MATERIAL

The Supplementary Material for this article can be found online at: https://www.frontiersin.org/articles/10.3389/fphys.2021.719346/full#supplementary-material

Supplementary Figure 1 | Cynomolgus macaque semen was stained with DAPI. No somatic cells were observed in the semen.

REFERENCES

Bogle, O. A., Kumar, K., Attardo-Parrinello, C., Lewis, S. E. M., Estanyol, J. M., Ballescà J. L., et al. (2017). Identification of protein changes in human spermatozoa throughout the cryopreservation process. *Andrology* 5, 10–22. doi: 10.1111/andr.12279

Chen, C. C., Wu, M. L., Ho, C. T., and Huang, T. C. (2015). Blockade of the Ras/Raf/ERK and Ras/PI3K/Akt pathways by monacolin K reduces the expression of GLO1 and Induces apoptosis in U937 cells. *J. Agric. Food Chem.* 63, 1186–1195. doi: 10.1021/jf505275s

Cheng, C. W., Kuo, C. Y., Fan, C. C., Fang, W. C., Jiang, S. S., Lo, Y. K., et al. (2013). Overexpression of Lon contributes to survival and aggressive phenotype of cancer cells through mitochondrial complex I-mediated generation of reactive oxygen species. *Cell Death Dis.* 4:e681. doi: 10.1038/cddis.2013.204

Cheng, C. Y., Chen, P. R., Chen, C. J., Wang, S. H., Chen, C. F., Lee, Y. P., et al. (2015). Differential protein expression in chicken spermatozoa before and after freezing–thawing treatment. *Anim. Reprod. Sci.* 152, 99–107. doi: 10.1016/j.anireprosci.2014.11.011

David, C. (2016). Monkey kingdom, *Nature* 532, 300–302. doi: 10.1038/532300a

Gao, D., and Critser, J. K. (2000). Mechanisms of cryoinjury in living cells. *ILAR J.* 41, 187–196. doi: 10.1093/ilar.41.4.187

Gillan, L., Evans, G., and Maxwell, W. M. (1997). Capacitation status and fertility of fresh and frozen–thawed ram spermatozoa. *Reprod. Fertil. Dev.* 9, 481–487. doi: 10.1071/R96046

Gould, K. G., and Mann, D. R. (1988). Comparison of electrostimulation methods for semen recovery in the rhesus monkey (*Macaca mulatta*). *J. Med. Primatol.* 17, 95–103. doi: 10.1111/j.1600-0684.1988.tb00366.x

Griffith, O. W., and Meister, A. (1979). Potent and specific inhibition of glutathione synthesis by buthionine sulfoximine (S-n-butyl homocysteine sulfoximine). *J. Biol. Chem.* 254, 7558–7560. doi: 10.1016/S0021-9258(18)35980-5

Jang, H., Kwon, H. J., Sun, W. S., Hwang, S., Hwang, I. S., Kim, S., et al. (2020). Effects of Leucosporidium-derived ice-binding protein (LeIBP) on bull semen cryopreservation. *Vet. Med. Sci.* 6, 447-453. doi: 10.1002/vms3.269

Johnson, L. A., Weitze, K. F., Fiser, P., and Maxwell, W. M. (2000). Storage of boar semen. *Anim. Reprod. Sci.* 62, 0–172. doi: 10.1016/S0378-4320(00)00157-3

Kim, H. J., Lee, J. H., Hur, Y. B., Lee, C. W., Park, S. H., and Koo, B. W. (2017). Marine antifreeze proteins: structure. function, and application to cryopreservation as a potential cryoprotectant. *Mar. Drugs.* 15:27. doi: 10.3390/md15020027

Kimura, R., Okouchi, M., Fujioka, H., Ichiyanagi, A., Ryuge, F., Mizuno, T., et al. (2009). Glucagon-like peptide-1 (GLP-1) protects against methylglyoxal-induced PC12 cell apoptosis through the PI3K/Akt/mTOR/GCLc/redox signaling pathway. *Neuroscience* 162, 1212–1219. doi: 10.1016/j.neuroscience.2009.05.025

Kwon, J. H., Lee, J., Kim, J., Kirchner, V. A., Jo, Y. H., Miura, T., et al. (2019). Upregulation of carbonyl reductase 1 by Nrf2 as a potential therapeutic intervention for ischemia/reperfusion injury during liver transplantation. *Mol. Cells* 42, 672–685. doi: 10.1016/j.hpb.2019.10.2338

Lee, H. H., Lee, H. J., Kim, H. J., Lee, J. H., Ko, Y., Kim, S. M., et al. (2015). Effects of antifreeze proteins on the vitrification of mouse oocytes: comparison of three different antifreeze proteins. *Hum. Reprod.* 30, 2110–2119. doi: 10.1093/humrep/dev170

Li, S., Ao, L., Yan, Y., Jiang, J., Chen, B., Duan, Y., et al. (2019). Differential motility parameters and identification of proteomic profiles of human sperm cryopreserved with cryostraw and cryovial. *Clin. Proteom.* 16:24. doi: 10.1186/s12014-019-9244-2

Lin, Y. N., Roy, A., Yan, W., Burns, K. H., and Matzuk, M. M. (2007). Loss of zona pellucida binding proteins in the acrosomal matrix disrupts acrosome biogenesis and sperm morphogenesis. *Mol. Cell. Biol.* 27, 6794–6805. doi: 10.1128/MCB.01029-07

Little, A. G., Lau, G., Mathers, K. E., Leary, S. C., and Moyes, C. D. (2018). Comparative biochemistry of cytochrome c oxidase in animals. *Comp. Biochem. Physiol. B. Biochem. Mol. Biol.* 224, 170–184. doi: 10.1016/j.cbpb.2017.11.005

McCarthy, M. J., and Meyers, S. A. (2011). Antioxidant treatment in the absence of exogenous lipids and proteins protects rhesus macaque sperm from cryopreservation-induced cell membrane damage. *Theriogenology* 76, 168–176. doi: 10.1016/j.theriogenology.2011.01.029

Muldrew, K., and McGann, L. E. (1994). The osmotic rupture hypothesis of intracellular freezing injury. *Biophys. J.* 66, 532–541. doi: 10.1016/S0006-3495(94)80806-9

Nagashima, K., Usui, T., and Baba, T. (2019). Behavior of ACRBP-deficient mouse sperm in the female reproductive tract. *J. Reprod. Dev.* 65, 97–102. doi: 10.1262/jrd.2018-137

Nigro, C., Leone, A., Raciti, G. A., Longo, M., Mirra, P., Formisano, P., et al. (2017). Methylglyoxal-glyoxalase 1 balance: the root of vascular damage. *Int. J. Mol. Sci.* 18:188. doi: 10.3390/ijms18010188

Parks, J. E., and Graham, J. K. (1992). Effects of cryopreservation procedures on sperm membranes. *Theriogenology* 38, 209–222. doi: 10.1016/0093-691X(92)90231-F

Pini, T., Rickard, J. P., Leahy, T., Crossett, B., Druart, X., and de Graaf, S. P. (2018). Cryopreservation and egg yolk medium alter the proteome of ram spermatozoa. *J. Proteom.* 181, 73–82. doi: 10.1016/j.jprot.2018.04.001

Robles, V., Valcarce, D. G., and Riesco, M. F. (2015). Up-regulation of CCT8 related to neuronal apoptosis after traumatic brain injury in adult rats. *Neurochem. Res.* 40, 1882–1891. doi: 10.1007/s11064-015-1683-1

Robles, V., Valcarce, D. G., and Riesco, M. F. (2019). The use of antifreeze proteins in the cryopreservation of gametes and embryos. *Biomolecules* 9:181. doi: 10.3390/biom9050181

Saeed, Z., Abdolhossein, S., Bita, E., and Marjan, S. (2020). A novel approach for human sperm cryopreservation with AFPIII. *Reprod. Biol.* 20, 169–174. doi: 10.1016/j.repbio.2020.03.006

Salamon, S., and Maxwell, W. M. (1995). Frozen storage of ram semen I. Processing. freezing, thawing and fertility after cervical insemination. *Anim. Reprod. Sci*. 37, 185–249. doi: 10.1016/0378-4320(94)01327-I

Salvay, A. G., Gabel, F., Pucci, B., Santos, J., Howard, E. I., and Ebel, C. (2010). Structure and interactions of fish type III antifreeze protein in solution. *Biophys. J*. 99, 609–618. doi: 10.1016/j.bpj.2010.04.030

Santucci, R., Sinibaldi, F., Cozza, P., Polticelli, F., and Fiorucci, L. (2019). Cytochrome c: an extreme multifunctional protein with a key role in cell fate. *Int. J. Biol. Macromol*. 136, 1237–1246. doi: 10.1016/j.ijbiomac.2019.06.180

Shetty, D. K., Kalamkar, K. P., and Inamdar, M. S. (2018). OCIAD1 controls electron transport chain complex I activity to regulate energy metabolism in human pluripotent stem cells. *Stem Cell Reports*. 11, 128–141. doi: 10.1016/j.stemcr.2018.05.015

Smiley, S. T., Reers, M., Mottola-Hartshorn, C., Lin, M., Chen, A., Smith, T. W., et al. (1991). Intracellular heterogeneity in mitochondrial membrane potentials revealed by a J-aggregate-forming lipophilic cation JC-1. *Proc. Natl. Acad. Sci. U. S. A*. 88, 3671–3675. doi: 10.1073/pnas.88.9.3671

Sousa Silva, M., Gomes, R. A., Ferreira, A. E., Ponces Freire, A., and Cordeiro, C. (2013). The glyoxalase pathway: the first hundred years... and beyond. *Biochem. J*. 453, 1–15. doi: 10.1042/BJ20121743

Stokman, G., Kors, L., Bakker, P. J., Rampanelli, E., Claessen, N., Teske, G. J. D., et al. (2017). NLRX1 dampens oxidative stress and apoptosis in tissue injury via control of mitochondrial activity. *J. Exp. Med*. 214, 2405–2420. doi: 10.1084/jem.20161031

Tucker, E. J., Wanschers, B. F., Szklarczyk, R., Mountford, H. S., Wijeyeratne, X. W., van den Brand, M. A., et al. (2013). Mutations in the UQCC1-interacting protein. UQCC2, cause human complex III deficiency associated with perturbed cytochrome b protein expression. *PLoS Genet*. 9:e1004034. doi: 10.1371/journal.pgen.1004034

Vilagran, I., Yeste, M., Sancho, S., Casas, I., Rivera del Álamo, M. M., and Bonet, S. (2014). Relationship of sperm small heat-shock protein 10 and voltage-dependent anion channel 2 with semen freezability in boars. *Theriogenology* 82, 418–426. doi: 10.1016/j.theriogenology.2014.04.023

Wang, G., Guo, Y., Zhou, T., Shi, X., Yu, J., Yang, Y., et al. (2013). In-depth proteomic analysis of the human sperm reveals complex protein compositions. *J. Proteom*. 79, 114–122. doi: 10.1016/j.jprot.2012.12.008

Wang, N., Maskomani, S., Meenashisundaram, G., Fuh, J., Dheen, S., and Anantharajan, S. (2020). A study of Titanium and Magnesium particle-induced oxidative stress and toxicity to human osteoblasts. *Mater. Sci. Eng. C Mater. Biol. Appl*. 117:111285. doi: 10.1016/j.msec.2020.111285

Wang, S., Duan, Y., Yan, Y., Adar, C., Braslavsky, I., Chen, B., et al. (2019). Improvement of sperm cryo-survival of Cynomolgus macaque (*Macaca fascicularis*) by commercial egg-yolk-free freezing medium with type III antifreeze protein. *Anim. Reprod. Sci*. 210:106177. doi: 10.1016/j.anireprosci.2019.106177

Wang, X., Li, N., Li, H., Liu, B., Qiu, J., Chen, T., et al. (2005). Silencing of human phosphatidylethanolamine-binding protein 4 sensitizes breast cancer cells to tumor necrosis factor-alpha-induced apoptosis and cell growth arrest. *Clin. Cancer Res*. 11, 7545–7553. doi: 10.1158/1078-0432.CCR-05-0879

Xia, T., Jiang, C., Li, L., Wu, C., Chen, Q., and Liu, S. S. (2002). A study on permeability transition pore opening and cytochrome c release from mitochondria induced by caspase-3 *in vitro*. *FEBS Lett*. 510, 62–66. doi: 10.1016/S0014-5793(01)03228-8

Xu, D., Wu, L., Yang, L., Liu, D., Chen, H., Geng, G., et al. (2020). Rutin protects boar sperm from cryodamage via enhancing the antioxidative defense. *Anim. Sci. J*. 91:e13328. doi: 10.1111/asj.13328

Yan, Y., Ao, L., Wang, H., Duan, Y., Chang, S., Chen, B., et al. (2016). Cryopreservation of *Cynomolgus macaque* (*Macaca fascicularis*) sperm by using a commercial egg-yolk-free freezing medium. *J. Am. Assoc. Lab. Anim. Sci*. 55, 744–748.

Yang, S., Ping, S., Si, W., He, X., Wang, X., Lu, Y., et al. (2011). Optimization of ethylene glycol concentrations. freezing rates and holding times in liquid nitrogen vapor for cryopreservation of rhesus macaque (*Macaca mulatta*) sperm. *J. Vet. Med. Sci*. 73, 717–723. doi: 10.1292/jvms.10-0398

Yin, H., Deng, Z., Li, X., Li, Y., Yin, W., Zhao, G., et al. (2019). Down-regulation of STIP1 regulate apoptosis and invasion of glioma cells via TRAP1/AKT signaling pathway. *Cancer Genet*. 237, 1–9. doi: 10.1016/j.cancergen.2019.05.006

Zhao, Q., Zhu, Y., Liu, L., Wang, H., Jiang, S., Hu, X., et al. (2018). STK39 blockage by RNA interference inhibits the proliferation and induces the apoptosis of renal cell carcinoma. *Onco. Targets. Ther*. 11, 1511–1519. doi: 10.2147/OTT.S153806

Zhao, W., Han, J., Hu, X., Zhou, Q., Qi, R., Sun, W., et al. (2020). PINK1/PRKN-dependent mitophagy in the burn injury model. *Burns* 47, 628–63. doi: 10.1016/j.burns.2020.07.026

Conflict of Interest: The authors declare that the research was conducted in the absence of any commercial or financial relationships that could be construed as a potential conflict of interest.

Publisher's Note: All claims expressed in this article are solely those of the authors and do not necessarily represent those of their affiliated organizations, or those of the publisher, the editors and the reviewers. Any product that may be evaluated in this article, or claim that may be made by its manufacturer, is not guaranteed or endorsed by the publisher.

frontiers in Endocrinology

ORIGINAL RESEARCH
published: 05 November 2021
doi: 10.3389/fendo.2021.763863

The Transgenerational Transmission of the Paternal Type 2 Diabetes-Induced Subfertility Phenotype

Eva Zatecka[1†], Romana Bohuslavova[2†], Eliska Valaskova[1], Hasmik Margaryan[1], Fatima Elzeinova[1], Alena Kubatova[1], Simona Hylmarova[2,3], Jana Peknicova[1‡] and Gabriela Pavlinkova[2‡]*

[1] Laboratory of Reproductive Biology, Institute of Biotechnology Czech Academy of Sciences (CAS), Biotechnology and Biomedicine Center of the Academy of Sciences and Charles University in Vestec (BIOCEV), Vestec, Czechia, [2] Laboratory of Molecular Pathogenetics, Institute of Biotechnology Czech Academy of Sciences (CAS), Biotechnology and Biomedicine Center of the Academy of Sciences and Charles University in Vestec (BIOCEV), Vestec, Czechia, [3] Department of Internal Medicine, Second Faculty of Medicine, Charles University in Prague and Motol University Hospital, Prague, Czechia

OPEN ACCESS

Edited by:
Honggang Li,
Huazhong University of Science and Technology, China

Reviewed by:
Francesca Mancuso,
University of Perugia, Italy
Anthony John Hannan,
University of Melbourne, Australia
Adam John Watkins,
University of Nottingham, United Kingdom

***Correspondence:**
Gabriela Pavlinkova
gpavlinkova@ibt.cas.cz

†These authors share first authorship

‡These authors share last authorship

Specialty section:
This article was submitted to Reproduction, a section of the journal Frontiers in Endocrinology

Received: *24 August 2021*
Accepted: *20 October 2021*
Published: *05 November 2021*

Citation:
Zatecka E, Bohuslavova R, Valaskova E, Margaryan H, Elzeinova F, Kubatova A, Hylmarova S, Peknicova J and Pavlinkova G (2021) The Transgenerational Transmission of the Paternal Type 2 Diabetes-Induced Subfertility Phenotype. Front. Endocrinol. 12:763863. doi: 10.3389/fendo.2021.763863

Diabetes is a chronic metabolic disorder characterized by hyperglycemia and associated with many health complications due to the long-term damage and dysfunction of various organs. A consequential complication of diabetes in men is reproductive dysfunction, reduced fertility, and poor reproductive outcomes. However, the molecular mechanisms responsible for diabetic environment-induced sperm damage and overall decreased reproductive outcomes are not fully established. We evaluated the effects of type 2 diabetes exposure on the reproductive system and the reproductive outcomes of males and their male offspring, using a mouse model. We demonstrate that paternal exposure to type 2 diabetes mediates intergenerational and transgenerational effects on the reproductive health of the offspring, especially on sperm quality, and on metabolic characteristics. Given the transgenerational impairment of reproductive and metabolic parameters through two generations, these changes likely take the form of inherited epigenetic marks through the germline. Our results emphasize the importance of improving metabolic health not only in women of reproductive age, but also in potential fathers, in order to reduce the negative impacts of diabetes on subsequent generations.

Keywords: sperm, diabetes, testes, fertility, offspring, molecular biomarkers, TERA, GAPDS

INTRODUCTION

Type 2 diabetes mellitus (T2D) combines insulin resistance and insulin secretion deficiency with the main characteristics of carbohydrate, protein, and lipid metabolism disorders (1, 2). The progression of the disease is clinically manifested by increasing weight gain, impaired glucose tolerance, and high plasma insulin, triglycerides, and fasting glucose. The worsening glycemic control causes the development of long-term complications, including diabetic retinopathy, nephropathy, peripheral neuropathy, autonomic neuropathy, and increases risk of cardiovascular disease (2). T2D is also an established risk factor for sexual dysfunction in both men and women (3). In men, diabetes is associated with erectile dysfunction, androgen deficiency, and disruption of the

hypothalamic-pituitary-gonadal axis (4–6). Additionally, clinical data from IVF clinics show that type 1 and type 2 diabetic male patients have lower *in vitro* fertilization success rates, suggesting that diabetes-exposed sperm are damaged, including increased sperm nuclear DNA fragmentation, altered sperm morphology, and reduced sperm motility (7–10). With the increasing prevalence and incidence of T2D, more men in their reproductive years will be affected, contributing to the increasing prevalence of subfertility. However, the molecular mechanisms responsible for diabetic environment-induced sperm damage and overall decreased reproductive outcomes are not fully established.

In addition, parental exposure to the diabetic environment represents a higher risk of adverse effects for the offspring, influencing effects on their cardiovascular and metabolic health, and increased susceptibility to metabolic and cardiovascular disorders later in life (11–18). The epidemiological evidence is supported by experimental animal studies that demonstrate the transmission of diabetic phenotypes to the offspring (19–24). The effects of maternal exposure to diabetes combine the direct effects of *in utero* exposure, genetic effects (nuclear and mitochondrial DNA), and epigenetic modifications of germ cells. Metabolic phenotypes can also be transmitted *via* the paternal lineage. Paternal effects that result from environmental exposures represent predominantly epigenetic modifications in sperm, although particular environmental factors can affect the composition of seminal fluid, which can produce placental and developmental effects (25). For example, high fat diet exposure of male rats reprograms ß cells in offspring (26), high-fat diet-induced paternal obesity modulates the sperm microRNA content and DNA methylation status (27), and paternal T2D alters DNA methylation patterns in sperm, involving changes in methylation of insulin signaling genes (28).

Although the molecular mechanisms associated with the transmission of the diabetic phenotype to the offspring have been investigated, the impact of paternal T2D exposure on the reproductive outcomes of subsequent generations remains unclear. Previously, we showed that paternal type I diabetes induced transgenerational changes in the testes, and increased sperm damage in the offspring across two generations (29). Here, we describe T2D exposure effects on the reproductive system and the reproductive outcome of fathers and their offspring, using a mouse model. This is the first complex analysis of the metabolic and reproductive system phenotypes of TD2 fathers and their descendants, demonstrating how paternal exposure to TD2 mediates intergenerational and transgenerational effects on the reproductive health of the offspring.

MATERIALS & METHODS

Experimental Animals

This study was conducted in accordance with the Guide for the Care and Use of Laboratory Animals (NIH Publication No. 85-23, revised 1996). The experimental protocol was approved by the Animal Care and Use Committee of the Institute of Molecular Genetics, CAS and carried out in accordance with the relevant guidelines and regulations. We used a T2D mouse model generated by a combination of high-fat diet and a low dose of streptozotocin (28, 30). Male inbred C57BL/6J mice (purchased from Charles River, Germany), aged 6 weeks, were divided into two groups and were fed either a high-fat diet (HFD: 60% of the metabolizable energy coming from fat, 20% from carbohydrates, and 20% from protein; ssniff® EF acc. D12492 from Ssniff Spezialdiäten GmbH, Germany) or a control standard chow diet (11% of the metabolizable energy coming from fat, 65% from carbohydrates, and 20% from protein, #1320 diet, Altromin, Germany). After 9 weeks of HFD, intraperitoneal injection of 100 mg/kg body weight of streptozotocin (STZ; Sigma) was applied. Body weight, and blood samples were taken after 6-h fasting at indicated time points during the experiment (Experimental schematics in **Figure 1**). Blood glucose levels were measured in animals by a glucometer (COUNTOUR TS, Bayer, Switzerland); blood glucose levels maintained above 13.9 mmol/L are classified as diabetic. Mice were kept under standard experimental conditions with constant temperature (23–24°C). Glucose tolerance tests (GTT) were performed in 6h-fasted males. Mice were injected intraperitoneally with glucose (2 g/kg). Blood glucose was measured at 0, 15, 30, 60, and 120 min after glucose administration. After 12 weeks in the experiment, T2D males were glucose intolerant with blood glucose levels maintained above 13.9 mmol/L.

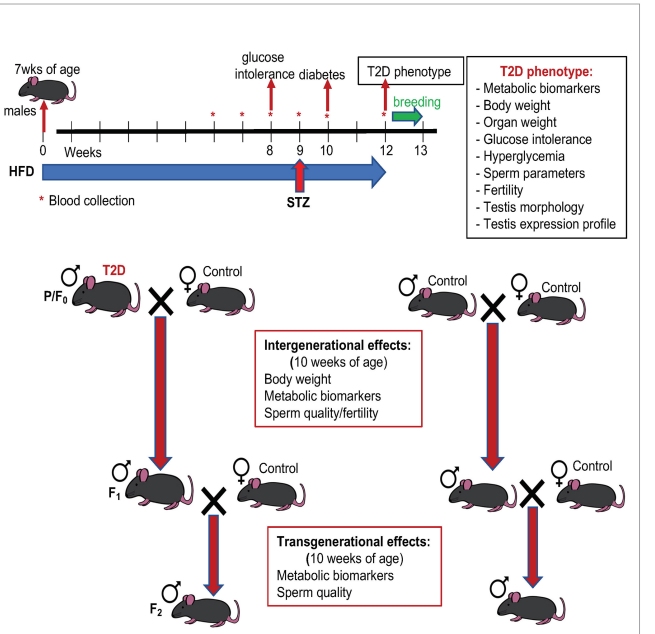

FIGURE 1 | Experimental schematics. Type 2 diabetes (T2D) was induced by a combination of high fat diet (HFD) and a low dose of streptozotocin (STZ): sexually matured males (7 weeks old) were kept on HFD for 12 weeks before mating and injected with STZ at week 9 of the HFD experiment. T2D males and standard diet (control) fed males (parental generation, P/F_0) were mated with standard diet fed females. After one week mating pairs were separated, males were killed, and tissues were collected for further analyses. The F_1 male offspring were mated at 9 weeks of age, after one week mating pairs were separated. F_1 males were killed, and analyses were performed at 10 weeks of age. Effects of diabetic paternal environment was also evaluated in the second (F_2) male offspring generation at 10 weeks of age. Both F_1 and F_2 males were maintained on standard diet.

At 18 weeks of age, male founders (P generation) were mated with females fed with the standard chow diet. Individual males were placed in a cage with 1 healthy adult female. The animals were kept together for a week with minimalized disruptions and therefore, a vaginal plug was not checked in female mice. During this week all mice were fed with a standard chow diet. Immediately after separation, the males were killed, tissues and blood were collected for analyses. The females were housed individually during the gestation period and the litter size was recorded. Only male pups, the F_1 offspring, were left in the litters to be used for following up transgenerational studies. At 9 weeks of age, randomly selected F_1 males were mated with females to produce the F_2 offspring. The offspring were fed only by the regular control diet. To minimize any additional environmental influence, molecular and cellular analyses were performed in both F_1 and F_2 male offspring at 10 weeks of age.

Biochemical Parameters

Blood serum was collected from non-diabetic and T2D males following a 6-h fast and was analyzed using a fully automated chemistry analyzer, Beckman Coulter AU480 (Beckman) according to the manufacturer's protocol in the Core Facility for Phenogenomics, Biocev. System Beckman Coulter AU480 reagents used for the quantification: glucose (OSR6621), AST (OSR6009), ALT (OSR6007), TG (OSR60118), insulin (33410), PAI-1 (plasminogen kit 20009000), and LDL (ODC0024).

Sperm Parameters

Mouse sperm cells were obtained from the left and right cauda epididymis. Spermatozoa from both caudae were left to release into warm (37 °C) PBS in a CO_2 incubator for 15 min. The resulting mixture was poured through a 30 μm filter (Partec) to obtain only the sperm fraction and PBS was added to 1 mL of final volume (31). Sperm were counted in a Bürker chamber under the light microscope, and sperm concentration, sperm morphology, and sperm head separation were determined as described previously (32). Sperm morphology was evaluated in 200 cells per each animal. Sperm viability was analyzed with SYBR14 from Live/Dead sperm viability kit (Molecular Probes, USA) and by flow cytometry (LSRII, blue laser 488 nm, Becton Dickinson, USA), minimum 15,000 events were evaluated. An annexin V–FITC apoptosis kit (Sigma) and chromomycin A_3 staining (CMA3, Sigma) were used to assess the sperm damage (29). The molecular and functional quality of sperm was further evaluated by the expression of two molecular biomarkers, sperm acrosomal transitional endoplasmic reticulum ATPase (TER ATPase, TERA) and glyceraldehyde-3-phosphate dehydrogenase-S (GAPDS), using monoclonal antibodies Hs-14 (33) and Hs-8 (34), respectively (EXBIO Ltd., Czechia). These antibodies are used for pathological human sperm and reproductive diagnostics, and evaluation of dysfunctional spermatogenesis (33, 35–37). A minimum of 200 spermatozoa per each animal was examined with a Nikon Eclipse E400 fluorescent microscope equipped with a Nikon Plan Apo VC 60/1.40 oil objective (Nikon Corporation Instruments Company) and photographed with a ProgRes MF CCD camera (Jenoptik, Germany) with the aid of NIS-ELEMENTS imaging software (Laboratory Imaging, Ltd.). Protamine 1 and 2 ratio was obtained from 4 x 10^6 sperm cells per each sample, as described previously (29).

Morphological and Immunohistochemical Analyses of Testes

Dissected testes were fixed with 4% paraformaldehyde in PBS (pH 7.4) at 4°C overnight, and embedded in paraffin. Paraffin-embedded tissues were cut into 8 μm sections, de-paraffinized and rehydrated sections were stained with hematoxylin & eosin or used for immunohistochemistry. Citrate buffer (pH 6.0) was used as a heat-induced antigen retriever. Evaluation of meiotic cells and the 12 stages of production of spermatozoa in the mouse seminiferous epithelium was done using immunolabeling of the axial element of the synaptonemal complex (SYCP3, mouse anti-SCP3 #ab97672, 1:1000 dilution, Abcam). Rabbit anti-CX43 (#C6219, 1:2000 dilution, Sigma) was used to evaluate gap junctions. The secondary antibodies Alexa Fluor® 488 AffiniPure Goat Anti-Mouse IgG (Jackson ImmunoResearch Laboratories 115-545-146), and Alexa Fluor® 594 AffiniPure Goat Anti-Rabbit IgG (Jackson ImmunoResearch Laboratories 111-585-144) were used in a 1:400 dilution. Samples were incubated with primary antibodies at 4°C for 24 hours. After several PBS washes, secondary antibodies were added and incubated at 4°C for 24 hours. The sections were counterstained with Hoechst 33342 (#14533 Sigma) and imaged with a confocal microscope (ZEISS LSM 880 NLO) or with a fluorescence microscope (Nikon Eclipse E400). A relative quantification of Cx43 staining in Leydig cells was done using ImageJ software. Morphometric evaluations of seminiferous tubule diameter and thickness of the seminiferous epithelium were performed. The diameter of a seminiferous tubule was defined as the shortest distance between two parallel tangent lines of the outer edge of the tubule. Paraffin sections (8 μm) were stained with Periodic acid–Schiff to visualize advanced glycation end products (Periodic acid–Schiff (PAS) kit; 395B-1KT, Sigma).

Real-Time Reverse-Transcription PCR

RT-qPCR was performed as previously described (29). Briefly, cDNA was prepared using 2 μg of total RNA isolated from the testes. We used RevertAid Reverse Transcriptase (Thermo Fisher Scientific), 1 μL Oligo(dT) and random hexamer primers (Thermo Fisher Scientific) in reverse transcription (RT). Quantitative real-time PCR (qPCR) was performed with a final concentration of cDNA 10 ng/μL using a CFX 384 – qPCR cycler (BioRad). The relative expression of a target gene was calculated, based on the quantification cycle (Cq) difference (Δ) of an experimental sample *versus* control. The control was set at 100% and experimental samples were compared to the control (29). The β-actin (*Actb*) and Peptidylprolyl isomerase A (*Ppia*) genes were used as the reference genes. Primer sequences are listed in **Supplementary Table S1**.

Statistical Analysis

The comparisons between diabetic and control mice were done using STATISTICA 7.0. (Statsoft, Czech Republic) and GraphPad Prism 7.0 (GraphPad Software, Inc., USA).

Differences in organ weights were tested by ANCOVA with body weight as covariate. Differences in sperm parameters, testis morphology, and gene expression between control and T2D groups were assessed by t-test. One-way ANOVA, follow by Tukey's *post hoc* tests for multiple comparisons was used to assess differences among offspring generations. Repeated measure-based parameters (such as weight gain over time, GTT, or blood glucose levels) were analyzed using two-way ANOVA for repeated measures. P value < 0.05 was considered to be statistically significant. Sample sizes and individual statistical results for all analyses are provided in the figure legends and tables.

RESULTS

Experimental Paradigm

We used a non-genetic type 2 diabetes (T2D) mouse model that manifests the metabolic abnormalities associated with human prediabetes and type 2 diabetes (28, 30). This model involves a combination of a high fat diet (HFD) to induce insulin resistance and hyperinsulinemia, and a low dose STZ, which reduces β-cell mass but does not cause diabetes in control-fed mice, to bring about glucose intolerance and hyperglycemia (28, 38) (**Figure 1** Experimental schematics). Together these two stressors have been designed to mimic the pathology and the multi-genetic/environmental background of T2D in humans (39–41). We continuously monitored the metabolic changes in our T2D model. As expected, after 8 weeks of HFD, all male C57BL/6J male mice in the experiment had significantly higher fasting plasma insulin levels and were glucose intolerant, as shown by glucose tolerance tests, indicating compromised insulin response (**Figure 2A**). Body weight of the T2D mice increased progressively over time compared to control mice maintained on a normal standard chow diet (**Figure 2B**). After STZ treatment, mice became hyperglycemic with blood glucose levels maintained above 13.9 mmol/l, classified as diabetic (**Figure 2C**). Fasting plasma levels of glucose and insulin were significantly higher in the T2D group (**Figure 3A**). Correspondingly to the diabetic phenotype, after STZ treatment, plasma glucose levels were increased. Plasma insulin levels, which were initially increased in response to the fat-enriched diet in T2D mice, decreased after STZ-induced β-cell reduction but remained at higher levels than insulin levels in control mice. After 12 weeks, compared to control males, T2D mice displayed significant changes in serum metabolic biomarkers, including increased serum glucose, triglycerides, low-density lipoprotein (LDL), plasminogen activator inhibitor 1 (PAI-1, a marker of insulin resistance), metabolic liver enzymes, alanine aminotransferase (ALT) and aspartate aminotransferase (AST) (**Figure 3B**). Metabolic differences were also manifested by increased body weight, and liver weight of T2D males (**Figure 3C**). These physiological and metabolic changes confirmed decreased insulin sensitivity and impaired glucose tolerance associated with the development of type 2 diabetes mellitus. To analyze the effects of the T2D environment on the reproductive system and reproductive outcomes, we mated these T2D males or control males to female mice maintained on a control chow diet through the course of the experiment (**Figure 1**). After 1 week of mating, males were removed, limiting their influence on their progeny to the mating itself.

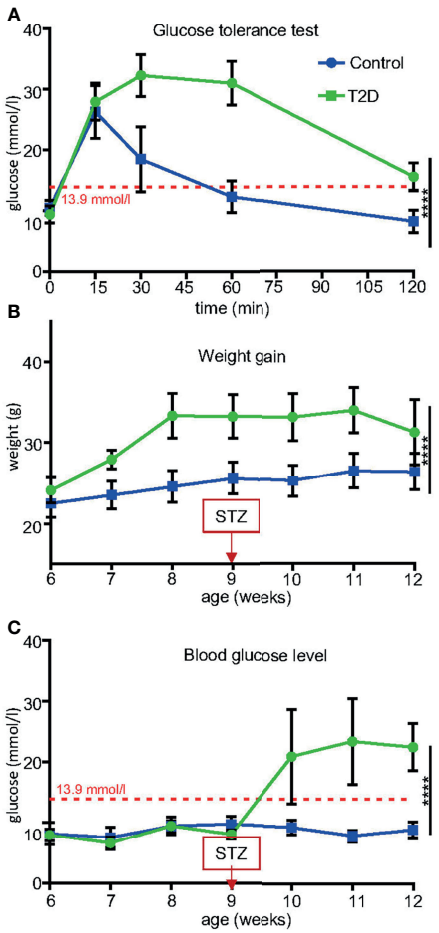

FIGURE 2 | Temporal changes induced in T2D males before mating. **(A)** After 8 weeks of HFD, all males were glucose intolerant compared to control males fed by standard diet. **(B)** Body weight trajectories in T2D males and control males. Note decreased weight gain starting week 11 due to worsening diabetes (hyperglycemia). **(C)** Blood glucose levels significantly increased after a low dose of STZ treatment in combination with HFD, as measured using a glucometer in blood collected from the tail vein after 6-hr fast. Blood glucose levels maintained above 13.9 mmol/l are classified as diabetic (red broken line). Data are presented as the mean ± SD (n = 10 Control and 8 T2D mice). Differences between groups were tested by Two-Way ANOVA for repeated measures, showing significant interactions between time x treatment as repeated measures. ****P < 0.0001.

Effects of T2D on the Reproductive Performance, Reproductive Organs, and Sperm Parameters of the Paternal Generation

All diabetic males, with the exception of one mouse, were able to mate in the period of one week. The rate of pregnancy was in the

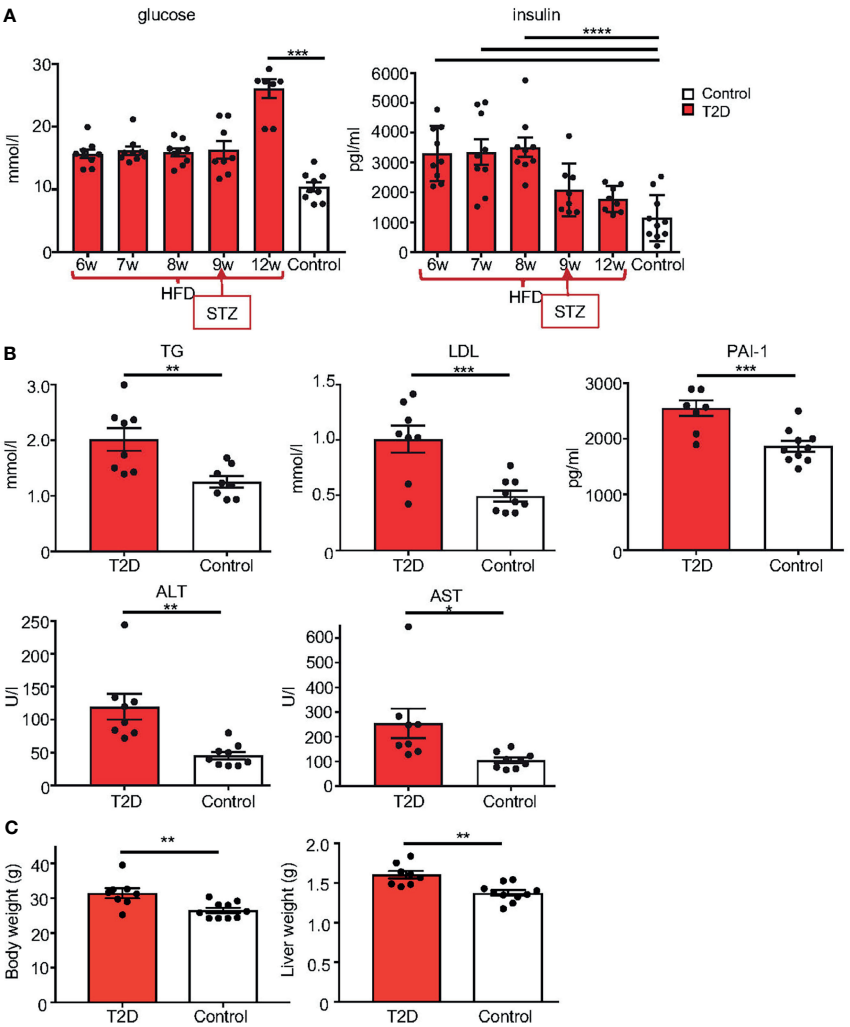

FIGURE 3 | Metabolic phenotype of T2D mouse model. **(A)** Temporal changes in fasting plasma levels of glucose and insulin in T2D males compare to the average level of male controls. Differences were tested by one-way ANOVA with Tukey's multiple comparisons test. **(B)** Fasting plasma levels of TG, triglycerides; LDL, low-density lipoprotein; marker of insulin resistance, PAI-1, plasminogen activator inhibitor 1; ALT, alanine aminotransferase; and AST, aspartate aminotransferase, in T2D males compared to controls at 12 weeks of age. **(C)** Body and liver weight. Data are presented as the mean ± SEM. Differences between groups were tested by *t*-test (GraphPad Prism 7.0). Differences in liver weight between groups were tested by ANCOVA with body weight as covariate (Ancova – STATISTICA 7.0). *P < 0.05, **P < 0.01, ***P < 0.001, ****P < 0.0001.

limits of the rate of pregnancy in our C57BL/6J colony (typically 70–80%, unpublished observation), indicating that overall reproductive performance of T2D males was comparable to controls. However, the litter size of T2D males was more variable (5.63 ± 1.35, n = 6 litters) compared to controls (7 ± 0.53, n = 7 litters, **Table 1**). The weights of the reproductive organs, epididymis and seminal vesicles, and the anogenital distance (AGD), as an androgen-responsive outcome, were unaffected in T2D mice, except for the prostate (**Supplementary Table S2**).

We performed a sperm quality assessment of collected caudal epididymal sperm. No significant effects were found in sperm concentration, viability, apoptosis, or in the packaging quality of the chromatin (as assessed by chromomycin A_3 staining) between T2D and control males (**Supplementary Table S3**). The abnormalities in sperm head morphology were increased in T2D males compared to controls (**Figure 4A**). To further assess sperm quality, we analyzed protamine 1 and protamine 2 ratios, which affect DNA stability, and play a role in the establishment of epigenetic marks (42, 43). The protamine 1 and protamine 2 ratios were altered in the paternal T2D generation (**Figure 4A**). Additionally, the expression of biomarkers of sperm dysfunction, transitional endoplasmic reticulum ATPase (TERA) and glyceraldehyde-3-phosphate dehydrogenase-S (GAPDS) was evaluated. TERA is expressed in the acrosomal part of the sperm head (33), whereas GAPDS is located mainly in the

TABLE 1 | Reproductive effects of T2D in males (parental generation, P).

Group	n	Number of litters	Litter size	Male offspring	Female offspring	Pregnancy rate (%)
Control	7	7	7.00 ± 0.53	4.29 ± 0.52	2.71 ± 0.42	100
T2D	8	6	5.63 ± 1.35	2.75 ± 0.70	2.88 ± 0.91	75

Data are presented as the mean ± SEM.

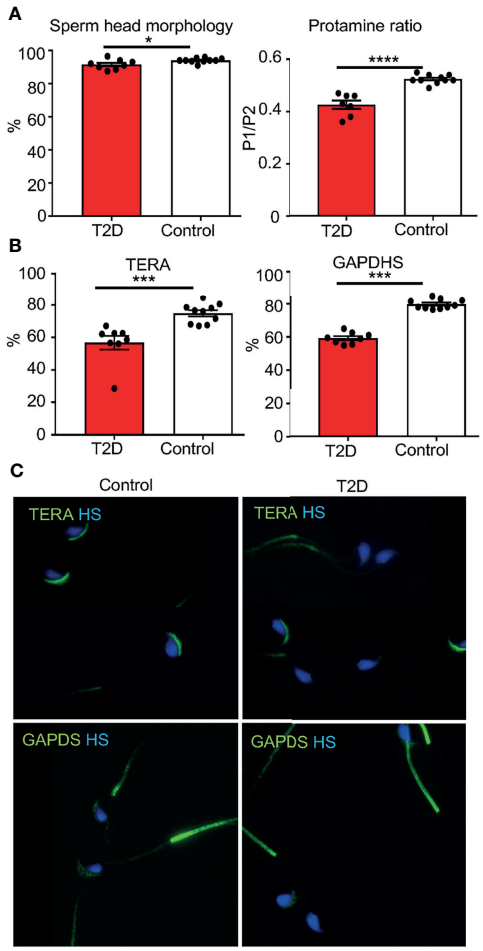

FIGURE 4 | Changes in sperm parameters of the paternal T2D generation. **(A)** Evaluations of caudal epididymal sperm from T2D and control males: abnormalities in the sperm head morphology and protamine 1 and protamine 2 ratios. **(B)** Evaluation of the expression of TERA and GAPDS. **(C)** Representative images of immunolabeling of TERA in the sperm acrosome and GAPDS mainly localized in the principal piece of the flagellum of caudal epidymal sperm from T2D and control males (600x magnification). Data are presented as the mean ± SEM. Differences between groups were tested by *t*-test (GraphPad Prism 7.0). *P < 0.05, ***P < 0.001, ****P < 0.0001. TERA, transitional endoplasmatic reticulum ATPase; GAPDS, glyceraldehyde 3-phosphate dehydrogenase-S.

principal piece of the sperm flagellum and in lesser amount in the acrosome (34, 44). The expression of both TERA and GAPDS was reduced in sperm from T2D males compared to sperm from control males (**Figures 4B, C**).

Morphological and Molecular Changes in the Testes of the T2D Paternal Generation

In mature testes, sperm are produced in the seminiferous epithelium during the cycle of I to XII stages of spermatogenesis, which are defined by the differentiation steps of germ cells, and occur continuously (45). In order to evaluate the morphology of the seminiferous epithelium at different stages of the differentiation of spermatogenic cells, we focused on four broad categories of the differentiation - spermatogonia, spermatocytes, spermatids, and spermatozoa (Schematic drawing in **Figure 5A**). We did not find any pronounced morphological abnormalities, such as testicular atrophy, deficiency, or loss of the seminiferous epithelium between the control and T2D testes. Immunolabeling of a meiotic marker, synaptonemal complex protein 3 (SYCP3) (46), revealed that T2D testes contained all stages of meiotic cells similar to controls (**Figures 5B–D**). Although all the distinct developmental stages of spermatogenesis were identified in similar percentages in both control and T2D testes, a significantly thinner germinal epithelium was found in all cycle stages in the testes of diabetic mice and the diameter of seminiferous tubules was reduced in diabetic testes compared to controls (**Tables 2**, **3** and **Supplementary Table S4**). To evaluate early markers of diabetes-induced tissue damage, the expression of gap junction protein connexin 43 (Cx43) and production of advanced glycation end products (AGE) in the testes was compared between control and T2D mice. Cx43 levels were increased specifically in the interstitial tissue containing Leydig cells, which are adjacent to the seminiferous tubules in the testes, suggesting altered intercellular communications between neighboring Leydig cells in the T2D testes (**Figures 5E–G**). Leydig cells are the primary source of testosterone or androgens in males, under the regulation of the hypothalamic-pituitary axis, and are vital for spermatogenesis (47). We also found an increased production of AGE in the testicular tissue from T2D males (**Figures 5H–I"**). As AGE are implicated in diabetes related complications, consequently, the formation of AGE may contribute to testicular dysfunction.

Having recognized the effects of T2D on testis morphology, we next wanted to assess the effects of the diabetic environment on mRNA expression in testicular tissue. Out of a selection of germ cell marker genes, we found two with altered expression: the expression of *Sycp1* in spermatocytes was reduced and *Prm1* levels were increased correspondingly with changes in the protamine ratio found in sperm from T2D males (**Figure 6A**). We also measured expression of a selection of blood testis barrier markers amongst which we found a significant increase in the expression of *Cldn11*, and *Cdh2* in the testes from T2D males compared to control testes (**Figures 6B, C**).

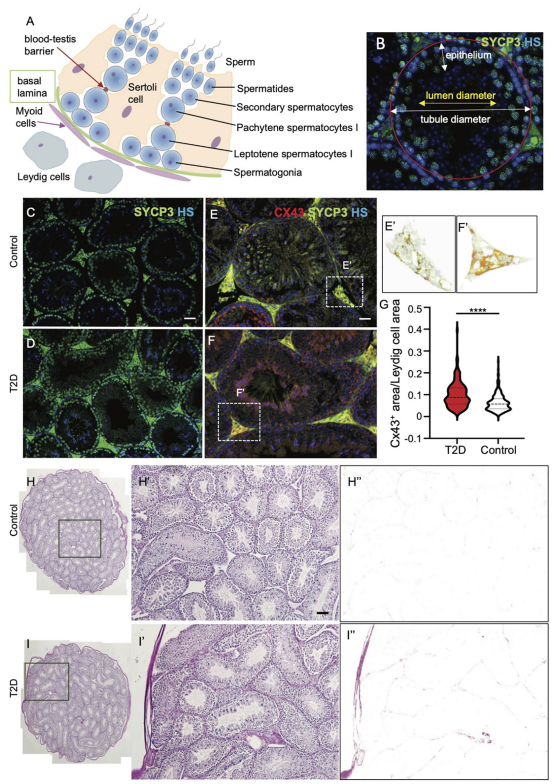

FIGURE 5 | Morphological and expressional changes in the testes of T2D males. **(A)** Schematic cross-section through a testicular tubule, showing germ cells at different stages of spermatogenesis embedded within the somatic Sertoli cells. Leydig cells are present in the interstitium. The blood-testis barrier facilitates the migration of spermatocytes in addition to the maintenance of the microenvironment. **(B)** Morphological evaluation of seminiferous tubules included the measurements of tubule diameter and epithelium thickness for different spermatogenesis stages. **(C, D)** Representative images of cross sections of control and T2D testes after immunolabeling of meiotic marker SYCP3, an axial element of the synaptonemal complex, show the germinal epithelium lining seminiferous tubules at different stages of spermatogenesis. Nuclei are counterstained with Hoechst 33342 (HS, blue). **(E–G)** Immunolabeling of tissue sections shows increased Cx43 expression in the interstitial tissue of the testes of T2D males compared to controls. **(E', F')** Delineated $Cx43^+$ area in the testis sections by ImageJ program. A relative quantification of staining determined as a ratio of $Cx43^+$ areas per the total Leydig cell areas by ImageJ. Stacked violin plot shows the differential expression of Cx43 in control and T2D. Data are presented as the mean ± SEM (n = 6 controls/271 Leydig cell areas, and 6 T2D/198 Leydig cell areas). Differences between groups were tested by *t*-test (GraphPad Prism 7.0). ****$P < 0.0001$. Nuclei are counterstained with Hoechst 33342 (blue). **(H–I')** Representative images of PAS staining of the control and T2D testes show increased advanced glycation end-products in the interstitial tissue of the testes from T2D males. **(H'', I'')** Delineated PAS^+ area in the testes by ImageJ. Scale bars, 50 µm.

Paternal T2D Alters the Metabolic and Reproduction Parameters of Male F_1 and F_2 Offspring

To assess whether the paternal response to a diabetic environment affects the reproductive system of male offspring, males on either diet were mated to females. Fathers were removed after mating, limiting influence on their offspring only to the mating itself. The females were housed individually during the gestation period and the litter size was recorded. All females and the offspring generations were fed by the standard, control diet. Only male pups, the F_1 offspring, were left in the litters to be used for following up transgenerational studies. The F_2 offspring were produced from the mating of randomly selected F_1 males with control females (n = 10 males/group). To evaluate paternal effects and minimize any additional environmental influence, all molecular and cellular analyses of both F_1 and F_2 offspring were performed at 10 weeks of age, when adult male mice are considered sexually mature (48, 49).

First, to determine the potential effect of paternal T2D on the F_1 and F_2 generations, we examined physiological and metabolic changes in the offspring. At 10 weeks of age, the body and liver weights were significantly increased in the F_1 offspring of T2D males (**Figures 7A, B**). Most analyzed serum biomarkers were unaffected in the F_1 and F_2 offspring with the exception of glucose and ALT (**Figures 7C, D**). Plasma glucose levels were increased in the F_1 males at 10 weeks of age, however, these F_1 males had no impairment of glucose tolerance, as shown by a glucose tolerance test. Interestingly, ALT was increased in F_2 males, indicating a transgenerational effect of T2D exposure.

Next, we evaluated the effects of paternal T2D on the reproductive system and reproductive parameters of the F_1 and F_2 male offspring. The testicular morphology of the F_1 offspring from control and T2D fathers was comparable, including the thickness of the germinal epithelium and diameter of the seminiferous tubules. Accordingly, the mRNA expression of selected genes in the testes was not different between the F_1 offspring groups (**Supplementary Figure S1**). However, the weight of testes of the F_1 offspring from T2D fathers was significantly smaller compared to the control F_1 offspring (**Supplementary Table S5**). Additionally, significantly reduced fertility was found in the F_1 males from the T2D parental generation with a pregnancy rate of 63% compared to a 90% pregnancy rate in the F_1 control generation (**Table 4**). Of eight F_1 males in the experiment, only five males were able to mate in the period of one week and produce progeny with the average litter size of 4.63 ± 1.41 (n = 5 litters) compared to the F_1 control cohort with the litter size of 6.44 ± 1.14 (n = 9 litters). The sex ratio of born pups was not significantly different (**Table 4**).

Paternal T2D Alters Sperm Parameters in Two Subsequent Offspring Generations

Caudal epididymal sperm were collected from the F_1 and F_2 offspring for a sperm quality assessment. Similar to the paternal T2D males, we found no changes in sperm concentration, viability, and cell apoptosis in the F_1 and F_2 offspring generations (**Supplementary Table S6**). The packaging quality of the sperm chromatin in the F_1 and F_2 offspring was not affected by the T2D parental exposure, as evaluated by chromomycin A_3 staining of sperm, and by protamine 1 and protamine 2 ratios (**Supplementary Table S6**). However, abnormalities in sperm head morphology were increased in both the F_1 and F_2 generations from T2D fathers compared to the control offspring generations (**Figure 8A**). Additionally, the

TABLE 2 | Tubule diameter (μm) for different stages of sperm production in the testes.

Group	I – III	IV – VI	VII – VIII	IX – XII
Control	182.781 ± 4.093	186.915 ± 2.415	191.109 ± 2.325	187.220 ± 2.512
T2D	164.399 ± 4.852*	176.009 ± 3.039**	174.310 ± 2.609***	167.963 ± 3.437***

*Data are presented as the mean ± SEM (n = 10 controls, 206 tubules; n = 8 T2D males, 254 tubules). Differences between groups were tested by t-test (GraphPad Prism 7.0). *P < 0.05, **P < 0.01, ***P < 0.001.*

TABLE 3 | The seminiferous epithelium thickness (μm) for different stages of sperm production.

Group	I – III	IV – VI	VII – VIII	IX – XII
Control	102.465 ± 4.466	105.582 ± 2.859	115.561 ± 2.264	99.791 ± 2.317
T2D	73.778 ± 4.230***	90.187 ± 2.885***	108.736 ± 2.438*	84.105 ± 2.555***

*Data are presented as the mean ± SEM (n = 10 controls, 206 tubules; 8 T2D males, 254 tubules). Differences between groups were tested by t-test (GraphPad Prism 7.0). *P < 0.05, ***P < 0.001.*

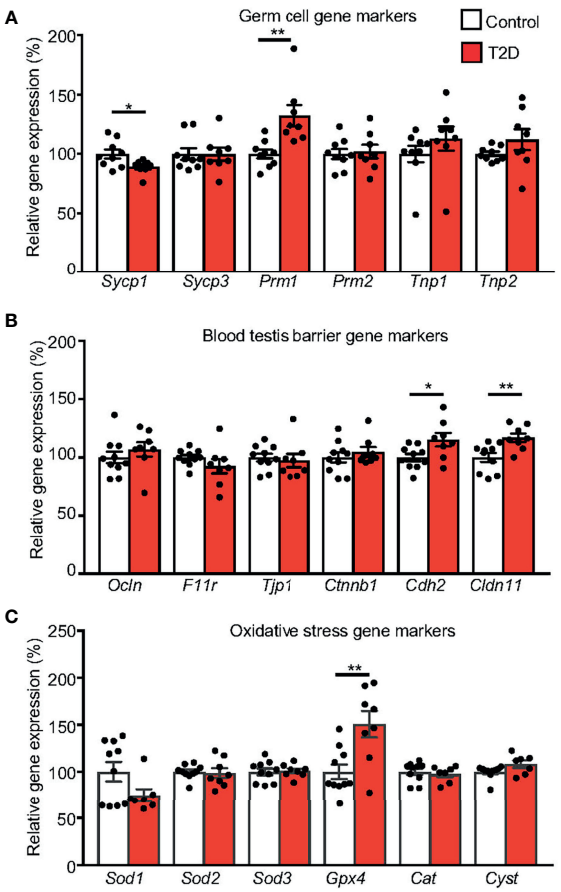

FIGURE 6 | Expression changes in the testes of the parental generation. **(A)** qPCR analysis of markers for spermatogenesis and spermiogenesis: *Sycp1*, synaptonemal complex protein 1; *Sycp3*, synaptonemal complex protein 3; *Prm1*, protamine 1; *Prm1*, protamine 2; *Tnp1*, transition protein 1 and *Tnp2*, transition protein 2; **(B)** Blood testis barrier markers: *Ocln*, occludin; *F11r*, F11 receptor; *Tjp1*, tight junction protein 1; *Ctnnb1*, catenin beta 1; *Cdh2*, cadherin 2; *Cldn11*, claudin 11 and **(C)** oxidative stress markers: *Sod1, Sod2, and Sod3*, superoxide dismutase 1, 2, and 3; *Gpx4*, glutathione peroxidase 4; *Cat*, catalase; and *Cyct*, cytochrome c. The control group represents 100% of relative gene expression. The values are means ± SEM, tested by *t*-test (GraphPad Prism 7.0). *P < 0.05, **P < 0.01.

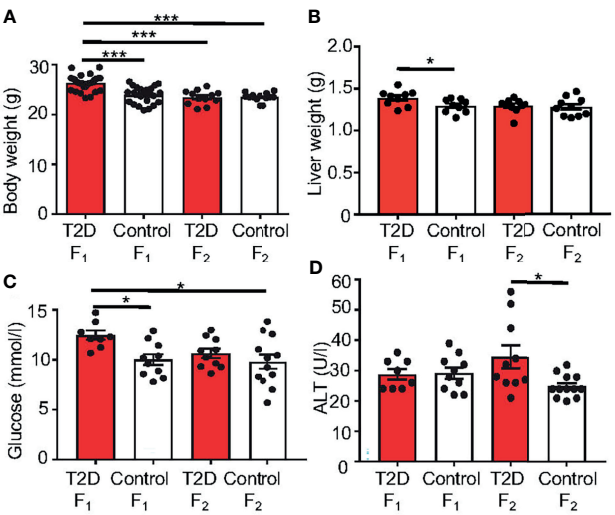

FIGURE 7 | Changes in metabolic characteristics of the offspring generations. **(A)** Body weight and **(B)** liver weight at 10 weeks of age. Differences in liver weight between groups were tested by ANCOVA with body weight as covariate (Ancova – STATISTICA 7.0). **(C)** Fasting plasma glucose and **(D)** alanine aminotransferase (ALT) levels at 10 weeks of age. Data are presented as the mean ± SEM. Differences were tested by one-way ANOVA, follow by Tukey's *post hoc* tests for multiple comparisons (GraphPad Prism 7.0). *P < 0.05, ***P < 0.001.

levels of TERA and GAPDS were reduced in the offspring of diabetic males in both F_1 and F_2 generations (**Figures 8B, C**), indicating not only intergenerational but also transgenerational transmission of negative effects of the diabetic environment.

DISCUSSION

In this study, we show that T2D affects not only metabolic health but also the reproductive system through the male lineage to the F_2 offspring. Paternal T2D exposure causes increased body weight gain and fasting plasma glucose, and significantly impaired reproductive functions of the F_1 males and sperm

TABLE 4 | Reproductive effects of T2D in parental generation on the F_1 offspring.

Group	n	Number of litters	Litter size	Male offspring	Female offspring	Pregnancy rate (%)
Control F_1	10	9	6.44 ± 1.14	3.56 ± 0.65	2.89 ± 0.59	90
T2D F_1	8	5	4.63 ± 1.41	1.88 ± 0.58	2.75 ± 0.86	63*

*Data are presented as the mean ± SEM. Pregnancy rate, Binomial test GraphPad Prism 7. *P <0.05.*

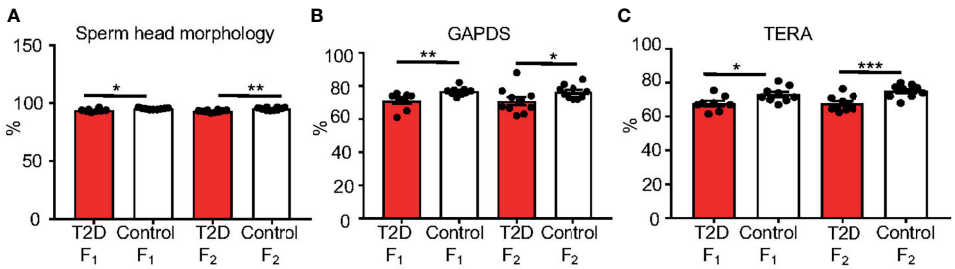

FIGURE 8 | Changes in sperm characteristics of the F_1 and F_2 offspring. **(A)** Evaluations of sperm head abnormalities of caudal epididymal sperm from the offspring F_1 and F_2 generations from T2D and control fathers. **(B)** The protein levels of glyceraldehyde 3-phosphate dehydrogenase-S (GAPDS) and **(C)** transitional endoplasmatic reticulum ATPase (TERA), as detected by immunolabeling of caudal epidymal sperm from the F_1 and F_2 offspring. All analyses were done at 10 weeks of age. Data are presented as the mean ± SEM. (n = 10 for all groups except n = 9 for T2D F_1 males/200 cells per each animal). Differences between groups were tested by *t*-test (GraphPad Prism 7.0). *P < 0.05, **P < 0.01, ***P < 0.001.

abnormalities in the F_1 male offspring. Furthermore, F_2 males had altered sperm parameters. Thus, the observed transgenerational non-genetic transmission of sperm damage caused by T2D in fathers indicate programmed sperm perturbations likely in the form of inherited epigenetic marks.

Both fertility and paternally transmitted effects are associated with changes in the sperm epigenome, including non-coding RNAs, DNA methylation, histones, and protamines (28, 50–53). Epigenetic paternal inheritance involving non-coding RNAs has been established in paternal metabolic disorder models. The intergenerational transmission of a paternal HFD-induced metabolic disorder was linked to a subset of sperm transfer RNA-derived small RNAs (tsRNAs) (53). Another study found changes in sperm miRNA profiles and germ cell methylation status in two offspring generations following diet-induced paternal obesity (27). Differential DNA methylation profiles have been identified in multiple regions of the sperm DNA because of environment-induced epigenomic reprogramming (28, 54–56). For example, numerous genes were differently methylated in sperm of prediabetic/T2D fathers, with a significant proportion of differentially methylated genes overlapping with hypermethylated genes in pancreatic islets of the offspring and corresponding to the prediabetes-associated physiological and metabolic phenotype (28). In a model of caloric restriction during *in utero* development, the germline DNA methylation was altered in the adult male offspring (57). Histone variants and histone modifications represent additional modes of paternal transmission of environmental information to the offspring. In contrast to somatic cells, male germ cells have more histone variants and their incorporation into the nucleosome may influence the activation of germline-specific genes and repression of the somatic gene expression program [reviewed in (50, 58)]. Some of the histone variants are exclusively detected on germ cells in testes and seem to also be important in the chromatin condensation process (59). The altered histone modifications may also contribute to transgenerational phenotypes through the male germline, as shown in a transgenic mouse model with histone demethylase KDM1A overexpression, resulting in increased H3K4me3 histone methylation in sperm, a transgenerational phenotype of impaired fertility, and severe birth defects in offspring (51). Similarly, deletion of the H3K4me2 demethylase leads to a transgenerational progressive decline in spermatogenesis (60). Specific histone modifications promote chromatin remodeling and histone-to-protamine replacement, which reshapes the nucleus and compacts chromatin [reviewed in (50, 58)]. The histone-to-protamine transition is a tightly controlled process, as premature expression of protamine 1 or disruption of protamine genes results in male infertility in mice (52, 61). Like histones, protamines have post-translational modifications, which are essential for the histone-to-protamine transitions, and abnormalities in protamine modifications may result in impaired spermiogenesis (62, 63). Epigenetic changes during histone-to-protamine transition may not only lead to reduced fertility but are also transmitted to the offspring (52, 62). Protamine 2-deficient mice demonstrate reduced integrity of sperm DNA, altered compaction of the chromatin, and developmental arrest of embryos (64). Furthermore, alterations in the protamine 1/protamine 2 ratio are related to infertility in humans (43, 65), correlate with worsened assisted reproduction outcomes (66), and aberrant protamine replacement may affect the sperm epigenome [reviewed in (65)]. The role of a 'protamine code' in addition to the 'histone code' in transgenerational epigenetic inheritance remains to be further investigated. Although adverse metabolic phenotypes correlate with reduced sperm concentration, motility, and increase sperm DNA damage in humans (67–69), a causal relationship by which paternal

exposures affect the phenotype of offspring has not been established. Nevertheless, epigenetic changes in sperm are implicated as potential mediators of paternal effects and it is essential to understand how epigenetic patterning is produced and how it is influenced by environmental factors resulting in a greater susceptibility to disease in offspring.

Our study used a well characterized model of type 2 diabetes (28, 30, 70). A combination of high-fat diet and low dose STZ resulted in increased body weight gain, glucose intolerance, and altered metabolic parameters, associated with insulin resistance and hyperglycemia, replicating metabolic changes in T2D patients [reviewed in (71)]. The major advantage of this T2D model is that it provides a more accurate model of the human multi-genetic/environmental T2D phenotype compared to monogenic mouse models, such as the mutant with deficiency in leptin (39, 40) or with deficiency in the leptin receptor (41).

We demonstrated that paternal T2D exposure induces a metabolic shift in glucose and fat metabolism in F_1 male offspring, as demonstrated by increased plasma glucose together with increased liver weight and body weight. Although the T2D metabolic perturbation phenotype is gradually reversed in the subsequent male generations, increased plasma levels of liver enzyme ALT in the F_2 males indicate a higher risk for susceptibility to metabolic syndrome and T2D (72, 73).

For the first time, we provide a complex molecular and morphological analysis of the effects of TD2 on the male reproductive system and the effects of TD2 paternal exposure on the reproductive health of two subsequent male offspring generations. Although the testis morphology of T2D mice appeared grossly normal without any atrophy or destruction of the seminiferous epithelium, immunohistological analysis showed a significant reduction of seminiferous tubule diameter and thickness of the seminiferous epithelium for all cycle stages of sperm production in the testes of T2D mice (**Tables 2**, **3**). In line with a lower severity of testicular damage in T2D males, we found only a few expression changes, particularly, altered expression of cell junction proteins, e.g. gap junction protein Cx43 in Leydig cells, and blood-testis-barrier components, tight junction protein, claudin 11 (74), and the adhesion junction component, cadherin 2 (75). Alternations in cell junctions, indicating abnormalities in cell-cell communications, are an early sign of diabetes-induced tissue damage (76). While the F_1 offspring of T2D males had no detectable molecular and morphological changes in the testes, the weight of testes of the F_1 offspring of T2D fathers was significantly smaller compared to the control F_1 males.

A significant finding of this study is the transgenerational transmission of sperm perturbations from T2D fathers through the male lineage to the F_2 offspring. The direct impact of metabolic diseases, such as obesity and diabetes, on sperm quality in men as well as in animal models is well documented. These negative changes include decreased sperm viability and motility, and increased DNA damage, and sperm morphology abnormalities (67, 77–81). Despite these observations, at present, there is only scant evidence for the impact of paternal exposure on sperm quality and the reproductive viability of subsequent generations. Previously, we showed that type 1 diabetes in male mice induces DNA damage, apoptosis, and alters nuclear protamine ratios in sperm in two subsequent male offspring generations (29). Another study, using a diet-induced obesity mouse model, demonstrated that increased sperm DNA damage and reduced motility was transmitted through the paternal line to the first male offspring generation (82). Similarly, Crisostomo et al. (83) reported irreversible changes in sperm quality in correlation with altered testicular metabolism induced by HFD feeding. Here we focused on the effects of T2D on reproductive health of the young adult offspring. We showed that T2D substantially decreased sperm quality in two subsequent F_1 and F_2 offspring male generations. A sperm impairment phenotype consisting of increased sperm head abnormalities and decreased expression of the sperm dysfunctional biomarkers, TERA and GAPDS, resulted in decreased reproductive function of the F_1 males. Since similar sperm defects were found in the F_2 offspring, we can speculate that the reproductive function of F_2 males may also be compromised. TERA is a member of the AAA ATPase family of proteins, and is found in the sperm acrosome (33). Consistent with the role of TERA in capacitation and the acrosome reaction (84), decreased expression of TERA correlates with reduced fertility in humans (33, 35). GAPDS is one of the sperm specific glycolytic enzymes localized primarily in the principal piece of the sperm flagellum and secondary in the acrosomal part of the sperm head (34, 85). It is essential for sperm metabolism, motility and sperm-oocyte binding, and reduced GAPDS is associated with infertility (34, 35, 44, 86).

In conclusion, our data demonstrate that the impaired reproductive system and sperm quality of T2D fathers negatively effects the reproductive health of F_1 male offspring, which persists into the subsequent F_2 male generation. Given the transgenerational impairment of reproductive and metabolic parameters through two generations, these changes likely take the form of inherited epigenetic marks through the germline. One possible way could be *via* alterations in protamine 1 and protamine 2 ratios, as we observed changes in this ratio in parental generation. Nevertheless, further investigation of the epigenetic alterations in sperm that result from paternal exposure to T2D are warranted. Consequently, new strategies to improve metabolic health not only in women of reproductive age but also in potential fathers are necessary in order to reduce the negative impacts on subsequent generations.

DATA AVAILABILITY STATEMENT

The original contributions presented in the study are included in the article/**Supplementary Material**. Further inquiries can be directed to the corresponding author.

ETHICS STATEMENT

The animal study was reviewed and approved by the Animal Care and Use Committee of the Institute of Molecular Genetics, CAS.

AUTHOR CONTRIBUTIONS

All authors have read and approved the manuscript. JP and GP conceived the study, designed experiments, and GP wrote the manuscript. FE, HM, and RB conducted animal study, morphological evaluations, and statistical analyses. EZ and EV designed and performed qPCR. SH and AK performed sperm analyses and Western blotting. HM, EZ, and RB performed immunohistological evaluations. All authors contributed to the article and approved the submitted version.

ACKNOWLEDGMENTS

Biochemical parameter analyses were done by the Czech Centre for Phenogenomics supported by LM2015040. We thank Imaging Methods Core Facility at BIOCEV supported by the MEYS CR (Large RI Project LM2018129 Czech-BioImaging) and ERDF (project No. CZ.02.1.01/0.0/0.0/18_046/0016045) for its support with obtaining imaging data presented in this paper. We thank A. Pavlinek (King's College London) for editing the manuscript.

FUNDING

This work was supported by the institutional support of the Czech Academy of Sciences RVO: 86652036 and the Czech Health Research Council #NU20J-02-00035.

SUPPLEMENTARY MATERIAL

The Supplementary Material for this article can be found online at: https://www.frontiersin.org/articles/10.3389/fendo.2021.763863/full#supplementary-material

REFERENCES

1. Fonseca VA. Defining and Characterizing the Progression of Type 2 Diabetes. *Diabetes Care* (2009) 32 Suppl 2:S151–6. doi: 10.2337/dc09-S301
2. A. American Diabetes. Diagnosis and Classification of Diabetes Mellitus. *Diabetes Care* (2014) 37 Suppl 1:S81–90. doi: 10.2337/dc14-S081
3. Maiorino MI, Bellastella G, Esposito K. Diabetes and Sexual Dysfunction: Current Perspectives. *Diabetes Metab Syndr Obes* (2014) 7:95–105. doi: 10.2147/DMSO.S36455
4. Hylmarova S, Stechova K, Pavlinkova G, Peknicova J, Macek M, Kvapil M. The Impact of Type 1 Diabetes Mellitus on Male Sexual Functions and Sex Hormone Levels. *Endocr J* (2020) 67:59–71. doi: 10.1507/endocrj.EJ19-0280
5. Andersson DP, Ekstrom U, Lehtihet M. Rigiscan Evaluation of Men With Diabetes Mellitus and Erectile Dysfunction and Correlation With Diabetes Duration, Age, BMI, Lipids and HbA1c. *PloS One* (2015) 10:e0133121. doi: 10.1371/journal.pone.0133121
6. Dhindsa S, Furlanetto R, Vora M, Ghanim H, Chaudhuri A, Dandona P. Low Estradiol Concentrations in Men With Subnormal Testosterone Concentrations and Type 2 Diabetes. *Diabetes Care* (2011) 34:1854–9. doi: 10.2337/dc11-0208
7. Mulholland J, Mallidis C, Agbaje I, McClure N. Male Diabetes Mellitus and Assisted Reproduction Treatment Outcome. *Reprod BioMed Online* (2011) 22:215–9. doi: 10.1016/j.rbmo.2010.10.005
8. La Vignera S, Condorelli R, Vicari E, D'Agata R, Calogero AE. Diabetes Mellitus and Sperm Parameters. *J Androl* (2012) 33:145–53. doi: 10.2164/jandrol.111.013193
9. Agbaje IM, Rogers DA, McVicar CM, McClure N, Atkinson AB, Mallidis C, et al. Insulin Dependant Diabetes Mellitus: Implications for Male Reproductive Function. *Hum Reprod* (2007) 22:1871–7. doi: 10.1093/humrep/dem077
10. Bhattacharya SM, Ghosh M, Nandi N. Diabetes Mellitus and Abnormalities in Semen Analysis. *J Obstet Gynaecol Res* (2014) 40:167–71. doi: 10.1111/jog.12149
11. Oyen N, Diaz LJ, Leirgul E, Boyd HA, Priest J, Mathiesen ER, et al. Prepregnancy Diabetes and Offspring Risk of Congenital Heart Disease: A Nationwide Cohort Study. *Circulation* (2016) 133:2243–53. doi: 10.1161/CIRCULATIONAHA.115.017465
12. Ornoy A, Reece EA, Pavlinkova G, Kappen C, Miller RK. Effect of Maternal Diabetes on the Embryo, Fetus, and Children: Congenital Anomalies, Genetic and Epigenetic Changes and Developmental Outcomes. *Birth Defects Res C Embryo Today* (2015) 105:53–72. doi: 10.1002/bdrc.21090
13. West NA, Crume TL, Maligie MA, Dabelea D. Cardiovascular Risk Factors in Children Exposed to Maternal Diabetes In Utero. *Diabetologia* (2011) 54:504–7. doi: 10.1007/s00125-010-2008-1
14. Dabelea D, Hanson RL, Lindsay RS, Pettitt DJ, Imperatore G, Gabir MM, et al. Intrauterine Exposure to Diabetes Conveys Risks for Type 2 Diabetes and Obesity: A Study of Discordant Sibships. *Diabetes* (2000) 49:2208–11. doi: 10.2337/diabetes.49.12.2208
15. Martin AO, Simpson JL, Ober C, Freinkel N. Frequency of Diabetes Mellitus in Mothers of Probands With Gestational Diabetes: Possible Maternal Influence on the Predisposition to Gestational Diabetes. *Am J Obstet Gynecol* (1985) 151:471–5. doi: 10.1016/0002-9378(85)90272-8
16. Sobngwi E, Boudou P, Mauvais-Jarvis F, Leblanc H, Velho G, Vexiau P, et al. Effect of a Diabetic Environment *In Utero* on Predisposition to Type 2 Diabetes. *Lancet* (2003) 361:1861–5. doi: 10.1016/S0140-6736(03)13505-2
17. Manderson JG, Mullan B, Patterson CC, Hadden DR, Traub AI, McCance DR. Cardiovascular and Metabolic Abnormalities in the Offspring of Diabetic Pregnancy. *Diabetologia* (2002) 45:991–6. doi: 10.1007/s00125-002-0865-y
18. Loffredo CA, Wilson PD, Ferencz C. Maternal Diabetes: An Independent Risk Factor for Major Cardiovascular Malformations With Increased Mortality of Affected Infants. *Teratology* (2001) 64:98–106. doi: 10.1002/tera.1051
19. Cerychova R, Bohuslavova R, Papousek F, Sedmera D, Abaffy P, Benes V, et al. Adverse Effects of Hif1a Mutation and Maternal Diabetes on the Offspring Heart. *Cardiovasc Diabetol* (2018) 17:68. doi: 10.1186/s12933-018-0713-0
20. Dunn GA, Bale TL. Maternal High-Fat Diet Effects on Third-Generation Female Body Size *via* the Paternal Lineage. *Endocrinology* (2011) 152:2228–36. doi: 10.1210/en.2010-1461
21. Gniuli D, Calcagno A, Caristo ME, Mancuso A, Macchi V, Mingrone G, et al. Effects of High-Fat Diet Exposure During Fetal Life on Type 2 Diabetes Development in the Progeny. *J Lipid Res* (2008) 49:1936–45. doi: 10.1194/jlr.M800033-JLR200
22. Sasson IE, Vitins AP, Mainigi MA, Moley KH, Simmons RA. Pre-Gestational *vs* Gestational Exposure to Maternal Obesity Differentially Programs the Offspring in Mice. *Diabetologia* (2015) 58:615–24. doi: 10.1007/s00125-014-3466-7
23. Aerts L, Van Assche FA. Animal Evidence for the Transgenerational Development of Diabetes Mellitus. *Int J Biochem Cell Biol* (2006) 38:894–903. doi: 10.1016/j.biocel.2005.07.006
24. Huypens P, Sass S, Wu M, Dyckhoff D, Tschop M, Theis F, et al. Epigenetic Germline Inheritance of Diet-Induced Obesity and Insulin Resistance. *Nat Genet* (2016) 48:497–9. doi: 10.1038/ng.3527
25. Patti ME. Intergenerational Programming of Metabolic Disease: Evidence From Human Populations and Experimental Animal Models. *Cell Mol Life Sci* (2013) 70:1597–608. doi: 10.1007/s00018-013-1298-0
26. Ng SF, Lin RC, Laybutt DR, Barres R, Owens JA, Morris MJ. Chronic High-Fat Diet in Fathers Programs Beta-Cell Dysfunction in Female Rat Offspring. *Nature* (2010) 467:963–6. doi: 10.1038/nature09491
27. Fullston T, Ohlsson Teague EM, Palmer NO, DeBlasio MJ, Mitchell M, Corbett M, et al. Paternal Obesity Initiates Metabolic Disturbances in Two Generations of Mice With Incomplete Penetrance to the F2 Generation and Alters the Transcriptional Profile of Testis and Sperm microRNA Content. *FASEB J* (2013) 27:4226–43. doi: 10.1096/fj.12-224048

28. Wei Y, Yang CR, Wei YP, Zhao ZA, Hou Y, Schatten H, et al. Paternally Induced Transgenerational Inheritance of Susceptibility to Diabetes in Mammals. *Proc Natl Acad Sci USA* (2014) 111:1873–8. doi: 10.1073/pnas.1321195111
29. Pavlinkova G, Margaryan H, Zatecka E, Valaskova E, Elzeinova F, Kubatova A, et al. Transgenerational Inheritance of Susceptibility to Diabetes-Induced Male Subfertility. *Sci Rep* (2017) 7:4940. doi: 10.1038/s41598-017-05286-0
30. Winzell MS, Ahren B. The High-Fat Diet-Fed Mouse: A Model for Studying Mechanisms and Treatment of Impaired Glucose Tolerance and Type 2 Diabetes. *Diabetes* (2004) 53 Suppl 3:S215–9. doi: 10.2337/diabetes.53.suppl_3.S215
31. Dostalova P, Zatecka E, Ded L, Elzeinova F, Valaskova E, Kubatova A, et al. Gestational and Pubertal Exposure to Low Dose of Di-(2-Ethylhexyl) Phthalate Impairs Sperm Quality in Adult Mice. *Reprod Toxicol* (2020) 96:175–84. doi: 10.1016/j.reprotox.2020.06.014
32. Elzeinova F, Novakova V, Buckiova D, Kubatova A, Peknicova J. Effect of Low Dose of Vinclozolin on Reproductive Tract Development and Sperm Parameters in CD1 Outbred Mice. *Reprod Toxicol* (2008) 26:231–8. doi: 10.1016/j.reprotox.2008.09.007
33. Capkova J, Margaryan H, Kubatova A, Novak P, Peknicova J. Target Antigens for Hs-14 Monoclonal Antibody and Their Various Expression in Normozoospermic and Asthenozoospermic Men. *Basic Clin Androl* (2015) 25:11. doi: 10.1186/s12610-015-0025-0
34. Margaryan H, Dorosh A, Capkova J, Manaskova-Postlerova P, Philimonenko A, Hozak P, et al. Characterization and Possible Function of Glyceraldehyde-3-Phosphate Dehydrogenase-Spermatogenic Protein GAPDHS in Mammalian Sperm. *Reprod Biol Endocrinol* (2015) 13:15. doi: 10.1186/s12958-015-0008-1
35. Tepla O, Peknicova J, Koci K, Mika J, Mrazek M, Elzeinova F. Evaluation of Reproductive Potential After Intracytoplasmic Sperm Injection of Varied Human Semen Tested by Antiacrosomal Antibodies. *Fertil Steril* (2006) 86:113–20. doi: 10.1016/j.fertnstert.2005.12.019
36. Capkova J, Kubatova A, Ded L, Tepla O, Peknicova J. Evaluation of the Expression of Sperm Proteins in Normozoospermic and Asthenozoospermic Men Using Monoclonal Antibodies. *Asian J Androl* (2016) 18:108–13. doi: 10.4103/1008-682X.151400
37. Peknicova J, Chladek D, Hozak P. Monoclonal Antibodies Against Sperm Intra-Acrosomal Antigens as Markers for Male Infertility Diagnostics and Estimation of Spermatogenesis. *Am J Reprod Immunol* (2005) 53:42–9. doi: 10.1111/j.1600-0897.2004.00245.x
38. Luo J, Quan J, Tsai J, Hobensack CK, Sullivan C, Hector R, et al. Nongenetic Mouse Models of Non-Insulin-Dependent Diabetes Mellitus. *Metabolism* (1998) 47:663–8. doi: 10.1016/S0026-0495(98)90027-0
39. Zhang Y, Proenca R, Maffei M, Barone M, Leopold L, Friedman JM. Positional Cloning of the Mouse Obese Gene and Its Human Homologue. *Nature* (1994) 372:425–32. doi: 10.1038/372425a0
40. D'Souza A M, Johnson JD, Clee SM, Kieffer TJ. Suppressing Hyperinsulinemia Prevents Obesity But Causes Rapid Onset of Diabetes in Leptin-Deficient Lep (ob/ob) Mice. *Mol Metab* (2016) 5:1103–12. doi: 10.1016/j.molmet.2016.09.007
41. Leifheit-Nestler M, Wagner NM, Gogiraju R, Didie M, Konstantinides S, Hasenfuss G, et al. Importance of Leptin Signaling and Signal Transducer and Activator of Transcription-3 Activation in Mediating the Cardiac Hypertrophy Associated With Obesity. *J Transl Med* (2013) 11:170. doi: 10.1186/1479-5876-11-170
42. Castillo J, Amaral A, Oliva R. Sperm Nuclear Proteome and Its Epigenetic Potential. *Andrology* (2014) 2:326–38. doi: 10.1111/j.2047-2927.2013.00170.x
43. Oliva R. Protamines and Male Infertility. *Hum Reprod Update* (2006) 12:417–35. doi: 10.1093/humupd/dml009
44. Miki K, Qu W, Goulding EH, Willis WD, Bunch DO, Strader LF, et al. Glyceraldehyde 3-Phosphate Dehydrogenase-S, a Sperm-Specific Glycolytic Enzyme, Is Required for Sperm Motility and Male Fertility. *Proc Natl Acad Sci USA* (2004) 101:16501–6. doi: 10.1073/pnas.0407708101
45. Eddy EM, O'Brien DA, Welch JE. *Mammalian Sperm Development In Vivo and In Vitro*. Boston: CRC Press (1991).
46. Yuan L, Liu JG, Zhao J, Brundell E, Daneholt B, Hoog C. The Murine SCP3 Gene Is Required for Synaptonemal Complex Assembly, Chromosome Synapsis, and Male Fertility. *Mol Cell* (2000) 5:73–83. doi: 10.1016/S1097-2765(00)80404-9
47. Zhou R, Wu J, Liu B, Jiang Y, Chen W, Li J, et al. The Roles and Mechanisms of Leydig Cells and Myoid Cells in Regulating Spermatogenesis. *Cell Mol Life Sci* (2019) 76:2681–95. doi: 10.1007/s00018-019-03101-9
48. Dutta S, Sengupta P. Men and Mice: Relating Their Ages. *Life Sci* (2016) 152:244–8. doi: 10.1016/j.lfs.2015.10.025
49. Flurkey K, Currer JM, Harrison DE. *Mouse Models in Aging Research*. Cambridge, Massachusetts: Academic Press (2007).
50. Kimmins S, Sassone-Corsi P. Chromatin Remodelling and Epigenetic Features of Germ Cells. *Nature* (2005) 434:583–9. doi: 10.1038/nature03368
51. Lismer A, Siklenka K, Lafleur C, Dumeaux V, Kimmins S. Sperm Histone H3 Lysine 4 Trimethylation Is Altered in a Genetic Mouse Model of Transgenerational Epigenetic Inheritance. *Nucleic Acids Res* (2020) 48:11380–93. doi: 10.1093/nar/gkaa712
52. Cho C, Willis WD, Goulding EH, Jung-Ha H, Choi YC, Hecht NB, et al. Haploinsufficiency of Protamine-1 or -2 Causes Infertility in Mice. *Nat Genet* (2001) 28:82–6. doi: 10.1038/ng0501-82
53. Chen Q, Yan M, Cao Z, Li X, Zhang Y, Shi J, et al. Sperm tsRNAs Contribute to Intergenerational Inheritance of an Acquired Metabolic Disorder. *Science* (2016) 351:397–400. doi: 10.1126/science.aad7977
54. Lambrot R, Xu C, Saint-Phar S, Chountalos G, Cohen T, Paquet M, et al. Low Paternal Dietary Folate Alters the Mouse Sperm Epigenome and Is Associated With Negative Pregnancy Outcomes. *Nat Commun* (2013) 4:2889. doi: 10.1038/ncomms3889
55. Carone BR, Fauquier L, Habib N, Shea JM, Hart CE, Li R, et al. Paternally Induced Transgenerational Environmental Reprogramming of Metabolic Gene Expression in Mammals. *Cell* (2010) 143:1084–96. doi: 10.1016/j.cell.2010.12.008
56. Anway MD, Cupp AS, Uzumcu M, Skinner MK. Epigenetic Transgenerational Actions of Endocrine Disruptors and Male Fertility. *Science* (2005) 308:1466–9. doi: 10.1126/science.1108190
57. Radford EJ, Ito M, Shi H, Corish JA, Yamazawa K, Isganaitis E, et al. *In Utero* Effects. *In Utero* Undernourishment Perturbs the Adult Sperm Methylome and Intergenerational Metabolism. *Science* (2014) 345:1255903. doi: 10.1126/science.1255903
58. Bao J, Bedford MT. Epigenetic Regulation of the Histone-to-Protamine Transition During Spermiogenesis. *Reproduction* (2016) 151:R55–70. doi: 10.1530/REP-15-0562
59. Martianov I, Brancorsini S, Catena R, Gansmuller A, Kotaja N, Parvinen M, et al. Polar Nuclear Localization of H1T2, a Histone H1 Variant, Required for Spermatid Elongation and DNA Condensation During Spermiogenesis. *Proc Natl Acad Sci USA* (2005) 102:2808–13. doi: 10.1073/pnas.0406060102
60. Greer EL, Beese-Sims SE, Brookes E, Spadafora R, Zhu Y, Rothbart SB, et al. A Histone Methylation Network Regulates Transgenerational Epigenetic Memory in C. Elegans. *Cell Rep* (2014) 7:113–26. doi: 10.1016/j.celrep.2014.02.044
61. Lee K, Haugen HS, Clegg CH, Braun RE. Premature Translation of Protamine 1 mRNA Causes Precocious Nuclear Condensation and Arrests Spermatid Differentiation in Mice. *Proc Natl Acad Sci USA* (1995) 92:12451–5. doi: 10.1073/pnas.92.26.12451
62. Wu JY, Ribar TJ, Cummings DE, Burton KA, McKnight GS, Means AR. Spermiogenesis and Exchange of Basic Nuclear Proteins Are Impaired in Male Germ Cells Lacking Camk4. *Nat Genet* (2000) 25:448–52. doi: 10.1038/78153
63. Brunner AM, Nanni P, Mansuy IM. Epigenetic Marking of Sperm by Post-Translational Modification of Histones and Protamines. *Epigenet Chromatin* (2014) 7:2. doi: 10.1186/1756-8935-7-2
64. Cho C, Jung-Ha H, Willis WD, Goulding EH, Stein P, Xu Z, et al. Protamine 2 Deficiency Leads to Sperm DNA Damage and Embryo Death in Mice. *Biol Reprod* (2003) 69:211–7. doi: 10.1095/biolreprod.102.015115
65. Carrell DT, Emery BR, Hammoud S. The Aetiology of Sperm Protamine Abnormalities and Their Potential Impact on the Sperm Epigenome. *Int J Androl* (2008) 31:537–45. doi: 10.1111/j.1365-2605.2008.00872.x
66. de Mateo S, Gazquez C, Guimera M, Balasch J, Meistrich ML, Ballesca JL, et al. Protamine 2 Precursors (Pre-P2), Protamine 1 to Protamine 2 Ratio (P1/P2), and Assisted Reproduction Outcome. *Fertil Steril* (2009) 91:715–22. doi: 10.1016/j.fertnstert.2007.12.047
67. Kort HI, Massey JB, Elsner CW, Mitchell-Leef D, Shapiro DB, Witt MA, et al. Impact of Body Mass Index Values on Sperm Quantity and Quality. *J Androl* (2006) 27:450–2. doi: 10.2164/jandrol.05124

68. Jensen TK, Andersson AM, Jorgensen N, Andersen AG, Carlsen E, Petersen JH, et al. Body Mass Index in Relation to Semen Quality and Reproductive Hormones Among 1,558 Danish Men. *Fertil Steril* (2004) 82:863–70. doi: 10.1016/j.fertnstert.2004.03.056
69. Magnusdottir EV, Thorsteinsson T, Thorsteinsdottir S, Heimisdottir M, Olafsdottir K. Persistent Organochlorines, Sedentary Occupation, Obesity and Human Male Subfertility. *Hum Reprod* (2005) 20:208–15. doi: 10.1093/humrep/deh569
70. Mansor LS, Gonzalez ER, Cole MA, Tyler DJ, Beeson JH, Clarke K, et al. Cardiac Metabolism in a New Rat Model of Type 2 Diabetes Using High-Fat Diet With Low Dose Streptozotocin. *Cardiovasc Diabetol* (2013) 12:136. doi: 10.1186/1475-2840-12-136
71. Fang JY, Lin CH, Huang TH, Chuang SY. *In Vivo* Rodent Models of Type 2 Diabetes and Their Usefulness for Evaluating Flavonoid Bioactivity. *Nutrients* (2019) 11:530. doi: 10.3390/nu11030530
72. Pinhas-Hamiel O, Zeitler P. Acute and Chronic Complications of Type 2 Diabetes Mellitus in Children and Adolescents. *Lancet* (2007) 369:1823–31. doi: 10.1016/S0140-6736(07)60821-6
73. Hanley AJ, Williams K, Festa A, Wagenknecht LE, D'Agostino RBJr., Kempf J, et al. Elevations in Markers of Liver Injury and Risk of Type 2 Diabetes: The Insulin Resistance Atherosclerosis Study. *Diabetes* (2004) 53:2623–32. doi: 10.2337/diabetes.53.10.2623
74. Gow A, Southwood CM, Li JS, Pariali M, Riordan GP, Brodie SE, et al. CNS Myelin and Sertoli Cell Tight Junction Strands Are Absent in Osp/claudin-11 Null Mice. *Cell* (1999) 99:649–59. doi: 10.1016/S0092-8674(00)81553-6
75. Jiang X, Ma T, Zhang Y, Zhang H, Yin S, Zheng W, et al. Specific Deletion of Cdh2 in Sertoli Cells Leads to Altered Meiotic Progression and Subfertility of Mice. *Biol Reprod* (2015) 92:79. doi: 10.1095/biolreprod.114.126334
76. Eftekhari A, Vahed SZ, Kavetskyy T, Rameshrad M, Jafari S, Chodari L, et al. Cell Junction Proteins: Crossing the Glomerular Filtration Barrier in Diabetic Nephropathy. *Int J Biol Macromol* (2020) 148:475–82. doi: 10.1016/j.ijbiomac.2020.01.168
77. Chavarro JE, Toth TL, Wright DL, Meeker JD, Hauser R. Body Mass Index in Relation to Semen Quality, Sperm DNA Integrity, and Serum Reproductive Hormone Levels Among Men Attending an Infertility Clinic. *Fertil Steril* (2010) 93:2222–31. doi: 10.1016/j.fertnstert.2009.01.100
78. Palmer NO, Fullston T, Mitchell M, Setchell BP, Lane M. SIRT6 in Mouse Spermatogenesis Is Modulated by Diet-Induced Obesity. *Reprod Fertil Dev* (2011) 23:929–39. doi: 10.1071/RD10326
79. Bakos HW, Mitchell M, Setchell BP, Lane M. The Effect of Paternal Diet-Induced Obesity on Sperm Function and Fertilization in a Mouse Model. *Int J Androl* (2011) 34:402–10. doi: 10.1111/j.1365-2605.2010.01092.x
80. Navarro-Casado L, Juncos-Tobarra MA, Chafer-Rudilla M, de Onzono LI, Blazquez-Cabrera JA, Miralles-Garcia JM. Effect of Experimental Diabetes and STZ on Male Fertility Capacity. Study in rats. *J Androl* (2010) 31:584–92. doi: 10.2164/jandrol.108.007260
81. Crisostomo L, Rato L, Jarak I, Silva BM, Raposo JF, Batterham RL, et al. A Switch From High-Fat to Normal Diet Does Not Restore Sperm Quality But Prevents Metabolic Syndrome. *Reproduction* (2019) 158:377–87. doi: 10.1530/REP-19-0259
82. Fullston T, Palmer NO, Owens JA, Mitchell M, Bakos HW, Lane M. Diet-Induced Paternal Obesity in the Absence of Diabetes Diminishes the Reproductive Health of Two Subsequent Generations of Mice. *Hum Reprod* (2012) 27:1391–400. doi: 10.1093/humrep/des030
83. Crisostomo L, Jarak I, Rato LP, Raposo JF, Batterham RL, Oliveira PF, et al. Inheritable Testicular Metabolic Memory of High-Fat Diet Causes Transgenerational Sperm Defects in Mice. *Sci Rep* (2021) 11:9444. doi: 10.1038/s41598-021-88981-3
84. Ficarro S, Chertihin O, Westbrook VA, White F, Jayes F, Kalab P, et al. Phosphoproteome Analysis of Capacitated Human Sperm. Evidence of Tyrosine Phosphorylation of a Kinase-Anchoring Protein 3 and Valosin-Containing Protein/P97 During Capacitation. *J Biol Chem* (2003) 278:11579–89. doi: 10.1074/jbc.M202325200
85. Bunch DO, Welch JE, Magyar PL, Eddy EM, O'Brien DA. Glyceraldehyde 3-Phosphate Dehydrogenase-S Protein Distribution During Mouse Spermatogenesis. *Biol Reprod* (1998) 58:834–41. doi: 10.1095/biolreprod58.3.834
86. Zatecka E, Castillo J, Elzeinova F, Kubatova A, Ded L, Peknicova J, et al. The Effect of Tetrabromobisphenol A on Protamine Content and DNA Integrity in Mouse Spermatozoa. *Andrology* (2014) 2:910–7. doi: 10.1111/j.2047-2927.2014.00257.x
87. Ausio J. Presence of a Highly Specific Histone H1-Like Protein in the Chromatin of the Sperm of the Bivalve Mollusks. *Mol Cell Biochem* (1992) 115:163–72. doi: 10.1007/BF00230327

Conflict of Interest: The authors declare that the research was conducted in the absence of any commercial or financial relationships that could be construed as a potential conflict of interest.

Publisher's Note: All claims expressed in this article are solely those of the authors and do not necessarily represent those of their affiliated organizations, or those of the publisher, the editors and the reviewers. Any product that may be evaluated in this article, or claim that may be made by its manufacturer, is not guaranteed or endorsed by the publisher.

frontiers in Endocrinology

ORIGINAL RESEARCH
published: 09 November 2021
doi: 10.3389/fendo.2021.774260

DNA Methylation Differences Between Zona Pellucida-Bound and Manually Selected Spermatozoa Are Associated With Autism Susceptibility

Longda Wang[†], *Mengxiang Chen*[†], *Gaofeng Yan* and *Shuhua Zhao*[*]

Department of Reproduction and Genetics, First Affiliated Hospital of Kunming Medical University, Kunming, China

OPEN ACCESS

Edited by:
Honggang Li,
Huazhong University of Science and Technology, China

Reviewed by:
Jana Peknicova,
Institute of Biotechnology (ASCR), Czechia
Janine M. LaSalle,
University of California, Davis, United States
Moshe Szyf,
McGill University, Canada

***Correspondence:**
Shuhua Zhao
kmshh1982@126.com

[†]*These authors have contributed equally to this work and share first authorship*

Specialty section:
This article was submitted to Reproduction, a section of the journal Frontiers in Endocrinology

Received: *11 September 2021*
Accepted: *25 October 2021*
Published: *09 November 2021*

Citation:
Wang L, Chen M, Yan G and Zhao S (2021) DNA Methylation Differences Between Zona Pellucida-Bound and Manually Selected Spermatozoa Are Associated With Autism Susceptibility. Front. Endocrinol. 12:774260. doi: 10.3389/fendo.2021.774260

Children conceived through intracytoplasmic sperm injection (ICSI) have been reported to have a higher risk of many abnormalities and disorders, including autism and intellectual disability, which may be due to bypassing of the natural sperm selection process during ICSI. Zona pellucida (ZP)-bound spermatozoa (ZPBS) have normal morphology and nuclear DNA. Using these spermatozoa for ICSI results in better outcomes compared with conventional ICSI. However, differences besides morphology that exist between sperm selected by ZP and by an embryologist and whether these differences affect the risk of autism in offspring after ICSI are unclear. To explore these questions, we compared genome-wide DNA methylation profiles between ZPBS and manually selected spermatozoa (MSS)using single-cell bisulfite sequencing. Global DNA methylation levels were significantly lower in ZPBS than in MSS. Using gene ontology (GO) analysis, genes overlapping differentially methylated regions (DMRs) were enriched in biological processes involving neurogenesis. Furthermore, we found that 47.8% of autism candidate genes were associated with DMRs, compared with 37.1% of matched background genes (P<0.001). This was mainly because of the high proportion of autism candidate genes with bivalent chromatin structure. In conclusion, bivalent chromatin structure results in large differences in the methylation of autism genes between MSS and ZPBS. ICSI using MSS, which increases the risk of methylation mutations compared with ZPBS, may lead to a higher risk of autism in offspring.

Keywords: sperm, DNA methylation, autism, zona pellucida binding assay, ICSI

INTRODUCTION

Infertility is one of the most common health disorders globally, affecting approximately 15% of the reproductive-aged population, with male infertility accounting for 30-50% of cases (1). A large proportion of these patients undergo intracytoplasmic sperm injection (ICSI), which involves the injection of a single spermatozoon into an oocyte cytoplasm using a glass micropipette. ICSI is currently used far beyond its original application to overcome the most severe forms of male

infertility. In the United States, the use of ICSI for all non-male factor infertility cases increased from 15.4% in 1996 to 66.9% in 2012 (2). Although ICSI may benefit couples by increasing the fertilization rate and decreasing the fertilization failure rate, there are concerns that the indiscriminate use of ICSI may lead to adverse health consequences for the offspring (3). For example, the risks of congenital malformations, epigenetic disorders, chromosomal abnormalities, subfertility, cancer, delayed psychological and neurological development, and impaired cardiometabolic profiles have been shown to be greater in infants born as a result of ICSI than in naturally conceived children (3).

A meta-analysis has reported a higher incidence of intellectual disability and autism, a set of heterogeneous neurodevelopmental conditions characterized by early-onset difficulties in social communication and unusually restricted, repetitive behavior and interests, in children conceived with ICSI (4). Importantly, the association between autism and ICSI is stronger among children conceived with ICSI for non-male factors, suggesting that autism may be associated with factors besides male infertility factors (5).During ICSI, the direct injection of a single spermatozoon into the egg bypasses the processes of natural sperm selection that occur during normal fertilization, which may increase the risk of transmission of genetic or epigenetic mutations in spermatozoa that are naturally unable to bind and enter eggs.

However, evidence supporting the link between ICSI sperm selection and autism is lacking. There is evidence showing the superiority of spermatozoa naturally selected by zona pellucida (ZP), a transparent, extracellular matrix composed of defined glycoproteins and containing receptors that are crucial for sperm-egg binding, sperm selection, and fertilization (6). Compared with unselected sperm, ZP-bound sperm (ZPBS) have significantly higher rates of normal morphology and nuclear DNA (7, 8). ICSI using ZPBS results in improved embryo quality and higher implantation rate than ICSI using spermatozoa manually selected by embryologists (9–11). These differences may be due to the high heterogeneity of spermatozoa even from the same ejaculate. Because of variations in motility and morphology, only 14% of spermatozoa from normozoospermic men can bind to ZP (12). In addition to morphological and functional heterogeneity, sperm heterogeneity is also found at the DNA level. Breuss et al. (13) reported sperm mosaicism using deep whole-genome sequencing and identified single nucleotide, structural, and short tandem repeat variants. Notably, the quantification of sperm mosaicism can stratify the risk of autism recurrence due to *de novo* mutations, and novel mosaic risk variants are able to be transmitted to offspring.

Compared with nucleotide mutations, DNA methylation alterations are more like to occur after exposure to risk factors. Jenkins et al. (14) reported intra-sample heterogeneity of sperm DNA methylation by comparing methylation profiles between high- and low-quality sperm separated using gradient separation. However, even among "high-quality" sperm, the proportion of functionally normal sperm is low (12, 15). Whether DNA methylation differences exist between naturally selected (functionally normal) sperm and unselected sperm or embryologist-selected sperm for ICSI, and whether these differences are related to male infertility and/or the health of children conceived after ICSI, have not been determined. To answer these questions, we compared whole-genome methylation profiles between ZBPS and manually selected spermatozoa (MSS) using single-cell genome-wide bisulfite sequencing. We found significant global DNA methylation differences. We also found that autism candidate genes had a greater number of differentially methylated regions (DMRs), due to the high proportion of autism genes with bivalent chromatin structures.

MATERIALS AND METHODS

Semen Collection, Routine Semen Analysis, and Sperm Purification

Semen samples were collected from four healthy, fertile men. After retrieval, the semen samples were liquefied at a constant temperature of 37°C for 30–60min. After liquefaction, sperm parameters were determined using a computer-assisted sperm analysis system (Sperm Class Analyzer; Microptic, Barcelona, Spain). The spermatozoa were purified by gradient centrifugation using 90% and 45%gradients (SpermGrad; Vitrolife, Kungsbacka, Sweden) at 300 × g for 20min.The resulting supernatant was removed, and the sperm pellets were washed twice with G-IVF medium(G-IVF; Vitrolife, Kungsbacka, Sweden). Finally, the spermatozoa were cultured in G-IVF medium at a concentration of approximately 10×10^6/mL.

Sperm Selection

Immature oocytes were donated by couples who underwent ICSI. To collect ZPBS, approximately 10,000 spermatozoa were co-incubated with two or three immature oocytes in a50 μL G-IVF microdroplet covered with oil in an incubator with 6% CO_2 for 2 hours. These oocytes were then washed in clear G-IVF microdroplets to remove loosely adhered spermatozoa. Sequentially, 30-50 spermatozoa bound to the ZP were collected using a micro-injection needle (Sunlight Medical, Jacksonville, FL, USA), and transferred to a PCR tube containing 10 μL of lysis buffer. To collect the MSS, another fraction of spermatozoa (10,000) was incubated under the same conditions as the ZPBS for 2 hours. Then, 30-50 spermatozoa in the microdroplet were collected by an embryologist trained to perform ICSI using a micro-needle under a microscope at 400× magnification (ZEISS, Jena, Germany), and transferred to a PCR tube containing 10 μL of lysis buffer. Thus, paired ZPBS and MSS samples were collected from one donor (e.g. ZPBS1 and MSS1 were recovered from donor1).

Single-Cell Bisulfite Sequencing

Single-cell bisulfite sequencing (scBS-seq) was performed by Annoroad Gene Tech. Co., Ltd. (Beijing, China). The single-

cell library was prepared as previously described using the following steps: bisulfite conversion, first-strand DNA synthesis, first-strand DNA purification, second-strand DNA synthesis, PCR amplification, library quantification, and sequencing (16). The sequencing data have been deposited in the SRA (https://www.ncbi.nlm.nih.gov/sra) under accession number PRJNA762253.

Data Analysis

Raw reads were trimmed using Trimmomatic (v0.36, http://www.usadellab.org/cms/?page=trimmomatic) to remove the first nine base pairs, contaminating adapter sequences, poor quality read, and the bases at both ends and to discard reads with a length < 36nt (17). Clean reads were mapped to the human genome (Homo_sapiens. GRCh38.87v2) using Bismark (v0.16.3, https://www.bioinformatics.babraham.ac.uk/projects/bismark/) (18). We converted residual Gs in the reads to As and Cs to Ts *in silico* for the reads and the reference genome. We mapped both strands of the reads and the reference genome to each other and chose the best mapped read from four aligned results. We used uniquely mapped reads to calculate methylation rates.

Global methylation rates were calculated as the total number of methylated CpGs divided by the total number of covered CpGs × 100%.Global methylation rates were compared between ZPBS and MSS using Student's t-test. For cluster analysis, we first searched the shared CpGs among all the samples and calculated the methylation rate for each shared CpG. We then constructed the methylation level clusters for these CpGs. For correlation analysis (Pearson's), we used 2kb sliding windows to calculate the methylation rate among the whole genome and calculated Pearson's correlation coefficient between samples. Mean correlations were compared between ZPBS and MSS using Student's t-test. DMRs were identified using the Dispersion Shrinkage for Sequencing data (DSS) with the Wald test, based on the β-binomial distribution model. DMRs were defined as regions containing at least three CpGs, with a methylation rate difference between groups >0.2 and a *q*-value (Bonferroni-corrected P-value) <0.05 by Wald test. The proportion of genes with a DMR were compared by the chi-square test. Gene ontology (GO) analysis of the DMR-associated genes was performed using the Gene Ontology Resource (http://geneontology.org/). Functional elements, including promoters, exons, introns, and untranslated regions (UTRs), were determined using gene transfer format (GTF) files of the reference genome. False discovery rate (FDR)was calculated for each term and terms with FDR <0.05 were considered as significantly enriched. The promoters were defined as regions 2,000 bp upstream of the transcriptional start site. Methylation rate of a functional element was calculated as the number of methylated CpGs in the element divided by the total number of covered CpGs × 100% in this element. Comparisons of the proportion of DMRs among sub-groups at different elements were performed by the chi-square test. The comparisons of methylation levels of DMEs and standard deviations (SDs) between sub-groups were performed using a nonparametric test. A *P* value <0.05 was considered statistically significant. SPSS 19.0 (SPSS Inc., Chicago, IL, USA) and R (19) were used for data analysis.

Autism candidate genes were downloaded from the SFARI database (https://gene.sfari.org/database/human-gene/). Autism genes are significantly longer than random background genes with more introns and exons, which have a great influence to DMR rate. To avoid this bias, a three-to-one nearest neighbor caliper matching method without replacement was used to match the numbers of mapped introns and exons between the background and autism genes with a 0.2 SD caliper. Only protein-coding genes were included in the matching.

RESULTS

Sperm samples were donated by four men at the ages between 29 and 31. All of these men had normal semen parameters according to the WHO guidelines (2010) (**Table 1**).The genome-wide methylation level of each ZPBS and MSS sample with 30-50 spermatozoa was detected by bisulfite sequencing. There were 104 to 152 million clean reads per sample, and more than 50% of the clean reads were mapped to the reference genome (**Supplementary Table 1**). For each sample, 45.6% to 48.6% of the CpGs in the genome were covered, and about 30% CpGs were covered twice or more times (**Supplementary Table 2**). The average of mean coverage for covered CpGs was 2.6.Sample purity was tested by calculating the methylation levels of imprinted genes. As expected, imprinting control region 1 (ICR1) of the paternally imprinted gene,*H19*, was hyper-methylated, while the DMR of the maternally imprinted gene, *MEST*, was hypo-methylated in all samples (**Supplementary Figure 1**). There were no significant differences in the methylation rates of ICR1 (ZPBS *vs* MSS: 95.0 ± 2.2% *vs* 89.9 ± 4.8%, *P*>0.05) or *MEST* (ZPBS *vs* MSS: 3.4 ± 1.7% *vs* 2.4 ± 1.3%, *P*>0.05) between groups.

To compare the DNA methylation profiles of different samples, the methylation rates of CpGs covered in all eight samples were calculated and clustered. The results showed that the ZPBS and MSS from the same ejaculate clustered together (**Supplementary Figure 2A**). We also compared the correlations between each sample for the eight samples and found that the correlation coefficient was slightly higher among ZPBS samples than MSS samples (0.822*vs*0.807, *P*=0.045, **Supplementary Figure 2B**). As a feature of single-cell methylation sequencing, the methylation rates of most CpGs were either 0% or 100% (**Figure 1A**). The global methylation levels of ZPBS were

TABLE 1 | Donor characteristics.

Donor	Age (y)	BMI (km/m^2)	Volume (mL)	Sperm concentration (x10^6/mL)	Sperm motility (%)	PR (%)
1	31	20.8	2.3	98.3	77.7	41.9
2	30	19.5	2	134.7	85.7	57.3
3	29	20.8	6.7	43.3	74	49.7
4	29	19.6	6.4	164.7	79.8	42.4

BMI, body mass index; PR, progressive motility rate.

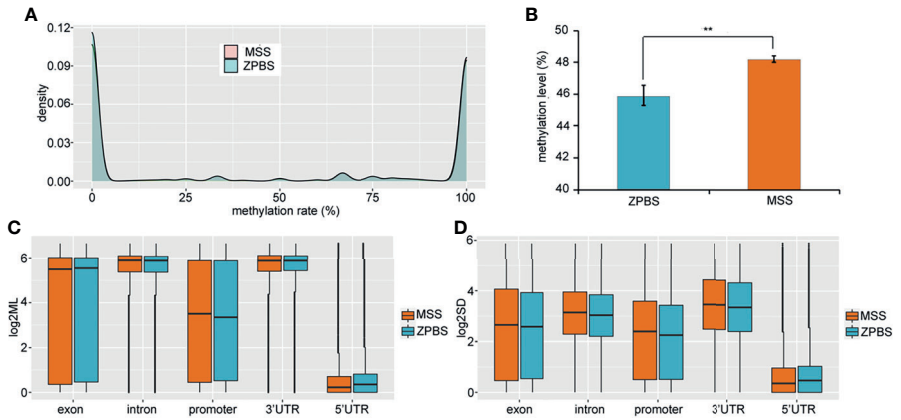

FIGURE 1 | The genome-wide methylation pattern of ZPBS and MSS. **(A)** The distribution of methylation levels in shared CpGs among samples. **(B)** A comparison of global methylation levels between ZPBS and MSS. **(C)** A comparison of methylation rates in different functional elements. **(D)** A comparison of standard deviations of element methylation levels among samples between ZPBS and MSS.**< 0.01.

significantly lower than those of MSS (**Figure 1B**). We further compared the methylation levels of different functional elements. The introns and 3′-UTRs were hyper-methylated while the 5′-UTRs were hypo-methylated (**Figure 1C**). The methylation levels of the exons and promoters were diverse, with wide ranges (**Figure 1C**). To compare inter-sample heterogeneity, we calculated the SDs of each element for ZPBS and MSS samples. The SDs in ZPBS were lower in exons, introns, promoters, and 3′-UTRs but not 5′-UTRs, suggesting lower inter-sample heterogeneity in most elements of ZPBS compared with those of MSS (**Figure 1D**).

A DMR was defined as a region including at least three CpGs with significantly different DNA methylation levels between the ZPBS and MSS groups. There were 11,175 DMRs identified throughout the whole genome, 52.3% of which were hypo-methylated in ZPBS (**Supplementary Table 3**). A DMR-related gene was defined as one gene overlapping with at least one DMR in its promoter and/or gene body. Of 7,641 DMR-related genes, 5,656 genes were annotated for biological processes in a GO analysis. The top five enriched GO terms were anterior/posterior axon guidance (GO:0033564), cerebrospinal fluid secretion (GO:0033326), synaptic transmission, glycinergic (GO:0060012), transmembrane receptor protein tyrosine phosphatase signaling pathway (GO:0007185), and semaphorin-plexin signaling pathway involved in neuron projection guidance (GO:1902285). These five biological processes included 32 DMR-associated genes (**Supplementary Table 4**), of which seven genes, including *TRIO*(high confidence),*DCC*(strong candidate), *PLXNA4*(strong candidate), *PLXNB1*(strong candidate), *GLRA2*(suggestive evidence), *NRP2*(suggestive evidence), and *PLXNA3*(suggestive evidence), were autism candidate genes reported in the SFARI database (https://gene.sfari.org/database/human-gene/).To avoid enrichment biases derived by gene length, genes with DMRs in promoters were analyzed by GO. These genes were also enriched in biological processes involved in neural development (**Figure 2A**). Then, genes with ZPBS-hyper-methylated DMRs and ZPBS-hypo-methylated DMRs in promoter were enriched separately. Interestingly, hyper-DMR related genes were enriched in terms related with neural development (**Figure 2B**), while hypo-DMR related genes were enriched in terms involving in ATP synthesis (**Figure 2C**).

To explore the relationship between sperm selection and the risk of autism in children conceived by ICSI, we analyzed the methylation status of 1,003 autism candidate genes reported in the SFARI database (**Supplementary Table 5**). We first compared the methylation profiles of autism genes between ZPBS and MSS, and found that the methylation rates of ZPBS functional elements showed more centralized profiles at about 68% compared with MSS (**Supplementary Figure 3**), indicating a lower methylation variability in ZPBS. Then, we compared the proportions of DMR-related genes between autism and background genes. We found more autism genes with DMRs in their promoter (**Figure 3A**). In accordance with GO analysis, there were more promoters overlapping with hyper-DMRs (**Figure 3B**), but not hypo-DMRs (**Figure 3C**), in autism genes compared with background genes.

Just like genes with DMRs in promoters, We also found more genes with DMRs in promoters and/or gene bodies in autism candidates than background genes (**Figure 4A**). However, as autism genes were significantly longer than random genes, there were more introns and exons in autism genes, which would great influence the number of DMRs. To avoid this bias, we defined a group of background genes with matched number of introns and exons (**Supplementary Table 6**). A total of2806 background protein-coding genes were matched to 951autism genes. The rate of DMR-related genes was still higher in these autism genes (47.8%) than matched background genes (37.1%) (**Figure 4B**).

Schrott et al. (20) showed that autism candidate genes are significantly enriched for bivalent chromatin structures, which makes the methylation of these genes vulnerable to environmental exposure. We sought to determine whether this

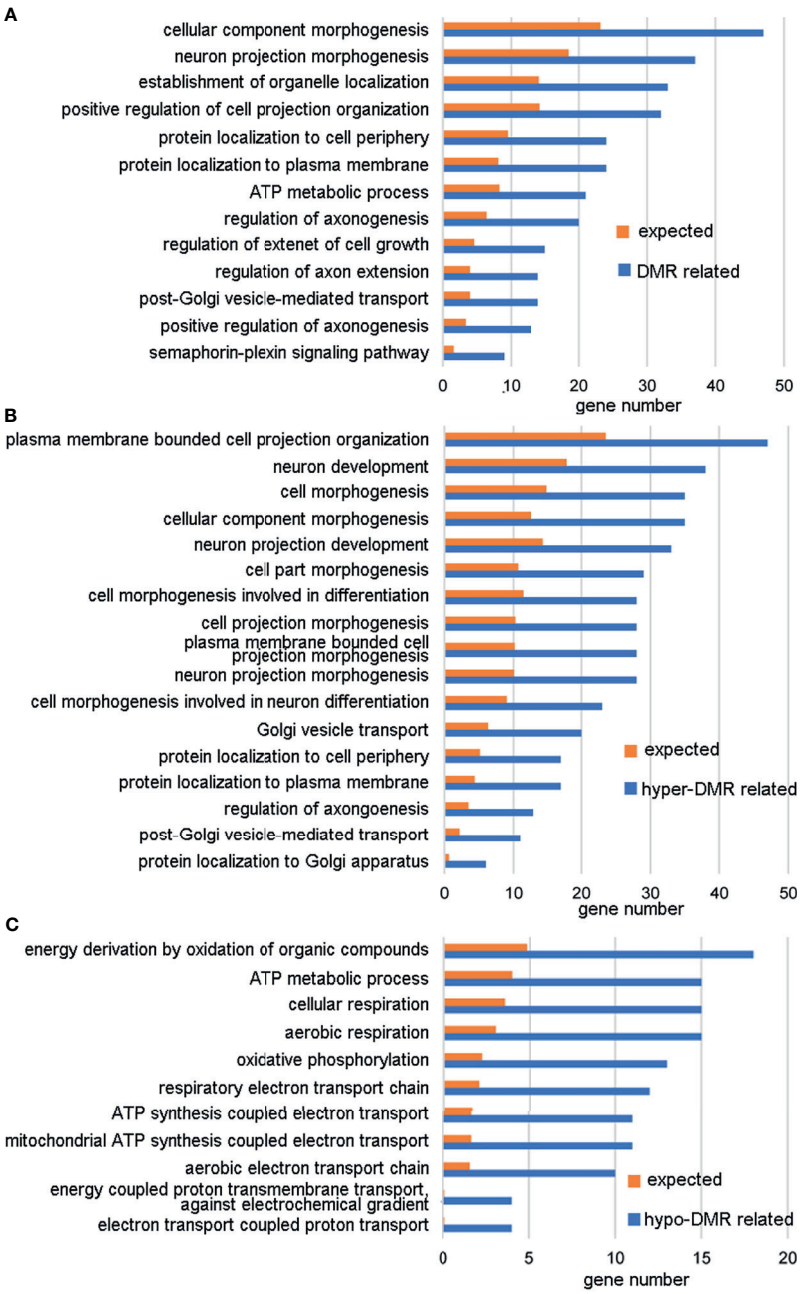

FIGURE 2 | GO analysis of genes with DMRs in promoters. **(A)** GO terms with enrichment ≥2 and FDR < 0.05 for genes with hyper-DMRs and/or hypo-DMRs in promoters. **(B)** GO terms with enrichment ≥2 and FDR < 0.05 for genes with hyper-DMRs in promoters. **(C)** GO terms with enrichment ≥ 2 and FDR < 0.05 for genes with hypo-DMRs in promoters.

bivalent structure also contributed to the higher DMR rate in autism genes between ZPBS and MSS. Indeed, there was a higher proportion of genes with bivalent chromatin (21) among autism genes than among matched background genes (**Figure 4C**). Moreover, the proportion of genes with DMRs was higher among genes with bivalent structures, both for autism candidate genes and matched background genes (**Figure 4D**).

DISCUSSION

The spermatozoa are a group of specialized cells with high heterogeneity. DNA methylation levels vary between different ejaculates from the same man and between high- and low-quality fractions of the same ejaculate (14). The morphological or functional differences between spermatozoa from the same ejaculate may be

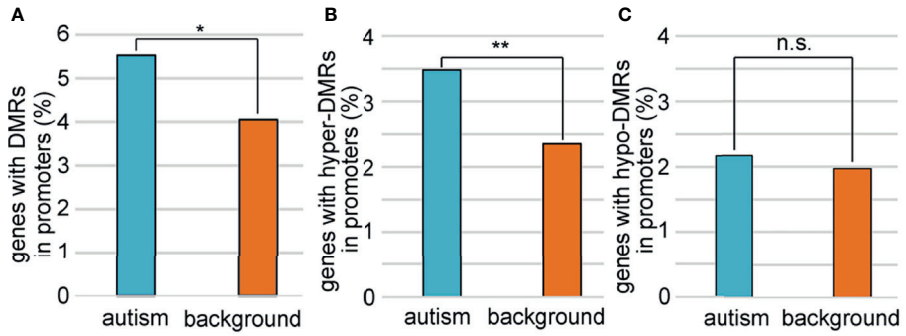

FIGURE 3 | Comparisons of genes with DMRs in promoters between autism and background genes. **(A)** The proportion of genes with DMRs in promoters was higher among autism genes than among background genes. **(B)**The proportions of genes with hyper-DMRs in promoter were higher among autism genes than among background genes. **(C)** The proportions of genes with hypo-DMRs in promoter were similar among autism genes with among background genes. *P < 0.05; **P < 0.01; n.s., not significant.

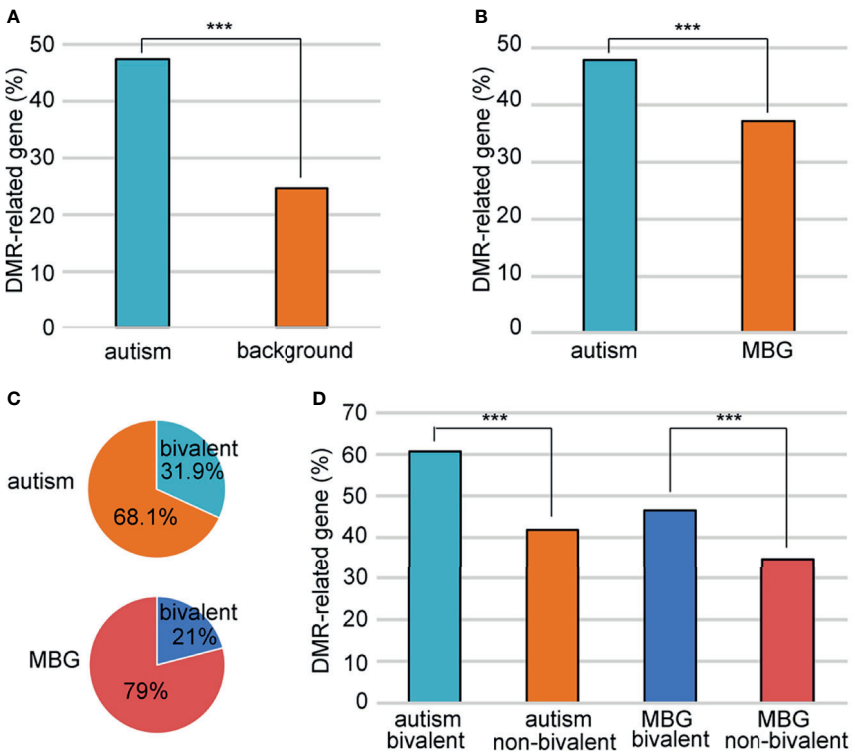

FIGURE 4 | Association of the bivalent chromatin structure and high DMR rates. **(A)** A comparison of DMR-related gene rate between autism and background genes. **(B)** A comparison of DMR-related gene rate between autism and matched background genes (MBG). **(C)** Bivalent chromatin structure was more common in autism genes than in background genes. **(D)** Bivalent chromatin structure was associated with a higher frequency of DMRs. MBG, matched background genes; ***P < 0.001.

due to epigenetic factors. We compared the genome-wide DNA methylation profiles between ZPBS and MSS and found global methylation differences and differences at a number of specific genes. We also found that these methylation differences were enriched in autism genes, which provides an explanation for the higher rate of autism in offspring conceived *via* ICSI.

During spermatogenesis, the genome undergoes demethylation and *de novo* methylation (22). Aberrant methylation during this process affects gene expression, imprinting, protamine transition, and chromosome structure, leading to abnormal sperm count, motility, and morphology (23). Several studies have linked aberrant DNA methylation in

sperm to a decrease in semen parameters. Houshdaran et al. (24) found that sperm DNA is hyper-methylated in samples with poor sperm concentration, motility, and morphology. Sujit et al. (25) reported that the sperm DNA methylation levels of spermatogenesis-related genes are higher in men with oligozoospermia than in men with normal semen parameters. These results are consistent with our findings that global DNA methylation levels were higher in MSS than in ZPBS (Fig. 1B). In addition, genes with ZPBS-hypo-DMRs in promoters were significantly enriched in processes involving in ATP synthesis which was essential for sperm motility, acrosin activity, acrosome reaction capability and chromatin integrity (26–28).Thus, DNA hyper-methylation in sperm may affect energy synthesis leading to reduced sperm fertilization ability.

Several studies have suggested that children born through ICSI have an increased risk of autism and intellectual disability, which may be influenced by paternal characteristics linked to male infertility or the processes of ICSI treatment (4, 5, 29, 30). Kissin et al. (5) reported a higher incidence of autism in children conceived after ICSI compared with those conceived *via* conventional IVF in a cohort study of 42,383 children conceived with assisted reproductive technology (1997–2006). Importantly, they further reported that the association between autism and ICSI was stronger among children conceived with ICSI for non-male factors, suggesting that a diagnosis of male infertility was not associated with an increased risk of autism. These results may be explained by the hypothesis that the bypassing of the natural sperm selection process during ICSI may result in the injection of a spermatozoon carrying genetic or epigenetic mutations related to autism, leading to an increased risk of autism. Our study provided evidence supporting this hypothesis. On one hand, the proportion of autism candidate genes with at least one DMR between ZPBS and MSS was significantly higher than the corresponding proportion among matched background genes (**Figure 4B**). On the other hand, genes with DMRs in promoter were enriched in functions related to neuron projection, axonogenesis, axon extension, semaphoring-plexin signaling pathway (**Figure 2**). These processes are all closely associated with the prevalence of autism.

Few studies have linked DNA methylation alterations in autism candidate genes with sperm selection during fertilization. However, there is evidence for a relationship between autism and locus-specific and genome-wide changes in DNA methylation. Garrido et al. (31) compared genome-wide methylation levels between sperm samples obtained from fathers of children with and without autism and found that genes associated with the DMRs are linked to previously known autism spectrum disorder genes and other neurobiology-related genes. Advanced paternal age has been suggested as a risk factor for autism (32). Global or locus-specific DNA methylation levels are reported to increase in sperm as men age (33). Some of the age-related changes in sperm DNA methylation occur at genes associated with neuropsychiatric disorders (33).

The prevalence of autism is increasing. In the United States, the prevalence reported by the Centers for Disease Control and Prevention was 1 in 150 in 2000, but reached 1 in 54 in 2016 (https://www.cdc.gov/ncbddd/autism/data.html). Environmental factors are thought to contribute to the increased prevalence of autism. Epigenetic factors play an important role in bridging the environment and disease. Two studies from one group reported that the methylation of autism candidate genes in rat sperm is affected by environmental exposure to tetrahydrocannabinol and nicotine (20, 34). They also discovered that autism candidate genes are significantly enriched for bivalent chromatin structure and proposed that this configuration may increase the vulnerability of genes in sperm to disrupted methylation (20). In the current study, a higher rate of DMRs between MSS and ZPBS was found in autism genes than in matched background genes, suggesting higher DNA methylation variability of autism genes in sperm (**Figure 4B**). This may be the result of special methylation features of autism genes. Indeed, we found that the number of DMRs was higher in autism candidate genes with a bivalent structure (**Figure 4D**).

The above findings provide insights into the reason for the association between ICSI and the risk of autism in offspring. The methylation of autism candidate genes in sperm is vulnerable because of the unique bivalent chromatin structure. This susceptibility of autism genes leads to higher DNA methylation heterogeneity between spermatozoa. Spermatozoa selected by an embryologist for ICSI escape the natural selection process and have a higher risk of carrying more DNA methylation alterations in autism candidate genes, resulting in abnormal expression of these genes and eventually leading to a higher risk of autism in offspring conceived by ICSI using these spermatozoa.

To the best of our knowledge, this is the first study to compare methylation levels between ZPBS and MSS. Using scBS-seq, approximately half of all CpGs were detected. However, due to the limited number of ZPBS samples and the nature of scBS-seq, the sequencing depth was limited. The mean coverage for covered CpGs was only 2.6. Therefore, intermediate methylation information was missing for a lot of single CpGs. However, the methylation levels of most CpGs in spermatozoa have been reported to be either 0 or 100% (35, 36), which may eliminate the potential bias introduced by this sequencing technique.

The global methylation levels in current study were about 46-48% which was similar with those in previous studies using Infinium Human Methylation beadchip and reduced representation bisulfite sequencing (RRBS) (35, 36). But comparing with whole genome bisulfite sequencing (WGBS), the global methylation levels in this study were much lower, which may due to the uneven distribution of reads (35, 37). It has been reported that the enrichment towards exons, promoters and CGIs is exaggerated in scBS-Seq libraries (38). Promoters and CGIs are hypo-methylated in sperm (39). Chan et al. (35) have compared methylation levels of sperm using WGBS between two studies, and found that the average methylation level was lower (69.4% *vs* 80.5%) in the study (WGBS-Prev) with lower coverage rate. This result was explained by the fact that a greater proportion of highly covered sites from the WGBS-Prev was found within promoter-transcriptional start site (TSS) regions as well as within CpG islands.

In summary, this study compared the methylation profiles of ZP-bound and manually selected spermatozoa and found differential methylation levels globally and at specific loci. DMR-related genes were enriched in biological processes related to the onset of autism. The frequency DMRs was higher in autism genes as a result of the specific bivalent structure of these genes. Our results provide an explanation for the higher risk of autism in offspring conceived by ICSI, and suggest that it should be taken seriously in selecting ICSI over conventional IVF for non-male factor infertility during assisted reproduction technology.

DATA AVAILABILITY STATEMENT

The datasets presented in this study can be found in online repositories. The names of the repository/repositories and accession number(s) can be found in the article/**Supplementary Material**.

ETHICS STATEMENT

The studies involving human participants were reviewed and approved by Ethics Committee of the First Affiliated Hospital of Kunming Medical University. The patients/participants provided their written informed consent to participate in this study.

AUTHOR CONTRIBUTIONS

LW and MC conducted the research. All authors provided contributions to analysis and interpretation of data. SZ designed and supervised the study, and drafted the manuscript. LW and MC contributed equally as corresponding authors. All authors contributed to the article and approved the submitted version.

FUNDING

This work was supported by the Natural National Science Foundation of China, under grant number 81760269, the Yunnan Provincial Science and Technology Department, under grant numbers 2018FB126 and 2017HB046, and the Health Commission of Yunnan Province, under grant number D-2017021. The open access publication fees were supported by the First Affiliated Hospital of Kunming Medical University.

SUPPLEMENTARY MATERIAL

The Supplementary Material for this article can be found online at: https://www.frontiersin.org/articles/10.3389/fendo.2021.774260/full#supplementary-material

REFERENCES

1. Ferlin A, Raicu F, Gatta V, Zuccarello D, Palka G, Foresta C. Male Infertility: Role of Genetic Background. *Reprod BioMed Online* (2007) 14(6):734–45. doi: 10.1016/s1472-6483(10)60677-3
2. Boulet SL, Mehta A, Kissin DM, Warner L, Kawwass JF, Jamieson DJ. Trends in Use of and Reproductive Outcomes Associated With Intracytoplasmic Sperm Injection. *JAMA* (2015) 313(3):255. doi: 10.1001/jama.2014.17985
3. Esteves SC, Roque M, Bedoschi G, Haahr T, Humaidan P. Intracytoplasmic Sperm Injection for Male Infertility and Consequences for Offspring. *Nat Rev Urol* (2018) 15(9):535–62. doi: 10.1038/s41585-018-0051-8
4. Djuwantono T, Aviani JK, Permadi W, Achmad TH, Halim D. Risk of Neurodevelopmental Disorders in Children Born From Different ART Treatments: A Systematic Review and Meta-Analysis. *J Neurodev Disord* (2020) 12(1):33. doi: 10.1186/s11689-020-09347-w
5. Kissin DM, Zhang Y, Boulet SL, Fountain C, Bearman P, Schieve L, et al. Association of Assisted Reproductive Technology (ART) Treatment and Parental Infertility Diagnosis With Autism in ART-Conceived Children. *Hum Reprod* (2015) 30(2):454–65. doi: 10.1093/humrep/deu338
6. Oehninger S. Biochemical and Functional Characterization of the Human Zona Pellucida. *Reprod BioMed Online* (2003) 7(6):641–8. doi: 10.1016/s1472-6483(10)62086-x
7. Liu DY, Baker HW. Acrosome Status and Morphology of Human Spermatozoa Bound to the Zona Pellucida and Oolemma Determined Using Oocytes That Failed to Fertilize *In Vitro*. *Hum Reprod* (1994) 9 (4):673–9. doi: 10.1093/oxfordjournals.humrep.a138570
8. Liu DY, Baker HWG. Human Sperm Bound to the Zona Pellucida Have Normal Nuclear Chromatin as Assessed by Acridine Orange Fluorescence. *Hum Reprod* (2007) 22(6):1597–602. doi: 10.1093/humrep/dem044
9. Jin R, Bao J, Tang D, Liu F, Wang G, Zhao Y, et al. Outcomes of Intracytoplasmic Sperm Injection Using the Zona Pellucida-Bound Sperm or Manually Selected Sperm. *J Assist Reprod Gen* (2016) 33(5):597–601. doi: 10.1007/s10815-016-0676-6
10. Liu F, Qiu Y, Zou Y, Deng Z, Yang H, Liu DY. Use of Zona Pellucida–Bound Sperm for Intracytoplasmic Sperm Injection Produces Higher Embryo Quality and Implantation Than Conventional Intracytoplasmic Sperm Injection. *FertilSteril* (2011) 95(2):815–8. doi: 10.1016/j.fertnstert.2010.09.015
11. Paes AFDB, Iaconelli AJ, Cassia SDFR, Madaschi C, Semiao-Francisco L, Borges EJ. Outcome of ICSI Using Zona Pellucida-Bound Spermatozoa and Conventionally Selected Spermatozoa. *Reprod BioMed Online* (2009) 19 (6):802–7. doi: 10.1016/j.rbmo.2009.09.020
12. Liu DY, Garrett C, Baker HW. Low Proportions of Sperm Can Bind to the Zona Pellucida of Human Oocytes. *Hum Reprod* (2003) 18(11):2382–9. doi: 10.1093/humrep/deg456
13. Breuss MW, Antaki D, George RD, Kleiber M, James KN, Ball LL, et al. Autism Risk in Offspring Can be Assessed Through Quantification of Male Sperm Mosaicism. *Nat Med* (2020) 26(1):143–50. doi: 10.1038/s41591-019-0711-0
14. Jenkins TG, Aston KI, Trost C, Farley J, Hotaling JM, Carrell DT. Intra-Sample Heterogeneity of Sperm DNA Methylation. *Mol Hum Reprod* (2015) 21(4):313–9. doi: 10.1093/molehr/gau115
15. Liu DY, Stewart T, Baker HW. Normal Range and Variation of the Zona Pellucida-Induced Acrosome Reaction in Fertile Men. *FertilSteril* (2003) 80 (2):384–9. doi: 10.1016/s0015-0282(03)00603-4
16. Clark SJ, Smallwood SA, Lee HJ, Krueger F, Reik W, Kelsey G. Genome-Wide Base-Resolution Mapping of DNA Methylation in Single Cells Using Single-Cell Bisulfite Sequencing (scBS-Seq). *Nat Protoc* (2017) 12(3):534–47. doi: 10.1038/nprot.2016.187
17. Bolger AM, Lohse M, Usadel B. Trimmomatic: A Flexible Trimmer for Illumina Sequence Data. *Bioinformatics* (2014) 30(15):2114–20. doi: 10.1093/bioinformatics/btu170
18. Krueger F, Andrews SR. Bismark: A Flexible Aligner and Methylation Caller for Bisulfite-Seq Applications. *Bioinformatics* (2011) 27(11):1571–2. doi: 10.1093/bioinformatics/btr167
19. R core team. *R: A Language and Environment for Statistical Computing*. (2021).

20. Schrott R, Rajavel M, Acharya K, Huang Z, Acharya C, Hawkey A, et al. Sperm DNA Methylation Altered by THC and Nicotine: Vulnerability of Neurodevelopmental Genes With Bivalent Chromatin. *Sci Rep Uk* (2020) 10 (1):16022. doi: 10.1038/s41598-020-72783-0
21. Court F, Arnaud P. An Annotated List of Bivalent Chromatin Regions in Human ES Cells: A New Tool for Cancer Epigenetic Research. *Oncotarget* (2017) 8(3):4110–24. doi: 10.18632/oncotarget.13746
22. Trasler JM. Epigenetics in Spermatogenesis. *Mol Cell Endocrinol* (2009) 306 (1-2):33–6. doi: 10.1016/j.mce.2008.12.018
23. Rajender S, Avery K, Agarwal A. Epigenetics, Spermatogenesis and Male Infertility. *Mutat Res* (2011) 727(3):62–71. doi: 10.1016/j.mrrev.2011.04.002
24. Houshdaran S, Cortessis VK, Siegmund K, Yang A, Laird PW, Sokol RZ, et al. Widespread Epigenetic Abnormalities Suggest a Broad DNA Methylation Erasure Defect in Abnormal Human Sperm. *PloS One* (2007) 2(12):e1289–9. doi: 10.1371/journal.pone.0001289
25. Sujit KM, Singh V, Trivedi S, Singh K, Gupta G, Rajender S. Increased DNA Methylation in the Spermatogenesis-Associated (SPATA) Genes Correlates With Infertility. *Andrology-Us* (2020) 8(3):602–9. doi: 10.1111/andr.12742
26. Zhang G, Wang Z, Ling X, Zou P, Yang H, Chen Q, et al. Mitochondrial Biomarkers Reflect Semen Quality: Results From the MARCHS Study in Chongqing, China. *PloS One* (2016) 11(12):e0168823. doi: 10.1371/journal.pone.0168823
27. Zhang G, Yang W, Zou P, Jiang F, Zeng Y, Chen Q, et al. Mitochondrial Functionality Modifies Human Sperm Acrosin Activity, Acrosome Reaction Capability and Chromatin Integrity. *Hum Reprod* (2019) 34(1):3–11. doi: 10.1093/humrep/dey335
28. Paoli D, Gallo M, Rizzo F, Baldi E, Francavilla S, Lenzi A, et al. Mitochondrial Membrane Potential Profile and Its Correlation With Increasing Sperm Motility. *FertilSteril* (2011) 95(7):2315–9. doi: 10.1016/j.fertnstert.2011.03.059
29. Knoester M, Helmerhorst FM, van der Westerlaken LAJ, Walther FJ, Veen S. Matched Follow-Up Study of 5 8-Year-Old ICSI Singletons: Child Behaviour, Parenting Stress and Child (Health-Related) Quality of Life. *Hum Reprod* (2007) 22(12):3098–107. doi: 10.1093/humrep/dem261
30. Sandin S, Nygren KG, Iliadou A, Hultman CM, Reichenberg A. Autism and Mental Retardation Among Offspring Born After. *Vitro Fertilization JAMA* (2013) 310(1):75–84. doi: 10.1001/jama.2013.7222
31. Garrido N, Cruz F, Egea RR, Simon C, Sadler-Riggleman I, Beck D, et al. Sperm DNA Methylation Epimutation Biomarker for Paternal Offspring Autism Susceptibility. *Clin Epigenet* (2021) 13(1):6. doi: 10.1186/s13148-020-00995-2
32. Oldereid NB, Wennerholm U, Pinborg A, Loft A, Laivuori H, Petzold M, et al. The Effect of Paternal Factors on Perinatal and Paediatric Outcomes: A Systematic Review and Meta-Analysis. *Hum Reprod Update* (2018) 24(3):320–89. doi: 10.1093/humupd/dmy005
33. Jenkins TG, Aston KI, Pflueger C, Cairns BR, Carrell DT. Age-Associated Sperm DNA Methylation Alterations: Possible Implications in Offspring Disease Susceptibility. *PloS Genet* (2014) 10(7):e1004458. doi: 10.1371/journal.pgen.1004458
34. Schrott R, Acharya K, Itchon-Ramos N, Hawkey AB, Pippen E, Mitchell JT, et al. Cannabis Use Is Associated With Potentially Heritable Widespread Changes in Autism Candidate Genedlgap2 DNA Methylation in Sperm. *Epigenetics-Us* (2020) 15(1-2):161–73. doi: 10.1080/15592294.2019.1656158
35. Chan D, Shao X, Dumargne M, Aarabi M, Simon M, Kwan T, et al. Customized MethylC-Capture Sequencing to Evaluate Variation in the Human Sperm DNA Methylome Representative of Altered Folate Metabolism. *Environ Health Persp* (2019) 127(8):87002. doi: 10.1289/EHP4812
36. Jenkins TG, James ER, Alonso DF, Hoidal JR, Murphy PJ, Hotaling JM, et al. Cigarette Smoking Significantly Alters Sperm DNA Methylation Patterns. *Andrology-Us* (2017) 5(6):1089–99. doi: 10.1111/andr.12416
37. Guo H, Zhu P, Yan L, Li R, Hu B, Lian Y, et al. The DNA Methylation Landscape of Human Early Embryos. *Nature* (2014) 511(7511):606–10. doi: 10.1038/nature13544
38. Smallwood SA, Lee HJ, Angermueller C, Krueger F, Saadeh H, Peat J, et al. Single-Cell Genome-Wide Bisulfite Sequencing for Assessing Epigenetic Heterogeneity. *Nat Methods* (2014) 11(8):817–20. doi: 10.1038/nmeth.3035
39. Dere E, Huse S, Hwang K, Sigman M, Boekelheide K. Intra- and Inter-Individual Differences in Human Sperm DNA Methylation. *Andrology-Us* (2016) 4(5):832–42. doi: 10.1111/andr.12170

Conflict of Interest: The authors declare that the research was conducted in the absence of any commercial or financial relationships that could be construed as a potential conflict of interest.

frontiers in Endocrinology

REVIEW
published: 23 November 2021
doi: 10.3389/fendo.2021.788321

An Update on the Relationship of SARS-CoV-2 and Male Reproduction

Juncen Guo[1,2], *Kai Sheng*[3,4], *Sixian Wu*[1,2], *Hanxiao Chen*[1,2] *and Wenming Xu*[1,2]*

[1] Sichuan University-The Chinese University of Hong Kong (SCU-CUHK) Joint Laboratory for Reproductive Medicine, Key Laboratory of Obstetric, Gynaecologic and Paediatric Diseases and Birth Defects of Ministry of Education, West China Second University Hospital, Sichuan University, Chengdu, China, [2] Reproductive Endocrinology and Regulation Laboratory, Department of Obstetric and Gynaecologic, West China Second University Hospital, Sichuan University, Chengdu, China, [3] Department of Orthopedic Surgery, Shriners Hospital for Children, Montreal, QC, Canada, [4] Orthopaedic Research Laboratory, Department of Orthopedic Surgery, McGill University, Montreal, QC, Canada

OPEN ACCESS

Edited by:
Honggang Li,
Huazhong University of Science and Technology, China

Reviewed by:
Laura Maria Mongioì,
University of Catania, Italy
Andrea Sansone,
University of Rome Tor Vergata, Italy

***Correspondence:**
Wenming Xu
xuwenming@scu.edu.cn

Specialty section:
This article was submitted to Reproduction, a section of the journal Frontiers in Endocrinology

Received: *02 October 2021*
Accepted: *29 October 2021*
Published: *23 November 2021*

Citation:
Guo J, Sheng K, Wu S, Chen H and Xu W (2021) An Update on the Relationship of SARS-CoV-2 and Male Reproduction. Front. Endocrinol. 12:788321. doi: 10.3389/fendo.2021.788321

Since the outbreak of the COVID-19, up to now, infection cases have been continuously rising to over 200 million around the world. Male bias in morbidity and mortality has emerged in the COVID-19 pandemic. The infection of SARS-CoV-2 has been reported to cause the impairment of multiple organs that highly express the viral receptor angiotensin-converting enzyme 2 (ACE2), including lung, kidney, and testis. Adverse effects on the male reproductive system, such as infertility and sexual dysfunction, have been associated with COVID-19. This causes a rising concern among couples intending to have a conception or who need assisted reproduction. To date, a body of studies explored the impact of SARS-CoV-2 on male reproduction from different aspects. This review aims to provide a panoramic view to understand the effect of the virus on male reproduction and a new perspective of further research for reproductive clinicians and scientists.

Keywords: COVID-19, male reproduction, angiotensin-converting enzyme 2, erectile dysfunction, drug toxicity

INTRODUCTION

At the end of 2019, a novel coronavirus, named SARS-CoV-2, was found in patients with severe pneumonia and has become a worldwide pandemic with a rapidly growing number of infection cases up to now. SARS-CoV-2 and SARS-CoV-1 belong to the same coronavirus subfamily named the beta coronaviruses (1, 2). SARS-CoV-2 and SARS-CoV-1 share the same receptors named ACE2 residing in many different human organs (3). Previously, several research groups have revealed that SARS-CoV-1 patients have post-infection reproductive system complications (4, 5). Thus, in the present review, we demonstrate the molecular mechanism of the viral tropism, post-infected pathological features, and potentially detrimental effects in the male reproductive system in the

COVID-19 patients. The review aims to draw appropriate conclusions about the impact of COVID-19 on male reproduction and put forward some new ideas for further research.

THE MOLECULAR MECHANISM OF THE INFECTION IN THE MALE REPRODUCTIVE SYSTEM

In early 2020, it was demonstrated that the transmission mode of SARS-CoV-2 is mainly by droplets containing pathogens in the air (6). Droplets enter the nose and mouth and then carry pathogens to infect the upper respiratory tract. Firstly, SARS-CoV-2 entry into the host cells depends on the recognition of the angiotensin-converting enzyme 2 (ACE2) receptor (7). Since viral spike protein binds to the extracellular domain of ACE2, another critical factor, transmembrane protease serine protease-2 (TMPRSS2), mediates cleavage at the S1/S2 site of S protein, which is indispensable for viral membrane fusion (7). The viral RNA genome begins to replicate and instruct host-cell ribosomes to translate its structural proteins and polyproteins for viral capsid after SARS-CoV-2 enters the host cells (8). Viral particles are assembled in reticulum-Golgi intermediate compartment (ERGIC) (9) and subsequently are released by means of exocytosis for the spread of the infection (8).

ACE2 is regarded as the most essential key for viral entry; thus, expression patterns of ACE2 in different tissues and organs have become a focus in many research works, which may suggest potential routes of SARS-CoV-2 infection in humans. Previous studies have shown that ACE2 expression is abundant in the testis (10, 11). The proportion of ACE2-positive cells in the testis is more than that in the lung, which indicated that the testis might serve as a high-risk potential infection organ (12). Using single-cell RNA sequencing (scRNA-seq), it is reported that ACE2 is primarily expressed in Sertoli cells, which have the highest expression level, and then Leydig cells (LCs) and spermatogonia (13). It suggests a possible tropism of SARS-CoV-2 to the testis. The virus may infect Sertoli cells, disturbing the physiological process in which Sertoli cells control the germ cell environment by the secretion and transport of nutrients and regulatory factors, which is strongly related to spermatogenesis. Sertoli cells also play an important role in constituting the blood–testis barrier (BTB) (14). The BTB gives testes immune privilege separating autoantigens and host immune cells from germ cells and Sertoli cells. The Leydig cells are located in the interstitium of the testis where they are most vulnerable within the testis against the virus. LCs secrete androgen, which is indispensable in spermatogenesis and in maintaining secondary sex characteristics (15). Moreover, LCs also regulate testicular macrophage and lymphocyte numbers (16). Collectively, if SARS-CoV-2 infects these types of cells, the disruption of spermatogenesis will occur. In addition, a human sperm proteomic database reveals the presence of ACE2 in the human sperm while it is not detected through scRNA-seq (17). Furthermore, TMPRSS2 is expressed abundantly in prostasomes and is released into the seminal fluid from the prostate gland at ejaculation (18), which makes it possible for sperm to be vulnerable to SARS-CoV-2 infection.

Besides, the viral infection of cells requires cofactors, such as TMPRSS2 (19) and CD147 (20), to promote its invasion. TMPRSS2 is highly expressed in the kidney, epididymis, prostate, and seminal vesicles. TMPRSS2 expression was concentrated in spermatogonia and spermatids with relatively low levels in other cell types of testes (13). Stanley et al. used the scRNA-seq method to find that the proportion of co-expression of ACE2 and TMPRSS2 in testicular cells is less than 0.05% (21), which indicated that human testis is not susceptible to viral attack. However, transcript-level expression cannot represent the protein expression profiles of the human reproductive system. Additionally, most studies evaluated the risk of viral infection by examining the expression of ACE2 and TMPRSS2, which is sort of arbitrary, because other co-receptors promote the entry of SARS-CoV-2 in cells of the respiratory system. That is why the lung is the most susceptible organ to SARS-CoV-2, while single-cell sequencing data show that ACE2 expression was expressed in fewer than 0.1% of cells in the lung (22). Therefore, further studies are warranted to focus on protein expression of more viral receptors in testicular cells so that we could better elucidate the tropism of SARS-CoV-2 in the human reproduction system.

THE IMPACTS OF COVID-19 ON THE MALE REPRODUCTIVE SYSTEM

Testicular Damage and Viral Transmission in the Semen of the COVID-19 Patients

Several studies focus on the reproductive pathology of COVID-19 patients. Ma et al. compared five COVID-19 patients with control patients and found that numerous degenerated germ cells (GCs) had sloughed into the lumen of seminiferous tubules (23). Two of five COVID-19 patients even showed symptoms similar to Sertoli cell-only syndrome. To ascertain the reason for the massive loss of GC, they found the significant presence of apoptotic cells and the infiltration of T lymphocytes, B lymphocytes, and macrophages in COVID-19 testes, which suggests that patients with COVID-19 had viral orchitis causing dysfunction of spermatogenesis. Yang et al. examined 12 postmortem testis samples of COVID-19 patients (24). They found that Sertoli cells showed swelling, vacuolation, and cytoplasmic rarefaction, and detachment from tubular basement membranes, and the number of Leydig cells was reduced, which is responsible for the decreased production of testosterone. Moreover, COVID-19 testes exhibited interstitial edema and mild lymphocytic inflammation corresponding to symptoms of orchitis. However, this study did not find significant alterations in spermatogenesis. Another research has reported damage of testes in autopsied testicular specimens consistent with autoimmune orchitis (25). Additionally, they also observed epididymitis in all cases. Two reports refer to the positive detection of SARS-CoV-2. Ma et al. have detected two testis samples of five positive for SARS-CoV-2 nucleic acid (23). Yao et al. examined 26 autopsy cases from deceased COVID-19 patients and found that SARS-CoV-2 spike

existed in endothelia of the BTB, seminiferous tubules, and sperm in the epididymis in 3 of 26 cases (26). Yang et al. found only 1 case out of 10 was positive for the virus in the testis, whereas the positive one resulted from the blood with a high viral load rather than testicular tissue affection (24). However, the study of Song et al. showed that the SARS-CoV-2 is absent from both the semen and testis specimens of the COVID-19 patient (27). In addition, Peirouvi et al. observed an elevated level of pro-inflammatory cytokines, including TNF-α, IL-1b, and IL-6, and decreased expressions of genes related to BTB, claudin, occludin, and connexin-43 in testis tissues, which indicates that COVID-19 infection would disrupt BTB integrity (28). Collectively, SARS-CoV-2 is more inclined to affect the function of the testis by triggering autoimmune orchitis leading to the destruction of BTB. Whether testis injury is attributed to viral direct infection on testicular cells or uncontrolled autoimmune is still unclear. Testicular organoids may be a suitable platform for further research to investigate the molecular mechanism of viral impact on male reproduction.

There are several viruses reported that could cross the BTB and can be transmitted sexually, such as Zika (29) and HIV (30). Currently, the existence of SARS-CoV-2 in semen is controversial. It was reported that a semen test of 38 specimens found that 6 samples (15.8%) were positive for SARS-CoV-2, namely, 4 of 15 patients (26.7%) with the acute stage of infection and 2 of 23 patients (8.7%) recovering from COVID-19 (31). This result could be due to the fact that patients of the acute stage have a high blood viral load, which allows the virus to have more chance to reach the testes and enter the BTB mediated by local and/or systemic inflammation. Most studies suggested that there was no viral detection in the semen (23, 27, 32, 33). Considering the results of the aforementioned studies, it seems that in mild COVID-19 cases, the seminal presence of SARS-CoV-2 is unlikely or rare, while there is a lack of evidence to draw a firm conclusion in severe acute cases. Recently there are skeptical views on the positive results since the process of ejaculation and semen collection may be contaminated (34). Further data following the WHO guideline to avoid virus contamination is needed to clarify the issue (35). Nonetheless, in almost all cases, the sensitivity and specificity of the RT-PCR methods used to detect SARS-CoV-2 in seminal fluid have not been evaluated (36). It is not clear that current detection methods applied to nasopharyngeal swabs are properly available in viral detections in semen. Although most studies indicate a low risk of seminal infection, infection in semen and gametes remains a pending issue, which requires substantial epidemiological data concerning viral transmission from male recovered patients to previously unaffected sexual partners (34). In particular, it is noteworthy to evaluate the presence of SARS-CoV-2 for semen cryopreservation, because the virus can retain its biological pathogenicity in liquid nitrogen (37).

Sperm Parameter Alterations in the COVID-19 Patients

The impact of SARS-CoV-2 on semen parameters has become an increasingly concerning issue to provide biological evidence for clinical recommendations in assisted reproduction centers. Holtmann et al. recruited 18 men, divided into mild and moderate groups, and a control group of 14 uninfected men (32). They examined sperm concentrations, the total number of sperm per ejaculate, the total number of progressive motility, and the total number of complete motility. Sperm concentrations, total progressive motility, and total sperm count of patients with moderate infection were significantly lower than the parameters of controls. However, there are limitations of this study in that the small sample can introduce sampling errors and it could not be compared with self-condition before infection. Li et al. observed that 9 out of 23 had decreased sperm concentration, representing the symptoms of oligozoospermia compared with the controls (25). Furthermore, all these patients with oligozoospermia have offspring, which demonstrated that they had intact fertility before infection. Segars et al. (38) indicated that male fertility may be severely affected for 72–90 days after infection due to decreased sperm concentration and motility (38). Furthermore, SARS-CoV-2, similar to other influenzas, could activate the cellular oxidative stress, leading to sperm DNA fragmentation, which is correlated to poor embryo development, lower implantation rate, and higher miscarriage rate (39–41). Febrility is one of the common symptoms of COVID-19 patients. The association of temporary alteration and sperm quality has been well studied (42). A fever can have significant effects on semen parameters and sperm DNA integrity, which suggests that a 3-month delay should be taken for COVID-19 male patients if they intend to have a conception or need an assisted reproductive techniques (ART) program. Furthermore, these adverse outcomes could be attributed to viral infections and may cause abnormal testosterone and LH levels and orchitis. To note, potential epigenome modifications of recovered patients' gametes should be taken into consideration in future studies.

Erectile Dysfunction in COVID-19 Patients

Because of the high transmissibility of the infection and the higher severity rates among men than women (43, 44), there is a worry that erectile dysfunction (ED) is a possible consequence of COVID-19 for survivors. A preliminary study concluded that ED and COVID-19 seemed to be strongly associated after removing the possible bias resulting from age and BMI, factors that contribute to both increased prevalence of ED (45). The mechanisms may lie in the following aspects (**Figure 1**). Studies reported that most male participants with COVID-19 had decreased testosterone, suggesting hypogonadism (46, 47). Testis damage, including reduced Leydig cells, resulting in impaired steroidogenesis, may cause the hypogonadism in patients with COVID-19 (48). Low testosterone suppresses the expression of nitric oxide synthase and causes vascular smooth muscle cell atrophy (49). Furthermore, testosterone has an immunosuppressive function. Rastrelli et al. reported that the low testosterone in COVID-19 patients could predict poor prognosis and mortality (50). Hypogonadal patients have a higher level of TNF-α, IL-6, and IL-1β, which has a higher risk of vascular impairment (51). Therefore, the state of hypogonadism may play a crucial role in the onset of ED. Sexual activity is closely associated with psychological health. Psychological distress universally occurs and is affected by COVID-19. Due to the lockdown of many cities, the loss of

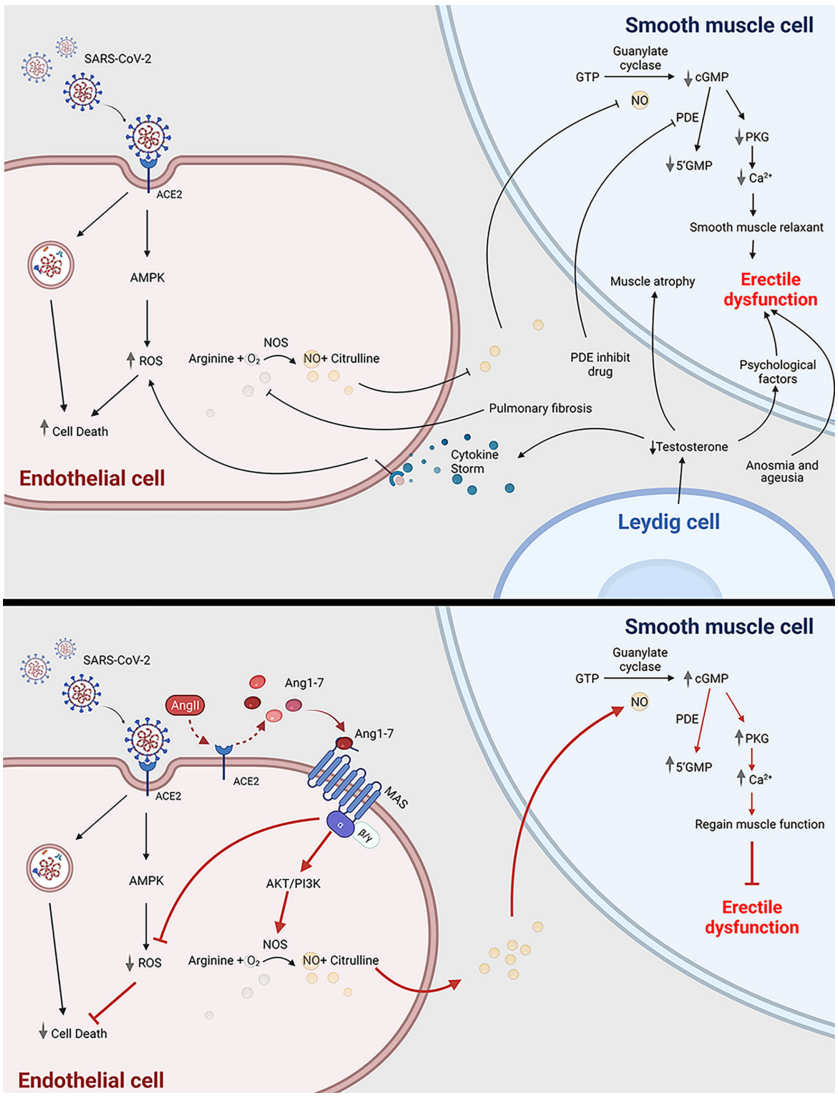

FIGURE 1 | COVID-19 can cause erectile dysfunction. The potential mechanism of how COVID-19 infection is related to erectile dysfunction through impairing endothelial cell and smooth muscle cell (top panel); Ang1-7 is a potential novel drug target to treat erectile dysfunction in COVID-19 patients (bottom panel). ACE2, angiotensin-converting enzyme 2; SARS-CoV-2, severe acute respiratory syndrome coronavirus 2; ED, erectile dysfunction; ROS, reactive oxygen species; AMPK, AMP-activated protein kinase; Ang1-7, angiotensin 1-7; Ang II, angiotensin 2; PDE, phosphodiesterase; 5'GMP, Guanosine-5'-monophosphate; cGMP, cyclic guanosine monophosphate; PKG, Cyclic GMP–dependent protein kinase; NOS, nitric oxide synthase. This scheme was created using BioRender, accessed on Sept. 29, 2021.

freedom can lead to secondary losses such as losses of relationship, recreation, social support, and even income sources (52). The loss of relatives and friends can also trigger an increasing rate of depression. In addition, psychological factors resulting from low testosterone also contribute to ED (53). Endothelial dysfunction and cardiovascular impairment are other etiological factors. As the endothelium expresses ACE2 (54), SARS-CoV-2 is likely to affect the vascular endothelium including the penis during the systemic infection. Kresch et al. firstly reported the presence of SARS-COV-2 in the penis long after the initial infection in humans (55). On the other hand, the spike protein of the virus can alone damage endothelial cells by impairing the mitochondrial function, reducing eNOS activity and increasing ROS production through the deactivation of AMPK (56). The penile endothelial bed maintains vascular pressure, patency, and perfusion; inhibits thrombosis; and regulates the behavior of the neighboring vascular smooth muscle, all of which is crucial for erections (57). Additionally, erectile function is regarded as a predictor of heart disease (58, 59). ED can partially reflect the cardiovascular systemic state in COVID-19 patients. When the acute cytokine storm impairs their own organs, the cytokine storm may lead to the ROS-dependent

apoptosis in vascular endothelial cells (60), which also contributes to the onset of ED. Another hypothesis that accounts for ED in the COVID-19 is decreased oxygen saturation as the result of pulmonary fibrosis hampers the availability of NO in the corpus cavernosum (61, 62). Another cause contributing to the potential onset of ED is anosmia and ageusia. Anosmia and ageusia, which play crucial roles in sexual activities, are symptoms of COVID-19 patients at the initial stage (63). The maintenance of penis erection requires both of them to trigger exciting messages to the brain (48, 64). PDE inhibitors are prevalent for drug treatment of ED because PDE inhibitors suppress degradation of cGMP, resulting in prolonged or enhanced erections (65). However, men with vascular-related diseases, such as diabetes, commonly do not respond well to PDE inhibitors (66). Novel approaches for ED treatment turn to novel drug target and stem cell therapy (67). The ACE2–Angiotensin-(1-7)–Mas axis may become an effective target to treat ED in COVID-19 patients. The mechanisms of this drug target is elucidated in **Figure 1**. Angiotensin 1-7 [Ang-(1-7)] is an endogenous heptapeptide from the renin–angiotensin system (RAS) with a cardioprotective role. Ang-(1-7) is proved to play an important role in eNOS activation and NO release by the PI3K/Akt pathway (68). Additionally, Ang-(1-7) also decreases the production of ROS (69), which may counteract the cytokine-induced dysfunction. In conclusion, further studies are needed to explore the pathogenesis of ED and investigate whether the occurrence of ED is just temporary or chronic.

THE REPRODUCTIVE TOXICITY OF DRUG TREATMENT OF COVID-19

During the treatment of COVID-19, the use of antiviral drugs often neglects the potential reproductive toxicity. The following are the drugs that may be used/exploited for treatment referring to current guidelines (70). Remdesivir is approved by the FDA for the treatment of COVID-19 in hospitalized adult and pediatric patients (70). Up to now, there have been no reports of Remdesivir concerning the adverse effect on the human productive system despite one investigation suggesting the reproductive toxicity of Remdesivir, which was withdrawn by the authors for better experimental design (71). IFN-α is known for antiviral, antiproliferative, and immunoregulatory activities (72). de Lima Rosa et al. concluded that IFN-α within the normal dose range did not significantly influence sperm production, maturation, and motility, as well as levels of gonadal hormones (73). Ribavirin is used widely as an antiviral drug, which is a candidate for COVID-19 treatment due to the inhibition of viral RNA-dependent RNA polymerase (74). It is generally accepted that ribavirin exposure should be avoided during pregnancy due to the potential teratogen (75). Besides, the impact of ribavirin on spermatogenesis should be emphasized. Narayana et al. revealed that ribavirin significantly decreased the sperm count in a dose- and time-dependent pattern in rats. Additionally, ribavirin could cause a reversible decrease in sperm parameters including decreased sperm motility, DNA packaging abnormalities, and increase in sperm DNA fragmentation up to 8 months after drug discontinuation (76), which indicates that mandatory contraception should be taken after treatment discontinuation. Corticosteroids are used widely in the clinic for the reason that their potent anti-inflammatory effects might prevent or mitigate these deleterious effects. There is no evidence supporting adverse effects on human sperm, while corticosteroids possibly indirectly affect spermatogenesis and oocyte competence through the hypothalamic–pituitary–gonadal axis (77, 78). Broad-spectrum antibiotics are being widely used in patients with COVID-19 (79). Although most relevant studies are inconclusive, the potential reproductive toxicity of antibiotics should be considered (80). Hargreaves et al. found that amoxicillin impaired sperm viability at high doses (81). Another group demonstrated that therapeutic doses of penicillin G resulted in spermatogenic arrest in rats after treatment for 8 days (82). Moreover, high doses of nitrofurantoin can cause spermatogenic arrest, reduced sperm counts, and sperm immobilization, which is probably due to the failure of testicular cells to use carbohydrates and oxygen (83, 84). There are two drugs mispresented as "miracle drugs" by media misinformation and forged studies. However, both are not approved to treat COVID-19 patients. Chloroquine, an immunomodulant drug, is effective in reducing viral replication in SARS-CoV-2 infections, supported by *in vitro* data and clinical studies involving humans (85). Rat models showed that chloroquine reduces motility and fertilizing capacity of sperm (86, 87). However, there is a lack of sufficient data to make recommendations. Ivermectin has been shown to inhibit the replication of SARS-CoV-2 *in vitro* (88). Moreira et al. found a significant decrease in striatal dopaminergic system activity including dopamine release and lower testosterone levels in male rats, leading to a reduction in motor coordination (89). Above all, couples who have used related drugs are advised to seek professional advice and fertility check before planning to conceive.

NOVEL MODEL FOR FUTURE INVESTIGATION OF FERTILITY IN COVID-19

Humanized ACE2 (hACE2) mice, which have overcome the natural insensitivity of mice to SARS-CoV-2 infection, are widely exploited for infection models and drug development. However, they are not an economical tool due to their high breeding fee and the lack of a qualified animal laboratory. Organoids are increasingly utilized for drug screening, toxicity assessment, and viral infection progression. Existing methods to evaluate the potential reproductive toxicity of drugs and viral infection require a large amount of animal sacrifice and could not ignore the individual differences. Organoids could provide more controllable, high-throughput, and faster evaluation techniques to simulate the microenvironment *in vivo*. In COVID-19, multiple research groups have resorted to organoid approaches to understand the tissue tropism of SARS-CoV-2. Penninger et al. established the capillary organoids and kidney organoids from human iPSCs and demonstrated that SARS-CoV-2 could directly infect cells in the capillary and kidney, which explains the spread of the virus throughout the body and the loss of kidney function in

several severely infected cases (90). Another research group utilized human ASC-derived intestinal organoids to prove that SARS-CoV-2 could infect intestinal epithelium, the enterocyte, and replicate in intestines, suggesting that the intestine is a susceptible site of SARS-CoV-2 (91). To note, Lancaster and colleagues used brain organoids to investigate viral neurotropism and discovered that SARS-CoV-2 mainly infects the choroid plexus leading to damage to this brain barrier (92), and it should be emphasized that testis has a similar structure composed of cell–cell tight junctions. There is a restricted number of research groups that have reported and characterized human testicular organoids. Daniel and his colleagues developed the human testicular organoid to investigate the impact of ZIKV infection on testis (93). Until now, testicular organoids have not been used in studies about COVID-19 possibly because of difficulties of building human testicular organoids. Thus, further improvement of strategies to establish testicular organoids is needed. There is no denying that testicular organoid is a novel and efficient tool to investigate the susceptibility of testis to SARS-CoV-2 and to understand the alterations of post-infected reproductive capacity.

CONCLUSION

It appears that COVID-19 influences different aspects of male reproduction including reproductive tracts, hormone, gametes, and sexual function. COVID-19 may trigger orchitis or epididymitis, thus impairing testis integrity and spermatogenesis. COVID-19 patients have decreased sperm concentration and motility. However, there seems to be a lack of consensus in the presence of SARS-COV-2 in semen and testis. Moreover, COVID-19 patients are exposed to a high risk of ED and thus we suggested Angiotensin-(1-7) as a novel drug target for ED in COVID-19. The current review also discusses the reproductive tract toxicity of drugs targeting COVID-19, and it also sheds new light on research on related fields and how the emerging model, such as the organoid, can be used to accelerate understanding of the related topic. Taken together, the impact of COVID-19 on the reproductive system still has outstanding unsolved questions. We need extensive clinical research and more efforts to investigate the long-term influence on male reproduction.

AUTHOR CONTRIBUTIONS

JG wrote the manuscript. KS performed the figure design and gave valuable advice. SW and HC contributed to collect relevant materials. All authors listed have made a substantial, direct, and intellectual contribution to the work, and approved it for publication.

FUNDING

Our work was supported by National Key Research & Development grant (No. 2018YFC1003603) and the National Nature Science Fund of China (No. 81971445).

REFERENCES

1. Peiris JS, Yuen KY, Osterhaus AD, Stohr K. The Severe Acute Respiratory Syndrome. *N Engl J Med* (2003) 349(25):2431–41. doi: 10.1056/NEJMra032498
2. Zhou P, Yang XL, Wang XG, Hu B, Zhang L, Zhang W, et al. A Pneumonia Outbreak Associated With a New Coronavirus of Probable Bat Origin. *Nature* (2020) 579(7798):270–3. doi: 10.1038/s41586-020-2012-7
3. Zhang H, Penninger JM, Li Y, Zhong N, Slutsky AS. Angiotensin-Converting Enzyme 2 (ACE2) as a SARS-CoV-2 Receptor: Molecular Mechanisms and Potential Therapeutic Target. *Intensive Care Med* (2020) 46(4):586–90. doi: 10.1007/s00134-020-05985-9
4. Zhao JM, Zhou GD, Sun YL, Wang SS, Yang JF, Meng EH, et al. Clinical Pathology and Pathogenesis of Severe Acute Respiratory Syndrome. *Zhonghua Shi Yan He Lin Chuang Bing Du Xue Za Zhi* (2003) 17(3):217–21.
5. Xu J, Qi L, Chi X, Yang J, Wei X, Gong E, et al. Orchitis: A Complication of Severe Acute Respiratory Syndrome (SARS). *Biol Reprod* (2006) 74(2):410–6. doi: 10.1095/biolreprod.105.044776
6. Czypionka T, Greenhalgh T, Bassler D, Bryant MB. Masks and Face Coverings for the Lay Public: A Narrative Update. *Ann Intern Med* (2021) 174(4):511–20. doi: 10.7326/M20-6625
7. Hoffmann M, Kleine-Weber H, Schroeder S, Kruger N, Herrler T, Erichsen S, et al. SARS-CoV-2 Cell Entry Depends on ACE2 and TMPRSS2 and Is Blocked by a Clinically Proven Protease Inhibitor. *Cell* (2020) 181(2):271–280 e8. doi: 10.1016/j.cell.2020.02.052
8. Li X, Geng M, Peng Y, Meng L, Lu S. Molecular Immune Pathogenesis and Diagnosis of COVID-19. *J Pharm Anal* (2020) 10(2):102–8. doi: 10.1016/j.jpha.2020.03.001
9. Fung TS, Liu DX. Human Coronavirus: Host-Pathogen Interaction. *Annu Rev Microbiol* (2019) 73:529–57. doi: 10.1146/annurev-micro-020518-115759
10. Douglas GC, O'Bryan MK, Hedger MP, Lee DK, Yarski MA, Smith AI, et al. The Novel Angiotensin-Converting Enzyme (ACE) Homolog, ACE2, Is Selectively Expressed by Adult Leydig Cells of the Testis. *Endocrinology* (2004) 145(10):4703–11. doi: 10.1210/en.2004-0443
11. Barbagallo F, Calogero A, Cannarella R, Condorelli R, Mongioì L, Aversa A, et al. The Testis in Patients With COVID-19: Virus Reservoir or Immunization Resource? *Transl Androl Urol* (2020) 9(5):1897–900. doi: 10.21037/tau-20-900
12. Shen Q, Xiao X, Aierken A, Yue W, Wu X, Liao M, et al. The ACE2 Expression in Sertoli Cells and Germ Cells may Cause Male Reproductive Disorder After SARS-CoV-2 Infection. *J Cell Mol Med* (2020) 24(16):9472–7. doi: 10.1111/jcmm.15541
13. Wang Z, Xu X. scRNA-Seq Profiling of Human Testes Reveals the Presence of the ACE2 Receptor, A Target for SARS-CoV-2 Infection in Spermatogonia, Leydig and Sertoli Cells. *Cells* (2020) 9(4):920. doi: 10.3390/cells9040920
14. Mruk DD, Cheng CY. The Mammalian Blood-Testis Barrier: Its Biology and Regulation. *Endocr Rev* (2015) 36(5):564–91. doi: 10.1210/er.2014-1101
15. Heinrich A, DeFalco T. Essential Roles of Interstitial Cells in Testicular Development and Function. *Andrology* (2020) 8(4):903–14. doi: 10.1111/andr.12703
16. Meinhardt A, Bacher M, Wennemuth G, Eickhoff R, Hedger M. Macrophage Migration Inhibitory Factor (MIF) as a Paracrine Mediator in the Interaction of Testicular Somatic Cells. *Andrologia* (2000) 32(1):46–8.
17. Castillo J, Jodar M, Oliva R. The Contribution of Human Sperm Proteins to the Development and Epigenome of the Preimplantation Embryo. *Hum Reprod Update* (2018) 24(5):535–55. doi: 10.1093/humupd/dmy017
18. Chen YW, Lee MS, Lucht A, Chou FP, Huang W, Havighurst TC, et al. TMPRSS2, A Serine Protease Expressed in the Prostate on the Apical Surface of Luminal Epithelial Cells and Released Into Semen in Prostasomes, Is

Misregulated in Prostate Cancer Cells. *Am J Pathol* (2010) 176(6):2986–96. doi: 10.2353/ajpath.2010.090665
19. Djomkam ALZ, Olwal CO, Sala TB, Paemka L. Commentary: SARS-CoV-2 Cell Entry Depends on ACE2 and TMPRSS2 and Is Blocked by a Clinically Proven Protease Inhibitor. *Front Oncol* (2020) 10:1448. doi: 10.3389/fonc.2020.01448
20. Wang K, Chen W, Zhang Z, Deng Y, Lian J, Du P, et al. CD147-Spike Protein Is a Novel Route for SARS-CoV-2 Infection to Host Cells. *Signal Transduct Target Ther* (2020) 5(1):283. doi: 10.1038/s41392-020-00426-x
21. Stanley K, Thomas E, Leaver M, Wells D. Coronavirus Disease-19 and Fertility: Viral Host Entry Protein Expression in Male and Female Reproductive Tissues. *Fertil Steril* (2020) 114(1):33–43. doi: 10.1016/j.fertnstert.2020.05.001
22. Wang S, Qiu Z, Hou Y, Deng X, Xu W, Zheng T, et al. AXL Is a Candidate Receptor for SARS-CoV-2 That Promotes Infection of Pulmonary and Bronchial Epithelial Cells. *Cell Res* (2021) 31(2):126–40. doi: 10.1038/s41422-020-00460-y
23. Ma X, Guan C, Chen R, Wang Y, Feng S, Wang R, et al. Pathological and Molecular Examinations of Postmortem Testis Biopsies Reveal SARS-CoV-2 Infection in the Testis and Spermatogenesis Damage in COVID-19 Patients. *Cell Mol Immunol* (2021) 18(2):487–9. doi: 10.1038/s41423-020-00604-5
24. Yang M, Chen S, Huang B, Zhong J, Su H, Chen Y, et al. Pathological Findings in the Testes of COVID-19 Patients: Clinical Implications. *Eur Urol Focus* (2020) 6(5):1124–9. doi: 10.1016/j.euf.2020.05.009
25. Li H, Xiao X, Zhang J, Zafar M, Wu C, Long Y, et al. Impaired Spermatogenesis in COVID-19 Patients. *EClinicalMedicine* (2020) 28:100604. doi: 10.1016/j.eclinm.2020.100604
26. Yao X, Luo T, Shi Y, He Z, Tang R, Zhang P, et al. A Cohort Autopsy Study Defines COVID-19 Systemic Pathogenesis. *Cell Res* (2021) 31(8):836–46. doi: 10.1038/s41422-021-00523-8
27. Song C, Wang Y, Li W, Hu B, Chen G, Xia P, et al. Absence of 2019 Novel Coronavirus in Semen and Testes of COVID-19 Patientsdagger. *Biol Reprod* (2020) 103(1):4–6. doi: 10.1093/biolre/ioaa050
28. Peirouvi T, Aliaghaei A, Eslami Farsani B, Ziaeipour S, Ebrahimi V, Forozesh M, et al. COVID-19 Disrupts the Blood-Testis Barrier Through the Induction of Inflammatory Cytokines and Disruption of Junctional Proteins. *Inflamm Res* (2021) 70(10–12):1165–75. doi: 10.1007/s00011-021-01497-4
29. Mansuy J, Dutertre M, Mengelle C, Fourcade C, Marchou B, Delobel P, et al. Zika Virus: High Infectious Viral Load in Semen, a New Sexually Transmitted Pathogen? *Lancet Infect Dis* (2016) 16(4):405. doi: 10.1016/s1473-3099(16)00138-9
30. Anderson J, Ping L, Dibben O, Jabara C, Arney L, Kincer L, et al. HIV-1 Populations in Semen Arise Through Multiple Mechanisms. *PloS Pathog* (2010) 6(8):e1001053. doi: 10.1371/journal.ppat.1001053
31. Li D, Jin M, Bao P, Zhao W, Zhang S. Clinical Characteristics and Results of Semen Tests Among Men With Coronavirus Disease 2019. *JAMA Netw Open* (2020) 3(5):e208292. doi: 10.1001/jamanetworkopen.2020.8292
32. Holtmann N, Edimiris P, Andree M, Doehmen C, Baston-Buest D, Adams O, et al. Assessment of SARS-CoV-2 in Human Semen-a Cohort Study. *Fertil Steril* (2020) 114(2):233–8. doi: 10.1016/j.fertnstert.2020.05.028
33. Paoli D, Pallotti F, Colangelo S, Basilico F, Mazzuti L, Turriziani O, et al. Study of SARS-CoV-2 in Semen and Urine Samples of a Volunteer With Positive Naso-Pharyngeal Swab. *J Endocrinol Invest* (2020) 43(12):1819–22. doi: 10.1007/s40618-020-01261-1
34. Paoli D, Pallotti F, Turriziani O, Mazzuti L, Antonelli G, Lenzi A, et al. SARS-CoV-2 Presence in Seminal Fluid: Myth or Reality. *Andrology* (2021) 9(1):23–6. doi: 10.1111/andr.12825
35. World Health Organization. *WHO Laboratory Manual for the Examination and Processing of Human Semen. Sixth ed*. Geneva: World Health Organization (2021). p. 276.
36. Madjunkov M, Dviri M, Librach C. A Comprehensive Review of the Impact of COVID-19 on Human Reproductive Biology, Assisted Reproduction Care and Pregnancy: A Canadian Perspective. *J Ovarian Res* (2020) 13(1):140. doi: 10.1186/s13048-020-00737-1
37. Corona G, Baldi E, Isidori A, Paoli D, Pallotti F, De Santis L, et al. SARS-CoV-2 Infection, Male Fertility and Sperm Cryopreservation: A Position Statement of the Italian Society of Andrology and Sexual Medicine (SIAMS) (Società Italiana Di Andrologia E Medicina Della Sessualità). *J Endocrinol Invest* (2020) 43(8):1153–7. doi: 10.1007/s40618-020-01290-w
38. Segars J, Katler Q, McQueen D, Kotlyar A, Glenn T, Knight Z, et al. Prior and Novel Coronaviruses, Coronavirus Disease 2019 (COVID-19), and Human Reproduction: What Is Known? *Fertil Steril* (2020) 113(6):1140–9. doi: 10.1016/j.fertnstert.2020.04.025
39. Borges E, Zanetti B, Setti A, Braga D, Provenza R, Iaconelli A. Sperm DNA Fragmentation Is Correlated With Poor Embryo Development, Lower Implantation Rate, and Higher Miscarriage Rate in Reproductive Cycles of Non-Male Factor Infertility. *Fertil Steril* (2019) 112(3):483–90. doi: 10.1016/j.fertnstert.2019.04.029
40. Homa S, Vassiliou A, Stone J, Killeen A, Dawkins A, Xie J, et al. A Comparison Between Two Assays for Measuring Seminal Oxidative Stress and Their Relationship With Sperm DNA Fragmentation and Semen Parameters. *Genes (Basel)* (2019) 10(3):236. doi: 10.3390/genes10030236
41. Anifandis G, Messini C, Daponte A, Messinis I. COVID-19 and Fertility: A Virtual Reality. *Reprod Biomed Online* (2020) 41(2):157–9. doi: 10.1016/j.rbmo.2020.05.001
42. Sergerie M, Mieusset R, Croute F, Daudin M, Bujan L. High Risk of Temporary Alteration of Semen Parameters After Recent Acute Febrile Illness. *Fertil Steril* (2007) 88(4):970.e1–7. doi: 10.1016/j.fertnstert.2006.12.045
43. Patel DP, Punjani N, Guo J, Alukal JP, Li PS, Hotaling JM. The Impact of SARS-CoV-2 and COVID-19 on Male Reproduction and Men's Health. *Fertil Steril* (2021) 115(4):813–23. doi: 10.1016/j.fertnstert.2020.12.033
44. La Vignera S, Cannarella R, Condorelli R, Torre F, Aversa A, Calogero A. Sex-Specific SARS-CoV-2 Mortality: Among Hormone-Modulated ACE2 Expression, Risk of Venous Thromboembolism and Hypovitaminosis D. *Int J Mol Sci* (2020) 21(8):2948. doi: 10.3390/ijms21082948
45. Sansone A, Mollaioli D, Ciocca G, Colonnello E, Limoncin E, Balercia G, et al. "Mask Up to Keep It Up": Preliminary Evidence of the Association Between Erectile Dysfunction and COVID-19. *Andrology* (2021) 9(4):1053–9. doi: 10.1111/andr.13003
46. Schroeder M, Tuku B, Jarczak D, Nierhaus A, Bai T, Jacobsen H, et al. The Majority of Male Patients With COVID-19 Present Low Testosterone Levels on Admission to Intensive Care in Hamburg, Germany: A Retrospective Cohort Study. *MedRxiv[Preprint]* (2020) 10(1):1807–18. doi: 10.1101/2020.05.07.20073817
47. Kadihasanoglu M, Aktas S, Yardimci E, Aral H, Kadioglu A. SARS-CoV-2 Pneumonia Affects Male Reproductive Hormone Levels: A Prospective, Cohort Study. *J Sex Med* (2021) 18(2):256–64. doi: 10.1016/j.jsxm.2020.11.007
48. Sansone A, Mollaioli D, Ciocca G, Limoncin E, Colonnello E, Vena W, et al. Addressing Male Sexual and Reproductive Health in the Wake of COVID-19 Outbreak. *J Endocrinol Invest* (2021) 44(2):223–31. doi: 10.1007/s40618-020-01350-1
49. Blute M, Hakimian P, Kashanian J, Shteynshluyger A, Lee M, Shabsigh R. Erectile Dysfunction and Testosterone Deficiency. *Front Horm Res* (2009) 37:108–22. doi: 10.1159/000176048
50. Rastrelli G, Di Stasi V, Inglese F, Beccaria M, Garuti M, Di Costanzo D, et al. Low Testosterone Levels Predict Clinical Adverse Outcomes in SARS-CoV-2 Pneumonia Patients. *Andrology* (2021) 9(1):88–98. doi: 10.1111/andr.12821
51. Mohamad N, Wong S, Wan Hasan W, Jolly J, Nur-Farhana M, Ima-Nirwana S, et al. The Relationship Between Circulating Testosterone and Inflammatory Cytokines in Men. *Aging Male* (2019) 22(2):129–40. doi: 10.1080/13685538.2018.1482487
52. Zhai Y, Du X. Loss and Grief Amidst COVID-19: A Path to Adaptation and Resilience. *Brain Behav Immun* (2020) 87:80–1. doi: 10.1016/j.bbi.2020.04.053
53. Shabsigh R. Hypogonadism and Erectile Dysfunction: The Role for Testosterone Therapy. *Int J Impot Res* (2003) 15 Suppl 4:S9–13. doi: 10.1038/sj.ijir.3901030
54. Lovren F, Pan Y, Quan A, Teoh H, Wang G, Shukla PC, et al. Angiotensin Converting Enzyme-2 Confers Endothelial Protection and Attenuates Atherosclerosis. *Am J Physiol Heart Circ Physiol* (2008) 295(4):H1377–84. doi: 10.1152/ajpheart.00331.2008
55. Kresch E, Achua J, Saltzman R, Khodamoradi K, Arora H, Ibrahim E, et al. COVID-19 Endothelial Dysfunction Can Cause Erectile Dysfunction: Histopathological, Immunohistochemical, and Ultrastructural Study of the Human Penis. *World J Mens Health* (2021) 39(3):466–9. doi: 10.5534/wjmh.210055

56. Lei Y, Zhang J, Schiavon CR, He M, Chen L, Shen H, et al. SARS-CoV-2 Spike Protein Impairs Endothelial Function *via* Downregulation of ACE 2. *Circ Res* (2021) 128(9):1323–6. doi: 10.1161/CIRCRESAHA.121.318902
57. Castela A, Costa C. Molecular Mechanisms Associated With Diabetic Endothelial-Erectile Dysfunction. *Nat Rev Urol* (2016) 13(5):266–74. doi: 10.1038/nrurol.2016.23
58. Corona G, Forti G, Maggi M. Why can Patients With Erectile Dysfunction be Considered Lucky? The Association With Testosterone Deficiency and Metabolic Syndrome. *Aging Male* (2008) 11(4):193–9. doi: 10.1080/13685530802468497
59. Kloner RA. Erectile Dysfunction as a Predictor of Cardiovascular Disease. *Int J Impot Res* (2008) 20(5):460–5. doi: 10.1038/ijir.2008.20
60. Winn RK, Harlan JM. The Role of Endothelial Cell Apoptosis in Inflammatory and Immune Diseases. *J Thromb Haemost* (2005) 3(8):1815–24. doi: 10.1111/j.1538-7836.2005.01378.x
61. Graney BA, Wamboldt FS, Baird S, Churney T, Fier K, Korn M, et al. Looking Ahead and Behind at Supplemental Oxygen: A Qualitative Study of Patients With Pulmonary Fibrosis. *Heart Lung* (2017) 46(5):387–93. doi: 10.1016/j.hrtlng.2017.07.001
62. Verratti V, Di Giulio C, Berardinelli F, Pellicciotta M, Di Francesco S, Iantorno R, et al. The Role of Hypoxia in Erectile Dysfunction Mechanisms. *Int J Impot Res* (2007) 19(5):496–500. doi: 10.1038/sj.ijir.3901560
63. Vaira L, Salzano G, Deiana G, De Riu G. Anosmia and Ageusia: Common Findings in COVID-19 Patients. *Laryngoscope* (2020) 130(7):1787. doi: 10.1002/lary.28692
64. Bertolo R, Cipriani C, Bove P. Anosmia and Ageusia: A Piece of the Puzzle in the Etiology of COVID-19-Related Transitory Erectile Dysfunction. *J Endocrinol Invest* (2021) 44(5):1123–4. doi: 10.1007/s40618-021-01516-5
65. Dolci S, Belmonte A, Santone R, Giorgi M, Pellegrini M, Carosa E, et al. Subcellular Localization and Regulation of Type-1C and Type-5 Phosphodiesterases. *Biochem Biophys Res Commun* (2006) 341(3):837–46. doi: 10.1016/j.bbrc.2006.01.035
66. Albersen M, Shindel A, Mwamukonda K, Lue T. The Future Is Today: Emerging Drugs for the Treatment of Erectile Dysfunction. *Expert Opin Emerg Drugs* (2010) 15(3):467–80. doi: 10.1517/14728214.2010.480973
67. Alwaal A, Zaid U, Lin C, Lue T. Stem Cell Treatment of Erectile Dysfunction. *Adv Drug Deliv Rev* (2015) 82–83:137–44. doi: 10.1016/j.addr.2014.11.012
68. Sampaio WO, Souza dos Santos RA, Faria-Silva R, da Mata Machado LT, Schiffrin EL, Touyz RM. Angiotensin-(1-7) Through Receptor Mas Mediates Endothelial Nitric Oxide Synthase Activation *via* Akt-Dependent Pathways. *Hypertension* (2007) 49(1):185–92. doi: 10.1161/01.HYP.0000251865.35728.2f
69. Rabelo LA, Alenina N, Bader M. ACE2-Angiotensin-(1-7)-Mas Axis and Oxidative Stress in Cardiovascular Disease. *Hypertens Res* (2011) 34(2):154–60. doi: 10.1038/hr.2010.235
70. *COVID-19 Treatment Guidelines. 2021/5/14 ed*. (2021). Available at: https://www.covid19treatmentguidelines.nih.gov/.
71. Fan J, Luo J, Zhao D, Deng T, Weng Y, Sun Y, et al. A Preliminary Study on the Reproductive Toxicity of GS-5734 on Male Mice. *MedRxiv[Preprint]* (2020). doi: 10.1101/2020.04.21.050104v1
72. Yazdani Brojeni P, Matok I, Garcia Bournissen F, Koren G. A Systematic Review of the Fetal Safety of Interferon Alpha. *Reprod Toxicol* (2012) 33 (3):265–8. doi: 10.1016/j.reprotox.2011.11.003
73. Rosa JL, Cavariani M, Borges CS, Leite G, Anselmo-Franci J, Kempinas W. Lack of Reproductive Toxicity in Adult Male Rats Exposed to Interferon-Alpha. *J Toxicol Environ Health A* (2015) 78(20):1288–98. doi: 10.1080/10937404.2015.1083518
74. Sanders JM, Monogue ML, Jodlowski TZ, Cutrell JB. Pharmacologic Treatments for Coronavirus Disease 2019 (COVID-19): A Review. *JAMA* (2020) 323(18):1824–36. doi: 10.1001/jama.2020.6019
75. Sinclair SM, Jones JK, Miller RK, Greene MF, Kwo PY, Maddrey WC. The Ribavirin Pregnancy Registry: An Interim Analysis of Potential Teratogenicity at the Mid-Point of Enrollment. *Drug Saf* (2017) 40(12):1205–18. doi: 10.1007/s40264-017-0566-6
76. Pecou S, Moinard N, Walschaerts M, Pasquier C, Daudin M, Bujan L. Ribavirin and Pegylated Interferon Treatment for Hepatitis C was Associated Not Only With Semen Alterations But Also With Sperm Deoxyribonucleic Acid Fragmentation in Humans. *Fertil Steril* (2009) 91 (3):933.e17–22. doi: 10.1016/j.fertnstert.2008.07.1755
77. Yuan H, Han X, He N, Wang G, Gong S, Lin J, et al. Glucocorticoids Impair Oocyte Developmental Potential by Triggering Apoptosis of Ovarian Cells *via* Activating the Fas System. *Sci Rep* (2016) 6:24036. doi: 10.1038/srep24036
78. Whirledge S, Cidlowski J. Glucocorticoids, Stress, and Fertility. Glucocorticoids, Stress, and Fertility. *Minerva Endocrinol* (2010) 35(2):109–25.
79. Beović B, Doušak M, Ferreira-Coimbra J, Nadrah K, Rubulotta F, Belliato M, et al. Antibiotic Use in Patients With COVID-19: A 'Snapshot' Infectious Diseases International Research Initiative (ID-IRI) Survey. *J Antimicrob Chemother* (2020) 75(11):3386–90. doi: 10.1093/jac/dkaa326
80. Samplaski M, Nangia A. Adverse Effects of Common Medications on Male Fertility. *Nat Rev Urol* (2015) 12(7):401–13. doi: 10.1038/nrurol.2015.145
81. Hargreaves C, Rogers S, Hills F, Rahman F, Howell R, Homa S. Effects of Co-Trimoxazole, Erythromycin, Amoxycillin, Tetracycline and Chloroquine on Sperm Function *In Vitro*. *Hum Reprod* (1998) 13(7):1878–86. doi: 10.1093/humrep/13.7.1878
82. Timmermans L. Influence of Antibiotics on Spermatogenesis. *J Urol* (1974) 112(3):348–9. doi: 10.1016/s0022-5347(17)59727-x
83. Albert P, Mininberg D, Davis J. The Nitrofurans as Sperm Immobilising Agents: Their Tissue Toxicity and Their Clinical Application. *Br J Urol* (1975) 47(4):459–62. doi: 10.1111/j.1464-410x.1975.tb04008.x
84. Schlegel P, Chang T, Marshall F. Antibiotics: Potential Hazards to Male Fertility. *Fertil Steril* (1991) 55(2):235–42. doi: 10.1016/s0015-0282(16)54108-9
85. Juurlink DN. Safety Considerations With Chloroquine, Hydroxychloroquine and Azithromycin in the Management of SARS-CoV-2 Infection. *CMAJ* (2020) 192(17):E450–3. doi: 10.1503/cmaj.200528
86. Okanlawon A, Noronha C, Ashiru O. An Investigation Into the Effects of Chloroquine on Fertility of Male Rats. *West Afr J Med* (1993) 12(2):118–21.
87. Adeeko A, Dada O. Chloroquine Reduces Fertilizing Capacity of Epididyma Sperm in Rats. *Afr J Med Med Sci* (1998) 27:63–4.
88. Caly L, Druce J, Catton M, Jans D, Wagstaff K. The FDA-Approved Drug Ivermectin Inhibits the Replication of SARS-CoV-2 *In Vitro*. *Antiviral Res* (2020) 178:104787. doi: 10.1016/j.antiviral.2020.104787
89. Moreira N, Sandini T, Reis-Silva T, Navas-Suáresz P, Auada A, Lebrun I, et al. Ivermectin Reduces Motor Coordination, Serum Testosterone, and Central Neurotransmitter Levels But Does Not Affect Sexual Motivation in Male Rats. *Reprod Toxicol* (2017) 74:195–203. doi: 10.1016/j.reprotox.2017.10.002
90. Monteil V, Kwon H, Prado P, Hagelkrüys A, Wimmer R, Stahl M, et al. Inhibition of SARS-CoV-2 Infections in Engineered Human Tissues Using Clinical-Grade Soluble Human Ace2. *Cell* (2020) 181(4):905–13.e7. doi: 10.1016/j.cell.2020.04.004
91. Lamers M, Beumer J, van der Vaart J, Knoops K, Puschhof J, Breugem T, et al. SARS-CoV-2 Productively Infects Human Gut Enterocytes. *Science* (2020) 369(6499):50–4. doi: 10.1126/science.abc1669
92. Pellegrini L, Albecka A, Mallery D, Kellner M, Paul D, Carter A, et al. SARS-CoV-2 Infects the Brain Choroid Plexus And Disrupts the Blood-CSF Barrier in Human Brain Organoids. *Cell Stem Cell* (2020) 27(6):951–61.e5. doi: 10.1016/j.stem.2020.10.001
93. Strange D, Zarandi N, Trivedi G, Atala A, Bishop C, Sadri-Ardekani H, et al. Human Testicular Organoid System as a Novel Tool to Study Zika Virus Pathogenesis. *Emerg Microbes Infect* (2018) 7(1):82. doi: 10.1038/s41426-018-0080-7

Conflict of Interest: The authors declare that the research was conducted in the absence of any commercial or financial relationships that could be construed as a potential conflict of interest.

frontiers in Endocrinology

MINI REVIEW
published: 16 December 2021
doi: 10.3389/fendo.2021.800693

Impact of Circadian Desynchrony on Spermatogenesis: A Mini Review

Ferdinando Fusco[1], Nicola Longo[2], Marco De Sio[3], Davide Arcaniolo[3], Giuseppe Celentano[2], Marco Capece[2], Roberto La Rocca[2], Francesco Mangiapia[2], Gianluigi Califano[2], Simone Morra[2], Carmine Turco[2], Gianluca Spena[2], Lorenzo Spirito[2], Giovanni Maria Fusco[2], Luigi Cirillo[2], Luigi De Luca[2], Luigi Napolitano[2], Vincenzo Mirone[2] and Massimiliano Creta[2]*

[1] Urology Unit, Department of Woman, Child and General and Specialized Surgery, University of Campania "Luigi Vanvitelli", Caserta, Italy, [2] Department of Neurosciences, Reproductive Sciences and Odontostomatology, Urology Unit, University of Naples "Federico II", Naples, Italy, [3] Department of Woman, Child and General and Specialized Surgery, Urology Unit, University of Campania Luigi Vanvitelli, Naples, Italy

OPEN ACCESS

Edited by:
Qing Chen,
Army Medical University, China

Reviewed by:
Yongxin Ma,
Sichuan University, China
Mary Anna Venneri,
Sapienza University of Rome, Italy

***Correspondence:**
Ferdinando Fusco
ferdinando-fusco@libero.it

Specialty section:
This article was submitted to Reproduction, a section of the journal Frontiers in Endocrinology

Received: *23 October 2021*
Accepted: *24 November 2021*
Published: *16 December 2021*

Citation:
Fusco F, Longo N, De Sio M, Arcaniolo D, Celentano G, Capece M, La Rocca R, Mangiapia F, Califano G, Morra S, Turco C, Spena G, Spirito L, Fusco GM, Cirillo L, De Luca L, Napolitano L, Mirone V and Creta M (2021) Impact of Circadian Desynchrony on Spermatogenesis: A Mini Review. Front. Endocrinol. 12:800693. doi: 10.3389/fendo.2021.800693

The purpose of this mini review is to provide data about pre-clinical and clinical evidence exploring the impact of circadian desynchrony on spermatogenesis. Several lines of evidence exist demonstrating that disruption of circadian rhythms may interfere with male fertility. Experimental knock-out or knock-down of clock genes, physiologically involved in the regulation of circadian rhythms, are associated with impairments of fertility pathways in both animal and human models. Moreover, disruption of circadian rhythms, due to reduction of sleep duration and/or alteration of its architecture can negatively interfere in humans with circulating levels of male sexual hormones as well as with semen parameters. Unfortunately, current evidence remains low due to study heterogeneity.

Keywords: circadian desynchrony, circadian rhythms, clock genes, spermatogenesis, fertility

INTRODUCTION

Globally, it has been estimated that infertility affects approximately 8-12% of couples, with a male factor being a primary or contributing cause in about 50% of couples (1, 2). Unfortunately, the cause of male infertility is unknown in about 30% of these cases (3, 4). Environmental endocrine disruptors, often consequences of human activity, have been widely investigated as agents potentially involved into the pathogenesis of infertility in animals and humans (5, 6). Over the past 30 years primary focus has been directed to the effects of chemicals environmental endocrine disruptors found in plasticizers, pharmaceuticals, and pesticides such as bisphenol A or glyphosate (7, 8). In recent years, however, the effects of non-chemical environmental endocrine disruptors such as that interfering with circadian rhythms (CR) leading to circadian desynchrony (CD) also gained growing interest in the pathophysiology of male infertility (5). The aim of this mini review is to provide the latest information on pre-clinical and clinical evidence about the relationship between CD and spermatogenesis.

METHODS

The authors conducted a literature search of available sources evaluating the pathophysiology and clinical evidence about the relationship between CD and impaired male reproduction, with a special focus on spermatogenesis. Web of Science, PubMed, and Scopus databases were searched to find relevant articles. The information found in the selected studies was carefully evaluated and it is described and discussed in the following sections.

CR and CD: Definition and Pathophysiology

CR consist in daily oscillations in physiology processes (gene expression, metabolism, activity patterns and serum hormone levels) and behavior recurring with a 24h period. CR represent an ubiquitous feature in living organisms: they modulate function since unicellular life and gained an higher complexity multicellular organisms (9, 10).

In vertebrates, CR are hierarchically organized. They are both autonomous, based on cellular cycle which builds rhythmic activity of tissues, and controlled by synchronization through environmental signals (11). The main regulator of these rhythms is represented by the hypothalamic suprachiasmatic nucleus (SCN) (12). The cells in the SCN orchestrate rhythms in endocrine, physiological, and behavioral parameters through the activation of other central circadian oscillators (e.g., the hypothalamus and pituitary gland), with a period close to, but not exactly 24 hours (13, 14).

CR are strongly entrained by the daily photoperiod as they are influenced by the environmental light-dark cycle which has been reported to modulate the expression of several genes (15). Therefore, light is the most effective environmental synchronizing agent for the clock of human beings: it represents a direct drive to the nervous system through activation of intrinsic photosensitive retinal ganglion cells and transduced directly to the SCN through the retinohypothalamic tract (16), and an indirectly through the intergeniculate leaflet (17, 18).

Clock genes play a central role in orchestrating CR. In mammals, the main clock genes include: *Period* genes (*Per 1/2/3*, Period Circadian Regulator1/2/3), Circadian Locomotor Output Cycles Kaput (*Clock*) gene, *Cryptochrome* genes (*Cry 1/2*, Cryptochrome Circadian Regulator 1/2) *and* Aryl hydrocarbon receptor nuclear translocator-like protein 1 (ARNTL, also known as MOP3 or Bmal1) (19). Clock genes are involved in several physiological processes and diseases including ageing, metabolism, fertility, cardiovascular health, and cell proliferation (20, 21).

Throughout the last two centuries, modern lifestyles increasingly deprive us of natural zeitgebers (dt. time-givers) and technological advances have dramatically changed individual work and rest patterns (22–24). Electricity and constant accessibility to light, energy, food, the possibility to travel across time zones created an environment that is different from the one of the last two centuries. These environmental perturbances strongly contribute to the pathophysiology of CD, a condition defined for the first time by Sack & Lewy in 1997 as a specific type of circadian disruption occurring when endogenous rhythms become misaligned with daily photoperiodic cycles (25–27).

Growing evidence support the hypothesis that disruption of CR is involved in the pathophysiology of several diseases such as metabolic impairment, cardiovascular and sleep disorders, psychiatric illness, cancers such as urothelial carcinoma, and infertility (28–32).

CD and Male Infertility

Physiological processes regulating fertility need to be appropriately synchronized with the external environment to guarantee reproductive success. In the testis several models of temporal organization had been found. The complexity of its rhythmic function is linked to its structure divided into compartments (33). In the seminiferous tubule there is a spermatogenic wave that travels along in length to determine the timing of the commitment of spermatogonia to differentiate, the phases of meiotic division, and the rate of differentiation of the post-meiotic germ cells (33). Leydig cells, localized in the interstitial space, produce steroid hormones to ensure spermatozoa maturation and the sexual characteristics (33).

Several lines of evidence exist suggesting that disruption of mechanisms involved in CR may interfere with male fertility.

Mutations of Clock Genes and Male Infertility

Clock proteins have been reported to be expressed in male germ epithelium. In details, BMAL1 localizes mainly in Leydig cells but it can also be found in the nucleus and cytoplasm of germ cells and CLOCK was observed having a higher expression level in the cytoplasm of round spermatids (34).

Both pre-clinical and clinical evidence suggest the involvement of clock genes in the pathophysiology of male infertility.

Table 1 summarizes evidence from pre-clinical animal studies.

Alvarez et al. used *Bmal1* knockout (KO) mice in order to clarify the role of this circadian clock protein in the fertility process and its role in testosterone production (36). Authors found that male *Bmal1* KO mice were infertile and had lower testosterone and higher luteinizing hormone (LH) serum concentrations, compared to wild-type mice thus suggesting a defect in testicular Leydig cells. Testes and other steroidogenic tissues of *Bmal1* KO mice exhibited reduced expression of steroidogenic genes. Expression of the *steroidogenic acute regulatory protein* (*StAR*) gene and protein, which regulates the rate-limiting step of steroidogenesis, was decreased in testes from *Bmal1* KO mice. Microscopically, testes from *Bmal1* KO mice exhibited reduced average seminiferous tubule diameter (by approximately 20%) and the sperm counts were reduced by approximately 70%. Homozygous *Bmal1* KO mice were unable to breed with each other (36).

Peruquetti et al. analyzed the role of two genes (*Clock* and *Bmal1*) in the chromatoid body. This cytoplasmic organelle plays a crucial role in RNA post-transcriptional and translation regulation during the germ cell differentiation. They detect an alteration in the structure of chromatoid body of the spermatids of *Bmal1* KO and *Clock* KO mice (34).

Liang et al. knocked down the *Clock* gene expression in the testes of male mice and determined its effect on fertility. Authors

TABLE 1 | Findings from pre-clinical studies investigating the role of clock genes on spermatogenesis.

Author, year	Pre-clinical model	Clock genes evaluated	Findings
Morse et al. (35)	*Clock* mutant male mice	*Per1*	*Per1* expression is not altered in testes from *Clock* mutant mice
Alvarez JD et al. (36)	*Bmal1* KO male mice	*Bmal1*	Impaired steroidogenesis in *Bmal1* KO mice. Reduced average seminiferous tubule diameter and the sperm counts in *Bmal1* KO mice.
Peruquetti RL et al. (34)	*Bmal1* KO male mice *Clock* KO male mice	*Bmal1* *Clock*	Alteration in the structure of chromatoid body of the spermatids of *Bmal1* KO and *Clock* KO mice
Liang X et al. (37)	*Clock* KD male mice	*Clock*	Smaller litter size, lower *in vitro* fertility rate, lower blastula formation rate, and lower acrosin activity in *Clock* KD male mice.

KD, Knock-down; KO, Knockout.

recorded lower *in vitro* fertilization rate, lower blastula formation rate, and a lower acrosin activity in the *Clock* Knockdown sperms, as well as a delay in dispersing cumulus cells. These results demonstrate that acrosin activity could be regulated by *Clock* and that *Clock* contributes to the regulation of male fertility and blastula formation (37).

Cheng et al. further corroborated these observation: they verified that acrosin activity and *in vitro* fertilization rate were reduced in SERPINA3K-treated sperm, producing a pattern of phenotypes very similar to that previously observed in the *Clock* knockdown sperm (38).

Unfortunately, the circadian expression of clock genes in testis tissue remains controversial.

Morse et al. investigated the role and the expression of *Per1* in the mice testis, reporting a constant expression of the gene during the 12-h light and 12-h dark cycles. Moreover, the levels of *Per1* proteins were constant during the day (35).

Human studies also provided evidence about the involvement of clock genes in male infertility.

Zhang et al. demonstrated, for the first time, an association between *CLOCK* genetic variants and altered semen quality in a human population with idiopathic infertility (39). In details, authors investigated the association between genetic variants of *CLOCK* and semen quality in humans. Authors examined three Single-Nucleotide-Polimorfism (SNP) of the *CLOCK* gene, (i.e. rs3749474, rs1801260 and rs3817444) to assess the association between these variants and semen quality in men with idiopathic infertility. The results indicated a strong association between the C allele carriers (CC or CT) of rs374947 and significantly reduced semen volume and sperm number per ejaculate. Moreover, associations between the A allele carriers (CA or AA) of rs3817444 and significantly reduced semen volume as well as between both the rs3749474 CC genotype and rs1801260 TC genotype and significantly decreased sperm motility were found (40).

CD and Reproductive Hormones

Circulating levels of male sexual hormones are modulated by circadian clock, light exposure, and sleep duration. The circadian pattern of LH and testosterone have been widely investigated in healthy males. In healthy young men, serum testosterone concentrations rise with sleep onset, reaches the peak during the first REM episode, remains stable until awakening, and then rapidly declines (41). Sleep-related elevations in LH have been also reported. Total sleep time and durations of stage 2 and REM have been reported to be positively related to morning testosterone levels (41). Zhang et al. found a significant correlation between sleep duration (measured by actigraphy) and follicle stimulating hormone (FSH) levels as well as by rapid eye movement sleep and FSH in healthy young men (42).

Total sleep deprivation or sleep restriction have been shown to impair the secretory activity of the pituitary-testis axis.

Leproult et al. investigated the effect of 1 week of sleep restriction to 5 hours per night (a condition experienced by at least 15% of the US working population) on testosterone levels in young healthy men and found a daytime decrease of testosterone levels by 10% to 15% (43).

Schmid et al. aimed to discriminate the effects of sleep duration and sleep timing on serum concentrations of LH and testosterone (44). They failed to find differences in terms of serum LH and testosterone concentrations between patents with sleep time restriction to 4 h for two consecutive nights (bedtime, 02:45 -07:00 h) and a control condition of 8 h regular sleep (bedtime, 22:45-07:00 h). However, total sleep deprivation and 4·5 h of sleep restricted to the first night-half (bedtime, 22:30-03:30 h) markedly decreased morning testosterone concentrations (44).

Interestingly, testosterone level has been reported to recover basal concentrations after one night of recovery sleep. However, extending sleep duration by approximately 1.2 h/night over six nights has minimal effects on hormonal responses to total sleep deprivation (41).

Yoon et al. investigated the levels of urinary LH in normal young men aged between 19 and 30 years following early morning light exposure (05:00 – 06.00). They found that LH excretion was increased 69.5% after bright light exposure but was not changed by placebo light exposure (45).

Despite previous results, Chen et al. failed to find significant association between sleep duration and reproductive hormone levels (follicle-stimulating hormone, LH, estradiol, progesterone, testosterone, and prolactin (46).

CD and Spermatogenesis in Humans

Evidence about the influence of CD on spermatogenesis in humans derive mainly from studies about the relationship between sleep duration/architecture and sperm parameters (**Table 2**).

Zhang et al. found a significant correlation between sleep duration (measured by actigraphy) and testis volume (42).

TABLE 2 | Findings from clinical studies investigating the association between sleep duration/quality and semen parameters.

Author, year	Study population	Findings
Jensen et al. (47)	Healthy men (n=953)	Inverse U-shaped association between sleep disturbance score and sperm concentration, total sperm count, percent morphologically normal spermatozoa (poorer semen quality in men with a sleep score below or above 11– 20).
Eisenberg et al. (48)	Men during preconception period (n=456)	No significant association between night or shift work and semen parameters
Chen et al. (46)	Healthy men (n=796)	Inverse U-shaped association between sleep duration and semen volume and total sperm count.
Vigano et al. (49)	Inferile men (n=382)	Negative association between sleep quality (difficulty in initiating sleep or lying awake most of the night) and sperm parameters concentration or motility.
Liu et al. (50)	Healthy men (n=1346)	Lower total sperm count in rotating shift workers.
Shi et al. (51)	Healthy men (n=328)	Decreased sperm concentration in short (< 4.7h) sleepers. Higher sperm DNA fragmentation index in patients with irregular sleeping habits.
Pokhrel et al. (52)	Healthy men (n=1101)	No association between sleep duration and sperm parameters.
Chen et al. (53)	Healthy men candidates for being sperm donor (n=842)	Association between short (<6 h) or long (>9 h) sleep duration and reduced sperm motility. Association between bad sleep quality (total Pittsburgh Sleep Quality Index [PSQI] score >5.0) and lower total sperm count, total motility, and progressive motility.
Du et al. (54)	Infertile men (n=970)	Negative correlation between the general quality of sleep and total motility, progressive motility, concentration, total sperm number and normal morphology.
Green et al. (55)	Healthy men (n=116)	Positive correlation between sleep duration and total sperm count progressive motility. Negative correlation between the usage of digital devices at night and total motility, progressive motility, concentration. Positive correlation between the usage of digital devices at night and immotile sperm.
Hvidt et al. (56)	Infertile men (n=104)	Lower semen quality in short (7.0–7.49 h) and very short (< 7.0 h) sleepers. Association between late (≥11:30 PM) bedtime and reduced semen quality. No association between sleep quality and semen quality.

Chen Q. et al. recorded an inversed U-shaped association between the entire sleep duration and two of the semen parameter (semen volume and total sperm count) with 7.0-7.5 h/d as the "turning point": for those whose sleep duration was below 7.0 h/d the semen parameters increased with longer sleep duration; but the semen parameters decreased, with longer sleep duration, for those whose sleep duration was over 7.5 h/d (46).

Similarly, Chen H-G. et al. investigated association between sleep duration and quality of the semen samples (53). Authors found a better quality of the semen (sperm volume, concentration and total count) in men who slept between 8.0 and 8.5 hours per day (53). Men who slept less than 6.0 h/day and higher than 9.0 h/day had lower sperm volume of 12% and 3.9%, respectively. Men who slept less than 6.0 h/day had lower total and progressive sperm motility of 4.4% and 5.0%, respectively. Moreover, men reporting poor sleep quality (total Pittsburgh Sleep Quality Index [PSQI] score >5.0) had lower total sperm count, total motility, and progressive motility of 8.0%, 3.9%, and 4.0%, respectively (53).

Jensen et al. demonstrated an inverse U-shaped association between sleep disturbance score and sperm concentration, total sperm count, percent morphologically normal spermatozoa (47).

Du et al. recorded a negative correlation between the general quality of sleep and several semen parameters (total motility, progressive motility, concentration, total sperm number and normal morphology) although semen volume and reproductive hormones were not markedly altered (54).

Green et al. recorded a positive statistically significant correlation between sleep duration and some semen parameters (total sperm count and progressive motility) (55). Additionally, authors recorded for the first time a negative significant correlation between the usage of digital devices, especially smartphones, at night, and sperm quality (total motility, progressive motility, concentration) and a positive statistically significant correlation between the usage of these devices and immotile sperm. It was hypothesized that the pathological mechanism underlying this phenomenon was the alteration in melatonin secretion induced by the short wavelength light emitted from the screens of these electronic devices (55). These results were corroborated by several studies, that report an association between elevated melatonin levels and oligospermia or azoospermia in men (57, 58).

Liu et al. compared sperm parameters between rotating shift workers (RSW) and permanent shift workers (PSW). They recorded a significantly lower total sperm count in RSW, compared to PSW. RSW was associated with higher risk of low total sperm count, after adjusting for age, education level, average monthly household income, abstinence period, sampling time point, tobacco smoking, alcohol drinking and body mass index (50).

Liu et al. conducted the same analyses on a cohort of male undergraduates in order to identify semen quality differences associated with non-work-related CD between school days and days off. Total sperm count in men with less than 0.5 h of CD was significantly higher compared to men with more than 2 h of CD (50).

Hvidt et al. found that early bedtime (< 10:30 PM) was more often associated with normal semen quality compared with both regular (10:30 PM-11:29 PM) and late (≥11:30 PM) bedtime. Similarly, regular sleep duration (7.5–7.99 h) was more often associated with normal semen quality than both short (7.0–7.49 h) and very short (< 7.0 h) sleep duration (56).

Of note, Shi et al. found significant associations between sperm DNA fragmentation index and irregular sleep habits (51).

Despite previous evidence, other studies failed to find significant association between sleep duration and or quality and sperm parameters (48, 52).

DISCUSSION

The relationship between disruption of CR and male infertility is supported by several pre-clinical and clinical lines of evidence. First, experimental manipulation or spontaneous mutations of clock genes, such as *Bmal1* and *Clock* negatively interfere with fertility pathways in both pre-clinical models and humans. Second, alterations of CR due to altered sleep duration and/or impairment of sleep architecture may negatively interfere with circulating levels of reproductive hormones and semen parameters in humans. Unfortunately, the current level of evidence is still low, and findings are often controversial due to heterogeneity in terms of study design, study populations, and standardization of measurements. Therefore, further studies are needed to further elucidate the interactions between CR, CD, and male infertility. In details, the impact of the duration of CD, genetic predisposing factors, as well the reversibility of these alterations deserve further investigations. Based on available evidence, clinicians facing infertile males should discuss, in everyday clinical practice, the potential detrimental ole of reduced sleep duration, altered sleep architecture or exposure to artificial light at night on reproduction.

AUTHOR CONTRIBUTIONS

Conception and design: FF, NL, and MCr. Acquisition of data: LS, LL, GF, and LC. Analysis and interpretation of data: MS, DA, and LN. Drafting of the manuscript: SM, GCa, CT, and GS. Critical revision of the manuscript for important intellectual content: MCr, GCe, MCa, RR, FF, FM, VM, and NL. Supervision: FF, NL, and MCr. All authors contributed to the article and approved the submitted version.

REFERENCES

1. Agarwal A, Saradha B, Neel P, Chak-Lam C, Ralf H, Sarah V, et al. Male Infertility. *Lancet (London England)* (2021) 397(10271):319–35. doi: 10.1016/S0140-6736(20)32667-2
2. Verze P, Arcaniolo D, Imbimbo C, Cai T, Venturino L, Spirito L, et al. General and Sex Profile of Women With Partner Affected by Premature Ejaculation: Results of a Large Observational, Non-Interventional, Cross-Sectional, Epidemiological Study (IPER-F). *Andrology* (2018) 6(5):714–19. doi: 10.1111/andr.12545
3. Arcaniolo D, Favilla V, Tiscione D, Pisano F, Bozzini G, Creta M, et al. Is There a Place for Nutritional Supplements in the Treatment of Idiopathic Male Infertility? *Archivio Italiano Di Urologia Andrologia: Organo Ufficiale [Di] Societa Italiana Di Ecografia Urologica E Nefrologica* (2014) 86(3):164–70. doi: 10.4081/aiua.2014.3.164
4. Verze P, La Rocca R, Spirito L, Califano G, Venturino L, Napolitano L, et al. Premature Ejaculation Patients and Their Partners: Arriving at a Clinical Profile for a Real Optimization of the Treatment. *Archivio Italiano Di Urologia Andrologia: Organo Ufficiale [Di] Societa Italiana Di Ecografia Urologica E Nefrologica* (2021) 93(1):42–7. doi: 10.4081/aiua.2021.1.42
5. Russart KLG, Nelson RJ. Light at Night as an Environmental Endocrine Disruptor. *Physiol Behav* (2018) 190(June):82–9. doi: 10.1016/j.physbeh.2017.08.029
6. Napolitano L, Barone B, Morra S, Celentano G, La Rocca R, Capece M, et al. Hypogonadism in Patients With Prader Willi Syndrome: A Narrative Review. *Int J Mol Sci* (2021) 22(4):1993. doi: 10.3390/ijms22041993
7. Li C, Zhang L, Ma T, Gao L, Yang L, Wu M, et al. Bisphenol A Attenuates Testosterone Production in Leydig Cells *via* the Inhibition of NR1D1 Signaling. *Chemosphere* (2021) 263(January):128020. doi: 10.1016/j.chemosphere.2020.128020
8. Zhao L, Zhang J, Yang L, Zhang H, Zhang Y, Gao D, et al. Glyphosate Exposure Attenuates Testosterone Synthesis *via* NR1D1 Inhibition of StAR Expression in Mouse Leydig Cells. *Sci Total Environ* (2021) 785 (September):147323. doi: 10.1016/j.scitotenv.2021.147323
9. Balsalobre A, Damiola F, Schibler U. A Serum Shock Induces Circadian Gene Expression in Mammalian Tissue Culture Cells. *Cell* (1998) 93(6):929–37. doi: 10.1016/s0092-8674(00)81199-x
10. Rosbash M. Why the Rat-1 Fibroblast Should Replace the SCN as the in Vitro Model of Choice. *Cell* (1998) 93(6):917–19. doi: 10.1016/s0092-8674(00)81197-6
11. Peterlin A, Kunej T, Peterlin B. The Role of Circadian Rhythm in Male Reproduction:". *Curr Opin Endocrinol Diabetes Obes* (2019) 26(6):313–16. doi: 10.1097/MED.0000000000000512
12. Weaver DR. The Suprachiasmatic Nucleus: A 25-Year Retrospective. *J Biol Rhythms* (1998) 13(2):100–12. doi: 10.1177/074873098128999952
13. Reppert SM, Weaver DR. Coordination of Circadian Timing in Mammals. *Nature* (2002) 418(6901):935–41. doi: 10.1038/nature00965
14. Gamble KL, Resuehr D, Hirschie Johnson C. Shift Work and Circadian Dysregulation of Reproduction. *Front Endocrinol* (2013) 4:92. doi: 10.3389/fendo.2013.00092
15. Huang W, Ramsey KM, Marcheva B, Bass J. Circadian Rhythms, Sleep, and Metabolism. *J Clin Invest* (2011) 121(6):2133–41. doi: 10.1172/JCI46043
16. Reid KJ. Assessment of Circadian Rhythms. *Neurologic Clinics* (2019) 37 (3):505–26. doi: 10.1016/j.ncl.2019.05.001
17. Harrington ME. The Ventral Lateral Geniculate Nucleus and the Intergeniculate Leaflet: Interrelated Structures in the Visual and Circadian Systems. *Neurosci Biobehav Rev* (1997) 21(5):705–27. doi: 10.1016/s0149-7634(96)00019-x
18. Rüger M, Scheer FAJL. Effects of Circadian Disruption on the Cardiometabolic System. *Rev Endocrine Metab Disord* (2009) 10(4):245–60. doi: 10.1007/s11154-009-9122-8
19. Takahashi JS, Hong H-K, Ko CH, McDearmon EL. The Genetics of Mammalian Circadian Order and Disorder: Implications for Physiology and Disease. *Nat Rev Genet* (2008) 9(10):764–75. doi: 10.1038/nrg2430
20. Litlekalsoy J, Rostad K, Kalland K-H, J G. Hostmark, Didrik Laerum O. Expression of Circadian Clock Genes and Proteins in Urothelial Cancer Is Related to Cancer-Associated Genes. *BMC Cancer* (2016) 16(July):549. doi: 10.1186/s12885-016-2580-y
21. Morales-Santana S, Morell S, Leon J, Carazo-Gallego A, Jimenez-Lopez JC, Morell M. An Overview of the Polymorphisms of Circadian Genes Associated With Endocrine Cancer. *Front Endocrinol* (2019) 10:104. doi: 10.3389/fendo.2019.00104
22. Vetter C. Circadian Disruption: What Do We Actually Mean? *Eur J Neurosci* (2020) 51(1):531–50. doi: 10.1111/ejn.14255
23. Alterman T, Luckhaupt SE, Dahlhamer JM, Ward BW, Calvert GM. Prevalence Rates of Work Organization Characteristics Among Workers in the U.S.: Data From the 2010 National Health Interview Survey. *Am J Ind Med* (2013) 56(6):647–95. doi: 10.1002/ajim.22108
24. Centers for Disease Control and Prevention (CDC). Short Sleep Duration Among Workers–United States 2010. In: *MMWR. Morbidity and Mortality Weekly Report* vol. 61. Atlanta, GA, USA: Centers for Disease Control and Prevention (2012). p. 281–5.
25. Sack RL, Lewy AJ. Melatonin as a Chronobiotic: Treatment of Circadian Desynchrony in Night Workers and the Blind. *J Biol Rhythms* (1997) 12 (6):595–603. doi: 10.1177/074873049701200615
26. Castro JM, Stoerzinger A, Barkmeier D, Ellen P. Medial Septal Lesions: Disruptions of Microregulatory Patterns and Circadian Rhythmicity in Rats. *J Comp Physiol Psychol* (1978) 92(1):71–84. doi: 10.1037/h0077443
27. Stevens RG, Rea MS. Light in the Built Environment: Potential Role of Circadian Disruption in Endocrine Disruption and Breast Cancer. *Cancer Causes Control: CCC* (2001) 12(3):279–87. doi: 10.1023/a:1011237000609

28. Foster RG, Peirson SN, Wulff K, Winnebeck E, Vetter C, Roenneberg T. Sleep and Circadian Rhythm Disruption in Social Jetlag and Mental Illness. *Prog Mol Biol Trans Sci* (2013) 119:325–46. doi: 10.1016/B978-0-12-396971-2.00011-7
29. Fritschi L, Groß JV, Wild U, Heyworth JS, Glass DC, Erren TC. Shift Work That Involves Circadian Disruption and Breast Cancer: A First Application of Chronobiological Theory and the Consequent Challenges. *Occup Environ Med* (2018) 75(3):231–4. doi: 10.1136/oemed-2017-104441
30. Scheer FAJL, Hilton MF, Mantzoros CS, Shea SA. Adverse Metabolic and Cardiovascular Consequences of Circadian Misalignment. *Proc Natl Acad Sci USA* (2009) 106(11):4453–8. doi: 10.1073/pnas.0808180106
31. Califano G, Xylinas E. Re: Phase II Trial of Neoadjuvant Systemic Chemotherapy Followed by Extirpative Surgery in Patients With High Grade Upper Tract Urothelial Carcinoma. *Eur Urol* (2020) 78(1):113–45. doi: 10.1016/j.eururo.2020.04.008
32. Califano G, Ouzaid I, Verze P, Stivalet N, Hermieu J-F, Xylinas E. New Immunotherapy Treatments in Non-Muscle Invasive Bladder Cancer. *Archivos Espanoles Urologia* (2020) 73(10):945–535.
33. Bittman EL. Timing in the Testis. *J Biol Rhythms* (2016) 31(1):12–36. doi: 10.1177/0748730415618297
34. Peruquetti RL, de Mateo S, Sassone-Corsi P. Circadian Proteins CLOCK and BMAL1 in the Chromatoid Body, a RNA Processing Granule of Male Germ Cells." Edited by Laszlo Tora. *PloS One* (2012) 7(8):e426955. doi: 10.1371/journal.pone.0042695
35. Morse D, Cermakian N, Brancorsini S, Parvinen M, Sassone-Corsi P. No Circadian Rhythms in Testis: Period1 Expression Is Clock Independent and Developmentally Regulated in the Mouse. *Mol Endocrinol (Baltimore Md)* (2003) 17(1):141–51. doi: 10.1210/me.2002-0184
36. Alvarez JD, Hansen A, Ord T, Bebas P, Chappell PE, Giebultowicz JM. Carmen Williams, Stuart Moss, and Amita Sehgal. 2008. "The Circadian Clock Protein BMAL1 Is Necessary for Fertility and Proper Testosterone Production in Mice. *J Biol Rhythms* (2008) 23(1):26–36. doi: 10.1177/0748730407311254
37. Liang X, Cheng S, Jiang X, He X, Wang Y, Jiang Z, et al. The Noncircadian Function of the Circadian Clock Gene in the Regulation of Male Fertility. *J Biol Rhythms* (2013) 28(3):208–17. doi: 10.1177/0748730413486873
38. Cheng S, Liang X, Wang Y, Jiang Z, Liu Y, Hou W, et al. The Circadian Clock Gene Regulates Acrosin Activity of Sperm Through Serine Protease Inhibitor A3K. *Exp Biol Med* (2016) 241(2):205–15. doi: 10.1177/1535370215597199
39. Zhang J, Ding X, Li Y, Xia Y, Nie J, Yi C, et al. Association of CLOCK Gene Variants With Semen Quality in Idiopathic Infertile Han-Chinese Males. *Reprod BioMed Online* (2012) 25(5):536–42. doi: 10.1016/j.rbmo.2012.07.018
40. Shen O, Ding X, Nie J, Xia Y, Wang X, Tong J, et al. Variants of the CLOCK Gene Affect the Risk of Idiopathic Male Infertility in the Han-Chinese Population. *Chronobiology Int* (2015) 32(7):959–65. doi: 10.3109/07420528.2015.1056305
41. Arnal PJ, Drogou C, Sauvet F, Regnauld J, Dispersyn G, Faraut B, et al. Effect of Sleep Extension on the Subsequent Testosterone, Cortisol and Prolactin Responses to Total Sleep Deprivation and Recovery. *J Neuroendocrinol* (2016) 28(2):12346. doi: 10.1111/jne.12346
42. Zhang W, Piotrowska K, Chavoshan B, Wallace J, Liu PY. Sleep Duration Is Associated With Testis Size in Healthy Young Men. *J Clin Sleep Medicine: JCSM: Off Publ Am Acad Sleep Med* (2018) 14(10):1757–64. doi: 10.5664/jcsm.7390
43. Leproult R, Van Cauter E. Effect of 1 Week of Sleep Restriction on Testosterone Levels in Young Healthy Men. *JAMA* (2011) 305(21):2173–4. doi: 10.1001/jama.2011.710
44. Schmid SM, Hallschmid M, Jauch-Chara K, Lehnert H, Schultes B. Sleep Timing May Modulate the Effect of Sleep Loss on Testosterone. *Clin Endocrinol* (2012) 77(5):749–54. doi: 10.1111/j.1365-2265.2012.04419.x
45. Yoon I-Y, Kripke DF, Elliott JA, Youngstedt SD. Luteinizing Hormone Following Light Exposure in Healthy Young Men. *Neurosci Lett* (2003) 341(1):25–8. doi: 10.1016/s0304-3940(03)00122-8
46. Chen Q, Yang H, Zhou N, Sun L, Bao H, Tan L, et al. Inverse U-Shaped Association Between Sleep Duration and Semen Quality: Longitudinal Observational Study (MARHCS) in Chongqing, China. *Sleep* (2016) 39(1):79–86. doi: 10.5665/sleep.5322
47. Jensen TK, Andersson A-M, Skakkebaek NE, Joensen UN, Jensen MB, Lassen TH, et al. Association of Sleep Disturbances With Reduced Semen Quality: A Cross-Sectional Study Among 953 Healthy Young Danish Men. *Am J Epidemiol* (2013) 177(10):1027–37. doi: 10.1093/aje/kws420
48. Eisenberg ML, Chen Z, Ye A, Buck Louis GM. Relationship Between Physical Occupational Exposures and Health on Semen Quality: Data From the Longitudinal Investigation of Fertility and the Environment (LIFE) Study. *Fertility Sterility* (2015) 103(5):1271–77. doi: 10.1016/j.fertnstert.2015.02.010
49. Viganò P, Chiaffarino F, Bonzi V, Salonia A, Ricci E, Papaleo E, et al. Sleep Disturbances and Semen Quality in an Italian Cross Sectional Study. *Basic Clin Androl* (2017) 27:16. doi: 10.1186/s12610-017-0060-0
50. Liu K, Hou G, Wang X, Chen H, Shi F, Liu C, et al. Adverse Effects of Circadian Desynchrony on the Male Reproductive System: An Epidemiological and Experimental Study. *Hum Reprod* (2020) 35(7):1515–28. doi: 10.1093/humrep/deaa101
51. Shi X, Chan CPS, Waters T, Chi L, Yiu Leung Chan D, Li T-C. Lifestyle and Demographic Factors Associated With Human Semen Quality and Sperm Function. *Syst Biol Reprod Med* (2018) 64(5):358–67. doi: 10.1080/19396368.2018.1491074
52. Pokhrel G, Yihao S, Wangcheng W, Upadhyaya Khatiwada S, Zhongyang S, Jianqiao Y, et al. The Impact of Sociodemographic Characteristics, Lifestyle, Work Exposure and Medical History on Semen Parameters in Young Chinese Men: A Cross-Sectional Study. *Andrologia* (2019) 51(8):e133245. doi: 10.1111/and.13324
53. Chen H-G, Sun B, Chen Y-J, Chavarro JE, Hu S-H, Xiong C-L, et al. Sleep Duration and Quality in Relation to Semen Quality in Healthy Men Screened as Potential Sperm Donors. *Environ Int* (2020) 135(February):105368. doi: 10.1016/j.envint.2019.105368
54. Du C-Q, Yang Y-Y, Chen J, Feng L, Lin W-Q. Association Between Sleep Quality and Semen Parameters and Reproductive Hormones: A Cross-Sectional Study in Zhejiang, China. *Nat Sci Sleep* (2020) 12:11–8. doi: 10.2147/NSS.S235136
55. Green A, Barak S, Shine L, Kahane A, Dagan Y. Exposure by Males to Light Emitted From Media Devices at Night Is Linked With Decline of Sperm Quality and Correlated With Sleep Quality Measures. *Chronobiology Int* (2020) 37(3):414–24. doi: 10.1080/07420528.2020.1727918
56. Hvidt JEM, Knudsen UB, Zachariae R, Jakob Ingerslev H, Tholstrup Philipsen M, Frederiksen Y. Associations of Bedtime, Sleep Duration, and Sleep Quality With Semen Quality in Males Seeking Fertility Treatment: A Preliminary Study. *Basic Clin Andrology* (2020) 30:5. doi: 10.1186/s12610-020-00103-7
57. Sciarra F, Franceschini E, Campolo F, Gianfrilli D, Pallotti F, Paoli D, et al. Disruption of Circadian Rhythms: A Crucial Factor in the Etiology of Infertility. *Int J Mol Sci* (2020) 21(11):3943. doi: 10.3390/ijms21113943
58. Karasek M, Pawlikowski M, Nowakowska-Jankiewicz B, Kolodziej-Maciejewska H, Zieleniewski J, Cieslak D, et al. Circadian Variations in Plasma Melatonin, FSH, LH, and Prolactin and Testosterone Levels in Infertile Men. *J Pineal Res* (1990) 9(2):149–57. doi: 10.1111/j.1600-079x.1990.tb00703.x

Conflict of Interest: The authors declare that the research was conducted in the absence of any commercial or financial relationships that could be construed as a potential conflict of interest.

frontiers in Endocrinology

ORIGINAL RESEARCH
published: 24 December 2021
doi: 10.3389/fendo.2021.801125

Extensive Assessment of Underlying Etiological Factors in Primary Infertile Men Reduces the Proportion of Men With Idiopathic Infertility

*Eugenio Ventimiglia[1,2], Edoardo Pozzi[1,3], Paolo Capogrosso[1,2], Luca Boeri[1,3], Massimo Alfano[1], Walter Cazzaniga[1,2], Rayan Matloob[1], Costantino Abbate[1], Paola Viganò[4], Francesco Montorsi[1,2] and Andrea Salonia[1,2]**

[1] Division of Experimental Oncology/Unit of Urology, Urological Research Institute (URI), Istituto di Ricerca e Cura a Carattere Scientifico (IRCCS) Ospedale San Raffaele, Milan, Italy, [2] Department of Urology, University Vita-Salute San Raffaele, Milan, Italy, [3] Department of Urology, Istituto di Ricerca e Cura a Carattere Scientifico (IRCCS) Fondazione Ca' Granda – Ospedale Maggiore Policlinico, University of Milan, Milan, Italy, [4] Infertility Unit, Unit of Obstetrics/Gynecology, Istituto di Ricerca e Cura a Carattere Scientifico (IRCCS) Ospedale San Raffaele, Milan, Italy

OPEN ACCESS

Edited by:
Qing Chen,
Army Medical University, China

Reviewed by:
Roland Eghoghosoa Akhigbe,
Ladoke Akintola University of Technology, Nigeria
Giovanni Luca,
University of Perugia, Italy

***Correspondence:**
Andrea Salonia
salonia.andrea@hsr.it

Specialty section:
This article was submitted to Reproduction, a section of the journal Frontiers in Endocrinology

Received: 24 October 2021
Accepted: 03 December 2021
Published: 24 December 2021

Citation:
Ventimiglia E, Pozzi E, Capogrosso P, Boeri L, Alfano M, Cazzaniga W, Matloob R, Abbate C, Viganò P, Montorsi F and Salonia A (2021) Extensive Assessment of Underlying Etiological Factors in Primary Infertile Men Reduces the Proportion of Men With Idiopathic Infertility. Front. Endocrinol. 12:801125. doi: 10.3389/fendo.2021.801125

Objective: Up to 40% of infertile men remain without a recognized cause (i.e., idiopathic infertility). We aimed to identify, categorize, and report the supposed causes of male infertility in a cohort of white-European men presenting for primary couple's infertility, by using a thorough and extensive baseline diagnostic work-up.

Material and Methods: Cross-sectional study of 1,174 primary infertile men who underwent a thorough diagnostic work-up including: detailed medical history, physical examination, hormonal assessment, genetic testing, semen analyses; semen and urine cultures; testis color Duplex US. Men without any identified causal factor were considered as idiopathic. Six different etiological categories were established, and their prevalence was estimated. Logistic regression models estimated the risk of missing causal identification.

Results: A possible causal factor was identified in 928 (81%) men. Hypogonadism was the most frequent identified cause (37%), followed by varicocele (27%). Genetic abnormalities were found in 5% of patients. A causal factor was more easily identifiable for the more severe infertility cases, and azoospermic men were those less likely to be defined as idiopathic (OR and 95% CIs: 0.09; 0.04-0.20). Relative proportion of identified causes remained constant during the 10-year study period (p>0.43).

Conclusions: Due to a more comprehensive and extensive diagnostic work-up, at least one underlying cause of male infertility factor in 4 out of 5 infertile men can be identified. Men with a less severe phenotype remain a clinical challenge in terms of establishing a possible etiologic factor. Further studies are needed to assess which subset of infertile men deserves a more extensive work-up.

Keywords: infertility, male infertility, cause, idiopathic, risk factors

INTRODUCTION

Lack of both effective therapeutic strategies and identifiable underlying causes are common features in infertile men (1). Up to 60% of cases remain without a recognized cause, and are therefore referred to as idiopathic according to various series (1–3). Overall, this group of men is an interesting epidemiological cohort for several reasons. First, this sample represents an ideal cohort for studying new possible etiological factors linked to male subfertility and infertility (1–3). Second, the lack of an underlying etiologic factor may seriously limit further diagnostic work-up and, above all, possible therapeutic options (1). Third, in the context of clinical syndromes, it might anticipate future or yet occult health issues which would otherwise progress unnoticed in infertile, and therefore often young, men (4). Eventually, the lack of a clear explanation for their reproductive issue represents a factor of psychological distress in infertile men (5).

The definition of idiopathic infertility and its prevalence vary consistently according to previously published reports (2, 3), depending on the postulated possible causal factors and the baseline diagnostic work-up selected by the investigators. It was previously shown that a more accurate work-up may improve the diagnostic process increasing its accuracy during clinical evaluation of the infertile male (6, 7).

For these reasons, by using a thorough and extensive baseline diagnostic work-up, we aimed to identify, categorize, and report possible aetiologies of male factor infertility of a large homogenous cohort of white-European men presenting for primary couple's infertility, and to report the rate of those men with an identifiable cause that would have otherwise classified as having idiopathic infertility with the standard diagnostic work-up.

METHODS

Study Population

The analyses considered a homogenous cohort of 1,147 white-European men only belonging to primary infertile couples assessed between 2007 and 2016 at a single academic centre. Two different semen analyses were requested for every enrolled man and evaluated according to the 2010 WHO guidelines. Male factor infertility (MFI) was defined and identified as at least one impaired sperm parameter in at least two consecutive semen analyses and after a comprehensive gynaecological evaluation of the female partners. Data collection followed the principles outlined in the Declaration of Helsinki. All patients signed an informed consent form agreeing to share their own anonymous information for other future studies. The study was approved by the local ethic committee (IRCCS OSR Prot. 2014 – Pazienti Ambulatoriali).

Diagnostic Work-Up

We performed an extensive diagnostic work-up for every included man, irrespective of the baseline infertility severity. This work-up included: detailed patient history (specifically also inquiring cryptorchidism, puberty onset, history of mumps, genital infections, urogenital trauma, previous urogenital/pelvic surgery, cigarette smoking, use of illicit drugs (e.g., marijuana, cocaine, opioids), use of anabolic steroids, symptoms of testosterone deficiency; comorbidities were scored with the Charlson Comorbidity Index (CCI), which was categorised as 0, 1, ≥2); physical examination (e.g., testicular volume, varicocele, genital tract abnormalities); hormonal assessment (including, total testosterone, FSH, LH performed in a fasting state in every case before 10 AM and repeated in order to confirm abnormal values); genetic testing (karyotype analysis, Y-chromosome microdeletions, CFTR gene mutations); semen analyses; semen and urine cultures; and, testis color duplex-US. Based on the results of the diagnostic work-up, six different etiological categories were established: 1) men with genetic abnormalities; 2) men with history of cryptorchidism (without genetic abnormalities); 3) men with genital tract obstructions (without known genetic abnormalities and cryptorchidism); 4) men with biochemical hypogonadism (defined as FSH>7.8 mU/ml and/or total testosterone <3 ng/ml and/or LH >9.4 mU/ml; without genetic abnormalities, cryptorchidism, and genital tract obstructions) (8, 9); 5) men with clinical varicocele (color duplex-US confirmed, without genetic abnormalities, cryptorchidism, genital tract obstruction, and hypogonadism); and, 6) men with other factors (either current or history of seminal tract infections, medical or physical treatment likely to affect fertility, trauma, and other iatrogenic causes) in absence of varicocele, genetic abnormalities, cryptorchidism, genital tract obstructions, and hypogonadism. Thereof, men without any identified causal factor were considered idiopathic.

We further distinguished between isolated MFI or a mixed infertility factor. MFI was defined after a comprehensive diagnostic evaluation of all the female partners.

Statistical Analyses

Statistical analyses consisted of several steps. First, we assessed the prevalence of each specific cause in our population, assessing the proportion of idiopathic men following the proposed extensive work-up. Second, we analysed the prevalence of each specific cause over time seeking for possible time trends. Third, we evaluated the prevalence of idiopathic infertility and each specific cause according to different severity of baseline clinical presentation; for this specific purpose, we evaluated cause prevalence at different sperm concentration thresholds, under the assumption that this parameter represents a proxy of MFI severity. Eventually, logistic regression model estimated odds ratio (OR) and 95% confidence (95% CI) intervals of the idiopathic infertility, including as model covariates patient age, BMI, comorbidities, mean testicular volume, isolated MFI vs. mixed infertility factor, and azoospermia. Distribution of data was tested with the Shapiro–Wilk test. Data are presented as medians (interquartile range; IQR) or frequencies (proportions). All statistical tests were two-sided with a significance value set a 0.05.

RESULTS

Table 1 details descriptive statistics of the whole cohort of patients. Median (IQR) age of the study cohort was 37 (34-41) years. Most of the included men had an isolated MFI (791, 69%) and a CCI score of 0 (1080, 94%). Men with isolated MFI did not

considerably differ from men with a mixed infertility factor, except for higher sperm concentration (9 (1-35) vs. 4 (0-24) 10^6 spermatozoa/ml, p<0.001 at Mann-Whitney test).

We were able to identify and define a causal category for 928 out of 1,147 men (81%). The most common causal category was hypogonadism (420 men, 37%), whereas genetic factors were identified in 61 men (5%, **Table 1**).

During the analyzed 10-year study period we found no difference in prevalent causes of MFI over time (p=0.43 as for Chi square test, **Figure 1**).

As shown in **Figure 2**, men with a more severe MFI were less likely to be classified as idiopathic: a lower proportion of idiopathic cases was observed in men with azoospermia compared to men with sperm concentration > 10 million spermatozoa/ml (3% vs. 34%, p<0.01 as for Chi square test).

At multivariable logistic regression analysis (**Table 2**), men with a larger testicular volume (OR: 1.07; 1.04 - 1.10) were at higher risk of having an idiopathic MFI, whereas azoospermic men (OR: 0.09; 0.04 - 0.20) had a reduced risk of missing a causal identification.

DISCUSSION

In this study, we performed an extensive diagnostic work-up in 1,147 white-European men with MFI only belonging to couples complaining primary infertility in order to properly and precisely assess the possible underlying causal factors. By applying this extensive work-up, it was possible to identify a causal category for 81% of the study cohort. Moreover, men with

TABLE 1 | Descriptive characteristic of the whole cohort of patients [No. 1,147].

	MFI	Mixed factor	Overall
	n = 791	n = 356	n = 1147
Age (years)			
Median (IQR)	37 (34-40)	37 (34-41)	37 (34-41)
BMI (kg/m^2)			
Median (IQR)	25 (23-27)	25 (23-27)	25 (23-27)
CCI - n (%)			
0	748 (95)	332 (93)	1080 (94)
1	21 (3)	12 (3)	33 (3)
2+	22 (3)	12 (3)	34 (3)
Mean testicular volume (Prader)			
Median (IQR)	15 (12-20)	15 (12-20)	15 (12-20)
Total testosterone (ng/ml)			
Median (IQR)	4 (3-6)	5 (3-6)	4 (3-6)
FSH (mU/mL)			
Median (IQR)	6 (3-13)	5 (3-10)	6 (3-11)
Sperm concentration (10^6/ml)			
Median (IQR)	4 (0-24)	9 (1-35)	6 (0-26)
Varicocele - n (%)			
No	423 (53)	191 (54)	614 (54)
Yes	368 (47)	165 (46)	533 (46)
Cryptorchidism - n (%)			
No	703 (89)	326 (92)	1029 (90)
Yes	88 (11)	30 (8)	118 (10)
Karyotype abnormalities - n (%)			
Normal	499 (93)	233 (95)	732 (94)
XXY	12 (2)	5 (2)	17 (2)
Other abnormalities	24 (4)	7 (3)	31 (4)
CFTR - n (%)			
Normal	788 (100)	356 (100)	1144 (100)
Mutation	3 (0)	0 (0)	3 (0)
Y chromosome microdeletions - n (%)			
Normal	780 (99)	355 (100)	1135 (99)
Deletion	11 (1)	1 (0)	12 (1)
Cause of infertility - n (%)			
Idiopathic	142 (18)	77 (22)	219 (19)
Genetic abnormalities	48 (6)	13 (4)	61 (5)
Cryptorchidism	73 (9)	25 (7)	98 (9)
Obstructive	16 (2)	5 (1)	21 (2)
Hypogonadism	295 (38)	125 (35)	420 (37)
Varicocele	199 (25)	105 (30)	304 (27)
Other	11 (1)	3 (1)	14 (1)

The study cohort is stratified according to the presence of an isolated male factor infertility (MFI) or a mixed factor (MFI + female factor).
BMI, body mass index; CCI, Charlson comorbidity index; CFTR, cystic fibrosis conductance regulator; FSH, follicle stimulating hormone.

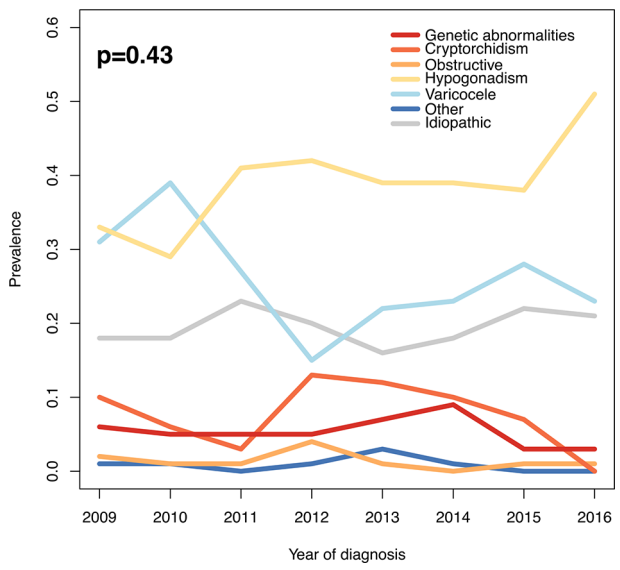

FIGURE 1 | Prevalence of different causes of male factor infertility during the study period. P-value as for Chi-square test.

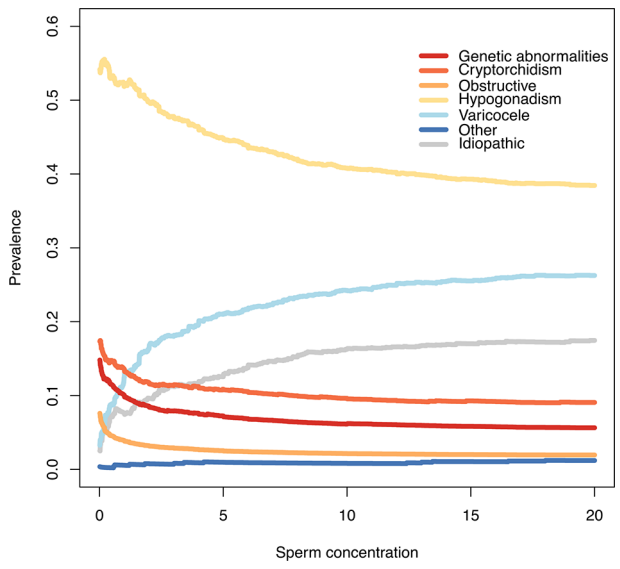

FIGURE 2 | Prevalence of different causes of male factor infertility according to different sperm concentration thresholds. At each sperm concentration threshold (x axis) is shown on the y-axis the relative proportion of men with a specific causal factor (eg: if x=5, on the y-axis is shown cause prevalence of men with sperm concentration < 5 million/ml).

a less severe MFI were those with the highest chance of missing a causal identification.

Uro-andrologists working in the reproductive medicine setting often face both lack of effective therapeutic options for MFI patients and a misclassification of the disease etiology (1).

TABLE 2 | Multivariable OR and 95% CI for the diagnosis of idiopathic infertility in the study cohort [No. 1,147].

	OR	95% CIs	p
Age			
years	1.03	1.00 - 1.05	0.05
BMI			
kg/m^2	0.97	0.93 - 1.02	0.26
CCI			
0	1.00	(Ref.)	
1	0.97	0.38 - 2.50	0.95
2+	1.64	0.69 - 3.88	0.26
Mean testicular volume			
prader	1.07	1.04 - 1.10	<0.001
Infertility factor			
MFI	1.00	(Ref.)	
Mixed factor	1.10	0.79 - 1.52	0.58
Azoospermia			
no	1.00	(Ref.)	
yes	0.09	0.04 - 0.20	<0.001

BMI, body mass index; CCI, Charlson comorbidity index; MFI, male factor infertility; Mixed factor MFI + female factor.

This has several drawbacks in terms of further diagnostic work-up and treatment (6, 7); it should be considered as well that the identification of possible causal factors might bring psychological relief to the infertile couple. Though several improvements were reported throughout the last years (10), the way we assess and treat infertile couple remains still unsatisfactory in a relevant proportion of cases.

The most comprehensive and recently available reports set the proportion of idiopathic cases between 35% and 60% (2, 3). Such wide differences depend both on selection criteria at study entry and the way causal categories were defined. Punab et al. (3) analyzed data from 1,737 men, establishing *a priori* seven causal factors (secondary hypogonadism, seminal tract obstruction, genetic causes, oncological diseases, severe sexual dysfunction, congenital uro-genital abnormalities, and acquired testicular damage) further sub-classified into absolute, severe, and plausible factors; the authors found that 40% of the study cohort was classified into the aforementioned categories. Of importance, varicocele was not considered as a causal factor. Conversely, Olesen et al. (2) established a wider pool of causes, including varicocele (13% of the analyzed cohort), limiting the idiopathic proportion of infertile men to one third of the whole cohort; the most frequently identified factor was cryptorchidism (17%). It should be noted that different selection criteria were used in the two aforementioned studies: Olesen et al. (2) selected men referred for diagnostic work-up prior to *in vitro* fertilization (IVF) or intra-cytoplasmatic sperm injection (ICSI) treatments, whereas Punab et al. (3) included infertile men with severe male factor infertility defined by total sperm count <39 million per ejaculate. Different inclusion criteria are likely to result in different prevalence of the underlying causal categories, since we clearly showed that cause-specific prevalence varies according to MFI severity. Moreover, not only inclusion criteria are likely to influence prevalence results: the selected work-up will similarly impact on study finding, since >30% of included men did not undergo genetic testing in the study by Punab et al. (3). Most of

the previous efforts in better ascertaining MFI were directed towards men with the most severe clinical presentation in terms of reproductive disorders, azoospermia (11, 12). Our group previously showed that a more extensive and tailored work-up is able to reduce the misdiagnosis of hypogonadism (7) and karyotype abnormalities in infertile men (6). Similarly, we show in this study that idiopathic cases can be limited by using a more extensive work-up. For these reasons, we aimed at designing a study capable of maximizing the ascertainment of possible causal factors (by means of an extensive work-up) in a cohort of men with MFI without entry restrictions. As a consequence, this allowed us to stratify cause prevalence according to MFI severity in the widest and most accurately ever analyzed homogenous sample of white-European primary infertile men.

There is still an ongoing and longstanding epidemiological debate regarding whether specific factors should be considered as either causal or risk factors (13). For the specific purpose of our study, we defined causal categories relying on previously published reports which examined consistently possible causes or strongly related risk factors, building a hierarchical classification up. At this regards, genetic abnormalities (GA; including karyotype abnormalities, CFTR mutations known to impair fertility, and Y-chromosome microdeletions) represent one of the very few indisputable and ascertained cause of male reproduction impairment (1). For this reason, we decided to give GA the highest position in our hierarchical classification.

Men with cryptorchidism and TDS symptoms but without genetic abnormalities ranked second in this hierarchical grouping. These men share a clear condition linked to MFI which dates back to the developmental age (14), despite lacking an identifiable shared genetic background (in its non-syndromic presentation) (15). At this regard, 9% of our cohort was included in this category, being more common in men with a more severe MFI.

We decided to consider men with biochemical hypogonadism as a category on its own for several reasons. For this specific purpose, we considered previously published European Male Aging Study (EMAS) criteria for defining biochemical hypogonadism (8) implementing them with FSH values according to Barbotin et al. (9). Notably, hypogonadal men represented the largest category in our population (37%). Including men with primary, secondary, and compensated hypogonadism allowed us to intercept a wide range of conditions eventually resulting in an alteration of the hormonal milieu (16), e.g. ranging from testicular deficiency to endocrine disruptors. We previously showed that not only hypogonadism is a frequent finding in infertile men, but it represents as well a heterogeneous category amenable to be further stratified into different and well defined prognostic categories (17).

We also decided to include clinical varicocele in our causal classification. It is still debated whether varicocele represents a condition unequivocally linked to MFI, and whether it should always be treated or not in this setting (1, 18, 19). In a subgroup analyses of five randomized control trials comparing treatment to observation in men with a clinical varicocele, oligozoospermia and otherwise unexplained infertility (i.e. the way we classified varicocele in this study), it was observed that varicocele repair improved pregnancy rate and live birth rate (20).

Our study is not devoid of limitations. First, the proposed extensive work-up inevitably results in overtreatment, with inherent extra costs. Future efforts will be devoted to better tailor such an extensive work-up without losing diagnostic powers. Second, there is a plethora of emerging metabolic and environmental factors detrimentally acting on male reproductive function (10, 16, 21–25), with a close interplay with general health status (25, 26); it will be interesting to see whether these factors, not considered in our classification, will gain the scientific dignity and eventually become causal factors. Third, the lack of a control group prevented us from inquiring the strengths of causal associations. Despite these limitations, we believe that the proposed user-friendly classification can be easily implemented and reproduced, casting light in a field where the everyday clinical practice still faces several grey areas.

CONCLUSIONS

By performing a more detailed and comprehensive diagnostic work up for men with male factor infertility, it is possible to identify at least one underlying cause of male factor infertility in 4 out of 5 of these men. In this regard, this subset of men would have been recognised as having idiopathic infertility, with standard diagnostic exams. It remains a clinical challenge to establish an identifiable aetiology among infertile men with a less severe phenotype.

DATA AVAILABILITY STATEMENT

The original contributions presented in the study are included in the article/supplementary material. Further inquiries can be directed to the corresponding author.

ETHICS STATEMENT

The studies involving human participants were reviewed and approved by "Pazienti ambulatoriali". The patients/participants provided their written informed consent to participate in this study.

AUTHOR CONTRIBUTIONS

Conception and design: EV and AS. Acquisition of data: EV, PC, LB, WC, RM, CA, and EP. Analysis and interpretation of data: EV and AS. Drafting of the manuscript: EV. Critical revision: AS, PV, MA, and FM. Statistical analysis: EV and AS. Administrative, technical, or material support: AS and FM. Supervision: AS and FM. All authors contributed to the article and approved the submitted version.

REFERENCES

1. Salonia A, Bettocchi C, Carvalho J, Corona G, Jones TH, Kadioğlu A, et al. EAU guidelines on Sexual and Reproductive Health. Available at: https://uroweb.org/guideline/sexual-and-reproductive-health/ (Accessed November 1, 2021).
2. Olesen IA, Andersson AM, Aksglaede L, Skakkebaek NE, Rajpert-de Meyts E, Joergensen N, et al. Clinical, Genetic, Biochemical, and Testicular Biopsy Findings Among 1,213 Men Evaluated for Infertility. *Fertil Steril* (2017) 107:74–82.e7. doi: 10.1016/j.fertnstert.2016.09.015
3. Punab M, Poolamets O, Paju P, Vihljajev V, Pomm K, Ladva R, et al. Causes of Male Infertility: A 9-Year Prospective Monocentre Study on 1737 Patients With Reduced Total Sperm Counts. *Hum Reprod* (2017) 32:18–31. doi: 10.1093/humrep/dew284
4. Ventimiglia E, Capogrosso P, Boeri L, Serino A, Colicchia M, Ippolito S, et al. Infertility as a Proxy of General Male Health: Results of a Cross-Sectional Survey. *Fertil Steril* (2015) 104:48–55. doi: 10.1016/j.fertnstert.2015.04.020
5. Verkuijlen J, Verhaak C, Nelen WLDM, Wilkinson J, Farquhar C. Psychological and Educational Interventions for Subfertile Men and Women. *Cochrane Database Syst Rev* (2016) 3:CD011034. doi: 10.1002/14651858.CD011034.pub2
6. Ventimiglia E, Capogrosso P, Boeri L, Pederzoli F, Montorsi F, Salonia A, et al. When to Perform Karyotype Analysis in Infertile Men? Validation of the European Association of Urology Guidelines With the Proposal of a New Predictive Model. *Eur Urol* (2016) 70(6):920–3. doi: 10.1016/j.eururo.2016.06.015
7. Ventimiglia E, Capogrosso P, Boeri L, Ippolito S, Scano R, Moschini M, et al. Validation of the American Society for Reproductive Medicine Guidelines/Recommendations in White European Men Presenting for Couple's Infertility. *Fertil Steril* (2016) 106(5):1076–82.e1. doi: 10.1016/j.fertnstert.2016.06.044
8. Tajar A, Forti G, O'Neill TW, Lee DM, Silman AJ, Finn JD, et al. Characteristics of Secondary, Primary, and Compensated Hypogonadism in Aging Men: Evidence From the European Male Ageing Study. *J Clin Endocrinol Metab* (2010) 95:1810–8. doi: 10.1210/jc.2009-1796
9. Barbotin A-L, Ballot C, Sigala J, Ramdane N, Duhamel A, Marcelli F, et al. The Serum Inhibin B Concentration and Reference Ranges in Normozoospermia. *Eur J Endocrinol* (2015) 172:669–76. doi: 10.1530/EJE-14-0932
10. Tournaye H, Krausz C, Oates RD. Novel Concepts in the Aetiology of Male Reproductive Impairment. *Lancet Diabetes Endocrinol* (2016) 8587:1–10. doi: 10.1016/S2213-8587(16)30040-7
11. Vincent M, Daudin M, Mas PDE, Massat G, Mieusset R, Pontonnier F, et al. Cytogenetic Investigations of Infertile Men With Low Sperm Counts: A 25-Year Experience Minireview. *J Androl* (2001) 18–22. doi: 10.1002/j.1939-4640.2002.tb02597.x
12. Dul EC, Groen H, Dijkhuizen T, Land JA. The Prevalence of Chromosomal Abnormalities in Subgroups of Infertile Men. *Hum Reprod* (2012) 27:36–43. doi: 10.1093/humrep/der374
13. Rothman KJ, Greenland S. Causation and Causal Inference in Epidemiology. *Am J Public Health* (2005) 95(Suppl 1):S144–50. doi: 10.2105/AJPH.2004.059204
14. Pettersson A, Richiardi L, Nordenskjold A, Kaijser M, Akre O. Age at Surgery for Undescended Testis and Risk of Testicular Cancer. *N Engl J Med* (2007) 356:1835–41. doi: 10.1056/NEJMoa067588
15. Chacko JK, Barthold JS. Genetic and Environmental Contributors to Cryptorchidism. *Pediatr Endocrinol Rev* (2009) 6:476–80.
16. Tournaye H, Krausz C, Oates RD. Concepts in Diagnosis and Therapy for Male Reproductive Impairment. *Lancet Diabetes Endocrinol* (2016) 8587:1–11. doi: 10.1016/S2213-8587(16)30040-7
17. Ventimiglia E. Primary , Secondary and Compensated Hypogonadism: A Novel Risk Stratification for Infertile Men. *Andrology* (2017) 505–10. doi: 10.1111/andr.12335
18. Ficarra V, Cerruto MA, Liguori G, Mazzoni G, Minucci S, Tracia A, et al. Treatment of Varicocele in Subfertile Men: The Cochrane Review–A Contrary Opinion. *Eur Urol* (2006) 49:258–63. doi: 10.1016/j.eururo.2005.11.023
19. Evers JHLH, Collins J, Clarke J. Surgery or Embolisation for Varicoceles in Subfertile Men. *Cochrane Database Syst Rev* (2008) CD000479. doi: 10.1002/14651858.CD000479.pub3
20. Kirby EW, Wiener LE, Rajanahally S, Crowell K, Coward RM. Undergoing Varicocele Repair Before Assisted Reproduction Improves Pregnancy Rate and Live Birth Rate in Azoospermic and Oligospermic Men With a Varicocele: A Systematic Review and Meta-Analysis. *Fertil Steril* (2016) 106:1338–43. doi: 10.1016/j.fertnstert.2016.07.1093
21. Cazzaniga W, Capogrosso P, Ventimiglia E, Pederzoli F, Boeri L, Frego N, et al. High Blood Pressure Is a Highly Prevalent But Unrecognised Condition in Primary Infertile Men: Results of a Cross-Sectional Study. *Eur Urol Focus* (2020) 6(1):178–83. doi: 10.1016/j.euf.2018.07.030
22. Ventimiglia E, Capogrosso P, Colicchia M, Boeri L, Serino A, Castagna G, et al. Metabolic Syndrome in White European Men Presenting for Primary Couple's Infertility: Investigation of the Clinical and Reproductive Burden. *Andrology* (2016) 4:944–51. doi: 10.1111/andr.12232
23. Michalakis K, Mintziori G, Kaprara A, Tarlatzis BC, Goulis DG. The Complex Interaction Between Obesity, Metabolic Syndrome and Reproductive Axis: A Narrative Review. *Metabolism* (2013) 62:457–78. doi: 10.1016/j.metabol.2012.08.012
24. Panara K, Masterson JM, Savio LF, Ramasamy R. Adverse Effects of Common Sports and Recreational Activities on Male Reproduction. *Eur Urol Focus* (2019) 5(6):1146–51. doi: 10.1016/j.euf.2018.04.013
25. Skakkebaek NE, Meyts ER, Louis GMB, Toppari J, Andersson A, Eisenberg ML, et al. Male Reproductive Disorders And Fertility Trends: Influences Of Environment And Genetic Susceptibility. *Physiol Rev* (2016) 55–97. doi: 10.1152/physrev.00017.2015
26. Eisenberg ML, Li S, Behr B, Pera RR, Cullen MR. Relationship Between Semen Production and Medical Comorbidity. *Fertil Steril* (2015) 103:66–71. doi: 10.1016/j.fertnstert.2014.10.017

Conflict of Interest: The authors declare that the research was conducted in the absence of any commercial or financial relationships that could be construed as a potential conflict of interest.

frontiers in Endocrinology

REVIEW
published: 24 December 2021
doi: 10.3389/fendo.2021.800327

Signaling Proteins That Regulate Spermatogenesis Are the Emerging Target of Toxicant-Induced Male Reproductive Dysfunction

Sheng Gao[1,2†], Xiaolong Wu[1,2†], Lingling Wang[1,2†], Tiao Bu[1,2†], Adolfo Perrotta[3], Giuseppe Guaglianone[4], Bruno Silvestrini[5], Fei Sun[1] and C. Yan Cheng[1,2*‡]*

[1] Department of Urology and Andrology, Sir Run Run Shaw Hospital, Zhejiang University School of Medicine, Hangzhou, China, [2] Institute of Reproductive Medicine, Nantong University School of Medicine, Nantong, China, [3] Department of Translational & Precision Medicine, Sapienza University of Rome, Rome, Italy, [4] Department of Hospital Pharmacy, "Azienda Sanitaria Locale (ASL) Roma 4", Civitavecchia, Italy, [5] Institute of Pharmacology and Pharmacognosy, Sapienza University of Rome, Rome, Italy

OPEN ACCESS

Edited by:
Qing Chen,
Army Medical University, China

Reviewed by:
Ying Gao,
Population Council, United States
Massimo Venditti,
Second University of Naples, Italy

***Correspondence:**
C. Yan Cheng
yancheng01@aol.com
Fei Sun
sunfeisrrsh@zju.edu.cn

†These authors have contributed equally to this work

‡Lead Author

Specialty section:
This article was submitted to Reproduction, a section of the journal Frontiers in Endocrinology

Received: 22 October 2021
Accepted: 22 November 2021
Published: 24 December 2021

Citation:
Gao S, Wu X, Wang L, Bu T, Perrotta A, Guaglianone G, Silvestrini B, Sun F and Cheng CY (2021) Signaling Proteins That Regulate Spermatogenesis Are the Emerging Target of Toxicant-Induced Male Reproductive Dysfunction. Front. Endocrinol. 12:800327. doi: 10.3389/fendo.2021.800327

There is emerging evidence that environmental toxicants, in particular endocrine disrupting chemicals (EDCs) such as cadmium and perfluorooctanesulfonate (PFOS), induce Sertoli cell and testis injury, thereby perturbing spermatogenesis in humans, rodents and also widelife. Recent studies have shown that cadmium (e.g., cadmium chloride, $CdCl_2$) and PFOS exert their disruptive effects through putative signaling proteins and signaling cascade similar to other pharmaceuticals, such as the non-hormonal male contraceptive drug adjudin. More important, these signaling proteins were also shown to be involved in modulating testis function based on studies in rodents. Collectively, these findings suggest that toxicants are using similar mechanisms that used to support spermatogenesis under physiological conditions to perturb Sertoli and testis function. These observations are physiologically significant, since a manipulation on the expression of these signaling proteins can possibly be used to manage the toxicant-induced male reproductive dysfunction. In this review, we highlight some of these findings and critically evaluate the possibility of using this approach to manage toxicant-induced defects in spermatrogenesis based on recent studies in animal models.

Keywords: testis, spermatogenesis, endocrine disrupting chemicals, Sertoli cells, cytoskeletons, male reproduction

1 INTRODUCTION

An endocrine disrupting chemical (EDC) is an exogenous chemical, usually an environmental toxicant, capable of interfering with the function of endogenous hormones that are essential to maintain body function including reproduction, development, growth, metabolism, behavior and/or cell/tissue/organ homeostasis in humans and other mammals. In fact, the list of EDCs has been growing for the last decade due to industrial activities in which pharmaceutical industry synthesize new chemicals for their use in consumer products (1–3). These include plastic softeners (also known

as plasticizers) for utensils and rubbers, stain- and stick-resistant chemicals to increase durability of clothing, fabrics, draperies, and vinyl flooring and wall covering products, as well as paints by modifying their components namely pigment, solvent and resin. These also include personal care products, such as nail polish, antiperspirants, deodorants, hair sprays, shampoos, soaps, and fragrance products. In fact, these chemicals are found in hundreds of products widely used by consumers across the globe. The EDCs include heavy metals (e.g., lead, mercury, cadmium), plasticizers (e.g., bisphenols, parabens, benzophenones, phthalates), and surfactants (e.g., PFOS, PFOA) (**Tables 1**, **2**) (3, 33–37). Studies have shown that many of these EDCs affects human reproductive function, pathogenesis of multiple diseases including carcinogenesis, obesity, diabetes, growth and development (in particular during fetal and child development) and others (37–39). For instance, recent studies have shown that exposure to EDCs is one of the major causes of idiopathic male infertility (40–43) and also reproductive dysfunction in females including primary ovarian insufficiency, endometriosis, preterm birth and earlier puberty (33, 43, 44).

More important, some EDCs have a very long half-life in humans. As such, high level of EDCs can be accumulated in the human body over an extended period of time, often years and also decades. For instance, cadmium has a half-life of >20 years (45, 46) *vs.* >5 years for PFOS in humans (47, 48). Furthermore, administration of a single EDC for a controlled study in rodents (or exposure of humans to a single EDC) may mask the physiological effects and its health risk since each animal (or person) is exposed to multiple EDCs simultaneously because of their widespread presence in our environment through foods, water, and air. Furthermore, selected life style, such as smoking, of the study subjects can also affect the outcome of a study. For instance, when laboratory animals were exposed to a mixture of phthalates in "dose addition model" and compared to results that obtained when toxicant was administered individually, the outcomes could be considerably different. Findings from the dose addition model studies have shown that a mixture of phthalates produce additive effects (49, 50), and the phenotypes are far worse than the sum of the combined individual effects. As such, changes that were found following low-dose exposure to a single EDC may not necessarily demonstrate the 'real' health risk. Thus, it is important to perform long-term studies using a combination of common EDCs to assess their health risks at doses that mimic the environmental (or industrial) exposure.

In this review, we focus our discussion based on recent reports on selected EDCs, namely cadmium and PFOS, that were found to perturb male reproductive function in particular spermatogenesis through putative signaling proteins and/or pathways. These findings are therapeutically important since the EDC-induced Sertoli cell or testis injury was shown to be blocked or rescued through an interference of the signaling proteins utilized by these EDCs in rodents (25, 51, 52), and in humans such as the use of primary human Sertoli cell cultures in

TABLE 1 | Effects of cadmium chloride ($CdCl_2$) on male reproductive function*.

Species/ cell line	Route of administration	Treatment dose	Observed effects	Refs
Human	*In vivo*	Natural environmental exposure	Sertoli cell injury; reduced inhibin B, AMH, and FSH in serum Reduced semen quality Reduced sperm concentration and motility Idiopathic oligoasthenozoospermic males had high levels of cadmium in serum, associated with impairment of sperm motility; higher sperm DNA fragmentation	(4–7)
Human sperm	*In vitro*	10 μM	Reduced sperm motility and DNA integrity; an increase in sperm DNA fragmentation and in intracellular oxidative stress in sperm	(8)
Human sperm	*In vitro*	20 μM	Reduced nucleus diameter; reduced mitochondrial membrane potential (MMP); an increase in DNA fragmentation.	(9)
Mouse	*In vivo*, i.p.	1 and 2.5 mg/kg b.w.	Reduced testis weight; reduced sperm survival and serum testosterone; an increase in sperm abnormality and ROS level.	(10)
Mouse	*In vivo*, i.p. *In vivo*, i.p. *In vivo*, oral	3 mg/kg b.w. 1.2 mg/kg b.w. 24 mg/kg b.w.	Germ cell exfoliation; Leydig cell degeneration; an increase in abnormal sperm morphology Seminiferous epithelial degeneration; Leydig cell injury; reduced serum testosterone; reduced Sertoli TJ function	(11, 12)
Mouse sperm	*In vitro*	14-55 μM	Reduced sperm motility	(13)
Rat	*In vivo*, oral *In vivo*, i.p. *In vivo*, i.p.	5 mg/kg b.w. 2 mg/kg b.w. 3 mg/kg b.w.	Reduced body weight, reduced sperm count, motility and viability; an increase in sperm defects; seminiferous epithelial degeneration Seminiferous epithelial injury; defects in spermatogenesis; intertubular haemorrahage; germ cell exfoliation Germ cell exfoliation; Sertoli cell injury with vacuoles found in cell cytosol; seminiferous epithelial disorganization	(14–16)
Rat Sertoli cell line	*In vitro*	1 μM	Sertoli cell injury; Sertoli cell tight junction disruption	(17)
Fish	*In vivo*, oral	5-40 μM	Germ cell exfoliation; germ cell injury with vacuoles in the cytosol of spermatogonia, spermatocytes, and spermatids; reduced semen quality	(18)
Chicken	*In vivo*, oral	140 mg/kg b.w.	Deformation of the seminiferous tubules; germ cell exfoliation	(19)

**This list is not intended to be exhaustive, it summarizes recent findings that illustrate effects of PFOS on male reproductive function based on studies in vivo and in vitro. AMH, anti-Mullerian hormone; FSH, follicle stimulating hormone; ROS, reactive oxygen species.*

TABLE 2 | Effects of perfluorooctane sulfonate (PFOS) on male reproductive function*.

Species/ cells	Route of administration	Treatment dose(s)	Phenotypes	References
Human	*In vivo*	Natural environmental exposure	Subfertility; reduced sperm count; reduced sperm motility; an increase in serum levels of LH and FSH but reduced inhibin B	(20)
			Germ cell chromosomal aneuploidies and DNA fragmentation; reduced sperm quality and an increase in the population oc immature sperm	(21, 22)
Human Sertoli cells	*In vitro*	20 and 40 μM	Sertoli cell injury manifested by truncated actin filaments and truncated microtubules across cell cytosol	(23)
Rat	*In vivo*, oral	0.5 - 6 mg/kg b.w.	Germ cell degeneration and testicle edema	(24)
Rat Sertoli cells	*In vitro*	20 μM	Sertoli cell injury manifested by truncation of actin filaments; TJ-barrier disruption; perturbed GJ communication	(25)
Mouse	*In vivo*, oral	0.5 or 10 mg/kg b.w.	An increase in germ cell apoptosis but reduced proliferation; reduced serum testosterone; reduced sperm count with vacuolations in spermatogonia, spermatocytes, and Leydig cells	(26)
Mouse	*In vivo*, oral	0.3 and 3 mg/kg b.w.	Low levels of adrenic acid and docosahexaenoic acid (DHA) in neonatal testes; reduced serum testosterone and reduced epididymal sperm count in postnatal mice	(27)
Mouse	*In vivo*, oral	0.5-10 mg/kg b.w.	Reduced sperm count in the epididymis and reduced serum testosterone; disrupted BTB and defects in spermatogenesis	(28)
Mouse Leydig cells	*In vitro*	15 and 30 mM	Reduced secretion of testosterone by Leydig cells due to defects in steroidogenesis	(29)
Mouse Sertoli cells	*In vitro*	5–60 μM	Disruption in Sertoli cell TJ-barrier function due to reduced expression of TJ and GJ proteins	(30)
Fish	*In vivo*	0.5 mM	Reduced sperm quality; structural defects in testis; an increase in serum E2; increased in estrogen receptor α1 levels	(31)
C. elegans	*In vivo*	0.375-10 mM	Reduced in germ cell population; reduced spermatid size and motility; an increase in spermatid defects	(32)

**This list is not intended to be exhaustive, it summarizes recent findings that illustrate effects of PFOS on male reproductive function based on studies in vivo and in vitro. BTB, blood-testis barrier, E2, estradiol-17β; GJ, gap junction; TJ, tight junction.*

studies (23, 53). As such, if these findings can be expanded in particular using other toxicants, some common signaling proteins and/or signaling cascades may be identified, in particular through the use of transcriptomics and pertinent omics including multiomics approaches. This information, in turn, can be helpful to alleviate toxicant-induced reproductive dysfunction. In brief, we narrowly focus on signaling proteins that are involved in EDC-induced Sertoli cell and/or testis injury based on studies in cadmium and PFOS. This approach is used since several eminent reviews on the larger topic of toxicant-induced reproductive dysfunction are found in the literature, many of which are cited here, to avoid redundancy.

2 PROTEIN KINASES CAPABLE OF ALLEVIATING EDC-INDUCED SERTOLI CELL INJURY IN RODENTS AND/OR HUMANS

2.1 Focal Adhesion Kinase (FAK)

2.1.1 Background

FAK is a known regulatory component of the focal adhesion complex (FAC, also called focal contact) at the cell-extracellular matrix (ECM or cell matrix) interface and an actin-based cell-matrix anchoring junction type (54, 55). FAK is also a crucial signaling protein that works in concert with integrins to relate integrin-based signaling cascade *via* its different interacting domains along its polypeptide sequence as shown in **Figure 1** (56). In fact, FAK is a prime target of anticancer therapy, being actively investigated by clinicians and scientists in recent years (57–59). FAK also involves in numerous cellular and physiological functions in cells and tissues, but also pathogenesis of diseases in particular carcinogenesis (57, 60). In the testis, FAK, however, is not found at the FAC since FAC is absent in the testis (61, 62). Instead, the only cell-matrix anchoring junction found in the testis is the intermediate filament-based hemidesmosome found at the base of the seminiferous epithelium, between basement membrane (a modified form of ECM in the testis) and the base of Sertoli cells (63, 64). Interestingly, FAK, and most notably its two activated/phosphorylated forms: p-FAK-Y397 (65, 66) and p-FAK-Y407 (67) (**Figure 1**) are constituent and regulatory component of the apical ES (apical ectoplasmic specialization) and basal ES (which together with tight junction (TJ) constitute the blood-testis barrier (BTB) in the testis), respectively. On the other hand, studies have shown that the robust expression of p-FAK-Y397 at the apical ES persists until late stage VIII tubules when the release of spermatozoa takes place near the edge of the tubule lumen (66, 68), suggesting it may be crucial to support spermatid adhesion at the apical ES. In fact, the α6ß1-integrin/p-FAK-Y397 complex is likely a crucial regulatory protein complex to modulate the release of sperm at spermiation (69–71). Interestingly, the use of a phosphomimetic mutant of p-FAK-Y397, namely p-FAK-Y397F, making it constitutively inactive was found to promote Sertoli cell TJ-barrier function making it tighter when overexpressed in the Sertoli cell

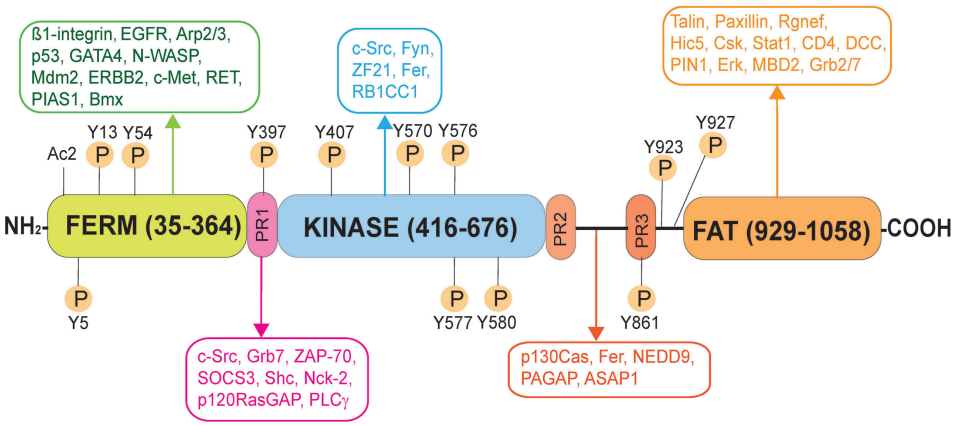

FIGURE 1 | Schematic illustration of the human focal adhesion kinase (FAK). FAK in humans is a polypeptide composed of 1058 amino acid residues (NP_001186578.1), comprised of different functional domains. The different functional domains along the FAK polypeptide from its N-terminus are the FERM (band 4.1, ezrin, radixin, moesin homology) domain, followed by the catalytic kinase domain, and the FAT (focal adhesion targeting) domain near its C-terminus, and also three Pro-rich regions (PR1, PR2 and PR3). There are multiple putative phosphorylation sites including Tyr-397, -407, -576, -577, -861, and Y927, which are well conserved across species. Following its activation through phosphorylation, FAK serves as a signaling platform wherein different regulatory proteins (e.g., c-Src, c-Yes, Fyn, Fer, Erk, Csk) and adaptors (e.g., talin, paxillin) can bind to FAK. As such, FAK can recruit additional signaling and regulatory proteins to its different functional domains to modulate cellular functions, such spermatogenesis. EGFR, epidermal growth factor receptor; Arp2/3, actin-related protein 2/3 complex; p53, tumor protein p53; GATA4, GATA binding protein 4; N-WASP, neuronal Wiskott-Aldrich syndrome protein; Mdm2, mouse double minute 2 homology (also known as E3 ubiquitin-protein ligase, a regulator of the p53 tumor suppressor); ERBB2, Rrb-b2 receptor tyrosine kinase 2; c-Met, MET proto-oncogene, receptor tyrosine kinase; RET, rearranged during transfction, a proto-oncogene; PIAS1, protein inhibitor of activated STAT 1; Bmx, BMX non-receptor tyrosine kinase; Fyn, FYN proto-oncogene, c-Src, cellular Src transforming kinase; ZF21, zinc finger FYVE-type containing 21; RB1CC1, RB1 inducible coiled-coil 1; Grb7, growth factor receptor bound protein 7; Rgnef, Rho guanine nucleotide exchange factor 28; Hic5, transforming growth factor ß1 induced transcript 1; Csk, C-terminal Src kinase; Stat1, signal transducer and activator of transcription 1; DCC, DCC netrin 1 receptor; PIN1, peptidylprolyl cis/trans isomerase, NIMA-interacting 1; Erk, mitogen-activated protein kinase 1; MBD2, methyl-CpG binding domain protein 2; STAT1, signal transducer and activator of transcription 1; SRC, SRC proto-oncogene, non-receptor tyrosine kinase; ZAP-70, zeta chain of T cell receptor associated protein kinase 70; SOCS3, suppressor of cytokine signaling 3; Shc, SHC-adaptor protein; Nck-2, NCK adaptor protein 2; p120RasGAP, RAS p21 protein activator 1; PLCγ, phospholipase C γ1; p130Cas, BCAR1 scaffold protein, Cas family member; ASAP1, ArfGAP with SH3 domain, ankyrin repeat and PH domain 1; NEDD9, neural precursor cell expressed, developmentally down-regulated 9; Graf, GTPase regulator associated with FAK; Fer, FER tyrosine kinase.

epithelium with an established TJ-barrier (67). This is analogous to expressing p-FAK-Y407E (a phosphomimetic and constitutively active mutant of p-FAK-Y407) in Sertoli cells when its overexpression promoted the Sertoli TJ-barrier, making the barrier tighter (67). On the other hand, the use of a p-FAK-Y407F (a phosphomimetic and constitutively inactive mutant of p-FAK-Y407) was found to perturb the Sertoli cell TJ-barrier following its overexpression (67). Other studies have shown that FAK involves in maintaining the phosphorylation status of the cell adhesion proteins at the BTB/basal ES site, such as occludin (72). For instance, FAK determines whether these proteins (e.g., occludin) stay at the Sertoli cell-cell interface to support the TJ-permeability function of the BTB, or these proteins (e.g., occludin) at the BTB site should be internalized (55, 67, 72). This thus provides a novel mechanism to induce transient "opening" of the BTB to facilitate the transport of preleptotene spermatocytes across the barrier at stages VII-VIII of the epithelial cycle when p-FAK-Y407 robustly expresses at the BTB (67). Studies have shown that FAK, in particular p-FAK-Y397 and p-FAK-Y407 exert their regulatory effects at the corresponding apical ES and basal ES/BTB through changes at the F-actin and microtubule cytoskeletal organization (67, 73). Importantly, the use of a biochemical assay that monitors the ability of lysates of primary Sertoli cells cultured *in vitro*, overexpression of p-FAK-Y407E in cells transfected with pCI-neo/p-FAK-Y407E mutant vs. control cells transfected with pCI-neo, is able to enhance actin polymerization considerably (67). On the other hand, overexpression of a human p-FAK-Y407E phosphomimetic (i.e., constitutively active) mutant in human Sertoli cells is also capable of blocking the PFOS-induced MT defragmentation (23), such that MTs stretched across the entire human Sertoli cell cytosol, analogous to control human Sertoli cells (23). Collectively, these findings are consistent with earlier studies in fibroblasts, and epithelial and endothelial cells in which FAK is involved in actin and MT polymerization (74–78). In brief, these two activated/phosphorylated forms of FAK (and mTORC1, see **Figure 2**) appear to serve as molecular switch to turn the apical ES and BTB/basal ES "on" or "off", depending on their expression status at the microdomain of these sites across the seminiferous epithelium (**Figures 2**, **3**).

2.1.2 Studies of the PFOS and Cadmium Models, and the Adjudin Pharmaceutical Model

The initial report that illustrates p-FAK-Y407 is involved in PFOS-induced Sertoli cell injury was first published in 2014 (52). This study showed that PFOS-mediated disruption of the Sertoli TJ-barrier function associated with a considerable down-regulation of p-FAK-Y407, but not p-FAK-Y397. Furthermore,

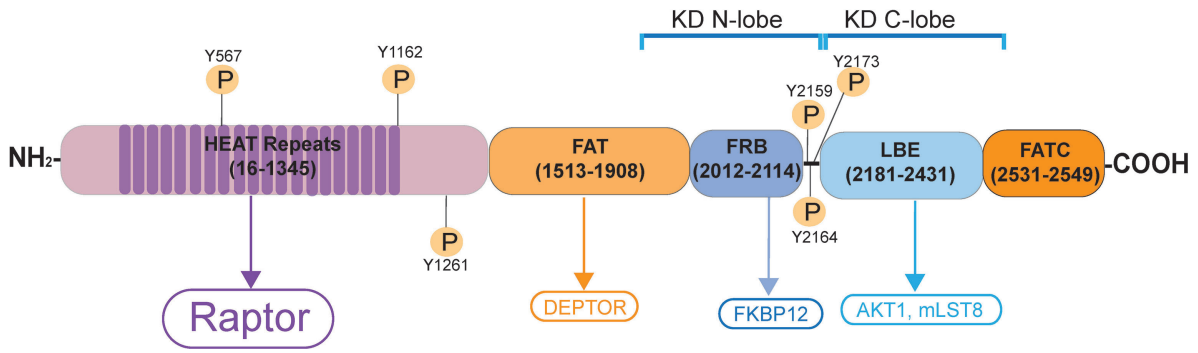

FIGURE 2 | Schematic illustration of the human mTORC1 signaling complex. mTORC1 (mammalian target of rapamycin, NP_001373429.1) is a non-receptor Ser/Thr protein kinase, when it binds to its adaptor protein Raptor (regulatory-associated protein of mTOR), this creates the mTORC1 (mammalian target of rapamycin complex 1) signal complex. mTOR contains two distinctive catalytic domain (KD) containing intrinsic protein kinase activity called KD N-lobe (near the N-terminus) and the KD C-lobe (near the C-terminus). It has 20 tandem HEAT repeats near its N-terminus, to be followed by the FAT domain, FRB domain, LBE domain and the FATC domain near its C-terminus. Akt1; transforming retrovirus Akt1, an onocogene, also known as PKB (protein kinase B); C-lobe, C-terminal lobe; DEP, Dishevelled, Egl-10 and Pleckstrin; DEPTOR, DEP domain-containing mTOR interacting protein; EF3, elongating factor 3; FAT domain, FRAP, ATM, TRAP domain; FATC, FAT domain at the C-terminus; FKBP12, FK506/rapamycin-binding protein; HEAT, Huntington, EF3, PP2A, TOR1; FRAP, FKBP rapamycin associated protein; FRB, FKBP132 rapamycin binding; KD, kinase domain; LBE, binding site for mLST8; mLST8, mammalian lethal with SEC thirteen 8, also known as mTOR associated protein LST8 homolog; N-lobe, N-terminal lobe; PKB, protein kinase B; Raptor, regulatory-associated protein of mTOR, an adaptor protein.

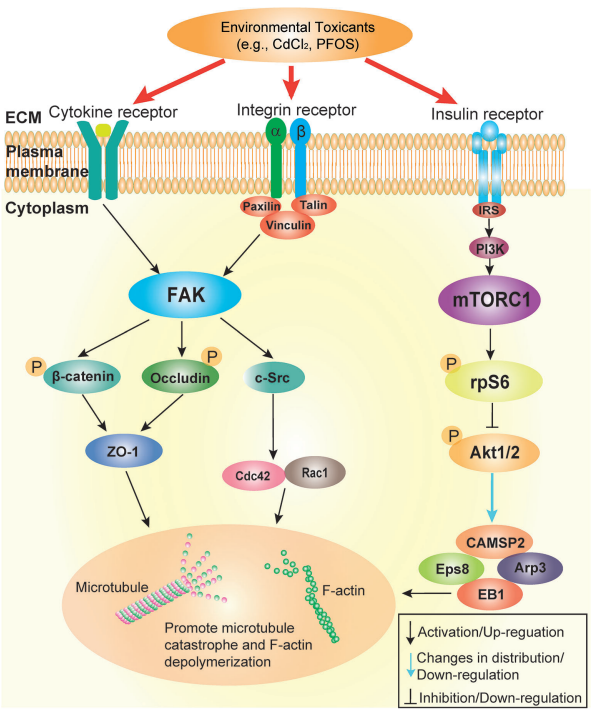

FIGURE 3 | Schematic illustration by which cadmium and PFOS induce Sertoli cell and/or testis injury *via* FAK and mTORC1. This schematic illustration was prepared based on findings using environmental toxicant models of $CdCl_2$ and PFOS. It is noted that the upstream ligand(s) utilized by cadmium and PFOS remain to be identified, but this likely involves either integrin-, cytokine- and/or insulin-based receptors. Both FAK and mTORC1 signaling protein/complex exert their corresponding effects downstream through different actin and microtubule (MT) regulatory proteins (*see text for details*). These changes, either through up- or down-regulation of the corresponding regulatory proteins, or distributions across the seminiferous epithelium, in turn, alter the structural organization of either actin- or MT-based cytoskeleton. The net result of these changes induce Sertoli cell or testis injury.

PFOS also considerably perturbed the cytoskeletal organization of F-actin across the Sertoli cell epithelium with an established functional TJ-barrier, in which actin filaments were considerably truncated and disorganized, analogous to the phenotypes when Sertoli cells were transfected with a specific FAK miRNA (called miR-135b, which is known to knockdown FAK (52, 79, 80). This report thus establishes the likely mechanism by which PFOS induces Sertoli cell injury, likely through a down-regulation of p-FAK-Y407, which in turn, perturbs the Sertoli cell F-actin organization (52) (**Figures 4**, **5**). This notion is also supported by an earlier report which has shown that p-FAK-Y407 indeed promotes Sertoli cell BTB function by stabilizing actin cytoskeleton at the Sertoli cell epithelium with a functional BTB *in vitro* (67). Interestingly, it was shown that overexpression of a phosphomimetic (and constitutively active) mutant of p-FAK-Y407, namely p-FAK-Y407E, in the Sertoli cell epithelium *in vitro*, was capable of blocking the PFOS-induced Sertoli cell injury by re-establishing the PFOS-mediated Sertoli cell TJ-barrier disruption (52). Overexpression of p-FAK-Y407E was also capable of inducing proper re-organization of the actin cytoskeleton which was perturbed by PFOS (52), likely through an increase in actin polymerization kinetics (67). An earlier report has also shown that FAK is capable of recruiting occludin to the Sertoli cell-cell interface, possibility through

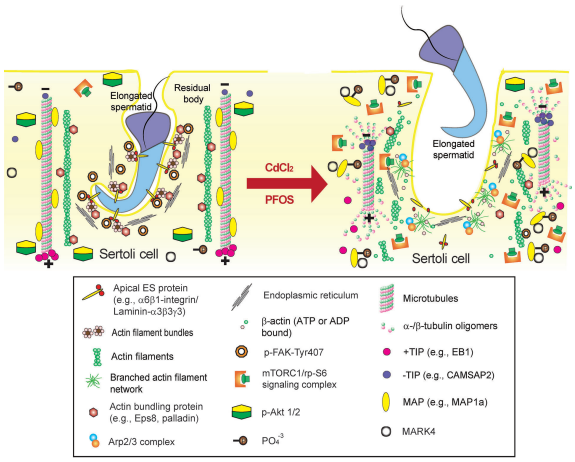

FIGURE 4 | Environmental toxicant-induced testis injury through changes in germ cell adhesion, leading to germ cell exfoliation. *Left* panel depicts schematic illustration of intact seminiferous epithelium, such as in a stage VII-early VIII tubule, wherein intact apical ES supports spermatid adhesion to the Sertoli cell in the seminiferous epithelium during the final stage of spermiogenesis. The integrity of MT cytoskeleton is maintained by binding of MAPs (e.g., MAP1a) to the MT protofilaments and MT stability is also maintained by binding of the +TIP (e.g., EB1), and the proper level of –TIP (e.g., CAMSAP2) at its corresponding plus (+) and minus (-) ends. On the other hand, the actin cytoskeleton is maintained by binding of the actin bundling proteins (e.g., palladin and actin barbed end capping and bundling protein Eps8) to maintain actin filament bundles at the apical ES but also across the epithelium as aggregates of actin filaments to support Sertoli cell structural integrity. This microenvironment is also maintained by robustly expression of p-FAK-Y407 and likely p-Akt1/2. However, the unexpected presence of either toxicant (e.g., cadmium or PFOS) alter the microenvironment of the testis. For instance, a surge in MARK4 induces phosphorylation of MAP1a, causing their detachment from MTs, which is coupled with a down-regulation of +TIP (e.g., EB1) and more –TIP (e.g., CAMSAP2) binding to the corresponding ends of the MT. These changes thus destabilize MTs, leading to MT catastrophe. The expression and/or distribution of actin bundling proteins (e.g., palladin, Eps8) are also affected, these changes, coupled with a surge in Arp2/3 complex, causing "debundling" of actin filaments at the apical ES since actin filaments becoming a branched network due to an increase in actin branched nucleation induced by the Arp2/3 complex, thereby destabilizing F-actin network. The disruptive changes in the microenvironment include a considerable decline in p-FAK-Y407 and a surge in mTORC1 (with a concomitant down-regulation of p-Akt1/2) expression. The net result leads to premature germ cell exfoliation as noted in the *right* panel (*see text for details*), thereby perturbing male fertility due to defects in spermatogenesis.

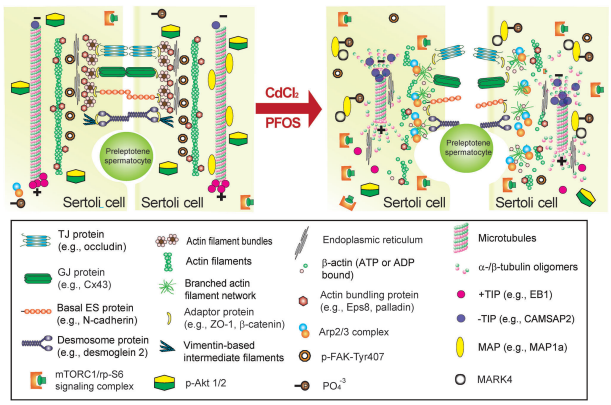

FIGURE 5 | Environmental toxicant-induced testis injury through changes in Sertoli cell adhesion at the BTB, leading to defects in spermatogenesis. *Left* panel depicts schematic illustration of intact seminiferous epithelium near the basement membrane at the site of the BTB, such as in a stage VII tubule, wherein intact basal ES maintains BTB integrity to support spermatogenesis. The integrity of MT cytoskeleton at the BTB and across the seminiferous epithelium is maintained by binding of MAPs (e.g., MAP1a) to the MT protofilaments, and MT stability is also maintained by binding of the +TIP (e.g., EB1) and the proper level of –TIP (e.g., CAMSAP2) at its corresponding plus (+) and minus (-) ends. On the other hand, the actin cytoskeleton is maintained by binding of the actin bundling proteins (e.g., palladin and Eps8) to maintain actin filament bundles at the basal ES/BTB but also across the epithelium as aggregates of actin filaments to support Sertoli cell structural integrity. This microenvironment is also maintained by robust expression of p-FAK-Y407 and likely p-Akt1/2. However, the unexpected presence of cadmium or PFOS alters the microenvironment of the testis at the BTB but also across the seminiferous epithelium. For instance, a surge in MARK4 induces phosphorylation of MAP1a, causing MAP detachment from MTs, which is coupled with a down-regulation of +TIP (e.g., EB1) and more –TIP (e.g., CAMSAP2) binding to the corresponding ends of the MT. These changes thus destabilize MTs, leading to MT catastrophe. The expression and/or distribution of actin bundling proteins (e.g., palladin, Eps8) are also affected, these changes, coupled with a surge in Arp2/3 complex, causing "debundling" of actin filaments at the basal ES/BTB since actin filaments becoming a branched network due to an increase in actin branched nucleation induced by the Arp2/3 complex, thereby destabilizing F-actin network. This disruptive change in the microenvironment is maintained by a considerable decline in p-FAK-Y407 and a surge in mTORC1 (with a concomitant down-regulation of p-Akt1/2). The net result leads to a loss of BTB integrity, making the barrier more permeable to toxicants/biomolecules as noted in the *right* panel (*see text for details*), thereby perturbing male fertility due to defects in spermatogenesis.

changes in the phosphorylation status of occludin (72). These changes, in turn, promoted proper distribution of the occludin-ZO-1 complex at the Sertoli cell-cell interface, thereby re-establishing the PFOS-induced disrupted TJ-barrier (52). More important, these findings were recently confirmed in primary Sertoli cell cultures *in vitro* in which PFOS not only perturbed the organization of actin- but also microtubule (MT)-based cytoskeletons (23). For instance, overexpression of a human p-FAK-Y407E phosphomimetic (and constitutively active) mutant was shown to re-establish the PFOS-induced human Sertoli cell TJ-barrier disruption, which is the result of a proper re-organization of actin and MT cytoskeletons across the human Sertoli cell epithelium (23). Collectively, these findings are important because they have unequivocally demonstrated for the first time that by manipulating a putative signaling protein, namely p-FAK-Y407 whose expression was down-regulated by PFOS, such as through overexpression of a phosphomimetic and constitutively active mutant p-FAK-Y407E, both in rodents and humans, the PFOS-induced Sertoli cell injury can be alleviated.

A recent report based on studies *in vivo* has also shown that cadmium chloride ($CdCl_2$)-induced testis injury (3 mg/kg b.w., *via* i.p.) was remarkably notable by as early as 6 hr by assessing changes in the organization of microtubule cytoskeleton across the seminiferous epithelium (81), consistent with more recent studies (82). This is also the time when the phenotypes across the seminiferous epithelium were not distinctively noted by histological analysis (81). Besides extensive truncation and disorganization of the MT protofilaments across the seminiferous epithelium, considerable disruption regarding distribution of the MT regulatory proteins MAP1a and CAMSAP2 were also notably detected (81). These findings are physiologically significant since MAP1a (microtubule associated proteins 1a, a MAP) is known to bind onto the microtubules to confer MT stability (83). On the other hand, CAMSAP2 (calmodulin-regulated spectrin-associated protein 2) is a microtubule minus (-) end targeting protein (-TIP) known to confer MT dynamics, determining the length of the MT protofilaments in response to changes in cellular environment (84), such as at different stages of the epithelial cycle in the testis. These findings suggest that toxicant-induced testis or Sertoli cell injury is more than a simple general cell toxicity cellular event, but involving a well defined toxicant-induced cascade of events including signaling and regulatory proteins. More important, these are the same signaling proteins that are being used by the testis to support testis function and spermatogenesis, illustrating that toxicants exert their toxic effects through defined signaling pathways. In this context, it is of interest to note that toxicants, including cadmium, also exert their disruptive effects in the testis through an increased oxidative damage in the seminiferous epithelium involving FAK (82, 85). It is obvious that much work is needed to relate these findings to p-FAK-Y407 in the cadmium model and to delineate the precise underlying molecular mechanism(s). The current concept by which PFOS and cadmium induce Sertoli cell and testis injury is summarized in **Figures 4**, **5**. Additionally, in parallel experiments that investigated changes in cytoskeletal organization and the downstream signaling proteins using the pharmaceutical model adjudin, we have discovered a remarkable negative correlation between p-FAK-Y407 expression and the adjudin-mediated defects in spermatogenesis in the testis *in vivo* (81). In this context, it is of interest to note that adjudin is a non-hormonal male contraceptive known to induce extensive germ cell exfoliation (86, 87) by primarily targeting the actin and microtubule cytoskeletons in the Sertoli cells across the seminiferous epithelium (81, 87–89). It has also been used to serve as a model to study Sertoli cell-cell and Sertoli-germ cell adhesion and BTB dynamics in the testis, making this a novel model to decipher the underlying mechanism(s) that regulate spermatogenesis (89–92). Using this pharmaceutical adjudin model, we have detected extensive disruption of the MT cytoskeletal organization across the seminiferous epithelium, which tightly associated with a considerable down-regulation of p-FAK-Y407 in testes (81). This finding is also consistent with earlier findings in which the spatiotemporal expression of p-FAK-Y407 in normal testes is tightly associated with the BTB in the testis, and overexpression of p-FAK-Y407E phosphomimetic (and constitutively active) mutant in Sertoli cell epithelium promotes BTB function making it "tighter" (67). On the other hand, p-FAK-Y407 is robustly expressed at the apical ES to confer spermatid adhesion onto Sertoli cells in the seminiferous epithelium, but its expression is remarkably reduced at the Sertoli cell-spermatid interface (i.e., apical ES) in late stage VIII when the release of sperm occurs (67). Collectively, these data thus indicate that findings obtained from the use of toxicant and/or pharmaceutical models are consistent with physiological data using normal testes *in vivo*. These changes also highlight the importance of delineating the downstream signaling proteins and the involving signaling cascade utilized by toxicants to induce male reproductive dysfunction. Since this information will be crucial to provide new approaches to manage toxicant-induced reproductive dysfunction and idiopathic infertility, and other pathological conditions, such as carcinogenesis.

2.2 mTORC1/rpS6/Akt1/2 Signaling Complex

2.2.1 Background

Studies have shown that the mTORC1 (mammalian target of rapamycin complex 1)/rpS6 (ribosomal protein S6)/Akt1/2 (transforming thymic lymphomas Akt1/2 kinase, also known as PKB, protein kinase B, a non-receptor Ser/Thr protein kinase) complex is one of the most prevalent signaling protein complexes that regulates cellular metabolism found in virtually all mammalian cells (93–95). mTORC1 is created by binding of the mTOR (mammalian target of rapamycin, a Ser/Thr non-receptor protein kinase) and its adaptor protein Raptor (regulatory-associated protein of mTOR) (**Figure 2**) (94). Besides energy metabolism in mammalian cells, mTORC1/p-rpS6/p-Akt1/2 is an emerging regulatory signaling complex crucial to support spermatogenesis through its effects on Sertoli cell function (95, 96) (**Figure 3**). The role of mTORC1 (and mTORC2) in regulating mammalian spermatogenesis in studies of the rat and mouse has been recently reviewed (95, 96),

so additional discussion is not included here to avoid redundancy. Nonetheless, studies using genetic models have also confirmed our earlier findings indicating the significance of both mTORC1 and mTORC2 in testis functions (97). For instance, Sertoli cell-specific deletion of mTOR led to infertility in mice, which associated with a surge in p-rpS6 expression, loss of Sertoli cell polarity, increased in germ cell apoptosis and extensive germ cell exfoliation, but also gap junction impairment due to mislocalization of connexin 43 (Cx43) (98). On the other hand, germ cell-specific deletion of mTOR also led to infertility in mice even though these mice were viable and apparently healthy (99). In adulthood, spermatogonial stem cells in these mice failed to proliferate and differentiate into spermatocytes to undergo meiosis, and seminiferous tubules were devoid of virtually all germ cells, leading to infertility (99). These findings also illustrate that these mTOR deletion mediated infertility is more than just defects in energy metabolism since developing germ cells rely on Sertoli cells for their energy needs. As such, specific deletion of mTOR in germ cells should not interfere with their energy metabolism since Sertoli cells remain in the testis to support their metabolic and nutritional needs. Studies have shown that this mTORC1-based signaling complex exerts its effects by modulating cytoskeletal organization of actin and MT in Sertoli cells across the seminiferous epithelium, involving changes in energy metabolism but also intrinsic activities and/or distribution of regulatory proteins of both cytoskeletons (95, 96). In brief, it is increasingly clear that the mTORC2 complex modulates cytoskeletal function by activating mTORC1 initially, to be followed by a surge in the expression of p-rpS6-S235/S236 and p-rpS-S240/S244, and then a down-regulation of the p-Akt1-S473 and p-Akt2-S474 expression (**Figure 1**) as noted in two reports (100, 101). Interestingly, this signaling complex has been shown to be involved in PFOS- and adjudin-mediated Sertoli cell or testis injury.

2.2.2 Studies of the PFOS and the Pharmaceutical Adjudin Models

Using the PFOS model in Sertoli cells cultured *in vitro* with an established TJ-permeability barrier, this environmental toxicant was found to perturb both actin and MT cytoskeletons through a down-regulation of the p-Akt1-S473 and p-Akt2-S474 (51). For instance, actin filaments that stretched across the entire Sertoli cell cytosol noted in control cells were considerably truncated and mis-aligned, no longer stretching properly across the Sertoli cell to support cell function, which in turn perturbed the TJ-barrier function (51). On the other hand, MT protofilaments that stretched across the entire Sertoli cell cytosol in control cells to support cell function were also considerably altered. For instance, MTs were considerably shortened and wrapped around the Sertoli cell nuclei instead (51). In order to confirm that PFOS exerts its disruptive effects to induce Sertoli cell injury is indeed involving p-Akt1/2, we used a specific Akt1/2 activator, namely SC79 (2-amino-6-chloro-α-cyano-3-(-ethoxycarbonyl)-4H-1-benzopyran-4-acetic acid ethyl ester, Mr 364.78) for the study. It is known that SC79 binds to the plecktrin homology (PH) domain of the Akt polypeptide, mimicking the binding of PtdIns(3,4,5)P3 to Alt to induce conformational change by enhancing its phosphorylation and activation at p-Akt1-T308 and p-Akt1-S473 sites (102). As anticipated, SC79 indeed was capable of blocking PFOS-mediated Sertoli cell injury by alleviating the PFOS-mediated Sertoli TJ-barrier disruption through corrective changes in the proper organization of actin- and MT-based cytoskeletons across the cell cytosol (51). In a recent *in vivo* study using the pharmaceutical adjudin model, we also reported a remarkable surge in the expression of p-rpS6-S235/S236 and p-rpS6-S240/S244 following treatment of adult rats with a single dose of adjudin at 50 mg/kg b.w. (oral gavage) (81). This observation is also consistent with an earlier study, reporting a surge in expression of mTOR and p-rpS6 (but not total rpS6) following treatment of adult rats with adjudin (single dose, 250 mg/kg b.w., oral gavage) (103). Collectively, these findings together with the data summarized and discussed in *Section 2.1* have provided compelling evidence that environmental toxicants exert their effects by disrupting key signaling proteins, most notably their phosphorylation status, which are necessary and essential to support spermatogenesis and testis function under physiological conditions (**Figures 3**–**5**). Furthermore, new activator(s) of p-Akt1/2, instead of SC79, with reduced cytotoxicity should be carefully evaluated in future studies.

3 CONCLUDING REMARKS AND FUTURE PERSPECTIVES

As discussed above, we have provided a critical summary on the two signaling proteins that are being used by the toxicants cadmium and POFS to induce male reproductive dysfunction, through changes in their phosphorylation status (**Figures 3**–**5**). In order to expand this work further prior to studies *in vivo*, it may be advantageous to develop an *in vitro* human testis model that mimics the testes *in vivo* for toxicity studies. This *in vitro* human testis model should have the capability of developing functional haploid spermatids from spermatogonical stem cells (SSCs), mimicking the testis *in vivo*. The use of such a model thus reduces the time it takes to translate findings from studies in rodents to humans. There are much interest in the field to develop polymer- or hydrogel-based microfluidic devices for tissue engineering that mimic ion channels in human cells/tissues, bone tissue regeneration for transplantation, and perhaps tubules found in kidneys, prostate and others (104–108). A major obstacle of developing an *in vitro* human testis model is that the polymer- or hydrogel-based microfluidic device, unlike the seminiferous tubules in the testis, is not a dynamic structure. Since these hydrogel- or biopolymer-based devices are not capable of undergoing disassembly, reassembly, and dynamic maintenance, similar to the actin- and MT-based cytoskeletons in the seminiferous tubules, in response to changes of the epithelial cycle during spermatogenesis in the testis. Nonetheless, it is our beliefs that such an *in vitro* human testis can be established in the near future due to advances in cell/tissue cultures and engineering technology. On the other hand, it remains to be established if these EDCs, such as cadmium and

PFOS, exert their disruptive effects directly, such as through direct changes on the phosphorylation status and/or distribution of the involving signaling proteins, or indirectly, such as through a down-regulation of the enzymes that change the testosterone availability through steroidogenesis. These possibilities should also be carefully evaluated in future studies.

AUTHOR CONTRIBUTIONS

CYC conceived the project and wrote the paper. SG, XW, LW, TB, and CYC researched on the topics and searched for relevant information in the literature at www.PubMed.com and relevant journal sites, which were discussed and cited in this review. SG and CYC prepared the Tables. SG and CC prepared the figures. SG, XW, LW, TB, AP, GG, BS, and FS discussed the concepts evaluated in this review. All authors contributed to the article and approved the submitted version.

FUNDING

This work was supported in part by grants from the National Key Research and Development Program of China (2018YFC1003500 to FS), and Fellowships from the Noopolis Foundation (Rome, Italy, to XW, LW, TB).

REFERENCES

1. Wong EWP, Yan HHN, Lie PPY, Mruk DD, Cheng CY. Cell Junctions in the Testis as Targets for Toxicants. In: McQueen CA, editor. *Comprehensive Toxicology*, *3rd Editiion*, vol. 4 . Oxford: Elsevier Science (2018). p. 128–46.
2. Wan HT, Mruk DD, Wong CKC, Cheng CY. Targeting Testis-Specific Proteins to Inhibit Spermatogenesis - Lession From Endocrine Disrupting Chemicals. *Expert Opin Ther Targets* (2013) 17:839–55. doi: 10.1517/14728222.2013.791679
3. Vandenberg LN, Pelch KE. Systematic Review Methodologies and Endocrine Disrupting Chemicals: Improving Evaluations of the Plastic Monomer Bisphenol A. *Endocr Metab Immune Disord Drug Targets* (2021). doi: 10.2174/1871530321666211005163614
4. Egger AE, Grabmann G, Gollmann-Tepeköylü C, Pechriggl EJ, Artner C, Türkcan A, et al. Chemical Imaging and Assessment of Cadmium Distribution in the Human Body. *Metallomics Integr Biometal Sci* (2019) 11:2010–9. doi: 10.1039/C9MT00178F
5. Li Y, Wu J, Zhou W, Gao E. Association Between Environmental Exposure to Cadmium and Human Semen Quality. *Int J Environ Health Res* (2016) 26:175–86. doi: 10.1080/09603123.2015.1061115
6. Pant N, Kumar G, Upadhyay AD, Gupta YK, Chaturvedi PK. Correlation Between Lead and Cadmium Concentration and Semen Quality. *Andrologia* (2015) 47:887–91. doi 10.1111/and.12342
7. Taha EA, Sayed SK, Ghandour NM, Mahran AM, Saleh MA, Amin MM, et al. Correlation Between Seminal Lead and Cadmium and Seminal Parameters in Idiopathic Oligoasthenozoospermic Males. *Cent Eur J Urol* (2013) 66:84–92. doi: 10.5173/ceju.2013.01.art28
8. Santonastaso M, Mottola F, Iovine C, Cesaroni F, Colacurci N, Rocco L. *In Vitro* Effects of Titanium Dioxide Nanoparticles (TiO(2)NPs) on Cadmium Chloride (CdCl(2)) Genotoxicity in Human Sperm Cells. *Nanomater (Basel Switzerland)* (2020) 10:1118. doi 10.3390/nano10061118
9. Etemadi T, Momeni HR, Ghafarizadeh AA. Impact of Silymarin on Cadmium-Induced Apoptosis in Human Spermatozoa. *Andrologia* (2020) 52:e13795. doi: 10.1111/and.13795
10. Han C, Zhu Y, Yang Z, Fu S, Zhang W, Liu C. Protective Effect of Polygonatum Sibiricum Against Cadmium-Induced Testicular Injury in Mice Through Inhibiting Oxidative Stress and Mitochondria-Mediated Apoptosis. *J Ethnopharmacol* (2020) 261:113060. doi: 10.1016/j.jep.2020.113060
11. Liu D, Wan J, Liu Z, Zhao Z, Zhang G, Leng Y. Determination of Cadmium Induced Acute and Chronic Reproductive Toxicity With Raman Spectroscopy. *Lasers Med Sci* (2020) 35:1919–26. doi: 10.1007/s10103-020-02976-6
12. Mouro VGS, Siman VA, da Silva J, Dias FCR, Damasceno EM, Cupertino MDC, et al. Cadmium-Induced Testicular Toxicity in Mice: Subacute and Subchronic Route-Dependent Effects. *Biol Trace Elem Res* (2020) 193:466–82. doi: 10.1007/s12011-019-01731-5
13. Zhao LL, Ru YF, Liu M, Tang JN, Zheng JF, Wu B, et al. Reproductive Effects of Cadmium on Sperm Function and Early Embryonic Development *In Vitro*. *PloS One* (2017) 12:e0186727. doi: 10.1371/journal.pone.0186727
14. Olaniyi KS, Amusa OA, Oniyide AA, Ajadi IO, Akinnagbe NT, Babatunde SS. Protective Role of Glutamine Against Cadmium-Induced Testicular Dysfunction in Wistar Rats: Involvement of G6PD Activity. *Life Sci* (2020) 242:117250. doi: 10.1016/j.lfs.2019.117250
15. Kheradmand A, Alirezaei M, Dezfoulian O. Biochemical and Histopathological Evaluations of Ghrelin Effects Following Cadmium Toxicity in the Rat Testis. *Andrologia* (2015) 47:634–43. doi: 10.1111/and.12311
16. Xiao X, Cheng CY, Mruk DD. Intercellular Adhesion Molecule-2 Is Involved in Apical Ectoplasmic Specialization Dynamics During Spermatogenesis in the Rat. *J Endocrinol* (2013) 216:73–86. doi: 10.1530/JOE-12-0434
17. Li L, Mao B, Wu S, Li H, Lv L, Ge R, et al. Endogenously Produced LG3/4/5-Peptide Protects Testes Against Toxicant-Induced Injury. *Cell Death Dis* (2020) 11:436. doi: 10.1038/s41419-020-2608-8
18. Vergilio CS, Moreira RV, Carvalho CE, Melo EJ. Evolution of Cadmium Effects in the Testis and Sperm of the Tropical Fish Gymnotus Carapo. *Tissue Cell* (2015) 47:132–9. doi: 10.1016/j.tice.2015.02.001
19. Wang H, Zhang R, Song Y, Li T, Ge M. Protective Effect of Ganoderma Triterpenoids on Cadmium-Induced Testicular Toxicity in Chickens. *Biol Trace Elem Res* (2019) 187:281–90. doi: 10.1007/s12011-018-1364-4
20. Den Hond E, Tournaye H, De Sutter P, Ombelet W, Baeyens W, Covaci A, et al. Human Exposure to Endocrine Disrupting Chemicals and Fertility: A Case-Control Study in Male Subfertility Patients. *Environ Int* (2015) 84:154–60. doi: 10.1016/j.envint.2015.07.017
21. Louis GM, Chen Z, Schisterman EF, Kim S, Sweeney AM, Sundaram R, et al. Perfluorochemicals and Human Semen Quality: The LIFE Study. *Environ Health Perspect* (2015) 123:57–63. doi: 10.1289/ehp.1307621
22. Governini L, Guerranti C, De Leo V, Boschi L, Luddi A, Gori M, et al. Chromosomal Aneuploidies and DNA Fragmentation of Human Spermatozoa From Patients Exposed to Perfluorinated Compounds. *Andrologia* (2015) 47:1012–9. doi: 10.1111/and.12371
23. Chen H, Gao Y, Mruk DD, Xiao X, John CM, Turek PJ, et al. Rescue of PFOS-Induced Human Sertoli Cell Injury by Overexpressing a P-FAK-Y407E Phosphomimetic Mutant. *Sci Rep* (2017) 7:15810. doi: 10.1038/s41598-017-15671-4
24. López-Doval S, Salgado R, Pereiro N, Moyano R, Lafuente A. Perfluorooctane Sulfonate Effects on the Reproductive Axis in Adult Male Rats. *Environ Res* (2014) 134:158–68. doi: 10.1016/j.envres.2014.07.006
25. Li N, Mruk DD, Chen H, Wong CK, Lee WM, Cheng CY. Rescue of Perfluorooctanesulfonate (PFOS)-Mediated Sertoli Cell Injury by Overexpression of Gap Junction Protein Connexin 43. *Sci Rep* (2016) 6:29667. doi: 10.1038/srep29667
26. Qu JH, Lu CC, Xu C, Chen G, Qiu LL, Jiang JK, et al. Perfluorooctane Sulfonate-Induced Testicular Toxicity and Differential Testicular Expression of Estrogen Receptor in Male Mice. *Environ Toxicol Pharmacol* (2016) 45:150–7. doi: 10.1016/j.etap.2016.05.025
27. Lai KP, Lee JC, Wan HT, Li JW, Wong AY, Chan TF, et al. Effects of *In Utero* PFOS Exposure on Transcriptome, Lipidome, and Function of Mouse Testis. *Environ Sci Technol* (2017) 51:8782–94. doi: 10.1021/acs.est.7b02102
28. Qiu L, Qian Y, Liu Z, Wang C, Qu J, Wang X, et al. Perfluorooctane Sulfonate (PFOS) Disrupts Blood-Testis Barrier by Down-Regulating Junction Proteins *via* P38 MAPK/ATF2/MMP9 Signaling Pathway. *Toxicology* (2016) 373:1–12. doi: 10.1016/j.tox.2016.11.003

29. Qiu L, Wang H, Dong T, Huang J, Li T, Ren H, et al. Perfluorooctane Sulfonate (PFOS) Disrupts Testosterone Biosynthesis *via* CREB/CRTC2/StAR Signaling Pathway in Leydig Cells. *Toxicology* (2021) 449:152663. doi: 10.1016/j.tox.2020.152663
30. Qiu L, Zhang X, Zhang X, Zhang Y, Gu J, Chen M, et al. Sertoli Cell Is a Potential Target for Perfluorooctane Sulfonate-Induced Reproductive Dysfunction in Male Mice. *Toxicol Sci* (2013) 135:229–40. doi: 10.1093/toxsci/kft129
31. Chen J, Wang X, Ge X, Wang D, Wang T, Zhang L, et al. Chronic Perfluorooctanesulphonic Acid (PFOS) Exposure Produces Estrogenic Effects in Zebrafish. *Environ Pollution (Barking Essex 1987)* (2016) 218:702–8. doi: 10.1016/j.envpol.2016.07.064
32. Yin J, Jian Z, Zhu G, Yu X, Pu Y, Yin L, et al. Male Reproductive Toxicity Involved in Spermatogenesis Induced by Perfluorooctane Sulfonate and Perfluorooctanoic Acid in Caenorhabditis Elegans. *Environ Sci Pollut Res Int* (2021) 28:1443–53. doi: 10.1007/s11356-020-10530-8
33. Lopez-Rodriguez D, Franssen D, Heger S, Parent AS. Endocrine-Disrupting Chemicals and Their Effects on Puberty. *Best Pract Res Clin Endocrinol Metab* (2021) 35:101579. doi: 10.1016/j.beem.2021.101579
34. López-Botella A, Velasco I, Acién M, Sáez-Espinosa P, Todolí-Torró JL, Sánchez-Romero R, et al. Impact of Heavy Metals on Human Male Fertility-An Overview. *Antioxid (Basel Switzerland)* (2021) 10:1473. doi 10.3390/antiox10091473
35. Robaire B, Delbes G, Head JA, Marlatt VL, Martyniuk CJ, Reynaud S, et al. A Cross-Species Comparative Approach to Assessing Multi- and Transgenerational Effects of Endocrine Disrupting Chemicals. *Environ Res* (2021) 204:112063. doi: 10.1016/j.envres.2021.112063
36. Padmanabhan V, Song W, Puttabyatappa M. Praegnatio Perturbatio-Impact of Endocrine-Disrupting Chemicals. *Endocr Rev* (2021) 42:295–353. doi: 10.1210/endrev/bnaa035
37. Sweeney MF, Hasan N, Soto AM, Sonnenschein C. Environmental Endocrine Disruptors: Effects on the Human Male Reproductive System. *Rev Endocr Metab Disord* (2015) 16:341–57. doi: 10.1007/s11154-016-9337-4
38. Eve L, Fervers B, Le Romancer M, Etienne-Selloum N. Exposure to Endocrine Disrupting Chemicals and Risk of Breast Cancer. *Int J Mol Sci* (2020) 21:9139. doi: 10.3390/ijms21239139
39. Francis CE, Allee L, Nguyen H, Grindstaff RD, Miller CN, Rayalam S. Endocrine Disrupting Chemicals: Friend or Foe to Brown and Beige Adipose Tissue? *Toxicology* (2021) 463:152972. doi: 10.1016/j.tox.2021.152972
40. Nordkap L, Joensen UN, Blomberg JM, Jorgensen N. Regional Differences and Temporal Trends in Male Reproductive Health Disorders: Semen Quality May Be a Sensitive Marker of Environmental Exposures. *Mol Cell Endocrinol* (2012) 355:221–30. doi: 10.1016/j.mce.2011.05.048
41. Krzastek SC, Farhi J, Gray M, Smith RP. Impact of Environmental Toxin Exposure on Male Fertility Potential. *Transl Androl Urol* (2020) 9:2797–813. doi: 10.21037/tau-20-685
42. Cheng CY, Wong EWP, Lie PPY, Li MWM, Su L, Siu ER, et al. Environmental Toxicants and Male Reproductive Function. *Spermatogenesis* (2011) 1:2–13. doi: 10.4161/spmg.1.1.13971
43. Mesquita I, Lorigo M, Cairrao E. Update About the Disrupting-Effects of Phthalates on the Human Reproductive System. *Mol Reprod Dev* (2021) 88:650–72. doi: 10.1002/mrd.23541
44. Priya K, Setty M, Babu UV, Pai KSR. Implications of Environmental Toxicants on Ovarian Follicles: How It Can Adversely Affect the Female Fertility? *Environ Sci Pollut Res Int* (2021). doi: 10.1007/s11356-021-16489-4
45. Bhardwaj JK, Panchal H, Saraf P. Cadmium as a Testicular Toxicant: A Review. *J Appl Toxicol* (2021) 41:105–17. doi: 10.1002/jat.4055
46. Genchi G, Sinicropi MS, Lauria G, Carocci A, Catalano A. The Effects of Cadmium Toxicity. *Int J Environ Res Public Health* (2020) 17:3782. doi: 10.3390/ijerph17113782
47. Mokra K. Endocrine Disruptor Potential of Short- and Long-Chain Perfluoroalkyl Substances (PFASs)-A Synthesis of Current Knowledge With Proposal of Molecular Mechanism. *Int J Mol Sci* (2021) 22:2148. doi: 10.3390/ijms22042148
48. Tarapore P, Ouyang B. Perfluoroalkyl Chemicals and Male Reproductive Health: Do PFOA and PFOS Increase Risk for Male Infertility? *Int J Environ Res Public Health* (2021) 18:3794. doi: 10.3390/ijerph18073794
49. Howdeshell KL, Wilson VS, Furr J, Lambright CR, Rider CV, Blystone CR, et al. A Mixture of Five Phthalate Esters Inhibits Fetal Testicular Testosterone Production in the Sprague-Dawley Rat in a Cumulative, Dose-Additive Manner. *Toxicol Sci* (2008) 105:153–65. doi: 10.1093/toxsci/kfn077
50. Howdeshell KL, Rider CV, Wilson VS, Gray LE Jr. Mechanisms of Action of Phthalate Esters, Individually and in Combination, to Induce Abnormal Reproductive Development in Male Laboratory Rats. *Environ Res* (2008) 108:168–76. doi: 10.1016/j.envres.2008.08.009
51. Gao Y, Chen H, Xiao X, Lui WY, Lee WM, Mruk DD, et al. Perfluorooctanesulfonate (PFOS)-Induced Sertoli Cell Injury Through a Disruption of F-Actin and Microtubule Organization Is Mediated by Akt1/2. *Sci Rep* (2017) 7:1110. doi: 10.1038/s41598-017-01016-8
52. Wan HT, Mruk DD, Wong CKC, Cheng CY. Perfluorooctanesulfonate (PFOS) Perturbs Male Rat Sertoli Cell Blood-Testis Barrier Function by Affecting F-Actin Organization *via* P-FAK-Tyr^{407} - An *In Vitro* Study. *Endocrinology* (2014) 155:249–62. doi: 10.1210/en.2013-1657
53. Xiao X, Mruk DD, Tang EI, Wong CKC, Lee WM, John CM, et al. Environmental Toxicants Perturb Human Serotli Cell Adhesive Function *via* Changes in F-Actin Organization Medicated by Actin Regulatory Proteins. *Hum Reprod* (2014) 29:1279–91. doi: 10.1093/humrep/deu011
54. Schaller MD. Cellular Functions of FAK Kinases: Insight Into Molecular Mechanisms and Novel Functions. *J Cell Sci* (2010) 123:1007–13. doi: 10.1242/jcs.045112
55. Cheng CY, Mruk DD. Regulation of Blood-Testis Barrier Dynamics by Focal Adhesion Kinase (FAK): An Unexpected Turn of Events. *Cell Cycle* (2009) 8:3493–9. doi: 10.4161/cc.8.21.9833
56. Li M, Wang Y, Li M, Wu X, Setrerrahmane S, Xu H. Integrins as Attractive Targets for Cancer Therapeutics. *Acta Pharm Sinica B* (2021) 11:2726–37. doi: 10.1016/j.apsb.2021.01.004
57. Dawson JC, Serrels A, Stupack DG, Schlaepfer DD, Frame MC. Targeting FAK in Anticancer Combination Therapies. *Nat Rev Cancer* (2021) 21:313–24. doi: 10.1038/s41568-021-00340-6
58. Rigiracciolo DC, Cirillo F, Talia M, Muglia L, Gutkind JS, Maggiolini M, et al. Focal Adhesion Kinase Fine Tunes Multifaced Signals Toward Breast Cancer Progression. *Cancers* (2021) 13:645. doi: 10.3390/cancers13040645
59. Chauhan A, Khan T. Focal Adhesion Kinase-An Emerging Viable Target in Cancer and Development of Focal Adhesion Kinase Inhibitors. *Chem Biol Drug design* (2021) 97:774–94. doi: 10.1111/cbdd.13808
60. Frame MC, Patel H, Serrels B, Lietha D, Eck MJ. The FERM Domain: Organizing the Structure and Function of FAK. *Nat Rev Mol Cell Biol* (2010) 11:802–14. doi: 10.1038/nrm2996
61. Siu MKY, Cheng CY. Dynamic Cross-Talk Between Cells and the Extracellular Matrix in the Testis. *BioEssays* (2004) 26:978–92. doi: 10.1002/bies.20099
62. Mruk DD, Cheng CY. Sertoli-Sertoli and Sertoli-Germ Cell Interactions and Their Significance in Germ Cell Movement in the Seminiferous Epithelium During Spermatogenesis. *Endocr Rev* (2004) 25:747–806. doi: 10.1210/er.2003-0022
63. Siu MKY, Cheng CY. Extracellular Matrix: Recent Advances on Its Role in Junction Dynamics in the Seminiferous Epithelium During Spermatogenesis. *Biol Reprod* (2004) 71:375–91. doi: 10.1095/biolreprod.104.028225
64. Dym M. Basement Membrane Regulation of Sertoli Cells. *Endocr Rev* (1994) 15:102–15. doi: 10.1210/edrv-15-1-102
65. Siu MKY, Mruk DD, Lee WM, Cheng CY. Adhering Junction Dynamics in the Testis Are Regulated by an Interplay of β1-Integrin and Focal Adhesion Complex (FAC)-Associated Proteins. *Endocrinology* (2003) 144:2141–63. doi: 10.1210/en.2002-221035
66. Siu MKY, Wong CH, Lee WM, Cheng CY. Sertoli-Germ Cell Anchoring Junction Dynamics in the Testis Are Regulated by an Interplay of Lipid and Protein Kinases. *J Biol Chem* (2005) 280:25029–47. doi: 10.1074/jbc.M501049200
67. Lie PPY, Mruk DD, Mok KW, Su L, Lee WM, Cheng CY. Focal Adhesion Kinase-Tyr^{407} and -Tyr^{397} Exhibit Antagonistic Effects on Blood-Testis Barrier Dynamics in the Rat. *Proc Natl Acad Sci USA* (2012) 109:12562–7. doi: 10.1073/pnas.1202316109
68. Beardsley A, Robertson DM, O'Donnell L. A Complex Containing α6β1-Integrin and Phosphorylated Focal Adhesion Kinase Between Sertoli Cells

and Elongated Spermatids During Spermatid Release From the Seminiferous Epithelium. *J Endocrinol* (2006) 190:759–70. doi: 10.1677/joe.1.06867
69. O'Donnell L, Nicholls PK, O'Bryan MK, McLachlan RI, Stanton PG. Spermiation: The Process of Sperm Release. *Spermatogenesis* (2011) 1:14–35. doi: 10.4161/spmg.1.1.14525
70. Siu MKY, Cheng CY. Interactions of Proteases, Protease Inhibitors, and the β1 Integrin/Laminin γ3 Protein Complex in the Regulation of Ectoplasmic Specialization Dynamics in the Rat Testis. *Biol Reprod* (2004) 70:945–64. doi: 10.1095/biolreprod.103.023606
71. Siu MKY, Wong CH, Xia W, Mruk DD, Lee WM, Cheng CY. The β1-Integrin-P-FAK-P130cas-DOCK180-RhoA-Vinculin Is a Novel Regulatory Protein Complex at the Apical Ectoplasmic Specialization in Adult Rat Testes. *Spermatogenesis* (2011) 1:73–86. doi: 10.4161/spmg.1.1.15452
72. Siu ER, Wong EWP, Mruk DD, Porto CS, Cheng CY. Focal Adhesion Kinase Is a Blood-Testis Barrier Regulator. *Proc Natl Acad Sci USA* (2009) 106:9298–303. doi: 10.1073/pnas.0813113106
73. Wan HT, Mruk DD, Li SYT, Mok KW, Lee WM, Wong CKC, et al. P-FAK-Tyr^{397} Regulates Spermatid Adhesion in the Rat Testis *via* Its Effects on F-Actin Organization at the Ectoplasmic Specialization. *Am J Physiol Endocrinol Metab* (2013) 305:E687–99. doi: 10.1152/ajpendo.00254.2013
74. Breuzard G, Pagano A, Bastonero S, Malesinski S, Parat F, Barbier P, et al. Tau Regulates the Microtubule-Dependent Migration of Glioblastoma Cells *via* the Rho-ROCK Signaling Pathway. *J Cell Sci* (2019) 132:jcs222851. doi: 10.1242/jcs.222851
75. Fan Z, Xu Q, Wang C, Lin X, Zhang Q, Wu N. A Tropomyosin-Like Meretrix Meretrix Linnaeus Polypeptide Inhibits the Proliferation and Metastasis of Glioma Cells *via* Microtubule Polymerization and FAK/Akt/MMPs Signaling. *Int J Biol Macromol* (2020) 145:154–64. doi: 10.1016/j.ijbiomac.2019.12.158
76. Peng Y, Qu R, Feng Y, Huang X, Yang Y, Fan T, et al. Regulation of the Integrin αvβ3- Actin Filaments Axis in Early Osteogenesis of Human Fibroblasts Under Cyclic Tensile Stress. *Stem Cell Res Ther* (2021) 12:523. doi: 10.1186/s13287-021-02597-y
77. Benwell CJ, Taylor J, Robinson SD. Endothelial Neuropilin-2 Influences Angiogenesis by Regulating Actin Pattern Development and α5-Integrin-P-FAK Complex Recruitment to Assembling Adhesion Sites. *FASEB J* (2021) 35:e21679. doi: 10.1096/fj.202100286R
78. Devi SS, Yadav R, Arya R. Altered Actin Dynamics in Cell Migration of GNE Mutant Cells. *Front Cell Dev Biol* (2021) 9:603742. doi: 10.3389/fcell.2021.603742
79. Linsen SE, de Wit E, de Bruijn E, Cuppen E. Small RNA Expression and Strain Specificity in the Rat. *BMC Genomics* (2010) 11:249. doi: 10.1186/1471-2164-11-249
80. Landgraf P, Rusu M, Sheridan R, Sewer A, Iovino N, Aravin A, et al. A Mammalian microRNA Expression Atlas Based on Small RNA Library Sequencing. *Cell* (2007) 29:1401–14. doi: 10.1016/j.cell.2007.04.040
81. Wang L, Yan M, Li H, Wu S, Ge R, Wong CKC, et al. The Non-Hormonal Male Contraceptive Adjudin Exerts Its Effects *via* MAPs and Signaling Proteins Mtorc1/Rps6 and FAK-Y407. *Endocrinology* (2021) 162:bqaa196. doi: 10.1210/endocr/bqaa196
82. Venditti M, Ben Rhouma M, Romano MZ, Messaoudi I, Reiter RJ, Minucci S. Evidence of Melatonin Ameliorative Effects on the Blood-Testis Barrier and Sperm Quality Alterations Induced by Cadmium in the Rat Testis. *Ecotoxicol Environ Saf* (2021) 226:112878. doi: 10.1016/j.ecoenv.2021.112878
83. Wang L, Yan M, Wong CKC, Ge R, Wu X, Sun F, et al. Microtubule-Associated Proteins (MAPs) in Microtubule Cytoskeletal Dynamics and Spermatogenesis. *Histol Histopathol* (2021) 36:249–65. doi: 10.14670/HH-18-279
84. Akhmanova A, Steinmetz MO. Control of Microtubule Organization and Dynamics: Two Ends in the Limelight. *Nat Rev Mol Cell Biol* (2015) 16:711–26. doi: 10.1038/nrm4084
85. Wong EWP, Cheng CY. Impacts of Environmental Toxicants on Male Reproductive Dysfunction. *Trends Pharmacol Sci* (2011) 32:290–9. doi: 10.1016/j.tips.2011.01.001
86. Cheng CY, Mruk DD, Silvestrini B, Bonanomi M, Wong CH, Siu MKY, et al. AF-2364 [1-(2,4-Dichlorobenzyl)-*1H*-Indazole-3-Carbohydrazide] Is a Potential Male Contraceptive: A Review of Recent Data. *Contraception* (2005) 72:251–61. doi: 10.1016/j.contraception.2005.03.008
87. Cheng CY. Toxicants Target Cell Junctions in the Testis - Insights From the Indazole-Carboxylic Acid Model. *Spermatogenesis* (2014) 4:e981485. doi: 10.4161/21565562.2014.9814895
88. Mruk DD, Cheng CY. Testin and Actin Are Key Molecular Targets of Adjudin, an Anti-Spermatogenic Agent, in the Testis. *Spermatogenesis* (2011) 1:137–46. doi: 10.4161/spmg.1.2.16449
89. Tang EI, Lee WM, Cheng CY. Coordination of Actin- and Microtubule-Based Cytoskeletons Supports Transport of Spermatids and Residual Bodies/Phagosomes During Spermatogenesis in the Rat Testis. *Endocrinology* (2016) 157:1644–59. doi: 10.1210/en.2015-1962
90. Mao B, Li L, Yan M, Wong CKC, Silvestrini B, Li C, et al. F5-Peptide and Mtorc1/Rps6 Effectively Enhance BTB Transport Function in the Testis-Lesson From the Adjudin Model. *Endocrinology* (2019) 160:1832–53. doi: 10.1210/en.2019-00308
91. Mao BP, Li L, Yan M, Ge R, Lian Q, Cheng CY. Regulation of BTB Dynamics in Spermatogenesis - Insights From the Adjudin Toxicant Model. *Toxicol Sci* (2019) 172:75–88. doi: 10.1093/toxsci/kfz180
92. Yan M, Li L, Mao BP, Li H, Li SYT, Mruk D, et al. Mtorc1/Rps6 Signaling Complex Modifies BTB Transport Function - An *In Vivo* Study Using the Adjudin Model. *Am J Physiol Endocrinol Metab* (2019) 317:E121–38. doi: 10.1152/ajpendo.00553.2018
93. Laplante M, Sabatini DM. mTOR Signaling in Growth Control and Disease. *Cell* (2012) 149:274–93. doi: 10.1016/j.cell.2012.03.017
94. Szwed A, Kim E, Jacinto E. Regulation and Metabolic Functions of Mtorc1 and Mtorc2. *Physiol Rev* (2021) 101:1371–426. doi: 10.1152/physrev.00026.2020
95. Mok KW, Mruk DD, Cheng CY. Regulation of Blood-Testis Barrier (BTB) Dynamics During Spermatogenesis *via* the "Yin" and "Yang" Effects of Mammalian Target of Rapamycin Complex 1 (Mtorc1) and Mtorc2. *Int Rev Cell Mol Biol* (2013) 301:291–358. doi: 10.1016/B978-0-12-407704-1.00006-3
96. Li N, Cheng CY. Mammalian Target of Rapamycin Complex (mTOR) Pathway Modulates Blood-Testis Barrier (BTB) Function Through F-Actin Organization and Gap Junction. *Histol Histopathol* (2016) 31:961–8. doi: 10.14670/HH-11-753
97. Wen Q, Tang EI, Gao Y, Jesus TT, Chu DS, Lee WM, et al. Signaling Pathways Regulating Blood-Tissue Barriers - Lesson From the Testis. *Biochim Biophys Acta* (2018) 1860:141–53. doi: 10.1016/j.bbamem.2017.04.020
98. Boyer A, Girard M, Thimmanahalli DS, Levasseur A, Celeste C, Paquet M, et al. mTOR Regulates Gap Junction Alpha-1 Protein Trafficking in Sertoli Cells and Is Required for the Maintenance of Spermatogenesis in Mice. *Biol Reprod* (2016) 95:13. doi: 10.1095/biolreprod.115.138016
99. Serra ND, Velte EK, Niedenberger BA, Kirsanov O, Geyer CB. Cell-Autonomous Requirement for Mammalian Target of Rapamycin (Mtor) in Spermatogonial Proliferation and Differentiation in the Mousedagger. *Biol Reprod* (2017) 96:816–28. doi: 10.1093/biolre/iox022
100. Mok KW, Chen H, Lee WM, Cheng CY. Rps6 Regulates Blood-Testis Barrier Dynamics Through Arp3-Mediated Actin Microfilament Organization in Rat Sertoli Cells. An *In Vitro* Study. *Endocrinology* (2015) 156:1900–13. doi: 10.1210/en.2014-1791
101. Mok KW, Mruk DD, Cheng CY. Rps6 Regulates Blood-Testis Barrier Dynamics Through Akt-Mediated Effects on MMP-9. *J Cell Sci* (2014) 127:4870–82. doi: 10.1242/jcs.152231
102. Jo H, Loison F, Luo HR. Microtubule Dynamics Regulates Akt Signaling *via* Dynactin P150. *Cell Signal* (2014) 26:1707–16. doi: 10.1016/j.cellsig.2014.04.007
103. Mok KW, Mruk DD, Silvestrini B, Cheng CY. RPS6 Regulates Blood-Testis Barrier Dynamics by Affecting F-Actin Organization and Protein Recruitment. *Endocrinology* (2012) 153:5036–48. doi: 10.1210/en.2012-1665
104. Yao Y, Fan Y. CO(2) Laser Fabrication of Hydrogel-Based Open-Channel Microfluidic Devices. *Biomed Microdevices* (2021) 23:47. doi: 10.1007/s10544-021-00584-x
105. Scott SM, Ali Z. Fabrication Methods for Microfluidic Devices: An Overview. *Micromachines* (2021) 12:319. doi: 10.3390/mi12030319
106. Annabestani M, Esmaeili-Dokht P, Fardmanesh M. A Novel, Low Cost, and Accessible Method for Rapid Fabrication of the Modifiable Microfluidic Devices. *Sci Rep* (2020) 10:16513. doi: 10.1038/s41598-020-73535-w

107. Roman J, Français O, Jarroux N, Patriarche G, Pelta J, Bacri L, et al. Solid-State Nanopore Easy Chip Integration in a Cheap and Reusable Microfluidic Device for Ion Transport and Polymer Conformation Sensing. *ACS sensors* (2018) 3:2129–37. doi: 10.1021/acssensors.8b00700
108. Riester O, Borgolte M, Csuk R, Deigner HP. Challenges in Bone Tissue Regeneration: Stem Cell Therapy, Biofunctionality and Antimicrobial Properties of Novel Materials and Its Evolution. *Int J Mol Sci* (2020) 22:192. doi: 10.3390/ijms22010192

Conflict of Interest: The authors declare that the research was conducted in the absence of any commercial or financial relationships that could be construed as a potential conflict of interest.

Publisher's Note: All claims expressed in this article are solely those of the authors and do not necessarily represent those of their affiliated organizations, or those of the publisher, the editors and the reviewers. Any product that may be evaluated in this article, or claim that may be made by its manufacturer, is not guaranteed or endorsed by the publisher.

frontiers in Endocrinology

ORIGINAL RESEARCH
published: 03 January 2022
doi: 10.3389/fendo.2021.807374

Analysis by Metabolomics and Transcriptomics for the Energy Metabolism Disorder and the Aryl Hydrocarbon Receptor Activation in Male Reproduction of Mice and GC-2spd Cells Exposed to $PM_{2.5}$

Fuquan Shi[1], Zhonghao Zhang[1], Jiankang Wang[1], Yimeng Wang[1], Jiuyang Deng[2], Yingfei Zeng[3], Peng Zou[1], Xi Ling[1], Fei Han[1], Jinyi Liu[1], Lin Ao[1] and Jia Cao[1]**

[1] Key Lab of Medical Protection for Electromagnetic Radiation, Ministry of Education of China, Institute of Toxicology, College of Preventive Medicine, Army Medical University (Third Military Medical University), Chongqing, China, [2] School of Public Health, Shanxi Medical University, Taiyuan, China, [3] School of Tropical Medicine and Laboratory Medicine, Hainan Medical University, Haikou, China

Fine particulate matter ($PM_{2.5}$)-induced male reproductive toxicity arouses global public health concerns. However, the mechanisms of toxicity remain unclear. This study aimed to further investigate toxicity pathways by exposure to $PM_{2.5}$ *in vitro* and *in vivo* through the application of metabolomics and transcriptomics. *In vitro*, spermatocyte-derived GC-2spd cells were treated with 0, 25, 50, 100 μg/mL $PM_{2.5}$ for 48 h. *In vivo*, the real-world exposure of $PM_{2.5}$ for mouse was established. Forty-five male C57BL/6 mice were exposed to filtered air, unfiltered air, and concentrated ambient $PM_{2.5}$ in Tangshan of China for 8 weeks, respectively. The results *in vitro* and *in vivo* showed that $PM_{2.5}$ exposure inhibited GC-2spd cell proliferation and reduced sperm motility. Mitochondrial damage was observed after $PM_{2.5}$ treatment. Increased Humanin and MOTS-c levels and decreased mitochondrial respiratory indicated that mitochondrial function was disturbed. Furthermore, nontargeted metabolomics analysis revealed that $PM_{2.5}$ exposure could disturb the citrate cycle (TCA cycle) and reduce amino acids and nucleotide synthesis. Mechanically, the aryl hydrocarbon receptor (AhR) pathway was activated after exposure to $PM_{2.5}$, with a significant increase in CYP1A1 expression. Further studies showed that $PM_{2.5}$ exposure significantly increased both intracellular and mitochondrial reactive oxygen species (ROS) and activated NRF2 antioxidative pathway. With the RNA-sequencing technique, the differentially expressed genes induced by $PM_{2.5}$ exposure were mainly enriched in the metabolism of xenobiotics by the cytochrome P450 pathway, of which *Cyp1a1* was the most significantly changed gene. Our findings demonstrated

OPEN ACCESS

Edited by:
Yankai Xia,
Nanjing Medical University, China

Reviewed by:
Aditya D. Joshi,
University of Oklahoma Health Sciences Center, United States
Cuiqing Liu,
Zhejiang Chinese Medical University, China

***Correspondence:**
Jia Cao
caojia1962@126.com
Lin Ao
aolin117@163.com

Specialty section:
This article was submitted to Reproduction, a section of the journal Frontiers in Endocrinology

Received: *02 November 2021*
Accepted: *08 December 2021*
Published: *03 January 2022*

Citation:
Shi F, Zhang Z, Wang J, Wang Y, Deng J, Zeng Y, Zou P, Ling X, Han F, Liu J, Ao L and Cao J (2022) Analysis by Metabolomics and Transcriptomics for the Energy Metabolism Disorder and the Aryl Hydrocarbon Receptor Activation in Male Reproduction of Mice and GC-2spd Cells Exposed to $PM_{2.5}$. Front. Endocrinol. 12:807374. doi: 10.3389/fendo.2021.807374

that $PM_{2.5}$ exposure could induce spermatocyte damage and energy metabolism disorder. The activation of the aryl hydrocarbon receptor might be involved in the mechanism of male reproductive toxicity.

Keywords: $PM_{2.5}$, GC-2spd, cell proliferation, aryl hydrocarbon receptor, mitochondrial dysfunction, energy metabolism, transcriptomics, metabolomics

INTRODUCTION

The impact of particulate matter (PM) on health has aroused widespread public concern around the world. Fine particulate matter ($PM_{2.5}$) is still one of the most common air pollutants in the world, especially in developing countries (1). In China, the average annual $PM_{2.5}$ concentration in 338 cities was 10 to 86 μg/m^3 (average: 43 μg/m^3) in 2017, which was much higher than the recommendation of the WHO air quality guidelines (10 μg/m^3) (2). $PM_{2.5}$ and its combined toxic components, including transition metals, polycyclic aromatic hydrocarbons (PAHs) and water-soluble ions (WSI) can penetrate into the gas exchange area of the lungs, pass through the respiratory barrier, enter the circulatory system, diffuse to the whole body (3), and ultimately damage the respiratory system, circulatory system (4), central nervous system (5) and reproductive system (6).

Numerous epidemiology studies have shown $PM_{2.5}$ could affect male reproduction and lead to a decrease in sperm quality (7–9). Our previous study also indicated $PM_{10\text{-}2.5}$ exposure was inversely associated with sperm concentration in a longitudinal study of 796 Chinese college students (10). Besides the epidemiological evidence, several toxicological studies in animals revealed decreased male reproductive capacity caused by $PM_{2.5}$. After $PM_{2.5}$ exposure *via* intratracheal instillation, injury of testicular tissue and reduced testosterone were occurred, the integrity of blood-testis barrier was destroyed, and finally sperm quality was significantly decreased (11–13). Up to now, the mechanisms of reproductive toxicity induced by $PM_{2.5}$ mainly focused on ROS generation, DNA damage, mitochondrial dysfunction and the disturbance of hypothalamic-pituitary-gonadal (HPG) axis. However, spermatogenesis is a complex process that requires the participation of various signal pathways, and $PM_{2.5}$, as a complex mixture, can carry various harmful substances, for instance, PAHs (14). Numerous studies have shown that PAHs exposure might induce various adverse health effects (15–17). In male reproduction, our recent study found that $PM_{2.5}$-bound PAHs, especially HMW PAHs decreased sperm normal morphology in the Male Reproductive Health in Chongqing College Students (MARHCS) cohort study (18). Besides, PAHs are well-known activators of the aryl hydrocarbon receptor (AhR). P. Esakky and K. Moley revealed that the PAHs of cigarette smoke condensate (CSC) showed a great effect on accelerating germ cell death through activation of AhR, which was present at all stages of spermatogenesis (19). These studies provided a possible mechanism of $PM_{2.5}$-induced spermatogenesis damage. Nonetheless, it is still unclear whether $PM_{2.5}$ exposure will activate AhR pathway in spermatogenesis.

Epidemiological and experimental studies have shown that mitochondria might be one of the target organelles damaged by environmental pollutants, including $PM_{2.5}$ (20, 21). Because of the lack of protective histones and DNA repair enzymes, mitochondrial DNA is particularly vulnerable to endogenous and exogenous damage factors, such as ROS or adducts (22, 23). Meanwhile, mitochondrial are involved in various important cellular functions, including oxidative phosphorylation of ATP synthesis, mitochondrial apoptosis pathway and ROS generation, etc. Therefore, mitochondrial damage will directly cause mitochondrial dysfunction and then mediate cytotoxicity. Moreover, previous studies found $PM_{2.5}$ can induce mitochondrial damage and activate mitochondrial apoptosis pathway in male reproduction (11, 24). Two major contributions of mitochondria in spermatogenesis involve energy generation and apoptosis (25). Because the process of spermatogenesis requires a lot of energy and the elimination of damaged spermatogenic cells, and mitochondria in sperm are arranged in the periphery of the tail microtubules to serve to energy demand for motility. It can be seen that mitochondria play a crucial part in spermatogenesis and sperm motility. However, whether $PM_{2.5}$ exposure can disturb energy metabolism through mitochondrial damage and dysfunction in spermatogenesis is still unclear.

To better understand the effects of $PM_{2.5}$ on male reproduction, we used GC-2spd cell line and real time whole-body $PM_{2.5}$ exposure mouse model to investigate the effects of $PM_{2.5}$ on mouse spermatocyte *in vitro* and *in vivo*. Then, metabolomics and transcriptomics were performed to probe into the role of energy metabolism and the aryl hydrocarbon receptor under $PM_{2.5}$ exposure.

MATERIALS AND METHODS

Particular Matter Suspension Preparation

Concerning the integrity of the experiment and immature technique of $PM_{2.5}$ extraction from sampling membrane, the SRM 1648a collected in an urban area in the USA was used in the study. It was purchased from the National Institute of Standards and Technology (NIST, USA), and composed mainly of inorganic substances and organic substances with polycyclic aromatic hydrocarbons (PAHs), nitro-substituted PAHs (nitro-PAHs), polychlorinated biphenyl (PCB) congeners, and chlorinated pesticides. In addition, the particular matter has good solubility and dispersion in PBS, and a previous study indicated that the size of PM in PBS solution is from 236.43 nm

to 1.98 μm (26). Thus, the PM was suspended and ultrasonicated for 2 hours in phosphate-buffered saline (PBS) to a final concentration of 10 mg/mL. All $PM_{2.5}$ stock solutions were stored at -80°C until biological analysis and ultrasound 30 min to avoid agglomeration of the suspended $PM_{2.5}$ prior to treatment.

Cell Culture and Cell Proliferation Assay

The GC-2spd cell line was purchased from American type culture collection (ATCC, CRL-2196) and cultured in Dulbecco's modified Eagle's medium (DMEM), supplemented with 10% FBS, 100 U/mL penicillin, and 100 μg/mL streptomycin at 37°C, 5% CO_2. Cells were labeled with Carboxyfluorescein diacetate, succinimidyl ester (CFDA-SE; C0051, Beyotime, Shanghai, China) and then plated onto 6-well plates at a density of 1×10^5 cells per well. $PM_{2.5}$ stock solution (10 mg/mL) was diluted to the final concentration of 12.5, 25, 50, 100, 200 μg/mL (0, 3.91, 7.81, 15.625, 31.25, 62.5 μg/cm^2) with complete medium. Then, cells were treated with different concentrations of $PM_{2.5}$ suspensions. Meanwhile, the control group was added with the normal culture medium and PBS. The final concentration of PBS was less than 1%. After 24 h or 48 h, the cells were harvested, washed with PBS, and resuspended in HBSS. The fluorescence intensity was measured by a BD Accuri™ C6 flow cytometer (BD Pharmingen, San Diego, CA, United States) at an excitation wavelength of 488 nm. The FL1 detection channel was used to perform analysis, and 10,000 events were collected for each sample.

Viability Assay for Live Cells

The cells were seeded in 6-well plates at a density of 1×10^5 cells per well overnight. After treatment with different doses of $PM_{2.5}$ (0, 25, 50, 100 μg/mL) for 48 h, the medium was removed and the cells were washed with PBS three times, The cells were stained with 2 μM Calcein AM (PF00008, Proteintech) and incubated for 15 min at room temperature in the dark. Images were obtained using a fluorescence microscope (Olympus IX-71, Japan) and the intensity of green fluorescent of each group was analyzed by ImageJ software.

Animal and Treatment Protocols

Forty-five male C57BL/6 mice (6–8-week-old) were purchased from Vital River Laboratory (Beijing Vital River Laboratory Animal Technology Co., Ltd, Beijing, China). All procedures of the study were approved by the Institution Animal Care and Use Committee (IACUC). All mice were treated humanely under good laboratory conditions, and free drinking distilled water and commercial standard pellet feed were provided. After a week of adaptation, these mice (15 per group) were randomly subjected to exposure to filtered air (FA), unfiltered air (UA) and concentrated ambient $PM_{2.5}$ (CAP) from November 18, 2019 to January 12, 2020 for a total duration of 2 months with a 12-h light/12-h dark cycle, the temperature at 24 to 26°C, and relative humidity of 40-60%. The sample size of 15 was calculated through the power analysis using an online calculator (www.stat.ubc.ca/~rollin/stats/ssize/n2.html) according to the published effect of CAP exposure on the sperm motility (27), and the statistic power is 0.90 (28). The FA-exposed mice received ambient air filtered by a high-efficient particulate air filter which was added to remove particles in the air. The UA-exposed mice were housed in the same chambers and exposed to ambient air conveyed through the pipeline. A previous study used the same apparatus had performed size classification for the particle matter in the UA chambers, and the results showed more than 90% of particle matters were less than 2.5 μm in diameter size (27). Mice exposed to concentrated ambient $PM_{2.5}$ were performed with a $PM_{2.5}$ concentration enrichment system (Beijing Huironghe Technology Co., Ltd, Beijing, China) located at the North China University of Science and Technology, Tangshan, China. The exposure protocol was 6 h/d, 5 days/week (only on weekdays). The real-time concentrations of $PM_{2.5}$ in chambers and the outdoor air were constantly measured by the aerosol monitor (TSI Instrument Co., Ltd, Minneapolis, USA). The average concentrations of $PM_{2.5}$ in the FA, UA and CAP chambers during the 2-month period were 0.39, 59.75 and 483.61 μg/m^3, respectively. During exposure, $PM_{2.5}$ particles were collected on quartz filter membranes (90 mm, Whatman, UK) and the membranes were weighed before and after sampling. Subsequently, analyses for water-soluble inorganic ions, metal elements and PAHs were performed in some representative membranes. Component analysis showed that $PM_{2.5}$ particles were mainly consisted of water-soluble inorganic ions (NO_3^-, SO_4^{2-}, NH_4^+ et al.) and major metals (S, Na, Ca, Fe, K et al.). Besides, $PM_{2.5}$ particles also contained abundant PAHs, of which benzo(b)fluoranthene (BbF) took the largest portion of PAHs, followed by fluoranthene (FLT), benzo(a)anthracene (BaA) and pyrene (PYR) (data not shown).

Assessment of Sperm Parameter in Epididymides

To measure sperm concentration and sperm motility, the epididymides were quickly collected and cut in 800 μL Ham's F-12 Nutrient Mixture (Gibco, USA) after the mice were anesthetized. After incubation at 37°C for 2 min, 5 μL sperm suspension was detected using a computer-assisted sperm assay (CASA; Suiplus, Beijing, China). The experimental staff were blinded to groups assignment.

Observation of Ultrastructure of Testis and GC-2spd

Cells and testes were collected and fixed in transmission electron microscopy (TEM) fixative (Servicebio, China) at 4°C. After washing the samples using 0.1 M PB (pH 7.4) three times, the samples were post-fixed with 1% OsO_4 in 0.1 M PB (pH 7.4) for 2 h at room temperature, then dehydrated with different proportions of ethanol. The ultrathin sections were obtained using a UC7 ultramicrotome (Leica, Germany) after Resin embedding, and then stained with 2% uranium acetate saturated alcohol solution. Finally, the ultrastructure was observed under TEM (HITACHI, Japan).

Measurements of Oxygen Consumption Rate (OCR)

The XFp cell mito stress test was conducted to measure mitochondrial function using the XFp 8-wells Extracellular Flux Analyzer (Seahorse Bioscience, North Billerica, MA, USA) according to manufacturer's instructions. Briefly, approximately 1,200 GC-2spd cells were seeded in the special 8-wells miniplates. After exposure to $PM_{2.5}$ for 48 h, cells were washed with XFp assay medium containing 10 mM glucose (Agilent Technologies, 103577), 2 mM L-glutamine (Agilent Technologies, 103579) and 1 mM sodium pyruvate (Agilent Technologies, 103578). OCR was analyzed by adding oligomycin, 1.5 μM; carbonyl cyanide 4-(trifluoromethoxy) phenylhydrazone (FCCP), 2 μM and Rotenone, 0.5 μM to evaluate basal respiration, maximal respiration, spare capacity, proton leak and ATP production. And the OCR was normalized to the protein concentration of each sample.

Measurements of Intracellular and Mitochondrial ROS

The intracellular and mitochondrial ROS production were detected using the oxidation-sensitive fluorescent probe CM-H2DCFDA (Invitrogen, USA) and MitoSOX Red (Invitrogen, USA), respectively. According to the manufacturer's instructions, the GC-2spd cells were seeded in 6-wells plates at a density of 1×10^5 cells per well. After treatment with 0, 25, 50, 100 μg/mL $PM_{2.5}$ for 48 h, the cells were harvested and washed in PBS, followed by incubation with 10 μM CM-H2DCFDA for 30 min at 37°C and 5 μM MitoSOX Red for 10 min at 37°C, respectively. The mean fluorescence intensity was measured by a BD Accuri™ C6 flow cytometer (BD Pharmingen, San Diego, CA, United States) and analyzed using FlowJo software (Tree Star, Inc., San Carlos, CA, USA).

Evaluations of Humanin and MOTS-c Levels

The levels of Humanin and MOTS-c in GC-2spd cells were measured using commercially available enzyme-linked immunosorbent assay (ELISA) kits (Shanghai Enzyme-linked Biotechnology Co., Ltd, Shanghai, China) according to the manufacturer's directions. The minimum detectable doses were both typically less than 0.1 ng/mL. The intra-assay CV (%) and inter-assay CV (%) were less than 15%, respectively. The final levels of Humanin and MOTS-c were normalized to total protein.

RNA Extraction and Quantitative Reverse-Transcription Polymerase Chain Reaction (qRT-PCR)

The total RNA from the cells and testes was isolated using TRIzol reagent (Invitrogen, Carlsbad, CA, USA) and converted to cDNA using RevertAid Master Mix (ThermoFisher, USA). PCR was performed on a CFX Real-Time System (Bio-Rad Laboratories Inc.) using GoTaq qPCR Master Mix (Promega, USA) and specific primers. The PCR amplification schedule started with 95°C for 10 min, followed by 45 cycles of 95°C for 30 s and 60°C for 30 s. The cycle threshold (Ct) values were recorded, and relative expression of the target gene was calculated through the $2^{-\triangle\triangle Ct}$ method. The primers (Sangon Biotech, Shanghai, China) were used as follows: ACTB (forward 5′-GTGA CGTTGACATCCGTAAAGA-3′, reverse 5′- GCCGGA CTCATCGTACTCC-3′); *Cyp1a1* (forward 5′-GGCCACT TTGACCCTTACAA-3′, reverse 5′- CAGGTAACGGA GGACAGGAA-3′).

Western Blot

Cells and testicular tissues were collected and lysed with a cell lysis buffer (Beyotime, Shanghai, China). Subsequently, 40-60 μg protein was resolved by 12% SDS-PAGE and then transferred to polyvinylidene difluoride (PVDF) membranes (Merck Millipore, Burlington MA, USA) for western blot analysis. Blots were blocked with 3% bovine serum albumin (BSA) in 0.15% Tris-Buffered Saline with Tween (0.15% TBST), and then probed with primary antibodies overnight at 4°C. The primary antibodies were used as follows: AHR Polyclonal Antibody (17840-1-AP, Proteintech); CYP1A1 Polyclonal Antibody (13241-1-AP, Proteintech); NRF2 Polyclonal Antibody (16396-1-AP, Proteintech); KEAP1 Polyclonal Antibody (10503-2-AP, Proteintech); β-actin Rabbit Antibody (4970S, Cell Signaling Technology, USA); Lamin B1 Rabbit Antibody (13435S, Cell Signaling Technology, USA). PCNA mouse Antibody (sc-56, Santa Cruz Biotechnology, USA). After three washes with 0.15% TBST, blots were treated with horseradish peroxidase-conjugated secondary antibodies (ab205718 and ab205719, Abcom, USA). Finally, protein bands were visualized using the enhanced chemiluminescence system, and the signals of blots were measured with ImageJ software. β-actin and Lamin B1 were utilized as the internal control for the normalization of the expression.

Extraction of Cytoplasmic and Nuclear Protein

To evaluate AhR and NRF2 nuclear translocation by Western blotting, cytoplasmic and nuclear proteins were separately extracted using Qproteome Nuclear Protein Kit (QIAGEN, Germany) following its instructions. In brief, after exposure to $PM_{2.5}$ for 48 h, cells were washed twice with ice-cold PBS, harvested using cell-scraper and centrifuged to remove supernatant. The cell pellets were resuspended in lysis buffer NL (supplemented with protease inhibitor solution and 0.1 M DTT) and incubated for 15 min on ice. Then, the detergent solution NP was added, and the cell suspensions were centrifuged for 5 min at 10,000 x g after vortex. The supernatants (cytoplasmic fraction) were transferred into new microcentrifuge tubes and stored at −80°C. The remaining pellets which contain cell nuclei were resuspended in nuclear protein lysis buffer NL (supplemented with protease inhibitor solution and 0.1 M DTT). After vortex and centrifugation, the nuclear pellets were obtained and resuspended in extraction buffer NX1 (supplemented with protease inhibitor solution). Finally, after incubation for 30 min and centrifugation at 12,000 x g for 10 min, the supernatants (nuclear fraction) were transferred into new tubes and stored at −80°C until use.

Metabolite Extraction, Dection, and Analysis

The GC-2spd cells with 80% confluency in a 10 cm dish were exposed to $PM_{2.5}$ (0, 100 μg/mL) for 48 h, and the medium was discarded followed by washing the cells three times with ice-cold PBS. Then the cells were harvested after adding trypsin and washed three times with ice-cold PBS, frozen and thawed with liquid nitrogen for 3 times, finally sonicated for 10 min in ice-water bath. 50 μL of homogenate was used to measure protein concentration. Then 600 μL acetonitrile: methanol = 1: 1 was added to the rest part and transferred to 2mL EP tube. After 30 s vortex, the samples were incubated at -40°C for 1 h and centrifuged at 12,000 rpm for 15 min at 4°C. 660 μL supernatant was transferred to an EP tube and dried in a vacuum concentrator. Then acetonitrile: methanol: water = 2: 2: 1, with isotopically-labelled internal standard mixture was added in proportion. After 30 s vortex, the samples were sonicated for 10 min in ice-water bath, centrifuged at 12,000 rpm for 15 min at 4°C. The resulting supernatant was transferred to a fresh glass vial for analysis, and the quality control (QC) sample was prepared by mixing an equal aliquot of the supernatants from all of the samples.

LC-MS/MS analyses were conducted by using an UHPLC system (Vanquish, Thermo Fisher Scientific) with a UPLC BEH Amide column (2.1 mm × 100 mm, 1.7 μm) coupled to Q Exactive HFX mass spectrometer (Orbitrap MS, Thermo). The mobile phase consisted of 25 mmol/L ammonium acetate and 25 ammonia hydroxide in water (pH = 9.75) (A) and acetonitrile (B). The auto-sampler temperature was 4°C, and the injection volume was 3 μL. The QE HFX mass spectrometer was used for its ability to acquire MS/MS spectra on information-dependent acquisition (IDA) mode in the control of the acquisition software (Xcalibur, Thermo). In this mode, the acquisition software continuously evaluated the full scan MS spectrum. The ESI source conditions were set as follows: sheath gas flow rate as 30 Arb, Aux gas flow rate as 25 Arb, capillary temperature 350°C, full MS resolution as 60000, MS/MS resolution as 7500, collision energy as 10/30/60 in NCE mode, spray Voltage as 3.6 kV (positive) or -3.2 kV (negative), respectively. For the raw data, we converted it to the mzXML format using ProteoWizard and processed using an in-house program, which was developed by R and based on XCMS, for peak detection, extraction, alignment, and integration. Then an in-house MS2 database (BiotreeDB) was applied in metabolite annotation. The cutoff for annotation was set at 0.3.

The final dataset containing the information of peak number, sample name and normalized peak area was imported to SIMCA16.0.2 software package (Sartorius Ste dim Data Analytics AB, Umea, Sweden) for principal component analysis (PCA) and orthogonal projections to latent structures-discriminate analysis (OPLS-DA). In addition, a 7-fold cross validation was performed to estimate the robustness and predictive ability of our model after 200 times permutations. According to OPLS-DA, a loading plot was constructed to show the contribution of variables to differences between the two groups. Furthermore, the value of variable importance in the projection (VIP) of the first principal component in OPLS-DA analysis was obtained, which summarized the contribution of each variable to the model. The metabolites with VIP>1 and $p<0.05$ (student's t-test) were considered as significantly changed metabolites. In addition, commercial databases including KEGG (http://www.genome.jp/kegg/) and MetaboAnalyst (http://www.metaboanalyst.ca/) were used for pathway enrichment analysis.

Transcriptome Analysis

Transcriptome analysis was applied to investigate global RNA changes after $PM_{2.5}$ exposure. The total RNA from the GC-2spd cells was isolated using TRIzol reagent (Invitrogen, Carlsbad, CA, USA). The RNA quantification and qualification were assessed using the NanoPhotometer® spectrophotometer (IMPLEN, CA, USA) and RNA Nano 6000 Assay Kit of the Bioanalyzer 2100 system (Agilent Technologies, CA, USA). A total amount of 1 μg RNA per sample was used for the RNA sample preparations. Sequencing libraries were structured with NEBNext® UltraTM RNA Library Prep Kit for Illumina® (NEB, USA) according to the manufacturer's recommendations. After cluster generation, the library preparations were sequenced on an Illumina Novaseq platform and 150 bp paired-end reads were generated. To ensure the quality and reliability of data analysis, the raw data were filtered, and all the downstream analyses were based on clean data with high quality. Next, we selected Hisat2 as the mapping tool to the reference genome. FPKM was calculated based on the length of the gene *via* featureCounts v1.5.0-p3. Differential expression analysis of two groups was proceeded with the DESeq2 R package. Genes with an adjusted p-value <0.05 found by DESeq2 were considered as differentially expressed genes (DEGs). Gene Set Enrichment Analysis (GSEA; http://www.broadinstitute.org/gsea/index.jsp) was conducted based on all changed genes.

Statistical Analyses

Quantitative data are expressed as the means ± standard deviation (SD) of three experiments unless noted otherwise. Statistical comparisons were performed by *t*-test and one-way ANOVA analysis of variance followed by the Dunnett's multiple comparison test. All subjective analyses were performed by individuals blinded to treatment groups. Statistical analysis was conducted using SPSS (version 26.0) and GraphPad Prism (version 8.4.0; GraphPad Software). A P-value < 0.05 was considered significance level.

RESULTS

$PM_{2.5}$ Inhibits Cell Proliferation in GC-2spd and Reduces Sperm Motility in Testes

The effect of $PM_{2.5}$ exposure on GC-2spd was examined firstly. As shown in **Figure 1A**, $PM_{2.5}$ exposure can significantly affect cell proliferation in a dose and time-dependent manner. The cell proliferation was significantly reduced in the doses of 200 μg/mL (equal to 62.5 $\mu g/cm^2$) after treatment for 24 h. When the exposure time was extended to 48 h, cell proliferation was

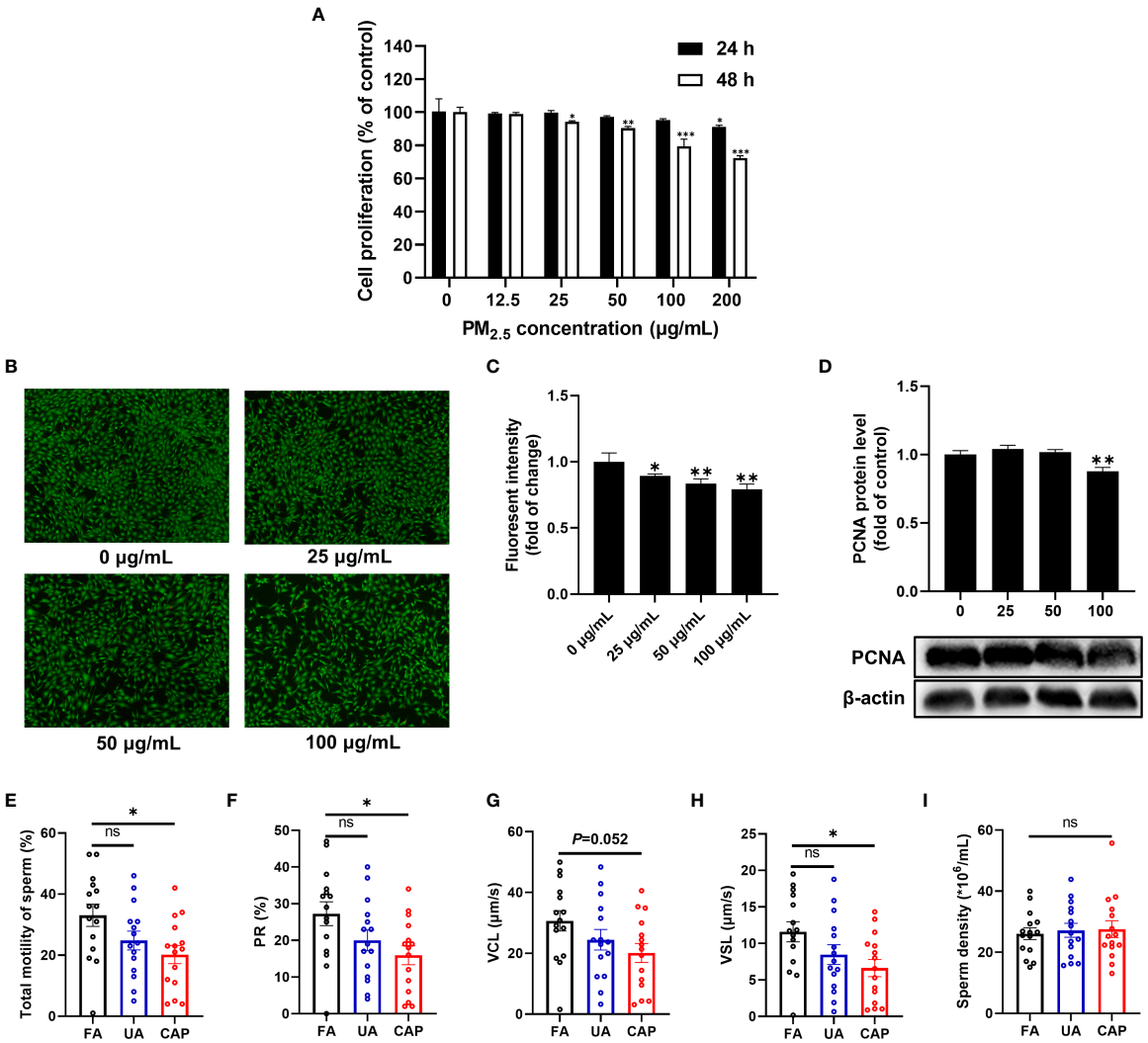

FIGURE 1 | $PM_{2.5}$ inhibits cell proliferation in GC-2spd and reduces sperm motility in testes. **(A)** Cells were treated with different concentrations of $PM_{2.5}$ (0, 12.5, 25, 50, 100, 200 μg/mL) for 24 or 48 h. Subsequently, cell proliferation was measured using CFDA-SE Cell Proliferation Assay and Tracking Kit. **(B)** Cells were treated with $PM_{2.5}$ (0, 25, 50, 100 μg/mL) for 48 h, and live cells were determined with Calcein AM staining followed by fluorescence microscope (100 X). **(C)** The intensity of green fluorescent was analyzed by ImageJ software. **(D)** The expression of PCNA was detected by western blot analysis, and the bar graph shows the quantification of PCNA. Values are presented as means ± SD (n=3). Sperm motility and sperm density changes of mice testes after exposure to $PM_{2.5}$. **(E)** Total motility of sperm; **(F)** PR% (progressive motility) of sperm; **(G)** VCL (curvilinear velocity) of sperm; **(H)** VSL (straight-line velocity) of sperm; **(I)** Sperm density. Data are presented as means ± SEM (n = 15). $^{*}P < 0.05$, $^{**}P < 0.01$, and $^{***}P < 0.001$. ns, not significant.

significantly inhibited from the dose of 25 μg/mL (equal to 7.81 $\mu g/cm^2$), and the inhibition ratio was about 20% in the dose of 100 μg/mL (equal to 31.25 $\mu g/cm^2$). In live cell staining experiment, the percentage of viable cells was about 80% when exposed to $PM_{2.5}$ (100 μg/mL) for 48 h (**Figures 1B, C**). Besides, the protein level of proliferating cell nuclear antigen (PCNA), a cell proliferation marker decreased markedly after $PM_{2.5}$ treatment for 48 h (**Figure 1D**). In consideration of the numbers and structures of viable cells, the largest dose of 100 μg/mL was adopted in the subsequent experiment.

In the animal study, we examined the sperm quality of mice testes using the whole-body $PM_{2.5}$ exposure mouse model. As shown in **Figure 1E**, exposure to CAP significantly decreased the total motility of sperm compared to the FA group. Likewise, significant changes were also observed in the motility parameters like PR% (progressive (motility), $P<0.05$) and VSL (straight-line velocity, $P<0.05$) (**Figures 1F–H**). However, no obvious change in sperm density was detected between FA and $PM_{2.5}$ groups (**Figure 1I**).

$PM_{2.5}$ Induces Mitochondrial Damage and Dysfunction in GC-2spd and Testes

The cellular ultrastructure was observed after $PM_{2.5}$ treatment for 48 h by using transmission electron microscopy. In the control group (0 μg/mL), the mitochondria were abundant and showed normal shape. The structure of mitochondrial cristae

was also clear and intact. While the ultrastructure of GC-2spd in 100 μg/mL $PM_{2.5}$ group displayed mitochondria swelling, cristae disruption, and even vacuolization (**Figure 2A**). In addition, aggregated $PM_{2.5}$ was found in the autolysosome (**Figure 2A**). Furthermore, the ultrastructure of mice testes showed that the spermatocyte displayed mitochondria swelling and cristae disruption in UA and CAP groups (**Figure 2B**).

Humanin and MOTS-c belong to mitochondrial derived peptide (MDP) which is a polypeptide encoded by short open reading frames in mitochondrial DNA (29). MDP is another type of retrograde signaling molecule with biological activity in response to cellular stress, and can reflect mitochondrial function to some extent (30). The ELISA kit revealed that exposure to $PM_{2.5}$ significantly increased humanin and MOTS-c level in a dose-dependent manner, and both humanin and MOTS-c levels were more than 2 times higher than control in the 100 μg/mL (**Figures 2C, D**). To provide a more comprehensive evaluation of mitochondrial function in GC-2spd, we examined the effects of $PM_{2.5}$ on oxidative phosphorylation and oxygen consumption rate (OCR) of cells using the Seahorse Mito stress test (**Figure 2E**). Compared with the control group (0 μg/mL), $PM_{2.5}$ exposure significantly decreased basal respiration, maximal respiration, spare capacity and proton leak (**Figures 2F–I**). ATP production was also reduced but no significant effect was found (**Figure 2J**).

$PM_{2.5}$ Activates AhR-CYP1A1 Pathway in GC-2spd and Testes

The SRM 1648a $PM_{2.5}$ contains abundant PAHs, and PAHs are well-known activators of the aryl hydrocarbon receptor (AhR) which is a ligand-activated transcription factor. Thus, we assessed the possible implication of AhR in our study. The status of AhR nuclear translocation was firstly examined using Western blotting by separately extracting cytoplasmic and nuclear protein. As shown in **Figure 3A**, the expression of AhR protein was significantly reduced in the cytoplasmic fraction even in a low concentration of $PM_{2.5}$, nevertheless it was obviously increased in the nuclear fraction comparing with the control group (**Figures 3B, C**). These results prompted $PM_{2.5}$-associated PAHs could bind to and activate AhR. CYP1A1, a xenobiotic-metabolizing phase I enzyme, is the target of the AhR. In our study, the *Cyp1a1* mRNA expression was significantly increased, more than 200 times higher than that in the control group (**Figure 3D**). Similarly, CYP1A1 protein expression was remarkably improved in a dose-dependent by $PM_{2.5}$ (about 6-fold increase in 100 μg/mL) (**Figures 3E, F**).

To explore the molecular mechanism by which $PM_{2.5}$ exposure-induced mitochondrial damage, we conducted RNA-sequencing analysis to investigate the changed genes and pathways. A total of 128 differentially expressed genes (DEGs) (31 upregulated DEGs and 97 downregulated DEGs) were identified (fold change >1 and $P<0.05$) in contrast with the control group, and the fold change of these DEGs was visualized by Volcano plot (**Figure 3G**). It was worth noting that *Cyp1a1* was the most significantly changed gene (468-fold increase in 100 μg/mL). To further investigate which signaling pathway was regulated by $PM_{2.5}$ exposure, all changed genes were further assessed *via* gene set enrichment analysis (GSEA). Consistently, GSEA showed that up-regulated genes were significantly enriched in the metabolism of xenobiotics by the cytochrome P450 pathway (**Figure 3H**). The RNA-Seq analysis confirmed that AhR-CYP1A1 pathway played a key role in mitochondrial damage caused by $PM_{2.5}$ exposure. Meanwhile, we examined the expression of CYP1A1 in mice testes. The results found that $PM_{2.5}$ exposure significantly increased the expressions of CYP1A1 in the mRNA and protein levels (**Figures 3I–K**).

$PM_{2.5}$ Induces ROS Production and Activates NRF2 Antioxidative Pathway in GC-2spd and Testes

Several studies indicate that PM and AhR-mediated induction of CYP1A1 lead to excessive production of ROS, which contributes to oxidative stress (16). Therefore, we examined mitochondrial ROS and intracellular ROS in GC-2spd after $PM_{2.5}$ exposure for 48 h using flow cytometry. As shown in **Figures 4A, B**, the mitochondrial ROS was significantly increased with the increase in doses (approximately 2-fold higher in 100 μg/mL) compared to the control group. Similarly, the intracellular ROS generation was also increased in a higher concentration of $PM_{2.5}$. NRF2, as an antioxidative transcription factor, can interact with AhR pathway. It is bound to the KEAP1 in the cytoplasm and activated by stress signals, such as ROS. After dissociation of KEAP1, NRF2 transfers to nuclear and binds to antioxidant response elements (AREs) (31). To know whether $PM_{2.5}$ is capable of activating the NRF2 antioxidative pathway, we next assessed the protein expressions of NRF2 and KEAP1. Western blotting showed the total NRF2 protein was significantly increased accompanied by a decrease in KEAP1 protein expression in GC-2spd (**Figures 4C, D**). Moreover, comparable results were found in mice testes (**Figures 4E, F**). The activation of NRF2 involves the process of cytoplasmic-to-nuclear translocation, thus the NRF2 nuclear translocation was confirmed by separately extracting cytoplasmic and nuclear protein. As shown in **Figures 4G–I**, NRF2 protein expression in the nuclear fraction was significantly increased, while the expression in the cytoplasmic fraction was decreased compared to the control group. These results indicated that exposure to $PM_{2.5}$ could cause ROS formation and activate NRF2 to defense oxidative stress.

$PM_{2.5}$ Inhibits Energy Metabolism and Thus Results in Deficiencies of Amino Acids and Nucleotides in GC-2spd

Energy metabolism is the process by which ATP is generated *via* oxidative phosphorylation in mitochondria (32). We confirmed $PM_{2.5}$ exposure could induce mitochondrial damage and disturb mitochondrial respiration. To further investigate whether $PM_{2.5}$ could affect energy metabolism, metabolomics analysis was conducted to estimate the metabolic variance induced by $PM_{2.5}$ exposure. As shown in **Figures 5A, B**, in the OPLS-DA score plot, the $PM_{2.5}$ exposure group was clearly separated from the control

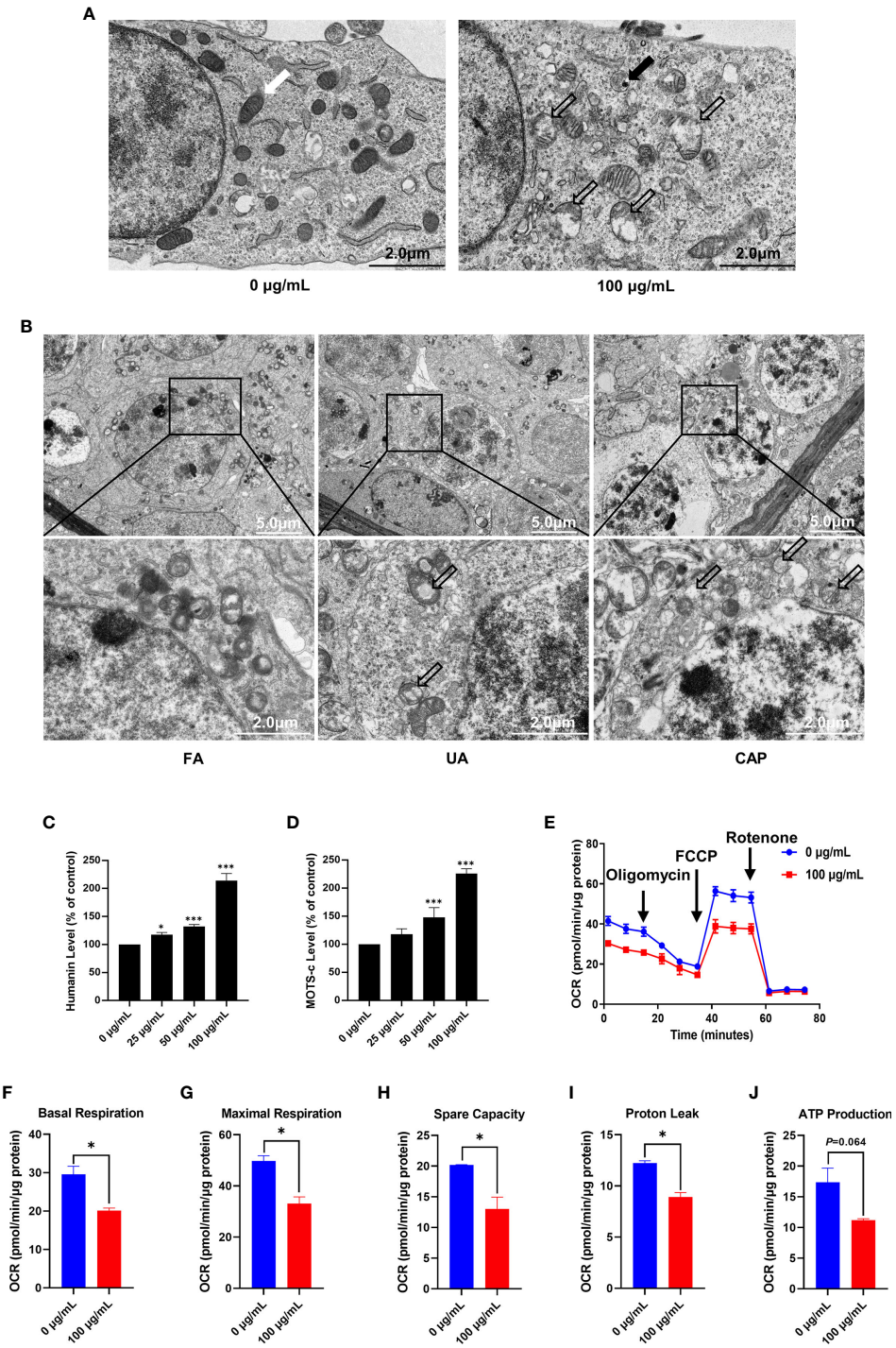

FIGURE 2 | $PM_{2.5}$ induces mitochondrial damage and dysfunction in GC-2spd and testes. **(A)** The ultrastructure of GC-2spd was observed by transmission electron microscopy after treatment with 0 or 100 μg/mL $PM_{2.5}$. The white arrow indicates normal mitochondria; the thick black arrow represents electron-dense $PM_{2.5}$ in the autolysosome; the hollow arrows represent swollen and cavitation of mitochondria. **(B)** The ultrastructure of spermatocyte in mice testes after exposure to $PM_{2.5}$. The hollow arrows represent swollen and cavitation of mitochondria. The humanin **(C)** and MOTS-c **(D)** levels were measured using ELISA kit. **(E)** The oxygen consumption rate (OCR) was measured in GC-2spd using the Seahorse XFp Cell Mito Stress test after injection of the mitochondrial ETC inhibitors oligomycin (an inhibitor of complex V), FCCP (which uncouples the proton gradient), and rotenone (an inhibitor of complex I). The basal respiration **(F)**, maximal respiration **(G)**, spare capacity **(H),** proton leak **(I)** and ATP production **(J)** were evaluated. $^{*}P < 0.05$ and $^{***}P < 0.001$. Values are presented as means ± SD (n = 3).

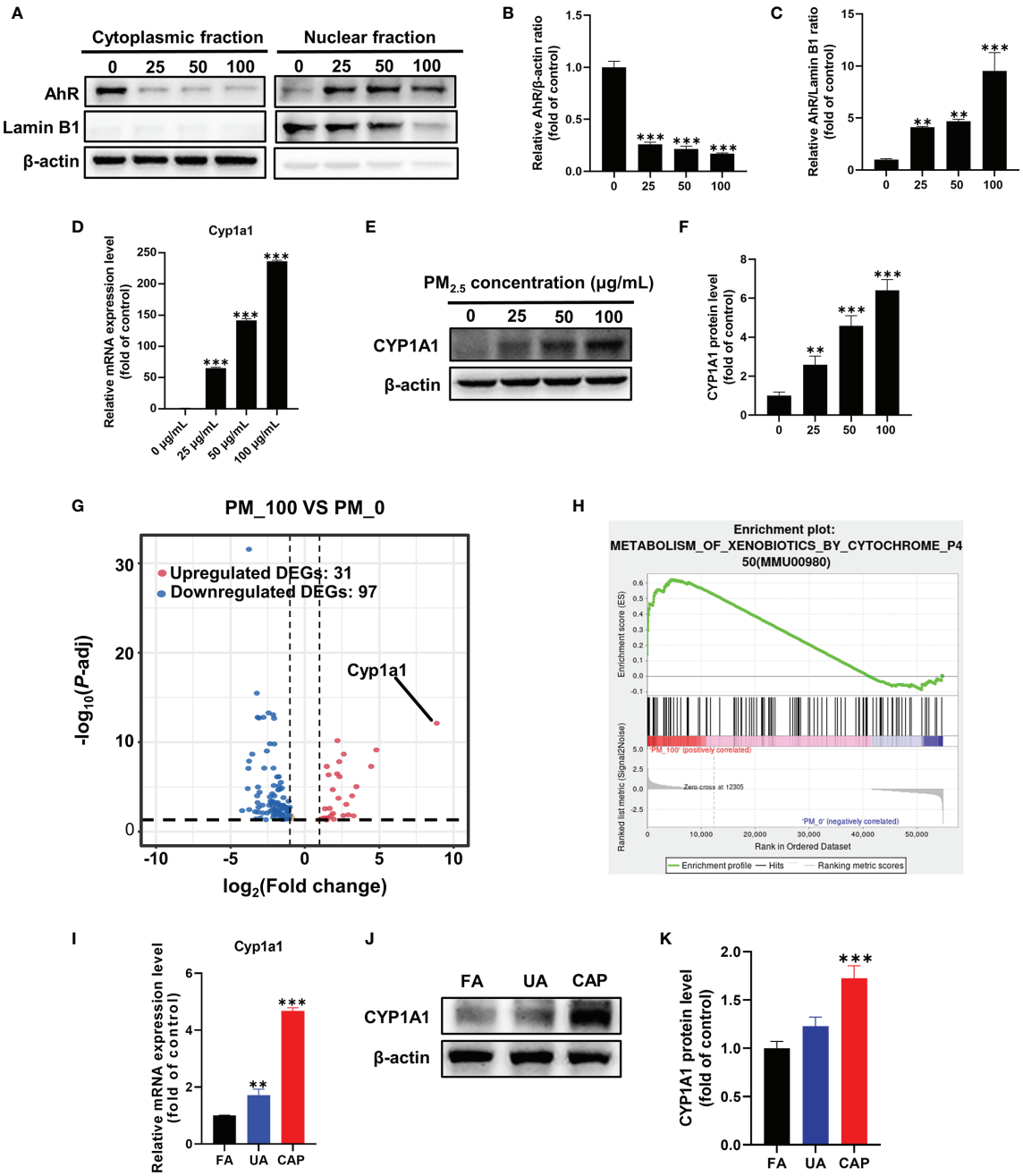

FIGURE 3 | $PM_{2.5}$ activates AhR-CYP1A1 pathway in GC-2spd and testes. GC-2spd cells were treated with $PM_{2.5}$ (0, 25, 50, 100 μg/mL) for 48 h and the cytoplasmic and nuclear fractions were separately extracted. **(A)** The nuclear translocation of AhR was examined by western blot analysis. The bar graphs show the quantifications of the indicated proteins, of which β-actin **(B)** and Lamin B1 **(C)** were used as internal controls of cytoplasmic or nuclear protein, respectively. The mRNA **(D)** and protein **(E)** expressions of CYP1A1 were measured in GC-2spd using qRT-PCR and western blotting, respectively. **(F)** The bar graph shows the quantification of CYP1A1 protein. The Volcano Plot **(G)** and GSEA result **(H)** were represented after transcriptome analysis. The mRNA **(I)** and protein **(J)** expressions of CYP1A1 in testes were measured using qRT-PCR and western blotting, respectively. **(K)** The bar graph shows the quantification of CYP1A1 protein. $^{**}P < 0.01$ and $^{***}P < 0.001$. Values are presented as means ± SD (n = 3).

group in both positive and negative ionization modes. The R^2 and Q^2 were 0.83 and 0.89 in the positive ionization mode, and 0.86 and 0.81 in the negative ionization mode, respectively (**Figures 5C, D**). These results indicated that the OPLS-DA model had good stability and no overfitting phenomenon. Between the control and $PM_{2.5}$ group, 317 and 128 significantly differential metabolites (SDMs) (P<0.05 and VIP>1, one-way ANOVA) were identified in the positive and negative ionization

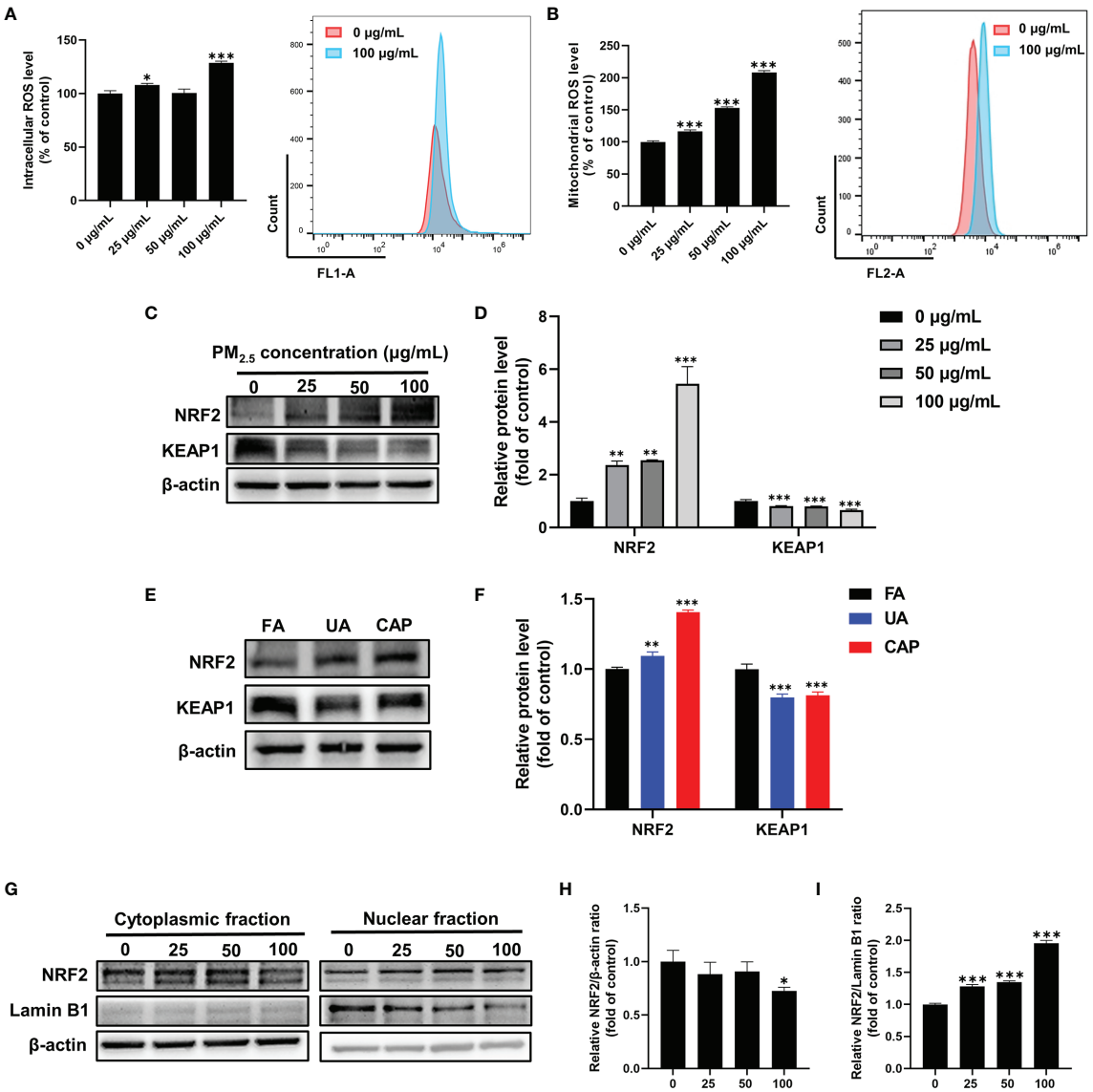

FIGURE 4 | $PM_{2.5}$ induces ROS production and activates NRF2 antioxidative pathway in GC-2spd. GC-2spd cells were treated with $PM_{2.5}$ (0, 25, 50, 100 μg/mL) for 48 h and the intracellular **(A)** and mitochondrial **(B)** ROS were measured by flow cytometry. **(C)** The protein expressions of NRF2 and KEAP1 were measured in GC-2spd by western blot analysis. **(D)** The bar graph shows the quantifications of NRF2 and KEAP1 in GC-2spd. **(E)** The protein expressions of NRF2 and KEAP1 were measured in testes by western blot analysis in mice testes. **(F)** The bar graph shows the quantifications of NRF2 and KEAP1 in mice testes. **(G)** The cytoplasmic and nuclear fractions were separately extracted and the nuclear translocation of NRF2 was examined by western blot analysis. The bar graphs show the quantifications of the indicated proteins, of which β-actin **(H)** and Lamin B1 **(I)** were used as internal controls of cytoplasmic or nuclear protein, respectively. $^{*}P < 0.05$, $^{**}P < 0.01$, and $^{***}P < 0.001$. Values are presented as means ± SD (n = 3).

modes, respectively. In addition, the altered metabolites were mainly involved in purine metabolism, pantothenate and CoA biosynthesis, glycerophospholipid metabolism, ascorbate and aldarate metabolism, pyrimidine metabolism and amino acids metabolism (**Figures 5E, F**).

Results of metabolomic analyses indicated that concentrations of total amino acids (∑amino acids) in GC-2spd exposed to $PM_{2.5}$ were significantly decreased by more than 30% and 15% in the positive and negative ionization modes, respectively (**Figure 6A**). Saccharopine was decreased by almost 70% compared to the control group. In addition, L-Histidine, S-Adenosylmethionine, L-Asparagine, L-Lysine, Citrulline, L-Methionine, L-Phenylalanine, L-Isoleucine, L-Valine were decreased by more than 30% compared to the control group. More detailed information was listed in **Supplemental Table 1**.

Among these significantly decreased amino acids, some of them were involved in central carbon metabolism, especially the citrate cycle (TCA cycle). Furthermore, citrate, succinate and malate in the TCA cycle were significantly decreased by 25%, 30% and 43% in GC-2spd exposed to $PM_{2.5}$, respectively

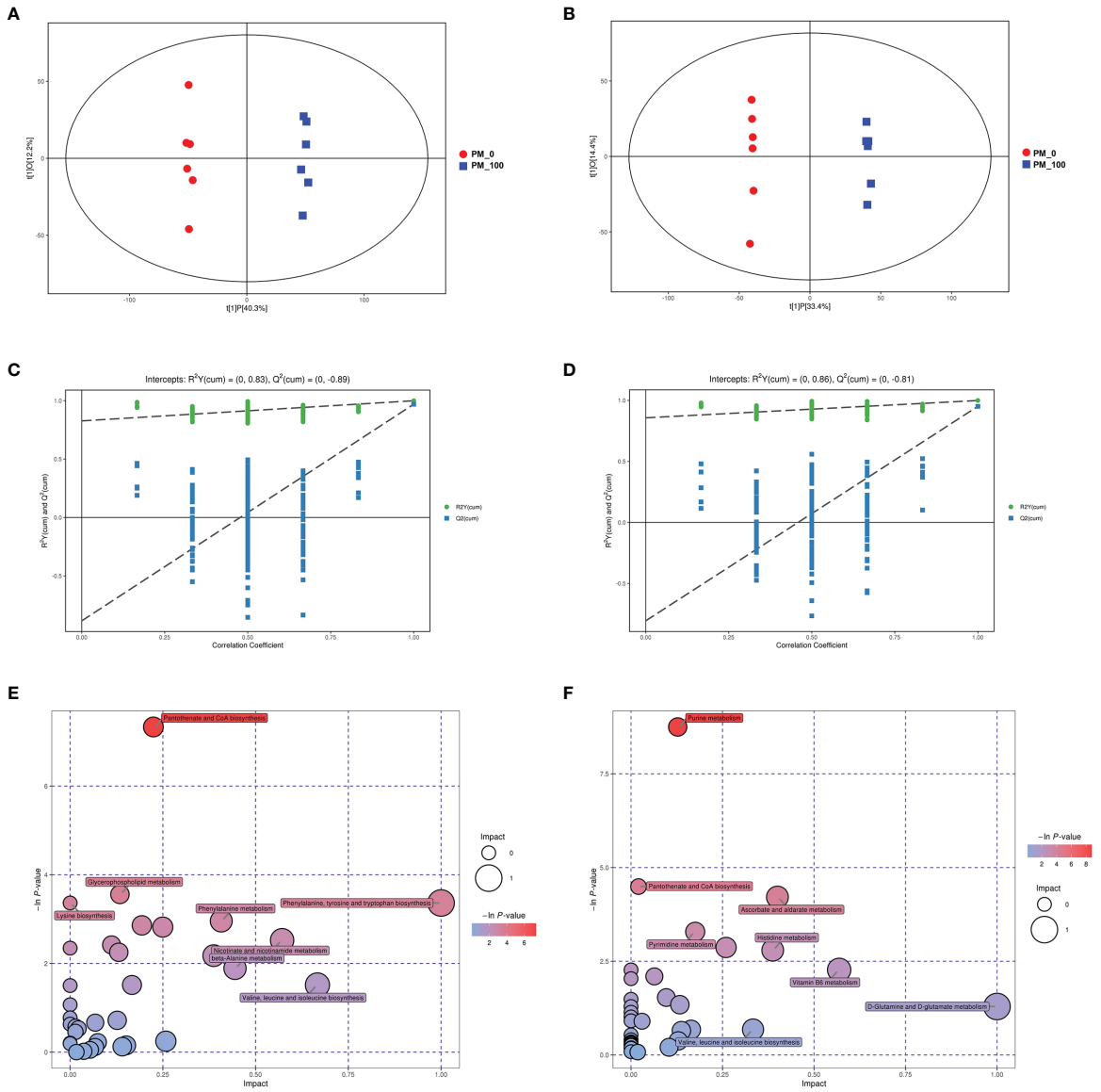

FIGURE 5 | Changes in metabolic profile in GC-2spd after exposure to $PM_{2.5}$ (0, 100 μg/mL) for 48 h. The OPLS–DA model **(A, B)** and permutation test of the OPLS–DA model **(C, D)** were derived from the LC/MS metabolomics profiles. **(E, F)** Analysis of the metabolic pathways of GC-2spd exposed to $PM_{2.5}$ are shown. Each circle represents a metabolic pathway, and the size of the circle indicates the relative impact value. **(A, C, E)** were derived from the positive ionization mode, and **(B, D, F)** were derived from the negative ionization mode.

(**Figures 6B, C**). These results suggested that $PM_{2.5}$ exposure suppressed the central hub of oxidative metabolism, and then affected amino-acids synthesis. Besides, in central carbon metabolism, pyruvate was associated with valine, leucine and isoleucine biosynthesis and glycine, serine and threonine metabolism (**Figure 6C**). Pentose phosphate pathway (PPP) is a way of oxidative decomposition of glucose, which provides variety of raw materials for synthesis and metabolism, like nucleotide synthesis and histidine metabolism (**Figure 6C**). The concentration of glucose 6-phosphate (G6P) had no significant change, however, gluconate, which converted from glucose was involved in PPP and significantly decreased compared to the control group (**Figure 6B**).

Total concentrations of purines (Σpurines) and pyrimidines (Σpyrimidines) were significantly decreased by more than 20% and 29% in GC-2spd exposed to $PM_{2.5}$, respectively (**Figures 7A, B**), which indicated that exposure to $PM_{2.5}$ could disrupt nucleotide synthesis. In purine metabolism, concentrations of dGTP, Guanosine, ADP, deoxyguanosine, deoxyinosine, adenosine and hypoxanthine were significantly decreased by more than 50% compared to the controls (**Supplemental Table 2**). In pyrimidine metabolism, concentrations of thymidine, thymine,

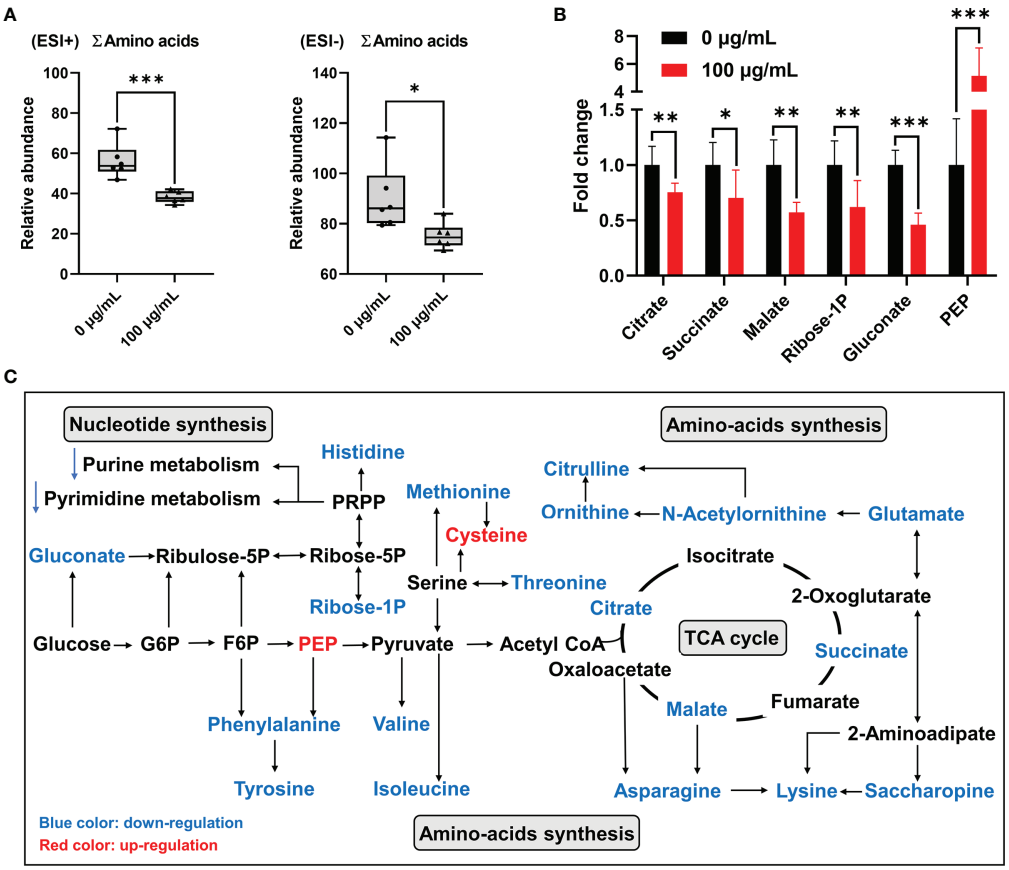

FIGURE 6 | Disorder of energy metabolism and amino acids synthesis in GC-2spd after exposure to $PM_{2.5}$ (0, 100 μg/mL) for 48 h. **(A)** Total concentrations of amino acids (Σamino acids). ESI+ indicates the positive ionization mode, and ESI- indicates the negative ionization mode. **(B)** $PM_{2.5}$-induced changes of the metabolic biomarkers related to central carbon metabolism. **(C)** Most relevant metabolites perturbed by $PM_{2.5}$ in central carbon metabolism and amino acids synthesis. G6P, glucose 6-phosphate; F6P, fructose 6-phosphate; PEP, phosphoenolpyruvate. $^{*}P < 0.05$, $^{**}P < 0.01$, and $^{***}P < 0.001$. Values are presented as means ± SD (n = 6).

deoxycytidine and dCMP were all 50% less than that in GC-2spd exposed to $PM_{2.5}$ (**Supplemental Table 3**). In addition, except for PPP, asparagine and glutamate were involved in purine and pyrimidine metabolism and were significantly decreased by more than 40% and 10% compared to the controls, respectively (**Figure 7C** and **Supplemental Table 1**).

DISCUSSION

In the present study, we found $PM_{2.5}$ induced the reduction of sperm motility and spermatocyte mitochondrial damage using the real time whole-body $PM_{2.5}$ exposure mouse model. To investigate the potential mechanism of male reproductive toxicity, the spermatocyte-derived GC-2spd was treated with $PM_{2.5}$. Our results indicated that $PM_{2.5}$ exposure inhibited GC-2spd cell proliferation and induced mitochondrial damage. Besides, increased Humanin and MOTS-c levels and decreased mitochondrial respiratory indicated that mitochondrial function was disturbed. Nontargeted metabolomics revealed that $PM_{2.5}$ exposure inhibited energy metabolism and thus resulted in the deficiencies of amino acids and nucleotides. On the other hand, The AhR pathway was activated and resulted in an increase in CYP1A1 expression, which was also observed in CAP-exposed mice. The transcriptomics also confirmed that *Cyp1a1* was the most significantly changed gene. Furthermore, exposure to $PM_{2.5}$ promoted ROS generation and activated NRF2 antioxidative pathway. These findings provided new insights into understanding the mechanisms of $PM_{2.5}$-induced male reproductive toxicity.

Sperm motility is one of the most important sperm parameters to evaluate male fertility (33). Our data demonstrated that exposure to CAP significantly reduced sperm motility, which is consistent with previous studies *via* the whole-body PM exposure model (27). Thus, the present study provided more substantial evidence for the reproductive toxicity by exposure to $PM_{2.5}$. Whereas, no significant change in sperm concentration was found in our study. Zhou et al. (27). and Li et al. (34). obtained the same effect when exposed for 8 weeks. But when the exposure time was extended to 4 months, there was a significant reduction

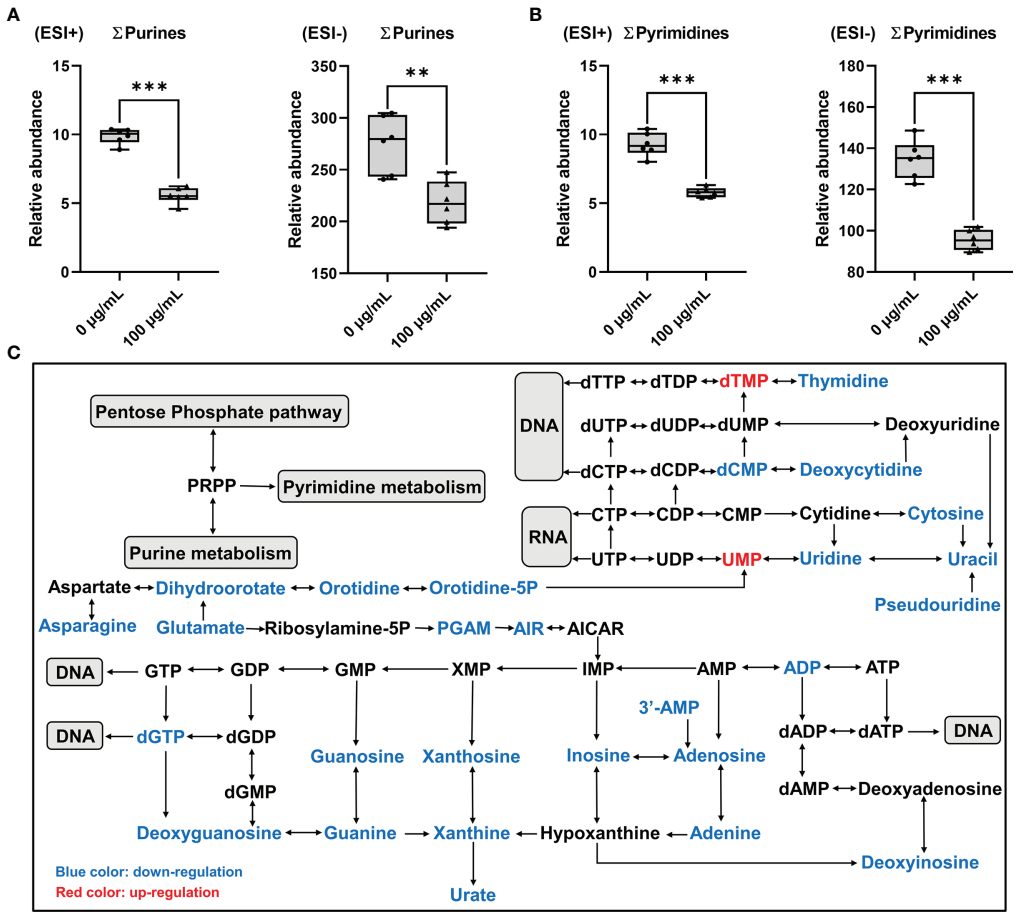

FIGURE 7 | Disorder of nucleotide metabolism in GC-2spd after exposure to $PM_{2.5}$ (0, 100 μg/mL) for 48 h. **(A)** Total concentrations of purines (Σpurines). **(B)** Total concentrations of pyrimidines (Σpyrimidines). ESI+ indicates the positive ionization mode, and ESI- indicates the negative ionization mode. **(C)** Most relevant metabolites perturbed by $PM_{2.5}$ in purine metabolism and pyrimidine metabolism. $^{**}P < 0.01$ and $^{***}P < 0.001$. Values are presented as means ± SD (n = 6).

in sperm concentration (27, 35, 36). Up to now, few researches explored the mechanism of reproductive toxicity reduced by $PM_{2.5}$ applying cell lines *in vitro*. Previous studies indicated that $PM_{2.5}$ could inhibit GC-2spd cell proliferation by ROS caused-DNA damage and induce cell apoptosis by RIPK1 and mitochondrial apoptosis pathways (11, 24). Similarly, our present results demonstrated that exposure to $PM_{2.5}$ could inhibit cell proliferation and lead to mitochondrial damage. What's more, we investigated two possible toxicological mechanisms for the first time including 1) $PM_{2.5}$ exposure might induce energy metabolism disorder by inhibiting mitochondrial respiratory, and thus result in the deficiencies of amino acids and nucleotides; 2) the AhR-CYP1A1 pathway was activated and might cause ROS generation after exposure to $PM_{2.5}$.

Energy metabolism is the process of ATP generation through oxidative phosphorylation and glycolysis. In the present study, exposure to $PM_{2.5}$ reduced the concentrations of succinate, citrate and malate, which indicated inhibition of the TCA cycle. The decreased concentration of succinate and inhibition of the TCA cycle would unavoidably reduce the efficiency of electron transfer to ubiquinone, and thus inhibit energy metabolism from oxidative phosphorylation (32). In mice testes, oxidative phosphorylation occurs in mitochondria, and $PM_{2.5}$ restrained oxidative phosphorylation implies that the mitochondrion is an important target of $PM_{2.5}$. In the present study, the observation of mitochondrial ultrastructure in GC-2spd and mice testes indicated that $PM_{2.5}$ exposure-induced mitochondrial damage. Moreover, we conducted Cell Mito Stress Test, which is a standard assay for measuring mitochondrial function in cells, to evaluate the mitochondrial respiratory. The results showed that a decrease in OCR was found, which was a clear indication of mitochondrial dysfunction. In addition, the reductions of basal respiration, maximal respiration, spare capacity, proton leak and ATP production indicated exposure to $PM_{2.5}$ could induce mitochondrial damage, reduce the capability of the cell to respond to an energetic demand and partly affect the mitochondrial ATP production. These findings supported the evidence of mitochondrial dysfunction and energy metabolism disorder induced by $PM_{2.5}$ exposure. As a result of the inhibition of energy metabolism, the active transport of

nutrients such as amino acids and nucleotides would inevitably be reduced, which might inhibit various biological reactions and ultimately affect cell growth. In our study, the concentrations of Σamino acids, Σpyrimidines and Σpurines were all significantly decreased in GC-2spd exposed to $PM_{2.5}$.

PAHs are well-known agonists of the AhR, a ligand-activated transcription factor in responding to environmental stress *via* regulating the expression of a diverse range of genes, especially monooxygenases cytochrome P450 (CYP) 1A1 and CYP1A2 (16). Previous studies reported that the SRM 1648a $PM_{2.5}$ contained abundant PAHs according to the research report from NIST (26, 37). In the present study, we confirmed that $PM_{2.5}$ exposure could activate AhR in GC-2spd and significantly promote the expression of CYP1A1 in GC-2spd and mice testes. Moreover, the results of RNA-seq analysis provided support to that $PM_{2.5}$-induced spermatocyte damage involved in the activation of AhR-CYP1A1 pathway. In addition, previous studies demonstrated that AhR-dependent production of CYP1A1 was a major source of ROS generation (16, 38). After binding to AhR, PAHs are oxidized by CYPs into epoxides and phenolic intermediates, which are further processed by phase II enzymes. The resulting 3,6-quinone undergoes redox cycles with generation of ROS and leads to oxidative stress (39, 40). Consistently, our data indicated that exposure to $PM_{2.5}$ induced ROS excessive production in GC-2spd and the NRF2 antioxidative pathway was activated in GC-2spd and mice testes. It is well-known that mitochondria are both the major site for ROS generation and the main target organelle of ROS attack. The present study showed that mitochondrial damage occurred both *in vivo* and *in vitro* study after exposure to $PM_{2.5}$. These results prompted that the activation of AhR-CYP1A1 pathway followed by ROS excessive generation might provide an explanation of mitochondrial damage and dysfunction. Additional, previous studies revealed that $PM_{2.5}$-induced ROS generation may induce spermatogenesis dysfunction *via* ROS-mediated MAPK signaling pathway or autophagy (41–43), which prompted that further studies should be performed to explore the potential interaction between AhR and MAPK signaling pathway, as well as autophagy in $PM_{2.5}$-induced reproductive damage.

The present study provided compelling evidence that $PM_{2.5}$ exposure-induced sperm motility decline and spermatocyte damage. Although we only provided preliminary data in this study, it has several advantages: We investigated the reproductive toxicity of $PM_{2.5}$ exposure *in vivo* and *in vitro*. In animal experiment, a whole-body $PM_{2.5}$ exposure mouse model was established to simulate exposure environment of humans in the real world. Furthermore, multiple omics techniques were applied to evaluate comprehensive biological changes in GC-2spd following exposure to $PM_{2.5}$. The nontargeted metabolomics confirmed that $PM_{2.5}$ exposure inhibited energy metabolism and thus resulted in the deficiencies of amino acids and nucleotides. And the results of transcriptomics raised the importance of the role of AhR-CYP1A1 pathway to $PM_{2.5}$-induced reproductive toxicity. However, there are also some limitations in this study: To further confirm agonism of $PM_{2.5}$ to AhR, expression or knockdown experiments should be conducted to make the conclusion more convincing. In addition, $PM_{2.5}$ is a very complex mixture. The substances that pass through the blood-testis barrier and play a role in male reproductive toxicity are mainly metabolites of toxic components. Previous study has shown that different methods of extraction of $PM_{2.5}$ can lead to different toxic effect (44). Thus, the method of $PM_{2.5}$ extraction and component identification should be considered in future study.

CONCLUSIONS

Overall, in the present study, we used GC-2spd cell line and a real time whole-body $PM_{2.5}$ exposure mouse model to examine $PM_{2.5}$-induced male reproductive toxicity *in vitro* and *in vivo*. Our results indicated that $PM_{2.5}$ exposure inhibited spermatocyte cell proliferation and reduced sperm motility. The reproductive toxicity might be partly explained by energy metabolism disorder induced by mitochondrial damage and dysfunction. The mechanism of mitochondrial damage might be through the AhR-CYP1A1 pathway which resulted in ROS production.

DATA AVAILABILITY STATEMENT

The datasets presented in this study can be found in online repositories. The names of the repository/repositories and accession number(s) can be found below: https://www.ncbi.nlm.nih.gov/geo/query/acc.cgi?acc=GSE189187.

ETHICS STATEMENT

The animal study was reviewed and approved by Ethics Council of the Army Medical University.

AUTHOR CONTRIBUTIONS

FS undertook the study, collected the data, analyzed the data, and drafted the manuscript. ZZ, JW, YW, JD, and YZ helped with the undertaking of the animal study. PZ, XL, FH, and JL helped with the analysis of omics data. LA and JC revised the manuscript, were responsible for the experimental design, and supervised the study. All authors contributed to the article and approved the submitted version.

FUNDING

This work was supported by the Key Program of the National Natural Science Foundation of China (No. 81630087), the National Natural Science Foundation of China (No. 82073590) and the National Key Research and Development Program of China (No. 2017YFC1002001).

ACKNOWLEDGMENTS

The authors thank the North China University of Science and Technology for their technical contributions and help in animal experiments.

SUPPLEMENTARY MATERIAL

The Supplementary Material for this article can be found online at: https://www.frontiersin.org/articles/10.3389/fendo.2021.807374/full#supplementary-material

REFERENCES

1. Landrigan PJ, Fuller R, Acosta NJR, Adeyi O, Arnold R, Basu NN, et al. The Lancet Commission on Pollution and Health. *Lancet (Lond Engl)* (2018) 391:462–512. doi: 10.1016/S0140-6736(17)32345-0
2. Huang X, Zhang B, Wu L, Zhou Y, Li Y, Mao X, et al. Association of Exposure to Ambient Fine Particulate Matter Constituents With Semen Quality Among Men Attending a Fertility Center in China. *Environ Sci Technol* (2019) 53:5957–65. doi: 10.1021/acs.est.8b06942
3. Lu F, Xu D, Cheng Y, Dong S, Guo C, Jiang X, et al. Systematic Review and Meta-Analysis of the Adverse Health Effects of Ambient PM2.5 and PM10 Pollution in the Chinese Population. *Environ Res* (2015) 136:196–204. doi: 10.1016/j.envres.2014.06.029
4. Sicard P, Khaniabadi YO, Perez S, Gualtieri M, De Marco A. Effect of O 3, PM 10 and PM 2.5 on Cardiovascular and Respiratory Diseases in Cities of France, Iran and Italy. *Environ Sci Pollut Res Int* (2019) 26:32645–65. doi: 10.1007/S11356-019-06445-8
5. Sram RJ, Veleminsky MJr, Veleminsky MSr, Stejskalová J. The Impact of Air Pollution to Central Nervous System in Children and Adults. *Neuro Endocrinol Lett* (2017) 38:389–96.
6. Wang L, Luo D, Liu X, Zhu J, Wang F, Li B, et al. Effects of PM2.5 Exposure on Reproductive System and its Mechanisms. *Chemosphere* (2021) 264:128436. doi: 10.1016/j.chemosphere.2020.128436
7. Zhang J, Cai Z, Ma C, Xiong J, Li H. Impacts of Outdoor Air Pollution on Human Semen Quality: A Meta-Analysis and Systematic Review. *BioMed Res Int* (2020) 2020:19–22. doi: 10.1155/2020/7528901
8. Guan Q, Chen S, Wang B, Dou X, Lu Y, Liang J, et al. Effects of Particulate Matter Exposure on Semen Quality: A Retrospective Cohort Study. *Ecotoxicol Environ Saf* (2020) 193:110139. doi: 10.1016/j.ecoenv.2020.110319
9. Qiu Y, Yang T, Seyler BC, Wang X, Wang Y, Jiang M, et al. Ambient Air Pollution and Male Fecundity: A Retrospective Analysis of Longitudinal Data From a Chinese Human Sperm Bank (2013–2018). *Environ Res* (2020) 186:109528. doi: 10.1016/j.envres.2020.109528
10. Zhou N, Jiang C, Chen Q, Yang H, Wang X, Zou P, et al. Exposures to Atmospheric PM10 and PM10-2.5 Affect Male Semen Quality: Results of MARHCS Study. *Environ Sci Technol* (2018) 52:1571–81. doi: 10.1021/acs.est.7b05206
11. Liu J, Zhang J, Ren L, Wei J, Zhu Y, Duan J, et al. Fine Particulate Matters Induce Apoptosis *via* the ATM/P53/CDK2 and Mitochondria Apoptosis Pathway Triggered by Oxidative Stress in Rat and GC-2spd Cell. *Ecotoxicol Environ Saf* (2019) 180:280–7. doi: 10.1016/j.ecoenv.2019.05.013
12. Liu J, Ren L, Wei J, Zhang J, Zhu Y, Li X, et al. Fine Particle Matter Disrupts the Blood–Testis Barrier by Activating TGF-β3/P38 MAPK Pathway and Decreasing Testosterone Secretion in Rat. *Environ Toxicol* (2018) 33:711–9. doi: 10.1002/tox.22556
13. Yang W, Xu Y, Pan H, Tian F, Wang Y, Xia M, et al. Chronic Exposure to Diesel Exhaust Particulate Matter Impairs Meiotic Progression During Spermatogenesis in a Mouse Model. *Ecotoxicol Environ Saf* (2020) 202:110881. doi: 10.1016/j.ecoenv.2020.110881
14. Kim KH, Kabir E, Kabir S. A Review on the Human Health Impact of Airborne Particulate Matter. *Environ Int* (2015) 74:136–43. doi: 10.1016/j.envint.2014.10.005
15. Hu C, Hou J, Zhou Y, Sun H, Yin W, Zhang Y, et al. Association of Polycyclic Aromatic Hydrocarbons Exposure With Atherosclerotic Cardiovascular Disease Risk: A Role of Mean Platelet Volume or Club Cell Secretory Protein. *Environ Pollut* (2018) 233:45–53. doi: 10.1016/j.envpol.2017.10.042
16. Vogel CFA, Van Winkle LS, Esser C, Haarmann-Stemmann T. The Aryl Hydrocarbon Receptor as a Target of Environmental Stressors – Implications for Pollution Mediated Stress and Inflammatory Responses. *Redox Biol* (2020) 34:101530. doi: 10.1016/j.redox.2020.101530
17. IARC. IARC Monographs on the Evaluation of Carcinogenic Risks to Humans: Some Non-Heterocyclic Polycyclic Aromatic Hydrocarbons and Some Related Exposures. *IARC Monogr Eval Carcinog Risks Hum* (2010) 93:1–853.
18. Chen Q, Wang F, Yang H, Wang X, Zhang A, Ling X, et al. Exposure to Fine Particulate Matter-Bound Polycyclic Aromatic Hydrocarbons, Male Semen Quality, and Reproductive Hormones: The MARCHS Study. *Environ Pollut* (2021) 280:116883. doi: 10.1016/j.envpol.2021.116883
19. Esakky P, Moley KH. Paternal Smoking and Germ Cell Death: A Mechanistic Link to the Effects of Cigarette Smoke on Spermatogenesis and Possible Long-Term Sequelae in Offspring. *Mol Cell Endocrinol* (2016) 435:85–93. doi: 10.1016/j.mce.2016.07.015
20. Hou L, Zhang X, Dioni L, Barretta F, Dou C, Zheng Y, et al. Inhalable Particulate Matter and Mitochondrial DNA Copy Number in Highly Exposed Individuals in Beijing, China: A Repeated-Measure Study. *Part Fibre Toxicol* (2013) 10:1–9. doi: 10.1186/1743-8977-10-17
21. Li R, Kou X, Geng H, Xie J, Tian J, Cai Z, et al. Mitochondrial Damage: An Important Mechanism of Ambient PM2.5 Exposure-Induced Acute Heart Injury in Rats. *J Hazard Mater* (2015) 287:392–401. doi: 10.1016/j.jhazmat.2015.02.006
22. Zhang G, Wang Z, Ling X, Zou P, Yang H, Chen Q, et al. Mitochondrial Biomarkers Reflect Semen Quality: Results From the MARCHS Study in Chongqing, China. *PLoS One* (2016) 11:e0168823. doi: 10.1371/journal.pone.0168823
23. Stepanov I, Hecht SS. Mitochondrial DNA Adducts in the Lung and Liver of F344 Rats Chronically Treated With 4-(Methylnitrosamino)-1-(3-Pyridyl)-1-Butanone and (S)-4-(Methylnitrosamino)-1-(3-Pyridyl)-1-Butanol. *Chem Res Toxicol* (2009) 22:406–14. doi: 10.1021/tx800398x
24. Zhang J, Liu J, Ren L, Wei J, Duan J, Zhang L, et al. PM2.5 Induces Male Reproductive Toxicity *via* Mitochondrial Dysfunction, DNA Damage and RIPK1 Mediated Apoptotic Signaling Pathway. *Sci Total Environ* (2018) 634:1435–44. doi: 10.1016/j.scitotenv.2018.03.383
25. Vertika S, Singh KK, Rajender S. Mitochondria, Spermatogenesis, and Male Infertility – An Update. *Mitochondrion* (2020) 54:26–40. doi: 10.1016/j.mito.2020.06.003
26. Wang Y, Tang M. PM2.5 Induces Ferroptosis in Human Endothelial Cells Through Iron Overload and Redox Imbalance. *Environ Pollut* (2019) 254:112937. doi: 10.1016/j.envpol.2019.07.105
27. Zhou L, Su X, Li B, Chu C, Sun H, Zhang N, et al. PM2.5 Exposure Impairs Sperm Quality Through Testicular Damage Dependent on NALP3 Inflammasome and miR-183/96/182 Cluster Targeting FOXO1 in Mouse. *Ecotoxicol Environ Saf* (2019) 169:551–63. doi: 10.1016/j.ecoenv.2018.10.108
28. Xu Y, Wang W, Zhou J, Chen M, Huang X, Zhu Y, et al. Metabolomics Analysis of a Mouse Model for Chronic Exposure to Ambient PM2.5. *Environ Pollut* (2019) 247:953–63. doi: 10.1016/j.envpol.2019.01.118
29. Kim SJ, Xiao J, Wan J, Cohen P, Yen K. Mitochondrially Derived Peptides as Novel Regulators of Metabolism. *J Physiol* (2017) 595:6613–21. doi: 10.1113/JP274472
30. Sreekumar PG, Ishikawa K, Spee C, Mehta HH, Wan J, Yen K, et al. The Mitochondrial-Derived Peptide Humanin Protects RPE Cells From Oxidative Stress, Senescence, and Mitochondrial Dysfunction. *Investig Ophthalmol Vis Sci* (2016) 57:1238–53. doi: 10.1167/iovs.15-17053
31. Tu W, Wang H, Li S, Liu Q, Sha H. The Anti-Inflammatory and Anti-Oxidant Mechanisms of the Keap1/Nrf2/ARE Signaling Pathway in Chronic Diseases. *Aging Dis* (2019) 10:637–51. doi: 10.14336/AD.2018.0513
32. Geng N, Ren X, Gong Y, Zhang H, Wang F, Xing L, et al. Integration of Metabolomics and Transcriptomics Reveals Short-Chain Chlorinated

Paraffin-Induced Hepatotoxicity in Male Sprague-Dawley Rat. *Environ Int* (2019) 133:105231. doi: 10.1016/j.envint.2019.105231
33. Lu JC, Huang YF, Lü NQ. Computer-Aided Sperm Analysis: Past, Present and Future. *Andrologia* (2014) 46:329–38. doi: 10.1111/and.12093
34. Li D, Zhang R, Cui L, Chu C, Zhang H, Sun H, et al. Multiple Organ Injury in Male C57BL/6J Mice Exposed to Ambient Particulate Matter in a Real-Ambient PM Exposure System in Shijiazhuang, China. *Environ Pollut* (2019) 248:874–87. doi: 10.1016/j.envpol.2019.02.097
35. Qiu L, Chen M, Wang X, Qin X, Chen S, Qian Y, et al. Exposure to Concentrated Ambient PM2.5 Compromises Spermatogenesis in a Mouse Model: Role of Suppression of Hypothalamus-Pituitary-Gonads Axis. *Toxicol Sci* (2018) 162:318–26. doi: 10.1093/TOXSCI/KFX261
36. Yang Y, Yang T, Liu S, Cao Z, Zhao Y, Su X, et al. Concentrated Ambient PM2.5 Exposure Affects Mice Sperm Quality and Testosterone Biosynthesis. *PeerJ* (2019) 2019:1–14. doi: 10.7717/peerj.8109
37. Wang Y, Wu T, Tang M. Ambient Particulate Matter Triggers Dysfunction of Subcellular Structures and Endothelial Cell Apoptosis Through Disruption of Redox Equilibrium and Calcium Homeostasis. *J Hazard Mater* (2020) 394:122439. doi: 10.1016/j.jhazmat.2020.122439
38. Knerr S, Schaefer J, Both S, Mally A, Dekant W, Schrenk D. 2,3,7,8-Tetrachlorodibenzo-P-Dioxin Induced Cytochrome P450s Alter the Formation of Reactive Oxygen Species in Liver Cells. *Mol Nutr Food Res* (2006) 50:378–84. doi: 10.1002/mnfr.200500183
39. Tanaka Y, Ito T, Tsuji G, Furue M. Baicalein Inhibits Benzo[a]Pyrene-Induced Toxic Response by Downregulating Src Phosphorylation and by Upregulating Nrf2-Hmox1 System. *Antioxidants* (2020) 9:1–20. doi: 10.3390/antiox9060507
40. Köhle C, Bock KW. Coordinate Regulation of Phase I and II Xenobiotic Metabolisms by the Ah Receptor and Nrf2. *Biochem Pharmacol* (2007) 73:1853–62. doi: 10.1016/j.bcp.2007.01.009
41. Liu B, De Wu S, Shen LJ, Zhao TX, Wei Y, Tang XL, et al. Spermatogenesis Dysfunction Induced by PM2.5 From Automobile Exhaust *via* the ROS-Mediated MAPK Signaling Pathway. *Ecotoxicol Environ Saf* (2019) 167:161–8. doi: 10.1016/j.ecoenv.2018.09.118
42. Wei Y, Cao XN, Tang XL, Shen LJ, Lin T, He DW, et al. Urban Fine Particulate Matter (PM2.5) Exposure Destroys Blood–Testis Barrier (BTB) Integrity Through Excessive ROS-Mediated Autophagy. *Toxicol Mech Methods* (2018) 28:302–19. doi: 10.1080/15376516.2017.1410743
43. Liu B, Shen LJ, Zhao TX, Sun M, Wang JK, Long CL, et al. Automobile Exhaust-Derived PM2.5 Induces Blood-Testis Barrier Damage Through ROS-MAPK-Nrf2 Pathway in Sertoli Cells of Rats. *Ecotoxicol Environ Saf* (2020) 189:110053. doi: 10.1016/j.ecoenv.2019.110053
44. Pardo M, Xu F, Shemesh M, Qiu X, Barak Y, Zhu T, et al. Nrf2 Protects Against Diverse PM 2.5 Components-Induced Mitochondrial Oxidative Damage in Lung Cells. *Sci Total Environ* (2019) 669:303–13. doi: 10.1016/j.scitotenv.2019.01.436

Conflict of Interest: The authors declare that the research was conducted in the absence of any commercial or financial relationships that could be construed as a potential conflict of interest.

Publisher's Note: All claims expressed in this article are solely those of the authors and do not necessarily represent those of their affiliated organizations, or those of the publisher, the editors and the reviewers. Any product that may be evaluated in this article, or claim that may be made by its manufacturer, is not guaranteed or endorsed by the publisher.

frontiers in Endocrinology

ORIGINAL RESEARCH
published: 03 January 2022
doi: 10.3389/fendo.2021.751915

Effects of Titanium Dioxide Nanoparticles on Porcine Prepubertal Sertoli Cells: An "*In Vitro*" Study

Francesca Mancuso[1†], Iva Arato[1†], Alessandro Di Michele[2†], Cinzia Antognelli[1,3], Luca Angelini[1], Catia Bellucci[1], Cinzia Lilli[1], Simona Boncompagni[4], Aurora Fusella[4], Desirée Bartolini[5], Carla Russo[5], Massimo Moretti[5], Morena Nocchetti[5], Angela Gambelunghe[1], Giacomo Muzi[1], Tiziano Baroni[1,3], Stefano Giovagnoli[5‡] and Giovanni Luca[1,3,6‡]*

[1] Department of Medicine and Surgery, University of Perugia, Perugia, Italy, [2] Department of Physics and Geology, University of Perugia, Perugia, Italy, [3] International Biotechnological Center for Endocrine, Metabolic and Embryo-Reproductive Translational Research (CIRTEMER), Department of Medicine and Surgery, University of Perugia, Perugia, Italy, [4] Center for Advanced Studies and Technology (CAST) and Department of Neuroscience, Imaging and Clinical Sciences (DNICS), University G. d'Annunzio (Ud'A) of Chieti-Pescara, Chieti, Italy, [5] Department of Pharmaceutical Sciences, University of Perugia, Perugia, Italy, [6] Division of Medical Andrology and Endocrinology of Reproduction, Saint Mary Hospital, Terni, Italy

OPEN ACCESS

Edited by:
Rossella Cannarella,
University of Catania, Italy

Reviewed by:
Anna Cariboni,
University of Milan, Italy
Roland Eghoghosoa Akhigbe
Ladoke Akintola University of Technology Nigeria
Eva Zatecka,
Institute of Biotechnology (ASCR), Czechia

***Correspondence:**
Francesca Mancuso
francesca.mancuso@unipg.it

[†]These authors have contributed equally to this work and share first authorship

[‡]These authors have contributed equally to this work and share last authorship

Specialty section:
This article was submitted to Reproduction, a section of the journal Frontiers in Endocrinology

Received: 02 August 2021
Accepted: 30 November 2021
Published: 03 January 2022

Citation:
Mancuso F, Arato I, Di Michele A, Antognelli C, Angelini L, Bellucci C, Lilli C, Boncompagni S, Fusella A, Bartolini D, Russo C, Moretti M, Nocchetti M, Gambelunghe A, Muzi G, Baroni T, Giovagnoli S and Luca G (2022) Effects of Titanium Dioxide Nanoparticles on Porcine Prepubertal Sertoli Cells: An "In Vitro" Study. Front. Endocrinol. 12:751915. doi: 10.3389/fendo.2021.751915

The increasing use of nanomaterials in a variety of industrial, commercial, medical products, and their environmental spreading has raised concerns regarding their potential toxicity on human health. Titanium dioxide nanoparticles (TiO_2 NPs) represent one of the most commonly used nanoparticles. Emerging evidence suggested that exposure to TiO_2 NPs induced reproductive toxicity in male animals. In this *in vitro* study, porcine prepubertal Sertoli cells (SCs) have undergone acute (24 h) and chronic (from 1 up to 3 weeks) exposures at both subtoxic (5 μg/ml) and toxic (100 μg/ml) doses of TiO_2 NPs. After performing synthesis and characterization of nanoparticles, we focused on SCs morphological/ultrastructural analysis, apoptosis, and functionality (AMH, inhibin B), ROS production and oxidative DNA damage, gene expression of antioxidant enzymes, proinflammatory/immunomodulatory cytokines, and MAPK kinase signaling pathway. We found that 5 μg/ml TiO_2 NPs did not induce substantial morphological changes overtime, but ultrastructural alterations appeared at the third week. Conversely, SCs exposed to 100 μg/ml TiO_2 NPs throughout the whole experiment showed morphological and ultrastructural modifications. TiO_2 NPs exposure, at each concentration, induced the activation of caspase-3 at the first and second week. AMH and inhibin B gene expression significantly decreased up to the third week at both concentrations of nanoparticles. The toxic dose of TiO_2 NPs induced a marked increase of intracellular ROS and DNA damage at all exposure times. At both concentrations, the increased gene expression of antioxidant enzymes such as SOD and HO-1 was observed whereas, at the toxic dose, a clear proinflammatory stress was evaluated along with the steady increase in the gene expression of IL-1α and IL-6. At both concentrations, an increased phosphorylation ratio of p-ERK1/2 was observed up to the second week followed by

the increased phosphorylation ratio of p-NF-kB in the chronic exposure. Although *in vitro*, this pilot study highlights the adverse effects even of subtoxic dose of TiO_2 NPs on porcine prepubertal SCs functionality and viability and, more importantly, set the basis for further *in vivo* studies, especially in chronic exposure at subtoxic dose of TiO_2 NPs, a condition closer to the human exposure to this nanoagent.

Keywords: ROS, comet, antioxidant enzymes, proinflammatory pathways, Sertoli cells, titanium dioxide nanoparticles

1 INTRODUCTION

The use of nanoparticles (NPs) has steadily increased over the past decade, due to their unique physical and chemical properties (1, 2) and has raised growing concern about their possible effects on human health (3). Given the small size and biocompatibility, NPs are potentially able to enter the body through different routes, such as inhalation, ingestion, skin uptake, injection, or implantation and interfere with several cellular physiological processes (4, 5). In particular, chronic exposure to NPs is associated with different disorders in animals, including pulmonary injury, hepatotoxicity, neurotoxicity, renal toxicity, and irreversible testis damage (6–12). TiO_2 NPs are among the top 5 NPs used in consumer products. In fact, they are added to cosmetics, chewing gum, beverage, sauces, printing ink, paper, sunscreens, car materials, and decomposing organic matters in water purification (13–15). It has been shown that TiO_2 NPs can be accumulated in the kidney (0.418 μg/g tissue), liver (5.78 μg/g tissue), lung (4.02 μg/g tissue), spleen (19.16 μg/g tissue), brain (145 ng/g tissue), and reproductive organs in animal models (75 ng/g tissue) (16–19).

A number of *in vivo* studies in mice or rats demonstrated that TiO_2 NPs are able to cross blood–testis barrier and accumulate in the testis resulting in the reduction of sperm numbers and motility, increased sperm morphological abnormalities, and germ cell apoptosis with histopathological changes in the testis and marked decrease in serum testosterone, LH, and FSH levels (20–24). Komatsu et al. (25) demonstrated that TiO_2 NPs affected the viability, proliferation, and gene expressions of mouse Leydig TM3 cells, the testosterone-producing cells of the testis. However, the molecular mechanisms of the observed impaired spermatogenesis nowadays are still discussed (26).

SCs play a critical role in the testis, providing the structural and metabolic supports for nourishing and developing germ cells by secreting many essential factors. Hence, any chemical agent that decreases the viability and the function of SCs may produce adverse effects on spermatogenesis and male infertility.

The very few studies describing the detrimental effect of TiO_2 NPs on SCs have been performed in mice and rat models under acute exposures (26–28). However, these experimental conditions may greatly differ from those under which human exposure can potentially occur and often result in conflicting data that are not applicable for risk assessment studies (29). Hence, to realistically mimic long-term exposure for toxicity testing, we here assessed the effect of TiO_2 NPs either under a subtoxic (5 μg/ml) or toxic dose (100 μg/ml) in an acute (24 h) and chronic exposure (up to 3 weeks), on an *in vitro* model of porcine prepubertal SCs, an experimental animal model sharing significant physiological similarity with humans. The concentrations were chosen according to 3-(4,5-dimethylthiazol-2-yl)-2,5-diphenyl-2H-tetrazolium bromide (MTT) results in our preliminary cytotoxicity tests as reported in the **Supplementary Material** and on the basis of literature data (26, 27).

Light microscopy and transmission electron microscopy (TEM) analysis revealed that TiO_2 NPs caused significant morphological and ultrastructural alterations at the toxic dose but, at subtoxic dose, ultrastructural alterations appeared at the third week.

The evaluation of caspase-3, as crucial mediator of apoptosis, showed at each concentration of NPs, an increase at the first and second week, with the cleavage of p35 into the p19 kDa active fragment.

TiO_2 NPs exposure negatively affected SCs functionality at both concentrations of NPs and induced reactive oxygen species (ROS) production and DNA oxidative damage at the toxic dose.

At both concentrations, an increased gene expression of antioxidant enzymes such as superoxide dismutase (SOD), heme oxygenase (HO-1) was observed, whereas, at the toxic dose, an evident proinflammatory condition was found, together with the steady increase in the gene expression of interleukin-1α (IL-1α) and interleukin 6 (IL-6). TiO_2 NPs treatment activated mitogen-activated protein kinase (MAPK) and nuclear factor kappa-light-chain-enhancer of activated B cell (NF-kB) signaling pathway.

Although *in vitro*, this pilot study highlights the adverse effects even of subtoxic dose of TiO_2 NPs on porcine SCs functionality and viability and, more importantly, set the basis for further *in vivo* studies, especially in chronic exposure at subtoxic dose of TiO_2 NPs, a condition closer to the human exposure to this nanoagent.

2 MATERIALS AND METHODS

2.1 TiO_2 NPs Synthesis and Characterization

The synthesis of the NPs was performed by sonochemical method using acoustic cavitation (30) at the Laboratory of Acoustic Cavitation of the Department of Physics and Geology of the University of Perugia. The ultrasound generator used was a

"Horn Type" working at 20 kHz and 750 W, using a 13-mm titanium probe (Sonics & Materials, Newtown, CT, USA). In particular, anatase phase of TiO_2 NPs was prepared dissolving 85 ml titanium (IV) butoxyde, (Sigma-Aldrich Co., St. Louis, MO, USA) in 200 ml of pure ethanol (Sigma-Aldrich Co., St. Louis, MO, USA), successively 200 ml of water (Sigma-Aldrich Co., St. Louis, MO, USA) were added dropwise under ultrasound irradiation for 90 min at 50% of amplitude. The obtained precipitate was centrifuged and calcinated at 400°C for 3 h. Chemical-structural characterization of the synthesized NPs was performed by X-ray diffraction (XRD) and electron scanning spectroscopy (SEM). XRD was evaluated at room temperature with the diffractometer Philips X'Pert PRO MPD (Malvern Panalytical Ltd., Royston, UK) operating at 40 kW/40 mA with step size of 0.017° and a step scan of 70 s, using a Cu Kα radiation and X-Celerator detector. SEM analysis was performed using a LEO 1525 Field Emission Scanning Electron Microscope, ZEISS (Jena, Germany). Size distribution of nanoparticle dispersion was performed by dynamic light scattering (DLS) using a Nicomp 380 ZLS spectrometer sorgent 35 mW He–Ne laser at 654 nm and Avalanche PhotoDiode (APD) detector (PSS NICOMP; Santa Barbara, CA, USA), Briefly, starting from a concentration of 1 mg/ml of TiO_2 NPs dissolved in endotoxin free water (Sigma-Aldrich, St. Louis, MO, USA) to obtain a stock dispersion and sonicated for 30 min to limit the formation of nanoaggregates, dilutions of 10 μg/ml were immediately prepared in different media in order to identify the best experimental conditions for NPs application and more precisely both in SCs culture medium, i.e., Hamster Ovary cells F-12 (HAMF-12), (Euroclone, Milan, Italy), supplemented with 0.166 nM retinoic acid (Sigma-Aldrich Co., St. Louis, MO, USA), 5 ml/500 ml of insulin-transferrin-selenium (ITS), (cat. no. 354352, BD Biosciences, Franklin Lakes, NJ, USA) and, based on literature data (31), Dulbecco's modified Eagle's medium (DMEM) (Euroclone, Milan, Italy) supplemented with 0.166 nM retinoic acid (Sigma-Aldrich, St. Louis, MO), 5 ml/500 ml ITS (cat. no. 354352, BD Biosciences, Franklin Lakes, NJ, USA), and 2 mg/ml bovine serum albumin (BSA) (Sigma-Aldrich Co., St. Louis, MO, USA).

2.2 SCs Isolation and Characterization

Animal studies were conducted in agreement with the guidelines adopted by the Italian Approved Animal Welfare Assurance (A-3143-01) and the European Communities Council Directive of November 24, 1986 (86/609/EEC). The experimental protocols were approved by the University of Perugia. Danish Duroc prepupertal pigs (15 to 20 days old) underwent bilateral orchidectomy after general anesthesia with ketamine (Ketavet 100; Intervet, Milan, Italy), at a dose of 40 mg/kg, and dexmedetomidine (Dexdomitor, Orion Corporation, Finland), at a dose of 40 g/kg (32), and were used as SC donors. Specifically, pure porcine prepupertal SCs were isolated and characterized, according to previously established methods (33, 34), as reported in the **Supplementary Material**.

2.3 Experimental Protocol

NPs working solutions, at a concentration of 5 and 100 μg/ml according to MTT analysis in the **Supplementary Material**, were prepared, administered to SCs for 24 h (acute exposure) and 1, 2, and 3 weeks (chronic exposure) where medium changes were performed every 72 h. The control group was the unexposed SCs (0 TiO_2 NPs μg/ml). Samples to perform all necessary analyses were collected at each experimental point.

2.4 TiO_2 NPs Uptake by SCs

Cellular uptake of TiO_2 NPs at 5 and 100 μg/ml was detected with different qualitative and quantitative techniques such as TEM and inductively coupled plasma-optical emission spectrometry (ICP-OES), respectively.

2.4.1 TEM

Briefly, TiO_2 NP-treated SCs were fixed with 4% glutaraldehyde in 0.1 M sodium cacodylate (NaCaCO) buffer for 30 min and stored at 4°C. Cells were postfixed in 2% osmium tetroxide (OsO_4) for 2 h and block stained in saturated uranyl acetate. After dehydration, specimens were embedded in epoxy resin (Epon 812), (Sigma-Aldrich Co., St. Louis, MO, USA). Ultrathin sections were cut using a Leica Ultracut R microtome (Leica Microsystem, Austria) with a Diatome knife (Diatome Ltd. CH-2501, Biel, Switzerland) and double stained with uranyl acetate replacement and lead citrate. Sections were viewed and photographed in a Morgagni Series 268D electron microscope (FEI Company, Brno, Czech Republic) equipped with a Megaview III digital camera and Analy-SIS software (Olympus Soft Imaging Solutions).

2.4.2 ICP-OES

TiO_2 NP-treated SCs were detached by trypsin/ethylenediaminetetraacetic acid (EDTA) (Lonza, Verviers, Belgium) at 37°C for 8 min, to promote the enzymatic reaction. After washing with 1 ml Hank's balanced salt solution (HBSS) (Sigma-Aldrich Co., St. Louis, MO, USA), samples were centrifuged at 150×*g* for 6 min, the supernatant was removed, the pellets were freeze-dried, and accurately weighed. Samples were dissolved by treatment with 10 ml of a mixture of sulfuric acid (H_2SO_4), (97% Sigma-Aldrich Co., St. Louis, MO, USA)/nitric acid (HNO_3 70%), (Sigma-Aldrich Co., St. Louis, MO, USA) (2:1). After solubilization, the obtained solutions were diluted with the EDTA solution (1:10) prior Ti^{4+} content determination using a Varian 700-Es series spectrometer (Agilent, Milan, Italy) in triplicate. Calibration was performed diluting a Ti^{4+} standard solution obtaining titanium solutions in the 1–15-μg/ml range. The Ti^{4+} content was expressed per unit weight of freeze-dried TiO_2 NP-treated SCs and % of the total amount added and the error expressed as SEM.

2.5 ROS Detection

Intracellular ROS were measured by treating unexposed and exposed SCs with 50 μM dichlorofluorescein diacetate (DCFH-DA) (Sigma-Aldrich Co., St. Louis, MO, USA) solution in Dulbecco's phosphate-buffered saline (D-PBS) (Sigma-Aldrich Co., St. Louis, MO, USA) at 37°C for 30 min. Fluorescence was read by using a plate reader (DTX 880 Multimode Detector, Beckman Coulter). Data were normalized for cell viability (MTT

assay) and expressed as the percentage of unexposed SCs. The sensitivity of the test was confirmed by adding 30 μM hydrogen peroxide (H_2O_2) (30 min) on unexposed SCs as positive control.

2.6 Oxidative DNA Damage Quantification by Single-Cell Microgel (Comet) Assay

To evaluate the oxidative DNA damage, unexposed and exposed SCs were processed in the comet assay under alkaline conditions (alkaline unwinding/alkaline electrophoresis, pH >13), basically following the original procedure (35). A positive control consisted in treating SCs with 1 μM 4-nitroquinoline N-oxide (4NQO) (Sigma-Aldrich, Milan, Italy) for 1 h at 37°C (36). At the end of treatments, the cells were washed twice with 5 ml ice-cold D-PBS (Sigma-Aldrich, St. Louis, MO, USA), pH 7.4, and detached with 300 μl of 0.05% trypsin (Invitrogen, Milan, Italy) in 0.02% Na_4EDTA (Invitrogen, Milan, Italy). After 3 min, trypsinization was stopped by adding 700 μl fetal bovine serum (FBS), (Sigma-Aldrich, St. Louis, MO, USA). Cells were then collected by centrifugation (70×*g*, 8 min, 4°C). Briefly, cell pellets were gently resuspended in 300 μl of 0.7% low-melting point agarose (Sigma-Aldrich, St. Louis, MO, USA) (in Ca^{2+}/Mg^{2+}-free D-PBS, w/v) at 37°C, layered onto a conventional microscope slide precoated with 1% normal-melting point agarose (in Ca^{2+}/Mg^{2+}-free D-PBS, w/v), and covered with a coverslip (Knittel-Glaser, Braunschweig, Germany). After brief agarose solidification at 4°C, the coverslip was removed and the slides were immersed in cold, freshly prepared lysing solution (2.5 M sodium chloride (NaCl), 100 mM Na_4EDTA, (Invitrogen, Milan, Italy); 10 mM tris (hydroxymethyl)aminomethane-hydrochloric acid (Tris-HCl) and sodium hydroxide (NaOH), pH 10, and 1% Triton X-100, (Sigma-Aldrich, Milan, Italy), added just before use, for at least 60 min at 4°C. The slides were then placed in a horizontal electrophoresis box (HU20, Scie-Plas, Cambridge, UK) filled with a freshly prepared solution (10 mM Na_4EDTA, 300 mM NaOH; pH 13, (Sigma-Aldrich, Milan, Italy). Prior to electrophoresis, the slides were left in the alkaline buffer for 20 min to allow DNA unwinding and expression of alkali-labile damage. Electrophoresis runs were then performed in an ice bath for 20 min by applying an electric field of 34 V (1 V/cm) and adjusting the current to 300 mA (Power Supply PS250, Hybaid, Chesterfield, MO, USA). The microgels were then neutralized with 0.4 M Tris-HCl buffer (pH 7.5), fixed 10 min in ethanol (10 min, Carlo Erba Reagenti, Milan, Italy), allowed to air-dry and stored in slide boxes at room temperature until analysis.

All the steps of the comet assay were conducted in yellow light to prevent the occurrence of additional DNA damage. Immediately before scoring, the air-dried slides were stained with 65 μl of ethidium bromide (EB), (Sigma-Aldrich, St. Louis, MO, USA) 20 mg/ml and covered with a coverslip. The comets in each microgel were analyzed (blind), at ×500magnification with an epi-fluorescent microscope (BX41, Olympus, Tokyo, Japan), equipped with a high sensitivity black and white charge-coupled device (CCD) camera (PE2020, Pulnix, UK), under a 100-W high-pressure mercury lamp (HSH-1030-L, Ushio, Japan), using appropriate optical filters (excitation filter 510–550 nm and emission filter 590 nm). Images were elaborated by Comet Assay III software (Perceptive Instruments, UK). A total of 100 randomly selected comets (50 cells/replicate slides) were evaluated for each experimental point.

2.7 RNA Isolation, Reverse Transcription, and Real-Time Reverse Transcriptase-Polymerase Chain Reaction Analyses

Total RNA was isolated with Tri-reagent (Sigma-Aldrich Co., St. Louis, MO, USA) and quantified by reading the optical density at 260 nm. Subsequently, 2.5 μg of total RNA was subjected to reverse transcription (RT Thermo Scientific, Waltham, MA, USA) in a final volume of 20 μl. Real-time reverse transcriptase-polymerase chain reaction (RT-PCR) was performed using 25 ng of the cDNA and SYBR Green master mix (Stratagene, Amsterdam, the Netherlands), as previously described (37).

Gene expression vs. β-actin was evaluated by RT-PCR on a MX3000P Real-Time PCR System (Agilent Technology, Milan, Italy). The sequences of the oligonucleotide primers are listed in **Table 1**. The thermal cycling conditions were 1 cycle at 95°C for 5 min, followed by 45 cycles at 95°C for 20 s and 58°C for 30 s. The data required for carrying out a comparative analysis of gene expression were obtained by means of the 2-(DDCT) method.

TABLE 1 | Primer sequences for PCR analyses.

Gene	Forward	Reverse
β-Actin	ATGGTGGGTATGGGTCAGAA	CTTCTCCATGTCGTCCCAGT
AMH	GCGAACTTAGCGTGGACCTG	CTTGGCAGTTGTTGGCTTGATATG
Inhibin B	TGGCTGGATGTCGTCCCAGT	CCGTGTGGAAGGATGAGG
SOD1	TCGGGAGACCATTCCATCAT	ACCTCTGCCCAAGTCATCT
HO-1	CTGGTGATGGCGTCCTTGTA	TTGTTGTGCTCAATCTCCTCCT
GHSPx	CGAGAAGTGTGAGGTGAATGG	GCGGAGGAAGGCGAAGAG
LDH A	GCACCCTGAATTAGGCACTGATG	ATAAGCACTGTCCACCACCTGTT
IL-1α	GCAAGTTCCTGTGACTCTAAGAAT	TTTGGATGGGCGGCTGAAT
IL-6	AATGCTCTTCACCTCTCC	TCACACTTCTCATACTTCTCA
TGF-β1	GCCCTGGACACCAACTATTGC	GCTGCACTTGCAGGAGCGCAC
IDO	ATGAAGGCGTTTGGGACACC	GAGGAATCCAGCAGCAGAGC

AMH, anti-Müllerian hormone, SOD1, superoxide dismutase 1, HO-1, heme-oxygenase 1; GHSPx, gluthatione peroxidase; LDH-A, lactate deidrogenase A; IL-1α, interleukin-1α; IL-6, interleukin-6; TGF-β1, transforming growth factor β1; IDO, indoleamine 2,3-dioxygenase.

2.8 Elisa Assay

Aliquots of the culture media from all the experimental groups were collected, stored at −20°C for the assessment of AMH (AMH Gen II ELISA, Beckman Coulter; intraassay CV = 3.89%; interassay CV = 5.77%) and inhibin B (inhibin B Gen II ELISA, Beckman Coulter, Webster, TX, USA; intraassay CV = 2.81%; interassay CV = 4.33%) secretion as previously described (34).

2.9 Protein Extraction and Western Blot Analysis

Total protein extracts were prepared by lysing the cells in 100 µl of radioimmunoprecipitation assay lysis buffer (RIPA buffer), (Santa Cruz Biotechnology Inc., Santa Cruz, CA, USA) as previously described (38).

After centrifuging the mixture at 1,000×*g* (Eppendorf, NY, USA) for 10 min, the supernatant was collected, and total protein content was determined by the Bradford method (39). Sample aliquots were stored at −20°C for WB analysis. The cell extracts were separated by 4%–12% sodium dodecyl sulfate-polyacrylamide gel electrophoresis (SDS-PAGE), and equal amounts of protein (70 µg protein/lane) were run and then blotted on nitrocellulose membranes (Bio-Rad, Hercules, CA, USA). The membranes were incubated overnight in a buffer containing 10 mM TRIS (Sigma-Aldrich Co., St. Louis, MO, USA), 0.5 M NaCl (Sigma-Aldrich Co., St. Louis, MO, USA), 1% (v/v) Tween 20 (Sigma-Aldrich Co., St. Louis, MO, USA), rabbit antiextracellular signal-regulated kinases 1–2 (ERK1–2) (1:2000; Millipore, Burlington, MA, USA), mouse antiphospho-ERK1-2 (1:100; Millipore, Burlington, MA, USA), rabbit anti-c-Jun N-terminal kinases (JNK) (1:1000; Millipore, Burlington, MA, USA), rabbit antiphospho-JNK (1:500; Millipore, Burlington, MA, USA), rabbit antiposphop38 (1:2000; Millipore, Burlington, MA, USA), mouse anti-p38 (1:2000; Millipore, Burlington, MA, USA), antiserine/threonine protein kinase (Akt) (1:100; Cell Signaling, Danvers, MA, USA), rabbit antiphospho-Akt (1:1000; Cell Signaling, Danvers, MA, USA), rabbit antiphospho-NF-kB p65 antibody (1:1000; AbCam, Cambridge, UK), rabbit anti-NF-kB p65 antibody (1:1000; AbCam, Cambridge, UK), rabbit anticaspase 3 antibody (1:1000; Cell Signaling, Danvers, MA, USA), and mouse anti-GAPDH (1:5000; Sigma-Aldrich Co., St. Louis, MO, USA) primary antibodies.

Primary antibody binding was then detected by incubating membranes for an additional 60 min in a buffer containing horseradish peroxidase conjugated antirabbit (1:5000; Sigma-Aldrich Co., St. Louis, MO, USA) and/or antimouse (1:5000; Santa Cruz Biotechnology Inc.) IgG secondary antibodies. The bands were detected by enhanced chemiluminescence and acquired by ChemiDoc imaging System (Bio-Rad, Hercules, CA, USA).

2.10 Statistical Analysis

Normality analysis was performed by Shapiro-Wilk test, and statistical comparisons were analyzed using one-way ANOVA followed by Tukey's HSD *post-hoc* test (SigmaStat 4.0 software, Systat Software Inc., CA, USA). Values were reported as the means ± SEM of three independent experiments, each performed in triplicate. Differences were considered statistically significant at $^{*}p < 0.05$ and $^{**}p < 0.001$ compared with unexposed SCs and $^{\#}p < 005$ with respect to 5 µg/ml of TiO_2 NPs.

3 RESULTS

3.1 Characterization and Size Distribution of TiO_2 NPs

XRD analysis, as a methodology used to determine the structure of inorganic compounds, confirmed the synthesis of TiO_2 NPs. In fact, the resulting diffractogram was characteristic of titanium dioxide crystals in anatase form (JCPDS 00-001-0562) (**Figure 1A**). https://doi.org/10.5061/dryad.7d7wm37wf.

SEM evaluation, through a nondestructive technique, allowed to perform morphological and measurement investigation of TiO_2 NP surfaces. A representative SEM image of TiO_2 NPs in dry form is showed in **Figure 1B**, and the mean size distribution reports values of 20 ± 5 nm diameter, calculated by measuring over 100 particles in random fields of view. Results showed that TiO_2 NPs tended to form aggregates of submicrometric dimensions.

DLS analysis, being able to measure the hydrodynamic diameter of NPs dispersed in a liquid, confirmed some aggregation of TiO_2 NPs in suspension. The mean hydrodynamic diameter of TiO_2 NPs mainly distributed in a range of 100–300 nm (**Figure 1C**). Additional information on NP suspension setups can be found in **Supplementary Material**.

3.2 Light Microscopy Analysis Revealed That TiO_2 NPs Caused Significant Morphological Alterations at the Toxic Dose

Light microscopy analysis was used to monitor over the course of the experiment any morphological changes in the SCs treated with the two TiO_2 NP concentrations with respect to the unexposed monolayer (**Figures 2A, D, G, J**). Morphological analysis revealed that SCs treated with 5 µg/ml TiO_2 NPs did not undergo substantial changes compared with the untreated monolayer at all times of exposure. In fact, cells exposed to TiO_2 NPs maintained the typical squamous shape of epithelial cells with vacuoles containing lipid hormones, well evident and abundantly distributed in the cell surface (**Figures 2B, E, H, K**). Conversely, SCs treated with 100 µg/ml TiO_2 NPs showed an evident reduction either of the cell number that constituted the monolayer (**Figure 2C**; **Supplementary Figure 2S**) and changes in the morphology of the remaining cells that showed a spindle-like shape, with very elongated cytoplasmic protrusions, typical of a cellular stress-associated condition by the end of the first week (**Figure 2F**) that progressively increased until the end of the third week (**Figures 2I, L**).

3.3 Qualitative (TEM) and Quantitative Analyses (ICP-OES) Confirmed the Uptake of TiO_2 NPs by SCs

TEM has been used both to verify the uptake of NPs and to assess any ultrastructural changes in SCs as a result of this interaction.

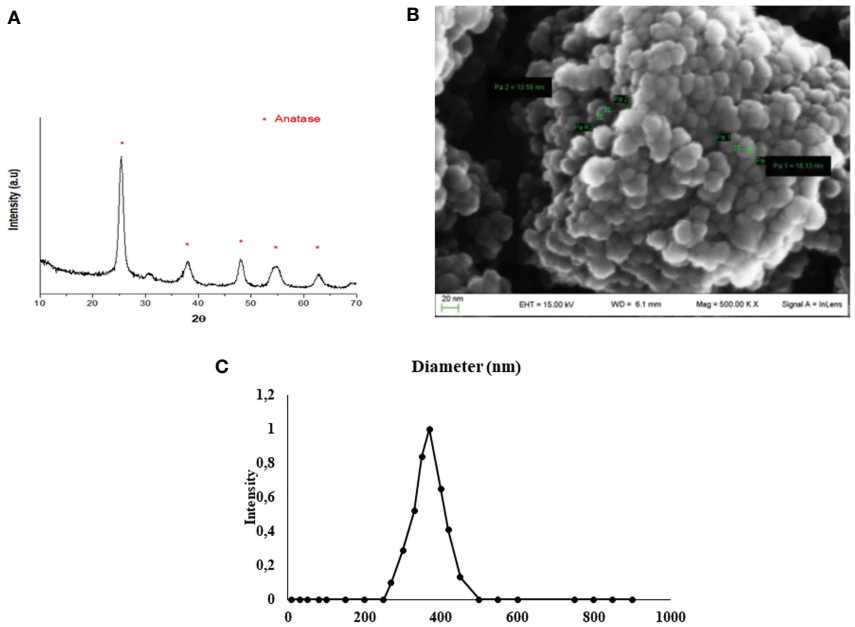

FIGURE 1 | TiO_2 NPs characterization. **(A)** XRD analysis: diffractogram confirmed the correct synthesis of TiO_2 NPs (JCPDS 00-001-0562) and * represents the peaks of TiO_2 NPs in anatase form. **(B)** SEM analysis: the mean size distribution of TiO_2 NPs in dry form was 20 ± 5 nm; image confirmed that TiO_2 NPs tend to form aggregates of submicrometric dimensions. **(C)** DLS analysis: mean hydrodynamic diameter of TiO_2 NPs at 10 μg/ml in culture medium.

TEM analysis of unexposed SCs outlined a typical architecture characterized by oval/elongated spindle-shaped morphology containing a quite large nucleus surrounded by abundant mitochondria and numerous aggregates of stacks of parallel and flat cisternae of endoplasmic reticulum membranes (**Figures 3A–C**). Although we did not notice substantial and/or severe ultrastructural alterations in SCs treated with 5 μg/ml TiO_2 NPs for 1 and 2 weeks (**Figures 3D, E**), in all the other exposure conditions (5 μg/ml for 3 weeks and 100 μg/ml for 1, 2, and 3 weeks), (**Figures 3F, I**) SCs showed several ultrastructural changes. Specifically, we noted a high percentage of severely damaged SCs, presenting different features of cell stress such as deeply invaginated and shrunk nuclei (**Figure 3G**), disorder/marginalization of chromatin components (**Figures 3G, I**), swollen very fragmented, or almost completely missing endoplasmic reticulum membranes (**Figures 3E, H**). In addition, mitochondrial morphology was severely affected (**Figure 3F**) and mitochondria number dramatically decreased. Finally, we noted the presence of several large vacuoles (**Figures 3H, I**) probably as a result of apoptotic mitochondria and/or enlarged endoplasmic reticulum and/or increased frequency of lipid droplets, https://doi.org/10.5061/dryad.7d7wm37wf.

ICP-OES was used to quantify the uptake of NPs expressed as the percentage of internalized NPs and the amount of metal adsorbed per cell number (expressed as ng/10^5), at each concentration, after 5 h of treatment (**Figure 4**). At the lowest concentration of 5 μg/ml, a 3% higher uptake rate was detected than at the 100-μg/ml concentration (1.3%) (**Figure 4**, dotted line). In contrast, the amount absorbed in ng/10^5 cells was greater at the highest concentration (28.6 ± 15.01 vs. 3.46 ± 1.3, **Figure 4**, black bars). This difference is likely attributable to gradual saturation of the particles within the cells with a progressive slowing of uptake as the concentration of NPs increases.

3.4 TiO_2 NPs Exposure Induced Apoptosis in SCs

We assessed, by Western blotting analysis, the involvement of caspase-3 pathway that is partially or totally responsible for the proteolytic cleavage of many key proteins, such as the nuclear enzyme poly (ADP-ribose) polymerase (PARP) (40). Activation of caspase-3 requires proteolytic processing of its inactive zymogen (p35) into activated p19 and p17 fragments (40).

We demonstrated that NPs exposure, at each concentration, induced the activation of caspase-3 at the first and second week, with the cleavage of p35 into the p19 kDa active fragment, to decrease at the third week, most likely due to the progress toward the final degradation phase of apoptosis (41).

Only at the toxic dose, we observed a statistical increase of active p19 with respect to the inactive p35 fragments, expression of a more prominent apoptotic process, as highlighted by TEM analysis (**Figures 5A, B**, $^{\#}p < 0.05$, $^{\#\#}p < 0.001$ vs. p35).

3.5 Effects of TiO_2 NPs on Intracellular ROS Production and DNA Damage

We evaluated the intracellular production of ROS and oxidative DNA damage, as the most important mechanisms activated by nanomaterial.

As shown in **Figure 6A**, the dose of 5 μg/ml TiO_2 NPs did not affect ROS intracellular level at 24 h and 1 week postexposure. On the contrary, at 2 and 3 weeks posttreatment, ROS level

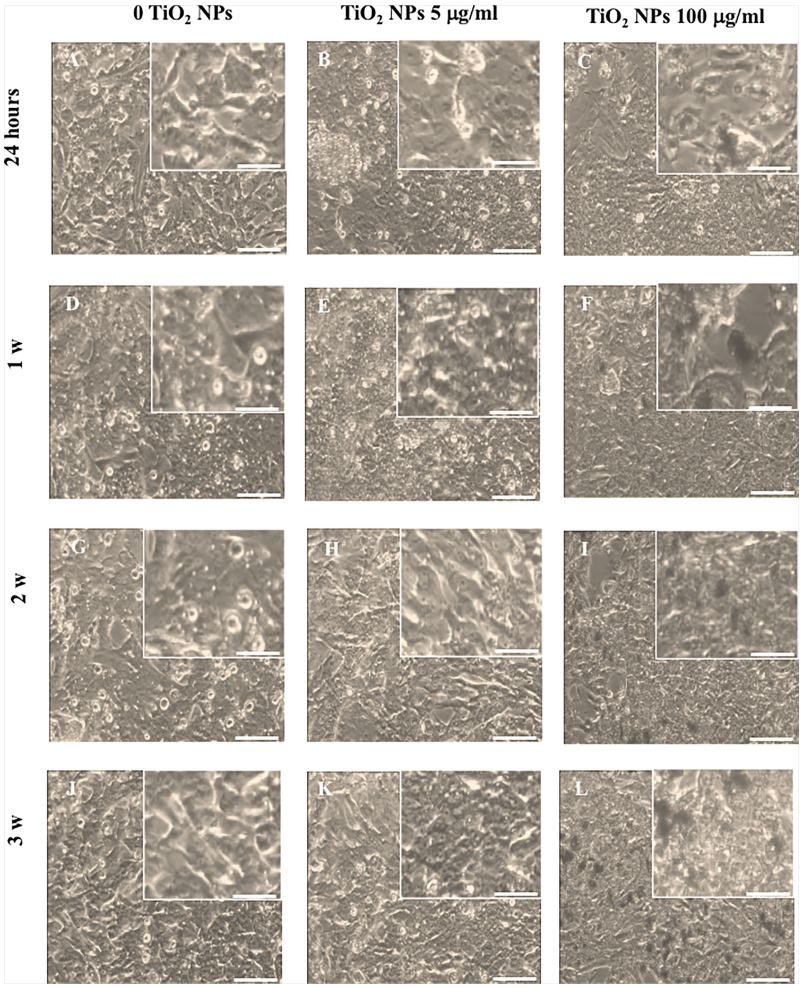

FIGURE 2 | Morphological characterization. Light microscope of unexposed (0 TiO_2 NPs) SCs **(A, D, G, J)**, TiO_2 NPs 5 **(B, E, H, K)**, and 100 µg/ml **(C, F, I, L)** exposed SCs at 24 h **(A–C)** and 1 **(D–F)**, 2 **(G–I)**, and 3 weeks **(L–N)**. The inserts show in detail the morphological characteristics of the respective images. The scale bar corresponds to 200 µm for **(A–N)** and 60 µm for the corresponding insets. The images are representative of three separate experiments.

significantly decreased with respect to unexposed SCs (set as 100 in the graphs and represented as a black dotted line, **Figure 6A**, $^{*}p < 0.05$). Conversely, 100 µg/ml TiO_2 NPs induced a significant increase of intracellular ROS amounts at the second and third week posttreatment with respect to unexposed SCs (set as 100 in the graphs and represented as a black dotted line, **Figure 6A**, $^{*}p < 0.05$ and $^{**}p < 0.001$) accompanied by a significant increase at the third week compared with 5 µg/ml of TiO_2 NPs, expression of oxidative stress onset with increasing concentration (**Figure 6A**, $^{\#}p < 0.05$ vs. 5 µg/ml of TiO_2 NPs). As expected, H_2O_2 (positive control) induced a significant increase in ROS intracellular levels (data not shown).

The levels of oxidative DNA damage induced by TiO_2 NPs were measured as the % of DNA in tail by the alkaline comet assay over time, after acute (24 h) and chronic exposures (from 1 to 3 weeks) to 5 and 100 µg/ml of TiO_2 NPs. At the dose of 5 µg/ml, the oxidative DNA damage was detected after 24 h of acute exposure (**Figure 6B**, $^{*}p < 0.05$). The follow-up study carried out after 1 and 3 weeks of chronic exposure exhibited an increase that however did not result in a significant difference compared with unexposed SCs (**Figure 6B**). Instead, the dose of 100 µg/ml induced a significant increase over time and until the end of treatment with respect to the unexposed SCs and from the second week compared with 5 µg/ml of TiO_2 NPs, as demonstrated by the increased oxidative DNA damage with increasing concentration (**Figure 6B**, $^{\#\#}p < 0.001$ vs. 5 µg/ml of TiO_2 NPs).

3.6 TiO_2 NPs Exposure Negatively Affected SCs Functionality

The effects of TiO_2 NPs exposure on SCs functional competence were studied through the evaluation of AMH and inhibin B gene expression and protein secretion, specific and important markers of SCs functionality.

Exposure of SCs toTiO_2 NPs induced a significant increase in AMH and inhibin B gene expression at 24 h followed by a

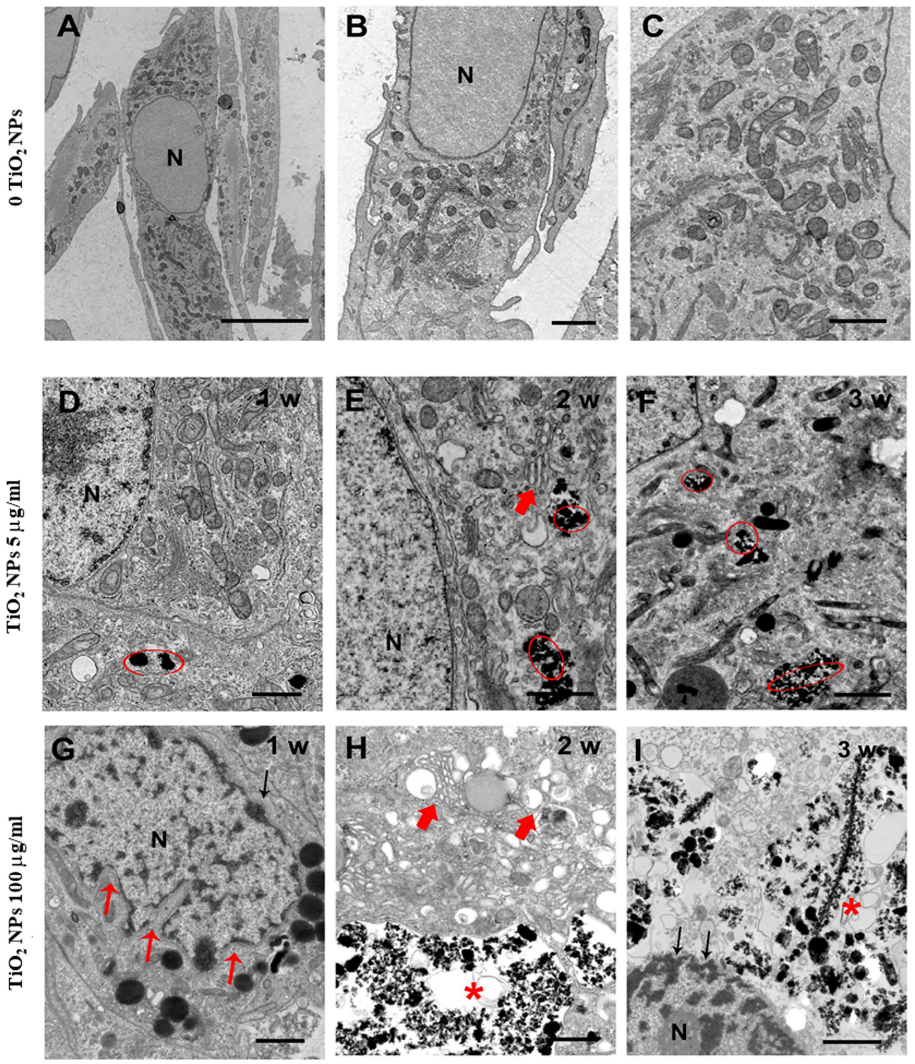

FIGURE 3 | Representative TEM images of unexposed SCs **(A–C)** and after treatment with TiO_2 NPs at 5 and 100 µg/ml for 1, 2, and 3 weeks of exposure **(D–I)**. **(A–C)** Elongated oval or spindle-shaped SCs containing quite large nuclei (N) and abundant mitochondria [better visible at higher magnification in **(C)**]. **(D–I)** SCs after treatment with TiO_2 NPs at 5 µg/ml **(D–F)** and 100 µg/ml/L **(G–I)** for 1, 2, and 3 weeks of exposure (chronic). Red circles and asterisks indicate TiO_2 NPs deposition. Small red arrows indicate nuclear membrane invaginations. Large red arrows indicate enlarged endoplasmic reticulum. Black arrows in **(I)** point to chromatin marginalization. The scale bar corresponds to 5 µm for **(A)**, 2 µm for the **(B)**, and 1 µm for **(C–I)**.

significant decrease after 1 week up to the third week, at both concentrations with respect to unexposed SCs (**Figures 7A, B**, $^{*}p < 0.05$ and $^{**}p < 0.001$ vs. unexposed SCs, set as 1 in the graphs and represented as a black dotted line). AMH secretion was significantly and steadily decreased at 24 h throughout the duration of the experiment, whereas inhibin secretion showed a significant decrease starting from the first week onwards (**Figures 7C, D**, $^{*}p < 0.05$ and $^{**}p < 0.001$ vs. unexposed SCs).

3.7 TiO_2 NPs Exposure Activated an Antioxidant Response and Damaged the Membrane Integrity

To investigate the role and effectiveness of phase II detoxification enzymes against ROS production, we evaluated SOD, glutathione peroxidase (GHSPx), and HO-1 gene expression. In addition, we studied lactate dehydrogenase-A (LDH-A) gene expression as a well-established and reliable indicator of cellular toxicity and plasma membrane damage.

The gene expression of SOD1 and HO-1 increased throughout the treatment at both TiO_2 NP concentrations (**Figures 8A, B**, $^{*}p < 0.05$, $^{**}p < 0.001$ vs. unexposed SCs, set as 1 in the graphs and represented as a black dotted line). The gene expression of GHSPx increased at the toxic dose of 100 µg/ml after the first and second week of exposure to undergo a significant reduction at the third week of the treatment (**Figure 8C**, $^{*}p < 0.05$ and $^{**}p < 0.001$ vs. unexposed SCs, set as 1 in the graphs and represented as a black dotted line). In particular, only at the second week, the dose of 100 µg/ml of TiO_2

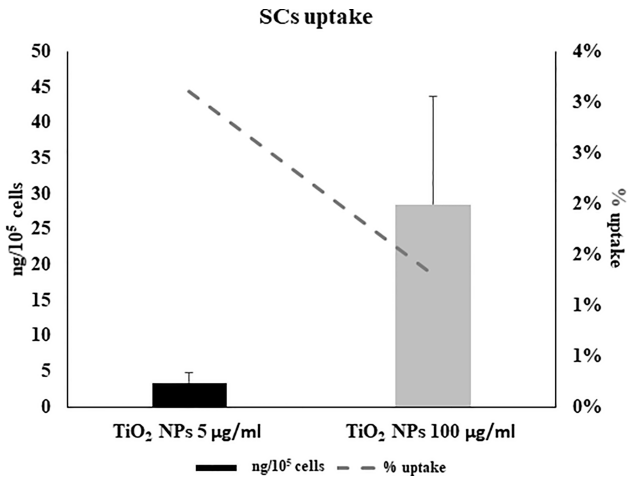

FIGURE 4 | Cellular uptake by inductively coupled plasma-optical emission spectrometry (ICP-OES). Percentage of internalized nanoparticles (dotted grey line) and amount of metal adsorbed per cell number (expressed as ng/10^5) in SCs 5 h of incubation with TiO_2 NPs 5 (black bar) and 100 µg/ml (grey bar) evaluated by ICP-OES analysis. Data represented as mean ± SEM of three independent experiments, each are performed in triplicate.

NPs showed a significant increase of HO-1 and GHSPx gene expression with respect to the dose of 5 µg/ml of TiO_2 NPs (**Figures 8B, C**, $^{\#}p < 0.05$ vs. 5 µg/ml of TiO_2 NPs).

A significant increase in LDH-A mRNA expression was observed at 100 µg/ml of TiO_2 NPs throughout the whole experiment with respect to the unexposed SCs. In addition, a significant increase was observed from the second week even when compared with the dose of 5 µg/ml of TiO_2 NPs (**Figure 8D**, $^{*}p < 0.05$ and $^{**}p < 0.001$ vs. unexposed SCs, set as 1 in the graphs and represented as a black dotted line; $^{\#}p < 0.05$ vs. 5 µg/ml of TiO_2 NPs).

3.8 TiO_2 NPs Exposure Stimulated Proinflammatory and Immunomodulatory Responses

To assess if TiO_2 NPs treatment could activate an inflammatory response, we evaluated the gene expression either of proinflammatory cytokines, such as, IL-1α, IL-6, and typical immunomodulatory factors expressed by SCs as transforming growth factor-β (TGF-β) and indoleamine 2,3-dioxygenase (IDO) (42).

The gene expression of IL-1α and IL-6 showed a significant increase at the first and second week of treatment with the subtoxic dose meanwhile at the toxic dose increased starting from the first week postexposure up to the end of the experiment (**Figures 9A, B**, $^{*}p < 0.05$, $^{**}p < 0.001$ vs. unexposed SCs, set as 1 in the graphs and represented as a black dotted line). Moreover, IL-1α gene expression showed a significant increase compared with the dose of 5 µg/ml of TiO_2 NPs only at the third week. IL-6 gene expression, at the highest dose, showed a statistical significant increase from the first week throughout the whole experiment with respect to the lowest dose as expression of an enhanced inflammatory state was probably linked to the increasing TiO_2 NP concentrations (**Figures 9A, B**, $^{\#}p < 0.05$ vs. 5 µg/ml of TiO_2 NPs).

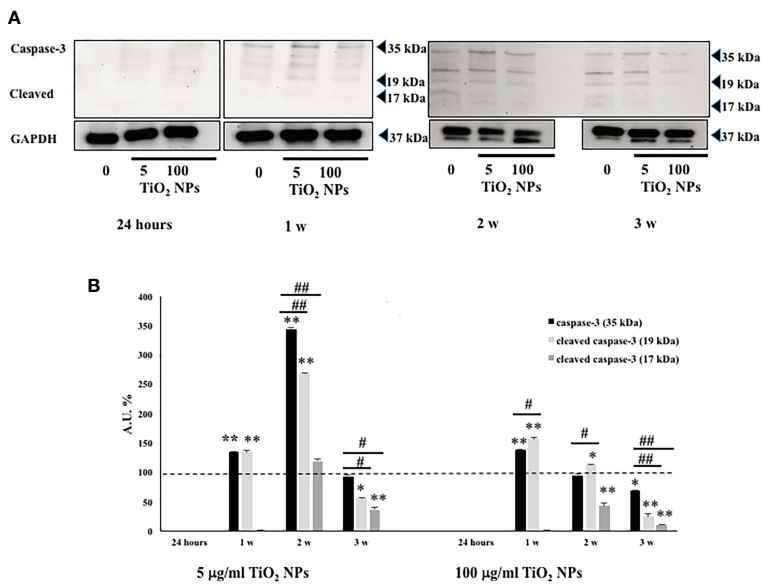

FIGURE 5 | WB analysis. **(A)** Immunoblots of caspase-3 p35, p19, and p17 in SCs at 24 h and 1, 2, and 3 weeks of incubation with TiO_2 NPs at 5 and 100 µg/ml. **(B)** Densitometric analysis of the protein bands of caspase-3 p35 (black bar), p19 (light grey bar), and p17 (dark grey bar) in SCs at 24 h and 1, 2, and 3 weeks of incubation with TiO_2 NPs 5 and 100 µg/ml. Data represent the mean ± SEM ($^{*}p < 0.05$,$^{**}p < 0.001$ vs. unexposed SCs (black dotted line) and $^{\#}p < 0.05$, $^{\#\#}p < 0.001$ vs. p35 of three independent experiments, each performed in triplicate).

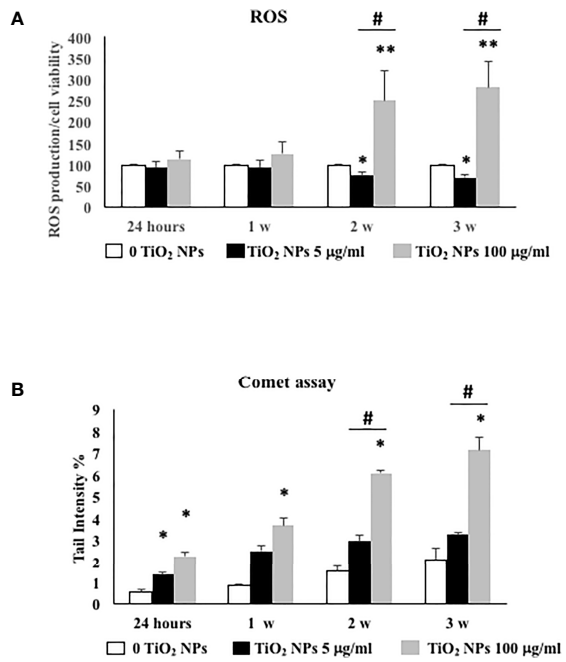

FIGURE 6 | ROS production and DNA damage under TiO_2 NPs treatment in SCs. **(A)** Total intracellular ROS production in SCs exposed to TiO_2 NPs 5 (black bar) and 100 µg/ml (grey bar) for 24 h and 1, 2, and 3 weeks. Data represent the mean ± SEM (*$p < 0.05$, **$p < 0.001$, with respect to unexposed SCs (black dotted line) and $^{\#}p < 0.05$ vs. 5 µg/ml of TiO_2 NPs of three independent experiments, $n = 8$). **(B)** DNA damage expressed as tail intensity % in unexposed SCs (white bar) and exposed to TiO_2 NPs 5 (black bar) and 100 µg/ml (grey bar) for 24 h and 1, 2, and 3 weeks. Data represent the mean ± SEM (*$p < 0.05$, **$p < 0.001$ vs. unexposed SCs and $^{\#}p < 0.05$ vs. 5 µg/ml of TiO_2 NPs of three independent experiments, $n = 8$).

The gene expression of TGF-β1 and IDO, at the subtoxic dose, showed an upregulation only at the first and second week respect to the unexposed SCs. At the toxic dose, the gene expression of TGF-β1 was upregulated at the first and second week; meanwhile, IDO showed an upregulation from the first to the third week with respect to the unexposed SCs (set as 1 in the graphs and represented as a black dotted line) and exhibited a significant increase compared with the lowest dose only at the third week (**Figures 9C, D**, *$p < 0.05$, **$p < 0.001$ vs. unexposed SCs; $^{\#}p < 0.05$ vs. 5 µg/ml of TiO_2 NPs).

3.9 TiO_2 NPs Treatment Activated MAPK and NF-kB Signaling Pathway

We performed Western blotting analysis to investigate the involvement and timing of activation of different MAPK family members (ERK1/2, JNK, and p38) and NF-kB signaling pathway after TiO_2 NPs exposure (**Figure 10A**).

The phosphorylation ratio of ERK1/2 showed a significant increase (**Figure 10B**, *$p < 0.05$, **$p < 0.001$ vs. unexposed SCs, set as 100 in the graphs and represented as a black dotted line) at 24 h postexposure that persisted until the second week posttreatment, to be downregulated at the third week postexposure, at both concentrations.

The phosphorylation ratio of JNK remained unaltered at both concentrations, at 24 h and 1 week postexposure, but showed a significant increase from the second and third week only at the highest concentration of 100 µg/ml (**Figure 10C**, **$p < 0.001$ vs. unexposed SCs, set as 100 in the graphs and represented as a black dotted line). In addition, the highest dose exhibited a significant increase starting from the second week in comparison with the lowest dose of NPs (**Figure 10C**, $^{\#}p < 0.05$ vs. 5 µg/ml of TiO_2 NPs).

The phosphorylation ratio of p38 showed a significant increase at 24 h, at the lowest dose of 5 µg/ml but was followed by a progressive decrease that became significant at the second and third week after exposure (**Figure 10D**, *$p < 0.05$, **$p < 0.001$ vs. unexposed SCs, set as 100 in the graphs and represented as a black dotted line). At the highest concentration of 100 µg/ml, p38-dependent pathway showed a significant increase with respect to the lowest dose from the second week (**Figure 10D**, *$p < 0.05$, **$p < 0.001$ vs. unexposed SCs, set as 100 in the graphs and represented as a black dotted line; $^{\#}p < 0.05$ vs. 5 µg/ml of TiO_2 NPs).

The phosphorylation ratio of AKT showed a significant increase throughout the whole experiment at the subtoxic dose but with an inverse time-dependent relationship (**Figure 10E**, *$p < 0.05$, **$p < 0.001$ vs. unexposed SCs (set as 100 in the graphs and represented as a black dotted line). At the toxic dose, a significant increase at 24 h was followed by a significant decrease over time (**Figure 10E**, *$p < 0.05$, **$p < 0.001$ vs. unexposed SCs (set as 100 in the graphs and represented as a black dotted line). In comparison with the lowest dose, the toxic dose showed a significant decrease from the first week (**Figure 10E**, $^{\#}p < 0.05$ vs. 5 µg/ml of TiO_2 NPs).

Finally, the phosphorylation ratio of p-NF-kB remained unchanged following acute exposure and at 1 week at both 5 and 100 µg/ml TiO_2 NPs. Subsequently, it showed a significant increase after the second and third week posttreatment at both concentrations (**Figure 10F**, *$p < 0.05$, **$p < 0.001$ vs. unexposed SCs, set as 100 in the graphs and represented as a black dotted line).

4 DISCUSSION

In the present study, we evaluated for the first time, to our knowledge, the effects of TiO_2 NPs on SCs from porcine prepubertal pig testes, an experimental animal model sharing significant physiological similarity with humans, thus providing novel results of a major translational importance.

It is important to note that primary SCs cultures have been recognized as a valuable *in vitro* system to study the effects of heavy metals and toxic substances (43–45).

To date, several *in vivo* and *in vitro* studies, mainly of mouse and rat origin, have evaluated the toxicological effects of TiO_2 NPs (19–24, 26, 27). Although interesting, the results are often contradictory, suggesting that the potential cell damage is

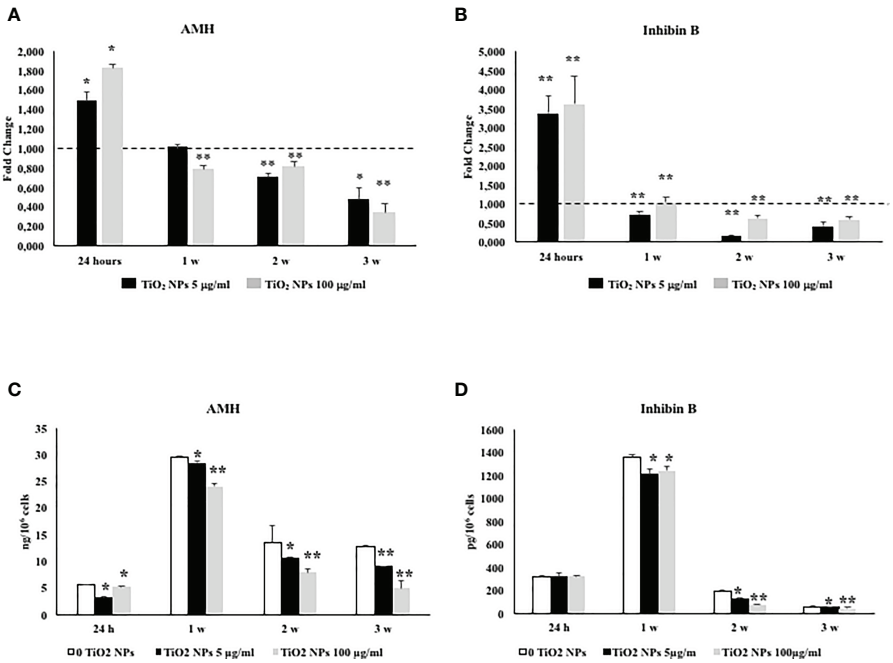

FIGURE 7 | Real-time PCR analysis of SCs functionality. Gene expression of AMH **(A)**, and inhibin B **(B)** in SCs at 24 h and 1, 2, and 3 weeks of incubation with TiO_2 NPs 5 (black bar) and 100 µg/ml (grey bar). ELISA assay of **(C)** AMH and **(D)** inhibin B secretion in SCs at 24 h and 1, 2, and 3 weeks of incubation with TiO_2 NPs 5 (black bar) and 100 µg/ml (grey bar). Data represent the mean ± SEM (*$p < 0.05$ and **$p < 0.001$ vs. unexposed SCs (0 TiO_2 NPs, black dotted line) of three independent experiments, each performed in triplicate).

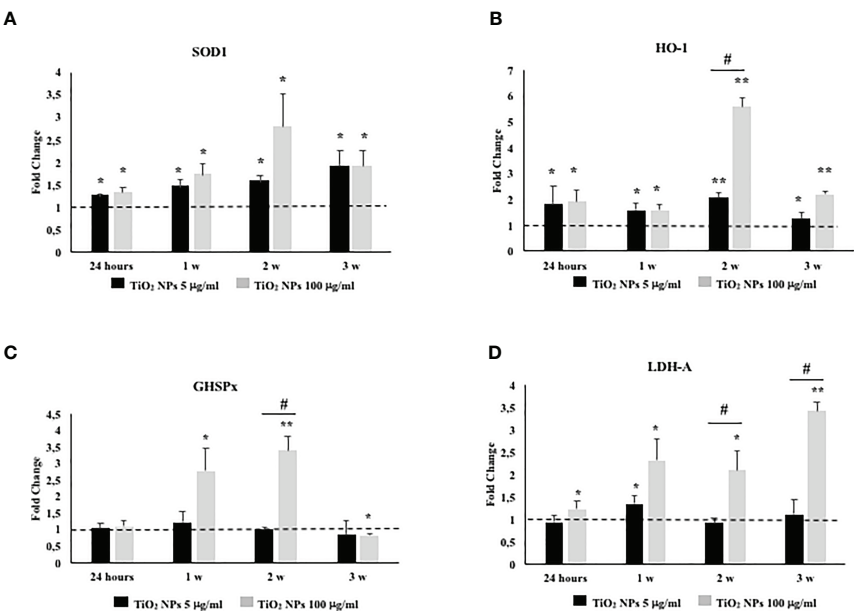

FIGURE 8 | Real-time PCR analysis of SCs antioxidant and metabolic enzymes. Gene expression of SOD1 **(A)**, HO-1 **(B)**, GHSPx **(C)**, and LDH A **(D)** in SCs at 24 h and 1, 2, and 3 weeks of incubation with TiO_2 NPs 5 (black bar) and 100 µg/ml (grey bar). Data represent the mean ± SEM (*$p < 0.05$, **$p < 0.001$ vs. unexposed SCs (black dotted line) and $^{\#}p < 0.05$ vs. 5 µg/ml of TiO_2 NPs of three independent experiments, each performed in triplicate).

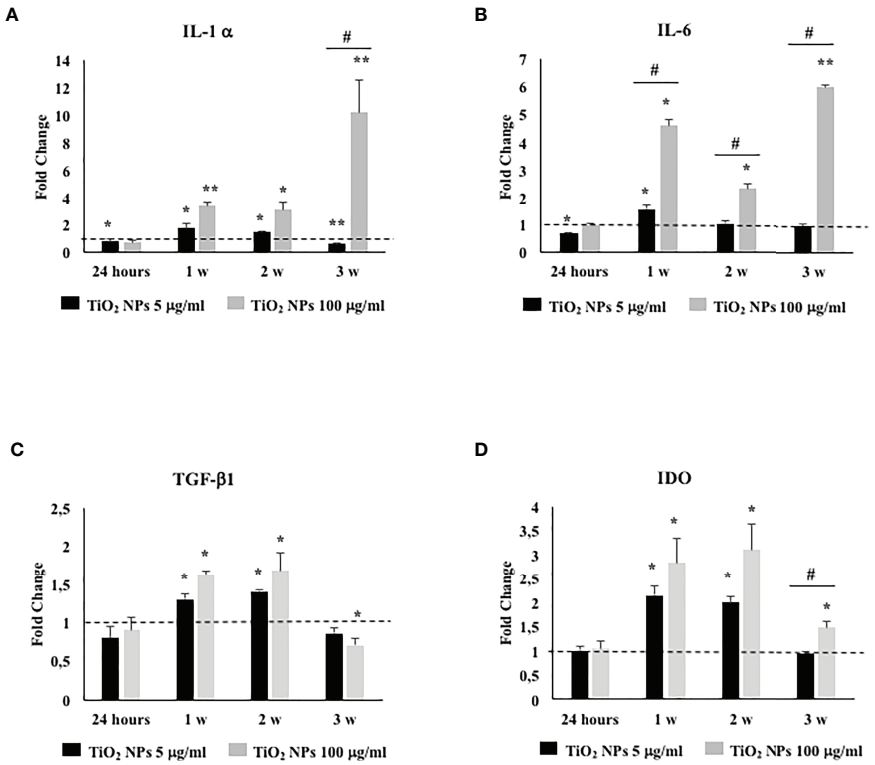

FIGURE 9 | Real-time PCR analysis of SCs proinflammatory and immunomodulatory response. Gene expression of IL-1α **(A)**, IL-6 **(B)**, TGF-β1 **(C)**, and IDO **(D)** in SCs at 24 h and 1, 2, and 3 weeks of incubation with TiO_2 NPs 5 (black bar) and 100 μg/ml (grey bar). Data represent the mean ± SEM (*$p < 0.05$, **$p < 0.001$ vs. unexposed SCs (black dotted line) and $^{\#}p < 0.05$ vs. 5 μg/ml of TiO_2 NPs of three independent experiments, each performed in triplicate).

affected by many factors including cell type, nanoparticle size, and dispersion protocols (46). In particular, the dimensions of TiO_2 NPs are critical from the toxicity point of view, because, as it is well known, NPs are more toxic and reactive than conventional TiO_2 particles (47).

Aggregates of NPs have been observed in Leydig-Sertoli cells and spermatids when mice were prenatally exposed to anatase TiO_2 NPs *via* subcutaneous injections (48, 49). In our study, several dispersion protocols were executed, followed by DLS analysis, in order to establish the best experimental condition, where the best choice resulted in DMEM with the addition of 2% BSA to obtain the smallest and stable nanoaggregates as reported in **Supplementary Materials**.

In particular, TiO_2 NP-treated SCs at 5 μg/ml apparently showed no morphological changes throughout the experimental treatment, but a deeper evaluation of this apparent health condition by MTT analysis revealed its cytotoxic effect under chronic exposure, with a 20% decrease in metabolically active cells (**Supplementary Material**), accompanied by important structural abnormalities revealed by TEM analysis at the third week.

At the concentration of 100 μg/ml TiO_2 NPs, SCs showed a spindle-like shape, with very elongated cytoplasmic protrusions, typical of a cellular stress-associated condition, by the end of the first week that progressively increased until the end of the third week, accompanied by a steady decrease around 50% of metabolically active cells (**Supplementary Material**). These important modifications were confirmed by TEM analysis that showed a high percentage of severely damaged SCs with nuclei deeply invaginated, shrunk, and disorder/marginalization of chromatin components, all typical features of apoptosis. In addition, we noted that endoplasmic reticulum membranes became swollen, very fragmented, or almost completely missing; mitochondrial morphology was severely affected and mitochondrial density dramatically decreased. Moreover, we observed the presence of several large vacuoles as the result of apoptotic mitochondria and/or enlarged endoplasmic reticulum.

To confirm the activation of apoptosis observed by TEM analysis, we performed the caspase-3 protein expression, crucial mediator of programmed cell death and essential for some of the characteristic changes in cell morphology associated with the execution and completion of apoptosis (40, 41). Our results, confirming previous *in vivo* (23) and *in vitro* (26) reports, showed at each concentration of NPs, a caspase-3 upregulation at the first and second week, with greater expression of p19 kDa active fragment only at toxic dose.

The increased intracellular production of ROS represents one of the most important mechanisms activated by nanomaterials.

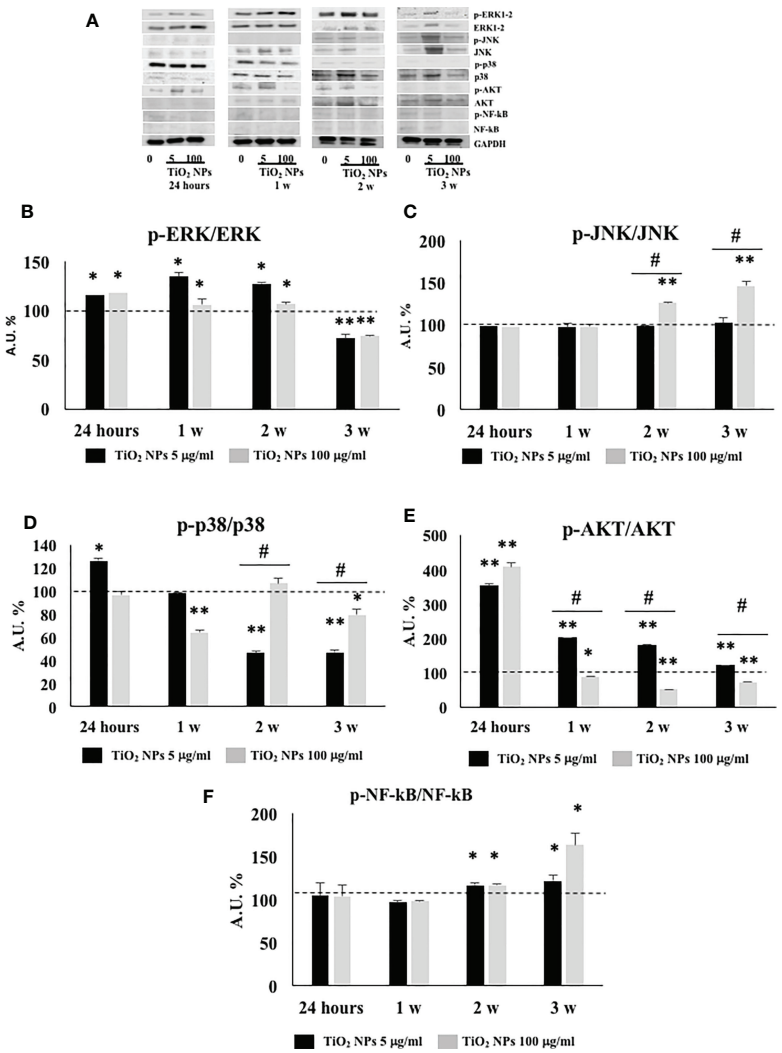

FIGURE 10 | WB analysis. **(A)** Immunoblots of phosphoERK1-2/ERK1-2, phosphoJNK/JNK, phosphop38/p38, phosphoAKT/AKT, posphoNF-kB p65/NF-kB, and GAPDH in SCs 24 h and 1, 2, and 3 weeks of incubation with TiO_2 NPs 5 and 100 µg/ml. Densitometric analysis of the protein bands of phosphoERK1-2/ERK1-2 **(B)**, phosphoJNK/JNK **(C)**, phosphop38/p38 **(D)**, phosphoAKT/AKT **(E)**, and phosphoNF-kB p65/NF-kB **(F)** in SCs 24 h and 1, 2, and 3 weeks of incubation with TiO_2 NPs 5 (black bar) and 100 µg/ml (grey bar). Data represent the mean ± SEM ($^*p < 0.05$, $^{**}p < 0.001$ vs. unexposed SCs (black dotted line) and $^{\#}p < 0.05$ vs. 5 µg/ml of TiO_2 NPs of three independent experiments, each performed in triplicate).

Typically, high doses of NPs, for example, 50 µg/ml in human fibroblasts (50) or 250 µg/ml in human hepatoma HepG2 (51), are associated with ROS generation.

In contrast, no intracellular production of ROS has been observed under either acute treatment (24 h), or chronic exposures (up to 4 weeks) (50) and either with the rutile and anatase forms (at a concentration of 50–500 µg/ml TiO_2 NPs) (51), and in different cell models such as human pulmonary fibroblast (52) and Caco-2 monolayer (at a concentration of 200 µg/ml TiO_2 NPs) (53).

Our data would agree with these latter results. In fact, in our model, the dose of 5 µg/ml TiO_2 NPs did not affect ROS intracellular level in contrast with the chronic exposure at the highest concentration, necessary condition to induce ROS production.

For deepening the analysis of ROS production, we evaluated the gene expression of antioxidative enzymes (ROS removal agents) including SOD, HO-1, and GHSPx as downstream molecules of Nrf2/ARE pathway (54–56). It is well known that Nrf2 is a crucial transcription factor in oxidative stress by regulating the expressions of phase II detoxification enzymes and antioxidant enzymes (56). Our results demonstrated that the exposure to TiO_2 NPs resulted primarily in SOD1 and HO-1 upregulation at both concentrations, then, only the dose of 100 µg/ml TiO_2 induced the upregulation of GHSPx. On this basis, we could hypothesize that the Nrf2/ARE pathway was sufficient to cope ROS production only at the subtoxic dose of TiO_2 NPs; meanwhile, its activation was not able to counteract the oxidative stress generated at the toxic dose. As future

perspective, to better understand the damage induced by ROS production, it will be useful to evaluate the involvement of the tyrosine kinase receptor HER2, involved in the epidermal growth factor-growth factor pathway (EGFG-GF), which is responsible for SCs proliferation, in addition to the assessment of ki67 and PCNA as indicators of germ cell mitotic and meiotic processes *in vivo* model (57).

Moreover, we investigated the gene expression of LDH-A as a marker of alteration of membrane integrity (26, 50), observing a significant increase only at the dose of 100 μg/ml TiO_2 NPs, confirming the detrimental effects of exposure to toxic dose of NPs on the membrane integrity.

Oxidative DNA damage is reported as another possible effect related to ROS production. However, the supposed genotoxic potential of TiO_2 NPs is debated because of conflicting results reported in the literature in both *in vivo* and *in vitro* models, most likely related to the different experimental conditions used.

To detect low-genotoxicity DNA damage induced by environmental contaminants, including nanomaterials, comet assay has been recognized as a reliable and sensitive technique (58, 59).

In our study, a statistically significant oxidative damage was observed at the lowest concentration of TiO_2 NPs at 24 h, whereas, only at the highest concentration of NPs, it was observed throughout the experiment with a time-dependent relationship. On the basis of what was observed, we could speculate that in our model the increased DNA damage observed at 24 h at the lowest concentration quickly activated the DNA repair systems as already observed by Zijno et al. (60) and that chronic exposure to subtoxic doses of TiO_2 NPs did not induce oxidative stress or genotoxic damage.

On the other hand, a significant increase of genotoxic damage before the oxidative one, observed after the exposure to toxic doses of TiO_2 NPs, could underline as the former is a much more sensitive and early marker than the latter.

The effects of TiO_2 NPs on SCs functionality were further evaluated by studying the levels of two specific SCs marker as AMH and inhibin B. AMH is a glycoprotein dimer belonging to the TGF-β family that is exclusively secreted by SCs, and it has become one of the most useful markers to study testicular function during the prepubertal period in males (61). Another specific and important marker of SCs action is inhibin B that provides for a negative feedback on FSH secretion and is clinically used to assess the presence and function of SCs during childhood (45).

In our study, the gene expression of both AMH and inhibin B was upregulated at 24 h and then downregulated over the course of the experiment at both concentrations, suggesting that TiO_2 NPs treatment impaired SCs functionality as expressed by the downregulation of both protein secretions overtime, inducing, at first, a transcriptional upregulation as a physiological response followed, in the end, by a definitive breakdown. These results were in agreement with other reports on porcine prepubertal SCs treated with other heavy metals (43, 45).

Another possible effect related to nanomaterial exposure is the activation of a proinflammatory response that ultimately could induce reproductive toxicity by disturbing the immune balance and immune privilege of the testis, leading to a chronic inflammation state. Grassian et al. (62) previously reported that mice subacutely exposed to 2–5 nm TiO_2 NPs showed a significant but moderate proinflammatory response. Park et al. (42) reported an activated inflammatory response through the upregulation of inflammatory cytokines in mouse bronchial alveolar lavage (BAL) fluid following exposure of TiO_2 NPs. Ye et al. (27) observed an increased inflammatory response in a primary cultured rat SCs following TiO_2 NPs administration characterized by the expression of IL-1β, TNF-α, IFN-γ, and IL-10. To evaluate the proinflammatory response, we focused on the analysis of the gene expression of IL-1α and IL-6 that showed, at 5 μg/ml of TiO_2 NPs, an increase limited to the first, maximal second week, time necessary for SCs to put in place responses to the perturbation caused by NPs exposure, and be able to counteract them. In contrast, the dose of 100 μg/ml TiO_2 NPs induced an obvious inflammatory state with a dose- and time-relationship increase.

Simultaneously, SCs tried to modulate an exacerbated *in vitro* proinflammatory response by the activation of the IDO-dependent mechanism TGF-β1 mediated as demonstrated by the further upregulation of TGF-β1 and IDO gene expression (63). Fallarino et al., for the first time, demonstrated the expression of IDO in SCs (63). In particular, they showed that IDO, with the involvement of the kynurenine pathway (the O_2-dependent oxidation of L-tryptophan), plays a key role in immune modulation (64). In our *in vitro* model, we observed at the subtoxic dose that, at the third week, the immunomodulatory response tended to normalize because the proinflammatory cytokines were reduced, while at the toxic dose, was still active as a response to the proinflammatory stress.

In order to identify the intracellular signaling pathways associated with TiO_2 NPs exposure and subsequent gene regulation, we investigated the phosphorylation ratio of some key signaling kinases by Western blot analysis. MAPKs (which are composed of three main members ERK, JNK, and p38) and PI3K/Akt signaling pathways are involved in a wide range of cellular processes, including NF-kB activation, an important nuclear transcription factor which regulates the expression of many genes involved in several cell responses such as inflammation and apoptosis (65, 66).

Treatment with both concentrations of NPs markedly increased the phosphorylation ratio of ERK1-2 up to the second week, demonstrating the involvement of this pathway in the responses initiated by the SCs after the exposure to NPs, as already reported by Han et al. in a model of porcine endothelial vascular cells treated with TiO_2 NPs (67).

The phosphorylation ratio of JNK was upregulated only at the dose of 100 μg/ml TiO_2 NPs from the second week of exposure throughout the end of experimentation, confirming its role as a kinase specifically activated by a significant cellular stress (66).

According to Ye et al. (27), who observed the activation of p-38 pathway in primary cultured rat SCs after an acute exposure at 5 μg/ml of TiO_2 NPs, we demonstrated the upregulation of phosphorylation ratio of p38 at 24 h and at the lowest dose of NPs, as a response to cell proliferation.

In contrast, p38 downregulation at high dose of NPs was expression of a really stressful and toxic condition to induce apoptosis and a reduction in the number of SCs already starting from the first week as observed by TEM analysis and cell number evaluation.

Akt phosphorylation at Ser473, a well-known signal pathway with antiapoptotic function, was activated only at subtoxic concentration, throughout the whole experiment; meanwhile, the concentration of 100 μg/ml, after an early activation at 24 h, silenced its expression, confirming again its detrimental effects on SCs viability (67).

Finally, we observed the increased phosphorylation ratio of NF-kB at both concentrations starting from the second week of treatment in contrast to Ye et al. (27) who observed its upregulation already at 24 h and at concentrations ranging from 10 to 50 μg/ml.

In our model, this delayed activation could be explained by the fact that ROS production, considered a key element in the activation of this nuclear transcription factor was demonstrated only at the highest concentration of NPs from the second week. Whereas, the activation of NF-kB at subtoxic concentration during the chronic exposure could be explained by its involvement in the apoptotic death, as previously reported (68) and confirmed in our *in vitro* model subjected to long-term exposure, by TEM analysis.

5 CONCLUSIONS

The results of our "*in vitro*" study confirmed the negative impact of TiO_2 NPs on porcine prepubertal SCs. In fact, SCs at a dose of 5 μg/ml seemingly maintained the morphological integrity, but a deeper analysis revealed how SCs were induced to activate a series of responses in an attempt to neutralize the harmful effects prompted by long time constant exposure that inevitably led to an altered ultrastructure, functionality, and viability.

Exposure to the dose of 100 μg/ml highlighted the negative effects of TiO_2 NPs on the morphological-ultrastructural integrity, apoptosis, alteration of functionality, and the induction of a proinflammatory state in SCs.

Although *in vitro* studies with NPs enable the identification of conceptual models of mechanistic interaction with cells, it is very important to consider that, they do not represent a full realistic model of how NPs will interact with the specific organ of the body *in vivo*. That said however, since our model is of a superior mammal, whose physiology is very similar to that of humans, our results pave the way for studying NPs toxicology in this latter species. Moreover, our study points out the importance of deepening the effects of TiO_2 NPs in *in vivo* animal model, especially at subtoxic dose and under chronic exposure because the impact of such a slow and insidious poisoning is not immediately perceivable and shows its side effects after a long-term treatment. Unfortunately, nowadays, no consistent epidemiologic studies exist on the association between reproductive health and the risk of TiO_2 NPs exposure in humans. Certainly, further screenings will be necessary to verify this association. Importantly, the acquired knowledge could help to adopt containment strategies and active surveillance programs in the next future as prevention measures before irreversible damage to SCs occurs and consequently affects spermatogenesis.

DATA AVAILABILITY STATEMENT

The datasets presented in this study can be found in online repositories. The names of the repository/repositories and accession number(s) can be found below: https://doi.org/10.5061/dryad.7d7wm37wf.

ETHICS STATEMENT

The animal studies were conducted in agreement with the guidelines adopted by the Italian Approved Animal Welfare Assurance (A-3143-01) and the European Communities Council Directive of November 24, 1986 (86/609/EEC). The experimental protocols were approved by the University of Perugia.

AUTHOR CONTRIBUTIONS

FM, IA, and AM designed the study and drafted the manuscript. AM synthesized TiO_2 NPs. FM, IA, and LA performed the experimental procedures. CB performed real-time PCR and analyzed the data. CL performed WB and analyzed the data. SB and AF performed TEM. MM and DB performed ROS analysis. MM and CR performed Comet analysis. MN performed ICP-OES analysis. AG, GM, and TB gave experimental guidance. CA, SG, and GL supervised and revised the manuscript. All authors have read and agreed to the published version of the manuscript.

FUNDING

This research was funded by Fondazione Cassa di Risparmio di Perugia, code of Project: 2019.0382.029.

ACKNOWLEDGMENTS

The authors would like to thank Altucell Inc., 3 Astor Court, Dix Hills, NY, USA.

SUPPLEMENTARY MATERIAL

The Supplementary Material for this article can be found online at: https://www.frontiersin.org/articles/10.3389/fendo.2021.751915/full#supplementary-material

REFERENCES

1. Powers KW, Carpinone PL, Siebein KN. Characterization of Nanomaterials for Toxicological Studies. *Methods Mol Biol* (2012) 926:13–32. doi: 10.1007/978-1-62703-002-1_2
2. Gambelunghe A, Giovagnoli S, Di Michele A, Boncompagni S, Dell'Omo M, Leopold K, et al. Redox-Sensitive Glyoxalase 1 Up-Regulation Is Crucial for Protecting Human Lung Cells From Gold Nanoparticles Toxicity. *Antioxidants* (2020) 9(8):697. doi: 10.3390/antiox9080697
3. Hoet PH, Brüske-Hohlfeld I, Salata OV. Nanoparticles – Known and Unknown Health Risks. *J Nanobiotechnol* (2004) 2:12. doi: 10.1186/1477-3155-2-12
4. Oberdörster G, Oberdörster E, Oberdörster J. Nanotoxicology: An Emerging Discipline Evolving From Studies of Ultrafine Particles. *Environ Health Perspect* (2005) 113(7):823–39. doi: 10.1289/ehp.7339
5. Oberdorster G. Toxicology of Air Born Environment and Occupational Particles. *Part Fibre Toxicol* (2006) 5(3):83–91. doi: 10.1289/ehp.7339
6. Derfus AM, Chan WCW, Bhatia SN. Probing the Cytotoxicity of Semiconductor Quantum Dots. *Nano Lett* (2004) 4(1):11–8. doi: 10.1021/nl0347334
7. Chou CC, Hsiao HY, Hong QS, Chen CH, Peng YW, Chen HW, et al. Single-Walled Carbon Nanotubes Can Induce Pulmonary Injury in Mouse Model. *Nano Lett* (2008) 8(2):437–45. doi: 10.1021/nl0723634
8. Lin P, Chen JW, Chang LW, Wu JP, Redding L, Chang H, et al. Computational and Ultrastructural Toxicology of a Nanoparticle, Quantum Dot 705, in Mice. *Environ Sci Technol* (2008) 42:6264–70. doi: 10.1021/es800254a
9. Schipper ML, Nakayama-Ratchford N, Davis CR, Kam NWS, Chu P, Liu Z, et al. A Pilot Toxicology Study of Single-Walled Carbon Nanotubes in a Small Sample of Mice. *Nat Nanotechnol* (2008) 3:216–21. doi: 10.1038/nnano.2008.68
10. Wu J, Liu W, Xue C, Zhou S, Lan F, Bi L, et al. Toxicity and Penetration of TiO 2 Nanoparticles in Hairless Mice and Porcine Skin After Subchronic Dermal Exposure. *Toxicol Lett* (2009) 191:1–8. doi: 10.1016/j.toxlet.2009.05.020
11. Bartneck M, Ritz T, Keul HA, Wambach M, Bornemann J, Gbureck U, et al. Peptide-Functionalized Gold Nanorods Increase Liver Injury in Hepatitis. *ACS Nano* (2012) 6:8767–77. doi: 10.1021/nn302502u
12. Vance ME, Kuiken T, Vejerano EP, McGinnis SP, Hochella MF Jr, Rejeski D, et al. Nanotechnology in the Real World: Redeveloping the Nanomaterial Consumer Products Inventory. *Beilstein J Nanotechnol* (2015) 6:1769–80. doi: 10.3762/bjnano.6.181
13. Fujishima A, Zhang X, Tryk DA. Ti Photocatalysis and Related Surface Phenomena. *Surface Sci Rep* (2008) 63:515–82. doi: 10.1016/j.surfrep.2008.10.001
14. Wang J, Chen C, Liu Y, Jiao F, Li W, Lao F, et al. Potential Neurological Lesion After Nasal Instillation of TiO(2) Nanoparticles in the Anatase and Rutile Crystal Phases. *Toxicol Lett* (2008) 183(1-3):72–80. doi: 10.1016/j.toxlet.2008.10.001
15. Trouiller B, Reliene R, Westbrook A, Solaimani P, Schiestl RH. Titanium Dioxide Nanoparticles Induce DNA Damage and Genetic Instability In Vivo in Mice. *Cancer Res* (2009) 69(22):8784–9. doi: 10.1158/0008-5472.CAN-09-2496
16. Elgrabli D, Beaudouin R, Jbilou N, Floriani M, Pery A, Rogerieux F, et al. Biodistribution and Clearance of TiO2 Nanoparticles in Rats After Intravenous Injection. *PloS One* (2015) 10(4):e0124490. doi: 10.1371/journal.pone.0124490
17. Iavicoli I, Leso V, Bergamaschi A. Toxicological Effects of Titanium Dioxide Nanoparticles: A Review of In Vivo Studies. *J Nanomater* (2012) 2012:964381. doi: 10.1155/2012/964381
18. La Z, Yang WX. Nanoparticles and Spermatogenesis: How do Nanoparticles Affect Spermatogenesis and Penetrate the Blood–Testis Barrier. *Nanomed (Lond)* (2012) 7:579–96. doi: 10.2217/nnm.12.20
19. Shi HB, Magaye R, Castranova V, Zhao JS. Titanium Dioxide Nanoparticles: A Review of Current Toxicological Data. *Part Fibre Toxicol* (2013) 10:15. doi: 10.1186/1743-8977-10-15
20. Guo LL, Liu XH, Qin DX, Gao L, Zhang HM, Liu J,Y, et al. Effects of Nano-Sized Titanium Dioxide on the Reproductive System of Male Mice. *Zhonghua Nan Ke Xue* (2009) 15:517–22 (in Chinese).
21. Takeda K, Suzuki K, Ishihara A, Kubo-Irie M, Fujimoto R, Tabata M, et al. Nanoparticles Transferred From Pregnant Mice to Their Offspring can Damage the Genital and Cranial Nerve System. *J Health Sci* (2009) 55:95–102. doi: 10.1248/jhs.55.95
22. Ema M, Kobayashi N, Naya M, Hanai S, Nakanishi J. Reproductive and Developmental Toxicity Studies of Manufactured Nanomaterials. *Reprod Toxicol* (2010) 30:343–52. doi: 10.1016/j.reprotox.2010.06.002
23. Gao G, Ze Y, Zhao X, Sang X, Zheng L, Ze X, et al. Titanium Dioxide Nanoparticle-Induced Testicular Damage, Spermatogenesis Suppression, and Gene Expression Alterations in Male Mice. *J Hazard Mater* (2013) 258–9:133–43. doi: 10.1016/j.jhazmat.2013.04.046
24. Jia F, Sun Z, Yan X, Zhou B, Wang J. Effect of Pubertal Nano-TiO2 Exposure on Testosterone Synthesis and Spermatogenesis in Mice. *Arch Toxicol* (2014) 88(3):781–8. doi: 10.1007/s00204-013-1167-5
25. Komatsu T, Tabata M, Kubo-Irie M, Shimizu T, Suzuki K, Nihei Y, et al. The Effects of Nanoparticles on Mouse Testis Leydig Cells In Vitro. *Toxicol In Vitro* (2008) 22(8):1825–31. doi: 10.1016/j.tiv.2008.08.009
26. Hong F, Zhao X, Si W, Ze Y, Wang L, Zhou Y, et al. Decreased Spermatogenesis Led to Alterations of Testis-Specific Gene Expression in Male Mice Following Nano-TiO2 Exposure. *J Hazard Mater* (2015) 300:718–28. doi: 10.1016/j.jhazmat.2015.08.010
27. Ye L, Hong F, Ze X, Li L, Zhou Y, Ze Y. Toxic Effects of TiO_2 Nanoparticles in Primary Cultured Rat Sertoli Cells Are Mediated *via* a Dysregulated Ca^{2+}/PKC/p38 MAPK/NF-κb Cascade. *J BioMed Mater Res A* (2017) 105 (5):1374–82. doi: 10.1002/jbm.a.36021
28. Wu N, Hong F, Zhou Y, Wang Y. Exacerbation of Innate Immune Response in Mouse Primary Cultured Sertoli Cells Caused by Nanoparticulate TiO_2 Involves the TAM/TLR3 Signal Pathway. *J BioMed Mater Res A* (2017) 105 (1):198–208. doi: 10.1002/jbm.a.35906
29. Vales G, Rubio L, Marcos R. Long-Term Exposures to Low Doses of Titanium Dioxide Nanoparticles Induce Cell Transformation, But Not Genotoxic Damage in BEAS-2B Cells. *Nanotoxicology* (2015) 9(5):568–78. doi: 10.3109/17435390.2014.957252
30. Ammar I, Wanichaya M, Wisanu P. Anatase/Rutile TiO2 Composite Prepared *via* Sonochemical Process and Their Photocatalytic Activity. *Mater Today: Proc* (2017) 4(5):6159–65. doi: 10.1016/j.matpr.2017.06.110
31. Zhang Y, Chen Y, Westerhoff P, Hristovski K, Crittenden JC. Stability of Commercial Metal Oxide Nanoparticles in Water. *Water Res* (2008) 42(8-9):2204–12. doi: 10.1016/j.watres.2007.11.036
32. De Monte V, Staffieri F, Di Meo A, Vannucci J, Bufalari A. Comparison of Ketamine-Dexmedetomidine-Methadone and Tiletamine-Zolazepam-Methadone Combinations for Short-Term Anaesthesia in Domestic Pig. *Vet J* (2015) 205(3):364–8. doi: 10.1016/j.tvjl.2015.05.011
33. Luca G, Mancuso F, Calvitti M, Arato I, Falabella G, Bufalari A, et al. Long-Term Stability, Functional Competence, and Safety of Microencapsulated Specific Pathogen-Free Neonatal Porcine Sertoli Cells: A Potential Product for Cell Transplant Therapy. *Xenotransplantation* (2015) 22(4):273–83. doi: 10.1111/xen.12175
34. Arato I, Luca G, Mancuso F, Bellucci C, Lilli C, Calvitti M, et al. An "*In Vitro*" Prototype of a Porcine Biomimetic Testis-Like Cell Culture System: A Novel Tool for the Study of Reassembled Sertoli and Leydig Cells. *Asian J Androl* (2018) 20(2):160–5. doi: 10.4103/aja.ja_47_17
35. Tice RR, Agurell E, Anderson D, Burlinson B, Hartmann A, Kobayashi H, et al. Single Cell Gel/COMET Assay: Guidelines for *In Vitro* and *In Vivo* Genetic Toxicology Testing, Environ. *Mol Mutagen* (2000) 35(3):206–21. doi: 10.1002/(SICI)1098-2280(2000)35:3b206::AIDEM8N3.0.CO;2-J
36. Giovagnoli S, Mancuso F, Vannini S, Calvitti M, Piroddi M, Pietrella D, et al. 'Microparticle-Loaded Neonatal Porcine Sertoli Cells for Cell-Based Therapeutic and Drug Delivery System'. *J Control Release* (2014) 192:249–61. doi: 10.1016/j.jconrel.2014.08.001
37. Arato I, Milardi D, Giovagnoli S, Grande G, Bellucci C, Lilli C, et al. "*In "Vitro"* Lps-Stimulated Sertoli Cells Pre-Loaded With Microparticles: Intracellular Activation Pathways. *Front Endocrinol* (2021) 11:611932. doi: 10.3389/fendo.2020.611932
38. Antognelli C, Mancuso F, Frosini R, Arato I, Calvitti M, Calafiore R, et al. Testosterone and Follicle Stimulating Hormone-Dependent Glyoxalase 1 Up-Regulation Sustains the Viability of Porcine Sertoli Cells Through the Control of Hydroimidazolone- and Argpyrimidine-Mediated NF-κb Pathway. *Am J Pathol* (2018) 188(11):2553–63. doi: 10.1016/j.ajpath.2018.07.01
39. Bradford MM. A Rapid and Sensitive Method for the Quantitation of Microgram Quantities of Protein Utilizing the Principle of Protein-Dye Binding. *Anal Biochem* (1976) 72:248–54. doi: 10.1016/0003-2697(76)90527-3

40. Fettucciari K, Ponsini P, Gioè D, Macchioni L, Palumbo C, Antonelli E, et al. Enteric Glial Cells Are Susceptible to *Clostridium Difficile* Toxin B. *Cell Mol Life Sci* (2017) 74:1527–155. doi: 10.1007/s00018-016-2426-4
41. Valencia-Cruz G, Shabala L, Delgado-Enciso I, Shabala S, Bonales-Alatorre E, Pottosin II, et al. K Bg and Kv1.3 Channels Mediate Potassium Efflux in the Early Phase of Apoptosis in Jurkat T Lymphocytes. *Am J Physiol Cell Physiol* (2009) 297:C1544–53. doi: 10.1152/ajpcell.00064.2009
42. Park EJ, Yoon J, Choi K, Yi J, Park K. Induction of Chronic Inflammation in Mice Treated With Titanium Dioxide Nanoparticles by Intratracheal Instillation. *Toxicology* (2009) 260(1-3):37–46. doi: 10.1016/j.tox.2009.03.005
43. Mancuso F, Arato I, Lilli C, Bellucci C, Bodo M, Calvitti M, et al. Acute Effects of Lead on Porcine Neonatal Sertoli Cells. *Vitro Toxicol In Vitro* (2018) 48:45–52. doi: 10.1016/j.tiv.2017.12.013
44. Marinucci L, Balloni S, Bellucci C, Lilli C, Stabile AM, Calvitti M, et al. Effects of Nicotine on Porcine Pre-Pupertal Sertoli Cells: An *In Vitro* Study. *Toxicol In Vitro* (2020) :67:104882. doi: 10.1016/j.tiv.2020.104882
45. Luca G, Lilli C, Bellucci C, Mancuso F, Calvitti M, Arato I, et al. Toxicity of Cadmium on Sertoli Cell Functional Competence: An In Vitro Study. *J Biol Regul Homeost Agents* (2013) 27(3):805–16.
46. Grande F, Tucci P. Titanium Dioxide Nanoparticles: A Risk for Human Health? *Mini Rev Med Chem* (2016) 16(9):762–9. doi: 10.2174/1389557516666160321114341
47. Liang G, Pu Y, Yin L, Liu R, Ye B, Su Y, et al. Influence of Different Sizes of Titanium Dioxide Nanoparticles on Hepatic and Renal Functions in Rats With Correlation to Oxidative Stress. *J Toxicol Environ Health A* (2009) 72 (11-12):740–5. doi: 10.1080/15287390902841516
48. De Jong WH, Borm PJ. Drug Delivery and Nanoparticles: Applications and Hazards. *Int J Nanomed* (2008) 3(2):133–49. doi: 10.2147/ijn.s596
49. Takahashi Y, Mizuo K, Shinkai Y, Oshio S, Takeda K. Prenatal Exposure to Titanium Dioxide Nanoparticles Increases Dopamine Levels in the Prefrontal Cortex and Neostriatum of Mice. *J Toxicol Sci* (2010) 35(5):749–56. doi: 10.2131/jts.35.749
50. Huang S, Chueh PJ, Lin YW, Shih TS, Chuang SM. Disturbed Mitotic Progression and Genome Segregation Are Involved in Cell Transformation Mediated by Nano-TiO2 Long-Term Exposure. *Toxicol Appl Pharmacol* (2009) 241(2):182–94. doi: 10.1016/j.taap.2009.08.013
51. Petković J, Küzma T, Rade K, Novak S, Filipič M. Pre-Irradiation of Anatase TiO2 Particles With UV Enhances Their Cytotoxic and Genotoxic Potential in Human Hepatoma HepG2 Cells. *J Hazard Mater* (2011) 196:145–52. doi: 10.1016/j.jhazmat.2011.09.004
52. Armand L, Dagouassat M, Belade E, Simon-Deckers A, Le Gouvello S, Tharabat C, et al. Titanium Dioxide Nanoparticles Induce Matrix Metalloprotease 1 in Human Pulmonary Fibroblasts Partly via an Interleukin-1β-Dependent Mechanism. *Am J Respir Cell Mol Biol* (2013) 48 (3):354–63. doi: 10.1165/rcmb.2012-0099OC
53. Gerloff K, Fenoglio I, Carella E, Kolling J, Albrecht C, Boots AW, et al. Distinctive Toxicity of TiO2 Rutile/Anatase Mixed Phase Nanoparticles on Caco-2 Cells. *Chem Res Toxicol* (2012) 3):646–55. doi: 10.1021/tx200334k
54. Gonzales S, Perez MJ, Perazzo JC, Tomaro ML. Antioxidant Role of Heme Oxygenase-1 in Prehepatic Portal Hypertensive Rats. *World J Gastroenterol* (2006) 12(26):4149–55. doi: 10.3748/wjg.v12.i26.4149
55. Maines MD, Kappas A. Studies on the Mechanism of Induction of Haem Oxygenase by Cobalt and Other Metal Ions. *Biochem J* (1976) 154(1):125–31. doi: 10.1042/bj1540125
56. Yang SH, Yu LH, Li L, Guo Y, Zhang Y, Long M, et al. Protective Mechanism of Sulforaphane on Cadmium-Induced Sertoli Cell Injury in Mice Testis *via* Nrf2/ARE Signaling Pathway. *Molecules* (2018) 23:1774. doi: 10.3390/molecules23071774
57. Ajayi AF, Akhigbe RE. *In Vivo* Exposure to Codeine Induces Reproductive Toxicity: Role of HER2 Andp53/Bcl-2 Signaling Pathway. *Heliyon* (2020) 6: e05589. doi: 10.1016/j.heliyon.2020.e05589
58. Dusinska M, Collins AR. The Comet Assay in Human Biomonitoring: Gene-Environment Interactions. *Mutagenesis* (2008) 23(3):191–205. doi: 10.1093/mutage/gen007
59. Magdolenova Z, Lorenzo Y, Collins A, Dusinska M. Can Standard Genotoxicity Tests be Applied to Nanoparticles? *J Toxicol Environ Health A* (2012) 75(13-15):800–6. doi: 10.1080/15287394.2012.690326
60. Zijno A, De Angelis I, De Berardis B, Andreoli C, Russo MT, Pietraforte D, et al. Different Mechanisms Are Involved in Oxidative DNA Damage and Genotoxicity Induction by ZnO and TiO2 Nanoparticles in Human Colon Carcinoma Cells. *Toxicol In Vitro* (2015) 29(7):1503–12. doi: 10.1016/j.tiv.2015.06.009
61. Josso N, Rey RA, Picard JY. Anti-Müllerian Hormone: A Valuable Addition to the Toolbox of the Pediatric Endocrinologist. *Int J Endocrinol* (2013) 2013:674105. doi: 10.1155/2013/674105
62. Grassian VH, O'shaughnessy PT, Adamcakova-Dodd A, Pettibone J–, Thorne PS. Inhalation Exposure Study of Titanium Dioxide Nanoparticles With a Primary Particle Size of 2 to 5 Nm. *Environ Health Perspect* (2007) 115 (3):397–402. doi: 10.1289/ehp.9469
63. Fallarino F, Luca G, Calvitti M, Mancuso F, Nastruzzi C, Fioretti MC, et al. Therapy of Experimental Type 1 Diabetes by Isolated Sertoli Cell Xenografts Alone. *J Exp Med* (2009) 206:2511–26. doi: 10.1084/jem.20090134
64. Mellor AL, Munn DH. IDO Expression by Dendritic Cells: Tolerance and Tryptophan Catabolism. *Nat Rev Immunol* (2004) 4:762–74. doi: 10.1038/nri1457
65. Sun Y, Liu WZ, Liu T, Feng X, Yang N, Zhou HF. Signaling Pathway of MAPK/ERK in Cell Proliferation, Differentiation, Migration, Senescence and Apoptosis. *J Recept Signal Transduct Res* (2015) 35(6):600–4. doi: 10.3109/10799893.2015.1030412
66. Zhang W, Liu HT. MAPK Signal Pathways in the Regulation of Cell Proliferation in Mammalian Cells. *Cell Res* (2002) 12(1):9–18. doi: 10.1038/sj.cr.7290105
67. Han SG, Newsome B, Hennig B. Titanium Dioxide Nanoparticles Increase Inflammatory 750 Responses in Vascular Endothelial Cells. *Toxicology* (2013) 306:1–8. doi: 10.1016/j.tox.2013.01.014
68. Liu X, Sun J. Endothelial Cells Dysfunction Induced by Silica Nanoparticles Through Oxidative Stress *via* JNK/P53 and NF-kappaB Pathways. *Biomaterials* (2010) 31:8198–209. doi: 10.1016/j.biomaterials.2010.07.069

Conflict of Interest: The authors declare that the research was conducted in the absence of any commercial or financial relationships that could be construed as a potential conflict of interest.

frontiers in Endocrinology

SYSTEMATIC REVIEW
published: 04 January 2022
doi: 10.3389/fendo.2021.802632

Relationship Among Traditional Semen Parameters, Sperm DNA Fragmentation, and Unexplained Recurrent Miscarriage: A Systematic Review and Meta-Analysis

Yanpeng Dai[1], *Junjie Liu*[2*], *Enwu Yuan*[1*], *Yushan Li*[2], *Ying Shi*[1] *and Linlin Zhang*[1]

[1] Department of Clinical Laboratory, The Third Affiliated Hospital of Zhengzhou University, Zhengzhou, China, [2] Henan Human Sperm Bank, The Third Affiliated Hospital of Zhengzhou University, Zhengzhou, China

Several studies have explored the relationship among traditional semen parameters, sperm DNA fragmentation (SDF), and unexplained recurrent miscarriage (RM); however, the findings remain controversial. Hence, we conducted a meta-analysis to explore the relationship among traditional semen parameters, SDF, and unexplained RM. Multiple databases, including PubMed, Google Scholar, MEDLINE, Embase, Cochrane Library, Web of Science, and China National Knowledge Infrastructure (CNKI), were searched to identify relevant publications. From the eligible publications, data were extracted independently by two researchers. A total of 280 publications were identified using the search strategy. According to the inclusion/exclusion criteria, 19 publications were eligible. A total of 1182 couples with unexplained RM and 1231 couples without RM were included in this meta-analysis to assess the relationship among traditional semen parameters, SDF, and unexplained RM. Our results showed that couples with unexplained RM had significantly increased levels of SDF and significantly decreased levels of total motility and progressive motility compared with couples without RM, although significant differences were not observed in the semen volume, sperm concentration, and total sperm count between couples with and without RM. The SDF assay may be considered for inclusion in evaluations of couples with unexplained RM.

Keywords: DNA fragmentation, semen quality, recurrent miscarriage, sperm, meta-analysis

OPEN ACCESS

Edited by:
Panagiotis Drakopoulos, University Hospital Brussels, Belgium

Reviewed by:
Cinzia Antognelli, University of Perugia, Italy
Andrea Garolla, University of Padua, Italy

****Correspondence:***
Enwu Yuan
diyudeshouhuzhe@126.com
Junjie Liu
13937112492@126.com

Specialty section:
This article was submitted to Reproduction, a section of the journal Frontiers in Endocrinology

Received: *27 October 2021*
Accepted: *13 December 2021*
Published: *04 January 2022*

Citation:
Dai Y, Liu J, Yuan E, Li Y, Shi Y and Zhang L (2022) Relationship Among Traditional Semen Parameters, Sperm DNA Fragmentation, and Unexplained Recurrent Miscarriage: A Systematic Review and Meta-Analysis. Front. Endocrinol. 12:802632. doi: 10.3389/fendo.2021.802632

INTRODUCTION

A uniform definition of recurrent miscarriage (RM) has not been established. The American Society for Reproductive Medicine (ASRM) defines RM as two or more consecutive miscarriages (1), while the Royal College of Obstetricians and Gynecologists (RCOG), the Chinese Society of Obstetrics and Gynecology, and the European Society of Human Reproduction and Embryology (ESHRE) guidelines define RM as three or more consecutive miscarriages (2–4). RM affects approximately 1% of couples trying to conceive (5). In almost half of the cases of RM, the etiology of the affected

couples remains unclear (1). Research has mainly focused on female factors for RM, but the role of male factors in RM has recently gained attention (6–8).

Male fertility is usually assessed by the semen volume, sperm concentration, total sperm count, progressive motility, and total motility according to WHO guidelines. However, traditional semen parameters have relatively poor predictive value for spermatozoa fertilizing capacity and reproductive outcomes (9). The integrity of sperm DNA is essential for the accurate transmission of genetic information from father to offspring. Sperm DNA fragmentation (SDF) is used to assess the integrity of sperm chromatin and has been increasingly recognized as crucial because of its diagnostic potential in terms of male fertility and pregnancy outcomes. There are three main hypotheses regarding the molecular mechanism of sperm DNA damage, including oxidative stress: chromatin packaging abnormalities, and apoptosis (10). A certain degree of sperm DNA damage can be repaired by the oocyte; however, when the damage exceeds the repair capacity of the oocyte, then adverse pregnancy outcomes may occur (11). Many clinical studies have investigated the relationship between SDF and reproductive outcomes, and several studies have suggested that SDF is associated with poor fertilization, suboptimal embryo quality, and lower pregnancy rates (12–15). Gandini et al. suggest that sperm with DNA damage are capable of fertilizing an oocyte (16). However, other studies have indicated that SDF is not associated with the fertilization rate or pregnancy outcome (17, 18). Thus, the implications of SDF on fertilization rate and pregnancy outcome remain controversial.

Many SDF assays have been developed, and the main methods are as follows: sperm chromatin dispersion (SCD) (19–23), terminal deoxyuridine nick end labeling (TUNEL) (24–28), acridine orange test (AOT) (29), sperm chromatin structure assay (SCSA) (27, 30–35), and aniline blue (AB) staining (36). TUNEL is a direct method of measuring single and double DNA strand breaks by using probes, while SCD, SCSA, AOT, and AB staining are indirect methods that use the increased susceptibility of sperm DNA damage to acid-induced denaturation.

This systematic review and meta-analysis aimed to assess the relationship among traditional semen parameters, SDF, and unexplained RM.

MATERIALS AND METHODS

Literature Search

The study was performed in accordance with the Preferred Reporting Items for Systematic Reviews and Meta-Analyses (PRISMA) guidelines (37). Multiple databases, including PubMed, Google Scholar, Cochrane Library, Embase, Web of Science, MEDLINE, and China National Knowledge Infrastructure (CNKI), were searched to identify relevant articles from inception to October 2021. The search was limited to human studies published in English and included using the following terms: "recurrent pregnancy loss", "repeated pregnancy loss", "recurrent abortions", "recurrent spontaneous abortion", "recurrent miscarriage", "sperm DNA fragmentation", "sperm DNA integrity", "sperm DNA damage", "SDF", "DFI", "traditional semen parameters", and "conventional semen parameters".

Selection Criteria

Studies that met the following criteria were included in this study: (1) original research; (2) the topic is unexplained RM; (3) natural conception; and (4) the data for traditional semen parameters and SDF are expressed as the means with standard deviations (SDs). The exclusion criteria were as follows: (1) reviews, letters, editorials, and abstracts; (2) inaccessible full articles; (3) case-only studies; and (4) duplicate publications.

Selection of Publications

Based on the predefined inclusion/exclusion criteria, all publications were independently selected for eligibility by two authors (Y.D. and J.L.). After removing duplicates, articles were selected by reviewing the titles and abstracts. The remaining publications were retrieved for full-text assessment if their appropriateness could not be determined. Any discrepancy was resolved through discussion with the third reviewer (E.Y.).

Data Extraction

From the eligible publications, data were extracted independently by two authors (Y.D. and J.L.). Any discrepancy between the two authors (Y.D. and J.L.) was resolved by discussion with the third reviewer (E.Y.). The following information was collected for each eligible publication: name of the first author, publication year, country of origin, ethnicity group, type of study design, sample size, and methods used to evaluate SDF. The main characteristics of the included studies are listed in **Table 1**.

Quality Assessment of the Included Publications

Quality assessments were performed using the Newcastle–Ottawa Scale (NOS) (39). A NOS score of ≥6 was considered high quality (40).

Statistical Analysis

All analyses were performed using Stata/SE 12.0 (StataCorp, College Station, Texas, USA). The heterogeneity between publications was calculated using the I^2 statistic and Cochran's Q test. Heterogeneity was considered significant at $P<0.10$ and/or $I^2<50\%$. Based on the heterogeneity assessment, random- or fixed-effects models were selected to calculate the weighted mean differences (WMDs) and their corresponding 95% confidence intervals (CIs). To explore the potential sources of heterogeneity, subgroup analyses were performed. To estimate the stability of the pooled results, a sensitivity analysis was conducted by excluding each publication. To estimate the possible publication bias, Egger's regression test and Begg's funnel plot were used. Statistical significance was set at $P<0.05$.

TABLE 1 | Main characteristics of the included studies in the meta-analysis.

Author (year)	Country	Ethnicity	Study design	Cases	Controls	Sample size Cases/ controls	Samples for DFI	Assay	Quality score
Absalan et al. (19)	Iran	Asian	Prospective	RPL≥ 3 times	Fertile	30/30	Fresh semen	SCD	7
Bareh et al. (24)	USA	Caucasian	Prospective	RPL≥ 2times	≥1 live birth	26/31	Fresh semen	TUNEL	7
Bhattacharya et al. (29)	India	Asian	Prospective	RPL≥ 2times	≥1 live birth	74/65	Fresh semen	AOT	7
Brahem et al. (25)	Tunisia	African	Prospective	RPL≥ 2times	Fertile	31/20	Frozen semen	TUNEL	7
Carlini et al. (26)	Italy	Caucasian	Prospective	RPL≥ 2times	≥1 live birth	112/114	Fresh semen	TUNEL	8
Carrell et al. (38)	USA	Caucasian	Prospective	RPL≥ 3 times	≥1 live birth	21/26	Frozen semen	TUNEL	7
Coughlan et al. (20)	UK	Caucasian	Prospective	RPL≥ 3 times	≥1 live birth	16/7	Fresh semen	SCD	8
Eisenberg et al. (30)	USA	Caucasian	Prospective	RPL≥ 2times	Currently pregnant	14/246	Frozen semen	SCSA	9
Gil-villa et al. (31)	USA	Caucasian	Prospective	RPL≥ 2times	≥1 live birth	23/11	Frozen semen	SCSA	7
Imam et al. (32)	India	Asian	Retrospective	RPL≥ 3 times	≥1 live birth	20/20	Frozen semen	SCSA	8
Kamkar et al. (27)	Iran	Asian	Retrospective	RPL≥ 2times	≥1 live birth	42/42	Frozen semen	SCSA and TUNEL	7
Khadem et al. (21)	Iran	Asian	Prospective	RPL≥ 3 times	Currently pregnant	30/30	Fresh semen	SCD	8
Kumar et al. (33)	India	Asian	Prospective	RPL≥ 3 times	≥1 live birth	45/20	Frozen semen	SCSA	7
Ribas-Maynou et al. (22)	Spain	Caucasian	Prospective	RPL≥ 2times	≥1 live birth	20/25	Frozen semen	SCD	8
Ruixue et al. (36)	China	Asian	Prospective	RPL≥ 3 times	Currently pregnant	68/63	Fresh semen	AB staining	7
Venkatesh et al. (34)	India	Asian	Prospective	RPL≥ 3times	≥1 live birth	16/20	Frozen semen	SCSA	7
Zhang et al. (23)	China	Asian	Prospective	RPL≥ 2times	≥1 live birth	111/30	Fresh semen	SCD	7
Zhu et al. (35)	China	Asian	Retrospective	RPL≥ 2times	Fertile	461/411	Fresh semen	SCSA	8
Zidi-Jrah et al. (28)	Tunisia	African	Prospective	RPL≥ 2times	≥1 live birth	22/20	Frozen semen	TUNEL	7

SCSA, sperm chromatin structure assay; SCD, sperm chromatin dispersion; TUNEL, terminal TdT-mediated dUTP-nick-end labeling; AOT, acridine orange test; AB staining, aniline blue staining.

RESULTS

Selection of Publications

Figure 1 shows the selection process of eligible publications. Based on our search strategy, 280 publications were initially identified through a database search. A total of 249 titles and abstracts of publications were reviewed after removing 31 duplicates. After screening the titles and abstracts of publications, 26 potentially relevant publications were found. The remaining publications were retrieved for full-text assessment. After full-text assessment of the remaining publications, 7 publications were excluded for various reasons. A total of 19 publications were finally included in the meta-analysis, which involved 2413 subjects (1182 couples with unexplained RM and 1231 couples without RM).

Characteristics of the Eligible Publications

Table 1 presents the main characteristics of the eligible publications. All included articles were of relatively high quality. None of the couples had received assisted reproductive treatments. Male partners of couples without unexplained RM had proven natural fertility with one or more live births. Female partners were under 40 years of age in all eligible studies. Female partners had normal ovarian function and a normal uterus (demonstrated by hysteroscopy, hysterosalpingography, and/or hysterosonography). Female partners with any of the following were excluded: abnormal karyotypes and uterine structural abnormalities.

Relation Between Traditional Semen Parameters and Unexplained RM

Sixteen studies explored the relation between traditional semen parameters and unexplained RM. For all eligible studies, the evaluation of traditional semen parameters was performed in fresh semen samples. The pooled results showed that there were no relations between unexplained RM and semen volume (WMD=-0.12, 95% CI=-0.32 to 0.08, P>0.05), sperm concentration (WMD=-2.28, 95% CI=-4.58 to 0.02, P>0.05), and total sperm count (WMD=-10.73, 95% CI=-22.11 to 0.66,

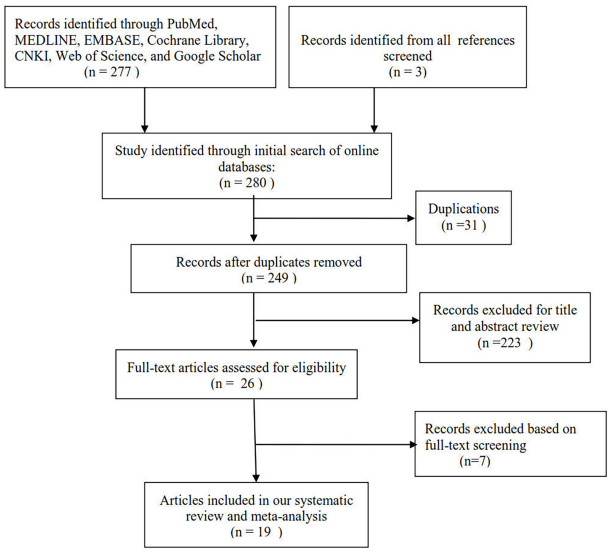

FIGURE 1 | Selection process for eligible publications.

P>0.05) (**Figure 2**). However, the pooled results showed that there were significant relations between unexplained RM and progressive motility (WMD=-4.75, 95% CI=-8.35 to -1.15, *P*<0.05) and total motility (WMD=-10.30, 95% CI=-15.03 to -5.57, *P*<0.05) (**Figure 2**). Since significant heterogeneity was observed for the total and progressive motility (I^2 = 82.3%, *P*<0.001; I^2 = 99.4%, *P*<0.001), subgroup analyses were performed by the study design type, RM definition, and ethnicity to explore the source of heterogeneity (**Figure 2**). For the majority of the subgroups, the percentages of total and progressive motility were significantly lower in couples with unexplained RM than in couples without RM (**Figures 3A–F**).

Relation Between SDF and Unexplained RM

Seventeen studies explored the relations between SDF and unexplained RM. For 8 of these studies, SDF was assessed using fresh semen samples. The pooled results showed that couples with unexplained RM had significantly increased levels of SDF compared with couples without RM (WMD=8.45, 95% CI=1.48 to 15.42, *P*=0.018) (**Table 2** and **Figure 4**). Because significant heterogeneity was observed for SDF (I^2 = 99.4%, *P*<0.001), subgroup analyses were performed by the assay type, RM definition, and ethnicity to explore the source of heterogeneity (**Table 2** and **Figure 4**). Subgroup analysis by SDF assay also showed a significant association between couples with and without RM for the SCD assay (WMD=2.15, 95% CI=1.62 to 2.68, *P*<0.001) (**Table 2** and **Figure 4A**). The subgroup analysis by the definition of RM showed that couples with a history of RM ≥2 times and ≥3 times had significantly increased levels of SDF compared with couples without RM (WMD=11.22, 95% CI=1.26 to 21.19, *P*=0.027 and WMD=3.33, 95% CI=1.20 to 5.46, *P*=0.002) (**Table 2** and **Figure 4B**). The subgroup analysis by ethnicity also showed similar results to the overall analysis in the Asian subgroup (WMD=5.90, 95% CI=2.30 to 9.50, *P*=0.001) (**Table 2** and **Figure 4C**).

Sensitivity Analyses

The sensitivity analysis showed that the pooled results were stable and reliable (**Figure 5**).

Publication Bias

As shown in **Table 2** and **Figure 6**, our results showed that there was no publication bias for the semen volume, sperm concentration, total sperm count, progressive motility, total motility, and SDF.

DISCUSSION

RM affects approximately 1% of couples trying to conceive (5). In almost half of the cases of RM, the etiology of the affected couples remains unclear (1). The role of female factors in RM has been studied intensively, but the role of male factors has been less thoroughly investigated (6–8).

Some studies have reported that male partners of couples with unexplained RM had significantly decreased levels of semen volume (26) and progressive motility (19, 27, 31, 34, 35) compared with couples without RM, but significant differences were not observed in sperm concentration (19–21, 23–31, 33, 35, 36, 38), total sperm count (23, 24, 26, 27, 29, 30) and total motility (20, 21, 24, 36) between the two groups. Some studies reported that couples with unexplained RM had significantly increased levels of sperm concentration (34) and total motility (25, 27–29) compared with couples without RM, but significant differences were not observed in semen volume (21, 23, 25, 27, 28, 30–35) and progressive motility (23, 26, 29) between the two groups. The combined results of this meta-analysis showed that couples with unexplained RM had significantly decreased levels of progressive motility and total motility than those of couples without RM. The combined results demonstrate that women whose partners had a higher percentage of progressive motility and total motility were more likely to have a successful pregnancy while women whose partners had a lower percentage of progressive motility and total motility were less likely to conceive and/or more likely to experience pregnancy loss.

Marked between-study heterogeneity was observed for progressive motility and total motility, and it could not be ignored. Therefore, subgroup analyses by the study design type, RM definition, and ethnicity were performed to explore the source of heterogeneity. However, heterogeneity was still observed despite performing the subgroup analyses. Such heterogeneity may be explained by differences in age and number of participants, duration of sexual abstinence, ethnicity, lifestyle habits, laboratory techniques, etc.

However, approximately 15% of male factor infertility patients show normal parameters in their ejaculates (41), suggesting that conventional semen parameters are poor predictors of reproductive outcome and that a definitive diagnosis of male

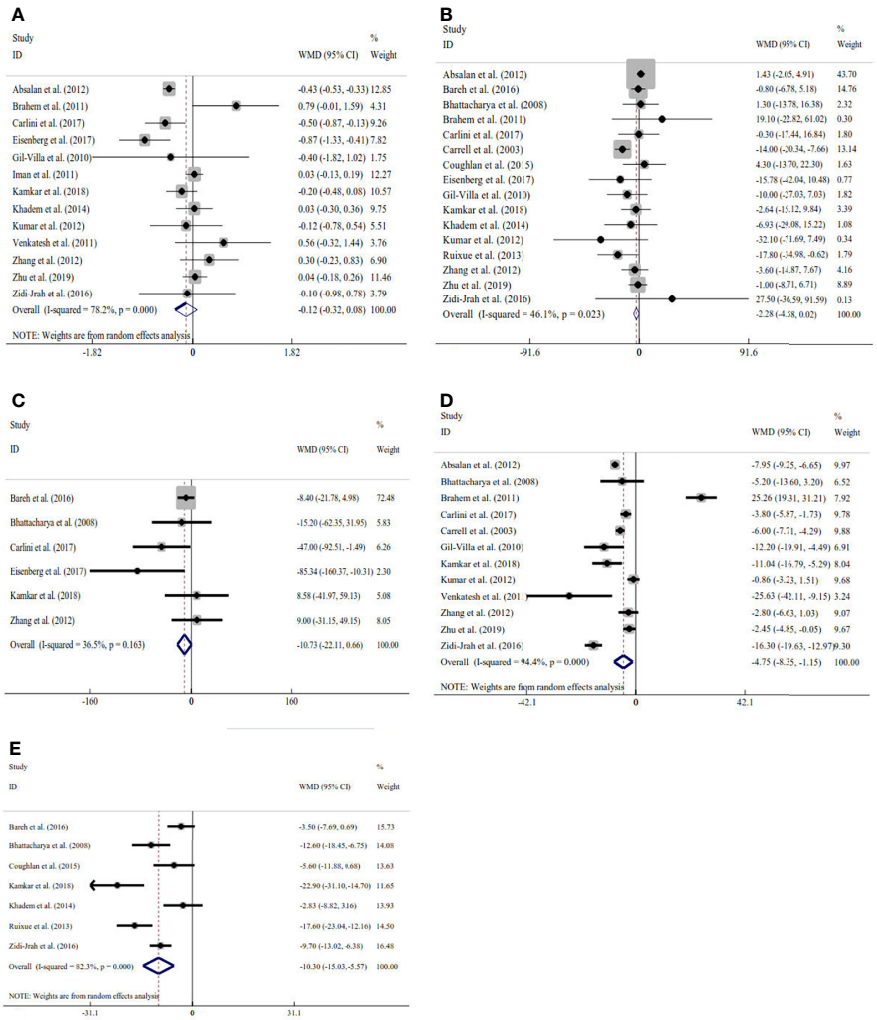

FIGURE 2 | Meta-analysis of the relations between traditional semen parameters and unexplained recurrent miscarriage. **(A)** Relation between volume and unexplained recurrent miscarriage; **(B)** relation between sperm concentration and unexplained recurrent miscarriage; **(C)** relation between total sperm count and unexplained recurrent miscarriage; **(D)** relation between progressive motility and unexplained recurrent miscarriage; and **(E)** relation between total motility and unexplained recurrent miscarriage.

infertility cannot be made by a routine semen analysis alone, which is because several factors other than conventional semen parameters affect the fertilization ability of spermatozoa.

Routine semen analysis does not assess all aspects of sperm quality. SDF is used to assess the integrity of sperm chromatin and may be a better predictor of male fertility and reproductive outcomes than conventional semen parameters. Sperm DNA integrity plays an important role in the initiation and maintenance of pregnancy (42). The study of sperm DNA integrity may be important for understanding the pathogenesis of unexplained RM. However, the relationship between sperm DNA integrity and unexplained RM remains controversial. Some studies (19, 20, 22, 24–29, 32, 33, 35, 36, 38) have reported that couples with unexplained RM had significantly increased levels of SDF compared with those of couples without RM. However, other studies (23, 30, 31) have reported no significant differences in SDF between couples with and without RM. For these studies, SDF was assessed using fresh or cryopreserved semen samples. The cryopreservation process can alter the sperm quality, particularly the motility and sperm DNA integrity (43–45). Only those studies that assessed SDF with fresh semen samples were included in this meta-analysis to evaluate the relationship between SDF and unexplained RM. The combined results of this meta-analysis demonstrated that couples with unexplained RM had significantly increased levels of SDF compared with couples without RM. Our results demonstrated that women whose partners had a lower percentage of SDF were more likely to have a successful pregnancy while women whose partners had a higher percentage of SDF were more likely to experience pregnancy loss. Our results also suggested that male factors may be involved in the pathogenesis of RM and that SDF might be used as a tool to evaluate the risk of RM. However, future large

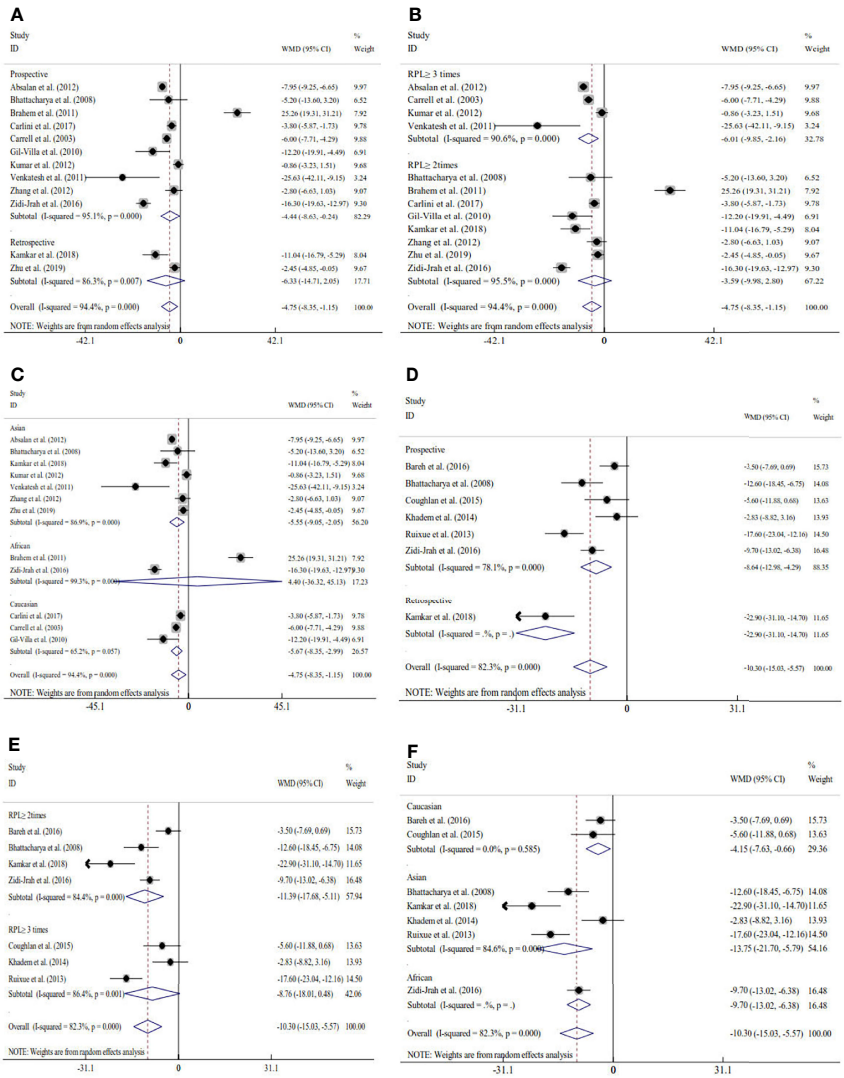

FIGURE 3 | Subgroup analyses for progressive motility by the type of study design **(A)**, definition of recurrent miscarriage **(B)**, and ethnicity **(C)**; subgroup analyses for total motility by type of study design **(D)**, definition of recurrent miscarriage **(E)**, and ethnicity **(F)**.

TABLE 2 | Subgroup analyses by sperm DNA fragmentation assay, definition of recurrent miscarriage, sperm preservation and ethnicity.

Outcomes	*N*	Model used	Heterogeneity		Pooled WMD		Begg's test *P*
			I^2 (%)	*P* value	WMD (95 CI)	*P* value	
Assay							
SCD	3	Fixed-effects	0.0	0.606	2.15 (1.62 to 2.68)	<0.001	
TUNEL	2	Random-effects	99.7	<0.001	16.70 (-4.27 to 37.68)	0.118	
AOT	1	NA	NA	NA	NA	NA	
SCSA	1	NA	NA	NA	NA	NA	
AB staining	1	NA	NA	NA	NA	NA	
Overall	8	Random-effects	99.4	<0.001	8.45 (1.48 to 15.42)	0.018	1.000
Definition of RPL							
RPL≥3 times	3	Random-effects	61.3	0.0076	3.33 (1.20 to 5.46)	0.002	
RPL≥2 times	5	Random-effects	99.4	<0.001	11.22 (1.26 to 21.19)	0.027	
Overall	8	Random-effects	99.4	<0.001	8.45 (1.48 to 15.42)	0.018	1,000
Ethnicity							
Asian	5	Random-effects	95.6	<0.001	5.90 (2.30 to 9.50)	0.001	
Caucasian	3	Random-effects	99.6	<0.001	12.40 (-3.89 to 28.69)	0.136	
Overall	8	Random-effects	99.4	<0.001	8.45 (1.48 to 15.42)	0.018	1.000

prospective studies are needed to evaluate the impact of elevated SDF on the risk of RM.

Marked between-study heterogeneity was observed, and it could not be ignored. Several factors may account for the measured heterogeneity. First, there are several methods used to assess SDF. Second, there are two definitions of unexplained RM. Third, the subjects included in the studies were of diverse ethnic backgrounds. All of these factors may have significantly affected the between-study heterogeneity. Subgroup analyses by the assay type, RM definition, and ethnicity were performed to explore the source of heterogeneity. However, heterogeneity was still observed despite performing these subgroup analyses. The results of the subgroups by the definition of RM showed that the couples with a history of RM≥2 times and ≥3 times had significantly increased levels of SDF. Given the limited sample size of the included studies and the significant heterogeneity between studies, further large prospective cohort studies are needed to validate these findings.

There were four strengths of this meta-analysis. First, more reliable results can be obtained as a result of the large sample size. Second, we also assessed the relation between traditional semen parameters and unexplained RM. Third, the subgroup analyses by the assay type, RM definition, and ethnicity were also conducted in this study. Fourth, no publication bias was found in this meta-analysis.

This meta-analysis has two limitations. First, between-study heterogeneity was found despite using strict inclusion/exclusion criteria. Second, the number of included publications was small in some subgroups.

Couples with unexplained RM had significantly increased levels of SDF compared with couples without RM, and they also had significantly decreased progressive motility and total motility. The SDF assay may be considered for inclusion in evaluations of couples with unexplained RM. Future large prospective studies are needed to evaluate the impact of elevated SDF on the risk of RM.

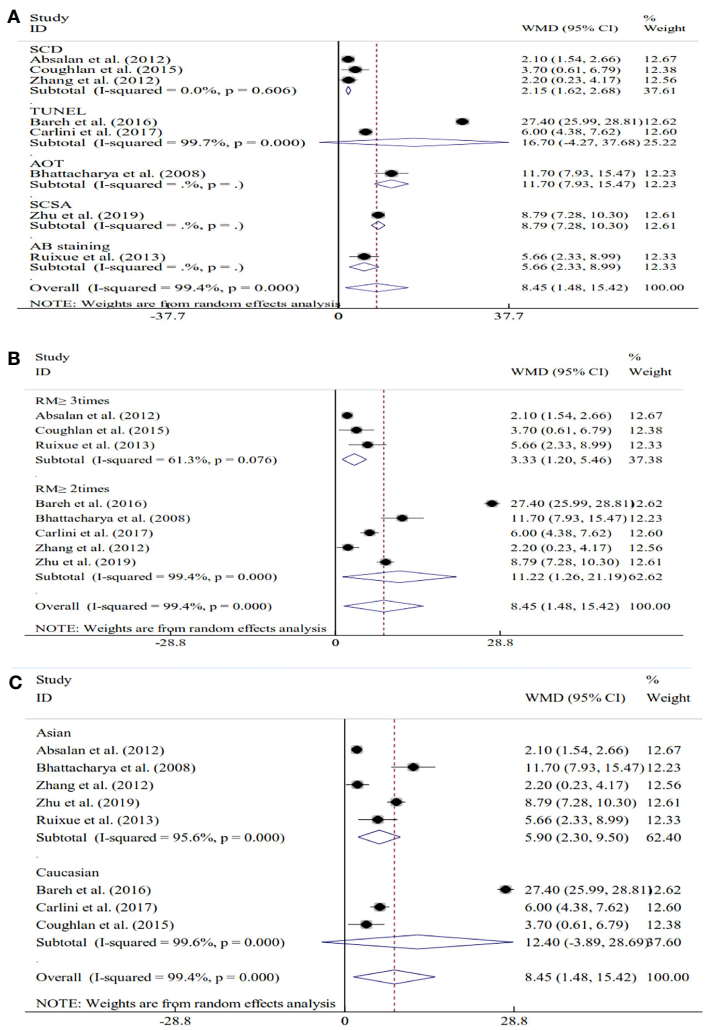

FIGURE 4 | Subgroup analyses based on the sperm DNA fragmentation assay **(A)**, the definition of recurrent miscarriage **(B)**, and ethnicity **(C)**.

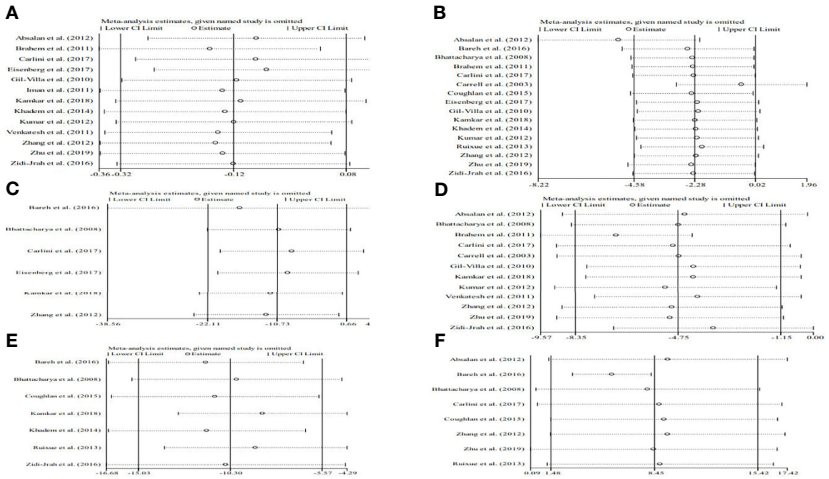

FIGURE 5 | Begg's funnel plot of the relationship among volume **(A)**, sperm concentration **(B)**, total sperm count **(C)**, progressive motility **(D)**, total motility **(E)**, and sperm DNA fragmentation **(F)** and unexplained recurrent miscarriage.

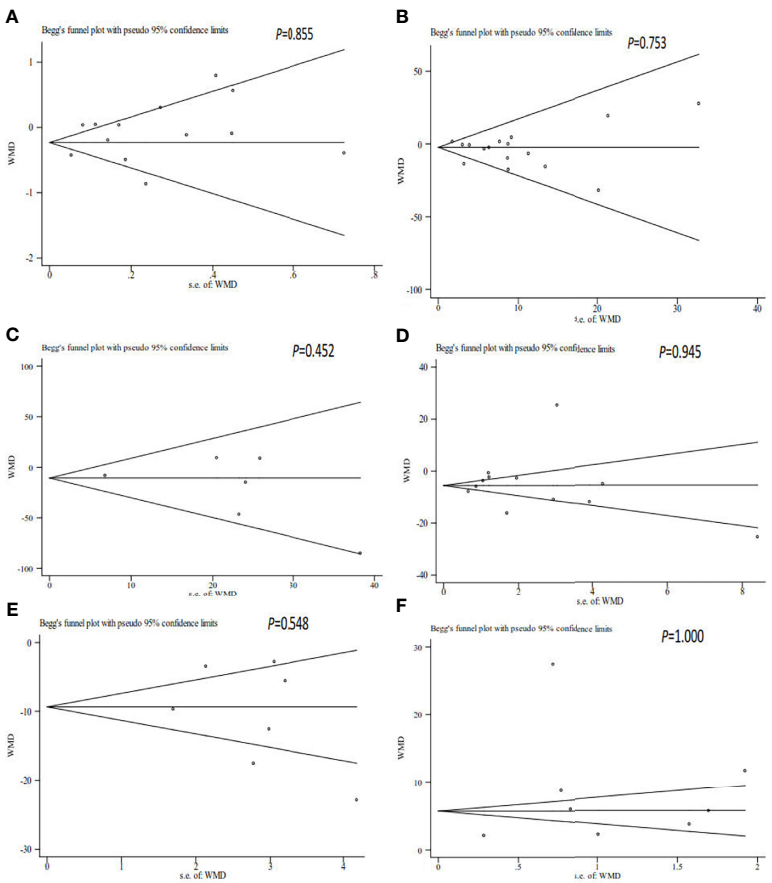

FIGURE 6 | Sensitivity analysis of the relationship among volume **(A)**, sperm concentration **(B)**, total sperm count **(C)**, progressive motility **(D)**, total motility **(E)**, and sperm DNA fragmentation **(F)** and unexplained recurrent miscarriage.

DATA AVAILABILITY STATEMENT

The original contributions presented in the study are included in the article/supplementary material. Further inquiries can be directed to the corresponding authors.

AUTHOR CONTRIBUTIONS

All authors contributed to the study's conception and design. YD and JL participated in drafting the manuscript and the study design. EY and YL searched and selected the relevant articles. YS and LZ contributed to the statistical analysis. All authors contributed to the article and approved the submitted version.

FUNDING

By Joint Construction Project of Henan Medical Science and Technology Research Plan (LHGJ20190396).

REFERENCES

1. Practice Committee of the American Society for Reproductive Medicine. Evaluation and Treatment of Recurrent Pregnancy Loss: A Committee Opinion. *Fertil Steril* (2012) 98(5):1103–11. doi: 10.1016/j.fertnstert.2012.06.048
2. Royal College of Obstetricians and Gynecologists. The Investigation and Treatment of Couples With Recurrent First-Trimester and Second-Trimester Miscarriage. *RCOG Green-top Guideline* (2011) 17:1–18.
3. Obstetrics Subgroup Chinese Society of Obstetrics and Gynecology. Chinese Expert Consensus on the Diagnosis and Tretment of Recurrent Spontaneous Abortion]. *Zhonghua Fu Chan Ke Za Zhi* (2016) 51(1):3–9. doi: 10.3760/cma.j.issn.0529-567X.2016.01.002
4. Bender Atik R, Christiansen OB, Elson J, Kolte AM, Lewis S, Middeldorp S, et al. ESHRE Guideline: Recurrent Pregnancy Loss. *Hum Reprod Open* (2018) 2018(2):1–12. doi: 10.1093/hropen/hoy004
5. Porter TF, Scott JR. Evidence-Based Care of Recurrent Miscarriage. *Best Pract Res Clin Obstet Gynaecol* (2005) 19(1):85–101. doi: 10.1016/j.bpobgyn.2004.11.005
6. Kumar N, Singh AK. Trends of Male Factor Infertility, an Important Cause of Infertility: A Review of Literature. *J Hum Reprod Sci* (2015) 8(4):191–6. doi: 10.4103/0974-1208.170370
7. Puscheck EE, Jeyendran RS. The Impact of Male Factor on Recurrent Pregnancy Loss. *Curr Opin Obstet Gynecol* (2007) 19(3):222–8. doi: 10.1097/GCO.0b013e32813e3ff0
8. Nanassy L, Carrell DT. Paternal Effects on Early Embryogenesis. *J Exp Clin Assist Reprod* (2008) 5:2. doi: 10.1186/1743-1050-5-2
9. Lewis SE. Is Sperm Evaluation Useful in Predicting Human Fertility? *Reproduction* (2007) 134(1):31–40. doi: 10.1530/REP-07-0152
10. Schulte RT, Ohl DA, Sigman M, Smith GD. Sperm DNA Damage in Male Infertility: Etiologies, Assays, and Outcomes. *J Assist Reprod Genet* (2010) 27(1):3–12. doi: 10.1007/s10815-009-9359-x
11. Bungum M, Bungum L, Lynch KF, Wedlund L, Humaidan P, Giwercman A. Spermatozoa DNA Damage Measured by Sperm Chromatin Structure Assay (SCSA) and Birth Characteristics in Children Conceived by IVF and ICSI. *Int J Androl* (2012) 35(4):485–90. doi: 10.1111/j.1365-2605.2011.01222.x
12. Agarwal A, Majzoub A, Esteves SC, Ko E, Ramasamy R, Zini A. Clinical Utility of Sperm DNA Fragmentation Testing: Practice Recommendations Based on Clinical Scenarios. *Transl Androl Urol* (2016) 5(6):935–50. doi: 10.21037/tau.2016.10.03
13. Evenson DP, Wixon R. Data Analysis of Two In Vivo Fertility Studies Using Sperm Chromatin Structure Assay-Derived DNA Fragmentation Index vs. Pregnancy Outcome. *Fertil Steril* (2008) 90(4):1229–31. doi: 10.1016/j.fertnstert.2007.10.066
14. Simon L, Lewis SE. Sperm DNA Damage or Progressive Motility: Which One Is the Better Predictor of Fertilization *In Vitro*? *Syst Biol Reprod Med* (2011) 57(3):133–8. doi: 10.3109/19396368.2011.553984
15. Velez de la Calle JF, Muller A, Walschaerts M, Clavere JL, Jimenez C, Wittemer C, et al. Sperm Deoxyribonucleic Acid Fragmentation as Assessed by the Sperm Chromatin Dispersion Test in Assisted Reproductive Technology Programs: Results of a Large Prospective Multicenter Study. *Fertil Steril* (2008) 90(5):1792–9. doi: 10.1016/j.fertnstert.2007.09.021
16. Gandini L, Lombardo F, Paoli D, Caruso F, Eleuteri P, Leter G, et al. Full-Term Pregnancies Achieved With ICSI Despite High Levels of Sperm Chromatin Damage. *Hum Reprod* (2004) 19(6):1409–17. doi: 10.1093/humrep/deh233
17. Niu ZH, Shi HJ, Zhang HQ, Zhang AJ, Sun YJ, Feng Y. Sperm Chromatin Structure Assay Results After Swim-Up Are Related Only to Embryo Quality But Not to Fertilization and Pregnancy Rates Following IVF. *Asian J Androl* (2011) 13(6):862–6. doi: 10.1038/aja.2011.77
18. Bungum M, Humaidan P, Axmon A, Spano M, Bungum L, Erenpreiss J, et al. Sperm DNA Integrity Assessment in Prediction of Assisted Reproduction Technology Outcome. *Hum Reprod* (2007) 22(1):174–9. doi: 10.1093/humrep/del326
19. Absalan F, Ghannadi A, Kazerooni M, Parifar R, Jamalzadeh F, Amiri S. Value of Sperm Chromatin Dispersion Test in Couples With Unexplained Recurrent Abortion. *J Assist Reprod Genet* (2012) 29(1):11–4. doi: 10.1007/s10815-011-9647-0
20. Coughlan C, Clarke H, Cutting R, Saxton J, Waite S, Ledger W, et al. Sperm DNA Fragmentation, Recurrent Implantation Failure and Recurrent Miscarriage. *Asian J Androl* (2015) 17(4):681–5. doi: 10.4103/1008-682X.144946
21. Khadem N, Poorhoseyni A, Jalali M, Akbary A, Heydari ST. Sperm DNA Fragmentation in Couples With Unexplained Recurrent Spontaneous Abortions. *Andrologia* (2014) 46(2):126–30. doi: 10.1111/and.12056
22. Ribas-Maynou J, Garcia-Peiro A, Fernandez-Encinas A, Amengual MJ, Prada E, Cortes P, et al. Double Stranded Sperm DNA Breaks, Measured by Comet Assay, Are Associated With Unexplained Recurrent Miscarriage in Couples Without a Female Factor. *PloS One* (2012) 7(9):e44679. doi: 10.1371/journal.pone.0044679
23. Zhang L, Wang L, Zhang X, Xu G, Zhang W, Wang K, et al. Sperm Chromatin Integrity may Predict Future Fertility for Unexplained Recurrent Spontaneous Abortion Patients. *Int J Androl* (2012) 35(5):752–7. doi: 10.1111/j.1365-2605.2012.01276.x
24. Bareh GM, Jacoby E, Binkley P, Chang TC, Schenken RS, Robinson RD. Sperm Deoxyribonucleic Acid Fragmentation Assessment in Normozoospermic Male Partners of Couples With Unexplained Recurrent Pregnancy Loss: A Prospective Study. *Fertil Steril* (2016) 105(2):329–36 e1. doi: 10.1016/j.fertnstert.2015.10.033
25. Brahem S, Mehdi M, Landolsi H, Mougou S, Elghezal H, Saad A. Semen Parameters and Sperm DNA Fragmentation as Causes of Recurrent Pregnancy Loss. *Urology* (2011) 78(4):792–6. doi: 10.1016/j.urology.2011.05.049
26. Carlini T, Paoli D, Pelloni M, Faja F, Dal Lago A, Lombardo F, et al. Sperm DNA Fragmentation in Italian Couples With Recurrent Pregnancy Loss. *Reprod BioMed Online* (2017) 34(1):58–65. doi: 10.1016/j.rbmo.2016.09.014
27. Kamkar N, Ramezanali F, Sabbaghian M. The Relationship Between Sperm DNA Fragmentation, Free Radicals and Antioxidant Capacity With Idiopathic Repeated Pregnancy Loss. *Reprod Biol* (2018) 18(4):330–5. doi: 10.1016/j.repbio.2018.11.002
28. Zidi-Jrah I, Hajlaoui A, Mougou-Zerelli S, Kammoun M, Meniaoui I, Sallem A, et al. Relationship Between Sperm Aneuploidy, Sperm DNA Integrity, Chromatin Packaging, Traditional Semen Parameters, and Recurrent Pregnancy Loss. *Fertil Steril* (2016) 105(1):58–64. doi: 10.1016/j.fertnstert.2015.09.041

29. Bhattacharya SM. Association of Various Sperm Parameters With Unexplained Repeated Early Pregnancy Loss–Which Is Most Important? *Int Urol Nephrol* (2008) 40(2):391–5. doi: 10.1007/s11255-007-9282-y
30. Eisenberg ML, Sapra KJ, Kim SD, Chen Z, Buck Louis GM. Semen Quality and Pregnancy Loss in a Contemporary Cohort of Couples Recruited Before Conception: Data From the Longitudinal Investigation of Fertility and the Environment (LIFE) Study. *Fertil Steril* (2017) 108(4):613–9. doi: 10.1016/j.fertnstert.2017.07.008
31. Gil-Villa AM, Cardona-Maya W, Agarwal A, Sharma R, Cadavid A. Assessment of Sperm Factors Possibly Involved in Early Recurrent Pregnancy Loss. *Fertil Steril* (2010) 94(4):1465–72. doi: 10.1016/j.fertnstert.2009.05.042
32. Imam SN, Shamsi MB, Kumar K, Deka D, Dada R. Idiopathic Recurrent Pregnancy Loss: Role of Paternal Factors; A Pilot Study. *J Reprod Infertil* (2011) 12(4):267–76.
33. Kumar K, Deka D, Singh A, Mitra DK, Vanitha BR, Dada R. Predictive Value of DNA Integrity Analysis in Idiopathic Recurrent Pregnancy Loss Following Spontaneous Conception. *J Assist Reprod Genet* (2012) 29(9):861–7. doi: 10.1007/s10815-012-9801-3
34. Venkatesh S, Thilagavathi J, Kumar K, Deka D, Talwar P, Dada R. Cytogenetic, Y Chromosome Microdeletion, Sperm Chromatin and Oxidative Stress Analysis in Male Partners of Couples Experiencing Recurrent Spontaneous Abortions. *Arch Gynecol Obstet* (2011) 284 (6):1577–84. doi: 10.1007/s00404-011-1990-y
35. Zhu XB, Chen Q, Fan WM, Niu ZH, Xu BF, Zhang AJ. Sperm DNA Fragmentation in Chinese Couples With Unexplained Recurrent Pregnancy Loss. *Asian J Androl* (2019) 22(3):296–301. doi: 10.4103/aja.aja_60_19
36. Ruixue W, Hongli Z, Zhihong Z, Rulin D, Dongfeng G, Ruizhi L. The Impact of Semen Quality, Occupational Exposure to Environmental Factors and Lifestyle on Recurrent Pregnancy Loss. *J Assist Reprod Genet* (2013) 30 (11):1513–8. doi: 10.1007/s10815-013-0091-1
37. Moher D, Liberati A, Tetzlaff J, Altman DG. Preferred Reporting Items for Systematic Reviews and Meta-Analyses: The PRISMA Statement. *BMJ* (2009) 339:b2535. doi: 10.1136/bmj.b2535
38. Carrell DT, Liu l, Peterson CM, Jones KP, Hatasaka HH, Erickson L, et al. Sperm DNA Fragmentation Is Increased in Couples With Unexplained Recurrent Pregnancy Loss. *Arch Androl* (2003) 49(1):49–55. doi: 10.1080/01485010290099390
39. Stang A. Critical Evaluation of the Newcastle-Ottawa Scale for the Assessment of the Quality of Nonrandomized Studies in Meta-Analyses. *Eur J Epidemiol* (2010) 25(9):603–5. doi: 10.1007/s10654-010-9491-z
40. Deng C, Li T, Xie Y, Guo Y, Yang QY, Liang X, et al. Sperm DNA Fragmentation Index Influences Assisted Reproductive Technology Outcome: A Systematic Review and Meta-Analysis Combined With a Retrospective Cohort Study. *Andrologia* (2019) 51(6):13263. doi: 10.1111/and.13263
41. Agarwal A, Allamaneni SS. Sperm DNA Damage Assessment: A Test Whose Time has Come. *Fertil Steril* (2005) 84(4):850–3. doi: 10.1016/j.fertnstert.2005.03.080
42. Agarwal A, Zini A, Sigman M. Is Sperm DNA Integrity Assessment Useful? *J Urol* (2013) 190(5):1645–7. doi: 10.1016/j.juro.2013.08.004
43. Raad G, Lteif L, Lahoud R, Azoury J, Azoury J, Tanios J, et al. Cryopreservation Media Differentially Affect Sperm Motility, Morphology and DNA Integrity. *Andrology* (2018) 6(6):836–45. doi: 10.1111/andr.12531
44. Lusignan MF, Li X, Herrero B, Delbes G, Chan PTK. Effects of Different Cryopreservation Methods on DNA Integrity and Sperm Chromatin Quality in Men. *Andrology* (2018) 6(6):829–35. doi: 10.1111/andr.12529
45. Zribi N, Chakroun N, Ben Abdallah F, Elleuch H, Sellami A, Gargouri J, et al. Effect of Freezing-Thawing Process and Quercetin on Human Sperm Survival and DNA Integrity. *Cryobiology* (2012) 65(3):326–31. doi: 10.1016/j.cryobiol.2012.09.003

Conflict of Interest: The authors declare that the research was conducted in the absence of any commercial or financial relationships that could be construed as a potential conflict of interest.

Publisher's Note: All claims expressed in this article are solely those of the authors and do not necessarily represent those of their affiliated organizations, or those of the publisher, the editors and the reviewers. Any product that may be evaluated in this article, or claim that may be made by its manufacturer, is not guaranteed or endorsed by the publisher.

frontiers in Physiology

ORIGINAL RESEARCH
published: 25 January 2022
doi: 10.3389/fphys.2021.819856

Glufosinate-Ammonium Induced Aberrant Histone Modifications in Mouse Sperm Are Concordant With Transcriptome in Preimplantation Embryos

Xuan Ma[1,2†], Yun Fan[1,2,3†], Wenwen Xiao[1,2†], Xingwang Ding[1,2], Weiyue Hu[1,4] and Yankai Xia[1,2*]*

[1] State Key Laboratory of Reproductive Medicine, Center for Global Health, School of Public Health, Nanjing Medical University, Nanjing, China, [2] Key Laboratory of Modern Toxicology of Ministry of Education, School of Public Health, Nanjing Medical University, Nanjing, China, [3] Department of Microbes and Infection, School of Public Health, Nanjing Medical University, Nanjing, China, [4] Department of Nutrition and Food Safety, School of Public Health, Nanjing Medical University, Nanjing, China

OPEN ACCESS

Edited by:
Md. Saidur Rahman,
Chung-Ang University, South Korea

Reviewed by:
Huan Shen,
Peking University, China
Elikanah Olusayo Adegoke,
Chung-Ang University, South Korea

****Correspondence:***
Yankai Xia
yankaixia@njmu.edu.cn
Weiyue Hu
weiyuehu@njmu.edu.cn

[†] These authors have contributed equally to this work and share first authorship

Specialty section:
This article was submitted to Reproduction, a section of the journal Frontiers in Physiology

Received: *22 November 2021*
Accepted: *31 December 2021*
Published: *25 January 2022*

Citation:
Ma X, Fan Y, Xiao W, Ding X, Hu W and Xia Y (2022) Glufosinate-Ammonium Induced Aberrant Histone Modifications in Mouse Sperm Are Concordant With Transcriptome in Preimplantation Embryos. Front. Physiol. 12:819856. doi: 10.3389/fphys.2021.819856

Glufosinate-ammonium (GLA) is a widely used herbicide with emerging concern over its male reproductive toxicity. Abnormalities in sperm histone modification induced by GLA exposure observed in our previous study aroused our interest in whether such alterations could further affect embryonic gene expression. Here we administered adult male mice with 0.2 mg/kg·day of GLA for 5 weeks to collect their sperm or 4-cell embryos after copulation. Cleavage Under Targets and Tagmentation (CUT&Tag) sequencing showed alterations of sperm H3 lysine 4 trimethylation (H3K4me3) and histone H3 lysine 27 acetylation (H3K27ac), which are active histone modification marks involved in embryo development, while RNA sequencing identified differentially expressed genes in 4-cell embryos. Differentially H3K4me3 and H3K27ac occupied regions were mainly distributed at the gene promoters and putative enhancers, and were enriched in pathways related to the immune system and nervous system. Integrative analysis of these sequencing data showed that genes such as *Mgl2* with increased H3K4me3 and H3K27ac in sperm were up-regulated in embryos, and *vice versa* for genes such as *Dcn*. Additionally, differentially occupied H3K4me3 and H3K27ac in sperm were linked to gene expression changes in both paternal and maternal alleles of 4-cell embryos. In conclusion, GLA-induced changes in sperm H3K4me3 and H3K27ac are concordant with gene expression in preimplantation embryos, which might further affect embryo development and offspring health.

Keywords: glufosinate-ammonium, H3K4me3, H3K27ac, sperm, embryo development

INTRODUCTION

Histones consisting of H2A, H2B, H3, and H4 are proteins that are critical in the packing of DNA into the cell. Lysine residues in N-terminal tails of histone H3 are the major targets for post-translational modifications (PTMs) such as methylation and acetylation, which are closely associated with gene transcription activities (Yan and Boyd, 2006). Unlike somatic cells, most

histones are replaced by protamines for condensed packaging of DNA during spermatogenesis, and only 1% histones are retained in mature mouse sperm (Siklenka et al., 2015). Although limited in quantity, the retained histones in sperm bearing abundant modifications are still essential in male reproduction (Liu et al., 2019), embryo development (Hammoud et al., 2009; Yoshida et al., 2018) and offspring health (Siklenka et al., 2015). Notably, histone H3 lysine 4 trimethylation (H3K4me3) and histone H3 lysine 27 acetylation (H3K27ac) have been well established as active promoter and enhancer marks respectively (Calo and Wysocka, 2013). It is reported that regions marked with H3K4me3 in sperm are mainly enriched at fertility and development related genes, and parts of them can be transmitted into embryos (Zhang et al., 2016; Lismer et al., 2020; Lambrot et al., 2021). Similarly, sperm H3K27ac is highly associated with *in vivo* fertility (Kutchy et al., 2018) and 3D chromatin architecture in embryos (Wike et al., 2021). Therefore, both sperm H3K4me3 and H3K27ac are essential for fertility and embryo development.

Sperm histone modifications are susceptible to environmental factors, such as diet (Carone et al., 2010; Lismer et al., 2021) and chemical exposures (Lombó and Herráez, 2021), leading to potential adverse outcome of offspring health from embryonic to adult stage. For example, sperm H3K4me3 at putative enhancers of developmental genes was altered by a folate-deficient diet, and then transmitted to preimplantation embryos resulting in deregulated embryonic gene expression (Lismer et al., 2021). For chemical exposures, paternal bisphenol A (BPA) exposure increased histone H3 lysine 9 acetylation (H3K9ac) and H3K27ac in zebrafish sperm, and further impaired heart development in progeny (Lombó et al., 2019; Lombó and Herráez, 2021). More findings are required to support the link between environmental factors-induced sperm H3K4me3/H3K27ac alterations and preimplantation embryos.

Glufosinate-ammonium (GLA), one of the most widely applied broad-spectrum herbicides, is highly hydrophilic and considered safe when properly used (Takano and Dayan, 2020). However, emerging evidence suggests its potential toxicity. An *in vivo* study on lizards observed GLA-induced severe testis lesions by oxidative damage (Zhang et al., 2019), while an *in vitro* study on human sperm recently revealed its impairment on sperm mitochondria respiration efficiency (Ferramosca et al., 2021), which indicates GLA toxicity on male reproduction. Our previous study (Ma et al., 2021) also showed its effects on male reproductive health with significantly altered DNA methylation, histone H3 lysine 27 trimethylation (H3K27me3) and histone H3 lysine 9 trimethylation (H3K9me3), as well as transcriptome in mouse sperm. The impact of GLA exposure on sperm histone modifications and transcriptome raised our awareness on its potential risks for embryo development, whereas no other data has shown such the risk to date. Given the role of sperm H3K4me3 and H3K27ac in gene transcription and embryo development, we hypothesized that GLA exposure would affect these two epigenetic marks in sperm, and thus disrupt embryonic gene expression.

In this study, after administration of GLA at a dose of 0.2 mg/kg·day to adult male mice for 5 weeks, we performed Cleavage Under Targets & Tagmentation (CUT&Tag) to demonstrate genome-wide H3K4me3 and H3K27ac profiles in sperm, and RNA sequencing (RNA-seq) to display transcriptome in 4-cell embryos derived from GLA exposed male mice. By integrating these sequencing data, we tried to answer whether GLA exposure affects H3K4me3 and H3K27ac profiles of sperm and transcriptome of preimplantation embryos.

MATERIALS AND METHODS

Animals and Glufosinate-Ammonium Administration

C57BL/6J male mice aged 6–8 weeks (purchased from Animal Core Facility of Nanjing Medical University) were housed in a constant environment, and they were randomly divided into two groups either for the control (CON) or GLA treatment after 1-week acclimation. The CON group had free access to ultrapure water, while the GLA group was treated with GLA (purity $\geq$ 98.0%; Sigma-Aldrich, 45520) through drinking water at a dose of 0.2 mg/kg·day, which was equivalent to the acceptable daily intake (ADI) of 0.01 mg/kg (JMPR, 2012) after conversion from human to mice (Nair and Jacob, 2016) and consistent with our previous study (Ma et al., 2021). Glass bottles of drinking water were renewed twice a week to keep the dose constant. After a 5-week administration, these male mice were mated with super-ovulated DBA/2 female mice (purchased from Beijing Vital River Laboratory Animal Technology Co., Ltd.) to obtain 4-cell embryos. GLA administration was continuous except during mating. Male mice were sacrificed for sperm collection once enough embryos were collected for further experiments. All animal procedures here were approved by the Institutional Animal Care and Use Committee (IACUC) of Nanjing Medical University (1811056–2).

Sperm Collection

After a successful mating within 1 week, male mice (n = 10 for each group) were sacrificed to collect mature sperm from bilateral cauda epididymidis as previously described (Sharma et al., 2016; Ma et al., 2021). Then, we counted 1,000 sperm under a microscope, and verified that the sperm purity was over 99.9%. Sperm from five mice were pooled as a biological replicate, and two biological replicates in each group were immediately subjected to the subsequent experiment.

CUT&Tag on Sperm and Library Preparation

To examine genome-wide H3K4me3 and H3K27ac enrichment on sperm DNA in the nucleus *in situ*, we performed chromatin profiling with CUT&Tag according to its latest protocol (Kaya-Okur et al., 2020). In brief, we permeabilized fresh sperm in ice-cold NE1 on ice for 10 min, followed by light crosslinking with formaldehyde to fix nuclei. Then, sperm nuclei bound to Concanavalin A-coated Magnetic Beads (Novoprotein Scientific Inc., N251). Next, H3K4me3 rabbit

pAb (1:100; PTM BIO, PTM-613) and H3K27ac rabbit pAb (1:100; PTM BIO, PTM-116) were employed as primary antibodies for nuclei binding, and Goat Anti-Rabbit IgG H&L (1:100; Abcam, ab6702) was used to bind primary antibodies. After binding pG-Tn5 adapter complex (1:100, Vazyme, S602), tagmentation was conducted, followed by DNA extraction with Phenol:Chloroform. After library preparation by PCR amplification (Vazyme, TD202 and TD601), DNA products were purified with Ampure XP beads (Beckman Coulter, A63881). After DNA quantification and qualification, all libraries were sequenced using NovaSeq, 6000 (Illumina, United States) by Beijing Novogene Bioinformatics Technology Co., Ltd., China.

CUT&Tag Data Processing

We conducted CUT&Tag data processing according to a step-by-step protocol described previously (Henikoff et al., 2020). In brief, all paired-end CUT&Tag reads after trimming were aligned to the mm10 genome using Bowtie2 v2.4.4 (Langmead and Salzberg, 2012). All unmapped reads, non-uniquely mapped reads and PCR duplicates were removed. Then, peaks and enriched regions typically for CUT&Tag profiling were called with SEACR v1.3 (Meers et al., 2019). Noisy peaks with very weak signals were removed in further analysis.

4-Cell Embryo Collection

To induce superovulation, 3–4-week-old DBA/2 female mice were intraperitoneally administered 5 IU of PMSG, followed by injection of 5 IU of hCG 48 h later. After injection of hCG, each female mouse was mated with one CON or GLA mice, and sacrificed 56 h after hCG administration to dissect its oviduct. Then, we flushed 4-cell embryos from oviducts with M2 medium. Embryos from three female mice were pooled as a biological replicate, and three biological replicates were contained in each group (n = 9). Embryos in M2 medium (at least 30 embryos in each replicate) were immediately used in the subsequent experiment.

RNA-Seq on 4-Cell Embryos and Library Preparation

To identify global mRNA transcripts in 4-cell embryos, we prepared cDNA library with Single Cell Full Length mRNA-Amplification Kit (Vazyme, N712) following manufacturer's instructions. In brief, embryos in M2 medium were washed in PBS and transferred to sample buffer for lysis. Then, reverse transcription of mRNA transcripts was conducted to obtain full length cDNA. Products of cDNA amplification were purified with Ampure XP beads (Beckman Coulter, A63881). Library preparation was performed with TruePrep^{TM} DNA Library Prep Kit V2 for Illumina (Vazyme, TD503) following manufacturer's instructions. After DNA quantification and qualification, all libraries were sequenced using NovaSeq, 6000 (Illumina, United States) by Beijing Novogene Bioinformatics Technology Co., Ltd., China.

RNA-Seq Data Processing

After trimming, all RNA-seq reads were aligned to the mm10 genome using STAR v2.7.6a (Dobin et al., 2013; Bray et al., 2016). All unmapped reads, multi-mapped reads and PCR duplicates were removed. By using FeatureCounts (Liao et al., 2014), aligned reads were counted against gene model annotation (Gencode.vM27). Differentially gene expression analysis was performed with an R package DESeq2 v1.34.0 (Love et al., 2014) with negative binomial generalized linear models.

Then, we determined parent-of-origin of uniquely aligned reads with SNPsplit v0.5.0 (Krueger and Andrews, 2016), and then summarized all SNP-containing reads for each gene for allele-specific expression analyses. Likewise, differential gene expression analysis was computed with the DESeq2 R package v1.34.0. Only genes with RPKM $>$ 1 in either group, P-value $<$ 0.05, and FoldChange $>$ 1.5 were considered as differentially expressed.

Bioinformatic Analysis

We merged replicates of each group for downstream analysis, normalized read counts into RPKM by counting the numbers of reads in each 100-bp bin and then summed these counts within each 2-kb window for the entire genome using deeptools2 v3.4.3 (Ramírez et al., 2016). Genome-wide visualization of CUT&Tag and RNA-seq signals were conducted with the Integrative Genomics Viewer (IGV). Additionally, R packages ChIPseeker v1.28.3 (Yu et al., 2015) and clusterProfiler v4.0.5 (Yu et al., 2012) were used for annotation and Gene Ontology (GO) enrichment analysis, respectively.

RESULTS

Cluster Characteristics of Integrated H3K4me3 and H3K27ac in CON Sperm

At first, we conducted CUT&Tag on sperm of the CON group and integrated H3K4me3 and H3K27ac data to display their physiological patterns (**Figure 1**). We performed genome-wide k-means clustering of H3K4me3 and H3K27ac regions, and then divided them into 4 clusters. As shown in **Figure 1A**-left, Cluster 1 to Cluster 4 are characterized by both strong signals, weak H3K4me3 and strong H3K27ac, strong H3K4me3 and weak H3K27ac, and both weak signals, respectively. Then, we categorized peaks of the first three clusters by their distances to the nearest transcription start sites (TSS) (**Figure 1A**-right). In general, the majority of peaks were located less than 1 kb from TSS, while those with strong H3K27ac signals in Cluster 2 were also found over 10 kb from TSS in intergenic regions.

To enable functional interpretation of distinct patterns of H3K4me3 and H3K27ac, we annotated peaks in Cluster 1–3 to their nearest genes and identified biological pathways by GO enrichment analysis (**Supplementary Table 1**). Results showed that genes with overlapped H3K4me3 and H3K27ac signals were mainly enriched in pathways such as myeloid cell differentiation, negative regulation of phosphorylation and autophagy (**Figure 1B**). Those predominantly bearing abundant

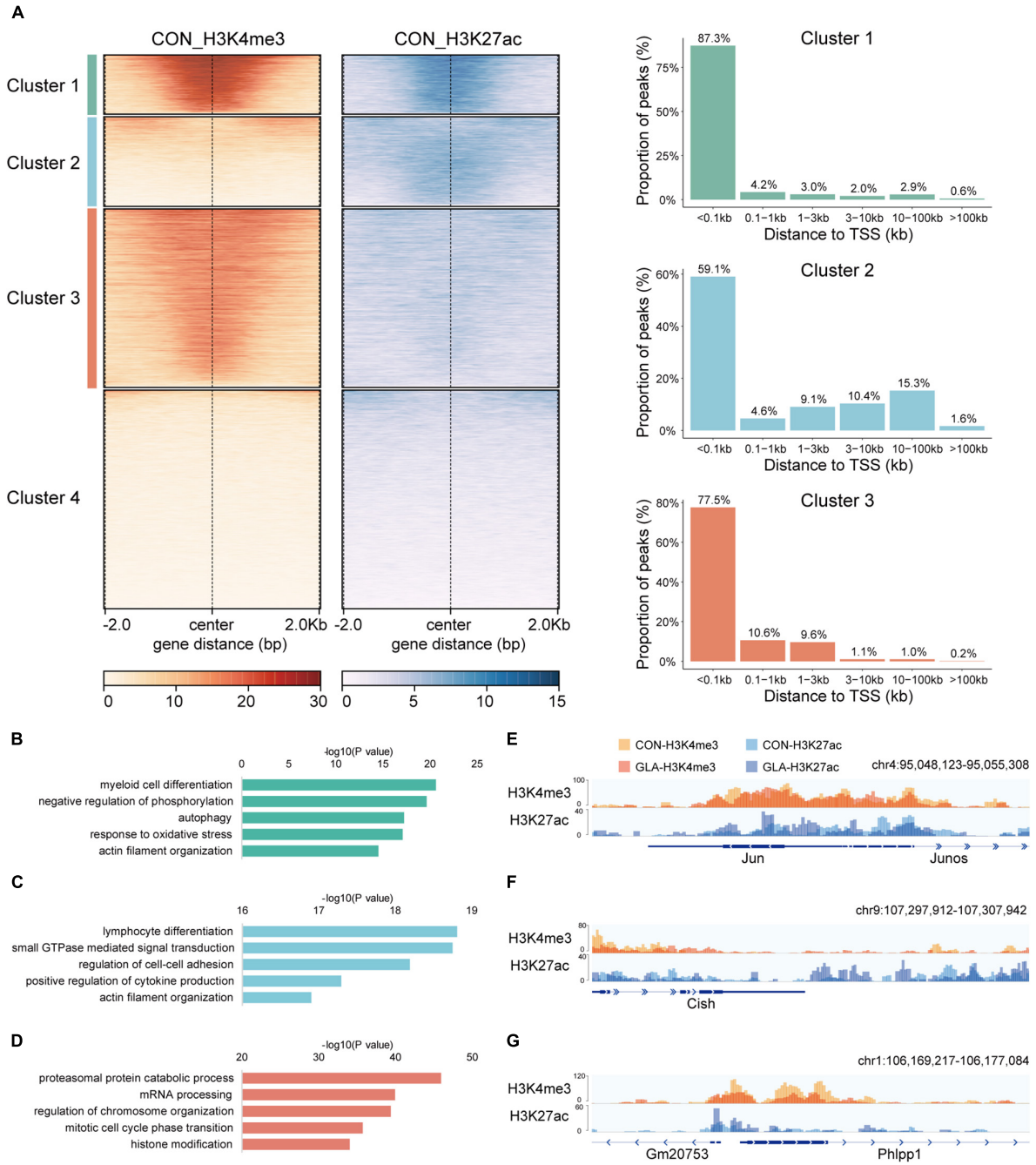

FIGURE 1 | Cluster characteristics of integrated H3K4me3 and H3K27ac in CON sperm. **(A)** Heatmap (left) of k-means clustering of genome-wide H3K4me3 and H3K27ac signals ± 2.0 kb the center of H3K4me3 and H3K27ac regions in CON sperm, and bar graph (right) showing distribution of regions in Cluster 1–3 relative to the nearest transcription start site (TSS). For each cluster, genes were arranged in order of decreasing signals from top to bottom. **(B–D)** Selected significant pathways from Gene Ontology analysis on genes from Cluster 1 **(B)**, Cluster 2 **(C)** and Cluster 3 **(D)** in CON sperm. **(E–G)** Integrative Genomics Viewer tracks showing H3K4me3 and H3K27ac signals on *Jun* **(E)** from Cluster 1, *Cish* **(F)** from Cluster 2 and *Phlpp1* **(G)** from Cluster 3 in CON and GLA sperm.

H3K27ac were enriched in pathways including GTPase signaling transduction and actin filament organization (**Figure 1C**). In addition, those with strong H3K4me3 signals in Cluster 3 were primarily enriched in mRNA and protein processing and chromosome organization (**Figure 1D**).

Next, we integrated H3K4me3 of CON and GLA sperm into one track, as well as H3K27ac of the two groups, and then zoomed in representative regions of these three clusters (**Figures 1E–G**). We found that overall GLA sperm had quite similar H3K4me3 and H3K27ac patterns with CON, while moderate intensity

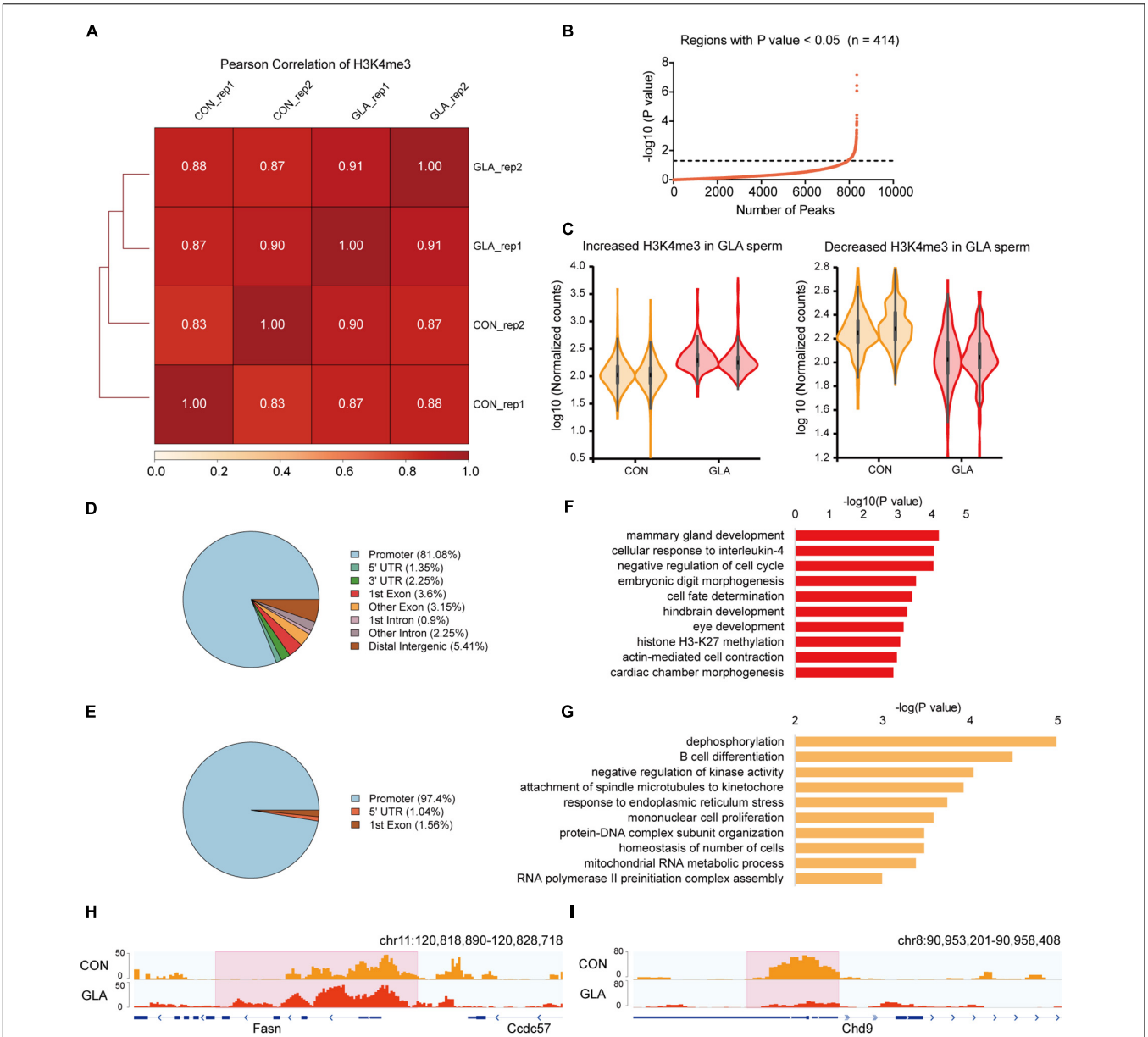

FIGURE 2 | GLA-induced H3K4me3 alterations in mouse sperm. **(A)** Correlation matrix showing Pearson correlation coefficient of H3K4me3 between replicates of CON and GLA sperm. **(B)** Selection of regions with *P*-value < 0.05. The black dashed line corresponds to the boundary of *P*-value = 0.05. **(C)** Violin plots showing increased and decreased H3K4me3 in GLA sperm. Two replicates in each group are in the same color. **(D,E)** Pie chart showing the genomic distribution of regions with increased **(D)** and decreased **(E)** H3K4me3 signals in GLA sperm. **(F,G)** Selected significant pathways from Gene Ontology analysis on genes with increased **(F)** or decreased **(G)** H3K4me3 signals in GLA sperm. **(H)** Integrative Genomics Viewer tracks showing increased H3K4me3 on *Fasn* in GLA sperm. **(I)** Integrative Genomics Viewer tracks showing decreased H3K4me3 on *Chd9* in GLA sperm. Pink box indicates regions with differential H3K4me3 signals (*P*-value < 0.05).

changes could still be observed in specific genomic loci such as decreased H3K4me3 in *Phlpp1* promoter of GLA sperm.

Glufosinate-Ammonium-Induced H3K4me3 and H3K27ac Alterations in Mouse Sperm

To assess whether GLA exposure would alter global profiles of H3K4me3 and H3K27ac in mouse sperm, we further analyzed their sequencing data separately. As for H3K4me3, Pearson correlation analysis showed that the correlation coefficients of H3K4me3 between each two replicates of CON and GLA sperm were over 0.83 (**Figure 2A**). Then we compared H3K4me3 levels between two groups and found 414 significantly differential peaks with a *P*-value < 0.05 (**Figures 2B,C** and **Supplementary Table 2**). Increased H3K4me3 occupied regions were primarily distributed in promoters (81.08%) and distal intergenic regions (5.41%) (**Figure 2D**), while most of decreased H3K4me3 were

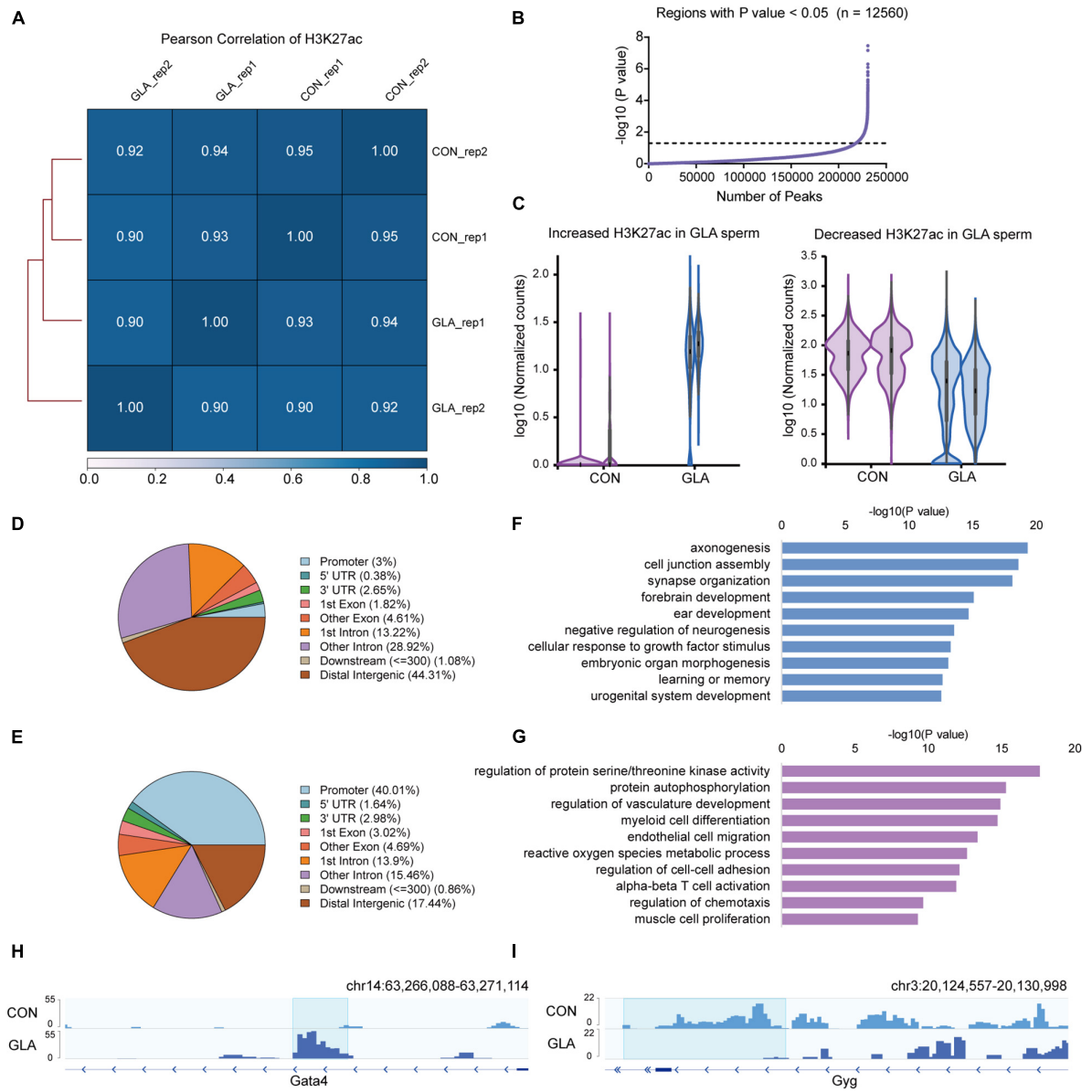

FIGURE 3 | GLA-induced H3K27ac alterations in mouse sperm. **(A)** Correlation matrix showing Pearson correlation coefficient of H3K27ac between replicates of CON and GLA sperm. **(B)** Selection of regions with *P*-value < 0.05. The black dashed line corresponds to the boundary of *P*-value = 0.05. **(C)** Violin plots showing increased and decreased H3K27ac in GLA sperm. Two replicates in each group are in the same color. **(D,E)** Pie chart showing the genomic distribution of regions with increased **(D)** and decreased **(E)** H3K27ac signals in GLA sperm. **(F,G)** Selected significant pathways from Gene Ontology analysis on genes with increased **(F)** or decreased **(G)** H3K27ac signals in GLA sperm. **(H)** Integrative Genomics Viewer tracks showing increased H3K27ac on *Gata4* in GLA sperm. **(I)** Integrative Genomics Viewer tracks showing decreased H3K27ac on *Gyg* in GLA sperm. Blue box indicates regions with differential H3K27ac signals (*P*-value < 0.05).

also located in promoters (97.4%) (**Figure 2E**). According to results of GO enrichment analysis (**Supplementary Table 2**), genes like *Fasn* annotated by increased H3K4me3 were mainly enriched in biological pathways including cellular response to interleukin-4, hindbrain development and histone H3-K27 methylation (**Figures 2F,H**). For genes with decreased H3K4me3 levels, such as *Chd9*, were enriched in dephosphorylation, B cell differentiation, and RNA polymerase II preinitiation complex assembly related pathways (**Figures 2G,I**).

Similarly, we did all these analyses on global H3K27ac level in sperm. All the Pearson correlation coefficients between each two replicates of CON and GLA sperm were over 0.90 (**Figure 3A**). In 12,560 differentially H3K27ac occupied regions (*P*-value < 0.05; **Figure 3B** and **Supplementary Table 3**), those with increased and decreased H3K27ac were analyzed separately (**Figure 3C**). Increased H3K27ac were mainly distributed in distal intergenic regions (44.31%) and introns (42.14%) (**Figure 3D**) while decreased H3K27ac were also primarily located in promoters

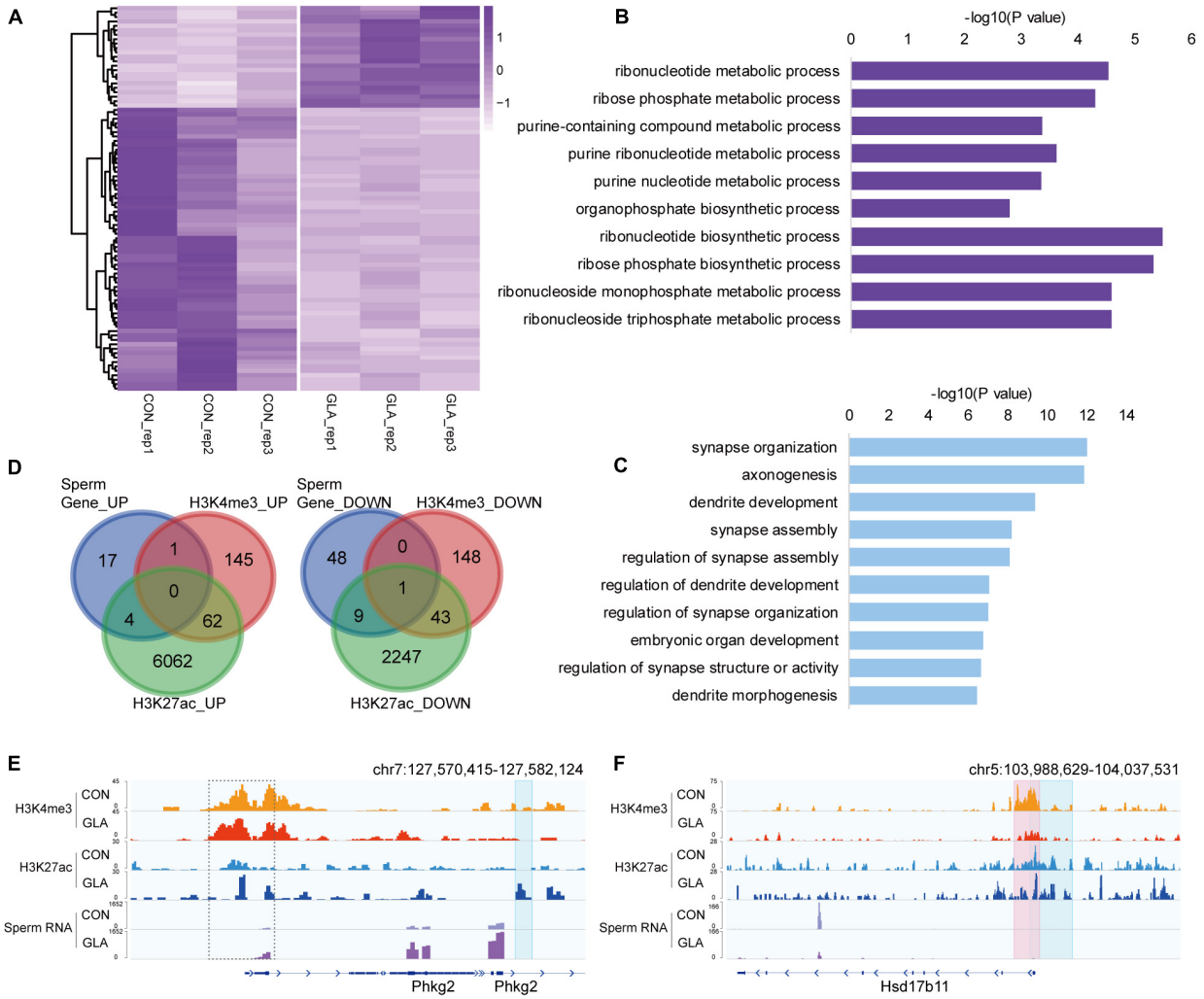

FIGURE 4 | Differential sperm mRNA transcripts in connection with H3K4me3 and H3K27ac alterations in GLA sperm. **(A)** Heatmap of normalized mRNA transcripts in CON and GLA sperm (n = 10, data from Ma et al., 2021). **(B,C)** Selected significant pathways from Gene Ontology analysis on up-regulated **(B)** or down-regulated **(C)** genes in GLA sperm. **(D)** Venn diagram showing the number of regions with different mRNA transcripts levels in GLA sperm that overlap regions with altered H3K4me3 and H3K27ac levels. Left, up-regulated regions overlapping regions with increased H3K4me3 and H3K27ac. Right, down-regulated regions overlapping regions with decreased H3K4me3 and H3K27ac. **(E)** Integrative Genomics Viewer tracks showing up-regulated *Phkg2* integrating with H3K4me3 and H3K27ac signals in GLA sperm. **(F)** Integrative Genomics Viewer tracks showing down-regulated *Hsd17b11* integrating with H3K4me3 and H3K27ac signals in GLA sperm. Pink box indicates regions with differential H3K4me3 signals (P-value < 0.05). Blue box indicates regions with differential H3K27ac signals (P-value < 0.05). Dashed box indicates regions with slightly differential histone methylation signals.

(40.01%) and distal intergenic regions (17.44%) (**Figure 3E**). GO enrichment analysis (**Supplementary Table 3**) showed that gene with increased H3K27ac were mainly enriched in axonogenesis, synapse organization and learning or memory related pathways (**Figure 3F**), while those with decreased H3K27ac were enriched in pathways including protein autophosphorylation, myeloid cell differentiation, and regulation of chemotaxis (**Figure 3G**). IGV tracks showed representative deposition of increased H3K27ac in *Gata4* (P-value = 0.0038; **Figure 3H**) and decreased deposition in *Gyg* (P-value = 8.12×10^{-7}; **Figure 3I**).

Taken together, GLA exposure alters H3K4me3 and H3K27ac profiles in mouse sperm, and their differentially occupied regions are distinct on genomic distribution and biological pathways.

Differential Sperm mRNA Transcripts in Connection With H3K4me3 and H3K27ac Alterations in Glufosinate-Ammonium Sperm

To better comprehend the alterations happened in GLA sperm, we integrated and analyzed H3K4me3 and H3K27ac profiles with sperm RNA-seq data from our previous study (Ma et al., 2021). RNA-seq data showed that a majority of detectable mRNA transcripts were decreased in GLA sperm (**Figure 4A**). GO enrichment analysis indicated distinct biological pathways involving these differentially expressed genes, such as ribonucleotide biosynthetic and metabolic process

in up-regulated pathways (**Figure 4B**) as well as synapse, axonogenesis and dendrite development in down-regulated pathways (**Figure 4C**). Given the positive correlation between these two active epigenetic marks and gene transcription, we hypothesized that GLA induced H3K4me3 and H3K27ac alterations would somewhat demonstrate those differentially expressed genes in sperm. Of the 22 up-regulated genes in sperm, only one overlapped with H3K4me3 increased regions, and 4 overlapped with H3K27ac increased regions, including *Phkg2* (**Figure 4D**-left). Then we zoomed our IGV plot of sperm H3K4me3, H3K27ac and mRNA tracks in the *Phkg2* locus, and found increased deposition of both H3K4me3 and H3K27ac (P-value = 0.0204) at its promoter, which was concordant with increased mRNA transcripts on the gene body (P-value = 6.97×10^{-5}; **Figure 4E**). Similarly, of the 58 down-regulated genes, there were 10 overlapping with H3K27ac decreased regions, and none of them overlapped with H3K4me3 decreased regions alone (**Figure 4D**-right). Interestingly, there was one gene occupied by both decreased H3K4me3 and H3K27ac, namely *Hsd17b11*. We found markedly decreased H3K4me3 (P-value = 0.0034) and H3K27ac (P-value = 0.0428) were distributed at the promoter region of *Hsd17b11*, which might account for the significant decline of mRNA transcripts (P-value = 0.0006; **Figure 4F**). It suggested that differential sperm mRNA transcripts were linked to alterations of H3K4me3 and H3K27ac profiles in GLA sperm.

Differential Gene Expression in 4-Cell Embryos in Connection With H3K4me3 and H3K27ac Alterations in Glufosinate-Ammonium Sperm

Considering the contribution of paternal chromosome to the embryonic development, we hypothesized that GLA exposure induced sperm H3K4me3 and H3K27ac alterations might associate with aberrant gene expression in preimplantation embryos. Thus, we collected 4-cell embryos as a critical period after fertilization and performed RNA-seq to measure transcriptomic profiles in 4-cell embryos. It was revealed that 37 genes were significantly up-regulated and 53 genes were significantly down-regulated in GLA embryos (**Figure 5A** and **Supplementary Table 4**). GO analysis (**Supplementary Table 4**) showed that those up-regulated genes were mainly enriched in biological pathways including mRNA splicing and apoptotic signaling (**Figure 5B**), while down-regulated genes were predominantly enriched in leukocyte homeostasis and mononuclear cell migration related pathways (**Figure 5C**). Then we used Venn diagram to check whether GLA sensitive H3K4me3 and H3K27ac regions in sperm overlapped with those differentially expressed genes in 4-cell embryos. We found that of the 37 up-regulated genes, only 8 overlapped with increased sperm H3K27ac, including *Mgl2* (**Figures 5D**-left,**E**). Similarly, of the 53 down-regulated genes in 4-cell embryos, only 9 genes overlapped with decreased H3K27ac signals in sperm, such as *Dcn* (**Figure 5D**-right,**F**). The *Dcn* profile showed a significantly declined H3K27ac deposited at its putative enhancer (P-value = 0.0040), and H3K4me3 signals at the promoter were also reduced in sperm. Overall, these overlapping regions indicated that paternal GLA exposure caused differential gene expression in 4-cell embryos, which might be associated with H3K4me3 and H3K27ac alterations in GLA sperm.

Differentially Parental-Origin Gene Expression in 4-Cell Embryos in Connection With H3K4me3 and H3K27ac Alterations in Glufosinate-Ammonium Sperm

By identifying differential gene expression in 4-cell embryos induced by paternal GLA exposure, it aroused our interest on whether these differences occurred at the paternal or the maternal alleles. To figure out such the problem, we assigned RNA-seq reads to its parent-of-origin by examining their single nucleotide polymorphisms (SNPs) derived from C57BL/6J male mice or DBA/2 female mice. As shown in **Figure 6A**, there were 5 significantly down-regulated and 4 significantly up-regulated paternal-origin genes (P-value < 0.05; **Supplementary Table 5**). We integrated histone modifications in sperm with biparental gene expression in 4-cell embryos, and found genes like *Usp36* and *Zfp81* were significantly down-regulated on paternal allele (*Usp36*: P-value = 1.52×10^{-5}; *Zfp81*: P-value = 1.89×10^{-7}) and almost unchanged on maternal allele in GLA 4-cell embryos, which might be regulated by decreased H3K4me3 and H3K27ac at their promoters in sperm (**Figure 6B**). As for maternal-origin genes, only 3 of them were significantly up-regulated, and other 17 genes were significantly down-regulated (P-value < 0.05; **Figure 6C** and **Supplementary Table 5**). Accordingly, we zoomed in integrated tracks of these genes and found that both of the *Anxa1* and *Sorl1* kept paternally silenced but significantly down-regulated in maternal allele (*Anxa1*: P-value = 0.0001; *Sorl1*: P-value = 0.0003), which were concordant with decreased H3K4me3 and H3K27ac at their promoters in sperm (**Figure 6D**). Taken together, we found that differentially occupied H3K4me3 and H3K27ac in sperm induced by GLA exposure were linked to gene expression changes in both paternal and maternal alleles of 4-cell embryos.

DISCUSSION

As an emerging herbicide widespread in the environment, GLA and its metabolites have been detected in human biofluids such as serum (Aris and Leblanc, 2011) and urine (Bienvenu et al., 2021) samples, and it requires more evidence on its toxicity. In this study, we investigated genome-wide H3K4me3 and H3K27ac in sperm and transcriptome in preimplantation embryos to identify the potential hazard of GLA exposure, and integrated these sequencing data to find some clues on their association. Our study revealed that GLA exposure altered H3K4me3 and H3K27ac profiles in mouse sperm, which was linked to aberrant gene expression in preimplantation embryos.

Global profiles of sperm H3K4me3 and H3K27ac in CON mouse showed distinct distribution in genomic loci and biological pathways in each cluster. Sperm H3K4me3 is mainly

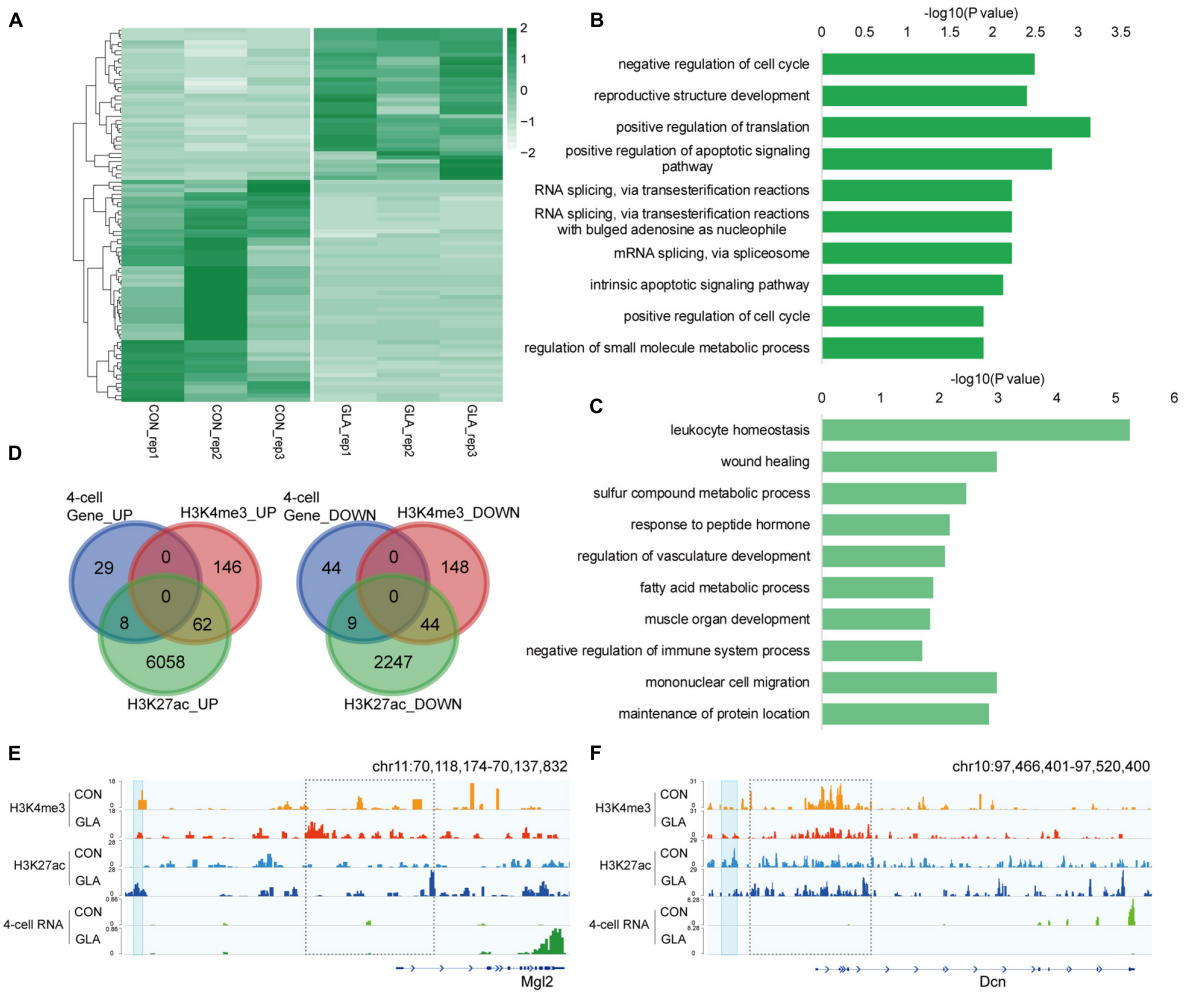

FIGURE 5 | Differential gene expression in 4-cell embryos in connection with H3K4me3 and H3K27ac alterations in GLA sperm. **(A)** Heatmap of normalized gene expression levels in CON and GLA 4-cell embryos. **(B,C)** Selected significant pathways from Gene Ontology analysis on up-regulated **(B)** or down-regulated **(C)** genes in GLA 4-cell embryos. **(D)** Venn diagram showing the number of regions with different gene expression levels in GLA 4-cell embryos that overlap regions with altered H3K4me3 and H3K27ac levels in GLA sperm. Left, up-regulated regions overlapping regions with increased H3K4me3 and H3K27ac. Right, down-regulated regions overlapping regions with decreased H3K4me3 and H3K27ac. **(E)** Integrative Genomics Viewer tracks showing up-regulated *Mgl2* in 4-cell embryos integrating with H3K4me3 and H3K27ac signals in GLA sperm. **(F)** Integrative Genomics Viewer tracks showing down-regulated *Dcn* integrating with H3K4me3 and H3K27ac signals in GLA sperm. Blue box indicates regions with differential H3K27ac signals (*P*-value < 0.05). Dashed box indicates regions with slightly differential histone methylation signals.

distributed at developmental promoters (Hammoud et al., 2009), while H3K27ac is superior to identify super-enhancers (Hnisz et al., 2013) compared to other enhancer marks such as histone H3 lysine 4 monomethylation (H3K4me1), DNase hypersensitivity and p300. In this study, consistent with those in a physiological manner, differentially H3K4me3 and H3K27ac occupied regions in sperm induced by GLA exposure were mainly located at promoters and putative enhancers, respectively, which is concordant with their role as active promoter and enhancer marks (Calo and Wysocka, 2013). As for the number of differentially occupied regions, sperm H3K27ac seemed more sensitive than H3K4me3 to GLA exposure. According to GO analyses, both differentially occupied regions of sperm H3K4me3 and H3K27ac were enriched in biological pathways related to the immune system and nervous system, while those down-regulated genes in 4-cell embryos were also mainly enriched in immune-related pathways, indicating potential immune impairment in preimplantation embryos induced by paternal GLA exposure. Additionally, up-regulated genes in GLA sperm were primarily enriched in ribonucleotide biosynthetic and metabolic process. Given that glutamine is an indispensable substrate in ribonucleotide biosynthesis, we hypothesized that such pathway might be disturbed due to the structure similarity between glutamate and GLA.

Despite of some constantly changed genes in both sperm and embryos, most genes marked with active promoters in sperm are not expressed until the embryonic stage. For example, monovalent genes marked with H3K4me3 are mainly

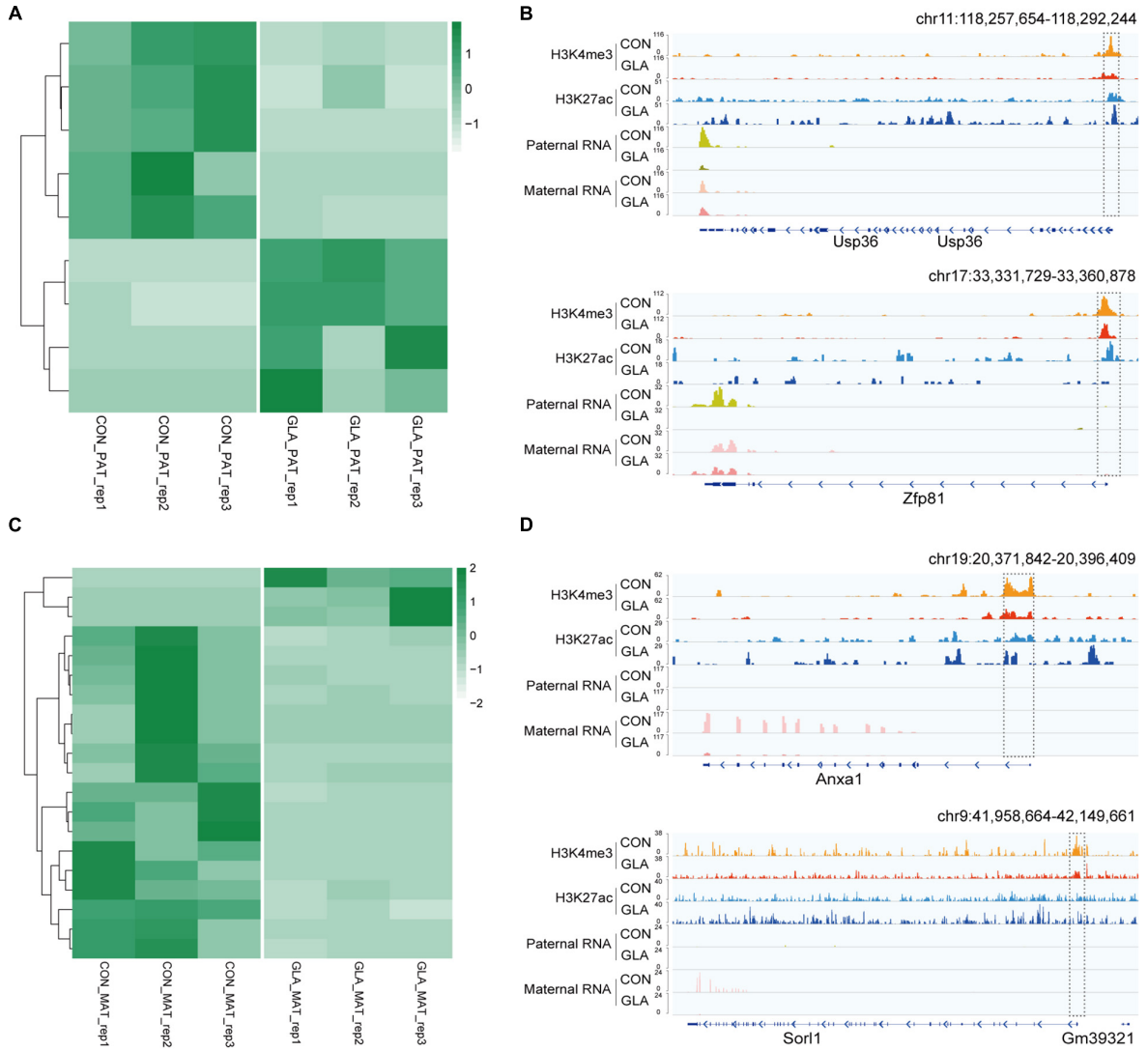

FIGURE 6 | Differentially parental-origin gene expression in 4-cell embryos in connection with H3K4me3 and H3K27ac alterations in GLA sperm. **(A)** Heatmap of normalized mRNA transcripts of paternal alleles in CON and GLA 4-cell embryos. **(B)** Integrative Genomics Viewer tracks showing RNA transcripts of parental-specific alleles (*Usp36* and *Zfp81*) in 4-cell embryos integrating with H3K4me3 and H3K27ac signals in GLA sperm. **(C)** Heatmap of normalized mRNA transcripts of maternal alleles in CON and GLA 4-cell embryos. **(D)** Integrative Genomics Viewer tracks showing RNA transcripts of parental-specific alleles (*Anxa1* and *Sorl1*) integrating with H3K4me3 and H3K27ac signals in GLA sperm. Dashed box indicates regions with slightly differential histone methylation signals.

active in late spermatogenesis, while bivalent genes marked with H3K4me3 and H3K27me3 keep silence until embryonic development (Tomizawa et al., 2018). Though extensively inhibited, sperm retains the transcription complex composed of RNA polymerase II (RNAPII) and the mediator complex at about 60% promoters flanking nucleosomes deposited with H3K4me3 marks for immediate transcription after fertilization (Jung et al., 2019). Therefore, differentially occupied H3K4me3 and H3K27ac in sperm might be more related to gene expression changes in embryos than in sperm. At fertilization, protamine on paternal genome is immediately replaced by histones, and histone modifications are established followed by further reorganization in preimplantation embryos (Morgan et al., 2005). During that process, sperm H3K4me3 is erased in zygotes and then regained after zygotic genome activation (ZGA) in late 2-cell embryos in mouse (Zhang et al., 2016; Jung et al., 2019) and the mid-blastula transition (MBT) in zebrafish (Zhu et al., 2019). As reported by Lismer et al. (2020) altered H3K4me3 enrichment was inherited from sperm of the histone demethylase KDM1A transgenic mice to preimplantation embryos. In their subsequent study, diet-induced changes in sperm H3K4me3 were also transmitted into preimplantation embryos (Lismer et al., 2021). Additionally, a study comparing H3K4me3 profiles among sperm, preimplantation embryos and male gonad primordial germ cells showed that H3K4me3 marks within promoters of RNA splicing genes could escape two rounds of paternal

reprogramming (Hao et al., 2021), which further proves the stability of H3K4me3 during the process of male reproduction and development.

When it comes to sperm H3K27ac, evidence becomes more limited. By immunostaining, the protein level of H3K27ac was similarly elevated both in sperm and embryos of zebrafish after paternal exposure to bisphenol A (BPA) (Lombó et al., 2019). Thus, it still needs further examination whether regions marked with H3K27ac in sperm could be inherited to embryos. Though we did not explore genome-wide profiles of H3K4me3 and H3K27ac in preimplantation embryos, transcriptome analysis indicated GLA altered embryonic gene expression. In addition, embryogenesis is a highly conserved process that involves cell fate decision. Many genes in early embryos have a dramatic impact on embryo development (Gardner and Lane, 2005; Leng et al., 2019) and offspring health (Shen et al., 2007; Zhao et al., 2013). Here we found that up-regulated genes in 4-cell embryos were mainly enriched in mRNA splicing related pathways, which reminded us the reprograming evasion of H3K4me3 marks mentioned above (Hao et al., 2021). By contrast, down-regulated genes were mostly enriched in immune related pathways. Therefore, such embryonic gene expression induced by paternal GLA exposure might threaten embryo development and offspring health, which requires further investigation.

Interestingly, we found differentially expressed genes in both paternal and maternal alleles of preimplantation embryos induced by paternal GLA exposure. Evidence reporting similar situation is quite limited even when it comes to lifestyle or other environmental stress, and its mechanism still remains unknown. Meanwhile, such differentially parental-origin gene expression caused non-canonical genomic imprinting in GLA embryos. For example, paternal GLA exposure newly generated a maternally expressed profile of *Zfp81* (**Figure 6B**), and made that of *Anxa1* disappeared (**Figure 6D**). Given to the crucial role of genomic imprinting in embryo and placenta development, fetus and neonate growth, as well as neurological behaviors and metabolism in adult offspring (Anckaert et al., 2013), differentially parental-origin gene expression in 4-cell embryos induced by GLA exposure might lead to unknown health risks in offspring developmental periods.

CONCLUSION

By examining genome-wide profiles of sperm H3K4me3 and H3K27ac, together with embryonic gene expression, we concluded that GLA exposure altered sperm H3K4me3 and H3K27ac. Most of them were distributed at gene promoters and enhancers and enriched in the immune and nervous system related pathways. Additionally, GLA exposure disrupted biparentally immune-related gene expression in preimplantation embryos, which was associated with sperm H3K4me3 and H3K27ac profile changes. Though it still needs further investigation on whether these changes in sperm H3K4me3 and H3K27ac persist in preimplantation embryos, alterations in embryonic gene expression observed in our study sounded the alarm for potential adverse impact of paternal GLA exposure on embryo development and offspring health.

DATA AVAILABILITY STATEMENT

The datasets presented in this study can be found in online repositories. The names of the repository/repositories and accession number(s) can be found below: Genome Sequence Archive (Genomics, Proteomics, and Bioinformatics 2021); GSA: CRA005732.

ETHICS STATEMENT

The animal study was reviewed and approved by the Institutional Animal Care and Use Committee (IACUC) of Nanjing Medical University (1811056–2).

AUTHOR CONTRIBUTIONS

XM: investigation, writing—original draft, reviewing, and editing. YF: software, formal analysis, and data curation. WX: investigation and validation. XD: investigation. WH: conceptualization, methodology, and supervision. YX: resources provision, funding acquisition, and supervision. All authors contributed to the article and approved the submitted version.

FUNDING

This work was supported by China-U.S. Program for Biomedical Collaborative Research (NSFC-NIH) (81961128022); the National Natural Science Foundation of China (81903351); and the Priority Academic Program Development of Jiangsu Higher Education Institutions (PAPD).

SUPPLEMENTARY MATERIAL

The Supplementary Material for this article can be found online at: https://www.frontiersin.org/articles/10.3389/fphys.2021.819856/full#supplementary-material

REFERENCES

Anckaert, E., De Rycke, M., and Smitz, J. (2013). Culture of oocytes and risk of imprinting defects. *Hum. Reprod. Update* 19, 52–66. doi: 10.1093/humupd/dms042

Aris, A., and Leblanc, S. (2011). Maternal and fetal exposure to pesticides associated to genetically modified foods in Eastern Townships of Quebec, Canada. *Reprod. Toxicol.* 31, 528–533. doi: 10.1016/j.reprotox.2011.02.004

Bienvenu, J. F., Bélanger, P., Gaudreau, É, Provencher, G., and Fleury, N. (2021). Determination of glyphosate, glufosinate and their major metabolites in urine by the UPLC-MS/MS method applicable to biomonitoring and epidemiological studies. *Anal. Bioanal. Chem.* 413, 2225–2234. doi: 10.1007/s00216-021-03194-x

Bray, N. L., Pimentel, H., Melsted, P., and Pachter, L. (2016). Near-optimal probabilistic RNA-seq quantification. *Nat. Biotechnol.* 34, 525–527. doi: 10.1038/nbt.3519

Calo, E., and Wysocka, J. (2013). Modification of enhancer chromatin: What, how, and why? *Mol. Cell* 49, 825–837. doi: 10.1016/j.molcel.2013.01.038

Carone, B. R., Fauquier, L., Habib, N., Shea, J. M., Hart, C. E., Li, R., et al. (2010). Paternally induced transgenerational environmental reprogramming of metabolic gene expression in mammals. *Cell* 143, 1084–1096. doi: 10.1016/j.cell.2010.12.008

Dobin, A., Davis, C. A., Schlesinger, F., Drenkow, J., Zaleski, C., Jha, S., et al. (2013). STAR: ultrafast universal RNA-seq aligner. *Bioinformatics* 29, 15–21. doi: 10.1093/bioinformatics/bts635

Ferramosca, A., Lorenzetti, S., Di Giacomo, M., Murrieri, F., Coppola, L., and Zara, V. (2021). Herbicides glyphosate and glufosinate ammonium negatively affect human sperm mitochondria respiration efficiency. *Reprod. Toxicol.* 99, 48–55. doi: 10.1016/j.reprotox.2020.11.011

Gardner, D. K., and Lane, M. (2005). Ex vivo early embryo development and effects on gene expression and imprinting. *Reprod. Fertil. Dev.* 17, 361–370. doi: 10.1071/rd04103

Hammoud, S. S., Nix, D. A., Zhang, H., Purwar, J., Carrell, D. T., and Cairns, B. R. (2009). Distinctive chromatin in human sperm packages genes for embryo development. *Nature* 460, 473–478. doi: 10.1038/nature08162

Hao, N., Xin, H., Shi, X., Xin, J., Zhang, H., Guo, S., et al. (2021). Paternal reprogramming-escape histone H3K4me3 marks located within promoters of RNA splicing genes. *Bioinformatics* 37, 1039–1044. doi: 10.1093/bioinformatics/btaa920

Henikoff, S., Henikoff, J. G., Kaya-Okur, H. S., and Ahmad, K. (2020). Efficient chromatin accessibility mapping in situ by nucleosome-tethered tagmentation. *Elife* 9:e63274. doi: 10.7554/eLife.63274

Hnisz, D., Abraham, B. J., Lee, T. I., Lau, A., Saint-André, V., Sigova, A. A., Hoke, H. A., et al. (2013). Super-enhancers in the control of cell identity and disease. *Cell* 155, 934–947. doi: 10.1016/j.cell.2013.09.053

JMPR (2012). *Report of the Joint Meeting of the FAO Panel of Experts on Residues in food and the Environment and the WHO Core Assessment Group on Pesticide Residues*. (Geneva: WHO), 547–652.

Jung, Y. H., Kremsky, I., Gold, H. B., Rowley, M. J., Punyawai, K., Buonanotte, A., et al. (2019). Maintenance of CTCF- and Transcription Factor-Mediated Interactions from the Gametes to the Early Mouse Embryo. *Mol. Cell* 75, 154–171.e5. doi: 10.1016/j.molcel.2019.04.014

Kaya-Okur, H. S., Janssens, D. H., Henikoff, J. G., Ahmad, K., and Henikoff, S. (2020). Efficient low-cost chromatin profiling with CUT&Tag. *Nat. Protoc.* 15, 3264–3283. doi: 10.1038/s41596-020-0373-x

Krueger, F., and Andrews, S. R. (2016). SNPsplit: allele-specific splitting of alignments between genomes with known SNP genotypes. *F1000Res.* 5:1479. doi: 10.12688/f1000research.9037.2

Kutchy, N. A., Menezes, E. S. B., Chiappetta, A., Tan, W., Wills, R. W., Kaya, A., et al. (2018). Acetylation and methylation of sperm histone 3 lysine 27 (H3K27ac and H3K27me3) are associated with bull fertility. *Acta Paediatr.* 50:e12915. doi: 10.1111/and.12915

Lambrot, R., Chan, D., Shao, X., Aarabi, M., Kwan, T., Bourque, G., et al. (2021). Whole-genome sequencing of H3K4me3 and DNA methylation in human sperm reveals regions of overlap linked to fertility and development. *Cell Rep.* 36:109418. doi: 10.1016/j.celrep.2021.109418

Langmead, B., and Salzberg, S. L. (2012). Fast gapped-read alignment with Bowtie 2. *Nat. Methods* 9, 357–359. doi: 10.1038/nmeth.1923

Leng, L., Sun, J., Huang, J., Gong, F., Yang, L., Zhang, S., et al. (2019). Single-cell transcriptome analysis of uniparental embryos reveals parent-of-origin effects on human preimplantation development. *Cell Stem Cell* 25, 697–712.e6. doi: 10.1016/j.stem.2019.09.004

Liao, Y., Smyth, G. K., and Shi, W. (2014). featureCounts: an efficient general purpose program for assigning sequence reads to genomic features. *Bioinformatics* 30, 923–930. doi: 10.1093/bioinformatics/btt656

Lismer, A., Dumeaux, V., Lafleur, C., Lambrot, R., Brind'Amour, J., Lorincz, M. C., et al. (2021). Histone H3 lysine 4 trimethylation in sperm is transmitted to the embryo and associated with diet-induced phenotypes in the offspring. *Dev. Cell* 56, 671–686.e6.

Lismer, A., Siklenka, K., Lafleur, C., Dumeaux, V., and Kimmins, S. (2020). Sperm histone H3 lysine 4 trimethylation is altered in a genetic mouse model of transgenerational epigenetic inheritance. *Nucleic Acids Res.* 48, 11380–11393. doi: 10.1093/nar/gkaa712

Liu, Y., Zhang, Y., Yin, J., Gao, Y., Li, Y., Bai, D., et al. (2019). Distinct H3K9me3 and DNA methylation modifications during mouse spermatogenesis. *J. Biol. Chem.* 294, 18714–18725. doi: 10.1074/jbc.RA119.010496

Lombó, M., Fernández-Díez, C., González-Rojo, S., and Herráez, M. P. (2019). Genetic and epigenetic alterations induced by bisphenol A exposure during different periods of spermatogenesis: from spermatozoa to the progeny. *Sci. Rep.* 9:18029.

Lombó, M., and Herráez, M. P. (2021). Paternal inheritance of bisphenol a cardiotoxic effects: the implications of sperm epigenome. *Int. J. Mol. Sci.* 22:2125. doi: 10.3390/ijms22042125

Love, M. I., Huber, W., and Anders, S. (2014). Moderated estimation of fold change and dispersion for RNA-seq data with DESeq2. *Genome Biol.* 15:550.

Ma, X., Wang, B., Li, Z., Ding, X., Wen, Y., Shan, W., et al. (2021). Effects of glufosinate-ammonium on male reproductive health: focus on epigenome and transcriptome in mouse sperm. *Chemosphere* 287(Pt 4):132395. doi: 10.1016/j.chemosphere.2021.132395

Meers, M. P., Tenenbaum, D., and Henikoff, S. (2019). Peak calling by Sparse Enrichment Analysis for CUT&RUN chromatin profiling. *Epigenetics Chromatin* 12:42.

Morgan, H. D., Santos, F., Green, K., Dean, W., and Reik, W. (2005). Epigenetic reprogramming in mammals. *Hum. Mol. Genet.* 14, R47–R58. doi: 10.1093/hmg/ddi114

Nair, A. B., and Jacob, S. (2016). A simple practice guide for dose conversion between animals and human. *J. Basic Clin. Pharm.* 7, 27–31. doi: 10.4103/0976-0105.177703

Ramírez, F., Ryan, D. P., Grüning, B., Bhardwaj, V., Kilpert, F., Richter, A. S., et al. (2016). deepTools2: a next generation web server for deep-sequencing data analysis. *Nucleic Acids Res.* 44, W160–W165. doi: 10.1093/nar/gkw257

Sharma, U., Conine, C. C., Shea, J. M., Boskovic, A., Derr, A. G., Bing, X. Y., et al. (2016). Biogenesis and function of tRNA fragments during sperm maturation and fertilization in mammals. *Science* 351, 391–396. doi: 10.1126/science.aad6780

Shen, J., Liu, J., Xie, Y., Diwan, B. A., and Waalkes, M. P. (2007). Fetal onset of aberrant gene expression relevant to pulmonary carcinogenesis in lung adenocarcinoma development induced by in utero arsenic exposure. *Toxicol. Sci.* 95, 313–320. doi: 10.1093/toxsci/kfl151

Siklenka, K., Erkek, S., Godmann, M., Lambrot, R., McGraw, S., Lafleur, C., et al. (2015). Disruption of histone methylation in developing sperm impairs offspring health transgenerationally. *Science* 350:aab2006. doi: 10.1126/science.aab2006

Takano, H. K., and Dayan, F. E. (2020). Glufosinate-ammonium: a review of the current state of knowledge. *Pest Manage. Sci.* 76, 3911–3925. doi: 10.1002/ps.5965

Tomizawa, S.-I., Kobayashi, Y., Shirakawa, T., Watanabe, K., Mizoguchi, K., Hoshi, I., et al. (2018). Kmt2b conveys monovalent and bivalent H3K4me3 in mouse spermatogonial stem cells at germline and embryonic promoters. *Development* 145:dev169102. doi: 10.1242/dev.169102

Wike, C. L., Guo, Y., Tan, M., Nakamura, R., Shaw, D. K., Díaz, N., et al. (2021). Chromatin architecture transitions from zebrafish sperm through early embryogenesis. *Genome Res.* 31, 981–994. doi: 10.1101/gr.269860.120

Yan, C., and Boyd, D. D. (2006). Histone H3 acetylation and H3 K4 methylation define distinct chromatin regions permissive for transgene expression. *Mol. Cell. Biol.* 26, 6357–6371.

Yoshida, K., Muratani, M., Araki, H., Miura, F., Suzuki, T., Dohmae, N., et al. (2018). Mapping of histone-binding sites in histone replacement-completed spermatozoa. *Nat. Commun.* 9:3885.

Yu, G., Wang, L. G., Han, Y., and He, Q. Y. (2012). clusterProfiler: an R package for comparing biological themes among gene clusters. *OMICS* 16, 284–287. doi: 10.1089/omi.2011.0118

Yu, G., Wang, L. G., and He, Q. Y. (2015). ChIPseeker: an R/Bioconductor package for ChIP peak annotation, comparison and visualization. *Bioinformatics* 31, 2382–2383. doi: 10.1093/bioinformatics/btv145

Zhang, B., Zheng, H., Huang, B., Li, W., Xiang, Y., Peng, X., et al. (2016). Allelic reprogramming of the histone modification H3K4me3 in early mammalian development. *Nature* 537, 553–557. doi: 10.1038/nature 19361

Zhang, L., Diao, J., Chen, L., Wang, Z., Zhang, W., Li, Y., et al. (2019). Hepatotoxicity and reproductive disruption in male lizards (Eremias argus) exposed to glufosinate-ammonium contaminated soil. *Environ. Pollut.* 246, 190–197. doi: 10.1016/j.envpol.2018. 12.004

Zhao, H. C., Zhao, Y., Li, M., Yan, J., Li, L., Li, R., et al. (2013). Aberrant epigenetic modification in murine brain tissues of offspring from preimplantation genetic diagnosis blastomere biopsies. *Biol. Reprod.* 89:117. doi: 10.1095/biolreprod. 113.109926

Zhu, W., Xu, X., Wang, X., and Liu, J. (2019). Reprogramming histone modification patterns to coordinate gene expression in early zebrafish embryos. *BMC Genomics* 20:248. doi: 10.1186/s12864-019-5611-7

Conflict of Interest: The authors declare that the research was conducted in the absence of any commercial or financial relationships that could be construed as a potential conflict of interest.

Publisher's Note: All claims expressed in this article are solely those of the authors and do not necessarily represent those of their affiliated organizations, or those of the publisher, the editors and the reviewers. Any product that may be evaluated in this article, or claim that may be made by its manufacturer, is not guaranteed or endorsed by the publisher.

frontiers in Physiology

ORIGINAL RESEARCH
published: 11 February 2022
doi: 10.3389/fphys.2022.843825

Epigenetic Regulation of TET1-SP1 During Spermatogonia Self-Renewal and Proliferation

*Lingling Liu, Jin Wang, Shenghua Wang, Mudi Wang, Yuanhua Chen and Liming Zheng**

School of Basic Medical Sciences, Anhui Medical University, Hefei, China

Spermatogonia are the source of spermatogenic waves. Abnormal spermatogonia can cause ab-normal spermatogenic waves, which manifest as spermatogenic disorders such as oligospermia, hypospermia, and azoospermia. Among them, the self-renewal of spermatogonia serves as the basis for maintaining the process of spermatogenesis, and the closely regulated balance between self-renewal and differentiation of spermatogonia can maintain the continuous production of spermatozoa. Tet methylcytosine dioxygenase 1(TET1) is an important epitope modifying enzyme that catalyzes the conversion of 5-methylcytosine (5-mC) to 5-hydroxymethylcytosine (5-hmC), thereby causing the methylation of specific genes site hydroxylation, enabling the DNA de-methylation process, and regulating gene expression. However, the hydroxymethylation sites at which TET1 acts specifically and the mechanisms of interaction affecting key differential genes are not clear. In the present study, we provide evidence that the expression of PLZF, a marker gene for spermatogonia self-renewal, was significantly elevated in the TET1 overexpression group, while the expression of PCNA, a proliferation-related marker gene, was also elevated at the mRNA level. Significant differential expression of SP1 was found by sequencing. SP1 expression was increased at both mRNA level and protein level after TET1 overexpression, while differential gene DAXX expression was downregulated at protein level, while the expression of its reciprocal protein P53 was upregulated. In conclusion, our results suggest that TET1 overexpression causes changes in the expression of SP1, DAXX and other genes, and that there is a certain antagonistic effect between SP1 and DAXX, which eventually reaches a dynamic balance to maintain the self-renewal state of spermatogonia for sustained sperm production. These findings may contribute to the understanding of male reproductive system disorders.

Keywords: TET1, SP1, epigenetic modification, self-renewal, spermatogonia

OPEN ACCESS

Edited by:
Rossella Cannarella, University of Catania, Italy

Reviewed by:
Elena Maria Scalisi, University of Catania, Italy
Andrea Crafa, University of Catania, Italy

****Correspondence:***
Liming Zheng
646797675@qq.com

Specialty section:
This article was submitted to Reproduction, a section of the journal Frontiers in Physiology

Received: *27 December 2021*
Accepted: *18 January 2022*
Published: *11 February 2022*

Citation:
Liu L, Wang J, Wang S, Wang M, Chen Y and Zheng L (2022) Epigenetic Regulation of TET1-SP1 During Spermatogonia Self-Renewal and Proliferation. Front. Physiol. 13:843825. doi: 10.3389/fphys.2022.843825

INTRODUCTION

According to research estimates, approximately 8–12% of couples worldwide are deeply affected by infertility, with approximately 50% of infertility being due to problems with the male partner (Minhas et al., 2021). The presence of male infertility may be associated with impaired sperm production due to congenital, genetic, or idiopathic factors (Vander Borght and Wyns, 2018). There is relevant evidence that when a mother conceives, the health status of the father

at this time can influence the level of reproductive health of the offspring through the inheritance of epigenetic modifications (Craig et al., 2017). Epigenetic modifications play an important role in germ cell function and post-fertilization embryonic development. In order to form terminally differentiated spermatozoa and promote the totipotency of fertilized eggs, these epigenetic modifications must be precisely regulated. Male infertility or early embryonic dysplasia may be associated with reproductive disorders resulting from epigenetic alterations associated with the male reproductive process (Liu et al., 2019). Epigenetic modifications can be involved in the spermatogenesis process and affect the fate of spermatogonia by regulating reproduction-specific genes. Self-renewal is fundamental to maintaining the spermatogenesis process, and abnormal self-renewal of spermato-gonia leads to reduced stability, causing decreased fertility, which eventually manifests as testicular atrophy or even infertility (Zheng et al., 2016).

The DNA hydroxymethylase TET1 is an important epitope-modifying enzyme (Ross and Bogdanovic, 2019). The TET1 protein possesses a catalytic structural domain with α-ketoglutarate (α-KG) and Fe2+ binding sites near the carbon terminus, a cyste-ine-rich region in front of the catalytic structural domain, and a CXXC structural domain with recognition function near the nitrogen terminus (Rasmussen and Helin, 2016), which can be directly recognized and bound to DNA to facilitate recruitment of genomic targets (Zhang et al., 2010). TET1 can catalyze the conversion of 5-methylcytosine (5-mC) to 5-hydroxymethylcytosine (5-hmC), which can further be converted to 5-formylcytosine (5fC) and 5 carboxycytosine (5caC). It is then recognized and excised by thymine—DNA glycosylase (TDG) and subsequently converted to cyto-sine *via* the base excision repair pathway (BER), which hydroxylates the methylation sites of specific genes, thus enabling the process of DNA demethylation and regulation of gene expression (Lio et al., 2019). Also, the hydroxylation product 5hmC can regulate gene transcription through its own recruitment (Cui et al., 2020). Localization distribution analysis at the genome-wide level revealed that TET1 and its hydroxylation product 5hmC are mainly distributed in many promoters, exons, transcription initiation regions and other important locations, which also suggests that TET1-mediated demethylation is closely linked to gene transcriptional activity (Wu and Morris, 2001; Wu et al., 2011).

Sp1 transcription factor (SP1) is a known member of the transcription factor family that also includes SP2, SP3, and SP4, which are involved in a variety of important biological processes (Peng et al., 2020). The structure of SP1 possesses three highly homologous C2H2 regions that feature direct binding to DNA and therefore enhance the transcriptional activity of genes (Memon and Lee, 2018). The SP family has a highly conserved DNA-binding structural domain (C-terminal structural domain), while the N-terminal region varies, so it is through this structural domain that many transcription factors regulate gene transcription (Zhang et al., 2013). The proteins encoded by SP1 can be involved in many cellular processes, such as cell growth, cell differentiation, apoptosis, immune response, chromatin remodeling, and DNA damage (Xu et al., 2019). Interestingly, SP1 not only initiates transcription but also has a regulatory role in activating or repressing processes (Vellingiri et al., 2020). It has been found that SP1 can activate gene transcription in many cells, and the promoter regions of these activated genes contain abundant GC binding sites (Vizcaíno et al., 2015). SP1 target genes are mainly involved in cell proliferation as well as tumorigenesis (Guo et al., 2019). Previous studies have found that the SP family is commonly over-expressed in certain human cancers and therefore is often considered as a negative prognostic factor (Beishline and Azizkhan-Clifford, 2015). When SP1 is overexpressed, it can contribute to the malignant phenotype of various human cancers by upregulating a number of genes associated with proliferation, invasion and metastasis, as well as certain genes with stem-ness and chemoresistance, resulting in a negative prognosis (Dupuis-Maurin et al., 2015).

The biological functions of DAXX (death domain associated protein) are complex. Previous studies have found a noteworthy commonality among various cancers in that DAXX is overexpressed in a variety of cancers and its possible association with tumorigenesis, disease progression and treatment resistance (Mahmud and Liao, 2019). DAXX was identified in 1997 as a regulator of FAS-binding protein and Jun N-terminal kinase (JNK)-mediated cell death (Yang et al., 1997; Chang et al., 1998). DAXX is almost ubiquitous in human tissues and its role in embryonic development is also crucial (Bogolyubova and Bogolyubov, 2021). DAXX can bind to a variety of DNA through transcription factors (TFs), chromatin-associated proteins, core histones, epigenetic regulators, etc., to regulate gene expression as transcriptional co-repressors or co-activators (Ivanauskiene et al., 2014; Nye et al., 2018; Wasylishen et al., 2018; Heaphy et al., 2020).

Previous studies have found that TET1 can participate in the spermatogenesis process and affect the self-renewal and proliferation of spermatogonial stem cells (SSCs; Zheng et al., 2016), but the hydroxymethylation sites of TET1 specific action and the mechanism of interactions affecting key differential genes are not clear. Therefore, in this study, by over-expressing TET1 in spermatogonia and discovering the differential methylation sites of TET1 hydroxylation by sequencing, and combining with mRNA level and protein level analysis, we further explain the epigenetic regulation mechanism of TET1 on spermatogonia self-renewal from the epigenetic level, which provides scientific basis for studying spermatogenesis, revealing the causes leading to spermatogenic disorders, and elucidating the mechanism of this will provide important scientific clues for the study of spermatogenesis, reveal the causes of spermatogenesis disorder, and elucidate its mechanism, and provide important scientific clues for cytogenetic treatment of male infertility.

MATERIALS AND METHODS

Cell Culture and Plasmid Transfection

Mouse spermatogonia GC-1 cells were used for cell culture, complete medium was made by adding 10% fetal bovine serum

(FBS) to the basal medium DMEM of Hyclone, and cells were cultured in a humidified environment containing 5% carbon dioxide at 37°C. Passage was performed every 3 days. At the time of passage, digestion was stopped by adding complete medium containing serum after digestion with trypsin digestion solution (Beyotime) containing .25% trypsin and .02% ethylene diamine tetraacetic acid (EDTA) for 2 min. When the Mouse spermatogonia GC-1 cells were cultured with the density of 75%, fresh DMEM consisted of FBS and other supplements were replaced. 30 min later, Lipofectamine 3000 reagent (Thermo) and plasmid (MYC and MYC-TET1) were, respectively, co-incubated with a volume V(MYC) = (2,500 ng/600 ng/ul) and V(MYC-TET1) = (2,500 ng/800 ng/ul) at room temperature for 15 min, then added to the medium and blended them. 12 h later, fresh DMEM contained all the supplements were replaced.

After 24–48 h Transfection, the Transfected Cells Were Collected for Subsequent Analysis. Real-Time Reverse Transcriptase Polymerase Chain Reaction

Twenty-four hours after cell transfection, transfected cells were collected, with Trizol (Thermo) Total RNA was purified and purified with cDNA was synthesized by a reverse transcription kit (SPARKscript II RT Plus Kit), followed by the use of SYBR Green qPCR Mix for SPARK and a fluorescence quantitative PCR instrument (ABI, QuantStudio6 Flex) Real-time reverse transcription-polymerase chain reaction (RT-PCR) was performed. GAPDH as a housekeeping gene for the normalization of gene expression. Primers were synthesized by Shanghai Shenggong. Primer pairs used in the experiments are listed in following **Table 1**.

Western Blot

After 48 h of cell transfection, transfected cells were collected. Proteins were extracted from transfected cells, and protein concentrations were determined with a BCA protein quantification kit (P0010S, Beyotime). Protein samples were denatured by 5% SDS-PAGE sample loading buffer, solubilized with 10% SDS-PAGE, and transferred to PVDF membranes. Detection was performed with β-actin (.5 ug/ml, GenScript#A00702S#Mouse) and anti-SP1 (1:1,000; Boster#A00110-1#Rabbit), anti-PLZF (1:1,000; Boster# PB1010#Rabbit), anti-GFRα1 (1:1,000; Boster#PB0199#Rabbit), anti-P53 (1:1,000; Bioworld#BS6437#Rabbit) and anti-DAXX (1:1,000; Bioworld#BS2411#Rabbit). Horseradish peroxidase-conjugated anti-rabbit (1:5,000, Boster#BA1054) and anti-mouse (1:10,000, Boster#BA1050) were used as secondary antibodies. The substrates were detected with a high-sensitivity ECL chemiluminescence kit (P0018S, Beyotime), and the results were analyzed with a Tanon-5200 automated gel imaging system.

Immunofluorescence Microscopy

Immunofluorescence staining of cells: cells cultured *in vitro* were washed twice with phosphate buffered saline (PBS), fixed with 4% paraformaldehyde (PFA) for 15 min at room temperature, and washed twice with PBS for 5 min each time. The membrane was permeabilized with .1% TritonX-100 for 10 min at room temperature and then washed twice with PBS for 5 min. If the protein is a membrane protein, omit this step. After washing with PBS three times for 5 min each, they were blocked with 1% bovine serum albumin (BSA) for 1 h at room temperature and then incubated with SP1 primary antibody (1:500, Boster#A00110-1#Rabbit) overnight at 4°C. After three washes with PBS, they were incubated with the appropriate secondary antibody (DyLight 488, Goat Anti-rabbit IgG, Boster# BA1127) for 40 min at room temperature. After the slides were washed with PBS, 1 μg/ml of nucleic acid fuel DAPI (biosharp#BS097) was added. Images were captured using a Nikon inverted fluorescence microscope.

Transcriptome Sequencing and Protein Sequencing Data

The data discussed in this publication have been deposited in NCBI's Gene Expression Omnibus and are accessible through GEO Series accession number GSE193717.[1]

The mass spectrometry proteomics data have been deposited to the ProteomeXchange Consortium *via* the PRIDE partner repository with the dataset identifier PXD030967.

[1]https://www.ncbi.nlm.nih.gov/geo/query/acc.cgi?acc=GSE193717

TABLE 1 | QRT-PCR primers.

Gene	Forward	Reverse
GAPDH	TGGCCTTCCGTGTTCCTAC	GAGTTGCTGTTGAAGTCGCA
TET1	GAGCCTGTTCCTCGATGTGG	CAAACCCACCTGAGGCTGTT
PLZF	CACCGCAACAGCCAGCACTAT	CAGCGTACAGCAGGTCATCCAG
GFRα1	GACCGTCTGGACTGTGTGAAAG	TTAGTGTGCGGTACTTGGTGC
PCNA	AGTGGAGAACTTGGAAATGGAA	GAGACAGTGGAGTGGCTTTTGT
Cylin A	TGGCTGTGAACTACATTGA	ACAAACTCTGCTACTTCTGG
Cylin E	GTGGCTCCGACCTTTCAGTC	CACAGTCTTGTCAATCTTGGCA
MAGE4	ATGGAAAATCCCGATAACACCC	AGGACTTGGTAATCCACTACTGT
PRDM1	TGGAGGACGCTGATATGACT	CTTACCACGCCAATAACCTC
VASA	GATAATCATTTAGCACAGCCTC	GTCAACAGATGCAAACACAG
DAZL	ATGTCTGCCACAACTTCTGAG	CTGATTTCGGTTTCATCCATCCT
C-KIT	CGCCTGCCGAAATGTATG	TCAGCGTCCCAGCAAGTC
SP1	GGCAGCGAGTCTTCCAAGAA	GATGATCTGTTGGTTTGCACCT

Statistical Analysis

Data were expressed as means ± SD ($n \geq 3$) and analyzed using GraphPad Prism 7 (GraphPad Software, San Diego, CA). Firstly, the data were verified to conform to normal distribution and homogeneity of variance. Comparison between two groups was analyzed using the *t*-test. Comparison among groups was analyzed using one-way ANOVA. If the data did not conform to normal distribution or homogeneity of variance, the rank-sum test was employed for the nonparametric analysis. Statistical significance was defined as $p < .001$(***), $p < .01$(**), or $p < .05$(*).

RESULTS

TET1 Overexpression Maintains Self-Renewal and Accelerates Proliferation of Spermatogonia

To identify the effect of TET1 overexpression on spermatogonia self-renewal and proliferation, we examined spermatogonia-specific related genes in the TET1 overexpression group and control cells, respectively. QRT-PCR results showed that the mRNA expression level of TET1 was significantly increased in TET1 overexpression cells (**Figure 1A**), and PLZF, which is related to spermatogonia self-renewal, had its mRNA level expression increased significantly (**Figure 1B**) and its protein level expression also increased to some extent (**Figures 1F,G**), the changes of mRNA expression level and protein level of GFRα1 were not obvious (**Figures 1C,H,I**), and the mRNA expression level of MAGE4 and PRDM1 decreased (**Figures 1D,E**), the above results indicate that TET1 has maintained the function of spermatogonia self-renewal.

Although the mRNA expression levels of Cylin A and Cylin E, which are related to the cell cycle, were somewhat decreased in TET1 overexpression cells (**Figures 2B,C**), the expression of PCNA, a gene specific for cell proliferation, was significantly increased at the mRNA level (**Figure 2A**). At the protein level, the expression level of PCNA decreased (**Figures 2D,E**), indicating that TET1 overexpression enhanced cell transcription and favored cell proliferation. The mRNA expression levels of VASA, DAZL, and C-KIT, which are associated with spermatogonial differentiation, were all increased to some extent (**Figures 3A–C**), indicating that TET1 can promote spermatogonial differentiation. All the above results indicate that TET1 overexpression can maintain the self-renewal state of spermatogonia, which leads to enhanced cell transcription and facilitates cell proliferation and differentiation.

Analysis of Global mRNA Levels After TET1 Overexpression

To identify the dynamic changes in the overall mRNA levels in spermatogonia after TET1 gene overexpression, we examined TET1 overexpression cells and control cells by RNA-seq and QRT-PCR techniques. We used differential multiplicity FC >=2 or FC <=.5 (that is, the absolute value of log2FC >= 1) and value of $p<.05$ as the criteria, and the genes thus screened were differentially expressed genes (DEGs). The sequencing results showed that there were 455 differentially expressed genes, of which 195 genes were upregulated at the mRNA level and 260 genes were downregulated at the mRNA level (**Figure 4A**). Using GO analysis, we found that genes involved in transcriptional regulation were significantly enriched in TET1 overexpressing spermatogonia (**Figure 4B**). This result suggests that TET1 overexpressing cells are more conducive to cellular transcription than control cells, resulting in enhanced cellular activity.

SP1 and DAXX Co-regulate Self-Renewal of Spermatogonia

After determining the fluctuating changes in overall mRNA levels after TET1 overexpression, we analyzed the 195 upregulated differential genes and found that SP1 was significantly different (**Figure 4A**). QRT-PCR results showed that the mRNA level expression of SP1 increased after TET1 overexpression (**Figure 5A**), and WB detection revealed that SP1 was also expressed at the protein level (**Figures 5B,C**), and then we performed immunofluorescence staining of the cells and found that the level of SP1 protein was significantly increased in the TET1 overexpressed cells (**Figures 6A,B**), indicating an increase in cell viability. The above results indicated that TET1 overexpression upregulated the SP1 expression level, accelerated the gene transcription of the cells, and facilitated cell proliferation. Subsequently, we analyzed among 260 downregulated differential genes and found that DAXX was also significantly differential (**Figure 4A**), and WB detection of DAXX and its downstream P53 revealed that DAXX and P53 were somewhat decreased in protein level expression (**Figures 5D–G**), which was consistent with the previous RNA sequencing results. The above results suggest that there may be some connection between SP1 and DAXX and P53, and that DAXX co-regulates transcription and affects cell proliferation by binding to transcription factor SP1, epigenetic modifiers and chromatin remodelers.

SP1-DAXX-TET1 Affect Self-Renewal of Spermatogonia *via* NF-Kappa B Signaling Pathway

We performed protein sequencing on TET1 overexpression cells and control cells, and KEGG analysis revealed a significant enrichment of differentially expressed genes in the NF-kappa B signaling pathway, suggesting a possible co-regulation of the NF-kappa B signaling pathway (**Figure 7A**). Subsequently, we found multiple protein interaction patterns between significantly differentially expressed genes in the protein interaction network map (**Figures 7B–D**), and analysis in connection with the KEGG signaling pathway revealed that in the apoptotic signaling pathway, DAXX affects the expression of P53 by regulating downstream Jun, thus playing a pro-apoptotic role, while our transcriptome sequencing results showed that DAXX is expressed in TET1 over expression was downregulated in TET1-overexpressing cells, leading to attenuation of the pro-apoptotic effect, which may be related to the inhibition of NFKB1 that accompanies the apoptotic signaling pathway, which promotes cell survival, and transcriptome sequencing

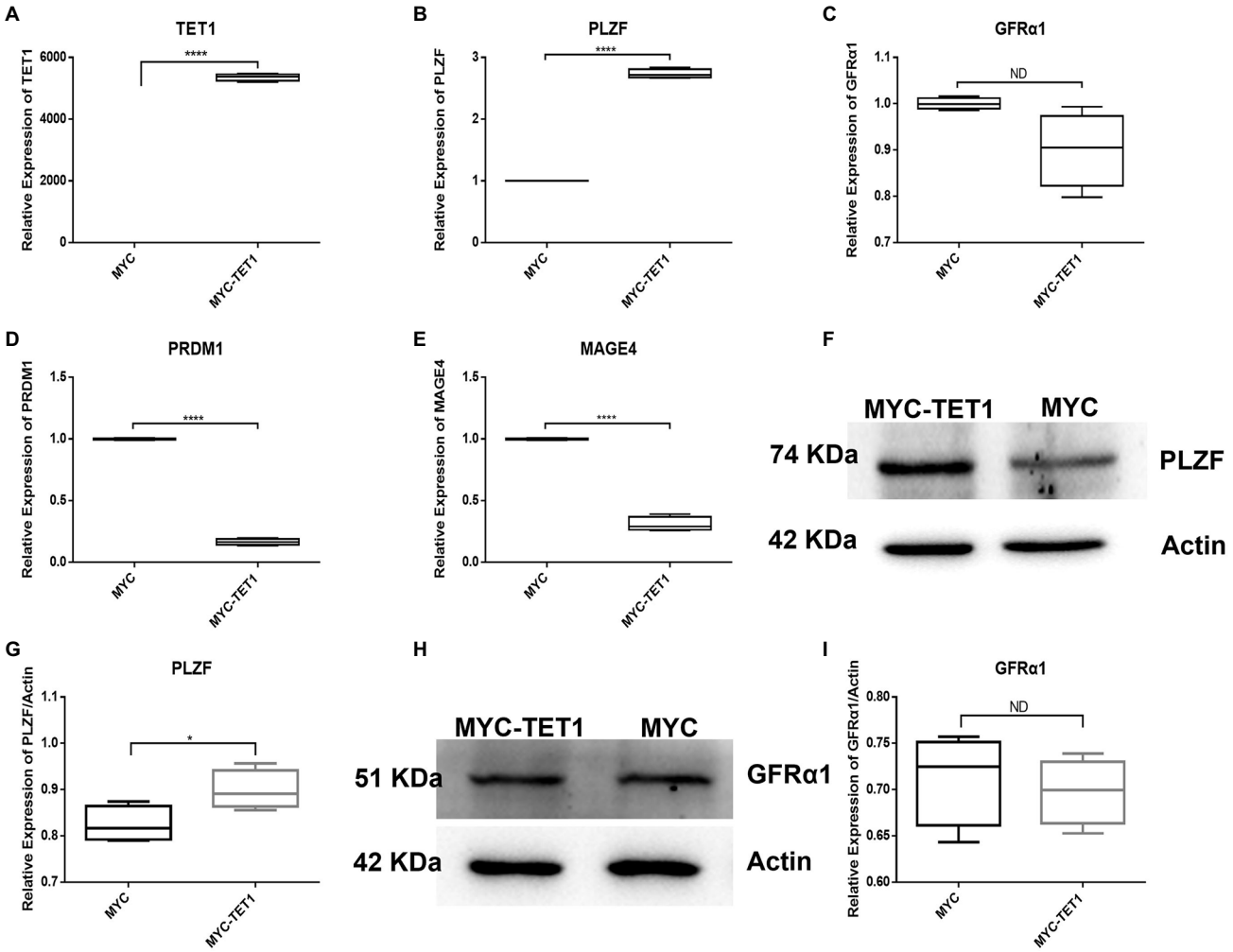

FIGURE 1 | Relative expression of specific genes in spermatogonial cells. **(A)** The mRNA expression of TET1 in spermatogonial cells was detected by QRT-PCR. **(B)** The mRNA expression of PLZF in spermatogonial cells was detected by QRT-PCR. **(C)** The mRNA expression of GFRα1 in spermatogonial cells was detected by QRT-PCR. **(D)** The mRNA expression of PRDM1 in spermatogonial cells was detected by QRT-PCR. **(E)** The mRNA expression of MAGE4 in spermatogonial cells was detected by QRT-PCR. **(F)** The expression of PLZF in TET1 overexpressed cells was detected by Western Blot. **(G)** Quantification of PLZF protein levels in TET1 overexpressed cells. **(H)** The expression of GFRα1 in TET1 overexpressed cells was detected by Western Blot. **(I)** Quantification of GFRα1 protein levels in TET1 overexpressed cells. $p < .0001$(****), $p < .001$(***), $p < .01$(**), $p < .05$(*).

results also showed upregulation of NFKB1 expression. Secondly, we also found that SP1 was highly expressed in TET1 overexpressing cells. SP1 and its reciprocal protein CDK9 jointly regulate the transcriptional signaling pathway, and high expression of CDK9 affects its downstream KLF3, PBX3 and UTX, playing a differentiation inhibitory, pro-proliferative role. The above results suggest that there may be some antagonistic effect between SP1 and DAXX, and finally reach a dynamic balance to maintain the self-renewal of spermatogonia.

DISCUSSION

In this study, we determined the differential methylation sites of TET1 hydroxylation by overexpression of TET1 in spermatogonia, and combined with mRNA level and protein level analysis to further explain the regulatory mechanism of TET1 on spermatogonia self-renewal at the epigenetic level. Studies on TET1 in recent years have focused on cancer, with generally low 5hmC expression levels in patients with breast, lung, liver, gastric and pancreatic cancers, suggesting that downregulation of TET1 expression may contribute to cancer and that TET1 plays a tumor suppressive role in epigenetic modifications (Cimmino et al., 2015; Park et al., 2016; Pei et al., 2016; Collignon et al., 2018; Wu et al., 2019; Zhang et al., 2019). Moreover, TET1 can function in different cell types through different regulatory pathways (Hill et al., 2018; Damal Villivalam et al., 2020; Li et al., 2020; Smeriglio et al., 2020). Previous studies have found that TET and its intermediate 5hmC can affect male spermatogenesis through epigenetic

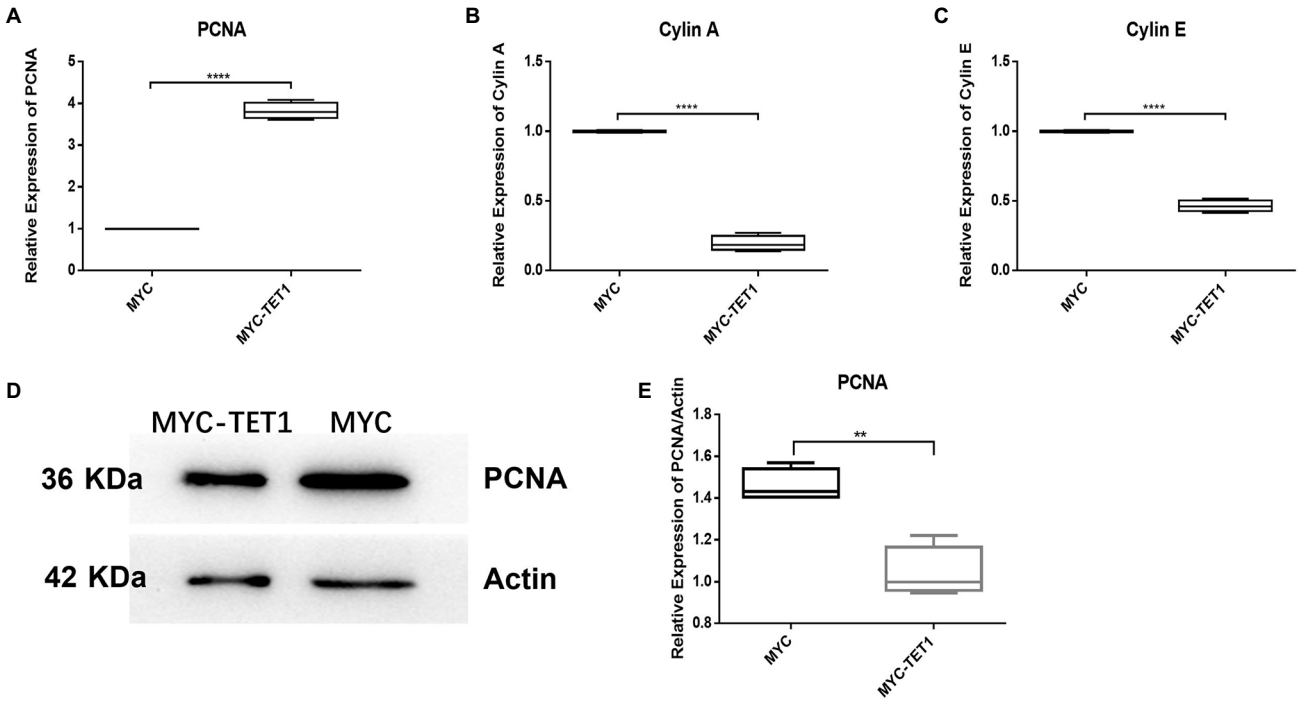

FIGURE 2 | Relative expression of specific genes in spermatogonial cells. **(A)** The mRNA expression of PCNA in spermatogonial cells was detected by QRT-PCR. **(B)** The mRNA expression of Cylin A in spermatogonial cells was detected by QRT-PCR. **(C)** The mRNA expression of Cylin E in spermatogonial cells was detected by QRT-PCR. **(D)** The expression of PCNA in TET1 overexpressed cells was detected by Western Blot. **(E)** Quantification of PCNA protein levels in TET1 overexpressed cells. $p < .0001$(****), $p < .001$(***), $p < .01$(**), $p < .05$(*).

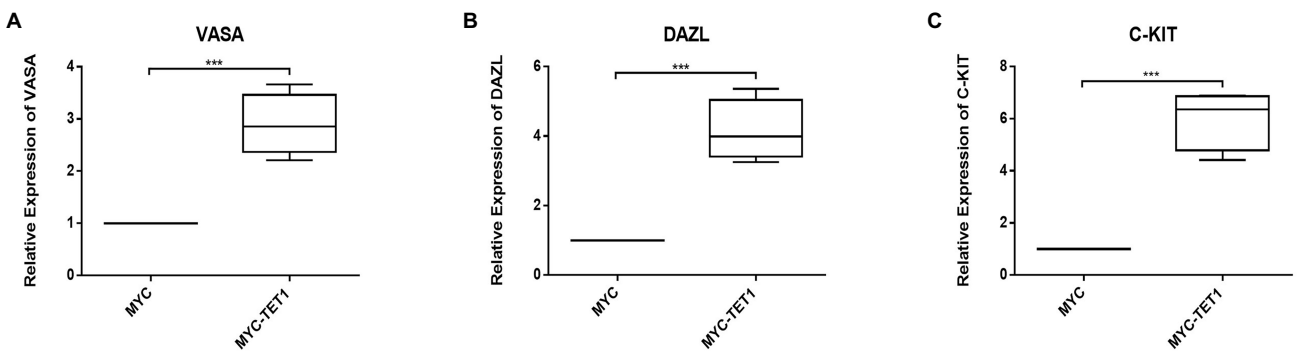

FIGURE 3 | Relative expression of specific genes in spermatogonial cells. **(A)** The mRNA expression of VASA in spermatogonial cells was detected by QRT-PCR. **(B)** The mRNA expression of DAZL in spermatogonial cells was detected by QRT-PCR. **(C)** The mRNA expression of C-KIT in spermatogonial cells was detected by QRT-PCR. $p < .001$(***), $p < .01$(**), $p < .05$(*).

modifications and have a crucial role in maintaining spermatogenesis (Ni et al., 2016). TET1 expression levels decline with age and TET1 is also associated with reduced fertility (Huang et al., 2020).

We examined spermatogonia-specific genes at mRNA level and protein level after TET1 overexpression and found that PLZF, a gene related to self-renewal, was upregulated at both mRNA level and protein level, indicating that TET1 has the function of maintaining spermatogonia self-renewal. The mRNA expression levels of Cylin A and Cylin E associated with cell cycle were somewhat decreased, but the expression of PCNA, a gene specific for cell proliferation, was significantly increased at the mRNA level, suggesting that TET1 overexpression did not exactly promote cell proliferation, but rather enhanced cell transcription. The mRNA expression levels of VASA, DAZL, and C-KIT, which are associated with spermatogonia differentiation, were all increased to some extent, indicating that TET1 can promote spermatogonia differentiation. All of these results verified that epigenetic modifications of TET1 play a key role in spermatogenesis and can maintain normal spermatogenesis (Zheng et al., 2016).

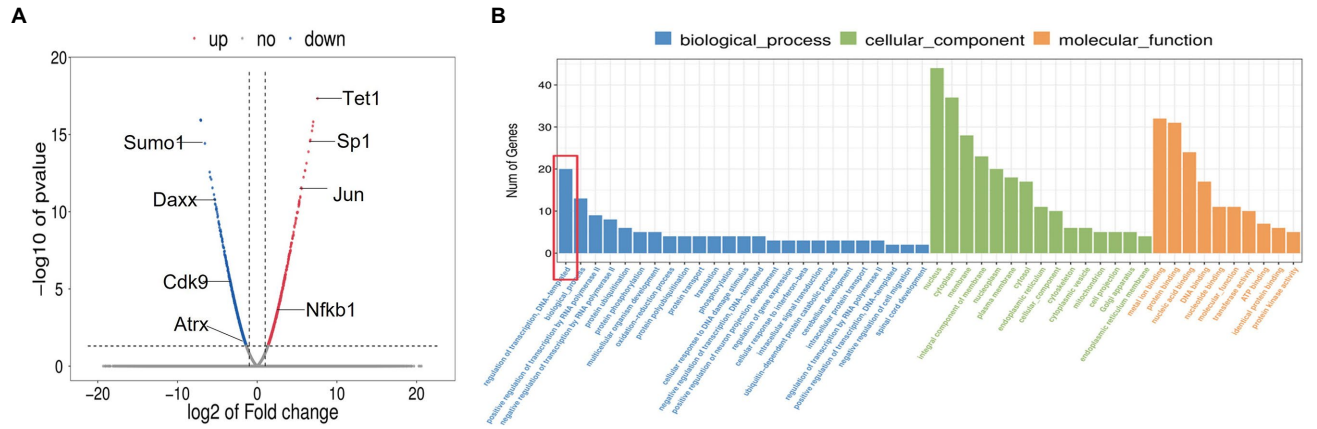

FIGURE 4 | Sequencing results of 36 h transcriptome of TET1 overexpression group and control group. **(A)** Transcriptome 36 h differential gene volcano map. The abscissa represents the differential expression multiple changes of genes in different samples. The ordinate represents the statistical significance of changes in gene expression levels. Red represents significantly upregulated differentially expressed genes, blue represents significantly downregulated differentially expressed genes, and gray dots represent nonsignificantly differentially expressed genes. **(B)** Histogram of GO enrichment of differential genes.

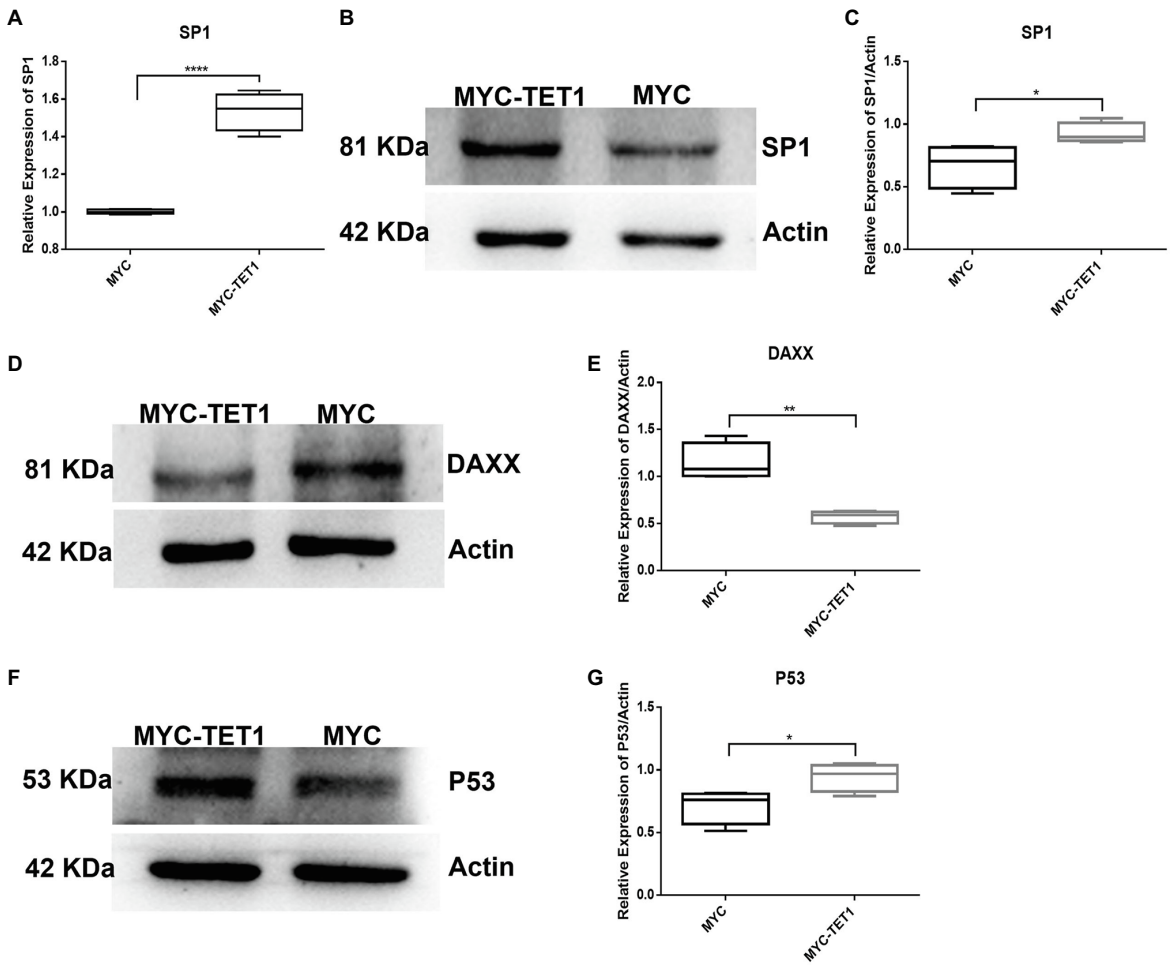

FIGURE 5 | mRNA and protein levels of TET1 and MYC-TET1 cells were detected. **(A)** The mRNA expression of SP1 in spermatogonial cells was detected by QRT-PCR. **(B)** The expression of SP1 in TET1 overexpressed cells was detected by Western Blot. **(C)** Quantification of SP1 protein levels in TET1 overexpressed cells. **(D)** The expression of DAXX in TET1 overexpressed cells was detected by Western Blot. **(E)** Quantification of DAXX protein levels in TET1 overexpressed cells. **(F)** The expression of P53 in TET1 overexpressed cells was detected by Western Blot. **(G)** Quantification of P53 protein levels in TET1 overexpressed cells. $p < .0001$(****), $p < .001$(***), $p < .01$(**), $p < .05$(*).

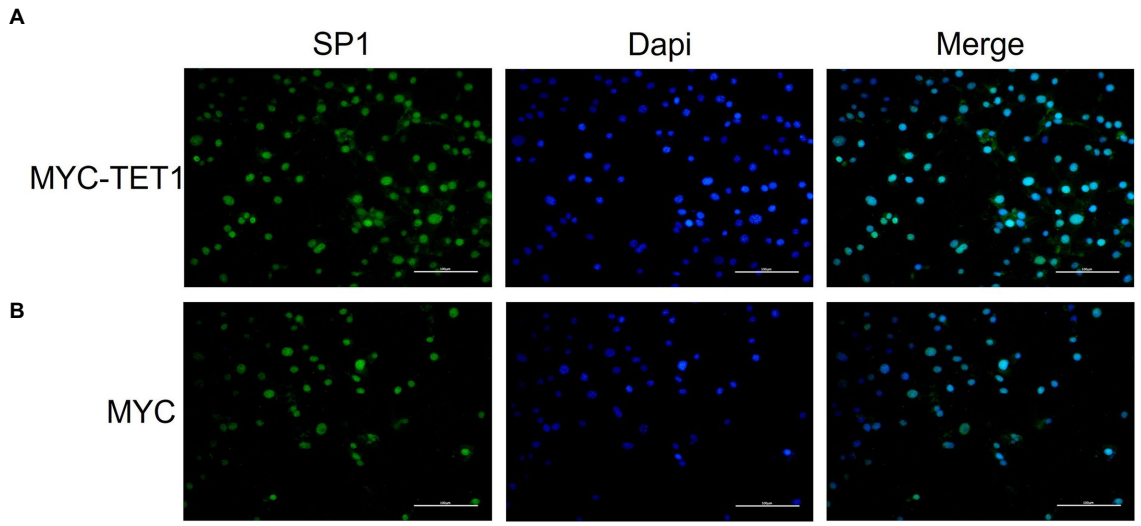

FIGURE 6 | Immunofluorescence staining of SP1 in overexpressed and control cells cultured *in vitro*. **(A)** Immunofluorescence staining of SP1 in overexpressed cells (MYC-TET1) cultured *in vitro*. **(B)** Immunofluorescence staining of SP1 in control cells (MYC) cultured *in vitro*.

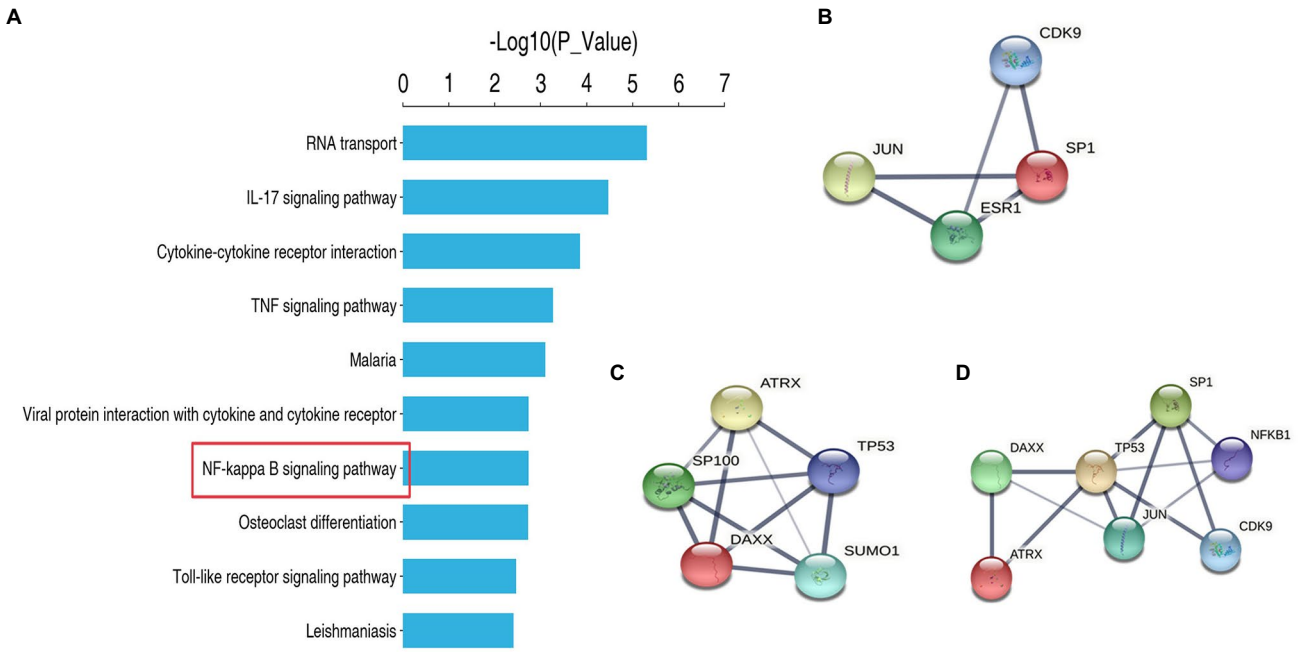

FIGURE 7 | Protein sequencing analysis and protein interaction analysis. **(A)** KEGG enrichment analysis. **(B)** Protein Interaction Analysis of SP1. **(C)** Protein Interaction Analysis of DAXX. **(D)** Protein Interaction Analysis of SP1 and DAXX.

Subsequently, we further sequenced TET1 overexpression cells and control cells, and our analysis revealed a total of 455 differentially expressed genes, of which 195 genes were upregulated in expression at the mRNA level and 260 genes were downregulated at the mRNA level. We then used GO enrichment analysis to find that genes involved in transcriptional regulation were significantly enriched in TET1 over-expressing spermatogonia. This result suggests that TET1 overexpressing cells are more conducive to cellular transcription and thus enhanced cellular activity compared to control cells. Among these differentially upregulated genes, we found a significant upregulation of SP1, the SP family that includes SP1, SP2, SP3 and SP4, which function in various important biological processes and have been shown to have biological importance in cell growth, differentiation, apoptosis and oncogenesis (Vizcaíno et al., 2015). SP1 target

genes are mainly involved in cell proliferation and tumorigenesis (Safe and Abdelrahim, 2005; Wierstra, 2008). In contrast, in previous experiments, we found that TET1 did not lead to a single proliferation due to high SP1 expression, but achieved a dynamic balance of proliferation, suggesting that SP1 may activate or repress the expression of some genes related to essential cellular functions. Our review of the literature shows the extreme complexity of SP1 function. SP1 not only activates, it also represses the expression of some essential oncogenes and tumor suppressors, and SP1 regulates some genes related to essential cellular functions, such as proliferation, differentiation, apoptosis, senescence, DNA damage response and angiogenesis. SP1 is also importantly associated with inflammation, genomic instability, and epigenetic silencing (Hanahan and Weinberg, 2000; Hanahan and Weinberg, 2011). We subsequently found significant downregulation of DAXX in differentially regulated genes. The biological function of DAXX is complex. Previous studies have identified a common denominator of interest in various cancers, namely that DAXX is overexpressed in a variety of cancers and its possible association with tumorigenesis, disease progression, and treatment resistance. DAXX can regulate transcription by binding to transcription factors, chromatin remodelers, and epigenetic modifiers. Their interactions can even directly affect apoptosis and cell signaling (Mahmud and Liao, 2019). Subsequently, we found that both SP1 and DAXX are proteins that interact with P53 through protein interaction analysis. A previous study showed that SP1 is a key factor in P53-mediated apoptosis (Li et al., 2014). Genome-wide analysis of the chromatin occupied by P53 and parallel analysis of gene expression have identified SP1 as one of the P53 regulators specific for P53-mediated transcriptional responses in the induction of apoptosis in tumor cells (Nikulenkov et al., 2012). Previous studies have identified a potential role of DAXX in the transcriptional, apoptotic and negative regulation of the P53 oncogenic pathway (Wasylishen et al., 2018). We sequenced proteins from TET1 overexpressing cells and control cells, and KEGG analysis revealed a significant enrichment of differentially expressed genes in the NF-kappa B signaling pathway and an overall upregulation of gene expression, suggesting that the NF-kappa B signaling pathway may be synergistically regulated. In the apoptotic signaling pathway, DAXX affects the expression of P53 by regulating downstream Jun, thus acting as a proapoptotic agent, while our transcriptome sequencing results showed that DAXX expression was downregulated in TET1 overexpressing cells, leading to a diminished pro-apoptotic effect, which may be related to the inhibition of NFKB1 that accompanies the apoptotic signaling pathway. KEGG analysis showed that NFKB1 could promote cell survival, and transcriptome sequencing results also showed upregulation of NFKB1 expression. Subsequently, we found that SP1 was highly expressed in TET1 overexpressing cells and that SP1 co-regulates the transcriptional signaling pathway with its counterpart, CDK9. CDK9 high expression affects its downstream KLF3, PBX3 and UTX, acting to inhibit differentiation and promote proliferation. We speculate that there may be some antagonistic effect between SP1 and DAXX, which eventually reaches a dynamic balance to maintain the self-renewal state of spermatogonia.

In summary, our results indicate that TET1 maintains self-renewal of mouse spermatogonia and facilitates cellular transcription, enhancing cellular activity, and we have identified key differential genes affected by the specific effects of TET1 and the mechanisms of interaction between these key differential genes, providing a scientific basis for studying spermatogenesis, revealing the causes of spermatogenic disorders, and elucidating their mechanisms, which may contribute to the understanding of male reproductive disorders.

DATA AVAILABILITY STATEMENT

The datasets presented in this study can be found in online repositories. The names of the repository/repositories and accession number(s) can be found at: GEO, GSE193717; ProteomeXchange, PXD030967.

AUTHOR CONTRIBUTIONS

LZ: conceptualization, resources, writing—review and editing, and funding acquisition. LL: methodology, formal analysis, and writing—original draft preparation. JW and SW: validation. JW: investigation. MW: data curation. YC: project administration. All authors contributed to manuscript revision, read, and approved the submitted version.

FUNDING

This work was supported by the National Natural Science Foundation of China (grant no. 31902225), the Anhui Province Natural Science Fund Project (grant no. 1908085QC92), the National Natural Science Foundation of China (82173559), and the Key Research and Development Projects of Anhui Province (202104j07020035).

REFERENCES

Beishline, K., and Azizkhan-Clifford, J. (2015). Sp1 and the 'hallmarks of cancer'. *FEBS J.* 282, 224–258. doi: 10.1111/febs.13148

Bogolyubova, I., and Bogolyubov, D. (2021). DAXX is a crucial factor for proper development of mammalian oocytes and early embryos. *Int. J. Mol. Sci.* 22. doi: 10.3390/ijms22031313

Chang, H. Y., Nishitoh, H., Yang, X., Ichijo, H., and Baltimore, D. (1998). Activation of apoptosis signal-regulating kinase 1 (ASK1) by the adapter protein Daxx. *Science* 281, 1860–1863. doi: 10.1126/science.281.5384.1860

Cimmino, L., Dawlaty, M. M., Ndiaye-Lobry, D., Yap, Y. S., Bakogianni, S., Yu, Y., et al. (2015). TET1 is a tumor suppressor of hematopoietic malignancy. *Nat. Immunol.* 16, 653–662. doi: 10.1038/ni.3148

Collignon, E., Canale, A., Al Wardi, C., Bizet, M., Calonne, E., Dedeurwaerder, S., et al. (2018). Immunity drives TET1 regulation in cancer through NF-κB. *Sci. Adv.* 4:eaap7309. doi: 10.1126/sciadv.aap7309

Craig, J. R., Jenkins, T. G., Carrell, D. T., and Hotaling, J. M. (2017). Obesity, male infertility, and the sperm epigenome. *Fertil. Steril.* 107, 848–859. doi: 10.1016/j.fertnstert.2017.02.115

Cui, X. L., Nie, J., Ku, J., Dougherty, U., West-Szymanski, D. C., Collin, F., et al. (2020). A human tissue map of 5-hydroxymethylcytosines exhibits tissue specificity through gene and enhancer modulation. *Nat. Commun.* 11:6161. doi: 10.1038/s41467-020-20001-w

Damal Villivalam, S., You, D., Kim, J., Lim, H. W., Xiao, H., Zushin, P. H., et al. (2020). TET1 is a beige adipocyte-selective epigenetic suppressor of thermogenesis. *Nat. Commun.* 11:4313. doi: 10.1038/s41467-020-18054-y

Dupuis-Maurin, V., Brinza, L., Baguet, J., Plantamura, E., Schicklin, S., Chambion, S., et al. (2015). Overexpression of the transcription factor Sp1 activates the OAS-RNAse L-RIG-I pathway. *PLoS One* 10:e0118551. doi: 10.1371/journal.pone.0118551

Guo, L., Fang, L., and Liu, Y. (2019). SP1-regulated LINC01638 promotes proliferation and inhibits apoptosis in non-small cell lung cancer. *Eur. Rev. Med. Pharmacol. Sci.* 23, 8913–8920. doi: 10.26355/eurrev_201910_19287

Hanahan, D., and Weinberg, R. A. (2000). The hallmarks of cancer. *Cell* 100, 57–70. doi: 10.1016/s0092-8674(00)81683-9

Hanahan, D., and Weinberg, R. A. (2011). Hallmarks of cancer: the next generation. *Cell* 144, 646–674. doi: 10.1016/j.cell.2011.02.013

Heaphy, C. M., Bi, W. L., Coy, S., Davis, C., Gallia, G. L., Santagata, S., et al. (2020). Telomere length alterations and ATRX/DAXX loss in pituitary adenomas. *Mod. Pathol.* 33, 1475–1481. doi: 10.1038/s41379-020-0523-2

Hill, P. W. S., Leitch, H. G., Requena, C. E., Sun, Z., Amouroux, R., Roman-Trufero, M., et al. (2018). Epigenetic reprogramming enables the transition from primordial germ cell to gonocyte. *Nature* 555, 392–396. doi: 10.1038/nature25964

Huang, G., Liu, L., Wang, H., Gou, M., Gong, P., Tian, C., et al. (2020). Tet1 deficiency leads to premature reproductive aging by reducing spermatogonia stem cells and germ cell differentiation. *iScience* 23:100908. doi: 10.1016/j.isci.2020.100908

Ivanauskiene, K., Delbarre, E., McGhie, J. D., Küntziger, T., Wong, L. H., and Collas, P. (2014). The PML-associated protein DEK regulates the balance of H3.3 loading on chromatin and is important for telomere integrity. *Genome Res.* 24, 1584–1594. doi: 10.1101/gr.173831.114

Li, H., Hu, Z., Jiang, H., Pu, J., Selli, I., Qiu, J., et al. (2020). TET1 deficiency impairs Morphogen-free differentiation of human embryonic stem cells to Neuroectoderm. *Sci. Rep.* 10:10343. doi: 10.1038/s41598-020-67143-x

Li, H., Zhang, Y., Ströse, A., Tedesco, D., Gurova, K., and Selivanova, G. (2014). Integrated high-throughput analysis identifies Sp1 as a crucial determinant of p53-mediated apoptosis. *Cell Death Differ.* 21, 1493–1502. doi: 10.1038/cdd.2014.69

Lio, C. J., Yuita, H., and Rao, A. (2019). Dysregulation of the TET family of epigenetic regulators in lymphoid and myeloid malignancies. *Blood* 134, 1487–1497. doi: 10.1182/blood.2019791475

Liu, Y., Zhang, Y., Yin, J., Gao, Y., Li, Y., Bai, D., et al. (2019). Distinct H3K9me3 and DNA methylation modifications during mouse spermatogenesis. *J. Biol. Chem.* 294, 18714–18725. doi: 10.1074/jbc.RA119.010496

Mahmud, I., and Liao, D. (2019). DAXX in cancer: phenomena, processes, mechanisms and regulation. *Nucleic Acids Res.* 47, 7734–7752. doi: 10.1093/nar/gkz634

Memon, A., and Lee, W. K. (2018). KLF10 as a tumor suppressor gene and its TGF-β signaling. *Cancers* 10:161. doi: 10.3390/cancers10060161

Minhas, S., Bettocchi, C., Boeri, L., Capogrosso, P., Carvalho, J., Cilesiz, N. C., et al. (2021). European Association of Urology Guidelines on Male Sexual and Reproductive Health: 2021 Update on Male Infertility. *Eur. Urol.* 80, 603–620. doi: 10.1016/j.eururo.2021.08.014

Ni, K., Dansranjavin, T., Rogenhofer, N., Oeztuerk, N., Deuker, J., Bergmann, M., et al. (2016). TET enzymes are successively expressed during human spermatogenesis and their expression level is pivotal for male fertility. *Hum. Reprod.* 31, 1411–1424. doi: 10.1093/humrep/dew096

Nikulenkov, F., Spinnler, C., Li, H., Tonelli, C., Shi, Y., Turunen, M., et al. (2012). Insights into p53 transcriptional function via genome-wide chromatin occupancy and gene expression analysis. *Cell Death Differ.* 19, 1992–2002. doi: 10.1038/cdd.2012.89

Nye, J., Melters, D. P., and Dalal, Y. (2018). The art of war: harnessing the epigenome against cancer. *F1000Res* 7:141. doi: 10.12688/f1000research.12833.1

Park, S. J., Lee, B. R., Kim, H. S., Ji, Y. R., Sung, Y. H., ShikChoi, K., et al. (2016). Inhibition of migration and invasion by Tet-1 overexpression in human lung carcinoma H460 cells. *Oncol. Res.* 23, 89–98. doi: 10.3727/096504015x14496932933539

Pei, Y. F., Tao, R., Li, J. F., Su, L. P., Yu, B. Q., Wu, X. Y., et al. (2016). TET1 inhibits gastric cancer growth and metastasis by PTEN demethylation and re-expression. *Oncotarget* 7, 31322–31335. doi: 10.18632/oncotarget.8900

Peng, F., Zhou, Y., Wang, J., Guo, B., Wei, Y., Deng, H., et al. (2020). The transcription factor Sp1 modulates RNA polymerase III gene transcription by controlling BRF1 and GTF3C2 expression in human cells. *J. Biol. Chem.* 295, 4617–4630. doi: 10.1074/jbc.RA119.011555

Rasmussen, K. D., and Helin, K. (2016). Role of TET enzymes in DNA methylation, development, and cancer. *Genes Devs.* 30, 733–750. doi: 10.1101/gad.276568.115

Ross, S. E., and Bogdanovic, O. (2019). TET enzymes, DNA demethylation and pluripotency. *Biochem. Soc. Trans.* 47, 875–885. doi: 10.1042/bst20180606

Safe, S., and Abdelrahim, M. (2005). Sp transcription factor family and its role in cancer. *Eur. J. Cancer* 41, 2438–2448. doi: 10.1016/j.ejca.2005.08.006

Smeriglio, P., Grandi, F. C., Davala, S., Masarapu, V., Indelli, P. F., Goodman, S. B., et al. (2020). Inhibition of TET1 prevents the development of osteoarthritis and reveals the 5hmC landscape that orchestrates pathogenesis. *Sci. Transl. Med.* 12:eaax2332. doi: 10.1126/scitranslmed.aax2332

Vander Borght, M., and Wyns, C. (2018). Fertility and infertility: definition and epidemiology. *Clin. Biochem.* 62, 2–10. doi: 10.1016/j.clinbiochem.2018.03.012

Vellingiri, B., Iyer, M., Devi Subramaniam, M., Jayaramayya, K., Siama, Z., Giridharan, B., et al. (2020). Understanding the role of the transcription factor Sp1 in ovarian cancer: from theory to practice. *Int. J. Mol. Sci.* 21:1153. doi: 10.3390/ijms21031153

Vizcaíno, C., Mansilla, S., and Portugal, J. (2015). Sp1 transcription factor: A long-standing target in cancer chemotherapy. *Pharmacol. Ther.* 152, 111–124. doi: 10.1016/j.pharmthera.2015.05.008

Wasylishen, A. R., Estrella, J. S., Pant, V., Chau, G. P., and Lozano, G. (2018). Daxx functions are p53-independent In vivo. *Mol. Cancer Res.* 16, 1523–1529. doi: 10.1158/1541-7786.Mcr-18-0281

Wierstra, I. (2008). Sp1: emerging roles--beyond constitutive activation of TATA-less housekeeping genes. *Biochem. Biophys. Res. Commun.* 372:18364237, 1–13. doi: 10.1016/j.bbrc.2008.03.074

Wu, C., and Morris, J. R. (2001). Genes, genetics, and epigenetics: a correspondence. *Science* 293, 1103–1105. doi: 10.1126/science.293.5532.1103

Wu, H., D'Alessio, A. C., Ito, S., Wang, Z., Cui, K., Zhao, K., et al. (2011). Genome-wide analysis of 5-hydroxymethylcytosine distribution reveals its dual function in transcriptional regulation in mouse embryonic stem cells. *Genes Dev.* 25, 679–684. doi: 10.1101/gad.2036011

Wu, J., Li, H., Shi, M., Zhu, Y., Ma, Y., Zhong, Y., et al. (2019). TET1-mediated DNA hydroxymethylation activates inhibitors of the Wnt/β-catenin signaling pathway to suppress EMT in pancreatic tumor cells. *J. Exp. Clin. Cancer Res.* 38:348. doi: 10.1186/s13046-019-1334-5

Xu, Y., Wu, W., Han, Q., Wang, Y., Li, C., Zhang, P., et al. (2019). Post-translational modification control of RNA-binding protein hnRNPK function. *Open Biol.* 9:180239. doi: 10.1098/rsob.180239

Yang, X., Khosravi-Far, R., Chang, H. Y., and Baltimore, D. (1997). Daxx, a novel Fas-binding protein that activates JNK and apoptosis. *Cell* 89, 1067–1076. doi: 10.1016/s0092-8674(00)80294-9

Zhang, B., Xiang, S., Yin, Y., Gu, L., and Deng, D. (2013). C-terminal in Sp1-like artificial zinc-finger proteins plays crucial roles in determining their DNA binding affinity. *BMC Biotechnol.* 13:106. doi: 10.1186/1472-6750-13-106

Zhang, H., Zhang, X., Clark, E., Mulcahey, M., Huang, S., and Shi, Y. G. (2010). TET1 is a DNA-binding protein that modulates DNA methylation and gene transcription via hydroxylation of 5-methylcytosine. *Cell Res.* 20, 1390–1393. doi: 10.1038/cr.2010.156

Zhang, P. F., Wei, C. Y., Huang, X. Y., Peng, R., Yang, X., Lu, J. C., et al. (2019). Circular RNA circTRIM33-12 acts as the sponge of MicroRNA-191 to suppress hepatocellular carcinoma progression. *Mol. Cancer* 18:105. doi: 10.1186/s12943-019-1031-1

Zheng, L., Zhai, Y., Li, N., Ma, F., Zhu, H., Du, X., et al. (2016). The modification of Tet1 in male Germline stem cells and interact with PCNA, HDAC1 to promote their self-renewal and proliferation. *Sci. Rep.* 6:37414. doi: 10.1038/srep37414

Conflict of Interest: The authors declare that the research was conducted in the absence of any commercial or financial relationships that could be construed as a potential conflict of interest.

Publisher's Note: All claims expressed in this article are solely those of the authors and do not necessarily represent those of their affiliated organizations, or those of the publisher, the editors and the reviewers. Any product that may be evaluated in this article, or claim that may be made by its manufacturer, is not guaranteed or endorsed by the publisher.

frontiers in Endocrinology

ORIGINAL RESEARCH
published: 18 February 2022
doi: 10.3389/fendo.2022.812974

Prevalence and Characteristics of Erectile Dysfunction in Obstructive Sleep Apnea Patients

Chen Feng[1,2,3†], Yan Yang[2,3†], Lixiao Chen[1], Ruixiang Guo[2,3], Huayang Liu[2,3], Chaojie Li[2,3], Yan Wang[2,3], Pin Dong[1] and Yanzhong Li[2,3*]*

[1] Department of Otolaryngology Head and Neck Surgery, Shanghai General Hospital, Shanghai Jiaotong University School of Medicine, Shanghai, China, [2] Department of Otorhinolaryngology, Qilu Hospital, Shandong University Cheeloo College of Medicine, Jinan, China, [3] NHC Key Laboratory of Otorhinolaryngology (Shandong University), Jinan, China

OPEN ACCESS

Edited by:
Qing Chen,
Army Medical University, China

Reviewed by:
Giovanni Luca,
University of Perugia, Italy
Heng-Gui Chen,
Fujian Medical University, China

***Correspondence:**
Pin Dong
dongpin64@aliyun.com
Yanzhong Li
liyanzhong@sdu.edu.cn

[†]These authors have contributed equally to this work

Specialty section:
This article was submitted to Reproduction, a section of the journal Frontiers in Endocrinology

Received: *11 November 2021*
Accepted: *12 January 2022*
Published: *18 February 2022*

Citation:
Feng C, Yang Y, Chen L, Guo R, Liu H, Li C, Wang Y, Dong P and Li Y (2022) Prevalence and Characteristics of Erectile Dysfunction in Obstructive Sleep Apnea Patients. Front. Endocrinol. 13:812974. doi: 10.3389/fendo.2022.812974

Background: Obstructive sleep apnea (OSA) is a common and severe social problem. Erectile dysfunction (ED) is an important health concern. The prevalence of OSA with ED is increasing, which significantly affects the quality of life and work efficiency of patients. However, the mechanism underlying the comorbidity of these two diseases remains unclear.

Objectives: (1) Investigate the prevalence of OSA with ED; (2) analyze the correlation between OSA and ED; and (3) explore the treatment response to and possible mechanism of uvulapalatopharyngoplasty (UPPP) in patients with OSA and ED. This study aims to provide a theoretical basis for the clinical diagnosis and comprehensive treatment of OSA with ED and improve prevention and treatment strategies.

Materials and Methods: In total, 135 subjects were enrolled in the study. Clinical data, polysomnography, the ESS score, Beck anxiety score, Beck depression score, IIEF-5 score and ASEX score were recorded before UPPP and 6 months after UPPP. Sex hormones were measured for all subjects using a Roche electrochemiluminescence analyzer.

Result: The prevalence of OSA with ED was 64.52%, and the prevalence of severe OSA with ED was 73.02%. The prevalence of OSA with ED increased with age, BMI and apnea-hypopnea index (AHI) value. Among polysomnography indicators, minimum oxygen saturation and average oxygen saturation may predict the occurrence of OSA with ED. Improving the patient's anxiety and depression is very important for treating OSA with ED. Sex hormone levels were not significantly correlated with the occurrence of OSA with ED.

Conclusion: ED is a common symptom of OSA patients. This study showed that sex hormone levels in OSA patients with ED were not significantly correlated with the condition, but further investigation of this relationship is worthwhile. It is recommended

that the free and combined types of sex hormones be further distinguished during testing because the free type is the active form. UPPP surgical treatment is effective for OSA with ED, and its possible mechanism is protection of the peripheral nerves of the sex organs by improving nighttime hypoxia and arousal.

Keywords: obstructive sleep apnea, erectile dysfunction, polysomnography, sex hormones, IIEF-5 questionnaire

INTRODUCTION

Obstructive sleep apnea (OSA) is a serious health hazard that requires long-term, multidisciplinary therapy and has a prevalence of 9% to 38% in the general population (1, 2). Previous studies have shown that OSA is a significant independent factor for hypertension, diabetes, coronary heart disease and other diseases (3–6). OSA has become a common and serious social problem that significantly affects the quality of life and work efficiency of patients, especially those who are overweight (7). Snoring, excessive daytime sleepiness, inattention, and erectile dysfunction (ED) are common comorbidities in OSA patients (8, 9).

Due to recurrent snoring, apnea and microarousal, OSA patients may have the following pathophysiological changes (10). First, repeated awakening at night can significantly reduce non-rapid eye movement (NREM) sleep and rapid eye movement (REM) sleep, resulting in sleep structure disorder, reduced sleep efficiency, daytime drowsiness, fatigue, memory loss and hormone secretion disorder. Second, chronic intermittent hypoxia can cause increased catecholamine secretion and vascular endothelial injury, leading to hypertension and atherosclerosis. Finally, decreased blood oxygen saturation is also closely related to arrhythmia, and increased erythropoietin levels can lead to increases in hemoglobin levels, the number of red blood cells, and platelet activity and reduced fibrinolytic activity and then induce coronary heart disease and cerebral thrombosis. The quality of REM sleep in OSA patients is generally worse than that of NREM sleep (11, 12). Series (12) has shown that in patients with OSA, the decrease in blood oxygen saturation (SaO_2) during REM sleep is greater than that during NREM sleep. Moreover, Findley (11) found that the sleep apnea duration during REM sleep is longer than that during NREM sleep, and hypoxemia is more severe. And Shi's study (13) showed sleep duration for men and women may be independent predictors of conception.

According to the National Institutes of Health Consensus meeting, ED is defined as a persistent inability to achieve or maintain an erection or sustain an adequate sexual relationship (14). Erection is an event involving the interaction of the psychological, neurological, endocrine and vascular systems. It is estimated that by 2025, 300 million men worldwide will be living with ED (15). Guilleminault (16) was the first to study the relationship between erectile function and OSA and showed a higher prevalence of ED in patients with severe OSA (48%). Subsequent epidemiological and clinical studies have supported the conclusion that OSA is associated with ED (17–22). Kellesarian (23) reported in the review that the prevalence of OSA patients with ED is between 40.9% and 80% and that the risk of ED in patients without OSA is significantly lower than that in OSA patients. Furthermore, Chen's study (19) showed that the prevalence of ED in OSA patients was 9.44 times higher than that in non-OSA patients and that OSA was an independent risk factor for the development of ED. Smith (24) reported that OSA with ED is closely related to patients' psychological states, such as depression and anxiety. Moreover, studies have shown that continuous positive airway pressure ventilation (CPAP) (17, 25–27) and oral orthotics (17) used to treat OSA can improve ED. However, Stannek (21) reported that the severity of OSA may not be related to the severity of ED. A correlation analysis between erectile function and polysomnography (PSG) results may suggest that factors such as decreased REM sleep can lead to peripheral nerve damage in the sexual organs in patients, resulting in ED (28). In the sleep state, the REM period is usually accompanied by erection, and most of the REM period occurs in the morning, so early morning erection is a common phenomenon (29). And Chen's study (30) found that sleep deprivation or oversleeping can also affect sperm quality. Notably, Andersen (20) reported that reduced REM sleep and increased arousal negatively affected erectile function in male rats. Chen (31) reported male sleep quality and duration may impact male fertility, an important consequence of poor semen quality.

The major factor associated with ED may be endothelial dysfunction, including reduced nitric oxide (NO) production and elevated endothelin levels (32, 33). NO, the most important mediator of penis swelling, plays a key role in the physiological process of erection by stimulating blood vessel dilation, increasing blood flow to the cavernous body and promoting smooth muscle relaxation (34–36), but the molecular levels of NO in OSA have been less studied. Studies have shown that both hypoxia and enhanced oxygen metabolism can stimulate the transcription of pre-endothelin, forming endothelin, the strongest vasoconstrictive substance (32, 33) known to date. Its long-lasting effect is an endogenous long-acting vasoconstrictive regulator that can cause the contraction of spongy smooth muscle cells (37), which has been verified in the experimental environment and OSA patients (38). In addition, there are other nonvascular mechanisms that can explain the mechanism of ED in OSA patients, including changes in hormone levels, as follows: hypothalamic-pituitary-gonadal (HPG) axis (39–41) regulation disorder leading to changes in hormone levels; neurological mechanisms, such as hypothalamic-pituitary-adrenal (HPA) axis (42) regulation disorders and neurological dysfunction; and psychological mechanisms, such as reduced libido and excessive fatigue (43). Although many studies have been conducted on OSA-related endocrine levels, few studies have investigated the HPG axis regulation mechanism in OSA patients

(41). There are still many unclear mechanisms in the relationship between OSA and ED, and there are few prospective studies and basic studies with large sample sizes, so no consistent conclusion has been reached. In this study, the clinical data of OSA patients were used to explore the correlation between OSA and ED.

MATERIALS AND METHODS

Research Process

First, the prevalence the cooccurrence of ED and OSA was investigated. Second, we explored the clinical characteristics of OSA and ED. Finally, the treatment response was assessed. The flow chart is shown in **Figure 1**.

Source of Cases

The subjects of the study were male patients had completed PSG for OSA at the sleep monitoring center from October 2019 to December 2020. The patients reported habitual snoring and daytime sleepiness, with or without nocturnal apnea. The patients were informed of the study plan, and the subjects voluntarily signed the informed consent form following the guidelines of the National Ethics Regulation Committee and in accordance with the Declaration of Helsinki.

Exclusion Criteria

To ensure scientific integrity, the following conditions were excluded: patients older than 60 years and younger than 18 years; patients taking medications that may affect erectile function, including cardiovascular drugs (beta-blockers, clonidine, diuretics and digoxin), antidepressants (tricyclic antidepressants and selective serotonin reuptake inhibitors), antipsychotics, antiepileptics, 5-reductase inhibitors, sedatives, cimetidine and opioids; patients with chronic oxygen-deficient respiratory diseases such as chronic obstructive pulmonary disease (COPD); and patients with a history of epilepsy, mental illness, and other disorders that cause erectile dysfunction.

Sample Size Calculation

We used formulas to estimate the sample size of the research. According to the literature (23) the prevalence of OSA with ED was the lowest 41.0%. We set the probability of the first type of error α=0.05, and used the software EXCEL to calculate the function: $Z_{\alpha/2}$=NORM.S.INV(1-α/2) =1.960. β was the probability of making the second type of error. The greater the test power required by the experimental research, the larger the sample size required. It was generally assumed that β=0.10, and the statistical power 1-β was 90%. The value range of δ was (0.25S, 0.50S), and we assumed that the allowable error δ=0.15. Then, we used the software EXCEL to calculate the function: sample size n= ((NORM.S.INV(1-α/2))/(ASIN(δ/(p*(1-p)) ^0.5)))^2. That is, when the sample size was 40.0, it could meet the inspection requirements. Therefore, our sample size was in line with the sample size estimate.

General Information

The enrollees were surveyed about general demographic data, including basic information about age, height, weight, blood

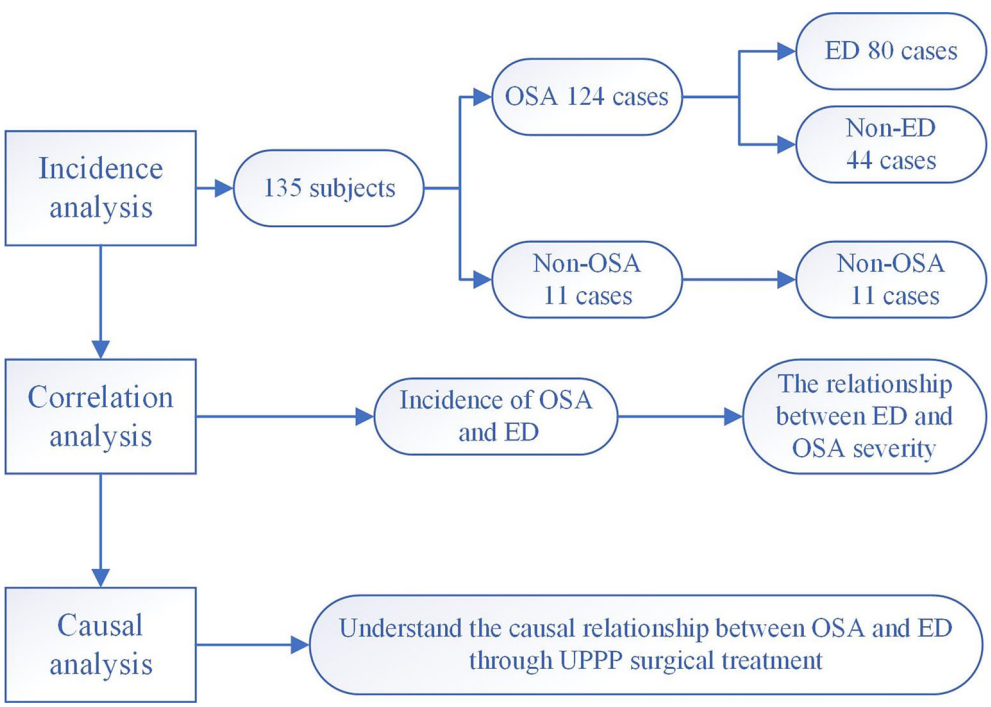

FIGURE 1 | Research flow chart. 135 male subjects with relevant clinical data were included to explore the mechanism underlying the comorbidity of OSA and ED.

pressure, smoking status, drinking status, neck circumference, waist circumference, and hip circumference, and the body mass index (BMI) value was calculated.

The BMI value adopts the Chinese adult standard (44), namely, a BMI value less than 18.5 means low body weight, a BMI value between 18.5 and 24.0 means normal weight, a BMI value between 24.0 and 28.0 means overweight, and a BMI value greater than or equal to 28.0 means obesity. To ensure the authenticity of the information, information collection and questionnaires were conducted anonymously, and specialized clinical technicians explained and verified the contents of the questionnaires.

PSG Data Acquisition and Interpretation Criteria

Overnight PSG includes encephalogram (EEG), electrooculogram (EOG), electromyography (EMG) of the chin muscles, electrocardiogram (ECG), nasal air measurement using pressure sensors, oral air measured with thermistors, chest and abdomen movements, snoring analysis, sleep posture, leg movements and finger pulse oxygen saturation (SO_2) detection. OSA was categorized as mild OSA (5-15 times/h), moderate OSA (15-30 times/h) and severe OSA (more than 30 times/h) according to the apnea-hypopnea index (AHI) value. Manual data analysis was performed by two experienced sleep technicians according to the scoring standards in the diagnostic and treatment guidelines of the American Academy of Sleep Medicine (AASM) (45).

Assessment of Erectile Function

The International Index of Erectile Function (IIEF-5) was used as the main diagnostic basis for erectile dysfunction and includes five aspects: erectile function, orgasm function, libido function, sexual satisfaction and overall satisfaction. An IIEF-5 score less than or equal to 7 indicates severe erectile dysfunction, between 8 and 11 indicates moderate erectile dysfunction, between 12 and 21 indicates mild erectile dysfunction, and greater than or equal to 22 indicates normal erectile function (46).

The Arizona Sexual Experience Scale (ASEX) was used as an auxiliary measure to assess sexual function. There are 5 questions on this scale, and each question is rated as 1-6 points according to sexual function hyperactivity and sexual function depression. The evaluation areas include sexual drive, sexual vigilance, penile erection, orgasm ability and sexual satisfaction. A comprehensive assessment of the patient's sexual function was carried out. Three or more items on the ASEX scale with a score greater than 4 points or any single item scoring greater than 5 or a total score greater than 19 points is indicative of sexual dysfunction (47). The contents of and instructions for the scale were introduced by specialized clinical technicians according to unified guidance, and subjects were given 10-20 minutes to complete it.

Sleep Quality Assessment

The Epworth Sleepiness Scale (ESS) was used to assess daytime sleepiness. There are 8 questions in the scale, and the probability of dozing in each question is "never", "mild", "moderate" and "severe". The scores are 0, 1, 2 and 3, with the highest total score being 24 points. An ESS score greater than 10 is classified as daytime sleepiness (48). The contents of and instructions for the scale were introduced by specialized clinical technicians according to unified guidance, and the time allotted was 5-10 minutes.

Assessment of Anxiety and Depression Symptoms

The Beck Anxiety Inventory (BAI) and the Beck Depression Inventory (BDI-II) were used to evaluate the subjective anxiety and depression status of the study subjects. There are 21 test dimensions in the BAI, and the four expressions correspond to the numbers 1, 2, 3, and 4. Number 1 represents nondisturbing anxiety, from milder to stronger, and number 4 represents symptoms of disturbing anxiety that can only barely be tolerated. The sum of the numbers is the evaluation result, and a score greater than or equal to 45 indicates that the patient is in an anxious state (49).

There are also 21 test dimensions in the BDI-II, which correspond to the numbers 0, 1, 2, and 3. The total score of the 21 items is the final test score. A total score of 0-13 means no depression, 14-19 means mild depression, 20-28 means moderate depression, and 29-63 means severe depression (50). The contents of and instructions for the scale were introduced by specialized clinical technicians according to the unified guidance, and the subjects were given 10-20 minutes for completion.

Peripheral Blood Collection for Assessment of Sex Hormones

At approximately 7:00 in the morning, approximately 3 ml of blood was drawn from the antecubital vein of each enrolled patient into a tube containing no anticoagulant, and the tubes were placed in a water bath for 10 minutes. The temperature was controlled at approximately 37°C. After removal, each sample was centrifuged at 2000 r/min for 10 minutes and then stored at -20°C. Tests for six sex hormones—follicle-stimulating hormone (FSH), luteinizing hormone (LH), testosterone (TEST), estradiol (E2), progesterone (PROG) and prolactin (PRL)—were performed by a Roche electrochemiluminescence analyzer.

OSA-Related Treatment

After the diagnosis of OSA in male patients with ED symptoms, uvulopalatopharyngoplasty (UPPP) was performed, and after treatment, the PSG and IIEF-5 scores of the patients were collected as described above.

Statistical Methods

SPSS 24.0, Prism 9 and Excel were used to process the data. Normally distributed measurement data are expressed as the mean ± standard deviation, and nonnormally distributed measurement data are expressed as the median (interquartile range) [M (Q25~Q75)]. For normally distributed measurement data, an independent-sample t-test or Pearson's chi-square test was used for comparisons between the two groups, and one-sample ANOVA was used for comparisons among three groups. For nonnormally distributed measurement data, the Mann-Whitney U test was used for comparisons between two groups,

and the Kruskal-Wallis H test was used for comparisons among three groups. Spearman's correlation analysis was used to test the correlation between nonnormally distributed measurement data, and Pearson's correlation analysis was used to test the correlation between normally distributed measurement data. Variables that were found to be significant in univariate analysis were included in multivariate analysis, and binary logistic regression analysis was performed. The receiver operating characteristic (ROC) curve was used to evaluate the AUC (area under the curve) of the relevant factors and then evaluate the performance of each factor as a criterion. Count data were used to calculate the composition ratio using the χ^2 test. For normally distributed measurement data, the paired-samples t-test was used to compare the differences before and after treatment. The inspection level was set at α=0.05.

RESULTS

General Conditions

Comparison of Basic Data

There were 30 male subjects with incomplete questionnaires, and 5 male subjects met the exclusion criteria. Ultimately, 135 male subjects with relevant clinical data were included. The median age was 37 years old, BMI was 28.55 ± 4.12 kg/m2, and AHI value was 35.89 ± 23.81 times/h. There were 11 non-OSA subjects, 61 patients with mild to moderate OSA and 63 patients with severe OSA. **Table 1** summarizes the demographic profile and related clinical phenotypes of the included population. The results show that among the non-OSA subjects, patients with mild to moderate OSA, and patients with severe OSA, the BMI (p=0.001), neck circumference (p=0.005), waist circumference (p=0.001), hip circumference (p=0.006), ESS score (p=0.003), Beck anxiety score (p<0.001) and ASEX score (p<0.001) showed a significant increase, while the IIEF-5 score (p<0.001) significantly decreased (**Figure 2A** and **Table 1**).

Comparison of Serum Sex Hormone Levels

Table 2 summarizes the sex hormone test data of the included population. The results show that no significant difference was found in the secretion levels of the six serum sex hormones among the three groups: PRL (p=0.728), FSH (p= 0.062), LH (p= 0.294), PROG (p=0.821), E2 (p= 0.686) and TEST (p= 0.056) (**Figure 2B**).

Prevalence of OSA and ED

There were 124 patients with confirmed OSA and 63 patients with severe OSA. The prevalence of OSA was 91.85% (124/135), with "snoring during sleep" as the chief complaint.

Prevalence of ED and OSA With ED

Figure S1 summarizes the IIEF-5 score of the included population. The results show that a total of 80 ED patients were included in the population, with an prevalence of 59.26% (80/135), and among these subjects, the prevalence of mild ED was 56.30% (76/135), the prevalence of moderate ED was 0.74% (1/135), and the prevalence of severe ED was 2.22% (3/135). There were a total of 80 patients with OSA with ED, with an prevalence of 64.52% (80/124), among whom the prevalence of mild ED was 61.29% (76/124), the prevalence of moderate ED

TABLE 1 | Basic demographics and related clinical phenotypes of the population included in the study.

Clinical Phenotype	Total (n=135)	OSA Patients			Non-OSA Subjects (n=11)	P
		Total (n=124)	Mild to Moderate (n=61)	Severe (n=63)		
Age	37.00 (31.00~44.00)	37.00 (31.00~44.00)	36.00 (30.50~45.00)	38.00 (32.00~43.00)	41.00 (29.00~47.00)	0.906
Smoking status (%)	60 (44.44)	51 (41.13)	21 (34.43)	30 (47.62)	8 (72.73)	0.064
Alcohol consumption (%)	90 (66.67)	83 (66.94)	41 (67.21)	42 (66.67)	6 (54.55)	0.537
BMI (kg/m^2)	28.55 ± 4.12	28.74 ± 4.09	27.60 ± 4.26	29.86 ± 3.61	25.87 ± 3.72	**0.001**
Neck circumference (cm)	42.00 (39.75~45.00)	42.00 (40.00~45.00)	41.00 (38.00~43.75)	43.00 (40.00~45.00)	40.50 (36.50~42.75)	**0.005**
Waist circumference (cm)	102.31 ± 11.96	103.15 ± 11.71	99.19 ± 12.18	105.70 ± 10.74	91.63 ± 10.36	**0.001**
Hip circumference (cm)	105.00 (101.00~111.00)	106.00 (102.00~111.00)	104.00 (99.13~109.75)	107.00 (103.00~112.25)	100.50 (94.75~104.50)	**0.006**
Systolic blood pressure (mmHg)	132.00 (124.50~140.00)	132.00 (125.75~140.00)	132.00 (123.00~140.00)	133.00 (128.00~140.00)	128.00 (109.00~138.00)	0.320
Diastolic blood pressure (mmHg)	83.80 ± 9.44	83.99 ± 9.45	83.42 ± 9.59	84.38 ± 9.41	80.86 ± 9.55	0.614
ESS score	9.00 (6.00~13.00)	9.00 (6.00~13.00)	7.00 (4.00~11.00)	10.00 (6.00~15.00)	6.00 (4.00~9.25)	**0.003**
Beck anxiety score	27.00 (22.00~33.00)	28.00 (22.00~33.75)	27.00 (22.50~32.50)	28.00 (24.00~34.00)	13.50 (12.00~15.75)	**<0.001**
Beck depression score	7.00 (3.75~11.25)	7.00 (4.00~12.00)	7.00 (3.50~11.00)	8.00 (4.00~13.00)	5.00 (0.75~7.25)	0.137
IIEF-5 score	20.00 (18.00~23.00)	20.00 (17.25~22.00)	21.00 (19.00~23.00)	19.00 (17.00~22.00)	24.00 (22.75~25.00)	**<0.001**
ASEX score	13.00 (11.00~15.00)	13.00 (11.00~15.00)	12.00 (11.00~14.00)	14.00 (12.00~16.00)	6.50 (5.00~9.25)	**<0.001**

The meaning of the bold values is p<0.05.

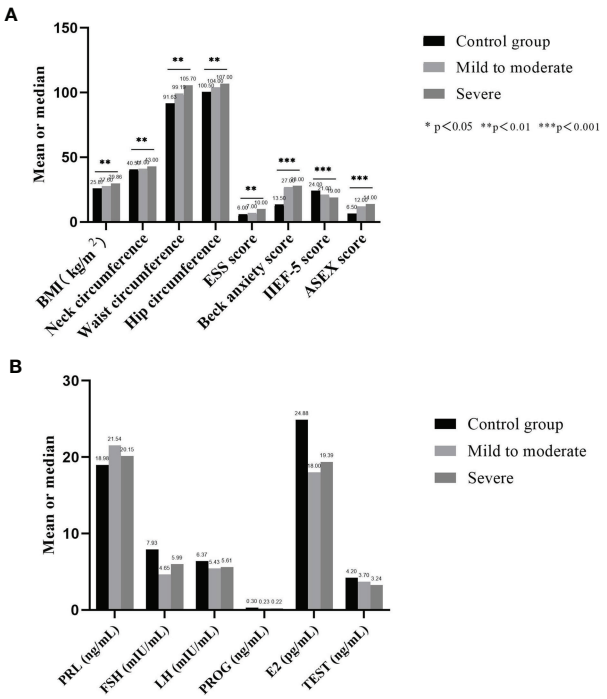

FIGURE 2 | Comparison of basic data and hormone secretion levels of each group. **(A)** shows that among the non-OSA subjects, patients with mild to moderate OSA, and patients with severe OSA, the BMI, neck circumference, waist circumference, hip circumference, ESS score, Beck anxiety score and ASEX score showed a significant increase, while the IIEF-5 score significantly decreased; **(B)** shows that no significant difference was found in the secretion levels of the six serum sex hormones among the three groups.

was 0.81% (1/124), and the prevalence of severe ED was 2.42% (3/124). For the 34 patients with mild to moderate OSA with ED, the prevalence rate was 55.74% (34/61), of which the prevalence of mild ED was 52.46% (32/61), the prevalence of moderate ED was 1.64% (1/61), and the prevalence of severe ED was 1.64% (1/61). A total of 46 patients with severe OSA with ED had an prevalence of 73.02% (46/63), among whom the prevalence of mild ED was 69.84% (44/63), the prevalence of severe ED was 3.17% (2/63), and the prevalence of moderate ED was 0 (statistical level). Mild to moderate OSA patients and severe OSA patients with OSA with ED were mainly characterized by mild ED.

Prevalence of OSA With ED in Different AHI Groups

To clarify the relationship between AHI values and the prevalence of OSA with ED, the patients in different AHI groups were analyzed, and it was found that with the increase in AHI values, the prevalence of OSA with ED gradually increased. When the AHI score was greater than or equal to 70 times/h, the prevalence OSA with ED reached a maximum of 81.82%; when the AHI score was 51 to 70 times/h, the prevalence was 71.88%; when the AHI score was 31 to 50 times/h, the prevalence was 70.00%; when the AHI was 16 to 30 times/h, the prevalence was 58.14%; and when the AHI score was 5 to 15 times/h, the minimum prevalence rate was 50.00% (**Figure 3A**).

The prevalence of OSA with ED increased with the increase in severity of OSA (OR=2.818, p<0.001); that is, for every increase in the AHI value of OSA patients by 1 time/h, the prevalence of OSA with ED increased by 2.818 times. The odds of patients with mild to moderate OSA having concurrent ED was OR=2.259, p=0.001; that is, every time the AHI value of patients with mild to moderate OSA increased by 1 time/h, the prevalence of ED increased by 2.259 times. The odds of patients with severe OSA having ED was OR=3.706, p<0.001; that is, every time the AHI value of patients with severe OSA increased by 1 time/h, the prevalence of ED increased by 3.706 times (**Table 3**).

Prevalence of OSA With ED in Different Age Groups

To clarify the relationship between age and the prevalence of OSA with ED, an analysis of patients in different age groups revealed that the prevalence of OSA with ED was 64.52% (80/124), and the highest prevalence rates were 70.59% in the 41-50 group, 64.29% in the 31-40 group, 59.09% in the 18-30 group, and 58.33% in the 51-60 group, indicating that the prevalence rate gradually increased with age before the age of 50. In the

TABLE 2 | Sex hormone test data of the population included in the study.

Sex Hormones	Total (n=135)	OSA patients			Non-OSA Subjects (n=11)	P
		Total (n=124)	Mild to moderate (n=61)	Severe (n=63)		
PRL (ng/mL)	18.88 (14.04~24.97)	18.88 (14.09~24.38)	18.81 (15.07~28.31)	19.29 (13.99~22.79)	19.55 (11.43~26.59)	0.728
FSH (mIU/mL)	5.10 (3.80~6.84)	5.00 (3.79~6.68)	4.76 (2.98~5.73)	5.26 (4.04~6.86)	7.30 (3.73~12.46)	0.062
LH (mIU/mL)	5.28 (3.85~6.76)	5.06 (3.83~6.69)	4.38 (3.82~6.90)	5.20 (3.83~6.28)	6.64 (5.36~7.47)	0.294
PROG (ng/mL)	0.20 (0.13~0.30)	0.20 (0.13~0.30)	0.21 (0.11~0.30)	0.20 (0.13~0.30)	0.22 (0.14~0.54)	0.821
E2 (pg/mL)	18.76 (12.82~22.95)	18.89 (12.89~22.79)	18.14 (15.46~20.37)	19.67 (11.86~23.82)	17.56 (10.26~44.79)	0.686
TEST (ng/mL)	3.42 ± 1.14	3.36 ± 1.15	3.70 ± 1.17	3.24 ± 1.12	4.20 ± 0.81	0.056

FSH, Follicle stimulating hormone; LH, luteinizing hormone; and TEST, testosterone; E2, estradiol; PROG, progesterone; and PRL, prolactin.

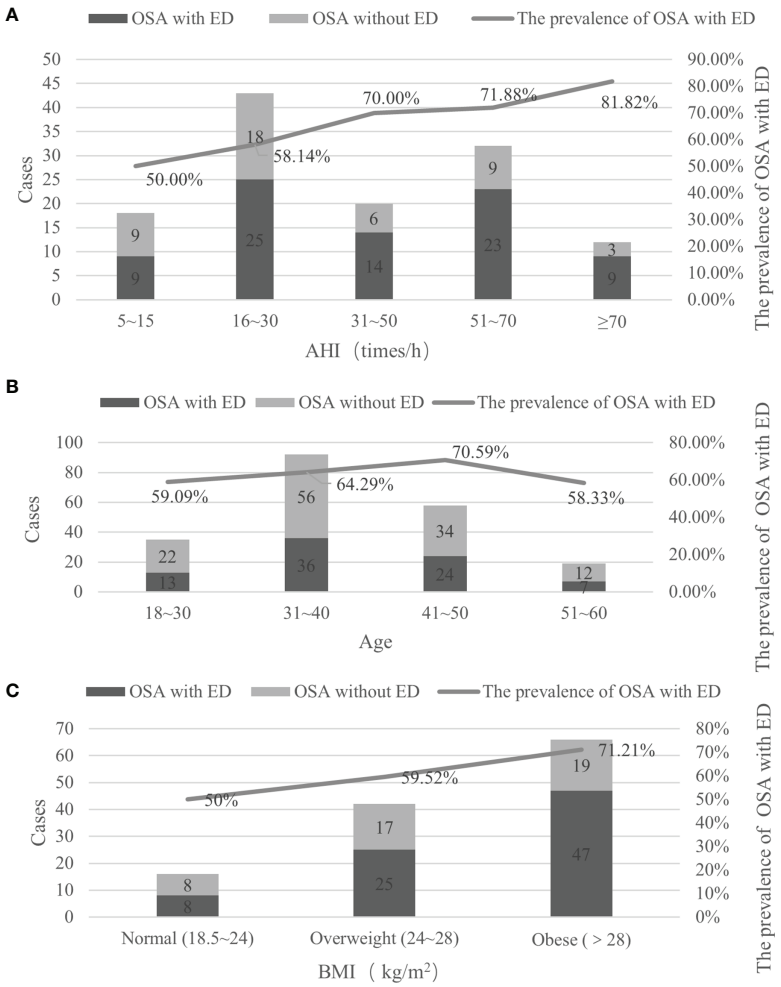

FIGURE 3 | The prevalence of OSA with ED in different AHI, age and BMI groups. **(A)** It was found that with the increase in AHI values, the prevalence of OSA with ED gradually increased; **(B)** the prevalence rate gradually increased with age before the age of 50; **(C)** Among OSA patients, as BMI increased, the prevalence of concurrent ED increased.

severe OSA population, the prevalence of OSA with ED was 74.60% (47/63); the highest prevalence rates were 85.71% in the 18-30-year-old group, followed by 80.00% in the 51-60-year-old group and 71.88% in the 31-40-year-old group, and the lowest prevalence was 68.42% in the 41-50-year-old group (**Figure 3B**).

The prevalence of OSA with ED increased with age (OR=2.444, p=0.001), which means that for every 1-year increase in age of OSA patients, the prevalence of ED increased by 2.444 times. The OR of the 31- to 40-year-old group was 2.800, p <0.001; that is, the prevalence of OSA with ED increased by 2.800 times when the age of OSA patients increased by 1-year in this group. The OR of the 41- to 50-year-old group was 3.400, p <0.001; that is, for every 1-year increase in age of OSA patients in this group, the prevalence of OSA with ED increased by 3.400 times. Finally, the OR of the 51- to 60-year-old group was 2.400, p = 0.002; that is, for every 1-year increase in the age among the OSA patients, the prevalence of ED increased by 2.400 times (**Table 3**).

Prevalence of OSA With ED in Different BMI Groups

To clarify the relationship between BMI and the prevalence of OSA with ED, an analysis of patients in different BMI groups was carried out. Among OSA patients, as BMI increased, the prevalence of concurrent ED increased, and the prevalence in the obesity group was as high as 71.21%, followed by 59.52% in the overweight group and 50.00% in the normal weight group. The same trend was observed in the severe OSA population. The obesity group had the highest prevalence rate of 76.92%, followed by the overweight group (68.18%), and the normal weight group had the lowest prevalence rate (50.00%) (**Figure 3C**).

The prevalence of ED among OSA patients increased as the BMI value increased. The OR of the normal weight group was 2.000, p = 0.005; that is, for every increase in BMI value of 1 kg/m^2 among OSA patients, the prevalence of ED increased by 2.000. The OR of the overweight group was 2.471, p <0.001; that is, for every increase of 1 kg/m^2 in BMI among OSA patients, the prevalence of ED increased by 2.471 times. The OR of the obese

TABLE 3 | The prevalence of ED in patients with OSA of different types of clinical data.

Types of Clinical Data	Grouping	OSA with ED	OSA Without ED	P	OR (95%CI)	OR (95%CI)
Different severity groups	Non-OSA subjects	0	11	–	–	–
	OSA patients	80	44	<0.001	2.818 (2.223-3.573)	
	Mild to moderate OSA	34	27	0.001	2.259 (1.705-2.994)	
	Severe OSA	46	17	<0.001	3.706 (2.469-5.563)	
Different age groups	Control	0	11		–	–
	18~30	13	9	0.001	2.444 (1.479-4.039)	
	31~40	36	20	<0.001	2.800 (1.970-3.979)	
	41~50	24	10	<0.001	3.400 (2.020-5.723)	
	51~60	7	5	0.002	2.400 (1.229-4.688)	
Different BMI groups	Control	0	11	–	–	–
	Normal (18.5~24)	8	8	0.005	2.000(1.225-3.265)	
	Overweight (24~28)	25	17	<0.001	2.471 (1.712-3.565)	
	Obese (>28)	47	19	<0.001	3.474 (2.377-5.077)	

group was 3.474, p<0.001; that is, for every increase of 1 kg/m^2 in BMI among OSA patients, the prevalence of ED increased by 3.474 times (**Table 3**).

Differences in Population Characteristics Between OSA Patients With ED and OSA Patients Without ED

Basic Demographics and Related Clinical Phenotypes of OSA With ED and OSA Without ED

A comparison of OSA patients with ED and OSA patients without ED showed that BMI (p=0.039), neck circumference (p=0.046), waist circumference (p=0.011), hip circumference (p=0.025), ESS score (p=0.040), Beck depression score (p=0.011) and ASEX score (p<0.001) were higher in the OSA with ED group than in the OSA without ED group (**Table 4** and **Figure 4A**).

PSG Data of OSA Patients With ED and OSA Patients Without ED

The comparison of OSA with ED and OSA without ED revealed that sleep efficiency (p=0.036), average oxygen saturation (p=0.018) and minimum oxygen saturation (p= 0.027) were significantly lower in the OSA with ED group than in the OSA without ED group.

Moreover, the total number of respiratory events (p=0.026), number of obstruction and hypopnea events (p=0.024), total proportion of the waking periods (p=0.030) and total proportion of the light sleep periods (p=0.034) were significantly higher in the OSA with ED group than in the OSA without ED group (**Table 4** and **Figure 4B**).

ROC Curve Analysis of Related Factors in OSA Patients

As shown in **Table 4**, both OSA with ED and OSA without ED are closely related to the following 14 factors: BMI, neck circumference, waist circumference, hip circumference, ESS score, Beck depression score, ASEX score, sleep efficiency, average oxygen saturation, minimum oxygen saturation, total number of respiratory events, number of obstruction and hypopnea events, total proportion of the waking periods and total proportion of the light sleep periods.

ROC analysis showed that ASEX score had the highest AUC (area under the curve) at 0.738, followed in descending order by waist circumference (0.703), total proportion of the light sleep periods (0.651), Beck depression score (0.638), hip circumference (0.638), total proportion of the waking periods (0.630), average oxygen saturation (0.629), obstruction and hypopnea events (0.625), total respiratory events (0.624), neck circumference (0.622), minimum oxygen saturation (0.621), sleep efficiency (0.619), ESS score (0.612) and BMI (0.611).Compared with the IIEF-5 scoring standard, ASEX score and waist circumference had general diagnostic value, and the 12 related factors had low diagnostic value (**Figure 5A**).

The Relationship of the IIEF-5 Score With the AHI Value and ASEX Score in OSA Patients

The IIEF-5 scores of 124 OSA patients were negatively correlated with the AHI value, and the Pearson correlation coefficient was r=-0.259, P=0.004 (**Figure 6A**). The IIEF-5 scores were negatively correlated with the ASEX score, and the Pearson correlation coefficient was r=-0.356, P<0.001 (**Figure 6B**). The IIEF-5 score was not significantly correlated with any of the other items (P>0.05).

Sex Hormone Secretion in OSA With ED and OSA Without ED

A comparison of OSA with ED and OSA without ED showed that the secretion levels of PRL (p=0.793), FSH (p=0.599), LH (p=0.676),

TABLE 4 | Basic demographics and related clinical phenotypes of OSA with ED and without ED.

Clinical Phenotype	OSA with ED (n=80)	OSA without ED (n=44)	P
Age	36.50 (31.00~44.75)	37.00 (31.25~43.75)	0.973
Smoking status (%)	38 (47.50)	13 (29.55)	0.059
Alcohol consumption (%)	56 (70.00)	27 (61.36)	0.420
BMI (kg/m^2)	29.31 ± 4.08	27.72 ± 3.94	**0.039**
Neck circumference (cm)	42.00 (40.00~45.00)	41.00 (38.00~43.00)	**0.046**
Waist circumference (cm)	105.18 ± 10.86	98.89 ± 12.44	**0.011**
Hip circumference (cm)	107.00 (103.00~112.00)	103.00 (99.25~110.50)	**0.025**
Systolic blood pressure (mmHg)	132.00 (128.00~140.25)	132.50 (120.50~140.00)	0.616
Diastolic blood pressure (mmHg)	85.23 ± 9.14	81.58 ± 9.70	0.060
ESS score	10.00 (6.00~15.00)	8.00 (5.25~11.00)	**0.040**
Beck anxiety score	28.00 (23.00~35.00)	27.00 (23.00~31.00)	0.367
Beck depression score	8.00 (5.00~13.00)	6.00 (2.25~8.00)	**0.011**
ASEX score	14.00 (12.00~16.00)	12.00 (10.00~13.00)	**<0.001**
AHI (times/h)	41.10 (16.90~60.23)	24.25 (17.45~50.40)	0.102
Sleep efficiency (%)	77.45 (67.00~87.68)	84.90 (74.63~91.23)	**0.036**
Average pause and hypopnea time (s)	22.00 (21.00~24.00)	22.00 (20.00~24.00)	0.317
Maximum pause and hypopnea time (s)	66.55 ± 15.32	64.48 ± 12.98	0.458
Total number of respiratory events (times)	181.50 (103.00~332.00)	134.00 (94.50~230.50)	**0.026**
Total time of respiratory event time (min)	52.50 (33.50~103.00)	48.00 (26.00~71.50)	0.147
Number of obstruction and hypopnea events (times)	178.00 (103.00~322.50)	129.00 (69.75~226.75)	**0.024**
Number of central respiratory events (times)	0.00 (0.00~2.00)	0.00 (0.00~0.00)	0.244
Number of mixed respiratory events (times)	3.00 (0.00~7.75)	2.00 (0.00~4.25)	0.225
Total proportion of the waking periods (%)	24.35 (14.03~34.25)	15.60 (11.25~26.00)	**0.030**
Total proportion of the REM periods (%)	17.18 ± 7.57	18.58 ± 7.19	0.365
Total proportion of the light sleep periods (%)	44.59 ± 12.75	50.08 ± 11.73	**0.034**
Total proportion of the deep sleep periods (%)	8.55 (4.70~14.55)	9.10 (4.55~15.45)	0.770
Average oxygen saturation (%)	93.55 (90.63~96.00)	96.05 (90.73~97.05)	**0.018**
Minimum oxygen saturation (%)	71.10 (60.93~83.03)	79.65 (66.25~88.48)	**0.027**
Oxygen depletion index (times/h)	31.00 (13.90~61.25)	20.10 (5.30~47.90)	0.076
Average heart rate (bpm)	66.50 (59.25~73.75)	66.00 (60.00~69.00)	0.590
Maximum heart rate (bpm)	100.00 (91.25~110.75)	99.00 (95.00~105.75)	0.699

The meaning of the bold values is p<0.05.

PROG (p=0.682) and TEST (p=0.431) were not significantly different between the groups (**Table 5** and **Figure 4C**).

Moreover, ROC analysis showed that TEST had the highest AUC at 0.554, followed in descending order by FSH (0.536), E2 (0.535), LH (0.529), PRL (0.518) and PROG (0.504). Compared with that of the IIEF-5 scoring standard, the diagnostic value of the six related factors was low (**Figure 5B**).

Binary Logistic Regression Analysis of Related Factors in OSA With ED

According to clinical characteristics of OSA with ED, BMI (p=0.209), ESS score (p=0.232), Beck depression score (p=0.190), average oxygen saturation (p=0.349) and minimum oxygen saturation (p=0.257) were subjected to binary logistic regression analysis, and no significant difference was found between the groups (p>0.05), indicating that these factors were not independent influencing factors (**Table S1**).

Treatment Response

Fifteen patients with mild to moderate OSA with ED and fifteen patients with severe OSA with ED were followed up. Six months after UPPP surgical treatment, AHI values*** of patients with mild to moderate OSA decreased from 16.55 ± 5.60 times/h to 4.33 ± 1.23 times/h, and the IIEF-5* score increased from 17.94 ± 3.70 to 24.61 ± 4.76; the AHI values*** of patients with severe OSA decreased from 58.27 ± 14.10 times/h to 13.56 ± 7.25 times/h, and the IIEF-5* score increased from 17.11 ± 3.97 to 22.51 ± 5.37 (*p<0.05, ***p<0.001, **Figure 7**).

DISCUSSION

This study explores the relationship between OSA and ED, which is a relatively small area in the study of OSA clinical symptoms. It focuses on the erectile function status of patients with OSA and explores the clinical connection between the two diseases, which has high clinical value.

Patients who are diagnosed with OSA can receive psychological counseling and take corresponding intervention measures to reduce the general symptoms of OSA while improving the erectile function to achieve the cotreatment of OSA-related diseases.

ED, Mainly Mild ED, Is a Common Symptom of OSA Patients

We found that ED was a common symptom of OSA patients and that symptoms were typically mild. The prevalence of OSA with ED was 64.52% (80/124), and the prevalence of severe OSA with ED was 73.02% (46/63). This figure is basically consistent with the following studies. Skoczynski (51) reported that the

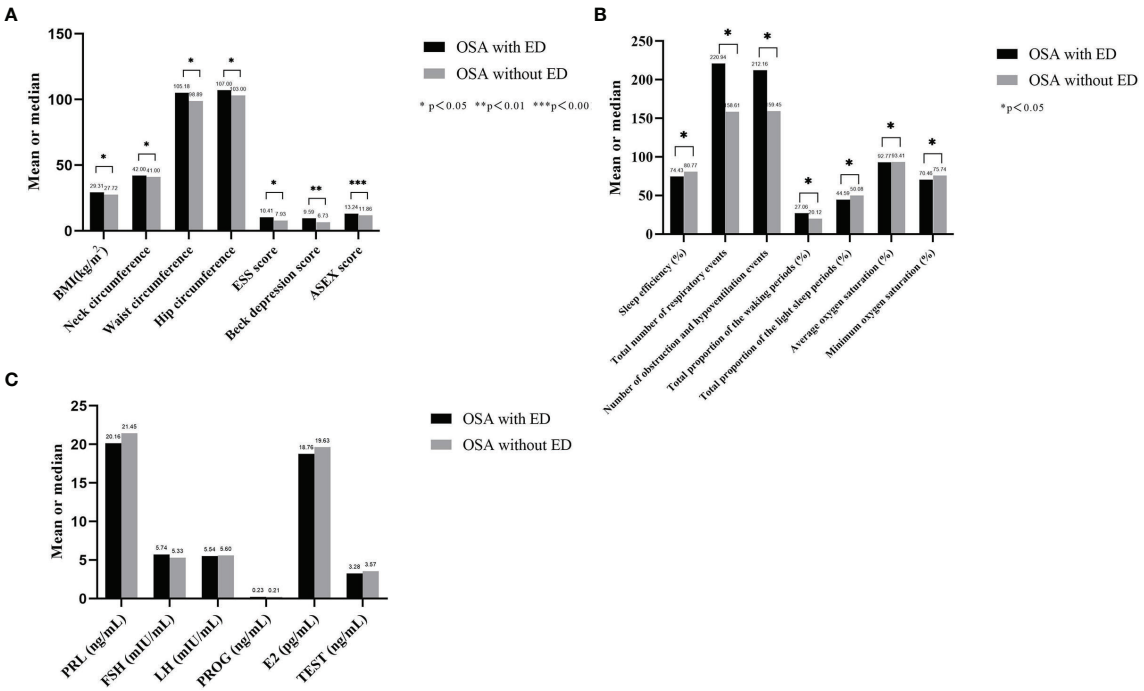

FIGURE 4 | Basic related clinical phenotypes, PSG data and sex hormone secretion of OSA with ED and without ED. **(A)** BMI, neck circumference, waist circumference, hip circumference, ESS score, Beck depression score and ASEX score were higher in the OSA with ED group than in the OSA without ED group; **(B)** Sleep efficiency, average oxygen saturation and minimum oxygen saturation were significantly lower in the OSA with ED group than in the OSA without ED group. Moreover, the total number of respiratory events, number of obstruction and hypopnea events, total proportion of the waking periods and total proportion of the light sleep periods were significantly higher in the OSA with ED group than in the OSA without ED group; **(C)** The secretion levels of PRL, FSH, LH, PROG and TEST were not significantly different between the groups.

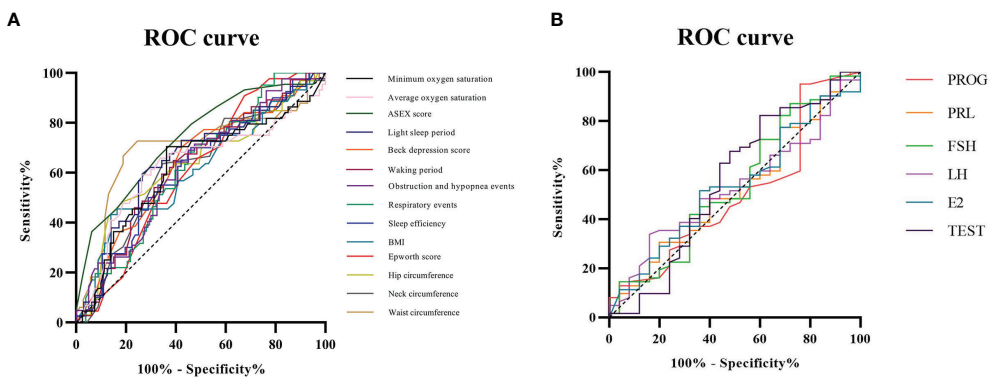

FIGURE 5 | ROC curve analysis of related factors in OSA patients. **(A)** Compared with the IIEF-5 scoring standard, ASEX score and waist circumference had general diagnostic value, and the 12 related factors had low diagnostic value; **(B)** Compared with that of the IIEF-5 scoring standard, the diagnostic value of the six related factors was low.

prevalence of ED in 61 Polish OSA patients was 72.1%; Popp (52) reported that the prevalence of ED in 246 German OSA patients was 65.0%; Budweiser (53) reported that the prevalence of ED in 91 German OSA patients was 61.5%; and Zhang (54) reported that the prevalence of ED in 207 Chinese OSA patients was 60.6% and that the prevalence of severe OSA with ED was 72.2%. Moreover, the prevalence of ED in 24 Turkish OSA patients was reported to be 54.2% by Gurbuz (55). Kellesarian (23) integrated several studies based on the IIEF questionnaire and found that the prevalence of OSA with ED was between 41% and 80%.

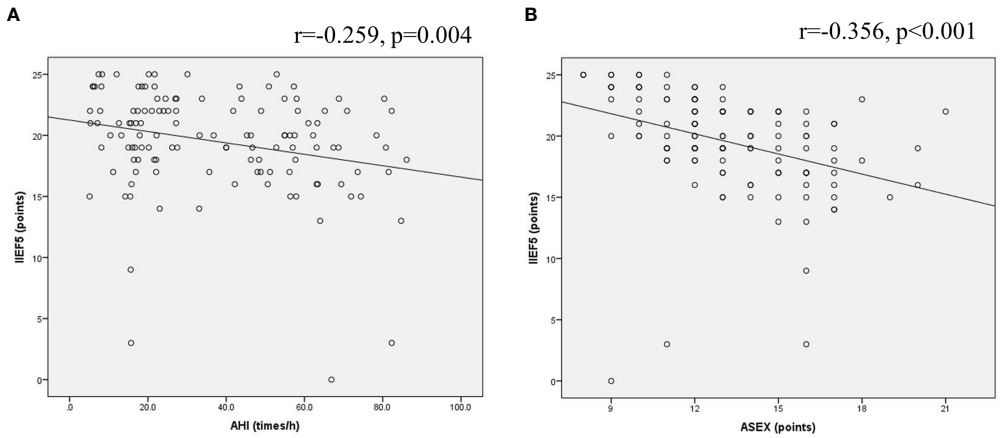

FIGURE 6 | Scatter plot of the relationship of OSA patients. **(A)** The IIEF-5 scores of 124 OSA patients were negatively correlated with the AHI value; **(B)** The IIEF-5 scores were negatively correlated with the ASEX score.

TABLE 5 | Sex hormone data of OSA with ED and OSA without ED.

Sex Hormones	OSA With ED (n=80)	OSA Without ED (n=44)	P
PRL (ng/mL)	19.08 (13.95~23.73)	18.74 (14.98~26.09)	0.793
FSH (mIU/mL)	4.81 (3.98~6.43)	5.10 (3.36~6.77)	0.599
LH (mIU/mL)	4.97 (3.80~6.77)	5.20 (4.05~6.28)	0.676
PROG (ng/mL)	0.23 ± 0.14	0.21 ± 0.11	0.533
E2(pg/mL)	18.76 ± 9.10	19.63 ± 8.52	0.682
TEST (ng/mL)	3.09 (2.53~3.87)	3.64 (2.31~4.68)	0.431

FSH, Follicle stimulating hormone; LH, luteinizing hormone; and TEST, testosterone; E2, estradiol; PROG, progesterone; and PRL, prolactin.

We also found that the factors associated with ED in OSA patients included the AHI value, age, BMI, ESS score, Beck depression score, sleep efficiency, total number of respiratory events, number of obstruction and hypopnea events, total proportion of the waking periods, total proportion of the light sleep periods, minimum oxygen saturation and average oxygen saturation. It is worth mentioning that the mechanisms related to these factors may be the causes of OSA with ED.

The Prevalence of OSA With ED Increases With Age and BMI

ED obviously increases with age. Andersen (20) found that the prevalence of ED in young people (20-29 years old) was 7.3% and that the prevalence in elderly people (>60 years old) was 63.25%. According to Tufik (56), the 60- to 80-year-old population has 34.5-fold increased likelihood of having OSA compared with the 20- to 29-year-old population, and the prevalence of ED also doubles. This study compared the prevalence of OSA with ED in different age groups and found that the prevalence gradually increased with age (before the age of 50) and that the prevalence was as high as 70.59% (41-50 years old group), especially in the population with severe OSA, in which it was as high as 85.71% (18- to 30-year-old group). The prevalence of OSA with ED increases with increasing age. The prevalence of OSA in the 18- to 30-year-old group increased each year, and the prevalence of ED showed a 2.444-fold increase. The prevalence of combined ED increased by 2.800 times for OSA patients in the 31- to 40-year-old group with each 1-year increase in age; in the 41- to 50-year-old group, this prevalence increased by 3.400 times for OSA patients with each year. However, the prevalence of combined ED increased by 2.400 times for OSA patients in the 51- to 60-year-old group for each 1-year increase in age. Nevertheless, in the data for OSA with ED and OSA without ED, age did not show a significant difference between the groups (p=0.973), which may be related to the small number of people included.

The prevalence of OSA has increased with the increase in obesity worldwide, and obesity is closely related to ED (57). Peppard (58) found that weight gain is one of the most important risk factors for the increase in AHI values and the development of OSA, especially in patients with moderate to severe OSA. When weight increases by 10%, the progression of OSA increases 6-fold. This study found that the BMI of non-OSA subjects, patients with mild to moderate OSA, and patients with severe OSA increased with disease severity (p=0.001). A comparison of the prevalence of OSA with ED among different BMI groups showed that the prevalence of ED gradually increased with increasing BMI. Furthermore, the prevalence of ED among OSA patients increased with the increase in BMI value. For every increase of 1 kg/m^2 in BMI of OSA patients, the prevalence of ED increased by 2.000 times in the normal weight group, by

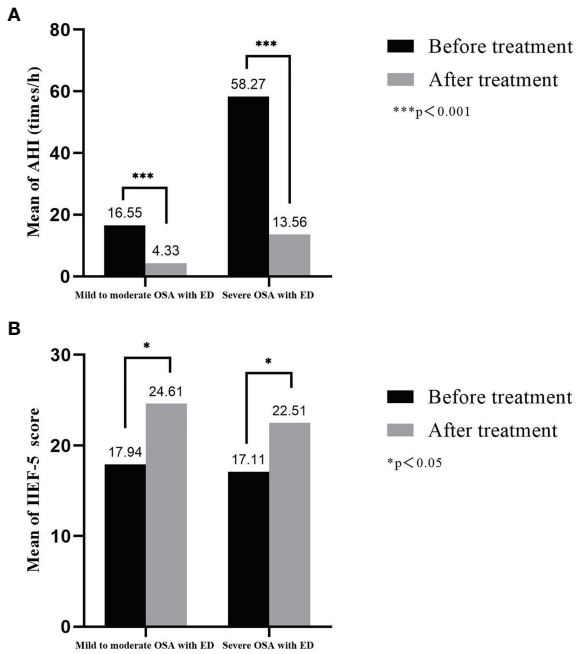

FIGURE 7 | Treatment response of AHI and IIEF-5 score in OSA with ED. **(A)** Six months after UPPP surgical treatment, AHI values of patients with mild to moderate OSA and patients with severe OSA decreased; **(B)** The IIEF-5 of patients with mild to moderate OSA and patients with severe OSA score increased.

2.471 times in the overweight group, and by 3.474 times in the obese group. In addition, OSA groups with and without ED, the BMI of patients in the OSA with ED group was significantly higher than that of patients in the OSA without ED group (BMI, 29.31 ± 4.08 kg/m2 vs. 27.72 ± 3.94 kg/m2, p=0.039).

The Prevalence of OSA With ED Increases With The Severity of OSA

A study by Margel (59) showed that the severity of OSA (mainly the AHI value) may be related to the severity of ED. Skoczynski (51) suggested that OSA will lead to cardiovascular complications with age, leading to an increase in AHI values, and will be accompanied by increased dyspnea, which ultimately leads to the occurrence of ED Liu (60) reported abnormal circadian rhythm is associated with a decrease in sperm count, and as the circadian rhythm improves, the sperm count can be restored. Moreover, Vincent (61) reported that when OSA worsens, it causes fear of heart failure symptoms and promotes general anxiety about sexual activity. There are also studies with contrasting opinions. Santos (62) found that ED has a higher prevalence in OSA patients and that the severity of ED is related to age and diabetes but not to OSA itself. This study compared the prevalence of OSA with ED among different AHI groups and found that it gradually increased with increasing AHI values. The prevalence of mild OSA (AHI: 5-15 times/h) was at least 50%, and the prevalence was as high as 81.82% when AHI was ≥70 times/h. As the severity of OSA increases, the prevalence of ED increases; that is, for each 1 time/h increase in the AHI value of OSA patients, the prevalence of combined ED increased by 2.818 times. Each 1 time/h increase in the AHI value of patients with mild to moderate OSA increased the prevalence of combined ED by 2.259 times; moreover, each 1 time/h increase in the AHI value of patients with severe OSA increased the prevalence of combined ED by 3.706 times. However, in the OSA with ED and OSA without ED groups, the AHI value was not significantly different (p=0.102), which may be related to the small number of people included or the age difference of the included people.

Arousal and lack of sleep can have many effects on the normal physiology of the body, especially endocrine abnormalities and abnormal sympathetic nerve activity (63). Petersen (64) reported that chronic intermittent hypoxemia can reduce sexual activity and spontaneous erections in mice. Goh (65) suggested that the concentration of sex hormones is significantly related to sleep time. However, Stannek (21) reported that the severity of OSA may not be related to the severity of ED. This study found that the sleepiness score (ESS score) increased sequentially (p =0.003) among the non-OSA subjects, patients with mild to moderate OSA and patients with severe OSA and that sleep efficiency (p=0.036), minimum oxygen saturation (p=0.027) and average oxygen saturation (p=0.018) were significantly lower in the OSA with ED group than in the OSA without ED group. However, the total number of respiratory events (p=0.026), number of obstructive and hypopnea events (p=0.024), total proportion of the waking periods (p=0.030) and total proportion of the light sleep periods (p=0.034) were significantly higher.

Andersen (20) reported that the decrease in rapid eye movement (REM) sleep and the increased number of waking periods have a negative impact on the erectile function of male rats. Luboshitzky (66) found that during the first REM sleep episode, the level of testosterone secretion was the highest. Moreover, Liu (28) reported that factors such as reduced sleep in the REM periods can lead to damage to the peripheral nerves of the patient's sexual organs, thereby causing ED. Furthermore, Gurbuz (55) found that an increase in the percentage of REM sleep has a negative impact on erectile function, while the total sleep time with a percentage of REM <20% seems to protect erectile function, but most of the research subjects were patients with psychological ED. Giles (67) showed that the REM period of the psychological ED group was longer than that of subjects without ED. This study found that the total proportion of the REM periods in the OSA with ED group was 17.18 ± 7.57%, while that in the OSA without ED group was 18.58 ± 7.19%, which was not significantly different (p=0.365) and may be related to the small number of people included.

Improving Patients' Anxiety and Depression Is Essential for the Treatment of OSA With ED

Papagiannopoulos (68) suggested that the contextual causes of psychological ED may include psychological distress (depression, job instability, and posttraumatic stress disorder), performance anxiety and partner-related difficulties (interpersonal instability). Zhang (54) reported that there is a well-known link between ED

and mental illness and that depression and anxiety are the main psychological risk factors for ED in young men. Furthermore, Bandini (69) and Smith (70) found that depression is closely related to the severity of ED among men with ED who seek help. McCabe (71) reported that ED is related to the occurrence of depression and that treatment of ED with PDE5 inhibitors can improve depression symptoms. In a retrospective population survey of approximately 3,500 Finnish men between the ages of 18 and 48, Jern (72) found that depression is an important predictor of ED. In addition, the current study also showed that anxiety symptoms play an important role and that men with more sexual experiences suffer from ED less frequently. As mentioned earlier, anxiety may be involved in the pathogenesis of ED, and Caskurlu (73) suggested that it usually occurs at the beginning of sexual life. Zou (74) found that poorer sleep quality of college students correlated with mental health problems. This study found that the Beck anxiety scores of the non-OSA subjects, patients with mild to moderate OSA and patients with severe OSA increased with OSA severity ($p<0.001$). A comparison of OSA with ED and OSA without ED showed that the Beck depression score ($p=0.011$) of the OSA with ED group was higher than that of the OSA without ED group. However, the Beck anxiety score ($p=0.367$) was not significantly different between the groups, which may be related to the small sample size. Therefore, there may be a vicious circle mechanism among the depressive state (and the anxiety state), OSA and ED. In summary, improving the patient's mental health is essential for the treatment of OSA.

OSA With ED May Not Be Caused by Abnormal Levels of Sex Hormones

Corona (75) and Zhang (54) have shown that endocrine dysfunction, including changes in the hypothalamic pituitary axis, adrenal insufficiency, diabetes, hyperprolactinemia, hyperthyroidism and hypothyroidism, is involved in the progression of ED. OSA patients have repeated cycles of upper airway collapse and awakening, leading to sleep disturbances, sleep deprivation and fragmentation, which are manifested by intermittent hypoxia and reoxygenation. ED caused by intermittent hypoxia may have the following mechanisms: 1) vascular endothelial function damage (76); 2) oxidative stress (77); and 3) inhibition of sex hormone secretion (78), which mainly suppresses the response of central gonadal organs, reduces the levels of luteinizing hormone and testosterone, and affects libido (63, 79). Studies have also shown that elevated estradiol (80) and serum leptin (80–82) in obese patients can cause decreased testosterone secretion and ED. Zhang (54) and Luboshitzky (63) reported that the levels of testosterone, dehydroepiandrosterone sulfate, dehydroepiandrosterone and prolactin in the serum of patients with OSA was decreased, thereby reducing the bioavailability of testosterone and leading to ED. And Chen (31) found long and short sleep duration, as well as poor sleep quality, were linked to poor sperm quality metrics, even to ED.

There are still some studies that do not support the above view. Ludwig (83) reported that only 4% of men under the age of 50 have low levels of testosterone secretion but that it was not clear whether this is the cause of ED. Buvat (84), Hatzimouratidis (85) and Basar (86) reported that testosterone had the greatest effect on libido but not on ED. Soukhova (87) supported the above view with an animal model of intermittent hypoxia, which caused a decrease in libido in the animal model but did not change testosterone levels. Celec (88) found that long-term continuous positive airway pressure (CPAP) treatment had no significant effect on the levels of testosterone or estradiol in patients with OSA and pointed out that the positive effects of CPAP on sexual function reported by other studies may be caused by factors other than endocrine effects, which is consistent with the report of Onem (89). Moreover, Gambineri (90) suggested that this may be due to the low testosterone levels reported in previous studies and proposed that the relationship between testosterone and OSA is unrelated to obesity. Schiavi (91) analyzed other studies and showed that the increased risk of OSA and decreased testosterone levels actually depend on age as the main pathogenic factor. Interestingly, studies by Hammoud (92) and Barrett (93) do not support the view that OSA inhibits the secretion of testosterone and other sex hormones through the central nervous system. Liu's study (94) showed that exogenous testosterone as a hormone replacement therapy can cause OSA. Even short-term treatment can aggravate sleep quality and OSA, but the mechanism is still unclear.

Killick (95) reported that testosterone had a limited therapeutic effect on OSA symptoms. The patient's oxygen saturation index increased after 7 weeks, but there was no significant change in symptoms after 18 weeks of testosterone treatment. Furthermore, Mohammadi (41) recently studied testosterone secretion in 16 healthy controls and 39 OSA patients (10 cases of mild OSA, 16 cases of moderate OSA, and 13 cases of severe OSA). Notably, the control group and OSA patients had no significant differences in total testosterone levels or free testosterone levels ($p>0.1$). Jiang (96) examined sex hormone levels in 48 patients with OSA, of whom 23 had OSA with ED and 25 had OSA without ED. There was no significant difference in the secretion levels of estradiol ($p=0.191$), follicle-stimulating hormone ($p=0.797$), luteinizing hormone ($p=0.412$), prolactin ($p=0.239$), progesterone ($p=0.964$) or testosterone ($p=0.07$). Chen (30) reported semen and peripheral blood samples were taken from 656 male students in China for analysis of sperm quality and reproductive hormone levels. There was no link discovered between sleep duration and reproductive hormone.

This study summarized the sex hormone test data of the included population, and the results showed that the secretion levels of prolactin ($p=0.728$), follicle-stimulating hormone ($p=0.062$), luteinizing hormone ($p= 0.294$), progesterone ($p=0.821$), estrogen ($p=0.686$) and testosterone ($p=0.056$) were not significantly different among the control group, mild to moderate OSA group, and severe OSA group. Comparing OSA with ED and OSA without ED revealed that the secretion levels of prolactin ($p=0.793$), follicle-stimulating hormone ($p=0.599$), luteinizing hormone ($p=0.676$), progesterone ($p=0.533$), estrogen ($p=0.682$), and testosterone ($p=0.431$) in the OSA

with ED group were not significantly different than those in the OSA without ED group. Compared with that of the IIEF-5 scoring standard, the sex hormone test had low diagnostic value. Therefore, it is speculated that OSA with ED may not be caused by abnormal levels of sex hormones but may be related to factors other than endocrine effects (such as obesity). Since free sex hormones are the main active form, it is recommended to use more advanced experimental equipment when studying sex hormones in the future to further distinguish between free and bound sex hormones.

Research Limitations

This study has the following limitations, which need to be resolved in future studies. First, several studies (11, 29) indicate that erectile function may be related to a reduction in REM sleep in OSA patients. This study did not find a significant correlation with REM sleep in either the OSA with ED group or the OSA without ED group. In addition, there were only 11 non-OSA subjects in the group. In the future, it will be necessary to organize large-sample, multicenter clinical research to improve the scientific nature of the research. Second, the participants were all men who had been diagnosed with OSA, which may not be generalizable to other ED-related populations. Third, objective measurements (nighttime penile erection monitoring equipment and Doppler ultrasound equipment) can evaluate ED more reliably than questionnaire surveys (97–99), but related studies have also confirmed the effectiveness of IIEF questionnaires for ED evaluation (59, 97, 100, 101). The main basis of this study was the IIEF-5 questionnaire, and the secondary basis was the ASEX questionnaire. In future studies, the diagnosis of ED should include evaluation of potential cardiovascular risk factors and current use of related drugs, especially objective measures, to evaluate erectile function. Fourth, due to limited resources in this study, the levels of sex hormones were tested only once, but the level of hormone secretion in the human body may vary from day to night. Future research needs to collect data multiple times according to the circadian rhythm, distinguish between free and combined sex hormones, and further study the relationship between hormone levels and OSA. Finally, this study failed to further explore the biomolecular mechanism, and research centers need to continue to investigate animal models for experimental research.

CONCLUSION

ED is a common symptom of OSA patients, and the symptoms are mainly mild. The prevalence of OSA with ED was 64.52%, and the prevalence of severe OSA with ED was 73.02%. The prevalence of OSA with ED increases with age, BMI, and AHI values. A mechanism related to the ESS score, sleep efficiency, total respiratory events, obstruction and hypopnea events, total waking periods, total light sleep periods, minimum blood oxygen saturation and average blood oxygen saturation may be the cause of ED in patients with OSA. Improving patient anxiety and depression is very important for the treatment of OSA with ED. The relationship between ED and sex hormone levels in OSA patients is still worthy of in-depth study. It is recommended that the free type and the combined type of sex hormones be further distinguished during testing, because the free type is the active form. Finally, UPPP surgical treatment is an effective treatment for OSA with ED. Its possible mechanism is protection of the peripheral nerves of the sex organs by improving nighttime hypoxia and arousal.

DATA AVAILABILITY STATEMENT

The original contributions presented in the study are included in the article/**Supplementary Material**. Further inquiries can be directed to the corresponding authors.

ETHICS STATEMENT

The studies involving human participants were reviewed and approved by the Internal Review Board of the Institutional Ethics Committee of Shanghai General Hospital. The patients/participants provided their written informed consent to participate in this study.

AUTHOR CONTRIBUTIONS

CF and YY have contributed equally to this work. CF and YL designed the study. YY, RG, HL, and CL performed the collection and handling of the data. LC, YW, and CF analyzed the data and wrote the manuscript. YL and PD revised the manuscript. All authors discussed the data and accepted the final draft. All authors contributed to the article and approved the submitted version.

FUNDING

This work was supported by the National Natural Science Foundation of Shandong Provincial (no. ZR2018MH017), the Key R&D Program Fund Project of Shandong Provincial (no. 2018GSF118001), the National Natural Science Foundation of China (no. 82072989) and the Fund Project of Shanghai Shen Kang Hospital Development Center (no.SHDC12020120).

SUPPLEMENTARY MATERIAL

The Supplementary Material for this article can be found online at: https://www.frontiersin.org/articles/10.3389/fendo.2022.812974/full#supplementary-material

Supplementary Figure S1 | Distribution of IIEF-5 scores in ED patients and control patients. Summarizes the IIEF-5 score of the included population.

REFERENCES

1. Young T, Palta M, Dempsey J, Skatrud J, Weber S, Badr S. The Occurrence of Sleep-Disordered Breathing Among Middle-Aged Adults. *N Engl J Med* (1993) 328(17):1230–5. doi: 10.1056/Nejm199304293281704
2. Le Grande M, Murphy B, Jackson A. Prevalence of Obstructive Sleep Apnoea in Cardiac Patients: A Systematic Review and Secondary Analysis. *Int J Behav Med* (2016) 23:S96–7. doi: 10.1213/ANE.0000000000002558
3. Ali SS, Oni ET, Warraich HJ, Blaha MJ, Blumenthal RS, Karim A, et al. Systematic Review on Noninvasive Assessment of Subclinical Cardiovascular Disease in Obstructive Sleep Apnea: New Kid on the Block! *Sleep Med Rev* (2014) 18(5):379–91. doi: 10.1016/j.smrv.2014.01.004
4. Aurora RN, Punjabi NM. Obstructive Sleep Apnoea and Type 2 Diabetes Mellitus: A Bidirectional Association. *Lancet Respir Med* (2013) 1(4):329–38. doi: 10.1016/S2213-2600(13)70039-0
5. Marshall NS, Wong KK, Cullen SR, Knuiman MW, Grunstein RR. Sleep Apnea and 20-Year Follow-Up for All-Cause Mortality, Stroke, and Cancer Incidence and Mortality in the Busselton Health Study Cohort. *J Clin Sleep Med* (2014) 10(4):355–62. doi: 10.5664/jcsm.3600
6. Pepin JL, Borel AL, Tamisier R, Baguet JP, Levy P, Dauvilliers Y. Hypertension and Sleep: Overview of a Tight Relationship. *Sleep Med Rev* (2014) 18(6):509–19. doi: 10.1016/j.smrv.2014.03.003
7. Shin HW, Rha YC, Han DH, Chung S, Yoon IY, Rhee CS, et al. Erectile Dysfunction and Disease-Specific Quality of Life in Patients With Obstructive Sleep Apnea. *Int J Impot Res* (2008) 20(6):549–53. doi: 10.1038/ijir.2008.39
8. Steinke E, Palm Johansen P, Fridlund B, Brostrom A. Determinants of Sexual Dysfunction and Interventions for Patients With Obstructive Sleep Apnoea: A Systematic Review. *Int J Clin Pract* (2016) 70(1):5–19. doi: 10.1111/ijcp.12751
9. Vinnikov D, Blanc PD, Alilin A, Zutler M, Holty JC. Fatigue and Sleepiness Determine Respiratory Quality of Life Among Veterans Evaluated for Sleep Apnea. *Health Qual Life Outcomes* (2017) 15(1):48. doi: 10.1186/s12955-017-0624-x
10. Gonzaga C, Bertolami A, Bertolami M, Amodeo C, Calhoun D. Obstructive Sleep Apnea, Hypertension and Cardiovascular Diseases. *J Hum Hypertens* (2015) 29(12):705–12. doi: 10.1038/jhh.2015.15
11. Findley LJ, Wilhoit SC, Suratt PM. Apnea Duration and Hypoxemia During Rem-Sleep in Patients With Obstructive Sleep-Apnea. *Chest* (1985) 87 (4):432–6. doi: 10.1378/chest.87.4.432
12. Series F, Cormier Y, Laforge J. Influence of Apnea Type and Sleep Stage on Nocturnal Postapneic Desaturation. *Am Rev Respir Dis* (1990) 141(6):1522–6. doi: 10.1164/ajrccm/141.6.1522
13. Shi F, Liu C, Liu K, Sun L, Yang H, Cao J, et al. Female and Male Sleep Duration in Association With the Probability of Conception in Two Representative Populations of Reproductive Age in Us and China. *Sleep Med* (2020) 74:9–17. doi: 10.1016/j.sleep.2020.05.026
14. Nih consensus conference. Impotence. Nih Consensus Development Panel on Impotence. *JAMA* (1993) 270(1):83–90.
15. Umeizudike KA, Iwuala SO, Ozoh OB, Ayanbadejo PO, Fasanmade OA. Association Between Periodontal Diseases and Systemic Illnesses: A Survey Among Internal Medicine Residents in Nigeria. *Saudi Dent J* (2016) 28 (1):24–30. doi: 10.1016/j.sdentj.2015.03.005
16. Guilleminault C, Simmons FB, Motta J, Cummiskey J, Rosekind M, Schroeder JS, et al. Obstructive Sleep-Apnea Syndrome and Tracheostomy - Long-Term Follow-Up Experience. *Arch Intern Med* (1981) 141(8):985–9. doi: 10.1001/archinte.141.8.985
17. Hoekema A, Stel AL, Stegenga B, van der Hoeven JH, Wijkstra PJ, van Driel MF, et al. Sexual Function and Obstructive Sleep Apnea-Hypopnea: A Randomized Clinical Trial Evaluating the Effects of Oral-Appliance and Continuous Positive Airway Pressure Therapy. *J Sex Med* (2007) 4(4 Pt 2):1153–62. doi: 10.1111/j.1743-6109.2006.00341.x
18. Koseoglu N, Koseoglu H, Itil O, Oztura B, Baklan B, Ikiz AO, et al. Sexual Function Status in Women With Obstructive Sleep Apnea Syndrome. *J Sex Med* (2007) 4(5):1352–7. doi: 10.1111/j.1743-6109.2006.00302.x
19. Chen KF, Liang SJ, Lin CL, Liao WC, Kao CH. Sleep Disorders Increase Risk of Subsequent Erectile Dysfunction in Individuals Without Sleep Apnea: A Nationwide Population-Base Cohort Study. *Sleep Med* (2016) 17:64–8. doi: 10.1016/j.sleep.2015.05.018
20. Andersen ML, Santos-Silva R, Bittencourt LRA, Tufik S. Prevalence of Erectile Dysfunction Complaints Associated With Sleep Disturbances in Sao Paulo, Brazil: A Population-Based Survey. *Sleep Med* (2010) 11 (10):1019–24. doi: 10.1016/j.sleep.2009.08.016
21. Stannek T, Hurny C, Schoch OD, Bucher T, Munzer T. Factors Affecting Self-Reported Sexuality in Men With Obstructive Sleep Apnea Syndrome. *J Sex Med* (2009) 6(12):3415–24. doi: 10.1111/j.1743-6109.2009.01486.x
22. Margel D, Cohen M, Livne PM, Pillar G. Severe, But Not Mild, Obstructive Sleep Apnea Syndrome Is Associated With Erectile Dysfunction. *Urology* (2004) 63(3):545–9. doi: 10.1016/j.urology.2003.10.016
23. Kellesarian SV, Malignaggi VR, Feng C, Javed F. Association Between Obstructive Sleep Apnea and Erectile Dysfunction: A Systematic Review and Meta-Analysis. *Int J Impot Res* (2018) 30(3):129–40. doi: 10.1038/s41443-018-0017-7
24. Smith S, Sullivan K, Hopkins W, Douglas J. Frequency of Insomnia Report in Patients With Obstructive Sleep Apnoea Hypopnea Syndrome (Osahs). *Sleep Med* (2004) 5(5):449–56. doi: 10.1016/j.sleep.2004.03.005
25. Petersen M, Kristensen E, Berg S, Midgren B. Sexual Function in Male Patients With Obstructive Sleep Apnoea After 1 Year of Cpap Treatment. *Clin Respir J* (2013) 7(2):214–9. doi: 10.1111/j.1752-699X.2012.00307.x
26. Melehan KL, Hoyos CM, Hamilton GS, Wong KK, Yee BJ, McLachlan RI, et al. Randomized Trial of Cpap and Vardenafil on Erectile and Arterial Function in Men With Obstructive Sleep Apnea and Erectile Dysfunction. *J Clin Endocrinol Metab* (2018) 103(4):1601–11. doi: 10.1210/jc.2017-02389
27. Schulz R, Bischof F, Galetke W, Gall H, Heitmann J, Hetzenecker A, et al. Cpap Therapy Improves Erectile Function in Patients With Severe Obstructive Sleep Apnea. *Sleep Med* (2019) 53:189–94. doi: 10.1016/j.sleep.2018.03.018
28. Liu LH, Kang R, Zhao SK, Zhang T, Zhu W, Li EM, et al. Sexual Dysfunction in Patients With Obstructive Sleep Apnea: A Systematic Review and Meta-Analysis. *J Sex Med* (2015) 12(10):1992–2003. doi: 10.1111/jsm.12983
29. Ware JC, Hirshkowitz M. Characteristics of Penile Erections During Sleep Recorded From Normal Subjects. *J Clin Neurophysiol* (1992) 9(1):78–87. doi: 10.1097/00004691-199201000-00009
30. Chen Q, Yang H, Zhou NY, Sun L, Bao HQ, Tan L, et al. Inverse U-Shaped Association Between Sleep Duration and Semen Quality: Longitudinal Observational Study (Marhcs) in Chongqing, China. *Sleep* (2016) 39 (1):79–86. doi: 10.5665/sleep.5322
31. Chen HG, Sun B, Chen YJ, Chavarro JE, Hu SH, Xiong CL, et al. Sleep Duration and Quality in Relation to Semen Quality in Healthy Men Screened as Potential Sperm Donors. *Environ Int* (2020) 135:105368. doi: 10.1016/j.envint.2019.105368
32. Kato M, Roberts-Thomson P, Phillips BG, Haynes WG, Winnicki M, Accurso V, et al. Impairment of Endothelium-Dependent Vasodilation of Resistance Vessels in Patients With Obstructive Sleep Apnea. *Circulation* (2000) 102(21):2607–10. doi: 10.1016/j.envint.2019.105368
33. Ip MSM, Lam B, Chan LY, Zheng L, Tsang KWT, Fung PCW, et al. Circulating Nitric Oxide Is Suppressed in Obstructive Sleep Apnea and Is Reversed by Nasal Continuous Positive Airway Pressure. *Am J Resp Crit Care* (2000) 162(6):2166–71. doi: 10.1164/ajrccm.162.6.2002126
34. Musicki B, Liu T, Lagoda GA, Bivalacqua TJ, Strong TD, Burnett AL. Endothelial Nitric Oxide Synthase Regulation in Female Genital Tract Structures. *J Sex Med* (2009) 6:247–53. doi: 10.1111/j.1743-6109.2008.01122.x
35. Traish AM, Botchevar E, Kim NN. Biochemical Factors Modulating Female Genital Sexual Arousal Physiology. *J Sex Med* (2010) 7(9):2925–46. doi: 10.1111/j.1743-6109.2010.01903.x
36. Monica FZ, Bian K, Murad F. The Endothelium-Dependent Nitric Oxide-Cgmp Pathway. *Adv Pharmacol* (2016) 77:1–27. doi: 10.1016/bs.apha.2016.05.001
37. Pelliccione F, D'Angeli A, Filipponi S, Falone S, Necozione S, Barbonetti A, et al. Serum From Patients With Erectile Dysfunction Inhibits Circulating Angiogenic Cells From Healthy Men: Relationship With Cardiovascular Risk, Endothelial Damage and Circulating Angiogenic Modulators. *Int J Androl* (2012) 35(5):645–52. doi: 10.1111/j.1365-2605.2012.01253.x

38. Phillips BG, Narkiewicz K, Pesek CA, Haynes WG, Dyken ME, Somers VK. Effects of Obstructive Sleep Apnea on Endothelin-1 and Blood Pressure. *J Hypertens* (1999) 17(1):61–6. doi: 10.1097/00004872-199917010-00010
39. Burschtin O, Wang J. Testosterone Deficiency and Sleep Apnea. *Urol Clin North Am* (2016) 43(2):233–+. doi: 10.1016/j.ucl.2016.01.012
40. Zhang XH, Melman A, DiSanto ME. Update on Corpus Cavernosum Smooth Muscle Contractile Pathways in Erectile Function: A Role for Testosterone? *J Sex Med* (2011) 8(7):1865–79. doi: 10.1111/j.1743-6109.2011.02218.x
41. Mohammadi H, Rezaei M, Sharafkhaneh A, Khazaie H, Ghadami MR. Serum Testosterone/Cortisol Ratio in People With Obstructive Sleep Apnea. *J Clin Lab Anal* (2020) 34(1):e23011. doi: 10.1002/jcla.23011
42. Ziegler MG, Milic M. Sympathetic Nerves and Hypertension in Stress, Sleep Apnea, and Caregiving. *Curr Opin Nephrol Hypertens* (2017) 26(1):26–30. doi: 10.1097/Mnh.0000000000000288
43. Zias N, Bezwada V, Gilman S, Chroneou A. Obstructive Sleep Apnea and Erectile Dysfunction: Still a Neglected Risk Factor? *Sleep Breath* (2009) 13 (1):3–10. doi: 10.1007/s11325-008-0212-8
44. Wang L, Zhou B, Zhao Z, Yang L, Zhang M, Jiang Y, et al. Body-Mass Index and Obesity in Urban and Rural China: Findings From Consecutive Nationally Representative Surveys During 2004-18. *Lancet* (2021) 398 (10294):53–63. doi: 10.1016/S0140-6736(21)00798-4
45. Berry RB, Budhiraja R, Gottlieb DJ, Gozal D, Iber C, Kapur VK, et al. Rules for Scoring Respiratory Events in Sleep: Update of the 2007 Aasm Manual for the Scoring of Sleep and Associated Events. Deliberations of the Sleep Apnea Definitions Task Force of the American Academy of Sleep Medicine. *J Clin Sleep Med* (2012) 8(5):597–619. doi: 10.5664/jcsm.2172
46. Rosen RC, Cappelleri JC, Smith MD, Lipsky J, Pena BM. Development and Evaluation of an Abridged, 5-Item Version of the International Index of Erectile Function (Iief-5) as a Diagnostic Tool for Erectile Dysfunction. *Int J Impot Res* (1999) 11(6):319–26. doi: 10.1038/sj.ijir.3900472
47. Nakhli J, El Kissi Y, Bouhlel S, Amamou B, Nabli TA, Nasr SB, et al. Reliability and Validity of the Arizona Sexual Experiences Scale-Arabic Version in Tunisian Patients With Schizophrenia. *Compr Psychiatry* (2014) 55(6):1473–7. doi: 10.1016/j.comppsych.2014.04.006
48. Sil A, Barr G. Assessment of Predictive Ability of Epworth Scoring in Screening of Patients With Sleep Apnoea. *J Laryngol Otol* (2012) 126(4):372–9. doi: 10.1017/S0022215111003082
49. Julian LJ. Measures of Anxiety: State-Trait Anxiety Inventory (Stai), Beck Anxiety Inventory (Bai), and Hospital Anxiety and Depression Scale-Anxiety (Hads-a). *Arthritis Care Res (Hoboken)* (2011) 63 Suppl 11:S467–472. doi: 10.1002/acr.20561
50. Beck AT, Steer RA, Ball R, Ranieri WF. Comparison of Beck Depression Inventories-Ia and -Ii in Psychiatric Outpatients. *J Pers Assess* (1996) 67 (3):588–97. doi: 10.1207/s15327752jpa6703_13
51. Skoczynski S, Nowosielski K, Minarowski L, Brozek G, Oraczewska A, Glinka K, et al. May Dyspnea Sensation Influence the Sexual Function in Men With Obstructive Sleep Apnea Syndrome? A Prospective Control Study. *Sex Med-Uk* (2019) 7(3):303–10. doi: 10.1016/j.esxm.2019.06.005
52. Popp R, Kleemann Y, Burger M, Pfeifer M, Arzt M, Budweiser S. Impaired Vigilance Is Associated With Erectile Dysfunction in Patients With Sleep Apnea. *J Sex Med* (2015) 12(2):405–15. doi: 10.1111/jsm.12789
53. Budweiser S, Luigart R, Jorres RA, Kollert F, Kleemann Y, Wieland WF, et al. Long-Term Changes of Sexual Function in Men With Obstructive Sleep Apnea After Initiation of Continuous Positive Airway Pressure. *J Sex Med* (2013) 10(2):524–31. doi: 10.1111/j.1743-6109.2012.02968.x
54. Zhang XB, Lin QC, Zeng HQ, Jiang XT, Chen B, Chen X, et al. Erectile Dysfunction and Sexual Hormone Levels in Men With Obstructive Sleep Apnea: Efficacy of Continuous Positive Airway Pressure. *Arch Sex Behav* (2016) 45(1):235–40. doi: 10.1007/s10508-015-0593-2
55. Gurbuz C, Okur HK, Demir S, Ordu S, Caskurlu T. Pure Obstructive Sleep Apnea Syndrome and Erectile Dysfunction. *Balkan Med J* (2011) 28(4):435–9. doi: 10.5152/balkanmedj.2011.011
56. Tufik S, Santos-Silva R, Taddei JA, Bittencourt LRA. Obstructive Sleep Apnea Syndrome in the Sao Paulo Epidemiologic Sleep Study. *Sleep Med* (2010) 11(5):441–6. doi: 10.1016/j.sleep.2009.10.005
57. Peppard PE, Young T, Barnet JH, Palta M, Hagen EW, Hla KM. Increased Prevalence of Sleep-Disordered Breathing in Adults. *Am J Epidemiol* (2013) 177(9):1006–14. doi: 10.1093/aje/kws342
58. Peppard PE, Young T, Palta M, Dempsey J, Skatrud J. Longitudinal Study of Moderate Weight Change and Sleep-Disordered Breathing. *Jama-J Am Med Assoc* (2000) 284(23):3015–21. doi: 10.1001/jama.284.23.3015
59. Warmoth L, Regalado MM, Kimball K, Wesson DE. Cigarette Smoking is Associated With Enhanced Rate of Gfr Decline in Severe But Not in Mild Primary Hypertension. *J Invest Med* (2004) 52(1):S318–8. doi: 10.1097/00042871-200401001-00895
60. Liu K, Hou G, Wang X, Chen H, Shi F, Liu C, et al. Adverse Effects of Circadian Desynchrony on the Male Reproductive System: An Epidemiological and Experimental Study. *Hum Reprod* (2020) 35(7):1515–28. doi: 10.1093/humrep/deaa101
61. Vincent EE, Singh SJ. Review Article: Addressing the Sexual Health of Patients With Copd: The Needs of the Patient and Implications for Health Care Professionals. *Chron Respir Dis* (2007) 4(2):111–5. doi: 10.1177/1479972306076105
62. Santos T, Drummond M, Botelho F. Erectile Dysfunction in Obstructive Sleep Apnea Syndrome-Prevalence and Determinants. *Rev Port Pneumol* (2012) 18(2):64–71. doi: 10.1016/j.rppneu.2011.10.004
63. Luboshitzky R, Aviv A, Hefetz A, Herer P, Shen-Orr Z, Lavie L, et al. Decreased Pituitary-Gonadal Secretion in Men With Obstructive Sleep Apnea. *J Clin Endocrinol Metab* (2002) 87(7):3394–8. doi: 10.1210/jc.87.7.3394
64. Petersen M, Kristensen E, Berg S, Midgren B. Sexual Function in Male Patients With Obstructive Sleep Apnoea. *Clin Respir J* (2010) 4(3):186–91. doi: 10.1111/j.1752-699X.2009.00173.x
65. Goh VHH, Tong TYY. Sleep, Sex Steroid Hormones, Sexual Activities, and Aging in Asian Men. *J Androl* (2010) 31(2):131–7. doi: 10.2164/jandrol.109.007856
66. Luboshitzky R, Zabari Z, Shen-Orr Z, Herer P, Lavie P. Disruption of the Nocturnal Testosterone Rhythm by Sleep Fragmentation in Normal Men. *J Clin Endocrinol Metab* (2001) 86(3):1134–9. doi: 10.1210/jcem.86.3.7296
67. Giles DE, Roffwarg HP, Schlesser MA, Rush AJ. Which Endogenous Depressive Symptoms Relate to Rem Latency Reduction. *Biol Psychiatry* (1986) 21(5-6):473–82. doi: 10.1016/0006-3223(86)90189-7
68. Papagiannopoulos D, Khare N, Nehra A. Evaluation of Young Men With Organic Erectile Dysfunction. *Asian J Androl* (2015) 17(1):11–6. doi: 10.4103/1008-682X.139253
69. Bandini E, Fisher AD, Corona G, Ricca V, Boddi V, Monami M, et al. Severe Depressive Symptoms and Cardiovascular Risk in Subjects With Erectile Dysfunction. *J Sex Med* (2010) 7:381–1.
70. Smith JF, Breyer BN, Eisenberg ML, Sharlip ID, Shindel AW. Sexual Function and Depressive Symptoms Among Male North American Medical Students. *J Sex Med* (2010) 7(12):3909–17. doi: 10.1111/j.1743-6109.2010.02033.x
71. McCabe MP, Althof SE. A Systematic Review of the Psychosocial Outcomes Associated With Erectile Dysfunction: Does the Impact of Erectile Dysfunction Extend Beyond a Man's Inability to Have Sex? *J Sex Med* (2014) 11(2):347–63. doi: 10.1111/jsm.12374
72. Jern P, Gunst A, Sandnabba K, Santtila P. Are Early and Current Erectile Problems Associated With Anxiety and Depression in Young Men? A Retrospective Self-Report Study. *J Sex Marital Ther* (2012) 38(4):349–64. doi: 10.1080/0092623x.2012.665818
73. Caskurlu T, Tasci AI, Resim S, Sahinkanat T, Ergenekon E. The Etiology of Erectile Dysfunction and Contributing Factors in Different Age Groups in Turkey. *Int J Urol* (2004) 11(7):525–9. doi: 10.1111/j.1442-2042.2004.00837.x
74. Zou P, Wang X, Sun L, Liu K, Hou G, Yang W, et al. Poorer Sleep Quality Correlated With Mental Health Problems in College Students: A Longitudinal Observational Study Among 686 Males. *J Psychosom Res* (2020) 136:110177. doi: 10.1016/j.jpsychores.2020.110177
75. Corona G, Isidori AM, Aversa A, Burnett AL, Maggi M. Endocrinologic Control of Men's Sexual Desire and Arousal/Erection. *J Sex Med* (2016) 13 (3):317–37. doi: 10.1016/j.jsxm.2016.01.007
76. Hoyos CM, Melehan KL, Phillips CL, Grunstein RR, Liu PY. To Ed or Not to Ed–is Erectile Dysfunction in Obstructive Sleep Apnea Related to Endothelial Dysfunction? *Sleep Med Rev* (2015) 20:5–14. doi: 10.1016/j.smrv.2014.03.004
77. Zhang GL, Dai DZ, Zhang C, Dai Y. Apocynin and Raisanberine Alleviate Intermittent Hypoxia Induced Abnormal Star and 3beta-Hsd and Low

Testosterone by Suppressing Endoplasmic Reticulum Stress and Activated P66shc in Rat Testes. *Reprod Toxicol* (2013) 36:60–70. doi: 10.1016/j.reprotox.2012.12.002
78. Macrea MM, Martin TJ, Zagrean L. Infertility and Obstructive Sleep Apnea: The Effect of Continuous Positive Airway Pressure Therapy on Serum Prolactin Levels. *Sleep Breath* (2010) 14(3):253–7. doi: 10.1007/s11325-010-0373-0
79. Luboshitzky R, Shen-Orr Z, Herer P. Seminal Plasma Melatonin and Gonadal Steroids Concentrations in Normal Men. *Arch Androl* (2002) 48 (3):225–32. doi: 10.1080/01485010252869324
80. Pitteloud N, Dwyer AA, DeCruz S, Lee H, Boepple PA, Crowley WF Jr, et al. The Relative Role of Gonadal Sex Steroids and Gonadotropin-Releasing Hormone Pulse Frequency in the Regulation of Follicle-Stimulating Hormone Secretion in Men. *J Clin Endocrinol Metab* (2008) 93(7):2686–92. doi: 10.1210/jc.2007-2548
81. Mammi C, Calanchini M, Antelmi A, Cinti F, Rosano GM, Lenzi A, et al. Androgens and Adipose Tissue in Males: A Complex and Reciprocal Interplay. *Int J Endocrinol* (2012) 2012:789653. doi: 10.1155/2012/789653
82. Schafer H, Pauleit D, Sudhop T, Gouni-Berthold I, Ewig S, Berthold HK, et al. Body Fat Distribution, Serum Leptin, and Cardiovascular Risk Factors in Men With Obstructive Sleep Apnea. *Chest* (2002) 122(3):829–39. doi: 10.1378/chest.122.3.829
83. Ludwig W, Phillips M. Organic Causes of Erectile Dysfunction in Men Under 40. *Urol Int* (2014) 92(1):1–6. doi: 10.1159/000354931
84. Buvat J, Maggi M, Guay A, Torres LO. Testosterone Deficiency in Men: Systematic Review and Standard Operating Procedures for Diagnosis and Treatment. *J Sex Med* (2013) 10(1):245–84. doi: 10.1111/j.1743-6109.2012.02783.x
85. Hatzimouratidis K, Amar E, Eardley I, Giuliano F, Hatzichristou D, Montorsi F, et al. Guidelines on Male Sexual Dysfunction: Erectile Dysfunction and Premature Ejaculation. *Eur Urol* (2010) 57(5):804–14. doi: 10.1016/j.eururo.2010.02.020
86. Basar MM, Aydin G, Mert HC, Keles I, Caglayan O, Orkun S, et al. Relationship Between Serum Sex Steroids and Aging Male Symptoms Score and International Index of Erectile Function. *Urology* (2005) 66 (3):597–601. doi: 10.1016/j.urology.2005.03.060
87. Soukhova-O'Hare GK, Shah ZA, Lei ZM, Nozdrachev AD, Rao CV, Gozal D. Erectile Dysfunction in a Murine Model of Sleep Apnea. *Am J Resp Crit Care* (2008) 178(6):644–50. doi: 10.1164/rccm.200801-190OC
88. Celec P, Mucska I, Ostatnikova D, Hodosy J. Testosterone and Estradiol are Not Affected in Male and Female Patients With Obstructive Sleep Apnea Treated With Continuous Positive Airway Pressure. *J Endocrinol Invest* (2014) 37(1):9–12. doi: 10.1007/s40618-013-0003-3
89. Onem K, Erol B, Sanli O, Kadioglu P, Yalin AS, Canik U, et al. Is Sexual Dysfunction in Women With Obstructive Sleep Apnea-Hypopnea Syndrome Associated With the Severity of the Disease? A Pilot Study. *J Sex Med* (2008) 5(11):2600–9. doi: 10.1111/j.1743-6109.2008.00934.x
90. Gambineri A, Pelusi C, Pasquali R. Testosterone Levels in Obese Male Patients With Obstructive Sleep Apnea Syndrome: Relation to Oxygen Desaturation, Body Weight, Fat Distribution and the Metabolic Parameters. *J Endocrinol Invest* (2003) 26(6):493–8. doi: 10.1007/Bf03345209
91. Schiavi RC, White D, Mandeli J. Pituitary-Gonadal Function During Sleep in Healthy Aging Men. *Psychoneuroendocrinology* (1992) 17(6):599–609. doi: 10.1016/0306-4530(92)90018-3
92. Hammoud AO, Walker JM, Gibson M, Cloward TV, Hunt SC, Kolotkin RL, et al. Sleep Apnea, Reproductive Hormones and Quality of Sexual Life in Severely Obese Men. *Obesity* (2011) 19(6):1118–23. doi: 10.1038/oby.2010.344
93. Barrett-Connor E, Dam TT, Stone K, Harrison SL, Redline S, Orwoll E, et al. The Association of Testosterone Levels With Overall Sleep Quality, Sleep Architecture, and Sleep-Disordered Breathing. *J Clin Endocrinol Metab* (2008) 93(7):2602–9. doi: 10.1210/jc.2007-2622
94. Liu PY, Yee B, Wishart SM, Jimenez M, Jung DG, Grunstein RR, et al. The Short-Term Effects of High-Dose Testosterone on Sleep, Breathing, and Function in Older Men. *J Clin Endocrinol Metab* (2003) 88(8):3605–13. doi: 10.1210/jc.2003-030236
95. Killick R, Wang D, Hoyos CM, Yee BJ, Grunstein RR, Liu PY, et al. The Effects of Testosterone on Ventilatory Responses in Men With Obstructive Sleep Apnea: A Randomised, Placebo-Controlled Trial. *J Sleep Res* (2013) 22 (3):331–6. doi: 10.1111/jsr.12027
96. Jiang KL, Qian W, Lin ZQ, Zhao L, Shao S, Muhammad AI. [Obstructive Sleep Apnea Affects the Sexual Function of the Male Patient]. *Zhonghua Nan Ke Xue* (2017) 23(10):883–8. doi: 10.13263/j.cnki.nja.2017.10.004
97. Budweiser S, Enderlein S, Jorres RA, Hitzl AP, Wieland WF, Pfeifer M, et al. Sleep Apnea is an Independent Correlate of Erectile and Sexual Dysfunction. *J Sex Med* (2009) 6(11):3147–57. doi: 10.1111/j.1743-6109.2009.01372.x
98. Beltrami R, Confalonieri L. Association Between Single Nucleotide Polymorphisms in Interleukin-6 Gene and Periodontal Disease: A Systematic Review and Meta-Analysis. *Oral Maxillofac Pathol* (2016) 7 (1):667–72. doi: 10.5005/jp-journals-10037-1063
99. Diehm N, Borm AK, Keo HH, Wyler S. Interdisciplinary Options for Diagnosis and Treatment of Organic Erectile Dysfunction. *Swiss Med Wkly* (2015) 145:w14268. doi: 10.4414/smw.2015.14268
100. Selvin E, Burnett AL, Platz EA. Prevalence and Risk Factors for Erectile Dysfunction in the Us. *Am J Med* (2007) 120(2):151–7. doi: 10.1016/j.amjmed.2006.06.010
101. Seftel AD, Strohl KP, Loye TL, Bayard D, Kress J, Netzer NC. Erectile Dysfunction and Symptoms of Sleep Disorders. *Sleep* (2002) 25(6):643–7. doi: 10.1016/j.amjmed.2006.06.010

Conflict of Interest: The authors declare that the research was conducted in the absence of any commercial or financial relationships that could be construed as a potential conflict of interest.

Publisher's Note: All claims expressed in this article are solely those of the authors and do not necessarily represent those of their affiliated organizations, or those of the publisher, the editors and the reviewers. Any product that may be evaluated in this article, or claim that may be made by its manufacturer, is not guaranteed or endorsed by the publisher.

frontiers in Endocrinology

REVIEW
published: 09 March 2022
doi: 10.3389/fendo.2021.799043

Assessment of the Emerging Threat Posed by Perfluoroalkyl and Polyfluoroalkyl Substances to Male Reproduction in Humans

Leah Calvert[1,2], *Mark P. Green*[3], *Geoffry N. De Iuliis*[1,2], *Matthew D. Dun*[2,4], *Brett D. Turner*[5,6], *Bradley O. Clarke*[7], *Andrew L. Eamens*[1,2], *Shaun D. Roman*[1,2,8] *and Brett Nixon*[1,2*]

[1] *Priority Research Centre for Reproductive Science, University of Newcastle, Callaghan, Newcastle, NSW, Australia,* [2] *Hunter Medical Research Institute, New Lambton Heights, Newcastle NSW, Australia,* [3] *School of BioSciences, Faculty of Science, University of Melbourne, VIC, Australia,* [4] *Cancer Signalling Research Group, School of Biomedical Sciences and Pharmacy, College of Health, Medicine and Wellbeing, University of Newcastle, Callaghan, NSW, Australia,* [5] *Centre for Technology in Water and Wastewater, School of Civil and Environmental Engineering, University of Technology Sydney, Ultimo, Sydney, NSW, Australia,* [6] *Priority Research Centre for Geotechnical Science and Engineering, University of Newcastle, Callaghan, NSW, Australia,* [7] *Australian Laboratory for Emerging Contaminants, School of Chemistry, University of Melbourne, Melbourne, VIC, Australia,* [8] *Priority Research Centre for Drug Development, University of Newcastle, Callaghan, NSW, Australia*

OPEN ACCESS

Edited by:
Claus Yding Andersen, University of Copenhagen, Denmark

Reviewed by:
Jens Peter Bonde, University of Copenhagen, Denmark
Chris K. C. Wong, Hong Kong Baptist University, Hong Kong SAR, China
Alan Ducatman, West Virginia University, United States
Giovanni Luca, University of Perugia, Italy

****Correspondence:***
Brett Nixon
brett.nixon@newcastle.edu.au

Specialty section:
This article was submitted to Reproduction, a section of the journal Frontiers in Endocrinology

Received: *21 October 2021*
Accepted: *30 December 2021*
Published: *09 March 2022*

Citation:
Calvert L, Green MP, De Iuliis GN, Dun MD, Turner BD, Clarke BO, Eamens AL, Roman SD and Nixon B (2022) Assessment of the Emerging Threat Posed by Perfluoroalkyl and Polyfluoroalkyl Substances to Male Reproduction in Humans. Front. Endocrinol. 12:799043. doi: 10.3389/fendo.2021.799043

Per-fluoroalkyl and polyfluoroalkyl substances (PFAS) are a diverse group of synthetic fluorinated chemicals used widely in industry and consumer products. Due to their extensive use and chemical stability, PFAS are ubiquitous environmental contaminants and as such, form an emerging risk factor for male reproductive health. The long half-lives of PFAS is of particular concern as the propensity to accumulate in biological systems prolong the time taken for excretion, taking years in many cases. Accordingly, there is mounting evidence supporting a negative association between PFAS exposure and an array of human health conditions. However, inconsistencies among epidemiological and experimental findings have hindered the ability to definitively link negative reproductive outcomes to specific PFAS exposure. This situation highlights the requirement for further investigation and the identification of reliable biological models that can inform health risks, allowing sensitive assessment of the spectrum of effects of PFAS exposure on humans. Here, we review the literature on the biological effects of PFAS exposure, with a specific focus on male reproduction, owing to its utility as a sentinel marker of general health. Indeed, male infertility has increasingly been shown to serve as an early indicator of a range of co-morbidities such as coronary, inflammatory, and metabolic diseases. It follows that adverse associations have been established between PFAS exposure and the incidence of testicular dysfunction, including pathologies such as testicular cancer and a reduction in semen quality. We also give consideration to the mechanisms that render the male reproductive tract vulnerable to PFAS mediated damage, and discuss novel remediation strategies to mitigate the negative impact of PFAS contamination and/or to ameliorate the PFAS load of exposed individuals.

Keywords: male fertility, male infertility, male reproduction, perfluoroalkyl and polyfluoroalkyl substances, PFAS, sperm, toxicants

INTRODUCTION

Perfluoroalkyl and polyfluoroalkyl substances (PFAS) are a diverse group of more than 4,700 synthetic, highly fluorinated, aliphatic chemicals with distinctive chemical properties [see review by Kirk et al. (1)], which render members of this chemical group incredibly stable and environmentally persistent (2, 3). Consequently, PFAS have been employed for a range of purposes including in the formulation of fire-fighting foams as well as in a variety of consumer products (4, 5), such as food packaging, cookware and water repellent clothing (6–9). Since the 1950s, the extensive manufacture, distribution, use and disposal of PFAS has resulted in the widespread environmental contamination and subsequent exposure of humans and animals. Despite endeavors to phase out the toxic eight chain PFAS initiated in 2000, the inherent stability of these compounds has resulted in omnipresence in the global environment (5, 9–11). Thus, many industrialized nations are seeking to implement measures to limit, detect and eradicate PFAS contamination (5, 9). Long-chain PFAS generally have longer environmental half-lives and a high propensity to accumulate in biological systems from which they may take many years to be fully excreted. For example, PFAS such as perfluorooctanoic acid (PFOA) and perfluorooctanesulfonic acid (PFOS) are the most extensively reported long-chain perfluoroalkyl acids described in scientific literature (5) and have a half-life in human serum of 3.8 and 5.4 years, respectively (**Table 1**) (13). Longer chain (≥ 6 carbon atoms) PFAS bioaccumulate to a greater extent than shorter chain analogues (14–17), and also possess longer half-lives (18, 19). Upon entering the body, PFAS bind to albumin in the blood stream and accumulate within the body's protein-rich tissues (6, 20). Consequently, PFAS are readily detectable throughout the human body as well as accumulating to detectable levels in most bodily fluids, including urine, breast milk, blood, and seminal plasma (21, 22). Notably, in support of the notion that albumin binding is one of the key reasons that PFAS are slowly excreted in urine, Jain and Ducatman have shown that serum PFAS levels decrease under conditions of albuminuria (23). This pathology, during which albumin is able to escape into the urine as a consequence of renal dysfunction, is presumed to result in increased excretion of bound PFAS.

PFOS and PFOA are the two most abundant PFAS found in human serum worldwide (7, 10, 24), with levels of each varying between countries, suggesting differences in the degree of exposure in each country (24, 25). Further, PFOS and PFOA have a propensity of accumulate in our food chains (10) and it is thought that dietary intake is a key pathway of exposure for the general population; either from food packaging or environmental contamination of food products (26–29). Other suggested routes of contamination include household dust (28, 30) or from the consumption of contaminated drinking water (29, 31, 32); although all paths of human exposure remain to be fully identified. Exposure levels vary between locations and individuals and range from background levels in the general population of up to around 14 ng/mL of PFOS and PFOA in the blood (33), through to considerably higher levels in individuals who have been occupationally exposed, or those who reside in contaminated areas (34). The highest concentrations have been detected in individuals employed in PFAS manufacturing facilities with a mean blood concentration of 1,000 to 2,000 ng/mL PFOS and 5,000 ng/mL PFOA (25, 35). Such findings are of particular concern in view of the potential of PFAS to elicit a range of adverse health outcomes.

Here, we review literature pertaining to the emerging threat posed by PFAS exposure, with a specific focus on the male reproductive tract and general male fertility, owing to its utility as a biomarker of general health. Indeed, in what has become a well-established paradigm, male infertility has been shown to serve as an early indicator of a range of co-morbidities such as coronary, inflammatory, and metabolic diseases; conditions that all have associated transgenerational effects (36–42). It follows that adverse associations have been established between PFAS and the incidence of testicular dysfunction, including pathologies such as testicular cancer (43–48) and a reduction in semen quality (35, 49, 50). Accordingly, we give consideration to the mechanisms that render the male reproductive tract vulnerable to PFAS mediated damage, as well as novel remediation strategies to mitigate the negative impact of PFAS contamination and/or ameliorate the concentration of PFAS that has accumulated in exposed individuals.

PFAS CHEMISTRY

The term 'fluorinated substances' encompasses an extensive array of organic and inorganic chemicals that contain a

TABLE 1 | Summary of a selection of common PFAS chemicals, detailing abbreviations, chemical formula, and half-life in humans.

Chemical Name	Abbreviation	Formula	Half-life in humans
Perfluorobutane sulfonic acid	PFBS	$C_4HF_9O_3S$	28 days
Perfluorohexane sulphonic acid	PFHxS	$C_6HF_{13}O_3S$	5.3 – 8.5 years
Perfluorooctane sulfonic acid	PFOS	$C_8F_{17}SO_3H$	3.5 – 5 years
Perfluorooctane sulfonamide	PFOSA	$C_8H_2F_{17}NO_2S$	Unknown
Perfluorobutanoic acid	PFBA	$C_4HF_7O_2$	3 days
Perfluoropentanoic acid	PFPeA	$C_5HF_9O_2$	Unknown
Perfluorohexanoic acid	PFHxA	$C_6HF_{11}O_2$	32 days
Hexafluoropropylene oxide dimer acid (MS-20244) (Q29388239)	GenX	$C_6HF_{11}O_3$	Unknown (estimated 4 hours to 6 days)
Perfluoroheptanoic acid	PFHpA	$C_7HF_{13}O_2$	1.2 – 2.5 years
Perfluorooctanoic acid	PFOA	$C_8HF_{15}O_2$	2.1 – 3.8 years
Perfluorononanoic acid	PFNA	$C_9HF_{17}O_2$	2.5 – 4.3 years
Perfluorodecanoic acid	PFDA	$C_{10}HF_{19}O_2$	Unknown

Table adapted from Fenton et al. (12).

minimum of one fluorine (F) atom, with each substance possessing different chemical, biological and physical properties (3). The properties of each compound are influenced by both the number of F atoms and their position in the molecule, with chemicals classed as partially fluorinated (polyfluoroalkyl), or fully fluorinated (perfluorinated) (4). The most common PFAS are the perfluorinated alkyl acids (PFAAs), which are amphiphilic and exhibit attraction to both aqueous and lipid media, mimicking phospholipid properties. Their structure contains a water-insoluble hydrophobic segment (the fluorinated carbon chain), and a water-soluble hydrophilic functional group such carboxylic acid or sulfonic acid (4). The structural formula of the resulting moiety is C_nF_{2n+1}-R, where R represents the functional group (**Figure 1**) (5). The PFAS moiety contains strong carbon-fluorine bonds conferring unique chemical properties that render these chemicals heat-resistant, water repellent, and exceptionally stable, to the point where they are almost indestructible under normal environmental conditions (5). The fluorination of the hydrocarbon chain drastically changes the chemical properties of the molecule, as the hydrophobic fluorinated segment repels water, while in parallel, the oleophobic properties also repel fat and oil (4). Thus, perfluorinated compounds can effectively lower surface tension and act as efficient surfactants for coatings on non-stick cookware and in food packaging and firefighting foam (1). Individual PFAS are distinguished from each other by 1) the properties of the functional group and 2) the length of the carbon backbone (**Figure 1**). However, PFAS molecules are also further categorized based on their usage, and the history of their manufacture. In this context, group members are described as either legacy PFAS, specifically those molecules with a long history of usage and/or environmental persistence, or as replacement PFAS, which include a new generation of compounds with different chemistries that were designed to replace the original and 'more' harmful legacy PFAS (51, 52).

ROUTES OF PFAS EXPOSURE

PFAS exposure can arise through several routes (**Figure 2**), with environmental contamination occurring at varying stages of production, usage, and waste disposal. In particular, PFAS have found application as a major component of aqueous film forming foams (AFFF) (53), which are widely used for firefighting, military training activities and at airports and thus has resulted in extensive contamination of nearby soil and waterways (31, 34, 54, 55). Elevated PFOS/PFOA levels have been detected in the serum of individuals living in areas with high levels of these chemicals in their drinking water (11, 31), including those communities located in close proximity to military bases, airports and PFAS manufacturing factories (31, 56). Not surprisingly, greater plasma contamination levels have also been detected in occupationally exposed individuals such as firefighters and factory workers manufacturing or using PFAS (31, 34, 55, 57, 58). Industry waste and AFFF usage has resulted in widespread contamination of groundwater, often used as drinking water, with dietary exposure suggested to be the main route of exposure for adults (29, 34, 56, 59). In addition, background levels of contamination are seen in the general population who are exposed to PFAS through drinking water (29, 60), house dust (61) and food consumption (27, 62, 63), with the latter arising from the extensive use of PFAS in consumer packaging. Compounding this situation, prenatal exposure can occur through the placenta (64, 65) and young babies can be exposed through breast milk (66, 67).

ACCUMULATION AND DISTRIBUTION OF PFAS IN THE BODY

PFAS enter the body through ingestion (31), inhalation (68) or dermal exposure (69). Once they have entered the bloodstream through gas-exchange or digestion, PFAS bind to serum proteins such as the major transport protein, human serum albumin (HSA) (70, 71). It appears PFOS has a greater binding affinity for HSA than PFOA, which correlates with the known longer half-life of PFOS (**Table 1**) (12, 72). Due to their biochemical stability, PFAS chemicals tend to accumulate within the body (1) and move from plasma into tissues, with the highest levels being found in human tissues with a larger blood supply such as the liver, lungs and kidneys (6, 20, 66). This is also reported in studies of mice where the highest accumulation of PFOS has been documented in the liver, lungs, kidney and bone marrow (73), as well as in primates, with the kidneys and blood also showing higher levels in comparison to other tissues (66). Notably, the tissue distribution of PFAS is influenced by multiple factors including species and gender, chemical characteristics such as chain length and functional group, as well as exposure dose (66, 74, 75). Most environmentally relevant PFAS have chain lengths between 4 and 13 fluorinated carbons (15, 76) giving rise to a variety of different structures such as branched forms (4, 76), although the most commonly detected PFAS in humans and wildlife are linear forms (**Figure 1**) (77). Longer chain PFAS have a greater potential to accumulate in living organisms than do shorter chain PFAS (<6 carbons) (14) due to the ability of longer chain PFAS such as PFOA, PFOS and perfluorohexanesulphonic acid (PFHxS) to bind to a wider range of serum proteins, including transferrin, plasma gamma-globulin and albumin (70). This is supported by evidence that PFAS accumulation occurs in protein-rich tissues such as the liver (66). Such evidence has led to the replacement of legacy and long-chain PFAS with structurally similar shorter chain variants, thought to be less toxic; for example, perfluorobutane sulfonic acid (PFBS) has been used to replace PFOS (51) and GenX (hexafluoropropylene oxide dimer acid) has replaced PFOA (16). Plasma concentrations support this rationale with longer chain PFAS such as PFOA and PFOS showing higher levels [3.9 and 20.7 μg/L, respectfully (21)] in comparison to the shorter chain replacements PFBS [typically below the detection limit of 4.2 μg/L (9)] and perfluorobutanoic acid (PFBA) [3.3 μg/L (78)]. However, little is currently known about the toxicology of these replacement chemicals (79). Additionally, bioaccumulation of PFAS appears to be influenced by the functional group(s) attached to the hydrocarbon backbone of each PFAS molecule. For example,

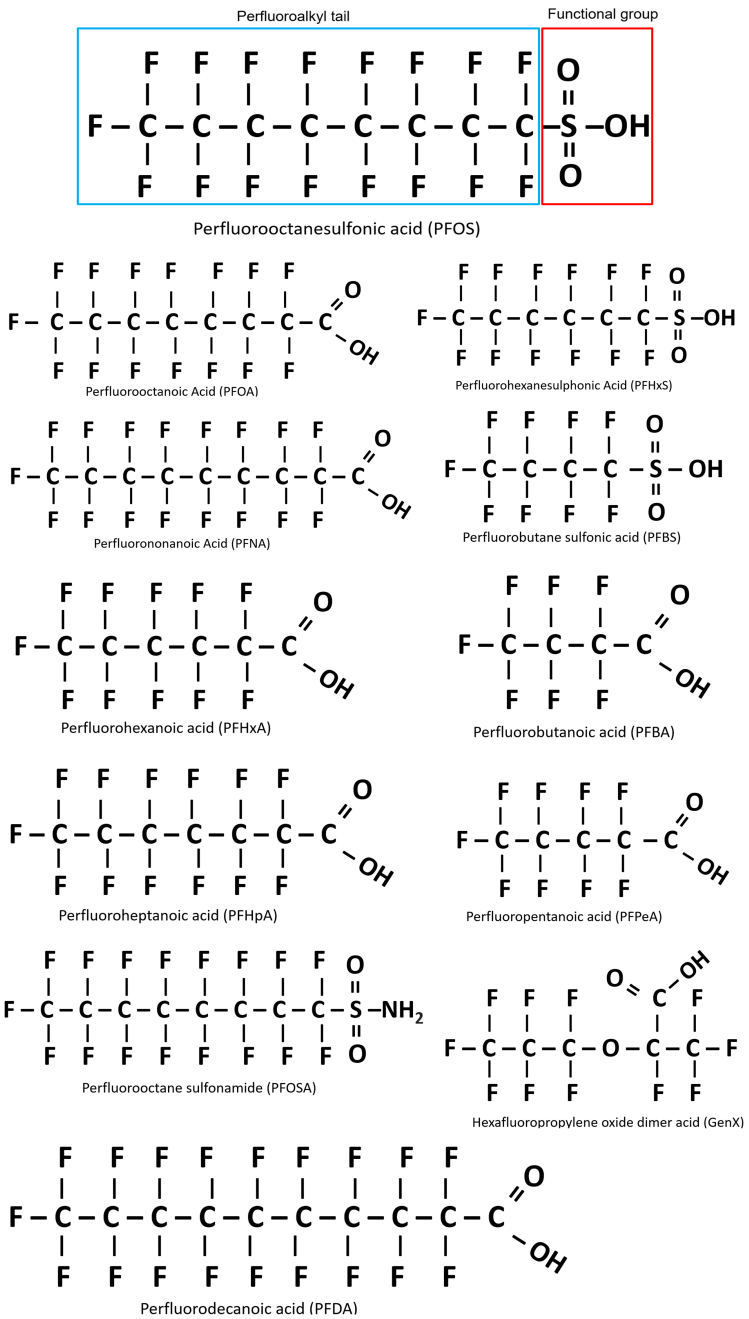

FIGURE 1 | Basic structure of perfluoroalkyl substances (PFAS), using perfluorooctanesulfonic acid (PFOS) as an example. Outlined in blue is the perfluoroalkyl tail (carbon/fluoride chain) and the functional group is outlined in red. All PFAS share these general features, with variation in the carbon chain length and functional group. Figure adapted from Blake and Fenton 2020 (51).

compounds that harbor an attached carboxylic acid functional group have been shown to accumulate less in fish, than those with a sulfonate functional group of the same carbon chain length (14, 18). Although the exact mechanisms behind this disparity are currently unknown, it may be due to the stronger affinity for proteins seen with longer chain length and in sulfonic acids (71).

PFAS HUMAN HEALTH ASSOCIATIONS

Increasing awareness of the dangers of PFAS and their propensity to bioaccumulate has led to a surge in scientific research and public interest, with PFAS being labelled as a potential risk for humans and the environment by the Scientific Committee on Health in 2018 (80). Studies have

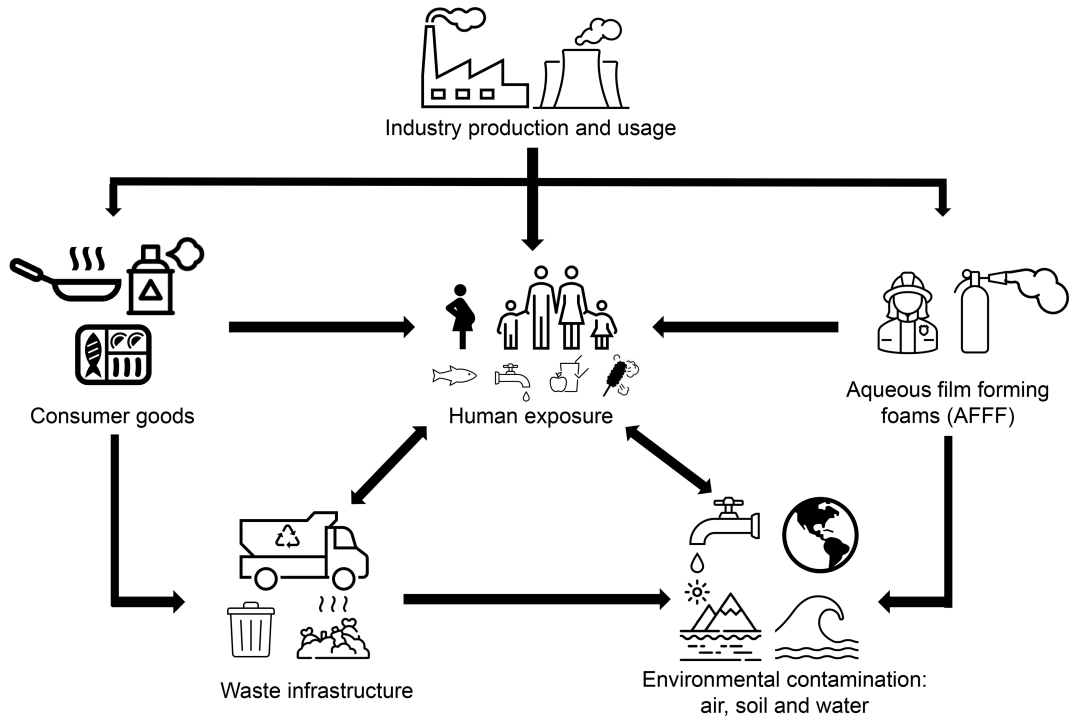

FIGURE 2 | Schematic diagram illustrating the routes of human PFAS exposure. Following production, PFAS are used in consumer products such as food packaging, cookware, water repellent clothing and non-stick fry pans. PFAS are also a main component in firefighting foam, which can leach into the environment, or are otherwise disposed of as industrial waste. Human exposure may occur through use of consumer products or from contaminated water supplies. Accordingly, environmental exposure can occur as a result of waste products contaminating waterways and soil through leaching of firefighting foam and waste from industry and consumers.

been conducted in both human and animal models to investigate possible health consequences arising from PFAS exposure (1, 43). The most commonly investigated PFAS with regards to human health are PFOS and PFOA (81), with a range of additional PFAS having been studied including PFHxS and PFBS (1) (**Table 1**). Mounting evidence from these studies supports an association between PFAS and an array of human diseases and disorders (1). However, it is somewhat difficult to definitively link causality to PFAS due to the variation in chemistries and potential biological activities between the different classes of PFAS, the duration and degree of exposure, potential synergistic or antagonistic effects of PFAS combinations in the body as well as the often-overlooked precursors of PFAS, which degrade to the terminal perfluoroalkyl acids (PFAAS) (82, 83). This situation is further compounded by the mechanisms of PFAS exposure, which vary both between and within communities, resulting in distinct PFAS profiles among individual subjects. Furthermore, disparities also exist in an individual's genetic and phenotypic constitution within affected populations, which could ultimately influence their PFAS clearance rates and susceptibility to the biological effects of these chemicals. Notwithstanding these limitations, the balance of evidence supports the potential for PFAS exposure to elicit adverse health sequelae at differing developmental stages and ages (66, 84–88). The C8 Health Project also bears out this conclusion; a comprehensive investigation of an entire community of 69,000 people exposed to PFAS *via* consumption of contaminated drinking water (43). This study revealed probable links between PFOA exposure and six diseases: kidney and testicular cancer, thyroid disease, high cholesterol, ulcerative colitis, and pregnancy-induced hypertension (43), findings that are supported by the International Agency for Research on Cancer evidence (48, 85). Although, it should be noted this evidence relates to PFOA exposure only, and therefore, further investigations of this nature are required for the remaining range of PFAS.

Building on this evidence, the greatest and most consistently reported metabolic consequence of PFAS exposure is dyslipidemia, with several notable studies finding links between serum PFAS and dysregulated lipid profiles (89), including increased low-density lipoprotein (90, 91), triglycerides (92) and total cholesterol (90, 91, 93, 94) in addition to diminished high-density lipoprotein (89). However, the extent of cholesterol dysregulation is variable across PFAS exposure levels as is the response to different forms of PFAS; with PFOA and PFOS demonstrating the most consistent effects between studies (62).

Epidemiological evidence has also linked PFAS exposure to the prevalence of testicular cancer, with the International Agency for Research on Cancer concluding PFOA is possibly carcinogenic to humans (48) and the United States Environment Protection Agency declaring it a likely carcinogen (95). In this context, studies by Barry et al. reported a strong association between

testicular cancer and PFOA exposure (hazard ratio of 1.34) in adults exposed through drinking water assessed as part of the C8 Health Project cohort (43, 44). Similarly, Vieira et al. identified a positive correlation in individuals exposed to very high PFOS levels, with an adjusted odds ratio of 2.8; although a potential limitation of this study was the relatively small sample number (45). Confounding this situation, three additional studies focusing on PFOA exposure and mortality from testicular cancer all failed to identify an association in occupationally exposed workers (87, 96, 97). Thus, whilst not universally demonstrated, the potential significance of these positive associations is highlighted by parallel correlations between the widespread increase in worldwide PFAS usage and the rising prevalence of testicular cancer; a pathology that has significantly increased in recent times to become the most common malignancy in young men aged 20-40 years (98–101). Although the characterization of testicular cancer remains incomplete, there is speculation that environmental factors, as opposed to genetic factors, are a key contributor to the etiology of this form of cancer (98, 102).

DIFFICULTIES ASSOCIATED WITH THE STUDY OF THE EFFECTS OF PFAS CHEMICALS ON HUMAN HEALTH

Many challenges exist that have hindered attempts to fully assess PFAS effects on health, including those directly related to tracing the mode and levels of PFAS exposure in the general population, consequences of PFAS precursors, compound effects of PFAS mixtures, as well as nuances specific to studies of animal models (103). The use of the latter has proven invaluable for studying the toxicology of PFAS exposure, albeit with variable outcomes (66, 104, 105). Laboratory rodents are the chief animal model employed, with zebrafish also being utilized in recent times, particularly in the context of assessing the impacts of PFOA and PFOS exposure (12). Amongst animal models, considerable interspecies variation has been noted, but thus far, the mechanistic basis of such inconsistency has not been entirely resolved. Known variables include biological mechanisms of PFAS action within target tissues, rates of PFAS metabolism and elimination, as well as assessment of different disease endpoints (12, 29, 51, 103). For instance, the half-life of PFOA in mice, at 6 days, is much shorter than in rats at 16 to 22 days and is generally significantly longer in humans (~2.1 to 3.8 years) (12). These differences are further confounded by differential responses between genders, with PFOA being eliminated much quicker from female rats (2-4 hours) compared to their male counterparts (4-6 days) (12, 106, 107). Li et al. (108) have reported similar results in humans with a significantly lower PFOS half-life being seen in women (3.1 years) compared to males (4.6 years). Similarly, Zhang et al. (109) reported that PFOS half-life was shorter in women under 50 years of age (6.2 years) in comparison to women over 50 and for males of all assessed age groups (27 years), although, the same trend was not seen with PFOA. However, it should be noted that this estimated half-life of 27 years for PFOS is higher than that calculated in similar studies, and as such, should be considered an upper limit estimation.

The manufacture and pervasive use of PFAS began in the 1950s (4), meaning that virtually all humans born after this time have potentially been exposed to some degree of PFAS contamination. As a consequence, there is a genuine difficulty in identifying a naïve unexposed control cohort, a situation that hinders the reliability of epidemiological models and cohort studies used to compare exposure groups and evaluate the risk of disease associated with varying PFAS exposure levels (51). Further, direct evaluation of the health outcomes of an individual resulting from PFAS exposure provides challenges due to the wide array of PFAS profiles detected in individuals within the same community, and between geographically distinct communities (51). Indeed, an individual's PFAS profile depends on several variables, such as the source of exposure, which can range from contamination associated with standard food packaging, through to the waste products encountered within the vicinity of a facility which manufactures PFAS (51). Exposure sources are also likely to differ over time due to fluctuations in PFAS usage as has been seen with the progressive phasing out of PFOS and PFOA chemicals in favor of alternative short chain PFAS derivatives (51). Additionally, possible synergistic or antagonist effects between different PFAS molecules may result in variable health outcomes between individuals (51), yet little is currently known of the repercussions of such chemical interplay (66). Variations in exposure also occur throughout the lifetime of an individual and can range from consistent chronic exposure to intermittent shorter periods of exposure. This exposure range has apparent consequences for an individual's PFAS profile making attempts to relate PFAS exposure to incident health outcomes difficult. Indeed, PFAS-related health outcomes emerging in adults may be attributed to exposure at one or more key stages of development such as the *in utero*, childhood or puberty stages (110), or alternatively, to chronic life-long exposure. Additionally, it cannot be determined whether an individual's PFAS contamination level is a result of a current exposure(s) or accumulation over a period of several years.

Another limitation of PFAS investigation is knowledge of the full assortment of contaminating PFAS chemicals. Initial identification of these chemicals in human serum was reported in 1980 when PFOA was discovered in a group of industrial plant workers exposed to fluorochemicals (111). A subsequent reduction in the manufacture, and phasing-out the use of PFAS classed as being damaging agents began in several countries in 2000 (5). Consequently, the original PFAS were replaced with other chemical analogues thought to be less toxic and which did not accumulate as readily in biological systems (79). Regrettably, the next generation of PFAS has subsequently been found to be detrimental to human health, with a prominent example being GenX, a branched short-chain PFAS that has subsequently been found to be more toxic than the PFOA it replaced (16). As a result, new PFAS are constantly being added to the list of hazardous and toxic chemicals (112, 113), which

emphasizes the necessity for increased investment into PFAS-related research.

Currently, determination of the PFAS profile of an individual is limited by available testing methods. Serum testing is performed most often using mass spectrometry paired with liquid chromatography (78). Mass spectrometry identifies organic compounds based on their molecular mass and can detect and quantify compounds with a high level of sensitivity. Many methods measure a limited subset of 20-30 PFAS, which potentially leads to inaccurate PFAS profiles, and should be considered when comparing PFAS studies (114). The limit of detection varies between PFAS (e.g., 1.10 ng/L for perfluoroheptanoic acid (PFHpA) to 25.1 ng/L for PFBA), with the limit of quantitation being even greater (e.g. 3.3 ng/mL for PFHpA, to 75.3 ng/L for PFBA) (78). If a particular PFAS is present below the method reporting limit in a sample it would be assumed not to be present in the assessed sample, thus introducing inaccuracies in the assignment of biological effects. These limitations in measurement techniques highlight the need to identify and understand new and emerging fluorinated compounds to allow an accurate determination of exposed communities and the efficacy of remediation strategies to reduce exposure.

The confounders documented above highlight the requirement for reliable markers of general health with which to determine the risk posed by PFAS exposure. Here, we explore the utility of employing male reproductive health as one such indicator to understand the molecular pathways by which PFAS drive pathophysiological responses, a strategy that builds on evidence that the male germline is vulnerable to a variety of environmental toxicants (1, 115).

THE RELATIONSHIP BETWEEN MALE INFERTILITY AND OVERALL HEALTH

Infertility is a reproductive system disease that impacts 16 to 25% of couples, with almost half of all cases attributed to male reproductive issues (116). Such problems are often connected to semen abnormalities, key contributors to which include body mass, lifestyle, age, and environmental exposures (116). Over the past few decades, decreasing trends in semen quality have been reported but there remains no clear explanation for the underlying causes of this decline (116). In recent years there has also been increased understanding that the general health of a male is closely related to his reproductive health (116), with strong associations established between male infertility and future health; especially the development of testicular cancer (117–120), and chronic non-malignant diseases such as ischemic heart disease and diabetes (36, 37, 40, 42, 116, 121). It has been proposed that shared genetic pathways, lifestyle factors and the environment, possibly acting *in utero*, could play a key role (122). Mounting evidence implies that semen quality can serve as a biological marker for future male health, as multiple epidemiological studies of notable size (>50,000 men) describe consistent associations between reduced semen quality and mortality. For instance, diminished semen parameters, such as sperm count, concentration, motility, and morphology, are related to a 2.3-fold greater risk of death in the following eight years: factors comparable to the risk of death due to diabetes or smoking (36, 42, 117). These studies reveal that men with atypical semen characteristics commonly die due to a higher prevalence of testicular cancer and/or altered androgen signaling, which culminate in the onset of metabolic, cardiovascular, or inflammatory diseases (123, 124); a disease set not too dissimilar to those suggested to onset due to PFAS exposure (1, 43).

Hence, current epidemiological evidence aligns with the association between male infertility and PFAS exposure, as seen with the link between male infertility and risk of chronic disease and mortality. Nevertheless, the scarcity of prospective studies and insufficient adjustment of confounders hinder the ability to ascertain the causality of these associations, and the pathogenic pathways linking these conditions are still ambiguous (1). Despite this, male fertility, particularly the clinical assessment of basic sperm parameters, allows for readily accessible biomarkers and presents as a potentially important resource to identify diseases promptly and predict the long-term health of an individual (36, 39–42). The theory that male reproductive pathologies are triggered by environmental exposure is not a new concept. Indeed, several studies have investigated a range of environmental contaminants (115) such as pesticides and herbicides (125), acrylamide (126), and radiation (127) and their implications for male fertility. In addition, these studies provide an important precedent for equivalent research to be performed on PFAS.

KNOWN EFFECTS OF PFAS EXPOSURE ON MALE FERTILITY

Despite the publication of several studies exploring the relationship between PFAS exposure and male fertility, the evidence presented is often conflicting (81, 128), and further such studies are hindered by the nature of the chemicals assessed and the pre-existing history of worldwide PFAS exposure. Notwithstanding the limitations imposed by these confounders, male ailments such as testicular cancer are perceived as a prominent endpoint of PFAS exposure (1, 43–47) (**Table 2**). Further evidence of testicular dysfunction is supported by large cohort studies assessing semen quality (49, 140). In this context, a dose-response relationship may exist between chronic PFOA and PFOS exposure and sperm production. A 35% decline in normal sperm production was observed in the upper tertile of PFOS concentration (> 27.3 μg/L), compared to that of the first tertile (< 11.9 μg/L) (35). Similarly, a 40% decrease in normal sperm production was recorded in high PFOS and PFOA exposed individuals, compared to men classed as having low exposure levels (129). Moreover, *in utero* exposure to PFOA was shown to lower total sperm count (130). Further to this, recent studies have described a significant association between PFAS exposure and several indicators of human sperm quality (49, 134). For instance, Toft and colleagues (35)

TABLE 2 | Summary of outcomes from studies investigating the impact of PFAS on human male reproductive function.

Assessed outcome	Serum PFAS assessed	Timing of PFAS exposure	Outcome	References
Prevalence of testicular cancer				
	PFOA	Adulthood	Increased	Frisbee et al. (43)
	PFHxS			Barry et al. (44)
				Kirk et al. (1)
				Vieira et al. (45)
				Bartell and Vieira (47)
	PFHxS	*In utero*	Increased	Lin et al. (46)
Sperm morphology				
	PFOS, PFHxS	Adulthood	Decrease in percentage of normal spermatozoa	Toft et al. (35)
	PFOA + PFOS			Joensen et al. (129)
	PFOSA			Louis et al. (49)
	PFOA, PFOS	*In utero*	No change	Vested et al. (130)
	Multiple	Adulthood	No change	Joensen et al. (131)
	PFOS, PFOA, PFNA, PFHxS			Petersen et al. (132)
Sperm count and concentration				
	PFOA	*In utero*	Decrease in sperm count and concentration	Vested et al. (130)
	PFOS, PFOA, PFNA, PFHxS	Adulthood	No change	Toft et al. (35)
				Joensen et al. (131)
				Petersen et al. (132)
				Raymer et al. (133)
	PFOS	*In utero*	No change	Vested et al. (130)
Sperm DNA quality				
	Multiple	Adulthood	Increased sperm DNA damage	Governini et al. (134)
	PFOS, PFOA, PFNA, PFHxS	Adulthood	No change in DNA integrity	Specht et al. (135)
	PFHxA			Emerce and Cetin (136)
	PFOS, PFOA, PFNA, PFHxS	Adulthood	No change in DNA methylation	Leter et al. (137)
Semen volume				
	PFOS, PFOA, PFNA, PFHxS	Adulthood	No change	Toft et al. (35)
				Joensen et al. (131)
				Joensen et al. (129)
				Vested et al. (130)
				Petersen et al. (132)
				Raymer et al. (133)
Sperm motility				
	PFOA	Adulthood	Increase	Toft et al. (35)
	PFOS, PFOA, PFHS	Adulthood	Decrease	Song et al. (78)
	Multiple	Adulthood	No change	Joensen et al. (131)
	PFOS, PFOA, PFNA, PFHxS			Joensen et al. (129)
				Petersen et al. (132)
				Raymer et al. (133)
	PFOA, PFOS	*In utero*	No change	Vested et al. (130)
Serum levels of testosterone				
	PFHxS	*In utero*	Increase	Nian et al. (138)
	PFOS	Adulthood	Decrease	Joensen et al. (131)
	PFOA, PFOS, PFNA	Adulthood	Decrease	Cui et al. (139)
	PFOS, PFOA, PFHxS, PFNA	Adulthood	No change	Joensen et al. (129)
				Petersen et al. (132)
				Raymer et al. (133)
	PFOS, PFOA	*In utero*	No change	Vested et al. (130)
Serum levels of sex hormone binding globulin				
	PFOA	Adulthood	Increase	Petersen et al. (132)
	PFOA, PFOS, PFNA	Adulthood	Decrease	Cui et al. (139)
	PFOS, PFOA, PFHxS, PFNA	Adulthood	No change	Joensen et al. (129)
				Joensen et al. (131)
				Petersen et al. (132)
	PFOS, PFOA	*In utero*	No change	Vested et al. (130)
Serum levels of luteinizing hormone				
	PFOA, PFOS	Adulthood	Increase	Petersen et al. (132)
				Raymer et al. (133)
	PFOA	*In utero*	Increase	Vested et al. (130)
	PFBS, PFHpA	*In utero*	Decrease	Nian et al. (138)
	PFOS, PFOA, PFHxS	Adulthood	No change	Joensen et al. (129)
				Cui et al. (139)

(Continued)

TABLE 2 | Continued

Assessed outcome	Serum PFAS assessed	Timing of PFAS exposure	Outcome	References
	PFOS	*In utero*	No change	Vested et al. (130)
Serum levels of follicle-stimulating hormone				
	PFOA	*In utero*	Increase	Vested et al. (130)
	PFBS	*In utero*	Decrease	Nian et al. (138)
	PFOS, PFOA, PFHxS, PFNA	Adulthood	No change	Joensen et al. (129) Petersen et al. (132) Raymer et al. (133)
	PFOS	*In utero*	No change	Vested et al. (130)

found no consistent associations between exposure to multiple PFAS and sperm concentration and count, or semen volume but did record a decrease in sperm cells with normal morphology in association with higher PFOS levels (35). Similarly, Joensen et al. reported equivalent results in their 2009 study with PFOA and PFOS (129), but these outcomes could not be reproduced in their later study published in 2013 (131), possibly due to lower levels of PFAS recorded in this later cohort (0.5% for PFOS), in which no participants were classified in the 'high exposure' category as per the criteria in the first study. Further studies also failed to find an association between PFAS and sperm quality (132, 133, 135–137); thus precluding the establishment of causative links (133, 136). Sperm motility has also been found to correlate both positively and negatively with PFOA exposure. One study investigating the implications of PFAS exposure on sperm parameters found greater sperm motility the study cohort with the highest serum PFOA levels (35). However, this observation was not consistent across all countries, nor the individual PFAS examined, and due to the many statistical tests performed in this study, the authors concluded such results might be due to chance events alone (35). In contrast, an independent study reported a significant negative correlation between several PFAS in semen, including PFOA, and sperm motility (78). This latter study also found associations between the PFAS concentration in semen and sperm motility, which indicates that seminal concentrations of PFAS may be more indicative of semen quality than that of serum PFAS levels. Such a finding has implications for the accuracy of extrapolating data from different sample sources across studies. Thus far, less than 15 studies have been conducted to investigate associations between PFAS levels and sperm parameters (1, 141) (**Table 2**). Half of these studies show no association while the other half report some associations. Yet, no studies consistently found the same set of altered sperm parameters due to PFAS exposure. Differing results may, in part, be attributed to the variation in the studied cohorts between countries; for example European and Arctic (35), versus Chinese populations (78), wherein participants are likely to have been exposed to different PFAS profiles depending on the source and route of contamination, not to mention other environmental factors to which they may be exposed, that could act synergistically or antagonistically. Although the variation in outcomes reported in these studies highlights the difficulties in directly comparing PFAS studies, the existence of positive correlations between PFAS exposure and abnormal sperm characteristics uphold the view that internalized PFAS do localize to the testis, along with other organs of the body, thereby forming a useful model to study PFAS-induced damage. However, it should be noted that using sperm parameters as a measure is quite a blunt tool and small changes are unlikely to be informative due to the wide variation seen between males and the low threshold for WHO defined parameters (142). Therefore, researchers should exercise caution when interpreting data on sperm parameter changes.

The impact of PFAS on a variety of additional reproductive characteristics has also been investigated, including dysregulation of reproductive hormone profiles (141, 143, 144). In one such study, significantly lower serum testosterone levels were detected in male mice following 21 days of high (10 mg/kg) PFOS administration *via* oral gavage, compared to untreated controls (145). This finding supports previous evidence from studies of adult male rats exposed to PFOA by gavage at a concentration of 25 mg/kg/day for 14 days (146) and of mice treated for 28 days with PFOA (147). In the latter study, a dose-responsive reduction in testosterone and progesterone levels in the testis was revealed. These animal data are commensurate with some human investigations, which have also attributed reduced testosterone levels in men to high PFOS (131) and PFOA (139) levels. Furthermore, Luteinizing hormone (LH) and sex hormone binding globulin (SHBG) levels have been reported to correlate with increasing plasma PFOA concentrations in adult males (132, 133). Additionally, increased LH and follicle-stimulating hormone (FSH) were detected in men who experienced prenatal exposure to PFOA (130), indicating that this developmental phase may be particularly sensitive to maternal PFAS exposure. However, several conflicting studies fail to show any associations between PFAS exposure and plasma reproductive hormone levels in males (testosterone, LH, FSH, SHBG and estradiol) (129, 148, 149). Further, Nian et al. revealed a negative trend with FSH and PFBS in cord blood from newborns exposed to PFAS during pregnancy (138). As an additional caveat, animal study evidence should be interpreted cautiously as information on PFAS effects and male fertility is often not at environmentally relevant concentrations due to the much shorter half-life and faster elimination rates seen in animals, which result in lower internal levels at doses equivalent to human exposures.

Mechanisms of PFAS Action on Reproductive Health

Testicular dysgenesis syndrome (TDS) is a term that encompasses a range of male reproductive disorders originating from fetal development (150) and which are

thought to be a consequence of environmental influences (150–152). Such issues share similarities with those attributed to PFAS exposure, such as undescended testes (cryptorchidism), fertility issues in adults, and testicular cancer (150, 151). Fetal development of the male reproductive system is sensitive to disturbance by environmental factors such as diethylstilbestrol, a synthetic estrogen prescribed to pregnant women in the mid-1900s (153) and cyclooxygenase inhibitors such as ibuprofen and paracetamol (154). An increased incidence of cryptorchidism has been identified in men exposed to these environmental toxicants *in utero*, with responses being particularly pronounced in those exposed during the critical programming windows of the first and second trimester (155, 156). Studies in rats have proposed the existence of male programming windows corresponding to weeks 8-14 of pregnancy in humans during which androgen-induced masculinization occurs, including programming of testes descent. Thus, environmental exposures encountered during this period have the potential to affect normal male reproductive development and reproductive hormone balance (156), suggesting a mechanism by which PFAS exposure during gestation may impact subsequent developmental events within the male reproductive system.

Endocrine disruptors are chemicals (both naturally occurring and synthetic) that interrupt the normal hormonal system of the body, either through direct hindrance of hormonal pathways or through mimicking the hormones within the endocrine system (157, 158). This can result in variable consequences such as dysregulation of immune, reproductive and developmental pathways (159–162). It follows that this diverse group of chemicals have been widely implicated in the development of reproductive abnormalities including TDS (150, 163–166). Indeed, the TDS hypothesis suggests that *in utero* exposure to endocrine disruptors damages testis development resulting in decreased function in adulthood, with symptoms ranging from moderately reduced semen quality through to the promulgation of testicular cancer (6, 167). PFAS display properties consistent with that expected of endocrine disruptors (1, 6, 168), and are widely reported as having endocrine disrupting actions (1, 6, 168–171). Accordingly, PFAS exposure often results in altered androgen and insulin-like factor 3 (INSL3) dependent processes (172–175) (**Figure 3**). There are two suggested mechanisms by which PFAS produce harmful endocrine effects: either by disturbing steroidogenesis (6) or by interfering with steroid hormone receptors (176, 177).

Specifically, at least some of the pathologies attributed to *in utero* PFAS exposure are hypothesized to arise due to abnormal Leydig cell development and/or function (6, 176). Leydig cells are a vital component of the male reproductive system responsible for synthesizing the steroid hormone testosterone, which is essential for sexual development and testis decedent in the fetal period (178), and the support of normal sperm production in the adult (179). Biegel et al. reported altered Leydig cell function *in vitro* with cells isolated from untreated rats, in which a dose-dependent decrease in testosterone was seen following a 5-hour treatment with PFOA (IC50 approximately 200 μM) (146). Additionally, *ex vivo* investigations with Leydig cells isolated from rats gavaged for 14 days with 25 mg/kg/day of PFOA showed these alterations are reversible following cessation of PFOA treatment (146). Such effects may be attributed to PFAS interfering with one, or more, of the enzymes involved in steroidogenesis. By way of example, PFAS may directly inhibit the catalytic activity of the 3β-hydroxysteroid dehydrogenase (HSD3B) enzyme by competing against its native pregnenolone substrate, thereby limiting the production of testosterone in rat Leydig cells (180). In humans, PFOS displays non-competitive inhibition of HSD17B3, another enzyme required for testosterone synthesis (176). Interference with steroid hormone receptors has also been documented, with the binding of PFAS leading to antagonism of androgen receptors (50), thereby blocking their activation by androgens, such as testosterone, in a dose-dependent manner (181). Other studies have reported a reduction in fetal Leydig cell number in male offspring exposed *in utero*, with mothers gavaged with 5 or 20 mg/kg of PFOS daily from gestational day 11 to 19 (182), which provides a tenable explanation for the reduction in testosterone levels seen in independent studies of rat models (146). Alternatively, elevated exposure to PFAS has been positively correlated with increased serum cholesterol in humans (1), which may lead to an increase in the production of steroid hormones. Of concern, the consequences of alterations resulting from prenatal PFAS exposure have the potential to be passed on to offspring through epigenetic transgenerational inheritance modalities (183) and may thus increase the susceptibility of future generations to disease, as demonstrated with other environmental factors (121, 184).

Further to this, at least two studies have shown that high PFOS exposure in adult men results in a higher proportion of morphologically abnormal sperm cells (35, 129). However, Vested et al. failed to identify any such association between PFOA exposure *in utero* and the proportion of morphologically normal spermatozoa (130). The authors did, however, report associations between PFOA exposure and total sperm count and concentration (130), which would suggest that the timing of exposure plays a part in the mechanism by which PFAS affects the fidelity of sperm production, that is; whether PFAS exposure gives rise to defects in sperm morphology or sperm count. This reasoning is plausible since sperm morphology and motility are primarily determined during sperm production and maturation in adulthood. In contrast, the capacity for sperm production is determined during the fetal period of sexual organ development (130). Furthermore, the relationship between sperm count/concentration and PFOA exposure suggests an effect on Sertoli cell development during the fetal period, as failure of Sertoli cell maturation and consequential inability to support spermatogenesis invariably results in lower rates of sperm cell production (185). This is supported by evidence demonstrating that *in vitro* PFAS exposure disturbs Sertoli cell function by altering the gap junction network with implications for the intracellular communication and cell-cell interactions (186–188) that are necessary for the support of spermatogenesis (189–192). Abnormal Sertoli cell development during the

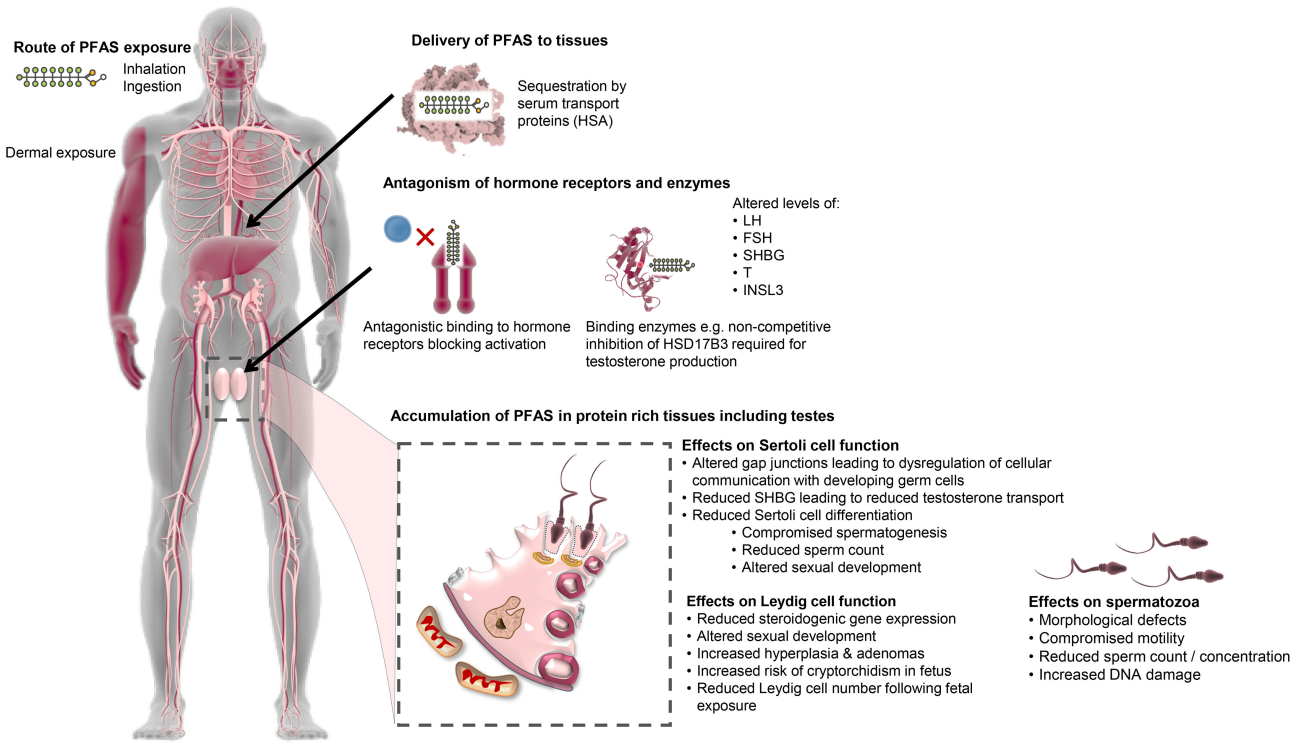

FIGURE 3 | Proposed mechanisms of PFAS action pertaining to the male reproductive system. PFAS have the potential to enter the body through multiple routes. Following entry, PFAS are capable of binding to fatty acid binding proteins and transport proteins in the blood such as human serum albumin (HSA) and thereafter are thought to be transported throughout the body eliciting harmful endocrine effects *via* two possible mechanisms: disturbing steroidogenesis (e.g. *via* allosteric inhibition of vital enzymes) or directly interfering with steroid hormone receptors. This results in altered levels of reproductive hormones such as luteinizing hormone (LH), follicle stimulating hormone (FSH), sex hormone binding globulin (SHBG), testosterone (T) and insulin-like peptide 3 (INSL3), which has subsequent effects on male reproductive processes. PFAS also accumulate in protein rich tissues, including the testes, which is facilitated by the high expression of fatty acid binding proteins. Here, PFAS impact testicular cell function, namely Leydig and Sertoli cells. Altered Leydig cell function leads to reduced testosterone production resulting in altered sexual development, increased incidence of hyperplasia and adenomas and increased risk of cryptorchidism in the fetus. This reduction in testosterone leads to attendant impacts on Sertoli cell function by reducing Sertoli cell differentiation and precipitating compromise of spermatogenesis, reduced sperm count and altered sexual development. Gap junctions between Sertoli cells and developing germ cells are also affected by PFAS, which reduces communication between the cells, negatively affecting spermatogenesis and resulting in a range of defects in the mature spermatozoa.

initial *in utero* stages of male reproductive tract development will also, in turn, impact Leydig cell function and subsequent masculinization events (193).

An *in vitro* study using a human stem cell model of spermatogenesis discovered a reduction in both spermatogonia and primary spermatocyte markers when cultures were treated with a mixture of PFOA, PFOS, and PFNA at levels consistent with general population exposure and occupationally exposed individuals, suggesting a potential long-term effect on fertility through exhausting the spermatogonial stem cell pool, rather than directly affecting cell viability (194). In agreement with this notion, an *in vivo* study in mice revealed a reduction in sperm count and testicular weight upon treatment with PFOS over five weeks (195), while in a zebrafish study the gonadal structure of juvenile males was altered by a 5-month treatment period with PFOS, ultimately resulting in fewer spermatogonia (196). Such results have been attributed to a combination of increased apoptosis and reduced proliferation of germ cells (195). However, the effects of PFAS exposure on the reproductive system differ depending on the specific PFAS and the toxicokinetics of the species studied (197). For example, PFOA mainly accumulates in the plasma and liver of rats, with the half-life in female rats at 1 day being much shorter than in males at 15 days (106). By comparison, high PFOS accumulation has been detected in the liver and lungs of humans (20, 198), with no differences in elimination between genders (12). Another mechanism by which PFAS mediated testicular issues may arise is through the binding of fatty acid binding-proteins (FABP), a family of proteins that bind fatty acids to enhance their solubility, and to aid in both the intracellular and extracellular transport of fatty acids (199). The most common FABP is albumin, which binds and transports fatty acids within the plasma and interstitial fluid (200, 201). There are distinct types of FABP, with each type exhibiting certain tissue distribution patterns and named accordingly (202). For example, mammalian testicular cells express high levels of the *Fabp9* gene (also known as testes FABP) (202), and *Fabp12* gene expression has been detected in adult rat testis (203). Due to the

distinct distribution and expression patterns of FABP encoding loci, it is suggested they may play a role in cell proliferation and differentiation (199, 204), specifically spermatogenesis in the testes (203). Therefore, the testes are a vulnerable organ for PFAS-mediated damage, owing to their abundant expression of FABPs that have a propensity to bind the perfluoroalkyl chains and lead to sequestration of PFAS.

REMEDIATION OF ENVIRONMENTAL PFAS CONTAMINATION

Extensive worldwide use of PFAS has led to pervasive contamination of land and water, which demand remediation if we are to have any prospect of combating the adverse health outcomes attributed to these chemicals, both in humans and wildlife. Environmental matrices that require targeting for remediation include groundwater, drinking and surface water, as well as soil and sediments (66, 205). However, this diversity of substrates provides unique challenges considering that different PFAS do not all interact with different matrices in the same manner (206), nor do they behave like other environmental contaminants (207). It is thus imperative that chemical features specific to PFAS are taken into consideration when designing remediation strategies to ensure thorough and long-lasting removal is achieved. Similarly, the logistics of the treatment, accessibility, and safety measures need to be taken into consideration. Regrettably, options for PFAS remediation remain limited, with most current technologies having originally been developed for the removal of other contaminants (208). Thus, there is considerable scope for the development of novel technologies to facilitate PFAS remediation, perhaps even employing a combination of treatment processes tailored to the site and/or PFAS profile to achieve the most cost-effective and efficient treatment process for each site (209). Illustrated in **Figure 4** are three remediation strategies that can be employed for effective treatment of PFAS water contamination (210–216). A novel technique has been proposed that utilizes plant proteins for effective removal of PFAS water contamination, through the pump-and-treat method (217). Such proteins contain both charged and uncharged residues on their surface, which allows them to form bonds with ligands through electrostatic interactions and/or hydrophobic/hydrophilic interactions (218), providing a method by which they could potentially remove PFAS contamination from water. Previous studies have shown PFOS forms a strong salt bridge with HSA, resulting in a high adsorption ratio of 45:1 PFOS to HSA (219). Building on these observations, Turner et al. (217) investigated the sequestration efficacy of six plant protein isolates and found that hemp protein has the highest removal rate for total PFAS at 92.5%, along with soy and pea proteins (around 82%), which is comparable to the granular activated carbon technique (95%). This technique provides a means by which plant proteins could be employed to reduce PFAS contamination within the body and thus warrants further investigation.

REMOVING PFAS ACCUMULATION IN THE HUMAN BODY

Unlike other environmental toxicants, such as parabens (220), the body cannot metabolize or facilitate the rapid removal of PFAS. Thus far, there has been limited investigation into the possibility of sequestering PFAS chemicals to reduce bioaccumulation within contaminated individuals in order to mitigate negative health outcomes. However, the adaption of existing techniques developed for other environmental contaminants may provide opportunities by which to reduce PFAS accumulation. Unfortunately, most of these techniques are only newly recognized and as such are still at an early stage of research with inadequate evidence of efficacy (221).

One process investigated for detoxification in humans is the exploitation of the body's natural excretion through perspiration, with an assortment of toxicants shown to be excreted in this manner, such as metals (222), phthalates (223) and bisphenol A (224). Studies have reported that induced perspiration treatment in individuals with toxicant accumulation, specifically polychlorinated biphenyls (PCBs) compounds, results in a statistically significant reduction in body burden (225, 226). Although promising, based on the limited available evidence, it seems that PFAS may not be readily excreted through sweat (227). Conversely, shorter half-lives are observed in women, which are proposed to result from increased PFAS elimination through menstruation, pregnancy or lactation (1, 109, 228). Accordingly, studies have shown regular phlebotomy or blood donation can also increase the elimination of PFAS (229, 230). Lorber et al. showed males undergoing regular blood withdrawals had 40% lower PFHxS, PFOA and PFOS levels in comparison to males in the general population (231), and suggested a 9% reduction in circulating blood volume was required to achieve significant reductions in PFAS levels. Additionally, evidence shows that bile acid sequestrants, such as cholestyramine, bind to PFAS toxicants within the gastrointestinal tract, thus preventing enterohepatic recirculation and increasing excretion of cholesterol and PFAS (227, 232). One case study with a single individual with high PFAS contamination showed increased levels of PFAS in stool samples following treatment with cholestyramine, with serum levels subsequently reducing with continued treatment (227). Ducatman and colleagues recently substantiated this evidence by analyzing the C8 Health Project Data (43) in which they found a reduction in serum PFAS levels (especially PFOS from 19 to 1 ng/mL) in individuals reporting to take regular cholestyramine medication, although data on duration and medication dosage administered was not reported (233). Of course, additional investigations are required to further corroborate these findings, but thus far evidence from these studies implies that utilizing cholestyramine treatment may allow for enhanced toxicant elimination.

CONCLUSION

Increasing awareness of the potential health implications of PFAS and realization of the extent of environmental

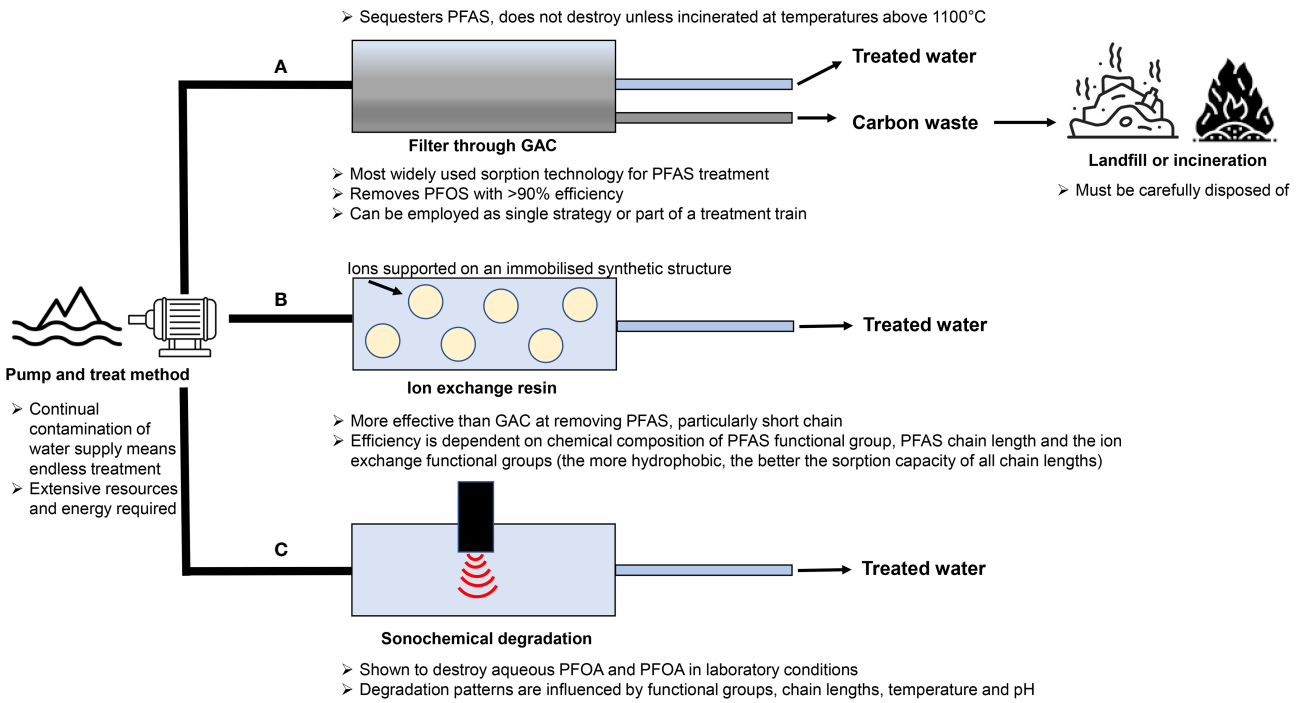

FIGURE 4 | Schematic diagram of three possible treatment mechanisms for PFAS contaminated water. **(A)** Carbon-rich sorbents such as granular activated carbon (GAC) have a long history of being utilised to remove a variety of organic contaminants from water and as such are by far the best studied and most widely used sorption technology for treating PFAS contaminated water sources (208). Granular activated carbon has been shown to reliably remove PFOS with over 90% efficiency (59, 210) and is thus now the reference point for comparison of all new PFAS water sorption technologies. This technology can be employed to treat water before it reaches consumers, either as a single strategy, or as part of an integrated treatment programme. This treatment often involves the pump and treat method in which groundwater is extracted and filtered (208, 211), with the sorbent then being disposed of in landfill sites, provided certain risk criteria are met and the chemicals remain sequestered. International conventions state that waste materials containing > 50 mg/kg of PFAS must be treated in such a way as to destroy these chemicals, which is often accomplished by incinerating at high temperatures (over 1100°C) (208, 212). **(B)** Ion exchange uses anion exchange to target a wider range of PFAS, allowing for more efficient removal. Removal occurs *via* electrostatic interactions between the charged functional groups of PFAS chemicals and ions supported on an immobilized synthetic structure (213). In comparison to activated carbon treatment, this method has been shown to be more effective in removing PFAS, particularly the short chain variants (205). However, the efficiency of ion exchange technologies is dependent on several factors, such as the chemical composition of PFAS functional group, PFAS chain length and the ion exchange functional groups (the more hydrophobic, the better the sorption capacity of all chain lengths) (213). The success of almost all remediation strategies employed has been shown to depend on the perfluoroalkyl chain length, with increased efficacy seen with smaller chain length (214). **(C)** However, simply removing PFAS from water does not destroy the chemical, hence why further processing or incineration is required, making removal techniques lengthy and potentially hazardous. Sonochemical degradation has been shown to destroy aqueous PFOA and PFOA in laboratory conditions (213), demonstrating sonic irradiation can be effectively employed to reduce PFAS contamination at environmentally relevant levels (215). The degradation patterns of PFAS chemicals are influenced by their functional groups and chain lengths as well as physical variables such as temperature and pH (216). Utilizing the method of groundwater pumping is seen as a potentially endless endeavor due to continual contamination from untreated water sources. This, in turn, raises questions as to whether the pump and treat method is sustainable in the long-term treatment of PFAS contamination due to extensive resources and energy required (208).

contamination has led to a rising demand for research into definitive health risks and effective remediation strategies. Animal models have been widely employed to investigate *in vitro* and *in vivo* consequences of PFAS exposure, as well as the toxicology of these chemicals. Such studies complement a growing body of evidence from human epidemiological studies. However, the literature abounds with conflicting evidence, and as such, it remains challenging to draw accurate conclusions regarding the causality of PFAS related health issues. This situation is exacerbated by the repeated demonstration that outcomes differ depending on factors such as the specific PFAS chemical(s) (of which there are over 4,700), stage of development (i.e., during fetal development or in later life) and duration of exposure, level and mix of contamination, route of exposure, and interaction with other environmental contaminants and toxicants, all of which are influenced by geographical location. These factors present significant difficulties for researchers in planning, executing, and interpreting studies, and thus hinder our ability to directly compare PFAS exposure studies. While standardization therefore remains an essential priority for future research, the identification of appropriate cellular model(s) with which to directly investigate and unlock the interaction of PFAS with the male reproductive system would also be advantageous. In addition, agreement is needed regarding endpoint measures, in which subtle changes, such as decreases in fertility or metabolic sequelae, may be used as early markers of PFAS-

mediated health effects, rather than more extreme factors such as tumors. In this regard, the male reproductive system offers notable advantages as a sensitive marker of human disease and may ultimately provide a unique opportunity for assessing the emerging threat to human health posed by PFAS exposure. Indeed, this model draws on a growing body of evidence of a strong association between a male's general health and reproductive potential, with infertility being strongly correlated with future health concerns such as testicular cancer, ischemic heart disease and diabetes.

FUTURE PERSPECTIVES

We contend that the identification of a reliable indicator of PFAS exposure would allow for the identification of reproductive health conditions resulting from PFAS bioaccumulation and aid in identifying, with certainty, the mechanisms by which PFAS impacts male reproductive health. Exploiting male reproductive function and sperm biology as a non-invasive means by which to investigate health outcomes is justified due to the responsiveness and sensitivity of the male reproductive system to environmental toxicants. Indeed, previous studies have employed this system as a marker to define the health effects of environmental factors such as acrylamide (234, 235), mobile phone radiation (236), and heat (237, 238). Additionally, the male reproductive system is known to be an early indicator for the onset of chronic diseases such as coronary and inflammatory diseases, making it a suitable indicator of general health. Strong associations have been seen between PFAS exposure and testicular dysfunction, indicating the male reproductive system is vulnerable to PFAS-mediated damage. In this context, perhaps the most suitable human cohorts to study are those that have received occupational PFAS exposure, such as firefighters, to determine the common effects of exposure and gain insight into possible mechanisms of action. It would then be pertinent to study individuals with idiopathic infertility to identify if any clear associations can be drawn between their diagnosis and PFAS levels, through assessment of detailed life history and daily routine/exposure information. These factors could then be used to screen for affected individuals within the general population. In addition to elucidating the toxicological effects of PFAS chemicals in humans, there is a need for data on a wider range of PFAS in order to regulate, legislate and ban those that are harmful, thus preventing further contamination from replacement PFAS, which may be just as harmful as the legacy variants.

AUTHOR CONTRIBUTIONS

LC conceived of the idea and wrote the first draft of the manuscript. MG, GI, MD, BT, BC, AE, SR and BN conceived of the idea, sourced funding, and edited the manuscript. All authors approved the final version of the manuscript.

FUNDING

This work was supported by funding from a National Health & Medical Research Council of Australia (NHMRC) Targeted Call for Research into Per- and Poly-Fluoroalkylated Substances (APP1189415) awarded to BN, MG, GI, MD, BT, BC, AE, and SR. BN is the recipitent of an NHMRC Senior Research Fellowship (APP1154837). MD is the recipient of an NHMRC Investigator Grant (APP1173892) and a Defeat DIPG ChadTough New Investigator Fellowship.

REFERENCES

1. Kirk M, Smurthwaite K, Bräunig J, Trevenar S, D'Este C, Lucas R, et al. *The PFAS Health Study: Systematic Literature Review*. Canberra: The Australian National University. (2018). p. 1–256.
2. OECD, Organisation for Economic Co-operation and Development. *Environment Directorate, Joint Meeting of the Chemicals Committee and the Working Party on Chemicals, Pesiticides and Biotechnology*. Paris: Organisation for Economic Co-operation and Development (2018).
3. Banks RE, Smart BE, Tatlow J. *Organofluorine Chemistry: Principles and Commercial Applications*. Birmingham: Springer Science & Business Media (1994).
4. Kissa E. *Fluorinated Surfactants and Repellents*. New York City: CRC Press (2001).
5. Buck RC, Franklin J, Berger U, Conder JM, Cousins IT, De Voogt P, et al. Perfluoroalkyl and Polyfluoroalkyl Substances in the Environment: Terminology, Classification, and Origins. *Integrated Environ Assess Manage* (2011) 7:513–41. doi: 10.1002/ieam.258
6. Jensen AA, Leffers H. Emerging Endocrine Disrupters: Perfluoroalkylated Substances. *Int J Androl* (2008) 31:161–9. doi: 10.1111/j.1365-2605.2008.00870.x
7. Lindstrom AB, Strynar MJ, Libelo EL. Polyfluorinated Compounds: Past, Present, and Future. *Environ Sci Technol* (2011) 45:7954–61. doi: 10.1021/es2011622
8. Renner R. Growing Concern Over Perfluorinated Chemicals. *Environ Sci Technol* (2001) 35:154a–60a. doi: 10.1021/es012317k
9. Olsen GW, Mair DC, Lange CC, Harrington LM, Church TR, Goldberg CL, et al. Per- and Polyfluoroalkyl Substances (PFAS) in American Red Cross Adult Blood Donors, 2000-2015. *Environ Res* (2017) 157:87–95. doi: 10.1016/j.envres.2017.05.013
10. Giesy JP, Kannan K. Global Distribution of Perfluorooctane Sulfonate in Wildlife. *Environ Sci Technol* (2001) 35:1339–42. doi: 10.1021/es001834k
11. Hölzer J, Midasch O, Rauchfuss K, Kraft M, Reupert R, Angerer J, et al. Biomonitoring of Perfluorinated Compounds in Children and Adults Exposed to Perfluorooctanoate-Contaminated Drinking Water. *Environ Health Perspect* (2008) 116:651–7. doi: 10.1289/ehp.11064
12. Fenton SE, Ducatman A, Boobis A, DeWitt JC, Lau C, Ng C, et al. Per- and Polyfluoroalkyl Substance Toxicity and Human Health Review: Current State of Knowledge and Strategies for Informing Future Research. *Environ Toxicol Chem* (2021) 40:606–30. doi: 10.1002/etc.4890
13. Olsen GW, Burris JM, Ehresman DJ, Froehlich JW, Seacat AM, Butenhoff JL, et al. Half-Life of Serum Elimination of Perfluorooctanesulfonate, Perfluorohexanesulfonate, and Perfluorooctanoate in Retired Fluorochemical Production Workers. *Environ Health Perspect* (2007) 115:1298–305. doi: 10.1289/ehp.10009
14. Martin JW, Mabury SA, Solomon KR, Muir DC. Dietary Accumulation of Perfluorinated Acids in Juvenile Rainbow Trout (Oncorhynchus Mykiss). *Environ Toxicol Chem* (2003) 22:189–95. doi: 10.1002/etc.5620220125

15. Conder JM, Hoke RA, De Wolf W, Russell MH, Buck RC. Are PFCAs Bioaccumulative? A Critical Review and Comparison With Regulatory Criteria and Persistent Lipophilic Compounds. *Environ Sci Technol* (2008) 42:995–1003. doi: 10.1021/es070895g
16. Gomis MI, Vestergren R, Borg D, Cousins IT. Comparing the Toxic Potency *In Vivo* of Long-Chain Perfluoroalkyl Acids and Fluorinated Alternatives. *Environ Int* (2018) 113:1–9. doi: 10.1016/j.envint.2018.01.011
17. Chambers WS, Hopkins JG, Richards SM. A Review of Per- and Polyfluorinated Alkyl Substance Impairment of Reproduction. *Front Toxicol* (2021) 3. doi: 10.3389/ftox.2021.732436
18. Martin JW, Mabury SA, Solomon KR, Muir DC. Bioconcentration and Tissue Distribution of Perfluorinated Acids in Rainbow Trout (Oncorhynchus Mykiss). *Environ Toxicol Chem* (2003) 22:196–204. doi: 10.1002/etc.5620220126
19. Lau C. Perfluorinated Compounds. *Exp Suppl* (2012) 101:47–86. doi: 10.1007/978-3-7643-8340-4_3
20. Pérez F, Nadal M, Navarro-Ortega A, Fàbrega F, Domingo JL, Barceló D, et al. Accumulation of Perfluoroalkyl Substances in Human Tissues. *Environ Int* (2013) 59:354–62. doi: 10.1016/j.envint.2013.06.004
21. Calafat AM, Wong LY, Kuklenyik Z, Reidy JA, Needham LL. Polyfluoroalkyl Chemicals in the U.S. Population: Data From the National Health and Nutrition Examination Survey (NHANES) 2003-2004 and Comparisons With NHANES 1999-2000. *Environ Health Perspect* (2007) 115:1596–602. doi: 10.1289/ehp.10598
22. Jian J-M, Chen D, Han F-J, Guo Y, Zeng L, Lu X, et al. A Short Review on Human Exposure to and Tissue Distribution of Per- and Polyfluoroalkyl Substances (PFASs). *Sci Total Environ* (2018) 636:1058–69. doi: 10.1016/j.scitotenv.2018.04.380
23. Jain RB, Ducatman A. Perfluoroalkyl Acids Serum Concentrations and Their Relationship to Biomarkers of Renal Failure: Serum and Urine Albumin, Creatinine, and Albumin Creatinine Ratios Across the Spectrum of Glomerular Function Among US Adults. *Environ Res* (2019) 174:143–51. doi: 10.1016/j.envres.2019.04.034
24. Kannan K, Corsolini S, Falandysz J, Fillmann G, Kumar KS, Loganathan BG, et al. Perfluorooctanesulfonate and Related Fluorochemicals in Human Blood From Several Countries. *Environ Sci Technol* (2004) 38:4489–95. doi: 10.1021/es0493446
25. Lau C, Butenhoff JL, Rogers JM. The Developmental Toxicity of Perfluoroalkyl Acids and Their Derivatives. *Toxicol Appl Pharmacol* (2004) 198:231–41. doi: 10.1016/j.taap.2003.11.031
26. Tittlemier SA, Pepper K, Edwards L. Concentrations of Perfluorooctanesulfonamides in Canadian Total Diet Study Composite Food Samples Collected Between 1992 and 2004. *J Agric Food Chem* (2006) 54:8385–9. doi: 10.1021/jf061713p
27. Tittlemier SA, Pepper K, Seymour C, Moisey J, Bronson R, Cao XL, et al. Dietary Exposure of Canadians to Perfluorinated Carboxylates and Perfluorooctane Sulfonate *via* Consumption of Meat, Fish, Fast Foods, and Food Items Prepared in Their Packaging. *J Agric Food Chem* (2007) 55:3203–10. doi: 10.1021/jf0634045
28. Haug LS, Huber S, Becher G, Thomsen C. Characterisation of Human Exposure Pathways to Perfluorinated Compounds–Comparing Exposure Estimates With Biomarkers of Exposure. *Environ Int* (2011) 37:687–93. doi: 10.1016/j.envint.2011.01.011
29. Vestergren R, Cousins IT. Tracking the Pathways of Human Exposure to Perfluorocarboxylates. *Environ Sci Technol* (2009) 43:5565–75. doi: 10.1021/es900228k
30. Shoeib M, Harner T, Webster MG, Lee SC. Indoor Sources of Poly- and Perfluorinated Compounds (PFCS) in Vancouver, Canada: Implications for Human Exposure. *Environ Sci Technol* (2011) 45:7999–8005. doi: 10.1021/es103562v
31. Emmett EA, Shofer FS, Zhang H, Freeman D, Desai C, Shaw LM. Community Exposure to Perfluorooctanoate: Relationships Between Serum Concentrations and Exposure Sources. *J Occup Environ Med* (2006) 48:759–70. doi: 10.1097/01.jom.0000232486.07658.74
32. Sinclair GM, Long SM, Jones OAH. What are the Effects of PFAS Exposure at Environmentally Relevant Concentrations? *Chemosphere* (2020) 258:127340. doi: 10.1016/j.chemosphere.2020.127340
33. Göckener B, Weber T, Rüdel H, Bücking M, Kolossa-Gehring M. Human Biomonitoring of Per- and Polyfluoroalkyl Substances in German Blood Plasma Samples From 1982 to 2019. *Environ Int* (2020) 145:106123. doi: 10.1016/j.envint.2020.106123
34. Fromme H, Tittlemier SA, Völkel W, Wilhelm M, Twardella D. Perfluorinated Compounds–Exposure Assessment for the General Population in Western Countries. *Int J Hyg Environ Health* (2009) 212:239–70. doi: 10.1016/j.ijheh.2008.04.007
35. Toft G, Jönsson BAG, Lindh CH, Giwercman A, Spano M, Heederik D, et al. Exposure to Perfluorinated Compounds and Human Semen Quality in Arctic and European Populations. *Hum Reprod* (2012) 27:2532–40. doi: 10.1093/humrep/des185
36. Jensen TK, Jacobsen R, Christensen K, Nielsen NC, Bostofte E. Good Semen Quality and Life Expectancy: A Cohort Study of 43,277 Men. *Am J Epidemiol* (2009) 170:559–65. doi: 10.1093/aje/kwp168
37. Del Giudice F, Kasman AM, Ferro M, Sciarra A, De Berardinis E, Belladelli F, et al. Clinical Correlation Among Male Infertility and Overall Male Health: A Systematic Review of the Literature. *Investig Clin Urol* (2020) 61:355–71. doi: 10.4111/icu.2020.61.4.355
38. Kasman AM, Del Giudice F, Eisenberg ML. New Insights to Guide Patient Care: The Bidirectional Relationship Between Male Infertility and Male Health. *Fertil Steril* (2020) 113:469–77. doi: 10.1016/j.fertnstert.2020.01.002
39. Glazer CH, Eisenberg ML, Tøttenborg SS, Giwercman A, Flachs EM, Bräuner EV, et al. Male Factor Infertility and Risk of Death: A Nationwide Record-Linkage Study. *Hum Reprod* (2019) 34:2266–73. doi: 10.1093/humrep/dez189
40. Eisenberg ML, Li S, Cullen MR, Baker LC. Increased Risk of Incident Chronic Medical Conditions in Infertile Men: Analysis of United States Claims Data. *Fertil Steril* (2016) 105:629–36. doi: 10.1016/j.fertnstert.2015.11.011
41. Latif T, Lindahl-Jacobsen R, Mehlsen J, Eisenberg ML, Holmboe SA, Pors K, et al. Semen Quality Associated With Subsequent Hospitalizations – Can the Effect be Explained by Socio-Economic Status and Lifestyle Factors? *Andrology* (2018) 6:428–35. doi: 10.1111/andr.12477
42. Eisenberg ML, Li S, Behr B, Cullen MR, Galusha D, Lamb DJ, et al. Semen Quality, Infertility and Mortality in the USA. *Hum Reprod* (2014) 29:1567–74. doi: 10.1093/humrep/deu106
43. Frisbee SJ, Brooks AP Jr, Maher A, Flensborg P, Arnold S, Fletcher T, et al. The C8 Health Project: Design, Methods, and Participants. *Environ Health Perspect* (2009) 117:1873–82. doi: 10.1289/ehp.0800379
44. Barry V, Winquist A, Steenland K. Perfluorooctanoic Acid (PFOA) Exposures and Incident Cancers Among Adults Living Near a Chemical Plant. *Environ Health Perspect* (2013) 121:1313–8. doi: 10.1289/ehp.1306615
45. Vieira VM, Hoffman K, Shin H-M, Weinberg JM, Webster TF, Fletcher T. Perfluorooctanoic Acid Exposure and Cancer Outcomes in a Contaminated Community: A Geographic Analysis. *Environ Health Perspect* (2013) 121:318–23. doi: 10.1289/ehp.1205829
46. Lin H-W, Feng H-X, Chen L, Yuan X-J, Tan Z. Maternal Exposure to Environmental Endocrine Disruptors During Pregnancy is Associated With Pediatric Germ Cell Tumors. *Nagoya J Med Sci* (2020) 82:323–33. doi: 10.18999/nagjms.82.2.323
47. Bartell SM, Vieira VM. Critical Review on PFOA, Kidney Cancer, and Testicular Cancer. *J Air Waste Manage Assoc* (2021) 71:663–79. doi: 10.1080/10962247.2021.1909668
48. IARC. *International Agency for Research on Cancer, IARC, Monograph, Perfluorooctanoic Acid*. Lyon: International Agency for Research on Cancer (2018).
49. Louis GM, Chen Z, Schisterman EF, Kim S, Sweeney AM, Sundaram R, et al. Perfluorochemicals and Human Semen Quality: The LIFE Study. *Environ Health Perspect* (2015) 123:57–63. doi: 10.1289/ehp.1307621
50. Di Nisio A, Sabovic I, Valente U, Tescari S, Rocca MS, Guidolin D, et al. Endocrine Disruption of Androgenic Activity by Perfluoroalkyl Substances: Clinical and Experimental Evidence. *J Clin Endocrinol Metab* (2019) 104:1259–71. doi: 10.1210/jc.2018-01855
51. Blake BE, Fenton SE. Early Life Exposure to Per- and Polyfluoroalkyl Substances (PFAS) and Latent Health Outcomes: A Review Including the Placenta as a Target Tissue and Possible Driver of Peri- and Postnatal Effects. *Toxicology* (2020) 443:152565. doi: 10.1016/j.tox.2020.152565

52. Brendel S, Fetter É, Staude C, Vierke L, Biegel-Engler A. Short-Chain Perfluoroalkyl Acids: Environmental Concerns and a Regulatory Strategy Under REACH. *Environ Sci Eur* (2018) 30:9. doi: 10.1186/s12302-018-0134-4
53. Vecitis CD, Wang Y, Cheng J, Park H, Mader BT, Hoffmann MR. Sonochemical Degradation of Perfluorooctanesulfonate in Aqueous Film-Forming Foams. *Environ Sci Technol* (2010) 44:432–8. doi: 10.1021/es902444r
54. Wang Z, DeWitt JC, Higgins CP, Cousins IT. A Never-Ending Story of Per- and Polyfluoroalkyl Substances (PFASs)? *Environ Sci Technol* (2017) 51:2508–18. doi: 10.1021/acs.est.6b04806
55. Olsen GW, Burris JM, Burlew MM, Mandel JH. Epidemiologic Assessment of Worker Serum Perfluorooctanesulfonate (PFOS) and Perfluorooctanoate (PFOA) Concentrations and Medical Surveillance Examinations. *J Occup Environ Med* (2003) 45:260–70. doi: 10.1097/01.jom.0000052958.59271.10
56. Hu XC, Andrews DQ, Lindstrom AB, Bruton TA, Schaider LA, Grandjean P, et al. Detection of Poly- and Perfluoroalkyl Substances (PFASs) in U.S. Drinking Water Linked to Industrial Sites, Military Fire Training Areas, and Wastewater Treatment Plants. *Environ Sci Technol Lett* (2016) 3:344–50. doi: 10.1021/acs.estlett.6b00260
57. Tanner EM, Bloom MS, Wu Q, Kannan K, Yucel RM, Shrestha S, et al. Occupational Exposure to Perfluoroalkyl Substances and Serum Levels of Perfluorooctanesulfonic Acid (PFOS) and Perfluorooctanoic Acid (PFOA) in an Aging Population From Upstate New York: A Retrospective Cohort Study. *Int Arch Occup Environ Health* (2018) 91:145–54. doi: 10.1007/s00420-017-1267-2
58. Rotander A, Kärrman A, Toms LM, Kay M, Mueller JF, Gómez Ramos MJ. Novel Fluorinated Surfactants Tentatively Identified in Firefighters Using Liquid Chromatography Quadrupole Time-of-Flight Tandem Mass Spectrometry and a Case-Control Approach. *Environ Sci Technol* (2015) 49:2434–42. doi: 10.1021/es503653n
59. Eschauzier C, Beerendonk E, Scholte-Veenendaal P, De Voogt P. Impact of Treatment Processes on the Removal of Perfluoroalkyl Acids From the Drinking Water Production Chain. *Environ Sci Technol* (2012) 46:1708–15. doi: 10.1021/es201662b
60. Ericson I, Nadal M, van Bavel B, Lindström G, Domingo JL. Levels of Perfluorochemicals in Water Samples From Catalonia, Spain: Is Drinking Water a Significant Contribution to Human Exposure? *Environ Sci Pollut Res Int* (2008) 15:614–9. doi: 10.1007/s11356-008-0040-1
61. Björklund JA, Thuresson K, De Wit CA. Perfluoroalkyl Compounds (PFCs) in Indoor Dust: Concentrations, Human Exposure Estimates, and Sources. *Environ Sci Technol* (2009) 43:2276–81. doi: 10.1021/es803201a
62. Sunderland EM, Hu XC, Dassuncao C, Tokranov AK, Wagner CC, Allen JG. A Review of the Pathways of Human Exposure to Poly- and Perfluoroalkyl Substances (PFASs) and Present Understanding of Health Effects. *J Expo Sci Environ Epidemiol* (2019) 29:131–47. doi: 10.1038/s41370-018-0094-1
63. Begley TH, Hsu W, Noonan G, Diachenko G. Migration of Fluorochemical Paper Additives From Food-Contact Paper Into Foods and Food Simulants. *Food Addit Contam Part A Chem Anal Control Expo Risk Assess* (2008) 25:384–90. doi: 10.1080/02652030701513784
64. Johnson PI, Sutton P, Atchley DS, Koustas E, Lam J, Sen S, et al. The Navigation Guide - Evidence-Based Medicine Meets Environmental Health: Systematic Review of Human Evidence for PFOA Effects on Fetal Growth. *Environ Health Perspect* (2014) 122:1028–39. doi: 10.1289/ehp.1307893
65. Apelberg BJ, Witter FR, Herbstman JB, Calafat AM, Halden RU, Needham LL, et al. Cord Serum Concentrations of Perfluorooctane Sulfonate (PFOS) and Perfluorooctanoate (PFOA) in Relation to Weight and Size at Birth. *Environ Health Perspect* (2007) 115:1670–6. doi: 10.1289/ehp.10334
66. ATSDR. *Toxicological Profile for Perfluoroalkyls: Draft for Public Comment, Agency for Toxic Substances and Disease Registry*. Atlanta: Agency for Toxic Substances and Disease Registry (2018).
67. Tao L, Ma J, Kunisue T, Libelo EL, Tanabe S, Kannan K. Perfluorinated Compounds in Human Breast Milk From Several Asian Countries, and in Infant Formula and Dairy Milk From the United States. *Environ Sci Technol* (2008) 42:8597–602. doi: 10.1021/es801875v
68. Hinderliter PM, DeLorme MP, Kennedy GL. Perfluorooctanoic Acid: Relationship Between Repeated Inhalation Exposures and Plasma PFOA Concentration in the Rat. *Toxicology* (2006) 222:80–5. doi: 10.1016/j.tox.2006.01.029
69. Franko J, Meade BJ, Frasch HF, Barbero AM, Anderson SE. Dermal Penetration Potential of Perfluorooctanoic Acid (PFOA) in Human and Mouse Skin. *J Toxicol Environ Health A* (2012) 75:50–62. doi: 10.1080/15287394.2011.615108
70. Han X, Snow TA, Kemper RA, Jepson GW. Binding of Perfluorooctanoic Acid to Rat and Human Plasma Proteins. *Chem Res Toxicol* (2003) 16:775–81. doi: 10.1021/tx034005w
71. Jones PD, Hu W, De Coen W, Newsted JL, Giesy JP. Binding of Perfluorinated Fatty Acids to Serum Proteins. *Environ Toxicol Chem* (2003) 22:2639–49. doi: 10.1897/02-553
72. Beesoon S, Martin JW. Isomer-Specific Binding Affinity of Perfluorooctanesulfonate (PFOS) and Perfluorooctanoate (PFOA) to Serum Proteins. *Environ Sci Technol* (2015) 49:5722–31. doi: 10.1021/es505399w
73. Bogdanska J, Borg D, Sundström M, Bergström U, Halldin K, Abedi-Valugerdi M, et al. Tissue Distribution of ^{35}S-Labelled Perfluorooctane Sulfonate in Adult Mice After Oral Exposure to a Low Environmentally Relevant Dose or a High Experimental Dose. *Toxicology* (2011) 284:54–62. doi: 10.1016/j.tox.2011.03.014
74. Kudo N, Sakai A, Mitsumoto A, Hibino Y, Tsuda T, Kawashima Y. Tissue Distribution and Hepatic Subcellular Distribution of Perfluorooctanoic Acid at Low Dose are Different From Those at High Dose in Rats. *Biol Pharm Bull* (2007) 30:1535–40. doi: 10.1248/bpb.30.1535
75. Cui L, Liao CY, Zhou QF, Xia TM, Yun ZJ, Jiang GB. Excretion of PFOA and PFOS in Male Rats During a Subchronic Exposure. *Arch Environ Contam Toxicol* (2010) 58:205–13. doi: 10.1007/s00244-009-9336-5
76. Prevedouros K, Cousins IT, Buck RC, Korzeniowski SH. Sources, Fate and Transport of Perfluorocarboxylates. *Environ Sci Technol* (2006) 40:32–44. doi: 10.1021/es0512475
77. De Silva AO, Mabury SA. Isolating Isomers of Perfluorocarboxylates in Polar Bears (Ursus Maritimus) From Two Geographical Locations. *Environ Sci Technol* (2004) 38:6538–45. doi: 10.1021/es049296p
78. Song X, Tang S, Zhu H, Chen Z, Zang Z, Zhang Y, et al. Biomonitoring PFAAs in Blood and Semen Samples: Investigation of a Potential Link Between PFAAs Exposure and Semen Mobility in China. *Environ Int* (2018) 113:50–4. doi: 10.1016/j.envint.2018.01.010
79. Wang Z, Cousins IT, Scheringer M, Hungerbühler K. Fluorinated Alternatives to Long-Chain Perfluoroalkyl Carboxylic Acids (PFCAs), Perfluoroalkane Sulfonic Acids (PFSAs) and Their Potential Precursors. *Environ Int* (2013) 60:242–8. doi: 10.1016/j.envint.2013.08.021
80. SCHEER, Scientific Committee on Health. *Environmental and Emerging Risks, Statement on Emerging Health and Environmental Issues*, Vol. 2018. Luxembourg City: Scientific Committee on Health, Environmental and Emerging Risks (2018).
81. Tarapore P, Ouyang B. Perfluoroalkyl Chemicals and Male Reproductive Health: Do PFOA and PFOS Increase Risk for Male Infertility? *Int J Environ Res Public Health* (2021) 18:3794. doi: 10.3390/ijerph18073794
82. Rand AA, Mabury SA. Is There a Human Health Risk Associated With Indirect Exposure to Perfluoroalkyl Carboxylates (PFCAs)? *Toxicology* (2017) 375:28–36. doi: 10.1016/j.tox.2016.11.011
83. Dagnino S, Strynar MJ, McMahen RL, Lau CS, Ball C, Garantziotis S, et al. Identification of Biomarkers of Exposure to FTOHs and PAPs in Humans Using a Targeted and Nontargeted Analysis Approach. *Environ Sci Technol* (2016) 50:10216–25. doi: 10.1021/acs.est.6b01170
84. N.T.P. *(NTP), National Toxicology Program Monograph on Immunotoxicity Associated With Exposures to Pfoa and Pfos*. Durham, North Carolina: National Toxicology Program (2016).
85. Benbrahim-Tallaa L, Lauby-Secretan B, Loomis D, Guyton KZ, Grosse Y, El Ghissassi F, et al. Carcinogenicity of Perfluorooctanoic Acid, Tetrafluoroethylene, Dichloromethane, 1,2-Dichloropropane, and 1,3-Propane Sultone. *Lancet Oncol* (2014) 15:924–5. doi: 10.1016/S1470-2045(14)70316-X
86. Olsen GW, Ley CA. Prostate Cancer and PFOA. *J Occup Environ Med* (2015) 57:e60. doi: 10.1097/JOM.0000000000000446
87. Gilliland FD, Mandel JS. Mortality Among Employees of a Perfluorooctanoic Acid Production Plant. *J Occup Med* (1993) 35:950–4. doi: 10.1097/00043764-199309000-00020
88. Mastrantonio M, Bai E, Uccelli R, Cordiano V, Screpanti A, Crosignani P. Drinking Water Contamination From Perfluoroalkyl Substances (PFAS): An

Ecological Mortality Study in the Veneto Region, Italy. *Eur J Public Health* (2017) 28:180–5. doi: 10.1093/eurpub/ckx066
89. Frisbee SJ, Shankar A, Knox SS, Steenland K, Savitz DA, Fletcher T, et al. Perfluorooctanoic Acid, Perfluorooctanesulfonate, and Serum Lipids in Children and Adolescents: Results From the C8 Health Project. *Arch Pediatr Adolesc Med* (2010) 164:860–9. doi: 10.1001/archpediatrics.2010.163
90. Sakr CJ, Kreckmann KH, Green JW, Gillies PJ, Reynolds JL, Leonard RC. Cross-Sectional Study of Lipids and Liver Enzymes Related to a Serum Biomarker of Exposure (Ammonium Perfluorooctanoate or APFO) as Part of a General Health Survey in a Cohort of Occupationally Exposed Workers. *J Occup Environ Med* (2007) 49:1086–96. doi: 10.1097/JOM.0b013e318156eca3
91. Steenland K, Tinker S, Frisbee S, Ducatman A, Vaccarino V. Association of Perfluorooctanoic Acid and Perfluorooctane Sulfonate With Serum Lipids Among Adults Living Near a Chemical Plant. *Am J Epidemiol* (2009) 170:1268–78. doi: 10.1093/aje/kwp279
92. Olsen GW, Zobel LR. Assessment of Lipid, Hepatic, and Thyroid Parameters With Serum Perfluorooctanoate (PFOA) Concentrations in Fluorochemical Production Workers. *Int Arch Occup Environ Health* (2007) 81:231–46. doi: 10.1007/s00420-007-0213-0
93. Sakr CJ, Leonard RC, Kreckmann KH, Slade MD, Cullen MR. Longitudinal Study of Serum Lipids and Liver Enzymes in Workers With Occupational Exposure to Ammonium Perfluorooctanoate. *J Occup Environ Med* (2007) 49:872–9. doi: 10.1097/JOM.0b013e318124a93f
94. Costa G, Sartori S, Consonni D. Thirty Years of Medical Surveillance in Perfluorooctanoic Acid Production Workers. *J Occup Environ Med* (2009) 51:364–72. doi: 10.1097/JOM.0b013e3181965d80
95. EPA. *EPA Advances Science to Protect the Public From PFOA and PFOS in Drinking Water, EPA*. Washington, DC: Environmental Protection Agency (2021).
96. Steenland K, Woskie S. Cohort Mortality Study of Workers Exposed to Perfluorooctanoic Acid. *Am J Epidemiol* (2012) 176:909–17. doi: 10.1093/aje/kws171
97. Leonard RC, Kreckmann KH, Sakr CJ, Symons JM. Retrospective Cohort Mortality Study of Workers in a Polymer Production Plant Including a Reference Population of Regional Workers. *Ann Epidemiol* (2008) 18:15–22. doi: 10.1016/j.annepidem.2007.06.011
98. McIver SC, Roman SD, Nixon B, Loveland KL, McLaughlin EA. The Rise of Testicular Germ Cell Tumours: The Search for Causes, Risk Factors and Novel Therapeutic Targets. *F1000Research* (2013) 2:55. doi: 10.12688/f1000research.2-55.v1
99. Baade P, Carrière P, Fritschi L. Trends in Testicular Germ Cell Cancer Incidence in Australia. *Cancer Causes Cont* (2008) 19:1043–9. doi: 10.1007/s10552-008-9168-z
100. Skakkebaek NE, Rajpert-De Meyts E, Jørgensen N, Main KM, Leffers H, Andersson AM, et al. Testicular Cancer Trends as 'Whistle Blowers' of Testicular Developmental Problems in Populations. *Int J Androl* (2007) 30:198–204; discussion 204-5. doi: 10.1111/j.1365-2605.2007.00776.x
101. Walschaerts M, Huyghe E, Muller A, Bachaud JM, Bujan L, Thonneau P. Doubling of Testicular Cancer Incidence Rate Over the Last 20 Years in Southern France. *Cancer Causes Cont* (2008) 19:155–61. doi: 10.1007/s10552-007-9081-x
102. Richiardi L, Pettersson A, Akre O. Genetic and Environmental Risk Factors for Testicular Cancer. *Int J Androl* (2007) 30:230–40; discussion 240-1. doi: 10.1111/j.1365-2605.2007.00760.x
103. Post GB, Cohn PD, Cooper KR. Perfluorooctanoic Acid (PFOA), an Emerging Drinking Water Contaminant: A Critical Review of Recent Literature. *Environ Res* (2012) 116:93–117. doi: 10.1016/j.envres.2012.03.007
104. Lau C, Anitole K, Hodes C, Lai D, Pfahles-Hutchens A, Seed J. Perfluoroalkyl Acids: A Review of Monitoring and Toxicological Findings. *Toxicol Sci* (2007) 99:366–94. doi: 10.1093/toxsci/kfm128
105. OECD, Organisation for Economic Co-operation and Development. *Co-Operation on Existing Chemicals. Hazard Assessment of Perfluorooctane Sulfonate (PFOS) and its Salts*. Paris: Organisation for Economic Co-operation and Development (2002).
106. Vanden Heuvel JP, Kuslikis BI, Van Rafelghem MJ, Peterson RE, distribution T. Metabolism, and Elimination of Perfluorooctanoic Acid in Male and Female Rats. *J Biochem Toxicol* (1991) 6:83–92. doi: 10.1002/jbt.2570060202
107. Hanhijärvi H, Ophaug RH, Singer L. The Sex-Related Difference in Perfluorooctanoate Excretion in the Rat. *Proc Soc Exp Biol Med* (1982) 171:50–5. doi: 10.3181/00379727-171-41476
108. Li Y, Fletcher T, Mucs D, Scott K, Lindh CH, Tallving P, et al. Half-Lives of PFOS, PFHxS and PFOA After End of Exposure to Contaminated Drinking Water. *Occup Environ Med* (2018) 75:46–51. doi: 10.1136/oemed-2017-104651
109. Zhang Y, Beesoon S, Zhu L, Martin JW. Biomonitoring of Perfluoroalkyl Acids in Human Urine and Estimates of Biological Half-Life. *Environ Sci Technol* (2013) 47:10619–27. doi: 10.1021/es401905e
110. Barker DJ. The Developmental Origins of Chronic Adult Disease. *Acta Paediatr Suppl* (2004) 93:26–33. doi: 10.1111/j.1651-2227.2004.tb00236.x
111. Ubel FA, Sorenson SD, Roach DE. Health Status of Plant Workers Exposed to Fluorochemicals–a Preliminary Report. *Am Ind Hyg Assoc J* (1980) 41:584–9. doi: 10.1080/15298668091425310
112. Scheringer M, Trier X, Cousins IT, de Voogt P, Fletcher T, Wang Z, et al. Helsingør Statement on Poly- and Perfluorinated Alkyl Substances (PFASs). *Chemosphere* (2014) 114:337–9. doi: 10.1016/j.chemosphere.2014.05.044
113. Blum A, Balan SA, Scheringer M, Trier X, Goldenman G, Cousins IT, et al. The Madrid Statement on Poly- and Perfluoroalkyl Substances (PFASs). *Environ Health Perspect* (2015) 123:A107–11. doi: 10.1289/ehp.1509934
114. Coggan TL, Anumol T, Pyke J, Shimeta J, Clarke BO. A Single Analytical Method for the Determination of 53 Legacy and Emerging Per- and Polyfluoroalkyl Substances (PFAS) in Aqueous Matrices. *Anal Bioanal Chem* (2019) 411:3507–20. doi: 10.1007/s00216-019-01829-8
115. Krzastek SC, Farhi J, Gray M, Smith RP. Impact of Environmental Toxin Exposure on Male Fertility Potential. *Transl Androl Urol* (2020) 9:2797–813. doi: 10.21037/tau-20-685
116. Glazer CH, Bonde JP, Eisenberg ML, Giwercman A, Hærvig KK, Rimborg S, et al. Male Infertility and Risk of Nonmalignant Chronic Diseases: A Systematic Review of the Epidemiological Evidence. *Semin Reprod Med* (2017) 35:282–90. doi: 10.1055/s-0037-1603568
117. Eisenberg ML, Li S, Behr B, Pera RR, Cullen MR. Relationship Between Semen Production and Medical Comorbidity. *Fertil Steril* (2015) 103:66–71. doi: 10.1016/j.fertnstert.2014.10.017
118. Hanson HA, Anderson RE, Aston KI, Carrell DT, Smith KR, Hotaling JM. Subfertility Increases Risk of Testicular Cancer: Evidence From Population-Based Semen Samples. *Fertil Steril* (2016) 105:322–8.e1. doi: 10.1016/j.fertnstert.2015.10.027
119. Walsh TJ, Croughan MS, Schembri M, Chan JM, Turek PJ. Increased Risk of Testicular Germ Cell Cancer Among Infertile Men. *Arch Intern Med* (2009) 169:351–6. doi: 10.1001/archinternmed.2008.562
120. Møller H, Skakkebaek NE. Risk of Testicular Cancer in Subfertile Men: Case-Control Study. *BMJ* (1999) 318:559–62. doi: 10.1136/bmj.318.7183.559
121. Xavier MJ, Roman SD, Aitken RJ, Nixon B. Transgenerational Inheritance: How Impacts to the Epigenetic and Genetic Information of Parents Affect Offspring Health. *Hum Reprod Update* (2019) 25:519–41. doi: 10.1093/humupd/dmz017
122. Bonde JP, Flachs EM, Rimborg S, Glazer CH, Giwercman A, Ramlau-Hansen CH, et al. The Epidemiologic Evidence Linking Prenatal and Postnatal Exposure to Endocrine Disrupting Chemicals With Male Reproductive Disorders: A Systematic Review and Meta-Analysis. *Hum Reprod Update* (2016) 23:104–25. doi: 10.1093/humupd/dmw036
123. Araujo AB, Dixon JM, Suarez EA, Murad MH, Guey LT, Wittert GA. Clinical Review: Endogenous Testosterone and Mortality in Men: A Systematic Review and Meta-Analysis. *J Clin Endocrinol Metab* (2011) 96:3007–19. doi: 10.1210/jc.2011-1137
124. Yeap BB, Alfonso H, Chubb SA, Handelsman DJ, Hankey GJ, Almeida OP, et al. In Older Men an Optimal Plasma Testosterone is Associated With Reduced All-Cause Mortality and Higher Dihydrotestosterone With Reduced Ischemic Heart Disease Mortality, While Estradiol Levels do Not Predict Mortality. *J Clin Endocrinol Metab* (2014) 99:E9–18. doi: 10.1210/jc.2013-3272
125. Mehrpour O, Karrari P, Zamani N, Tsatsakis AM, Abdollahi M. Occupational Exposure to Pesticides and Consequences on Male Semen and Fertility: A Review. *Toxicol Lett* (2014) 230:146–56. doi: 10.1016/j.toxlet.2014.01.029
126. Nixon BJ, Stanger SJ, Nixon B, Roman SD. Chronic Exposure to Acrylamide Induces DNA Damage in Male Germ Cells of Mice. *Toxicol Sci* (2012) 129:135–45. doi: 10.1093/toxsci/kfs178

127. De Felice F, Marchetti C, Marampon F, Cascialli G, Muzii L, Tombolini V. Radiation Effects on Male Fertility. *Andrology* (2019) 7:2–7. doi: 10.1111/andr.12562
128. Bach CC, Vested A, Jørgensen KT, Bonde JP, Henriksen TB, Toft G. Perfluoroalkyl and Polyfluoroalkyl Substances and Measures of Human Fertility: A Systematic Review. *Crit Rev Toxicol* (2016) 46:735–55. doi: 10.1080/10408444.2016.1182117
129. Joensen UN, Bossi R, Leffers H, Jensen AA, Skakkebæk NE, Jørgensen N. Do Perfluoroalkyl Compounds Impair Human Semen Quality? *Environ Health Perspect* (2009) 117:923–7. doi: 10.1289/ehp.0800517
130. Vested A, Ramlau-Hansen CH, Olsen SF, Bonde JP, Kristensen SL, Halldorsson TI, et al. Associations of *In Utero* Exposure to Perfluorinated Alkyl Acids With Human Semen Quality and Reproductive Hormones in Adult Men. *Environ Health Perspect* (2013) 121:453–8. doi: 10.1289/ehp.1205118
131. Joensen UN, Veyrand B, Antignac JP, Blomberg Jensen M, Petersen JH, Marchand P, et al. PFOS (Perfluorooctanesulfonate) in Serum is Negatively Associated With Testosterone Levels, But Not With Semen Quality, in Healthy Men. *Hum Reprod* (2013) 28:599–608. doi: 10.1093/humrep/des425
132. Petersen MS, Halling J, Jørgensen N, Nielsen F, Grandjean P, Jensen TK, et al. Reproductive Function in a Population of Young Faroese Men With Elevated Exposure to Polychlorinated Biphenyls (PCBs) and Perfluorinated Alkylate Substances (PFAS). *Int J Environ Res Public Health* (2018) 15:1880. doi: 10.3390/ijerph15091880
133. Raymer JH, Michael LC, Studabaker WB, Olsen GW, Sloan CS, Wilcosky T, et al. Concentrations of Perfluorooctane Sulfonate (PFOS) and Perfluorooctanoate (PFOA) and Their Associations With Human Semen Quality Measurements. *Reprod Toxicol* (2012) 33:419–27. doi: 10.1016/j.reprotox.2011.05.024
134. Governini L, Guerranti C, De Leo V, Boschi L, Luddi A, Gori M, et al. Chromosomal Aneuploidies and DNA Fragmentation of Human Spermatozoa From Patients Exposed to Perfluorinated Compounds. *Andrologia* (2015) 47:1012–9. doi: 10.1111/and.12371
135. Specht IO, Hougaard KS, Spanò M, Bizzaro D, Manicardi GC, Lindh CH, et al. Sperm DNA Integrity in Relation to Exposure to Environmental Perfluoroalkyl Substances - A Study of Spouses of Pregnant Women in Three Geographical Regions. *Reprod Toxicol* (2012) 33:577–83. doi: 10.1016/j.reprotox.2012.02.008
136. Emerce E, Çetin Ö. Genotoxicity Assessment of Perfluoroalkyl Substances on Human Sperm. *Toxicol Ind Health* (2018) 34:884–90. doi: 10.1177/0748233718799191
137. Leter G, Consales C, Eleuteri P, Uccelli R, Specht IO, Toft G, et al. Exposure to Perfluoroalkyl Substances and Sperm DNA Global Methylation in Arctic and European Populations. *Environ Mol Mutagen* (2014) 55:591–600. doi: 10.1002/em.21874
138. Nian M, Luo K, Luo F, Aimuzi R, Huo X, Chen Q, et al. Association Between Prenatal Exposure to PFAS and Fetal Sex Hormones: Are the Short-Chain PFAS Safer? *Environ Sci Technol* (2020) 54:8291–9. doi: 10.1021/acs.est.0c02444
139. Cui Q, Pan Y, Wang J, Liu H, Yao B, Dai J. Exposure to Per- and Polyfluoroalkyl Substances (PFASs) in Serum Versus Semen and Their Association With Male Reproductive Hormones. *Environ Pollut* (2020) 266:115330. doi: 10.1016/j.envpol.2020.115330
140. Pan Y, Cui Q, Wang J, Sheng N, Jing J, Yao B, et al. Profiles of Emerging and Legacy Per-/Polyfluoroalkyl Substances in Matched Serum and Semen Samples: New Implications for Human Semen Quality. *Environ Health Perspect* (2019) 127:127005. doi: 10.1289/EHP4431
141. Green MP, Harvey AJ, Finger BJ, Tarulli GA. Endocrine Disrupting Chemicals: Impacts on Human Fertility and Fecundity During the Peri-Conception Period. *Environ Res* (2021) 194:110694. doi: 10.1016/j.envres.2020.110694
142. Cooper TG, Noonan E, von Eckardstein S, Auger J, Baker HW, Behre HM, et al. World Health Organization Reference Values for Human Semen Characteristics. *Hum Reprod Update* (2010) 16:231–45. doi: 10.1093/humupd/dmp048
143. Lopez-Espinosa M-J, Mondal D, Armstrong BG, Eskenazi B, Fletcher T. Perfluoroalkyl Substances, Sex Hormones, and Insulin-Like Growth Factor-1 at 6-9 Years of Age: A Cross-Sectional Analysis Within the C8 Health Project. *Environ Health Perspect* (2016) 124:1269–75. doi: 10.1289/ehp.1509869
144. Wang Y, Aimuzi R, Nian M, Zhang Y, Luo K, Zhang J. Perfluoroalkyl Substances and Sex Hormones in Postmenopausal Women: NHANES 2013-2016. *Environ Int* (2021) 149:106408. doi: 10.1016/j.envint.2021.106408
145. Wan HT, Zhao YG, Wong MH, Lee KF, Yeung WS, Giesy JP, et al. Testicular Signaling is the Potential Target of Perfluorooctanesulfonate-Mediated Subfertility in Male Mice. *Biol Reprod* (2011) 84:1016–23. doi: 10.1095/biolreprod.110.089219
146. Biegel LB, Liu RC, Hurtt ME, Cook JC. Effects of Ammonium Perfluorooctanoate on Leydig Cell Function: *In Vitro*, *In Vivo*, and Ex Vivo Studies. *Toxicol Appl Pharmacol* (1995) 134:18–25. doi: 10.1006/taap.1995.1164
147. Zhang H, Lu Y, Luo B, Yan S, Guo X, Dai J. Proteomic Analysis of Mouse Testis Reveals Perfluorooctanoic Acid-Induced Reproductive Dysfunction *via* Direct Disturbance of Testicular Steroidogenic Machinery. *J Proteome Res* (2014) 13:3370–85. doi: 10.1021/pr500228d
148. Olsen GW, Gilliland FD, Burlew MM, Burris JM, Mandel JS, Mandel JH. An Epidemiologic Investigation of Reproductive Hormones in Men With Occupational Exposure to Perfluorooctanoic Acid. *J Occup Environ Med* (1998) 40:614–22. doi: 10.1097/00043764-199807000-00006
149. Tsai M-S, Lin C-Y, Lin C-C, Chen M-H, Hsu SHJ, Chien K-L, et al. Association Between Perfluoroalkyl Substances and Reproductive Hormones in Adolescents and Young Adults. *Int J Hyg Environ Health* (2015) 218:437–43. doi: 10.1016/j.ijheh.2015.03.008
150. Skakkebaek NE, Rajpert-De Meyts E, Main KM. Testicular Dysgenesis Syndrome: An Increasingly Common Developmental Disorder With Environmental Aspects. *Hum Reprod* (2001) 16:972–8. doi: 10.1093/humrep/16.5.972
151. Rajpert-De Meyts E. Developmental Model for the Pathogenesis of Testicular Carcinoma in Situ: Genetic and Environmental Aspects. *Hum Reprod Update* (2006) 12:303–23. doi: 10.1093/humupd/dmk006
152. Toppari J, Larsen JC, Christiansen P, Giwercman A, Grandjean P, Guillette LJ Jr, et al. Male Reproductive Health and Environmental Xenoestrogens. *Environ Health Perspect* (1996) 104(Suppl 4):741–803. doi: 10.1289/ehp.96104s4741
153. Palmer JR, Herbst AL, Noller KL, Boggs DA, Troisi R, Titus-Ernstoff L, et al. Urogenital Abnormalities in Men Exposed to Diethylstilbestrol *In Utero*: A Cohort Study. *Environ Health* (2009) 8:37. doi: 10.1186/1476-069X-8-37
154. Jensen MS, Rebordosa C, Thulstrup AM, Toft G, Sørensen HT, Bonde JP, et al. Maternal Use of Acetaminophen, Ibuprofen, and Acetylsalicylic Acid During Pregnancy and Risk of Cryptorchidism. *Epidemiology* (2010) 21:779–85. doi: 10.1097/EDE.0b013e3181f20bed
155. Fudvoye J, Bourguignon JP, Parent AS. Endocrine-Disrupting Chemicals and Human Growth and Maturation: A Focus on Early Critical Windows of Exposure. *Vitam Horm* (2014) 94:1–25. doi: 10.1016/B978-0-12-800095-3.00001-8
156. Welsh M, Saunders PT, Fisken M, Scott HM, Hutchison GR, Smith LB, et al. Identification in Rats of a Programming Window for Reproductive Tract Masculinization, Disruption of Which Leads to Hypospadias and Cryptorchidism. *J Clin Invest* (2008) 118:1479–90. doi: 10.1172/JCI34241
157. Gore AC, Chappell VA, Fenton SE, Flaws JA, Nadal A, Prins GS, et al. EDC-2: The Endocrine Society's Second Scientific Statement on Endocrine-Disrupting Chemicals. *Endocr Rev* (2015) 36:E1–e150. doi: 10.1210/er.2015-1010
158. Giulivo M, Lopez de Alda M, Capri E, Barceló D. Human Exposure to Endocrine Disrupting Compounds: Their Role in Reproductive Systems, Metabolic Syndrome and Breast Cancer. *A Review Environ Res* (2016) 151:251–64. doi: 10.1016/j.envres.2016.07.011
159. Damstra TB, Bergman S, Kavlock A, van der Kraak R, Van Der Kraak G. *Global Assessment of the State-of-the-Science of Endocrine Disruptors*. Geneva: World Health Organization (2002).
160. Alonso-Magdalena P, Vieira E, Soriano S, Menes L, Burks D, Quesada I, et al. Bisphenol A Exposure During Pregnancy Disrupts Glucose Homeostasis in Mothers and Adult Male Offspring. *Environ Health Perspect* (2010) 118:1243–50. doi: 10.1289/ehp.1001993
161. Ghassabian A, Trasande L. Disruption in Thyroid Signaling Pathway: A Mechanism for the Effect of Endocrine-Disrupting Chemicals on Child

Neurodevelopment. *Front Endocrinol (Lausanne)* (2018) 9:204. doi: 10.3389/fendo.2018.00204
162. Kopp R, Martínez IO, Legradi J, Legler J. Exposure to Endocrine Disrupting Chemicals Perturbs Lipid Metabolism and Circadian Rhythms. *J Environ Sci* (2017) 62:133–7. doi: 10.1016/j.jes.2017.10.013
163. Sifakis S, Androutsopoulos VP, Tsatsakis AM, Spandidos DA. Human Exposure to Endocrine Disrupting Chemicals: Effects on the Male and Female Reproductive Systems. *Environ Toxicol Pharmacol* (2017) 51:56–70. doi: 10.1016/j.etap.2017.02.024
164. Abaci A, Demir K, Bober E, Buyukgebiz A. Endocrine Disrupters - With Special Emphasis on Sexual Development. *Pediatr Endocrinol Rev* (2009) 6:464–75.
165. Axelstad M, Hass U, Scholze M, Christiansen S, Kortenkamp A, Boberg J, et al. Reduced Sperm Counts in Rats Exposed to Human Relevant Mixtures of Endocrine Disrupters. *Endocr Connect* (2018) 7:139–48. doi: 10.1530/EC-17-0307
166. Skakkebaek NE. A Brief Review of the Link Between Environment and Male Reproductive Health: Lessons From Studies of Testicular Germ Cell Cancer. *Horm Res Paediatr* (2016) 86:240–6. doi: 10.1159/000443400
167. Thorup J, McLachlan R, Cortes D, Nation TR, Balic A, Southwell BR, et al. What is New in Cryptorchidism and Hypospadias–a Critical Review on the Testicular Dysgenesis Hypothesis. *J Pediatr Surg* (2010) 45:2074–86. doi: 10.1016/j.jpedsurg.2010.07.030
168. Coperchini F, Awwad O, Rotondi M, Santini F, Imbriani M, Chiovato L. Thyroid Disruption by Perfluorooctane Sulfonate (PFOS) and Perfluorooctanoate (PFOA). *J Endocrinol Invest* (2017) 40:105–21. doi: 10.1007/s40618-016-0572-z
169. Rickard BP, Rizvi I, Fenton SE. Per- and Poly-Fluoroalkyl Substances (PFAS) and Female Reproductive Outcomes: PFAS Elimination, Endocrine-Mediated Effects, and Disease. *Toxicology* (2021) 465:153031. doi: 10.1016/j.tox.2021.153031
170. Coperchini F, Croce L, Ricci G, Magri F, Rotondi M, Imbriani M, et al. Thyroid Disrupting Effects of Old and New Generation PFAS. *Front Endocrinol (Lausanne)* (2020) 11:612320. doi: 10.3389/fendo.2020.612320
171. Rosenmai AK, Taxvig C, Svingen T, Trier X, van Vugt-Lussenburg BM, Pedersen M, et al. Fluorinated Alkyl Substances and Technical Mixtures Used in Food Paper-Packaging Exhibit Endocrine-Related Activity In Vitro. *Andrology* (2016) 4:662–72. doi: 10.1111/andr.12190
172. Bay K, Main KM, Toppari J, Skakkebæk NE. Testicular Descent: INSL3, Testosterone, Genes and the Intrauterine Milieu. *Nat Rev Urol* (2011) 8:187–96. doi: 10.1038/nrurol.2011.23
173. Toft G, Jönsson BA, Bonde JP, Nørgaard-Pedersen B, Hougaard DM, Cohen A, et al. Perfluorooctane Sulfonate Concentrations in Amniotic Fluid, Biomarkers of Fetal Leydig Cell Function, and Cryptorchidism and Hypospadias in Danish Boys (1980-1996). *Environ Health Perspect* (2016) 124:151–6. doi: 10.1289/ehp.1409288
174. Zimmermann S, Steding G, Emmen JM, Brinkmann AO, Nayernia K, Holstein AF, et al. Targeted Disruption of the Insl3 Gene Causes Bilateral Cryptorchidism. *Mol Endocrinol* (1999) 13:681–91. doi: 10.1210/mend.13.5.0272
175. Nef S, Parada LF. Cryptorchidism in Mice Mutant for Insl3. *Nat Genet* (1999) 22:295–9. doi: 10.1038/10364
176. Ye L, Su ZJ, Ge RS. Inhibitors of Testosterone Biosynthetic and Metabolic Activation Enzymes. *Molecules* (2011) 16:9983–10001. doi: 10.3390/molecules16129983
177. Azhagiya Singam ER, Tachachartvanich P, Fourches D, Soshilov A, Hsieh JCY, La Merrill MA, et al. Structure-Based Virtual Screening of Perfluoroalkyl and Polyfluoroalkyl Substances (PFASs) as Endocrine Disruptors of Androgen Receptor Activity Using Molecular Docking and Machine Learning. *Environ Res* (2020) 190:109920. doi: 10.1016/j.envres.2020.109920
178. Huhtaniemi I, Pelliniemi LJ. Fetal Leydig Cells: Cellular Origin, Morphology, Life Span, and Special Functional Features. *Proc Soc Exp Biol Med* (1992) 201:125–40. doi: 10.3181/00379727-201-43493
179. Awoniyi CA, Santulli R, Sprando RL, Ewing LL, Zirkin BR. Restoration of Advanced Spermatogenic Cells in the Experimentally Regressed Rat Testis: Quantitative Relationship to Testosterone Concentration Within the Testis. *Endocrinology* (1989) 124:1217–23. doi: 10.1210/endo-124-3-1217
180. Zhao B, Hu GX, Chu Y, Jin X, Gong S, Akingbemi BT, et al. Inhibition of Human and Rat 3beta-Hydroxysteroid Dehydrogenase and 17beta-Hydroxysteroid Dehydrogenase 3 Activities by Perfluoroalkylated Substances. *Chem Biol Interact* (2010) 188:38–43. doi: 10.1016/j.cbi.2010.07.001
181. Kjeldsen LS, Bonefeld-Jørgensen EC. Perfluorinated Compounds Affect the Function of Sex Hormone Receptors. *Environ Sci Pollut Res Int* (2013) 20:8031–44. doi: 10.1007/s11356-013-1753-3
182. Zhao B, Li L, Liu J, Li H, Zhang C, Han P, et al. Exposure to Perfluorooctane Sulfonate *In Utero* Reduces Testosterone Production in Rat Fetal Leydig Cells. *PloS One* (2014) 9:e78888. doi: 10.1371/journal.pone.0078888
183. Kim S, Thapar I, Brooks BW. Epigenetic Changes by Per- and Polyfluoroalkyl Substances (PFAS). *Environ Pollut* (2021) 279:116929. doi: 10.1016/j.envpol.2021.116929
184. Nilsson EE, Sadler-Riggleman I, Skinner MK. Environmentally Induced Epigenetic Transgenerational Inheritance of Disease. *Environ Epigenet* (2018) 4:dvy016. doi: 10.1093/eep/dvy016
185. Sharpe RM, McKinnell C, Kivlin C, Fisher JS. Proliferation and Functional Maturation of Sertoli Cells, and Their Relevance to Disorders of Testis Function in Adulthood. *Reproduction* (2003) 125:769–84. doi: 10.1530/rep.0.1250769
186. Upham BL, Deocampo ND, Wurl B, Trosko JE. Inhibition of Gap Junctional Intercellular Communication by Perfluorinated Fatty Acids is Dependent on the Chain Length of the Fluorinated Tail. *Int J Cancer* (1998) 78:491–5. doi: 10.1002/(SICI)1097-0215(19981109)78:4<491::AID-IJC16>3.0.CO;2-9
187. Wan HT, Mruk DD, Wong CK, Cheng CY. Perfluorooctanesulfonate (PFOS) Perturbs Male Rat Sertoli Cell Blood-Testis Barrier Function by Affecting F-Actin Organization *via* P-FAK-Tyr(407): An *In Vitro* Study. *Endocrinology* (2014) 155:249–62. doi: 10.1210/en.2013-1657
188. Gao Y, Chen H, Xiao X, Lui W-Y, Lee WM, Mruk DD, et al. Perfluorooctanesulfonate (PFOS)-Induced Sertoli Cell Injury Through a Disruption of F-Actin and Microtubule Organization is Mediated by Akt1/2. *Sci Rep* (2017) 7:1110–0. doi: 10.1038/s41598-017-01016-8
189. Mruk DD, Cheng CY. Sertoli-Sertoli and Sertoli-Germ Cell Interactions and Their Significance in Germ Cell Movement in the Seminiferous Epithelium During Spermatogenesis. *Endocrine Rev* (2004) 25:747–806. doi: 10.1210/er.2003-0022
190. Cheng CY, Mruk DD. Cell Junction Dynamics in the Testis: Sertoli-Germ Cell Interactions and Male Contraceptive Development. *Physiol Rev* (2002) 82:825–74. doi: 10.1152/physrev.00009.2002
191. Skinner MK, Norton JN, Mullaney BP, Rosselli M, Whaley PD, Anthony CT. Cell-Cell Interactions and the Regulation of Testis Function. *Ann N Y Acad Sci* (1991) 637:354–63. doi: 10.1111/j.1749-6632.1991.tb27322.x
192. Jégou B. The Sertoli-Germ Cell Communication Network in Mammals. *Int Rev Cytol* (1993) 147:25–96. doi: 10.1016/S0074-7696(08)60766-4
193. Mackay S. Gonadal Development in Mammals at the Cellular and Molecular Levels. *Int Rev Cytol* (2000) 200:47–99. doi: 10.1016/S0074-7696(00)00002-4
194. Steves AN, Turry A, Gill B, Clarkson-Townsend D, Bradner JM, Bachli I, et al. Per- and Polyfluoroalkyl Substances Impact Human Spermatogenesis in a Stem-Cell-Derived Model. *Syst Biol Reprod Med* (2018) 64:225–39. doi: 10.1080/19396368.2018.1481465
195. Qu JH, Lu CC, Xu C, Chen G, Qiu LL, Jiang JK, et al. Perfluorooctane Sulfonate-Induced Testicular Toxicity and Differential Testicular Expression of Estrogen Receptor in Male Mice. *Environ Toxicol Pharmacol* (2016) 45:150–7. doi: 10.1016/j.etap.2016.05.025
196. Chen J, Wang X, Ge X, Wang D, Wang T, Zhang L, et al. Chronic Perfluorooctanesulphonic Acid (PFOS) Exposure Produces Estrogenic Effects in Zebrafish. *Environ Pollut* (2016) 218:702–8. doi: 10.1016/j.envpol.2016.07.064
197. Li K, Gao P, Xiang P, Zhang X, Cui X, Ma LQ. Molecular Mechanisms of PFOA-Induced Toxicity in Animals and Humans: Implications for Health Risks. *Environ Int* (2017) 99:43–54. doi: 10.1016/j.envint.2016.11.014
198. Maestri L, Negri S, Ferrari M, Ghittori S, Fabris F, Danesino P, et al. Determination of Perfluorooctanoic Acid and Perfluorooctanesulfonate in Human Tissues by Liquid Chromatography/Single Quadrupole Mass Spectrometry. *Rapid Commun Mass Spectrom* (2006) 20:2728–34. doi: 10.1002/rcm.2661

199. Glatz JFC, van der Vusse GJ. Cellular Fatty Acid-Binding Proteins: Their Function and Physiological Significance. *Prog Lipid Res* (1996) 35:243–82. doi: 10.1016/S0163-7827(96)00006-9
200. Hamilton JA. Binding of Fatty Acids to Albumin: A Case Study of Lipid-Protein Interactions. *Physiology* (1992) 7:264–70. doi: 10.1152/physiologyonline.1992.7.6.264
201. Spector AA. [17] Structure and Lipid Binding Properties of Serum Albumin. *Methods Enzymol* (1986) 128:320–39. doi: 10.1016/0076-6879(86)28077-5
202. Yamamoto T, Yamamoto A, Watanabe M, Matsuo T, Yamazaki N, Kataoka M, et al. Classification of FABP Isoforms and Tissues Based on Quantitative Evaluation of Transcript Levels of These Isoforms in Various Rat Tissues. *Biotechnol Lett* (2009) 31:1695–701. doi: 10.1007/s10529-009-0065-7
203. Liu R-Z, Li X, Godbout R. A Novel Fatty Acid-Binding Protein (FABP) Gene Resulting From Tandem Gene Duplication in Mammals: Transcription in Rat Retina and Testis. *Genomics* (2008) 92:436–45. doi: 10.1016/j.ygeno.2008.08.003
204. Storch J, Thumser AEA. The Fatty Acid Transport Function of Fatty Acid-Binding Proteins. *Biochim Biophys Acta (BBA) - Mol Cell Biol Lipids* (2000) 1486:28–44. doi: 10.1016/S1388-1981(00)00046-9
205. Gagliano E, Sgroi M, Falciglia PP, Vagliasindi FGA, Roccaro P. Removal of Poly- and Perfluoroalkyl Substances (PFAS) From Water by Adsorption: Role of PFAS Chain Length, Effect of Organic Matter and Challenges in Adsorbent Regeneration. *Water Res* (2020) 171:115381. doi: 10.1016/j.watres.2019.115381
206. Kah M, Sigmund G, Xiao F, Hofmann T. Sorption of Ionizable and Ionic Organic Compounds to Biochar, Activated Carbon and Other Carbonaceous Materials. *Water Res* (2017) 124:673–92. doi: 10.1016/j.watres.2017.07.070
207. Mueller B, Yingling G, Schlosser KE, Goodrow S. *ITRC, PFAS Fact Sheets PFAS-1, Interstate Technology and Regulatory Council, Interstate Technology & Regulatory Council, PFAS Team*. Washington, DC: Interstate Technology and Regulatory Counci (2018).
208. Ross I, McDonough J, Miles J, Storch P, Thelakkat Kochunarayanan P, Kalve E, et al. A Review of Emerging Technologies for Remediation of PFASs. *Remediation J* (2018) 28:101–26. doi: 10.1002/rem.21553
209. Lu D, Sha S, Luo J, Huang Z, Zhang Jackie X. Treatment Train Approaches for the Remediation of Per- and Polyfluoroalkyl Substances (PFAS): A Critical Review. *J Hazard Mater* (2020) 386:121963. doi: 10.1016/j.jhazmat.2019.121963
210. Ochoa-Herrera V, Sierra-Alvarez R. Removal of Perfluorinated Surfactants by Sorption Onto Granular Activated Carbon, Zeolite and Sludge. *Chemosphere* (2008) 72:1588–93. doi: 10.1016/j.chemosphere.2008.04.029
211. Nancy Merino YQ, Deeb RA, Hawley EL, Hoffmann MR, Mahendra S. Degradation and Removal Methods for Perfluoroalkyl and Polyfluoroalkyl Substances in Water. *Environ Eng Sci* (2016) 33:615–49. doi: 10.1089/ees.2016.0233
212. *NEMP, PFAS National Environmental Management Plan Version 2.0 Heads of EPA Australia and New Zealand*. Canberra, ACT: Department of Agriculture, Water and the Environment (2020).
213. Zaggia A, Conte L, Falletti L, Fant M, Chiorboli A. Use of Strong Anion Exchange Resins for the Removal of Perfluoroalkylated Substances From Contaminated Drinking Water in Batch and Continuous Pilot Plants. *Water Res* (2016) 91:137–46. doi: 10.1016/j.watres.2015.12.039
214. Dickenson E, Higgins C. Treatment Mitigation Strategies for Poly-and Perfluoroalkyl Substances. *Water Res Foundation Web Rep* (2016) 4322:241–54.
215. Vecitis CD, Park H, Cheng J, Mader BT, Hoffmann MR. Enhancement of Perfluorooctanoate and Perfluorooctanesulfonate Activity at Acoustic Cavitation Bubble Interfaces. *J Phys Chem C* (2008) 112:16850–7. doi: 10.1021/jp804050p
216. Cui J, Gao P, Deng Y. Destruction of Per- and Polyfluoroalkyl Substances (PFAS) With Advanced Reduction Processes (ARPs): A Critical Review. *Environ Sci Technol* (2020) 54:3752–66. doi: 10.1021/acs.est.9b05565
217. Turner BD, Sloan SW, Currell GR. Novel Remediation of Per-and Polyfluoroalkyl Substances (PFASs) From Contaminated Groundwater Using Cannabis Sativa L. (hemp) Protein Powder. *Chemosphere* (2019) 229:22–31. doi: 10.1016/j.chemosphere.2019.04.139
218. Parsons DF, Duignan TT, Salis A. Cation Effects on Haemoglobin Aggregation: Balance of Chemisorption Against Physisorption of Ions. *Interface Focus* (2017) 7:20160137. doi: 10.1098/rsfs.2016.0137
219. Zhang X, Chen L, Fei X-C, Ma Y-S, Gao H-W. Binding of PFOS to Serum Albumin and DNA: Insight Into the Molecular Toxicity of Perfluorochemicals. *BMC Mol Biol* (2009) 10:1–12. doi: 10.1186/1471-2199-10-16
220. Shin M-Y, Shin C, Choi JW, Lee J, Lee S, Kim S. Pharmacokinetic Profile of Propyl Paraben in Humans After Oral Administration. *Environ Int* (2019) 130:104917. doi: 10.1016/j.envint.2019.104917
221. Sears ME, Genuis SJ. Environmental Determinants of Chronic Disease and Medical Approaches: Recognition, Avoidance, Supportive Therapy, and Detoxification. *J Environ Public Health* (2012) 2012:356798. doi: 10.1155/2012/356798
222. Genuis SJ, Birkholz D, Rodushkin I, Beesoon S. Blood, Urine, and Sweat (BUS) Study: Monitoring and Elimination of Bioaccumulated Toxic Elements. *Arch Environ Contam Toxicol* (2011) 61:344–57. doi: 10.1007/s00244-010-9611-5
223. Genuis SJ, Beesoon S, Lobo RA, Birkholz D. Human Elimination of Phthalate Compounds: Blood, Urine, and Sweat (BUS) Study. *ScientificWorldJournal* (2012) 2012:615068. doi: 10.1100/2012/615068
224. Genuis SJ, Beesoon S, Birkholz D, Lobo RA. Human Excretion of Bisphenol A: Blood, Urine, and Sweat (BUS) Study. *J Environ Public Health* (2012) 2012:185731. doi: 10.1155/2012/185731
225. Dahlgren J, Cecchini M, Takhar H, Paepke O. Persistent Organic Pollutants in 9/11 World Trade Center Rescue Workers: Reduction Following Detoxification. *Chemosphere* (2007) 69:1320–5. doi: 10.1016/j.chemosphere.2006.05.127
226. David WS, Ben M, Megan GS. Body Burden Reductions of PCBs, PBBs and Chlorinated Pesticides in Human Subjects. *Ambio* (1984) 13:378–80.
227. Genuis SJ, Birkholz D, Ralitsch M, Thibault N. Human Detoxification of Perfluorinated Compounds. *Public Health* (2010) 124:367–75. doi: 10.1016/j.puhe.2010.03.002
228. Wong F, MacLeod M, Mueller JF, Cousins IT. Enhanced Elimination of Perfluorooctane Sulfonic Acid by Menstruating Women: Evidence From Population-Based Pharmacokinetic Modeling. *Environ Sci Technol* (2014) 48:8807–14. doi: 10.1021/es500796y
229. Genuis SJ, Liu Y, Genuis QI, Martin JW. Phlebotomy Treatment for Elimination of Perfluoroalkyl Acids in a Highly Exposed Family: A Retrospective Case-Series. *PloS One* (2014) 9:e114295. doi: 10.1371/journal.pone.0114295
230. Rotander A, Toms LM, Aylward L, Kay M, Mueller JF. Elevated Levels of PFOS and PFHxS in Firefighters Exposed to Aqueous Film Forming Foam (AFFF). *Environ Int* (2015) 82:28–34. doi: 10.1016/j.envint.2015.05.005
231. Lorber M, Eaglesham GE, Hobson P, Toms LM, Mueller JF, Thompson JS. The Effect of Ongoing Blood Loss on Human Serum Concentrations of Perfluorinated Acids. *Chemosphere* (2015) 118:170–7. doi: 10.1016/j.chemosphere.2014.07.093
232. Genuis SJ, Curtis L, Birkholz D. Gastrointestinal Elimination of Perfluorinated Compounds Using Cholestyramine and Chlorella Pyrenoidosa. *ISRN Toxicol* (2013) 2013:657849. doi: 10.1155/2013/657849
233. Ducatman A, Luster M, Fletcher T. Perfluoroalkyl Substance Excretion: Effects of Organic Anion-Inhibiting and Resin-Binding Drugs in a Community Setting. *Environ Toxicol Pharmacol* (2021) 85:103650. doi: 10.1016/j.etap.2021.103650
234. Katen AL, Stanger SJ, Anderson AL, Nixon B, Roman SD. Chronic Acrylamide Exposure in Male Mice Induces DNA Damage to Spermatozoa; Potential for Amelioration by Resveratrol. *Reprod Toxicol* (2016) 63:1–12. doi: 10.1016/j.reprotox.2016.05.004
235. Trigg NA, Skerrett-Byrne DA, Xavier MJ, Zhou W, Anderson AL, Stanger SJ, et al. Acrylamide Modulates the Mouse Epididymal Proteome to Drive Alterations in the Sperm Small Non-Coding RNA Profile and Dysregulate Embryo Development. *Cell Rep* (2021) 37:109787. doi: 10.1016/j.celrep.2021.109787
236. Houston BJ, Nixon B, McEwan KE, Martin JH, King BV, Aitken RJ, et al. Whole-Body Exposures to Radiofrequency-Electromagnetic Energy can Cause DNA Damage in Mouse Spermatozoa *via* an Oxidative Mechanism. *Sci Rep* (2019) 9:17478. doi: 10.1038/s41598-019-53983-9

237. Hamilton TRDS, Mendes CM, de Castro LS, de Assis PM, Siqueira AFP, Delgado J, et al. Evaluation of Lasting Effects of Heat Stress on Sperm Profile and Oxidative Status of Ram Semen and Epididymal Sperm. *Oxid Med Cell Longev* (2016) 2016:1687657–1687657. doi: 10.1155/2016/1687657
238. Houston BJ, Nixon B, Martin JH, De Iuliis GN, Trigg NA, Bromfield EG, et al. Heat Exposure Induces Oxidative Stress and DNA Damage in the Male Germ Line†. *Biol Reprod* (2018) 98:593–606. doi: 10.1093/biolre/ioy009

Conflict of Interest: The authors declare that the research was conducted in the absence of any commercial or financial relationships that could be construed as a potential conflict of interest.

Publisher's Note: All claims expressed in this article are solely those of the authors and do not necessarily represent those of their affiliated organizations, or those of the publisher, the editors and the reviewers. Any product that may be evaluated in this article, or claim that may be made by its manufacturer, is not guaranteed or endorsed by the publisher.

frontiers in Physiology

ORIGINAL RESEARCH
published: 11 March 2022
doi: 10.3389/fphys.2022.828578

Long-Term Wi-Fi Exposure From Pre-Pubertal to Adult Age on the Spermatogonia Proliferation and Protective Effects of Edible Bird's Nest Supplementation

*Farah Hanan Fathihah Jaffar[1], Khairul Osman[2], Chua Kien Hui[1], Aini Farzana Zulkefli[1] and Siti Fatimah Ibrahim[1]**

[1] Department of Physiology, Faculty of Medicine, Universiti Kebangsaan Malaysia (UKM), Kuala Lumpur, Malaysia, [2] Faculty of Health Sciences, Universiti Kebangsaan Malaysia (UKM), Kuala Lumpur, Malaysia

OPEN ACCESS

Edited by:
Panagiotis Drakopoulos, University Hospital Brussels, Belgium

Reviewed by:
Laura Maria Mongioi, University of Catania, Italy
Kajal Khodamoradi, University of Miami, United States

***Correspondence:**
Siti Fatimah Ibrahim
timi@ukm.edu.my

Specialty section:
This article was submitted to Reproduction, a section of the journal Frontiers in Physiology

Received: *03 December 2021*
Accepted: *07 February 2022*
Published: *11 March 2022*

Citation:
Jaffar FHF, Osman K, Hui CK, Zulkefli AF and Ibrahim SF (2022) Long-Term Wi-Fi Exposure From Pre-Pubertal to Adult Age on the Spermatogonia Proliferation and Protective Effects of Edible Bird's Nest Supplementation. Front. Physiol. 13:828578. doi: 10.3389/fphys.2022.828578

Children are vulnerable to the radiofrequency radiation (RFR) emitted by Wi-Fi devices. Nevertheless, the severity of the Wi-Fi effect on their reproductive development has been sparsely available. Therefore, this study was conducted to evaluate the Wi-Fi exposure on spermatogonia proliferation in the testis. This study also incorporated an approach to attenuate the effect of Wi-Fi by giving concurrent edible bird's nest (EBN) supplementation. It was predicted that Wi-Fi exposure reduces spermatogonia proliferation while EBN supplementation protects against it. A total of 30 (N = 30) 3-week-old Sprague Dawley weanlings were divided equally into five groups; Control, Control EBN, Wi-Fi, Sham Wi-Fi, and Wi-Fi + EBN. 2.45 GHz Wi-Fi exposure and 250 mg/kg EBN supplementation were conducted for 14 weeks. Findings showed that the Wi-Fi group had decreased in spermatogonia mitosis status. However, the mRNA and protein expression of c-Kit-SCF showed no significant decrease. Instead, the reproductive hormone showed a reduction in FSH and LH serum levels. Of these, LH serum level was decreased significantly in the Wi-Fi group. Otherwise, supplementing the Wi-Fi + EBN group with 250 mg/kg EBN resulted in a significant increase in spermatogonia mitotic status. Even though EBN supplementation improved c-Kit-SCF mRNA and protein expression, the effects were insignificant. The improvement of spermatogonia mitosis appeared to be associated with a significant increase in blood FSH levels following EBN supplementation. In conclusion, the long-term Wi-Fi exposure from pre-pubertal to adult age reduces spermatogonia proliferation in the testis. On the other hand, EBN supplementation protects spermatogonia proliferation against Wi-Fi exposure.

Keywords: children, gonadotropin, mitosis, spermatogonia, sperm, Wi-Fi

INTRODUCTION

Amid the pandemic COVID-19 outbreak, Wi-Fi has become a daily necessity rather than a privilege ([MCMC] Malaysian Communications and Multimedia Commission, 2020). The worldwide lockdown had caused an increment of 500 and 155% of Wi-Fi users among children in the United States and Malaysia, respectively ([MCMC] Malaysian Communications and Multimedia Commission, 2020). In Malaysia, this involves children aged 5–17 years old ([MCMC] Malaysian Communications and Multimedia Commission, 2020). Children nowadays have been using Wi-Fi since before puberty and may continue to do so until adulthood. Therefore, the trend of using Wi-Fi early in childhood causes the children to receive radiofrequency radiation (RFR) emitted by the Wi-Fi devices for a more extended period than it will be to adults (Stewart et al., 2000; Moon, 2020).

In view of the fact that the testis is a sensitive organ to the RFR emitted by Wi-Fi (Zhu et al., 2014), the focus of this study was to evaluate the effect of Wi-Fi exposure on the testis when it receives early Wi-Fi exposure since childhood. The testis is an essential organ for male gamete production through spermatogenesis (Nishimura and L'Hernault, 2017). Spermatogenesis is a continuous process that begins at the onset of puberty to produce millions of spermatozoa (Feng et al., 2014). This process involves strict regulation of multifactorial niche in the testis microenvironment (Hai et al., 2014).

Before the onset of the first meiosis during puberty, spermatogonial stem cells (SSCs) located in the seminiferous tubule of the testis should undergo two processes. The first is mitosis for the maintenance of the SSC pool, and the second is differentiation to produce differentiated spermatogonia progenitor (Kanatsu-Shinohara and Shinohar, 2013). The differentiated spermatogonia are marked by the expression of c-Kit, a type III tyrosine kinase receptor (Ohta et al., 2000; Zhang et al., 2011; Babaei et al., 2016). c-Kit is a 145 kDa transmembrane glycoprotein coded by a gene located at the dominant white spotting (W) locus on chromosome 4q11-q12 in humans (Badr et al., 2018) and chromosome 5 in mice (Gomes et al., 2018).

The ligand for c-Kit is known as stem cell factor (SCF), a 45 kDa glycoprotein secreted by Sertoli cells and encoded by Steel (Sl) locus on chromosome 12 in humans and chromosome 10 in mice (Wiesner et al., 2008; Mansuroglu et al., 2009). Interaction and communication of c-Kit-SCF are crucial for the survival and proliferation of the differentiated spermatogonia and the onset of spermatogenesis (Prabhu et al., 2006). Subsequently, the proliferation of the differentiated spermatogonia is a critical stage to dictate the number of spermatogonia that will enter meiosis and determine the number of sperm yields (Xu et al., 2016).

Besides c-Kit-SCF interaction, important reproductive hormones also influence spermatogonia proliferation (Khanehzad et al., 2021). As the Wi-Fi exposure was done from pre-pubertal to adult age, the probability of hormonal disturbance on the testosterone, follicle-stimulating hormone (FSH), and luteinizing hormone (LH) is quite likely. However, whether early Wi-Fi exposure could impair spermatogonia proliferation and these prominent factors regulating them is still unknown.

Besides evaluating the effect of pre-pubertal Wi-Fi exposure on the testis, this study also incorporated edible bird's nest (EBN) supplementation to overcome the expected negative impact of Wi-Fi exposure. EBN is a bird's nest made of male swiftlet saliva, *Aerodramus fuciphagus*, particularly during the breeding season (Kuntjoro and Rachmadiarti, 2020). It is composed mainly of protein, carbohydrates, and a small amount of fat (Chua and Zukefli, 2016). Our previous study demonstrated a dose-dependent increase of sperm concentration, sperm motility, as well as testosterone, FSH, and LH serum hormonal level upon EBN supplementation (Jaffar et al., 2021).

There are two reasons why this study incorporates EBN. Firstly, EBN was reported to have a positive proliferative effect in *in vitro* study (Aswir and Wan Nazaimoon, 2011; Abidin et al., 2011; Roh et al., 2012). Second, EBN was also reported containing a few male reproductive hormones such as FSH, LH, and testosterone (Ma and Liu, 2012a) and showed potential as an alternative treatment for erectile dysfunction (Ma et al., 2012). These EBN characteristics align with the current study objective and therefore becomes the reason for this selection interest.

Hereby, this study was done to evaluate the effect of long-term Wi-Fi exposure from pre-pubertal until adult age and its impact on spermatogonia proliferation, several spermatogonia proliferation regulatory factors, and the protective effect of EBN supplementation against the Wi-Fi exposure. This study is imperative in understanding the consequences of long-term Wi-Fi exposure on children's reproductive development and the approach to overcome the Wi-Fi effect with continuous Wi-Fi exposure.

MATERIALS AND METHODS

Animals

Thirty (N = 30) male Sprague–Dawley rats at the age of 3 weeks with an initial body weight of 45 ± 5 g were acquired from the Laboratory Animal Research Unit (LARU) of the National University of Malaysia (UKM). This 3-week-old male rat pups representing 7-year-old children. Wi-Fi exposure was conducted for 14 weeks until the pups reached 17-week-old. The 17-week-old rats represent 33-year-old humans who have matured reproductive systems. This age comparison was performed according to the pre-pubertal period of rats compared to humans (Sengupta, 2013).

The rats were divided randomly and equally into five groups (**Table 1**), with six rats (n = 6) in each group. Each rat was housed individually in a plastic cage (43 cm length × 16 cm wide × 29 cm height) and have the privilege to move freely inside the cage without any movement restriction. The rats were fed with respective food pellets, supplied with clean water *ad libitum*, and kept in 12 h light: dark cycle at the ambient temperature of 22°C ± 5°C. In this study, all animal procedures were approved by the National University of Malaysia (UKM). The approval reference number for this study

TABLE 1 | Description of experimental group.

Group	Description
Control group	No Wi-Fi exposure from a Wi-Fi router + normal food pellet
Control EBN	No Wi-Fi exposure from a Wi-Fi router + EBN enriched food pellet
Wi-Fi	Wi-Fi exposure from an active Wi-Fi router + normal food pellet
Sham Wi-Fi	Exposure from an inactive Wi-Fi router + normal food pellet
Wi-Fi + EBN	Wi-Fi exposure from an active Wi-Fi router + EBN enriched food pellet

was FISIO/PP/2018/SITI FATIMAH/28-MAR./908-MAR.-2018-DEC.-2020.

Wi-Fi Exposure Setting

A Wi-Fi router, namely, TP-LINK AC750 Wireless Dual Band Wi-Fi Router Archer C20 (Shenzhen, China), was used. This Wi-Fi router consists of three omnidirectional antennas. Two antennas generate 2.45 GHz Wi-Fi frequency, while one antenna supports dual frequencies, 2.45 and 5 GHz. Only 2.45 GHz Wi-Fi frequency operating at 802.11b/g/n standards was used.

The Wi-Fi router was placed at a 20 cm distance from the animal cages (**Figure 1**). Wi-Fi group was exposed to a router maintained in an active state by constant communication (ping protocol via Bitvise SSH client software v8.18) with a Raspberry Pi computer. Ten pings were sent per minute throughout the exposure. In the Sham Wi-Fi group, the Wi-Fi router was maintained without the ping and considered to be in an inactive state. Exposure was conducted 24 h daily for 14 consecutive weeks.

Based on the Maximum Permissible Exposure report of TP-LINK AC750 Wireless Dual Band Wi-Fi Router Archer C20, the specific absorption rate (SAR) is approximately 0.41 W/kg.

Edible Bird's Nest Supplementation

The raw EBN was obtained from an identified swiftlet's house at Bera, State of Pahang, Peninsular Malaysia. The collected EBN were then processed, freeze-dried, and provided by Glycofood Sdn Bhd, Malaysia.

EBN 250 mg/kg supplementation was given to the Control EBN and Wi-Fi + EBN groups. The dose chosen and the method of supplementation was done based on our previous report (Jaffar et al., 2021).

Animal Euthanization and Tissue Sampling

After 14 weeks of Wi-Fi exposure, each animal was euthanized with a Ketamine-Tiletamine-Xylazine (KTX) cocktail intraperitoneally. Blood was drawn immediately from retro-orbital sinus and collected in BD Vacutainer SST II Advance Plus Blood Collection Tube (BD, United States). The blood was left undisturbed for at least 30 min at room temperature, and the collection tubes were centrifuged at 1,500 g for 10 min at 4°C. The obtained serum was aliquoted and stored at −80°C until analysis.

Both sides of the testis, epididymis and seminal vesicle were carefully dissected and cleaned from surrounding adipose tissue before weighing. The organ coefficient of each dissected reproductive organ was expressed according to the equation: the wet weight of organ (g)/body weight (g) × 100 (Feng et al., 2015). The right testis was fixed in 10% buffered neutral formalin (Merck, Germany), processed with standard protocol,

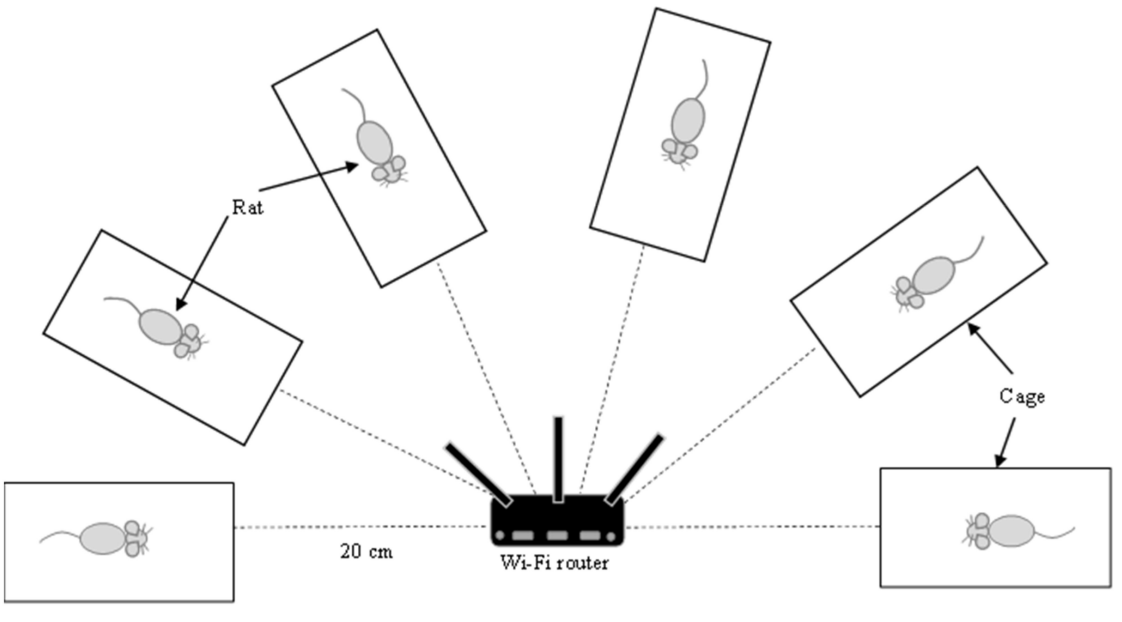

FIGURE 1 | The experimental setting for Wi-Fi exposure. Wi-Fi router was placed at 20 cm distance from the animal cages. The animal was caged individually without any movement restriction. Exposure was conducted 24 h daily for 14 consecutive weeks.

TABLE 2 | Sequence and code for primers of targeted and housekeeping genes.

Gene	Primer sequence 5′–3′/Primer code	NCBI accession number	Expected product size (bp)
c-Kit	QT00194145	NM_022264, XM_006250909	103
SCF	QT00411285	NM_021843, NM_021844, XM_008765339, XM_008765340	129
β-actin	Forward: TCT GTG TGG ATT GGT GGC TCT A Reverse: CTG CTT GCT GAT CCA CAT CTG	NM_031144_3	69

and embedded in paraffin wax (Merck, Germany). The left testis was immediately snap-frozen and stored at −80°C until analysis.

Evaluation of Spermatogonia Mitosis Status by Direct Immunofluorescence

Serial sections of 3-μm thick paraffin-embedded testis were prepared and mounted on poly-L-lysine slides. The sections were deparaffinized in xylene and then rehydrated in graded alcohols.

The tissue sections were heated in a microwave oven in pre-heated 10 mM sodium citrate buffer pH 6.0 for 5 min for antigen retrieval and permeabilized with 0.1% Triton-X 100 in PBS for 30 min. The slides were washed three times with PBS before incubation in Blocking One Solution (Nacalai Tesque, Kyoto, Japan) for 10 min to block non-specific binding. The slides were rewashed with PBS three times. The tissue sections were incubated overnight at 4°C with mouse monoclonal phosphohistone 3 (pHH3) antibody conjugated with Alexa Flour 594 (Santa Cruz Biotechnology, Texas, United States) at a dilution of 1:100.

After antibody binding, the slides were washed three times with PBS. DNA was counterstained with 10 μg/mL Hoechst 33342 and observed using Nikon Eclipse Ni fluorescent microscope under 400 × magnification. About 10–15 random fields were captured using Nikon Y-T TV. The intensity of the staining of 20 random seminiferous tubules was measured using Image J software v1.52a. The steps were repeated for rectum adenocarcinoma tissue (Kim et al., 2018) as a positive control for the staining.

qPCR Analysis of c-Kit and Stem Cell Factor in the Testis

Total RNA was extracted from the left testis using the NucleoSpin®RNA kit (Macherey-Nagel, Düren, Germany). The RNA was eluted with 60 μL of RNase-free water, and its concentration was determined using a NanoDrop DS-11 + Spectrophotometer (DeNovix, Wilmington, United States). Total RNA was converted into a more stable single-strand cDNA using commercially High-Capacity cDNA Reverse Transcription Kits (Applied Biosystems, California, United States). RNA stabilization was done by mixing 1,000 ng of total RNA in a master mix containing RT buffer, 100 mM dNTP mix, RT random primers, and MultiScribe® Reverse Transcriptase. The reaction was conducted for 10 min at 25°C, 120 min at 37°C, and 5 min at 85°C.

Quantitative Real-Time PCR (qPCR) reactions were conducted using the PrecisionPLUS qPCR master mix (Primer Design, United Kingdom). Dilution of 1:5 and 1:50 cDNA was applied for c-Kit and SCF, respectively. Approximately 1 μL of the respective cDNA dilution and 1 μL of each primer (**Table 2**) were added into the master mix. A final reaction volume of 20 μL was run in CFX96TM Real-Time System attached to C1000 Thermal Cycler (Bio-Rad, United States) under the following conditions: 95°C for 2 min, followed by 40 cycles of 95°C for 10 s, and 60°C for 60 s. A final melting step was performed under the following conditions: 65–95°C for 5 s, with 0.5°C increments, to ensure primer dimers' absence and confirm reaction specificity.

All reactions were run in triplicate. Each sample's threshold cycle value (Ct) was measured from the fluorescence signal at the end of every extension cycle. β-Actin was used as a housekeeping gene. The Ct values were used to calculate the relative expression levels compared with the housekeeping gene expression.

Standard plots were constructed for each target gene by using specific primers (**Table 2**). Each standard curve was generated by linear regression of the plotted points. The standard curves exhibited correlation coefficients not less than 0.99, and the efficiencies ranged between 100 and 110%.

Evaluation of c-Kit and Stem Cell Factor Protein Expression by Western Blot

The frozen rat testis was thawed and homogenized in radioimmunoprecipitation assay buffer (RIPA) buffer containing protease inhibitors. The samples were centrifuged at 12,000 rpm for 10 min at 4°C. The supernatant was extracted, aliquoted, and stored at 80°C. Bradford assay was performed to determine protein concentration in each homogenate sample. About 0.2 g of the protein sample was mixed with SDS 5 × loading buffer (Elabscience, Wuhan, China), incubated at 70°C for 5 min, and centrifuged at 12,000 rpm for 30 s. The proteins were electrophoresed on 10% polyacrylamide gels for c-Kit and 8% polyacrylamide gels for SCF.

The membranes were blocked using 5% (w/v) skim milk in Tween-containing Tris-buffered saline [TBST; 145.4 mM NaCl, 10 mM Tris-base, 0.1% (v/v) Tween20, pH 7.5] for 1 h. Then it was incubated in rabbit c-Kit polyclonal (1:1,000 in 5% skim milk) (Elabscience, Wuhan, China) and rabbit SCF polyclonal (1:1,000 in 5% skim milk) (Elabscience, Wuhan, China) primary antibodies overnight at 4°C. The membrane was washed with TBST and incubated with goat anti-rabbit Ig-G (H + L) conjugated with horseradish peroxidase (HRP) (1:5,000 in 2% skim milk) (Elabscience, Wuhan, China) for 1 h at room temperature. The membrane was rewashed with TBST, and the immunoreactive bands were detected using the Excellent Chemiluminescent Substrate (ECL) Kit (Elabscience, Wuhan, China). The membranes were stripped and re-blotted with an anti-β-actin antibody to determine equal loading.

Protein detection was then done on the membrane. It was performed using Gel Doc Amersham Imager 600 (GE Healthcare, United Kingdom). Digital images from the latter imager were immediately analyzed using Image J v. 1.52a. The band intensities of the protein were normalized to that of β -actin.

Serum Testosterone, Follicle-Stimulating Hormone, and Luteinizing Hormone Determination by ELISA

Serum testosterone was measured by competitive enzyme-linked immunosorbent assay (ELISA, Elabscience, Wuhan, China). Serum FSH and LH were measured by sandwich ELISA (Elabscience, Wuhan, China). Intra-assay and inter-assay variability (CV) for all ELISA kits was less than 10%.

All the assay procedures were conducted in duplicate according to the kit's instructions. In brief, 50 μL of the standard and serum were pipetted into a 96 well testosterone ELISA plate. The well was immediately added with 50 μL of biotinylated antibody, sealed, and incubated for 45 min at 37°C.

For FSH and LH hormone analyses, 100 μL of the standard and serum were pipetted into a 96 well ELISA plate. The plate was sealed and incubated for 90 min at 37°C, and all liquid was removed before adding 100 μL of respective biotinylated antibodies into the well. The well was then incubated for 1 h at 37°C.

After incubation with the respective biotinylated antibody, all the solution was removed from the well and washed three times. About 100 μL of horseradish peroxidase (HRP)-conjugated avidin was added into each well. The well was further incubated for another 30 min at 37°C and washed five times. The colorimetric reaction was allowed by adding 90 μL of the substrate reagent, covered from light, and incubated for another 15 min. The reaction was terminated by adding 50 μL of the stop solution. Absorbance was recorded at 450 nm. Testosterone, FSH, and LH serum levels were interpolated from an eight-point standard curve plotted according to a four-parameter logistic (4PL) by using MyAssays.com.

Statistical Analysis

Statistical analysis was performed using SPSS version 22.0 software (SPSS Inc., Chicago, IL, United States). One-way analysis of variance (ANOVA) followed by Tukey's *post hoc* analysis was conducted due to the data's normal distribution and variance homogeneity. The Kruskal-Wallis H test evaluated immunofluorescence intensity and sperm chromatin integrity because of the lack of normality of the data distribution. A p-value < 0.05 was considered statistically significant.

RESULTS

Organ Coefficient

No significant differences in the organ coefficients of the testis, epididymis, and seminal vesicles were found among the groups (**Table 3**).

TABLE 3 | Organ coefficient of testis, epididymis and seminal vesicle in each group.

Group/Organ	Testis	Epididymis	Seminal vesicle
Control	0.40 ± 0.02	0.17 ± 0.00	0.43 ± 0.05
Control EBN	0.34 ± 0.02[a]	0.16 ± 0.01	0.39 ± 0.02
Wi-Fi	0.38 ± 0.01	0.16 ± 0.01	0.36 ± 0.04
Sham Wi-Fi	0.36 ± 0.01	0.15 ± 0.00	0.39 ± 0.02
Wi-Fi + EBN	0.32 ± 0.01[a,b]	0.14 ± 0.00[a]	0.39 ± 0.02

Organ coefficient refers to the wet weight of organ (g)/body weight (g) × 100. Data is presented as mean ± SEM (n = 6).
[a]Represents significant difference compared to the Control group.
[b]Represents significant difference compared to the Wi-Fi group.

Spermatogonia Mitosis Status

The mitosis status of spermatogonia was evaluated by pHH3 expression, represented by red immunofluorescence staining (**Figure 2A**). The immunofluorescence staining of the testis tissue in each group demonstrated that Wi-Fi and Sham's groups exhibited reduced immunofluorescence red signal. The intensity of the red immunofluorescence signal was measured by Image J software and evaluated by the Kruskal-Wallis H test. A significant difference in the signal intensity was found among the groups (Chi-square = 24.84, $p = 0.000$, df = 2) (**Figure 2B**).

Evaluation of c-Kit and Stem Cell Factor mRNA Expression by qPCR

There were no significant changes in c-Kit and SCF mRNA expression in the Wi-Fi group compared with the Control group. However, the mRNA expression levels of c-Kit ($p = 0.007$) and SCF ($p = 0.000$) in the Wi-Fi group showed a statistically significant difference compared with those in the Sham group. The c-Kit ($p = 0.015$) mRNA expression was significantly higher in the Sham group than in the Control group (**Figure 3**). The SCF mRNA expression in the Sham group showed a similar trend with c-Kit mRNA expression, but it was not statistically significant compared with the Control group.

Evaluation of c-Kit and Stem Cell Factor Protein Expression by Western Blot

We further examined the protein levels of c-Kit (**Figures 4A,B**) and SCF (**Figures 4C,D**) in each group. The results of relative intensities with β-actin as standard showed that the protein expression levels of c-Kit ($p = 0.977$) and SCF ($p = 0.996$) in the Wi-Fi group showed no significant changes compared with those in the Control group. The c-Kit and SCF protein expression levels increased in the Sham group but were not statistically significant compared with those in Control (c-Kit $p = 0.071$; SCF $p = 0.428$) and Wi-Fi group (c-Kit $p = 0.205$; SCF $p = 0.634$). These patterns of protein expression indicate that changes in protein and mRNA levels are somehow parallel.

Serum Testosterone, Follicle-Stimulating Hormone, and Luteinizing Hormone

Serum testosterone level was not statistically different among the groups (**Figure 5A**). There was a gradual decrease in the serum FSH level but was not significant among the groups (**Figure 5B**).

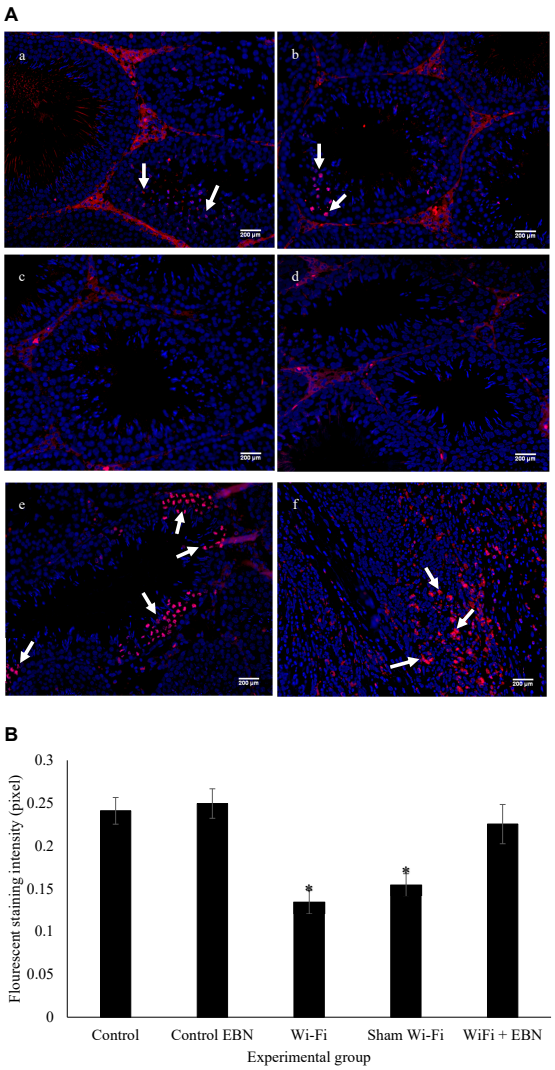

FIGURE 2 | (A) Immunofluorescence staining on sections of the testis for the expression of pHH3 by using Alexa Flour 594, with excitation and emission wavelengths of 590 and 618 nm, respectively. Positive staining is represented by red fluorescence signal (arrow). **(a)** Control group; **(b)** Control EBN group; **(c)** Wi-Fi group; **(d)** Sham Wi-Fi group; **(e)** Wi-Fi + EBN group **(f)** staining positive control by using rectum adenocarcinoma tissue section. For each section, Hoechst 33342 was used to counterstain the cell nuclei, as indicated by the blue signal. All observations were conducted under 200× magnification. **(B)** Immunofluorescence intensity measured by Image J is presented as median ± SEM (n = 6). Kruskal-Wallis H test showed significant differences * among the groups (Chi-square = 24.84, p = 0.000, df = 2).

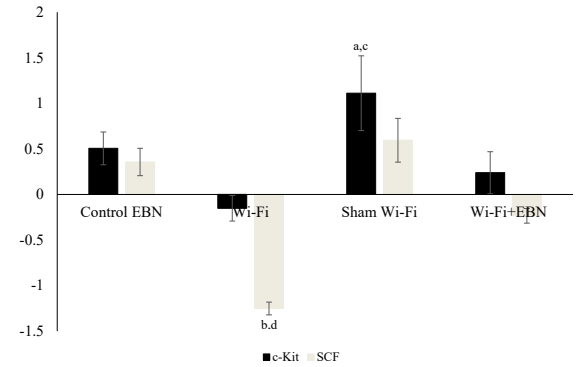

FIGURE 3 | Log_2 fold change of c-Kit and SCF mRNA expression in each group. mRNA expression was determined by qPCR after normalization with β-actin housekeeping gene. Data are expressed as fold change variation relative to the Control group (0 baselines) and presented as mean ± SEM (n = 6). [a]Represents a significant difference compared with the Control group. [b]Represents a significant difference compared with the Control EBN group. [c]Represents a significant difference compared with the Wi-Fi group. [d]Represents a significant difference compared with the Sham Wi-Fi group.

The serum LH level significantly decreased in Wi-Fi (p = 0.039) and Sham (p = 0.000) groups compared with that in the Control group (**Figure 5C**).

DISCUSSION

The discussion was separated into two sections to make it easier to understand. The first section will be explaining the effect of Wi-Fi exposure on the male reproductive system of Sprague Dawley pups. At the same time, the second section will demonstrate the possibility of EBN to overcome the effect of Wi-Fi exposure.

The Effect of Wi-Fi Exposure on Male Children Reproductive System

To date, only two studies have reported the effect of Wi-Fi exposure on the testis of rat pups, which represent children (Özorak et al., 2013; Šimaiová et al., 2019). Both studies only evaluated the effect of Wi-Fi up to several weeks of life. Nevertheless, the use of Wi-Fi is more protracted in the current pattern and often in a consistent manner that can seem to take up eternity. In this study, we applied long-term Wi-Fi exposure from pre-pubertal until adulthood. Findings showed that all the animals successfully achieved puberty following 2 weeks of Wi-Fi exposure. This is indicated by the enlargement of the testis. Long-term Wi-Fi exposure also did not affect the testis, epididymis, and seminal vesicle coefficient, which was not significantly different among the groups. However, both Wi-Fi and Sham Wi-Fi groups had caused a substantial decrease in the spermatogonia mitosis status in the testis. As mitosis of the spermatogonia is an essential step that contributes to the sperm concentration yields, this finding reflected the consistent report on sperm concentration reduction following Wi-Fi exposure in previous studies (Mahmoudi et al., 2015; Saygin et al., 2016).

This study evaluated the possible regulatory factors that may cause the reduction in the spermatogonia mitosis status following Wi-Fi exposure. Evaluation of the c-Kit-SCF regulatory factor showed a non-significant decrease in both mRNA expression in the Wi-Fi group compared to the Control group. On the other hand, it is interesting to note a significant increase of c-Kit-SCF mRNA expression in the Sham Wi-Fi group compared to the Control group. The mRNA expression of c-Kit-SCF was further evaluated by their respective protein expression. A slight reduction in c-Kit and SCF mRNA expression in the Wi-Fi group

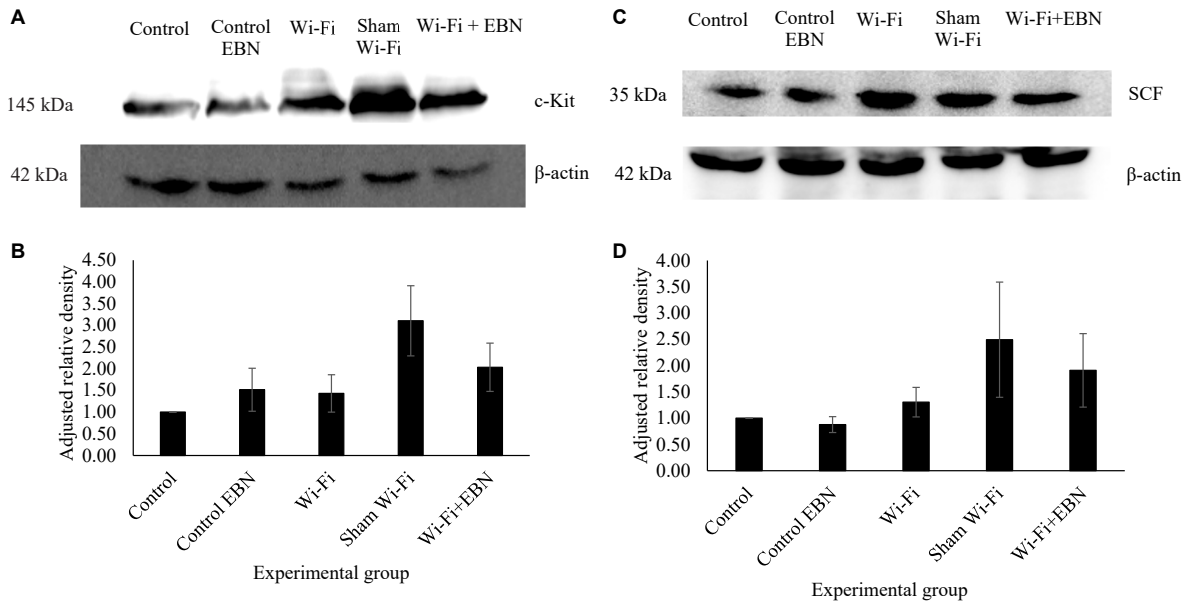

FIGURE 4 | Protein expression of c-Kit and SCF in each experimental group. **(A,C)** Are the representative blots of five different rats. The β-actin lanes belong to the same blot and have the same film exposure. **(B,D)** Represents relative intensities compared with β-actin measured by ImageJ. Data are expressed as mean ± SEM ($p > 0.05$; One-way ANOVA, $n = 5$).

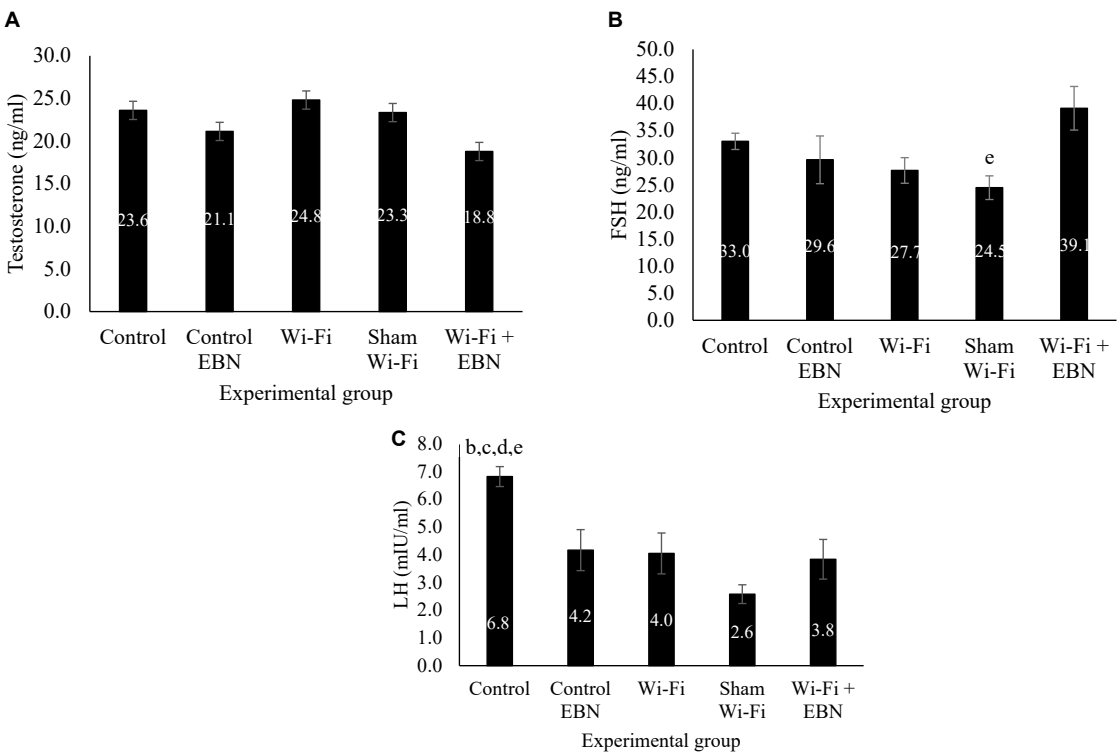

FIGURE 5 | Serum hormonal level of male reproductive hormones in each group following exposure. Data are presented as mean ± SEM ($n = 6$). **(A)** Serum testosterone level in each group following the Wi-Fi exposure. No significant difference was noted among the groups. **(B)** Serum FSH level in each group following the Wi-Fi exposure. [e]Significant difference compared with Wi-Fi + EBN group. **(C)** Serum LH level in each group following the Wi-Fi exposure. [b]Significant difference compared with the Control EBN group ($p = 0.030$), [c]Significant difference compared with the Wi-Fi group ($p = 0.039$), [d]significant difference compared with the Sham Wi-Fi group ($p = 0.000$), and [e]significant difference compared with the Wi-Fi + EBN group ($p = 0.011$).

did not affect the protein expression, and it is comparable to the expression in the Control group. On the other hand, the substantial increase in c-Kit and SCF mRNA expression in the Sham Wi-Fi group indicated an increase in the levels of the respective proteins. However, the increased expression of an individual protein in the Sham Wi-Fi group was also insignificant compared to the Control group.

The changes in the c-Kit-SCF mRNA and protein expression in both Wi-Fi and Sham Wi-Fi groups might relate to the different settings applied for the exposure. Wi-Fi group received Wi-Fi signals from an active router (data transfer is on) while Sham Wi-Fi group was only exposed to inactive Wi-Fi router (data transfer is off). It seems that the active Wi-Fi router had caused a higher RFR compared to the passive Wi-Fi router. This postulation was consistent with a previous study reported by Pachón-García et al. (2015) where they found that the maximum background exposure increases when the Wi-Fi network is in operation compared to when the Wi-Fi network is off.

The greater RFR emitted by an active router may cause the decrease of c-Kit-SCF mRNA expression. On the other hand, the probability of having a lower RFR emitted from an inactive Wi-Fi router may promote a positive effect in the testis and cause the increase of c-Kit-SCF mRNA expression in the Sham Wi-Fi group. The postulation about these findings seems to be consistent with biphasic dose-response explained in radiation hormesis theory (Jin et al., 2020). Although this theory is applied to ionizing radiation, it also suggests that low doses of radiation may exert protective effects and induce beneficial outcomes. In contrast, higher doses lead to detrimental effects (Jargin, 2020).

Delavarifar et al. (2020) observed a similar discovery of beneficial low-dose radiation generated by Wi-Fi routers. Their study applied a shorter exposure time (2 h daily for 4 days) at a greater distance from the router (100 and 150 cm). This setting resulted in a lower specific absorption rate (SAR). These exposure settings increased the sperm concentration and sperm histomorphometric parameters in Busulfan-induced oligospermic mice (Delavarifar et al., 2020).

To the best of our knowledge, this study is the first to report the association of Wi-Fi exposure with the c-Kit-SCF regulation system in the testis. Although the finding seems to be in line with radiation hormesis theory, we cannot rule out the possibility of the detrimental effect when c-Kit and SCF are overexpressed (Cardoso et al., 2017). We do not have the privilege to discuss our results further due to a lack of supporting information on bio-positive and/or bio-negative effects observed. Further studies may shed light on the exact mechanisms of how low and high RFR emitted by the Wi-Fi router affects the testis.

Since the protein expression of c-Kit and SCF in both groups was not affected, the communication between c-Kit and SCF has still occurred despite the Wi-Fi exposure given. However, the proliferation of the spermatogonia was significantly reduced in both groups. It thus suggested that the c-Kit-SCF crosstalk may have failed. As there were no changes in both proteins' expression, the reduction in spermatogonia mitosis may have been related to the protein structural changes upon Wi-Fi exposure. The structural changes of a protein due to EMF exposure have been previously proven by Todorova et al. (2016) Thus, the protein structural changes may have caused the impairment in the crosstalk between c-Kit-SCF and subsequently affected the spermatogonia mitosis status.

As the regulation of the spermatogonia proliferation involved a very complex interaction with other biomolecules, there is a possibility that factors other than c-Kit-SCF may also have been affected by the Wi-Fi exposure. Given that Wi-Fi exposure was conducted before puberty, major male reproductive hormones may have been affected following the exposure. Findings showed a decrease in gonadotropin, FSH and LH serum levels in Wi-Fi and Sham Wi-Fi groups. Whether serum FSH and LH levels are affected by the distinctive exposure of Wi-Fi, or a sign of a typical negative feedback mechanism remains unclear.

However, in terms of FSH action, it is the primary hormone that regulates germ cell numbers by increasing the proliferation of spermatogonia (Ding et al., 2011). So, a decrease in spermatogonia mitosis status may have enhanced the FSH secretion as a normal response in the negative feedback mechanism. As the FSH level in Wi-Fi and Sham Wi-Fi groups was lower than in the Control group, we speculate that the serum level of FSH may have been affected by the Wi-Fi exposure rather than a product of a negative feedback mechanism. A more significant decrease was observed in the serum level of LH in the Wi-Fi and Sham Wi-Fi groups.

The reduction of both gonadotropin hormones suggested that Wi-Fi exposure has affected the pituitary gland. A similar finding was reported by Kaur & Khera, which reported the decrease of FSH and LH secretion following RFR exposure of a cell phone toward male albino rats (Khaur and Khera, 2018). Aside from FSH and LH, the other pituitary hormone known as adrenocorticotropic hormone (ACTH) was also reported to be reduced (Eskander et al., 2012). As the average plasma level will remain constant from the start of puberty (Nassar et al., 2020), Wi-Fi exposure seems to "reprogram" the pituitary hormone and cause it to be secreted at a low level. Because this involves a region of the brain, the findings of this study and other previously confirmed evidence should raise worrisome concerns about the implications of Wi-Fi or cell phone use, particularly among children.

Interestingly, the serum testosterone level was not affected by Wi-Fi exposure. Despite the low serum LH level, the Leydig cells are still responsive and secrete testosterone. According to Santi et al. (2020) relatively low levels of LH may be adequate to maintain intra-testicular testosterone with the presence of FSH. This observation seems to confirm our LH and testosterone findings. The testosterone levels in the Wi-Fi group were similar to the control groups may have contributed to the testis enlargement during puberty, as noted in the preceding paragraph.

Effect of Edible Bird's Nest Supplementation in Wi-Fi Exposed Rats

Supplementation of 250 mg/kg EBN was given to evaluate its attenuation effect on the Wi-Fi exposure. However, the testis coefficient in the Control EBN group showed a significant

decrease compared to the Control group. The same result was recorded in the Wi-Fi + EBN group, which showed a significant reduction in testis and epididymal coefficients. These data indicate that supplementation of EBN 250 mg/kg to the pre-pubertal young has decreased testis and epididymal coefficients. This result contrasts with the supplementation of the EBN 250 mg/kg in the adult rats group, which did not cause any decrease in testis and epididymal coefficients (Jaffar et al., 2021).

The decrease in testis and epididymal organ coefficients following EBN supplementation to the young rats was likely due to estradiol (E2) hormone activity. This hormone was previously characterized to present in the EBN extract used in this study (Jaffar et al., 2021). Several previous studies have reported an association between the administration of the hormone E2 on the development of the reproductive system of male rats. These include significant testicular weight loss (Kula et al., 2001; Brouard et al., 2016), epididymis, and seminal vesicles (Goyal et al., 2003) when mice received E2 or other forms of estrogen. The decrease in organ weight is closely associated with a decrease in the percentage of seminiferous tubules with lumen (Brouard et al., 2016). Furthermore, the percentage of apoptosis in the Sertoli cell and spermatogonia was found to increase. This was accompanied by a decrease in the number of spermatocytes (Walczak-Jędrzejowska et al., 2013).

However, the changes in the testis microenvironment showed otherwise. The spermatogonia mitosis status in the Control EBN group showed no significant differences compared to the Control group. Yet, EBN supplementation in the Wi-Fi + EBN group showed an increase in the mitotic status of spermatogonia. These findings suggest that EBN can preserve and improve spermatogonia's proliferation, which is affected by Wi-Fi exposure. Several previous studies have shown that EBN can promote cell proliferation *in vitro*. EBN capability includes the proliferation of rabbit corneal keratocyte cell culture (Abidin et al., 2011) and human adipose-derived stem cells (hADSCs) (Roh et al., 2012). In *in vivo* studies, EBN supplementation has been reported to accelerate the proliferation and activation of B cell antibodies (Zhao et al., 2016) and stimulate the proliferation of uterine structures (Albishtue et al., 2018).

The study done by Roh et al. (2012) has reported that activation of cell proliferation by EBN occurs through mitogen-activated protein kinase (MAPK). MAPK is also among the activated pathways when c-Kit autophosphorylation occurs following SCF binding (Cardoso et al., 2014). Therefore, it can be assumed that the increase in spermatogonia mitosis status in this Wi-Fi + EBN group is due to the improvement in the expression of c-Kit and SCF proteins. Furthermore, our data suggest that it further enhances MAPK activation contributes to increased spermatogonia proliferation. However, the mechanisms involved in the activation of these downstream road sites are beyond the scope of the current study.

Evaluation of the c-Kit-SCF regulatory factor showed an insignificant increase in c-Kit and SCF mRNA expression of the Control EBN group compared to the Control group. The small changes in c-Kit and SCF mRNA expression did not provide any significant differences in the expression of c-Kit and SCF proteins in the Control EBN group. EBN supplementation in the Wi-Fi + EBN group also showed an increase in c-Kit mRNA expression compared to the Wi-Fi group. The SCF mRNA expression also showed an improvement compared to the Wi-Fi group. Consistent with these mRNA changes, the expression of both c-Kit and SCF proteins in the Wi-Fi + EBN group increased compared to the Wi-Fi group. Nevertheless, changes in the expression patterns of c-Kit and SCF proteins in the Wi-Fi + EBN group were insignificant compared to the Wi-Fi group. To some extent, supplementation of EBN showed that it could prevent the deterioration of the mRNA expression of c-Kit and SCF in the testis receiving Wi-Fi exposure.

The second spermatogonia proliferation regulatory factor showed a significant decrease in gonadotropin hormone levels following EBN supplementation. A significant reduction was recorded in LH hormonal levels. However, EBN supplementation did not cause a significant reduction in FSH and T serum hormonal levels. From these findings, EBN supplementation had caused a decrease in gonadotropin hormone levels, especially in LH hormonal levels. The reduction in LH hormone following EBN administration in rats that had not reached puberty was also reported to be closely related to E2 hormone activity (Gill-Sharma et al., 2001). Thus, the considerable decrease in LH was the second indication of E2 activity in EBN after significantly decreasing the testis and epididymis coefficient. As a result, despite EBN potential as a male fertility treatment, EBN consumers must be cautious of the presence of this specific hormone, which may produce adverse effects, especially in pre-pubertal children.

However, EBN supplementation to the Wi-Fi + EBN group had increased FSH hormonal levels. The mechanism by which EBN increases the FSH in this group is yet to be understood. The probable factors of the increase in serum FSH level may be due to the presence of FSH in the EBN itself (Ma and Liu, 2012b) or the EBN has stimulated FSH production after spermatogonia proliferation was found to be decreased due to Wi-Fi exposure. However, the pathway involved are unclear and need to be further evaluated in future studies. Somehow, the increase in the spermatogonia mitotic status observed in the Wi-Fi + EBN group was most likely due to the elevated FSH levels in this serum together with restoration of gene expression and c-Kit and SCF.

CONCLUSION

The long-term exposure of developing rat pups to Wi-Fi throughout the pre-pubertal age to adulthood has detrimental effects on their reproductive development. Although the Wi-Fi exposure did not significantly reduce the c-Kit-SCF proliferative regulatory system, it had decreased the spermatogonia mitosis activity. It is essential to note that the decrease in the spermatogonia mitosis status may be partly due to the effect of Wi-Fi on the hypothalamus-pituitary-gonadal (HPG) axis which caused the reduction in the gonadotropin hormone. This result was accomplished by using a 64 bps ping signal, significantly less than the amount of data traffic we encounter in our daily lives. Email, for example, requires at least 0.5 Mbps, video requires 1.5 Mbps, and HD video or two-way video games demand 4.0 Mbps

(Liu et al., 2018). A more severe effect could be expected because of the higher data transfer rate in our daily lives. However, until more research is done, it will remain a hypothesis. These findings may reflect the progression of infertility in children upon reaching reproductive age due to Wi-Fi exposure. Therefore, the use of Wi-Fi among children should be minimized due to the risk associated with prolonged radiation exposure.

Attenuation of long-term Wi-Fi exposure in young children with EBN had demonstrated a promising finding where it increases the spermatogonia proliferation despite the Wi-Fi exposure given. However, EBN supplementation at a dose of 250 mg/kg per day on young rats from pre-pubertal age until adulthood was found to have side effects. The side effect includes decreased testis and epididymis coefficient and decreased gonadotropin, LH, and FSH. It is most likely related to the hormone E2, which is also present in the EBN. Therefore, despite the high potential of EBN as a treatment for male infertility, the results presented in this study indicate that there is a need to monitor and verify various health claims made against EBN. This cautionary advice is not only for user's protection but also for ensuring the EBN can be developed safely for human consumption without any unwanted side effects.

DATA AVAILABILITY STATEMENT

The original contributions presented in the study are included in the article/supplementary material, further inquiries can be directed to the corresponding author/s.

ETHICS STATEMENT

The animal study was reviewed and approved by the UKM Animal Ethical Committee (FISIO/PP/2018/SITI FATIMAH/28-MAR./908-MAR.-2018-DEC.-2020).

AUTHOR CONTRIBUTIONS

FJ, SI, and KO designed the study. FJ and AZ conducted the data acquisition, interpreted, and analyzed the data. FJ drafted. SI, KO, and CH revised the manuscript and supervised the whole work. All authors read and approved the final manuscript.

FUNDING

This research was funded by the Ministry of Education (MOE) of Malaysia (grant no. FRGS/1/2019/SKK06/UKM/02/3) and the Faculty of Medicine, UKM (grant no. FF-2018-193) for the financial support.

ACKNOWLEDGMENTS

Our greatest attitude goes to Glycofood Sdn Bhd for providing the EBN extract. We also would like to express our appreciation to all laboratory personnel involved in keeping the animal and giving technical assistance during the molecular study.

REFERENCES

Abidin, F. Z., Hui, C. K., Luan, N. S., Ramli, E. S. M., Hun, L. T., and Ghafar, N. A. (2011). Effects of edible Bird's nest (EBN) on cultured rabbit corneal keratocytes. *BMC Complement. Altern. Med.* 11:94. doi: 10.1186/1472-6882-11-94

Albishtue, A. A., Yimer, N., Zakaria, M. Z. A., Haron, A. W., Yusoff, R., Assi, M. A., et al. (2018). Edible Bird's nest impact on rats' uterine histomorphology, expressions of genes of growth factors and proliferating cell nuclear antigen, and oxidative stress level. *Vet. World* 11, 71–79. doi: 10.14202/vetworld.2018.71-79

Aswir, A. R., and Wan Nazaimoon, W. M. (2011). Effect of edible bird's nest on cell proliferation and tumor necrosis factor-alpha (TNF-α) release in vitro. *Int. Food Res. J.* 18, 1123–1127.

Babaei, M. A., Kamalidehghan, B., Saleem, M., Huri, H. Z., and Ahmadipour, F. (2016). Receptor tyrosine kinase (c-Kit) inhibitors: a potential therapeutic target in cancer cells. *Drug Des. Devel. Ther.* 10, 2443–2459. doi: 10.2147/DDDT.S89114

Badr, P., Elsayed, G. M., Eldin, D. N., Riad, B. Y., and Hamdy, N. (2018). Detection of KIT mutations in core binding factor acute myeloid leukemia. *Leuk. Res. Rep.* 10, 20–25. doi: 10.1016/j.lrr.2018.06.004

Brouard, V., Guénon, I., Bouraima-Lelong, H., and Delalande, C. (2016). Differential effects of bisphenol a and estradiol on rat spermatogenesis' establishment. *Reprod. Toxicol.* 63, 49–61. doi: 10.1016/j.reprotox.2016.05.003

Cardoso, H. J., Figueira, M. I., Correia, S., Vaz, C. V., and Socorro, S. (2014). The SCF/c-KIT system in the male: survival strategies in fertility and cancer. *Mol. Reprod. Dev.* 81:12. doi: 10.1002/mrd.22430

Cardoso, H. J., Figueira, M. I., and Socorro, S. (2017). The stem cell factor (SCF)/c-KIT signalling in testis and prostate cancer. *J. Cell Commun. Signal.* 11, 297–307. doi: 10.1007/s12079-017-0399-1

Chua, L. S., and Zukefli, S. N. (2016). A comprehensive review of edible bird nests and swiftlet farming. *J. Integr. Med.* 14, 415–428. doi: 10.1016/S2095-4964(16)60282-0

Delavarifar, S., Razi, Z., Tamadon, A., Rahmanifar, F., Mehrabani, D., Owjfard, M., et al. (2020). Low-power density radiations emitted from common Wi-Fi routers influence sperm concentration and sperm histomorphometric parameters: a new horizon on male infertility treatment. *J. Biomed. Phy. Eng.* 10, 167–176. doi: 10.31661/jbpe.v0i0.581

Ding, L. J., Yan, G. J., Ge, Q. Y., Yu, F., Zhao, X., Diao, Z. Y., et al. (2011). FSH acts on the proliferation of type a spermatogonia via Nur77 that increases GDNF expression in the Sertoli cells. *FEBS Lett.* 585, 2437–2444. doi: 10.1016/j.febslet.2011.06.013

Eskander, E. F., Estefan, S. F., and Abd-Rabou, A. A. (2012). How does long term exposure to base stations and mobile phones affect human hormone profiles? *Clin. Biochem.* 45, 157–161. doi: 10.1016/j.clinbiochem.2011.11.006

Feng, C. W., Bowles, J., and Koopman, P. (2014). Control of mammalian germ cell entry into meiosis. *Mol. Cell. Endocrinol.* 382, 488–497. doi: 10.1016/j.mce.2013.09.026

Feng, D., Huang, H., Yang, Y., Yan, T., Jin, Y., Cheng, X., et al. (2015). Ameliorative effects of N-acetylcysteine on fluoride-induced oxidative stress and DNA damage in male rats' testis. *Mutat. Res. Genet. Toxicol. Environ. Mutagen.* 792, 35–45. doi: 10.1016/j.mrgentox.2015.09.004

Gill-Sharma, M. K., D'Souza, S., Padwal, V., Balasinor, N., Aleem, M., Parte, P., et al. (2001). Antifertility effects of estradiol in adult male rats. *J. Endocrinol. Invest.* 24, 598–607. doi: 10.1007/BF03343900

Gomes, S. A., Hare, J. M., and Rangel, E. B. (2018). Kidney-Derived c-Kit^{+} cells possess regenerative potential. *Stem Cells Transl. Med.* 7, 317–324. doi: 10.1002/sctm.17-0232

Goyal, H. O., Robateau, A., Braden, T. D., Williams, C. S., Srivastava, K. K., and Ali, K. (2003). Neonatal estrogen exposure of male rats alters reproductive functions at adulthood. *Biol. Reprod.* 68, 2081–2091. doi: 10.1095/biolreprod.102.010637

Hai, Y., Hou, J., Liu, Y., Liu, Y., Yang, H., Li, Z., et al. (2014). The roles and regulation of Sertoli cells in fate determinations of spermatogonial stem cells

and spermatogenesis. *Semin. Cell Dev. Biol.* 29, 66–75. doi: 10.1016/j.semcdb.2014.04.007

Jaffar, F. H. F., Osman, K., Hui, C. K., Zulkefli, A. F., and Ibrahim, S. F. (2021). Edible Bird's nest supplementation improves male reproductive parameters of sprague Dawley rat. *Front. Pharmacol.* 12:631402. doi: 10.3389/fphar.2021.631402

Jargin, S. V. (2020). Radiation safety and hormesis. *Front. Public Health* 8:278. doi: 10.3389/fpubh.2020.00278

Jin, S., Jiang, H., and Cai, Lu (2020). New understanding of the low-dose radiation-induced hormesis. *Radiat. Med. Prot.* 1, 2–6. doi: 10.1016/j.radmp.2020.01.004

Kanatsu-Shinohara, M., and Shinohar, T. (2013). Spermatogonial stem cell self-renewal and development. *Ann. Rev. Cell Dev. Biol.* 29, 163–187. doi: 10.1146/annurev-cellbio-101512-122353

Khanehzad, M., Abbaszadeh, R., Holakuyee, M., Modarressi, M. H., and Nourashrafeddin, S. M. (2021). FSH regulates RA signaling to commit spermatogonia into differentiation pathway and meiosis. *Reprod. Biol. Endocrinol.* 19:4. doi: 10.1186/s12958-020-00686-w

Khaur, M., and Khera, K. S. (2018). Impact of cell phone radiations on pituitary gland and biochemical parameters in albino rat. *Octa J. Biosci.* 6, 1–4.

Kim, M. J., Kwon, M. J., Kang, H. S., Choi, K. C., Nam, E. S., Cho, S. J., et al. (2018). . Identification of phosphohistone H3 cutoff values corresponding to original WHO grades but distinguishable in well-differentiated gastrointestinal neuroendocrine tumors. *Biomed Res. Int.* 2018:1013640. doi: 10.1155/2018/1013640

Kula, K., Walczak-Jêdrzejowska, R., Słowikowska-Hilczer, J., and Oszukowska, E. (2001). Estradiol enhances the stimulatory effect of FSH on testicular maturation and contributes to precocious initiation of spermatogenesis. *Mol. Cell. Endocrinol.* 178, 89–97. doi: 10.1016/S0303-7207(01)00415-4

Kuntjoro, S., and Rachmadiarti, F. (2020). Preference swiftlet bird (*Aerodramus fuciphagus*) nesting at different sites in an effort to increase nest production. *J. Phys. Conf. Ser.* 1569:042083. doi: 10.1088/1742-6596/1569/4/042083

Liu, Y. H., Prince, J., and Wallsten, S. (2018). Distinguishing bandwith and latency in households willingness to pay for broadband internet speed. *Inf. Econ. Policy* 45, 1–15. doi: 10.1016/j.infoecopol.2018.07.001

Ma, F., and Liu, D. (2012a). Sketch of the edible Bird's nest and its important bioactivities. *Food Res. Int.* 48, 559–567. doi: 10.1016/j.foodres.2012.06.001

Ma, F., and Liu, D. (2012b). Extraction and determination of hormones in the edible Bird's nest. *Asian J. Chem.* 24, 117–120.

Ma, F., Liu, D., and Dai, M. (2012). The effects of the edible Bird's nest on sexual function of male castrated rats. *Afr. J. Pharm. Pharmacol.* 6, 2875–2879.

Mahmoudi, R., Mortazavi, S. M. J., Safari, S., Nikseresht, M., Mozdarani, H., Jafari, M., et al. (2015). Effects of microwave electromagnetic radiations emitted from common Wi-Fi routers on rats' sperm count and motility. *Int. J. Radiat. Res.* 133, 363–368.

Mansuroglu, T., Ramadori, P., Dudás, J., Malik, I., Hammerich, K., Füzesi, L., et al. (2009). Expression of stem cell factor and its receptor c-Kit during the development of intrahepatic cholangiocarcinoma. *Lab. Invest* 89, 562–574. doi: 10.1038/labinvest.2009.15

[MCMC] Malaysian Communications and Multimedia Commission (2020). *Internet Users Survey*. Available online at: https://www.mcmc.gov.my/skmmgovmy/media/General/pdf/IUS-2020-Report.pdf (accessed May 4, 2021).

Moon, J. H. (2020). Health effects of electromagnetic fields on children. *Clin. Exp. Pediatr.* 63, 422–428. doi: 10.3345/cep.2019.01494

Nassar, G. N., Raudales, F., and Leslie, S. W. (2020). *Physiology, Testosterone*. Treasure Island, FL: StatPearls Publishing.

Nishimura, H., and L'Hernault, S. W. (2017). Spermatogenesis. *Curr. Biol.* 27, R988–R994. doi: 10.1016/j.cub.2017.07.067

Ohta, H., Yomogida, K., Dohmae, K., and Nishimune, Y. (2000). Regulation of proliferation and differentiation in spermatogonial stem cells: the role of c-kit and its ligand SCF. *Development* 127, 2125–2131. doi: 10.1242/dev.127.10.2125

Özorak, A., Nazıroğlu, M., Çelik, Ö, Yüksel, M., Özçelik, D., Özkaya, O., et al. (2013). Wi-Fi (2.45 GHz)-and mobile phone (900 and 1800 MHz)-induced risks on oxidative stress and elements in kidney and testis of rats during pregnancy and the development of offspring. *Biol. Trace. Elem. Res* 156, 221–229. doi: 10.1007/s12011-013-9836-z

Pachón-García, F. T., Fernández-Ortiz, K., and Paniagua-Sánchez, J. M. (2015). Assessment of Wi-Fi radiation in indoor environments characterizing the time and space-varying electromagnetic fields. *Measurement* 63, 309–321. doi: 10.1016/j.measurement.2014.12.002

Prabhu, S. M., Meistrich, M. L., McLaughlin, E. A., Roman, S. D., Warne, S., Mendis, S., et al. (2006). Expression of c-Kit receptor mRNA and protein in the developing, adult and irradiated rodent testis. *Reproduction* 131, 489–499. doi: 10.1530/rep.1.00968

Roh, K.-B., Lee, J., Kim, Y.-S., Park, J., Kim, J.-H., Lee, J., et al. (2012). Mechanisms of edible Bird's nest extract-induced proliferation of human adipose-derived stem cells. *Evid Based Complement. Alternat. Med.* 2012:797520. doi: 10.1155/2012/797520

Santi, D., Crépieux, P., Reiter, E., Spaggiari, G., Brigant, G., Casarini, L., et al. (2020). Follicle-stimulating hormone (FSH) action on spermatogenesis: a focus on physiological and therapeutic roles. *J. Clin. Med.* 9:1014. doi: 10.3390/jcm9041014

Saygin, M., Asci, H., Ozmen, O., Cankara, F. N., Dincoglu, D., and Ilhan, I. (2016). Impact of 2.45 GHz microwave radiation on the testicular inflammatory pathway biomarkers in young rats: the role of gallic acid. *Environ. Toxicol.* 31, 1771–1784. doi: 10.1002/tox.22179

Sengupta, P. (2013). The laboratory rat: relating its age with Human's. *Int. J. Prev. Med.* 4, 624–630.

Šimaiová, V., Almášiová, V., Holovská, K., Kisková, T., Horváthová, F., Ševčíková, Z., et al. (2019). The effect of 2.45 GHz non-ionizing radiation on the structure and ultrastructure of the testis in juvenile rats. *Histol. Histopathol.* 34, 391–403. doi: 10.14670/hh-18-049

Stewart, W., Callis, L., Barclay, L., Barton, M. N., Blakemore, C., Coggon, D., et al. (2000). "Mobile phones and health," in *Independent Expert Group on Mobile Phones*, (Oxon: National Radiological Protection Board), 1–160. .

Todorova, N., Bentvelzen, A., English, N. J., and Yarovsky, I. (2016). Electromagnetic effects on structure and dynamics of amyloidogenic peptides. *J. Chem. Phys.* 144:085101. doi: 10.1063/1.4941108

Walczak-Jędrzejowska, R., Marchlewska, K., Oszukowska, E., Filipiak, E., Słowikowska-Hilczer, J., and Kula, K. (2013). Estradiol and testosterone inhibit rat seminiferous tubule development in a hormone-specific way. *Reprod. Biol.* 13, 243–250. doi: 10.1016/j.repbio.2013.07.005

Wiesner, C., Nabha, S. M., Bonfil, R. D., Dos Santos, E. B., Yamamoto, H., Meng, H., et al. (2008). C-kit and its ligand stem cell factor: potential contribution to prostate cancer bone metastasis. *Neoplasia* 10, 996–1003. doi: 10.1593/neo.08618

Xu, H., Shen, L., Chen, X., Ding, Y., He, J., Zhu, J., et al. (2016). mTOR/P70S6K promotes spermatogonia proliferation and spermatogenesis in sprague dawley rats. *Reprod. Biomed. Online* 32, 207–217. doi: 10.1016/j.rbmo.2015.11.007

Zhang, L., Tang, J., Haines, C. J., Feng, H., Lai, L., Teng, X., et al. (2011). c-kit and its related genes in spermatogonial differentiation. *Spermatogenesis* 1, 186–194. doi: 10.4161/spmg.1.3.17760

Zhao, R., Li, G., Kong, X. J., Huang, X. Y., Li, W., Zeng, Y. Y., et al. (2016). The improvement effects of edible Bird's nest on proliferation and activation of B lymphocyte and its antagonistic effects on immunosuppression induced by cyclophosphamide. *Drug Des. Devel. Ther.* 10, 371–381. doi: 10.2147/DDDT.S88193

Zhu, H., Yan, R., Huang, Z., Li, R., and Wang, S. (2014). Experimental studies on leaked electromagnetic fields around radio frequency heating systems. *Appl. Eng. Agri.* 30:4. doi: 10.13031/aea.30.10597

Conflict of Interest: The authors declare that the research was conducted in the absence of any commercial or financial relationships that could be construed as a potential conflict of interest.

frontiers in Endocrinology

ORIGINAL RESEARCH
published: 23 March 2022
doi: 10.3389/fendo.2022.849534

Associations of Sperm mtDNA Copy Number, DNA Fragmentation Index, and Reactive Oxygen Species With Clinical Outcomes in ART Treatments

Wei-Hui Shi[1,2†], Mu-Jin Ye[1,2†], Ning-Xin Qin[3†], Zhi-Yang Zhou[1,2], Xuan-You Zhou[1,2], Nai-Xin Xu[1,2], Song-Chang Chen[4], Shu-Yuan Li[1,2] and Chen-Ming Xu[1,2,4*]*

[1] International Peace Maternity and Child Health Hospital, School of Medicine, Shanghai Jiao Tong University, Shanghai, China, [2] Shanghai Key Laboratory of Embryo Original Diseases, Shanghai, China, [3] Department of Assisted Reproductive Medicine, Shanghai First Maternity and Infant Hospital, School of Medicine, Tongji University, Shanghai, China, [4] Obstetrics and Gynecology Hospital, Institute of Reproduction and Development, Fudan University, Shanghai, China

OPEN ACCESS

Edited by:
Panagiotis Drakopoulos,
University Hospital Brussels, Belgium

Reviewed by:
Alex C. Varghese,
Astra Fertility Group, Canada
Borut Kovacic,
Maribor University Medical Centre, Slovenia

***Correspondence:**
Chen-Ming Xu
chenming_xu2006@163.com
Shu-Yuan Li
shuyuanli816@163.com

[†]These authors have contributed equally to this work

Specialty section:
This article was submitted to Reproduction, a section of the journal Frontiers in Endocrinology

Received: 06 January 2022
Accepted: 21 February 2022
Published: 23 March 2022

Citation:
Shi W-H, Ye M-J, Qin N-X, Zhou Z-Y, Zhou X-Y, Xu N-X, Chen S-C, Li S-Y and Xu C-M (2022) Associations of Sperm mtDNA Copy Number, DNA Fragmentation Index, and Reactive Oxygen Species With Clinical Outcomes in ART Treatments. Front. Endocrinol. 13:849534. doi: 10.3389/fendo.2022.849534

Recent studies have suggested that sperm mitochondrial DNA copy number (mtDNA-CN), DNA fragmentation index (DFI), and reactive oxygen species (ROS) content are crucial to sperm function. However, the associations between these measurements and embryo development and pregnancy outcomes in assisted reproductive technology (ART) remain unclear. Semen samples were collected from 401 participants, and seminal quality, parameters of sperm concentration, motility, and morphology were analyzed by a computer-assisted sperm analysis system. DFI, mtDNA-CN, and ROS levels were measured using sperm chromatin structure assay, real-time quantitative polymerase chain reaction, and ROS assay, respectively. Among the participants, 126 couples underwent ART treatments, including *in vitro* fertilization (IVF) and intracytoplasmic sperm injection (ICSI), and 79 of the couples had embryos transferred. In 401 semen samples, elevated mtDNA-CN and DFI were associated with poor seminal quality. In 126 ART couples, only mtDNA-CN was negatively correlated with the fertilization rate, but this correlation was not significant after adjusting for male age, female age, seminal quality, ART strategy, number of retrieved oocytes, controlled stimulation protocols, and cycle rank. Regarding pregnancy outcomes, sperm mtDNA-CN, ROS, and DFI were not associated with the clinical pregnancy rate or live birth rate in 79 transferred cases. In conclusion, increased mtDNA-CN and DFI in sperm jointly contributed to poor seminal quality, but sperm mtDNA-CN, ROS, and DFI were not associated with clinical outcomes in ART.

Keywords: sperm mitochondrial DNA copy number, DNA fragmentation index, reactive oxygen species, sperm quality, assisted reproductive technology

INTRODUCTION

It is estimated that over 186 million people are affected by infertility, and assisted reproductive technology (ART) treatments are continuously increasing worldwide (1). However, there is a challenge in that a large proportion of embryos during ART end with adverse outcomes, such as implantation failures and miscarriages (2). Abnormal gametes from parents impact embryo quality, and the effect of paternal factors has been increasingly explored in recent years (3, 4).

Previous studies have investigated the associations between seminal quality, including parameters of sperm concentration, motility, and morphology, and ART outcomes. It has been reported that both sperm concentration and motility are strongly correlated with the fertilization rate, and poor seminal quality may lead to developmental failures of embryos, mainly manifested as blastomere fragmentations (5). However, sperms with normal morphology were selected for the intracytoplasmic sperm injection (ICSI) process, and sperm concentration rarely affects this treatment. Thus, sperm motility plays a more significant role in embryo development in ICSI (6).

Researchers have investigated the relationship between sperm structural abnormalities and adverse pregnancy outcomes (7–9). As an indicator of sperm chromatin integrity, the DNA fragmentation index (DFI) has been suggested to have a negative correlation with embryo development and implantation rates in ICSI cycles (9), while some studies have indicated contrary results (10). Sperm mitochondria are essential to the normal reproductive process, as they are involved in multiple functions, including the production of adenine triphosphate and reactive oxygen species (ROS) as well as the regulation of apoptosis (11). Oxidative stress induced by excess ROS in sperm has been found to impair DNA demethylation in the paternal pronucleus and affects embryo development (8). A negative association has been observed between seminal ROS and pregnancy rates after *in vitro* fertilization (IVF) (12). Additionally, sperm mitochondrial DNA copy number (mtDNA-CN), a relative measure of mtDNA content, has also been reported to be negatively correlated with the fertilization rate (13). Rosati et al. (14) found that higher sperm mtDNA-CN is associated with lower pregnancy probability in couples without contraception, suggesting that mtDNA might be a potential clinical biomarker to predict male fecundity.

It remains unclear whether the measurements mentioned above, namely, DFI, mtDNA-CN, and ROS, are predictive of ART outcomes. Therefore, the present study aimed to investigate the correlations of sperm mtDNA-CN, ROS, and DFI with male fertility, embryo viability, and pregnancy outcomes.

METHODS

Subjects

All participants were recruited from July 2020 to September 2020 from the Outpatient Department of the Reproductive Center at the International Peace Maternity and Child Health Hospital (IPMCH), Shanghai Jiao Tong University School of Medicine. The inclusion criteria were as follows: 1) 20–50 years of age; 2) no *AZF* gene microdeletions; 3) no mycoplasma or chlamydia infections; 4) no medication taken within 3 months; and 5) sperm concentration ≥1 million/ml. Semen samples were collected by masturbation after 3–7 days of sexual abstinence. The present study was approved by the IPMCH Ethics Review Committee and performed according to the Declaration of Helsinki. Written consent forms were obtained from all participants.

Semen Analysis and Sperm Chromatin Structure Assay

After liquefaction, sperm concentration and motility were assessed by the computer-assisted sperm analysis (CASA) system (Hamilton Thorne IVOS II, USA), and sperm morphology was evaluated with Papanicolaou staining according to the World Health Organization (WHO) laboratory manual (15). Sperm DFI was determined by a sperm chromatin structure assay (8). In detail, sperm samples were first diluted to a concentration of 2×10^6/ml with TNE buffer (0.01 M Tris–HCl, pH 7.4, 0.15 M NaCl, 1 mM EDTA). Then, 100 μl of diluted sperm suspension was mixed with 200 μl of acid-detergent solution (pH 1.2; 0.08 N HCl, 0.15 M NaCl, 0.1% Triton X-100) and incubated for 30 s on ice. After adding 600 μl of acridine orange, the sample was incubated for 3 min and analyzed by the NovoCyte Flow Cytometer (Agilent, CA, USA).

Sperm DNA Extraction

Semen samples were washed three times with 1× PBS and centrifuged at 200 g for 5 min. Somatic cells were eliminated with 0.1% sodium dodecyl sulfate (3250GR500, BioFroxx) and 0.5% Triton™-X100 (X100, Sigma) in diethypyrocarbonate (DEPC)-treated water (AM9920, Invitrogen) at 4°C for 15 min. The spermatozoa were then homogenized with 1-mm beads in Tissue Lysis buffer (69504, Qiagen) containing 10 mg/ml Proteinase K and 150 mM DL-dithiothreitol (A100281, Sangon Biotech, China). Total sperm DNA was extracted using the DNeasy Blood & Tissue Kit (69504, Qiagen) following the manufacturer's instructions.

Quantification of mtDNA Copy Number

The mtDNA-CN was measured by real-time quantitative polymerase chain reaction (qPCR) using a QuantStudio™ 7 Flex real-time PCR machine (4485701, Applied Biosystems) (16). Briefly, TaqMan primers were designed in a stable segment in the minor arc of mtDNA (mtMinArc), and RNAse P (4403326, ThermoFisher, USA) was used as the genomic DNA reference. The detailed primer sequences are shown in **Supplementary Table S1**. Real-time PCR with three technical replicates was performed as previously described (16). The mtDNA-CN was calculated using the following formula: mtDNA-CN = $2^{\triangle CT\ (mtDNA\text{-}CN)}$, where $\triangle$CT (mtDNA-CN) = CTRNase P − CTmtMinArc.

Determination of Sperm Reactive Oxygen Species Levels

Sperm ROS content was measured by a ROS assay kit (S0033M, Beyotime Biotech, Shanghai, China) following the manufacturer's instructions. The collected sperm samples were washed three times with 1× PBS (200 g, 5 min) and then incubated with 2',7'-dichlorodihydrofluorescein diacetate (DCFH-DA; 10 μmol/L) at 37°C for 20 min. The samples were then washed three times with 1× PBS (200 g, 5 min), and the fluorescent signals of DCFH-DA oxidized products [2',7'-dichlorofluorescein (DCF)] were detected using a Synergy™ H1 Microplate Reader (BioTek Instruments, Inc., Vermont, USA) under 488-nm excitation. To normalize the ROS level, ROS per million sperm (ROS/MS) was used to represent the average ROS content in each seminal sample.

Assisted Reproductive Technology Procedure

Different protocols of controlled ovarian stimulation (COS), including gonadotrophin-releasing hormone agonist (GnRH-a) protocols (long, short, and ultra-long protocols), the GnRH antagonist protocol, and mild ovarian stimulation, were performed in 126 couples according to the women's age, ovarian reserve, and previous IVF outcomes (**Supplementary Table S2**). IVF of oocytes was carried out through inseminating oocytes with motile sperm or injecting a single sperm into the cytoplasm of an oocyte. The zygotes were cultured to blastocysts on Day 5 and freshly transferred into the uterus or cryopreserved and thawed at a suitable time of embryo transfer.

Outcome Assessment

In terms of ART, only those IVF/ICSI cycles performed within 3 months after the semen analysis were included. The embryonic outcomes included the fertilization rate, cleavage rate, and top-quality embryo rate. The fertilization rate was defined as the number of two pronuclear embryos devised by the retrieved cumulus–oocyte complex. The cleavage rate was the percentage of cleaving embryos on Day 3 in all fertilized oocytes. The cleaving zygotes were classified into Grades 1–5 according to the numbers and sizes of blastomeres and the percentage of cytoplasmic fragments (17). The top-quality embryo rate was calculated as the number of embryos evaluated as Grade 1 or 2 divided by the number of total embryos. In terms of embryos transferred into the uterus, pregnancy outcomes were evaluated in every transfer cycle. Clinical pregnancy was defined as the presence of an intrauterine gestational sac by ultrasound examination at a gestational age of 7 weeks.

Statistical Analysis

The characteristics of the participants were summarized. Continuous variables are presented as the median (interquartile range) and were compared with the Mann–Whitney U test. Categorical variables are presented as percentages and were compared using the chi-square test. Seminal quality was categorized as normal or abnormal sperm group. Sperm with at least one parameter, including sperm concentration, motility, and morphology, lower than the WHO criteria was categorized as abnormal sperm (concentration $\geq 15 \times 10^6$ per ml; total motility ≥40%; normal forms ≥4%). The associations between the three measurements (mtDNA-CN, ROS/MS, and DFI) and seminal quality were analyzed by binary logistic regression. Embryonic outcomes were analyzed with linear regression. The generalized linear model (GLM) was performed to adjust the covariates, including male age, female age, seminal quality, number of retrieved oocytes, ART strategy, and cycle rank. Regarding pregnancy outcomes, generalized estimating equations (GEEs) were used to address the correlation of different transfer cycles in the same patient. Odds ratios (ORs) and 95% confidence intervals (CIs) were calculated for the variates in the model. All statistical analyses were conducted with SPSS statistics 24 (IBM, Chicago, USA).

RESULTS

Demographic and Biochemical Characteristics of Participants

During the study period, 401 male participants who fulfilled the inclusion criteria were included in our study. Among them, 126 with their spouses were subjected to ART within 3 months after the semen analysis in our center. The demographic characteristics, sperm parameters, and three measurements are summarized in **Table 1**. Compared to the IVF cases, the ICSI cases showed lower

TABLE 1 | Sperm parameters and measurements in all participants and ART cases.

	All participants (n = 401)	IVF cases (n = 82)	ICSI cases (n = 44)	*P**
Male age, years	33 (31, 37)	33 (30, 36)	35.5(32, 40)	0.009
Female age, years		33 (29, 36)	34 (31, 38)	0.080
Percentage of male with abnormal sperms	71%	55%	59%	0.708
Morphology, %	3 (2, 4)	3 (2, 4)	3 (1, 4)	0.244
Sperm concentration, million/ml	36.99 (21.48, 59.29)	40.62 (26.21, 60.11)	36.26 (18.85, 53.64)	0.250
Total motility, %	41.90 (26.85, 52.30)	42.95 (29.75, 51.60)	34 (17.65, 49.05)	0.014
mtDNA-CN	3.80 (2.10, 7.38)	3.30 (1.96, 8.36)	4.37 (2.39, 9.07)	0.321
ROS/MS	81.33 (48.65, 174.80)	74.15 (49.89, 146.10)	73.00 (47.23, 154.66)	0.976
DFI	9.92 (5.61, 15.86)	7.98 (5.16, 14.56)	11.83 (6.59, 22.71)	0.005

The data were analyzed with the Mann–Whitney U test.

mtDNA-CN, mitochondrial DNA copy number; ROS/MS, reactive oxygen species per million sperm; DFI, DNA fragmentation index.

**P value indicates the comparison between IVF and ICSI cases.*

ART, assisted reproductive technology; IVF, in vitro fertilization; ICSI, intracytoplasmic sperm injection.

total motility and higher DFI levels ($P < 0.05$). For controlled ovarian stimulation, 80 cases underwent the GnRH antagonist protocol, 27 cases underwent mild ovarian stimulation, and 19 cases underwent GnRH agonist protocols, including long, short, and ultra-long protocols (**Supplementary Table S2**).

Associations of Sperm mtDNA-CN, DNA Fragmentation Index, and Reactive Oxygen Species With Seminal Quality

Univariate logistic regression showed that mtDNA-CN, ROS/MS, and DFI were all negatively associated with seminal quality (**Supplementary Table S3**). Based on the fifth WHO laboratory manual (15), the seminal samples were divided into two groups as follows: the normal sperm group (n = 116) and the abnormal sperm group (n = 285). As shown in **Figure 1**, the multivariate logistic regression suggested that only the mtDNA-CN (OR 1.102, 95% CI 1.042–1.166; $P = 0.001$) and DFI (OR 1.133, 95% CI 1.083–1.185; $P = 6.768 \times 10^{-8}$) were associated with seminal quality.

Correlations of Sperm mtDNA-CN, DNA Fragmentation Index, and Reactive Oxygen Species With Embryonic Outcomes

Regarding the three embryonic outcomes, a higher sperm mtDNA-CN level was associated with a lower fertilization rate in all ART cases (**Table 2**) ($\beta = -0.629$, 95% CI -1.175 to -0.083; $P = 0.024$). The quartile analysis showed a similar trend that the fourth quartile group of sperm mtDNA-CN had the lowest fertilization rate (**Table 3**). However, after adjustment for factors, including male age, female age, seminal quality, number of retrieved oocytes, ART strategy, COS protocols, and cycle rank, the adjusted model indicated that the association between sperm mtDNA-CN and fertilization rate was not significant (**Table 3**). There was no significant correlation between sperm mtDNA-CN and cleavage rate ($\beta = 0.108$, 95% CI -0.344 to 0.560; $P = 0.637$) or top-quality embryo rate ($\beta = 0.345$, 95% CI -0.345 to 1.034; $P = 0.325$) (**Table 2**).

Moreover, neither ROS/MS nor DFI was associated with three embryonic outcomes in all ART cases (**Table 2**). However, in 92 couples performed with the first ART cycle, there was a statistically significant association between the DFI and fertilization rate (**Supplementary Table S4**), which was not observed after adjustment for male age, female age, seminal

TABLE 3 | Association of mtDNA-CN with fertilization rate.

mtDNA-CN	Fertilization rate			
	OR (95% CI)	*P*	Adj OR (95% CI) [a]	*P*
Q1	Reference			
Q2	0.919 (0.818, 1.033)	0.158	0.921 (0.826, 1.028)	0.144
Q3	0.928 (0.826, 1.043)	0.211	0.968 (0.868, 1.079)	0.553
Q4	0.870 (0.773, 0.979)	0.021	0.915 (0.817, 1.025)	0.125

The data were analyzed with quartile analysis.
Q1–4, quartiles 1–4; OR, odds ratio.
[a]Adj OR was adjusted for male age, female age, seminal quality, number of retrieved oocytes, ART strategy (IVF/ICSI), COS protocols, and cycle rank.
CI, confidence interval.

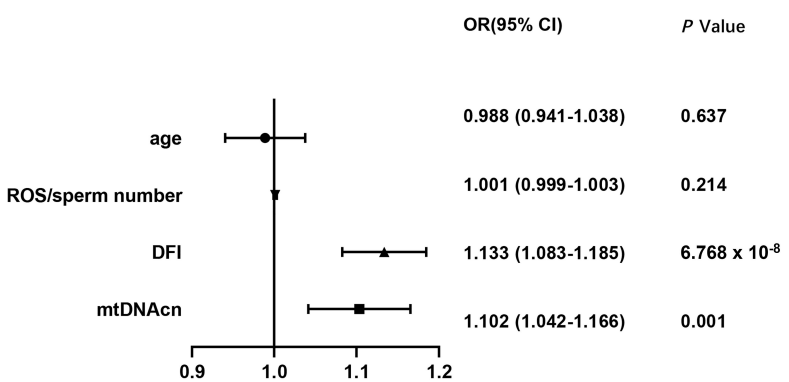

FIGURE 1 | Associations of mtDNA-CN, DFI, ROS, and male age with seminal quality. mtDNA-CN, mitochondrial DNA copy number; ROS, reactive oxygen species; DFI, DNA fragmentation index; OR, odds ratio; CI, confidence interval.

TABLE 2 | Embryonic outcomes of patients with ART.

	Fertilization rate (%)		Cleavage rate (%)		Top-quality embryo rate (%)	
	Coefficients (95% CI)	*P*	Coefficients (95% CI)	*P*	Coefficients (95% CI)	*P*
mtDNA-CN	-0.629 (-1.175, -0.083)	0.024	0.108 (-0.344, 0.560)	0.637	0.345 (-0.345, 1.034)	0.325
DFI	-0.128 (-0.567, 0.311)	0.564	0.127 (-0.229, 0.483)	0.482	0.377 (-0.165, 0.919)	0.171
ROS/MS	-0.012 (-0.035, 0.012)	0.325	0.005 (-0.013, 0.024)	0.566	0.009 (-0.20, 0.038)	0.532

The data were analyzed with linear regression (n = 126).
ART, assisted reproductive technology; mtDNA-CN, mitochondrial DNA copy number; ROS/MS, reactive oxygen species per million sperm; DFI, DNA fragmentation index; CI, confidence interval.

quality, number of retrieved oocytes, ART strategy, and COS protocols (**Supplementary Table S5**).

Pregnancy Outcomes

To date, 79 of 126 couples undergoing ART have undergone embryo transfer. In total, 114 transfer cycles were conducted, including 12 fresh embryo transfers and 102 frozen embryo transfers (**Supplementary Table S6**). In all transfer cycles, mtDNA-CN, DFI, and ROS/MS were not associated with clinical pregnancy rate and live birth rate (**Table 4**), and this lack of association remained after adjustment for male age, female age, seminal quality, types of embryo transfer (frozen or fresh), ART strategy, IVF cycle rank, COS protocols, and number of retrieved oocytes (**Supplementary Table S7**).

DISCUSSION

In the present study, we found that three sperm measurements, namely, mtDNA-CN, DFI, and ROS, were negatively associated with seminal quality. In 92 cases conducted with the first ART cycle, high levels of mtDNA-CN and DFI were correlated with a poor fertilization rate. However, this correlation was not significant after adjusting for male age, female age, seminal quality, ART strategy, number of retrieved oocytes, COS protocols, and cycle rank. Moreover, pregnancy outcomes were summarized in 79 cases of transferred embryos, and no associations were found between the three measurements and the clinical pregnancy rate or the live birth rate.

During spermatogenesis, most of the cytoplasm is discarded, while a proportion of mitochondria are retained in the midpiece of mature sperm to provide energy for flagellar beating (18). The role of mitochondria in sperm function, especially sperm motility, has been widely noted. It has been reported that abnormal mitochondrial structures and functions, such as short midpieces, abnormal assemblies, and membranous defects, are associated with poor seminal quality (19, 20). As an important component of mitochondria, mtDNA encodes 22 tRNAs, two rRNAs, and 13 proteins that are crucial for oxidative phosphorylation (21). Mutations and deletions of mtDNA have been reported in asthenozoospermia and shown to be correlated with male infertility when they present beyond a certain threshold level (22). In addition, amplification of sperm mtDNA-CN has been observed in sperm samples from infertile males (23).

TABLE 4 | Pregnancy outcomes of patients with embryo transfer.

	Clinical pregnancy		Live birth	
	OR (95% CI)	*P*	OR (95% CI)	*P*
mtDNA-CN	0.997 (0.943, 1.055)	0.927	1.014 (0.959, 1.071)	0.635
DFI	1.013 (0.969, 1.059)	0.575	1.011 (0.966, 1.058)	0.651
ROS/MS	1.001 (0.999, 1.004)	0.241	1.000 (0.998, 1.003)	0.784

The data were analyzed with generalized estimating equations.
mtDNA-CN, mitochondrial DNA copy number; ROS/MS, reactive oxygen species per million sperm; DFI, DNA fragmentation index; CI, confidence interval; OR, odds ratio.

Consistent with previous studies in various species (23–26), higher mtDNA-CN in abnormal sperm was observed in the present study. Although the underlying mechanism remains unclear, the elevated mtDNA-CN in abnormal sperm might be explained by abnormal gene expression, mtDNA mutations/deletions, and mitochondria *per se*. First, abnormal expression of genes that regulate mtDNA transcription and replication, such as mitochondrial transcription factor A (*TFAM*), may be responsible for the elevated mtDNA-CN. Because *TFAM* expression is positively associated with mtDNA-CN and negatively correlated with sperm motility (27), increased *TFAM* expression may lead to the aberrant replication of mtDNA in abnormal sperm. Second, increased mtDNA-CN may compensate for mitochondrial dysfunction caused by mtDNA mutations or deletions (28–30). Moreover, mtDNA-CN may accumulate due to the imbalance between mitochondrial fusion and fission. In mitochondrial fission factor (*Mff*) mutant mice, sperm mitochondria fail to divide and mitochondrial sheaths are disjointed, resulting in abnormal sperm morphology and motility, which ultimately cause reduced fertility in mice (31).

ROS, a variety of oxygen-derived free radicals, is essential for sperm maturation, capacitation, hyperactivation, and acrosome reactions at low levels (32). However, excess ROS leads to oxidative stress and DNA damage in sperm, including DNA fragmentation, mtDNA damage, telomere attrition, epigenetic abnormalities, and Y chromosome microdeletions (33). In the present study, ROS/MS was correlated with mtDNA-CN in both normal and abnormal sperm groups, while the association of ROS/MS and DFI was not observed (**Supplementary Figure S1**), indicating that the negative effects of ROS on mtDNA may be more serious than those on nuclear DNA. Compared to nuclear DNA, mtDNA is adjacent to the ROS source and more susceptible to oxidative stress due to a lack of protective histones and repair system. In the multivariate logistic regression analysis, the association with ROS/MS was not significant, yet mtDNA and DFI were still associated with seminal quality, suggesting that mtDNA and DFI are more predictive of seminal quality.

For embryo and pregnancy outcomes, it has been reported that abnormal seminal quality has negative paternal effects in IVF or ICSI procedures (5, 6, 34, 35). However, the effects of sperm mtDNA-CN, DFI, and ROS on embryo quality are ambiguous. In 2019, Wu et al. (13) found that sperm mtDNA-CN, as well as mtDNA deletions, is inversely associated with the odds of fertilization and high-quality embryos after adjusting for male age and measurement batches. In addition, a prospective study of couples discontinuing contraception has revealed that a higher mtDNA-CN is associated with a lower pregnancy probability (14). In contrast, it has been recently reported that sperm mtDNA-CN is not a prognostic factor for fertilization, usable blastocyst development, or live birth rates in couples who undergo ICSI (36). In this study, mtDNA-CN is negatively associated with the fertilization rate, but the association is not significant after adjusting for male age, female age, seminal quality, number of retrieved oocytes, ART strategy, and cycle

rank. Thus, further studies on the role of mtDNA-CN in embryo development are needed.

The role of DFI has been investigated over a longer time span, and many meta-analyses and systematic reviews have summarized the effect of sperm DNA damage on clinical outcomes after IVF or ICSI (37–41). Overall, these studies have suggested that there is a difference between the outcomes of IVF and ICSI. Most studies have reported no significant association of DFI and clinical outcomes in ICSI. Nevertheless, increased DFI leads to a negative impact on IVF outcomes, including fertilization rate, embryo quality, implantation rate, pregnancy rate, and live birth rate (41, 42). However, the correlation analysis of DFI and IVF outcomes in these studies was not adjusted for factors, such as seminal quality, COS protocols, and number of retrieved oocytes. In the present study, the correlation of DFI with fertilization rate was also observed in the first ART cycle of couples, but this correlation was not statistically significant in the adjusted model. Notably, in the study by Pregl Breznik et al. (42), washed sperm samples during IVF procedures were analyzed for hyaluronan-binding assays, DFI, and hyperactivity, which was a good strategy to attenuate the impact of fluctuations in sperm measurements on clinical outcomes.

Sperm ROS was reported to have a greater effect on embryo development than the fertilization process (43). However, negative associations of ROS with fertilization rate and pregnancy rate have also been reported (12, 44). In the present study, however, ROS/MS was not correlated with the fertilization rate, cleavage rate, top-quality embryo rate, or clinical pregnancy rate.

The present study prospectively investigated the relationships between three sperm measurements and clinical outcomes throughout the ART procedure, including seminal quality, fertilization rate, cleavage rate, clinical pregnancy rate, and live birth rate. A major limitation of this study was the limited sample size for the analysis of embryonic/pregnancy outcomes. Moreover, the sperm samples analyzed for the three measurements and sperm quality were collected before the ART procedure. Even though the analysis of IVF/ICSI cycles was restricted to within 3 months after the semen analysis, the fluctuations in sperm measurements and parameters could not be ignored. Multicenter studies with a larger sample size are warranted to validate these findings in the future.

CONCLUSIONS

In conclusion, sperm mtDNA-CN, ROS/MS, and DFI were separately associated with sperm parameters, while elevated sperm mtDNA-CN and DFI jointly contributed to poor seminal quality. Moreover, mtDNA-CN was negatively correlated with fertilization rate in ART cases, which was not significant after adjusting for male age, female age, seminal quality, ART strategy, number of retrieved oocytes, COS protocols, and cycle rank. For pregnancy outcomes, sperm mtDNA-CN, ROS/MS, and DFI were not associated with clinical pregnancy rate or live birth rate. Further studies are necessary to determine the role of sperm mtDNA-CN, ROS/MS, and DFI in embryonic and fetal development.

DATA AVAILABILITY STATEMENT

The original contributions presented in the study are included in the article/**Supplementary Material**. Further inquiries can be directed to the corresponding authors.

ETHICS STATEMENT

The studies involving human participants were reviewed and approved by the International Peace Maternity and Child Health Hospital Ethics Review Committee. The patients/participants provided their written informed consent to participate in this study.

AUTHOR CONTRIBUTIONS

WHS and MJY collected seminal samples and wrote the article. ZYZ and NXQ performed the experiments and analyzed the data. XYZ, NXX, and SCC collected the clinical outcomes of the participants. SYL and CMX designed the study and revised the article. All authors contributed to the article and approved the submitted version.

FUNDING

This work was supported by the National Natural Science Foundation of China (Nos. 81771638, 81971344, 81871136, and 81501231) and the Shanghai Municipal Health Commission (No. GW-10.1-XK07).

ACKNOWLEDGMENTS

We appreciate the support provided by the Youth Science and Technology Innovation Studio, Shanghai Jiao Tong University School of Medicine.

SUPPLEMENTARY MATERIAL

The Supplementary Material for this article can be found online at: https://www.frontiersin.org/articles/10.3389/fendo.2022.849534/full#supplementary-material

REFERENCES

1. Inhorn MC, Patrizio P. Infertility Around the Globe: New Thinking on Gender, Reproductive Technologies and Global Movements in the 21st Century. *Hum Reprod Update* (2015) 21(4):411–26. doi: 10.1093/humupd/dmv016
2. Kushnir VA, Barad DH, Albertini DF, Darmon SK, Gleicher N. Systematic Review of Worldwide Trends in Assisted Reproductive Technology 2004-2013. *Reprod Biol Endocrinol* (2017) 15(1):6. doi: 10.1186/s12958-016-0225-2
3. Colaco S, Sakkas D. Paternal Factors Contributing to Embryo Quality. *J Assist Reprod Genet* (2018) 35(11):1953–68. doi: 10.1007/s10815-018-1304-4
4. Imterat M, Agarwal A, Esteves SC, Meyer J, Harlev A. Impact of Body Mass Index on Female Fertility and ART Outcomes. *Panminerva Med* (2019) 61 (1):58–67. doi: 10.23736/s0031-0808.18.03490-0
5. Liao QY, Huang B, Zhang SJ, Chen J, Chen G, Li KZ, et al. Influence of Different Quality Sperm on Early Embryo Morphokinetic Parameters and Cleavage Patterns: A Retrospective Time-Lapse Study. *Curr Med Sci* (2020) 40 (5):960–7. doi: 10.1007/s11596-020-2272-3
6. Shoukir Y, Chardonnens D, Campana A, Sakkas D. Blastocyst Development From Supernumerary Embryos After Intracytoplasmic Sperm Injection: A Paternal Influence? *Hum Reprod* (1998) 13(6):1632–7. doi: 10.1093/humrep/13.6.1632
7. Yang Q, Zhao F, Dai S, Zhang N, Zhao W, Bai R, et al. Sperm Telomere Length is Positively Associated With the Quality of Early Embryonic Development. *Hum Reprod* (2015) 30(8):1876–81. doi: 10.1093/humrep/dev144
8. Wyck S, Herrera C, Requena CE, Bittner L, Hajkova P, Bollwein H, et al. Oxidative Stress in Sperm Affects the Epigenetic Reprogramming in Early Embryonic Development. *Epigenet Chromatin* (2018) 11(1):60. doi: 10.1186/s13072-018-0224-y
9. Borges EJr, Zanetti BF, Setti AS, Braga D, Provenza RR, Iaconelli AJr. Sperm DNA Fragmentation is Correlated With Poor Embryo Development, Lower Implantation Rate, and Higher Miscarriage Rate in Reproductive Cycles of non-Male Factor Infertility. *Fertil Steril* (2019) 112(3):483–90. doi: 10.1016/j.fertnstert.2019.04.029
10. Anifandis G, Bounartzi T, Messini CI, Dafopoulos K, Markandona R, Sotiriou S, et al. Sperm DNA Fragmentation Measured by Halosperm Does Not Impact on Embryo Quality and Ongoing Pregnancy Rates in IVF/ICSI Treatments. *Andrologia* (2015) 47(3):295–302. doi: 10.1111/and.12259
11. Durairajanayagam D, Singh D, Agarwal A, Henkel R. Causes and Consequences of Sperm Mitochondrial Dysfunction. *Andrologia* (2021) 53 (1):e13666. doi: 10.1111/and.13666
12. Zorn B, Vidmar G, Meden-Vrtovec H. Seminal Reactive Oxygen Species as Predictors of Fertilization, Embryo Quality and Pregnancy Rates After Conventional *In Vitro* Fertilization and Intracytoplasmic Sperm Injection. *Int J Androl* (2003) 26(5):279–85. doi: 10.1046/j.1365-2605.2003.00424.x
13. Wu H, Whitcomb BW, Huffman A, Brandon N, Labrie S, Tougias E, et al. Associations of Sperm Mitochondrial DNA Copy Number and Deletion Rate With Fertilization and Embryo Development in a Clinical Setting. *Hum Reprod* (2019) 34(1):163–70. doi: 10.1093/humrep/dey330
14. Rosati AJ, Whitcomb BW, Brandon N, Buck Louis GM, Mumford SL, Schisterman EF, et al. Sperm Mitochondrial DNA Biomarkers and Couple Fecundity. *Hum Reprod* (2020) 35(11):2619–25. doi: 10.1093/humrep/deaa191
15. World Health Organization, D.o.R.H.a.R. *WHO Laboratory Manual for the Examination and Processing of Human Semen*, *Fifth*. (2010). p. 287. Available at: https://www.who.int/publications/i/item/9789240030787.
16. Ye M, Shi W, Hao Y, Zhang L, Chen S, Wang L, et al. Associations of Mitochondrial DNA Copy Number and Deletion Rate With Early Pregnancy Loss. *Mitochondrion* (2020) 55:48–53. doi: 10.1016/j.mito.2020.07.006
17. Veeck LL. Oocyte Assessment and Biological Performance. *Ann N Y Acad Sci* (1988) 541:259–74. doi: 10.1111/j.1749-6632.1988.tb22263.x
18. Ho HC, Wey S. Three Dimensional Rendering of the Mitochondrial Sheath Morphogenesis During Mouse Spermiogenesis. *Microsc Res Tech* (2007) 70 (8):719–23. doi: 10.1002/jemt.20457
19. Gopalkrishnan K, Padwal V, D'Souza S, Shah R. Severe Asthenozoospermia: A Structural and Functional Study. *Int J Androl* (1995) 18 Suppl 1:67–74. doi: 10.1111/j.1365-2605.1995.tb00642.x
20. Pelliccione F, Micillo A, Cordeschi G, D'Angeli A, Necozione S, Gandini L, et al. Altered Ultrastructure of Mitochondrial Membranes is Strongly Associated With Unexplained Asthenozoospermia. *Fertil Steril* (2011) 95 (2):641–6. doi: 10.1016/j.fertnstert.2010.07.1086
21. Anderson S, Bankier AT, Barrell BG, de Bruijn MH, Coulson AR, Drouin J, et al. Sequence and Organization of the Human Mitochondrial Genome. *Nature* (1981) 290(5806):457–65. doi: 10.1038/290457a0
22. Vertika S, Singh KK, Rajender S. Mitochondria, Spermatogenesis, and Male Infertility - An Update. *Mitochondrion* (2020) 54:26–40. doi: 10.1016/j.mito.2020.06.003
23. May-Panloup P, Chrétien Mf Fau - Savagner F, Savagner F Fau - Vasseur C, Vasseur C Fau - Jean M, Jean M Fau - Malthièry Y, Malthièry Y Fau - Reynier P, et al. Increased Sperm Mitochondrial DNA Content in Male Infertility. *Hum Reprod* (2003) 18(3):550–6. doi: 10.1093/humrep/deg096
24. Darr CR, Moraes LE, Connon RE, Love CC, Teague S, Varner DD, et al. The Relationship Between Mitochondrial DNA Copy Number and Stallion Sperm Function. *Theriogenology* (2017) 94:94–9. doi: 10.1016/j.theriogenology.2017.02.015
25. Guo H, Gong Y, He B, Zhao R. Relationships Between Mitochondrial DNA Content, Mitochondrial Activity, and Boar Sperm Motility. *Theriogenology* (2017) 87:276–83. doi: 10.1016/j.theriogenology.2016.09.005
26. Hesser A, Darr C, Gonzales K, Power H, Scanlan T, Thompson J, et al. Semen Evaluation and Fertility Assessment in a Purebred Dog Breeding Facility. *Theriogenology* (2017) 87:115–23. doi: 10.1016/j.theriogenology.2016.08.012
27. Faja F, Carlini T, Coltrinari G, Finocchi F, Nespoli M, Pallotti F, et al. Human Sperm Motility: A Molecular Study of Mitochondrial DNA, Mitochondrial Transcription Factor A Gene and DNA Fragmentation. *Mol Biol Rep* (2019) 46(4):4113–21. doi: 10.1007/s11033-019-04861-0
28. Heidari MM, Khatami M, Danafar A, Dianat T, Farahmand G, Talebi AR. Mitochondrial Genetic Variation in Iranian Infertile Men With Varicocele. *Int J Fertil Steril* (2016) 10(3):303–9. doi: 10.22074/ijfs.2016.5047
29. Bahrehmand Namaghi I, Vaziri H. Sperm Mitochondrial DNA Deletion in Iranian Infertiles With Asthenozoospermia. *Andrologia* (2017) 49(3):e12627. doi: 10.1111/and.12627
30. Al Zoubi MA-O, Al-Batayneh K, Alsmadi M, Rashed M, Al-Trad BA-O, Al Khateeb W, et al. 4,977-Bp Human Mitochondrial DNA Deletion is Associated With Asthenozoospermic Infertility in Jordan. *Andrologia* (2020) 52(1):e13379. doi: 10.1111/and.13379
31. Varuzhanyan G, Chen H, Rojansky R, Ladinsky MS, McCaffery JM, Chan DC. Mitochondrial Fission Factor (Mff) is Required for Organization of the Mitochondrial Sheath in Spermatids. *Biochim Biophys Acta Gen Subj* (2021) 1865(5):129845. doi: 10.1016/j.bbagen.2021.129845
32. Aitken RA-OX. Reactive Oxygen Species as Mediators of Sperm Capacitation and Pathological Damage. *Mol Reprod Dev* (2017) 84(10):1039–52. doi: 10.1002/mrd.22871
33. Bui AD, Sharma RA-O, Henkel RA-O, Agarwal AA-O. Reactive Oxygen Species Impact on Sperm DNA and its Role in Male Infertility. *Andrologia* (2018) 50(8):e13012. doi: 10.1111/and.13012
34. Parinaud J, Mieusset R, Vieitez G, Labal B, Richoilley G. Influence of Sperm Parameters on Embryo Quality. *Fertil Steril* (1993) 60(5):888–92. doi: 10.1016/s0015-0282(16)56292-x
35. Janny L, Menezo YJ. Evidence for a Strong Paternal Effect on Human Preimplantation Embryo Development and Blastocyst Formation. *Mol Reprod Dev* (1994) 38(1):36–42. doi: 10.1002/mrd.1080380107
36. Tiegs AW, Tao X, Landis J, Zhan Y, Franasiak JM, Seli E, et al. Sperm Mitochondrial DNA Copy Number Is Not a Predictor of Intracytoplasmic Sperm Injection (ICSI) Cycle Outcomes. *Reprod Sci* (2020) 27(6):1350–6. doi: 10.1007/s43032-020-00163-0
37. Li Z, Wang L, Cai J, Huang H. Correlation of Sperm DNA Damage With IVF and ICSI Outcomes: A Systematic Review and Meta-Analysis. *J Assist Reprod Genet* (2006) 23(9-10):367–76. doi: 10.1007/s10815-006-9066-9
38. Zhao J, Zhang Q, Wang Y, Li Y. Whether Sperm Deoxyribonucleic Acid Fragmentation has an Effect on Pregnancy and Miscarriage After *In Vitro* Fertilization/Intracytoplasmic Sperm Injection: A Systematic Review and Meta-Analysis. *Fertil Steril* (2014) 102(4):998–1005.e1008. doi: 10.1016/j.fertnstert.2014.06.033
39. Simon L, Zini A, Dyachenko A, Ciampi A, Carrell DT. A Systematic Review and Meta-Analysis to Determine the Effect of Sperm DNA Damage on In

Vitro Fertilization and Intracytoplasmic Sperm Injection Outcome. *Asian J Androl* (2017) 19(1):80–90. doi: 10.4103/1008-682x.182822
40. Deng C, Li T, Xie Y, Guo Y, Yang QY, Liang X, et al. Sperm DNA Fragmentation Index Influences Assisted Reproductive Technology Outcome: A Systematic Review and Meta-Analysis Combined With a Retrospective Cohort Study. *Andrologia* (2019) 51(6):e13263. doi: 10.1111/and.13263
41. Ribas-Maynou J, Yeste M, Becerra-Tomás N, Aston KI, James ER, Salas-Huetos A. Clinical Implications of Sperm DNA Damage in IVF and ICSI: Updated Systematic Review and Meta-Analysis. *Biol Rev Camb Philos Soc* (2021) 96(4):1284-300. doi: 10.1111/brv.12700
42. Pregl Breznik B, Kovačič B, Vlaisavljević V. Are Sperm DNA Fragmentation, Hyperactivation, and Hyaluronan-Binding Ability Predictive for Fertilization and Embryo Development in *In Vitro* Fertilization and Intracytoplasmic Sperm Injection? *Fertil Steril* (2013) 99(5):1233–41. doi: 10.1016/j.fertnstert.2012.11.048
43. Kuroda S, Takeshima T, Takeshima K, Usui K, Yasuda K, Sanjo H, et al. Early and Late Paternal Effects of Reactive Oxygen Species in Semen on Embryo Development After Intracytoplasmic Sperm Injection. *Syst Biol Reprod Med* (2020) 66(2):122–8. doi: 10.1080/19396368.2020.1720865
44. Das S, Chattopadhyay R, Jana SK, Narendra BK, Chakraborty C, Chakravarty B, et al. Cut-Off Value of Reactive Oxygen Species for Predicting Semen Quality and Fertilization Outcome. *Syst Biol Reprod Med* (2008) 54(1):47–54. doi: 10.1080/19396360701883274

Conflict of Interest: The authors declare that the research was conducted in the absence of any commercial or financial relationships that could be construed as a potential conflict of interest.

Publisher's Note: All claims expressed in this article are solely those of the authors and do not necessarily represent those of their affiliated organizations, or those of the publisher, the editors and the reviewers. Any product that may be evaluated in this article, or claim that may be made by its manufacturer, is not guaranteed or endorsed by the publisher.

Advantages of publishing in Frontiers

OPEN ACCESS
Articles are free to read for greatest visibility and readership

FAST PUBLICATION
Around 90 days from submission to decision

HIGH QUALITY PEER-REVIEW
Rigorous, collaborative, and constructive peer-review

TRANSPARENT PEER-REVIEW
Editors and reviewers acknowledged by name on published articles

Frontiers
Avenue du Tribunal-Fédéral 34
1005 Lausanne | Switzerland

Visit us: www.frontiersin.org
Contact us: frontiersin.org/about/contact

REPRODUCIBILITY OF RESEARCH
Support open data and methods to enhance research reproducibility

DIGITAL PUBLISHING
Articles designed for optimal readership across devices

FOLLOW US
@frontiersin

IMPACT METRICS
Advanced article metrics track visibility across digital media

EXTENSIVE PROMOTION
Marketing and promotion of impactful research

LOOP RESEARCH NETWORK
Our network increases your article's readership